Karlsruhe Institute of Technology

Implementation of GDH model in TALYS-1.7 code

by A.Yu.Konobeyev[1], U.Fischer[1], P.E.Pereslavtsev[1], A.Koning[2], M.Blann[3]

KIT SCIENTIFIC WORKING PAPERS 45

[1] Institute for Neutron Physics and Reactor Technology, KIT
[2] Nuclear Data Section, International Atomic Energy Agency, Vienna
[3] 75-5865 Walua Rd. D423, Kailua-Kona, Hi. 967409, US

Impressum

Karlsruher Institut für Technologie (KIT)
www.kit.edu

2016

ISSN: 2194-1629

KIT Scientific Working Papers
ISSN 2194-1629
www.kit.edu

Abstract

The geometry dependent hybrid model proposed by M.Blann and supplied with models for the non-equilibrium cluster emission was implemented in the TALYS-1.74 code. A number of subprograms of ALICE and ALICE/ASH codes after an appropriate modification were added to TALYS. The value of the TALYS input variable *preeqmode* equal to five is reserved for the use of new approach. The calculated nucleon and light cluster energy distributions are compared with measured data.

CONTENTS

1. Introduction

More than forty years the geometry dependent hybrid model (GDH) proposed by M.Blann [1] is used successfully for the simulation of non-equilibrium emission of nucleon and light clusters in nuclear reactions at intermediate energies. An advance of the use of the GDH model with a combination with the Hauser-Feshbach model was clearly demonstrated [2,3].

The TALYS code [4] represents a new generation of nuclear model codes combining a number of well justified models and approaches for the simulation of particle interaction with nuclei. In practice the use of various alternative methods of calculations available by user's choice gives a unique possibility to understand a real uncertainty of theoretical predictions of calculated cross-sections and particle distributions.

The goal of the present work is an extension of the current version of the TALYS code by the implementation of the GDH model and performing test calculations.

A brief description of implemented models, changes in the TALYS text, and results of test calculations are given below.

2. Brief description of models implemented in TALYS

2.1 Pre-compound nucleon emission

In the GDH model the pre-equilibrium energy distribution of nucleons is calculated as follows [5]:

$$\frac{d\sigma}{d\varepsilon_x} = \pi\lambda \sum_{l=0}^{\infty} (2l+1)\, T_l \sum_{n=n_0} {}_nX_x \frac{\omega(p-1,h,U)}{\omega(p,h,E)} \frac{\lambda_x^e}{\lambda_x^e + \lambda_x^+} g\, D_n, \qquad (1)$$

where T_l is the transmission coefficient for l-th partial wave; ${}_nX_x$ is the number of nucleons of type "x" in the n-exciton state; ε_x is the channel energy of the nucleon; $\omega(p,h,E)$ is the density of exciton states with "p" particles and "h" holes ($p+h=n$) at the excitation energy E; U is the final excitation energy, $U=E-Q_x-\varepsilon_x$ and Q_x is the nucleon separation energy; D_n is the factor [6], which takes into account a "depletion" of the n-exciton state due to the nucleon emission; n_0 is the initial exciton number.

The nucleon emission rate λ_x^e is equal to

$$\lambda_x^e = \frac{(2S_x+1)\,\mu_x\,\varepsilon_x\,\sigma_x^{inv}(\varepsilon_x)}{\pi^2\,\hbar^2\,g_x}\,, \tag{2}$$

where S_x and μ_x are the spin and reduced mass of the outgoing nucleon of type "x", σ_x^{inv} is the inverse reaction cross-section and g_x is the single-nucleon state density.

The intranuclear transition rate λ_x^+ is defined as follows

$$\lambda_x^+ = V\,\sigma_0(\varepsilon_x)\,\rho_l\,, \tag{3}$$

where V is a velocity of a nucleon inside the nucleus, σ_0 is the nucleon-nucleon scattering cross-section corrected for the Pauli principle [5], ρ_l is the average nuclear matter density at the distance from $l\lambda\!\!\!^{-}$ to $(l+1)\lambda\!\!\!^{-}$.

For nucleon induced reactions the density of excited states with the number of excitons n=2 and 3 is calculated considering the finite depth of the nuclear potential well [7]

$$\omega(1,1,E) = \frac{g(gE_F)}{2}, \quad \text{if } E > E_F \tag{5}$$

$$\omega(1,1,E) = \frac{g(gE)}{2}, \quad \text{if } E \le E_F \tag{6}$$

$$\omega(2,1,E) = \frac{g^3\left[V(2E-E_F)\right]}{4}, \quad \text{if } E > E_F \tag{7}$$

$$\omega(2,1,E) = \frac{g^3E^2}{4}, \quad \text{if } E \le E_F \tag{8}$$

where E_F is the Fermi energy, and the finite potential depth is equal to $V + Q$, and Q is the nucleon binding energy.

The number of nucleons of x-type in the n-exciton state ${}_nX_x$ for incident neutrons is calculated as

$${}_3X_n = 2\,\frac{(\sigma_{np}/\sigma_{nn})Z + 2N}{2(\sigma_{np}/\sigma_{nn})Z + 2N}, \tag{9}$$

$${}_3X_p = 2 - {}_3X_n\,, \tag{10}$$

and for incident proton

$${}_3X_p = 2\,\frac{(\sigma_{pn}/\sigma_{pp})N + 2Z}{2(\sigma_{pn}/\sigma_{pp})N + 2Z}, \tag{11}$$

$$ {}_3X_n = 2 - {}_3X_p , \qquad (12) $$

where σ_{xy} is the nucleon - nucleon interaction cross-section in the nucleus.

The ratio of the nucleon-nucleon cross-sections calculated taking into account the Pauli principle and the nucleon motion is parameterized in the present work as

$$ \sigma_{pn}/\sigma_{pp} = \sigma_{np}/\sigma_{nn} = 1.375\times10^{-5}\, T^2 - 8.734\times10^{-3}\, T + 2.776, \qquad (13) $$

where T is the kinetic energy of the projectile outside the nucleus in MeV.

A correction has been made for the high energy tails of (p,xn) and (n,xp) reaction spectra calculated by the GDH model [8]. The details are given in Ref.[9].

Fig.1 shows an example of neutron energy distribution for the p+^{90}Zr reaction calculated using the GDH model implemented in TALYS and the common pre-equilibrium exciton model of TALYS.

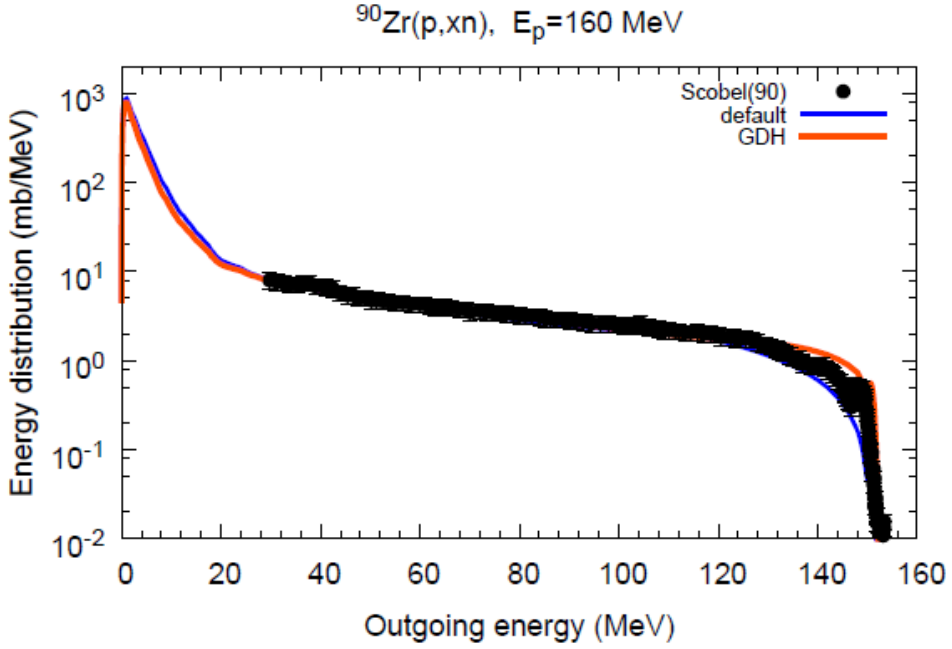

Fig.1 Neutron energy distribution for p+^{90}Zr reaction calculated using the GDH model and the “default” pre-equilibrium model of TALYS. Experimental data are discussed in the text.

2.2 Pre-compound α-particle emission

The pre-equilibrium α-particle emission spectrum for nucleon induced reaction is calculated as a sum of components corresponding to the mechanism of pick-up and knock-out

$$\frac{d\sigma}{d\varepsilon_\alpha} = \frac{d\sigma^{PU}}{d\varepsilon_\alpha} + \frac{d\sigma^{KO}}{d\varepsilon_\alpha} \tag{14}$$

The contribution of the pick-up mechanism is calculated with the help of the coalescence pick-up model [10,11] combined with the hybrid exciton model

$$\frac{d\sigma^{PU}}{d\varepsilon_\alpha} = \sigma_{non}(E_p) \sum_{n=n_0} \sum_{k+m=4} F_{k,m}(\varepsilon_\alpha) \frac{\omega(p-k,h,U)}{\omega(p,h,E)} \frac{\lambda_\alpha^e(\varepsilon_\alpha)}{\lambda_\alpha^e(\varepsilon_\alpha) + \lambda_x^+(\varepsilon_\alpha)} g_\alpha D_n , \tag{15}$$

where σ_{non} is the nonelastic interaction cross-section of the primary particle with a nucleus at kinetic energy E_p, $F_{k,m}(\varepsilon_\alpha)$ is the α-formation factor [10] equal to the probability that the α-particle is composed of "*k*" particles above Fermi level and "*m*" particles below, the residual excitation energy U is equal to $E - Q_\alpha - \varepsilon_\alpha$; λ_α^e is the emission rate of the α-particle; λ_α^+ is the intranuclear transition rate corresponding to the absorption of the α-particle in a nucleus; g_α is the intranuclear density of single particle states for the α-particle. The emission rate of α-particles is calculated as

$$\lambda_\alpha^e = \frac{(2S_\alpha + 1)\mu_\alpha \varepsilon_\alpha \sigma_\alpha^{inv}(\varepsilon_\alpha)}{\pi^2 \hbar \; g_\alpha}, \tag{16}$$

where S_α and μ_α are the spin and reduced mass of the outgoing α-particle, and the inverse reaction cross-section for α-particles, $\sigma_\alpha^{inv}(\varepsilon_\alpha)$ is calculated by the optical model with parameters discussed in Ref. [6]. The absorption rate of α-particles is defined as follows

$$\lambda_\alpha^+ = 2W_\alpha^{opt} / \hbar , \tag{17}$$

where W_α^{opt} is the imaginary part of the optical potential for α-particles.

The knock-out contribution to the α-particle energy distribution [12] is equal to

$$\frac{d\sigma^{knock-out}}{d\varepsilon_\alpha} = \sigma_{non}(E_p) \sum_{n=n_0} \phi_\alpha \frac{g}{g_\alpha p} \frac{\omega(p-1,h,U)}{\omega(p,h,E)} \frac{\lambda_\alpha^e(\varepsilon_\alpha)}{\lambda_\alpha^e(\varepsilon_\alpha) + \lambda_x^+(\varepsilon_\alpha)} g_\alpha D_n , \tag{18}$$

where the factor $g/(g_\alpha p)$ justifies the substitution of the level density $\omega(\pi,$ for the three-component system (neutron, proton, α-particle) [13,12] by the one-component state density $\omega(p,h,E)$ in Eq.(18), and φ_α is the probability of interaction of the incident particle with a "pre-formed" α-cluster resulting in its excitation in the nucleus [13].

The imaginary part of the optical potential for α-particles is calculated as follows: $W_\alpha^{opt} = (\varepsilon_\alpha/\varepsilon_0)W'$ at $\varepsilon_\alpha \le \varepsilon_0$, $W_\alpha^{opt} = W'$ at $\varepsilon_0 < \varepsilon_\alpha <$ 72 MeV, and $W_\alpha^{opt} = W' \cdot exp(0.06\varepsilon_\alpha -$ 4.32) at $\varepsilon_\alpha \ge$ 72 MeV, where $W' = \beta W_0$ and ε_0=0.228A, β=0.25. The value of W_0 is taken from Refs.[14,15] $W_0=10 +0.345(A-2Z)$ MeV. The value adopted for g_α is equal to $A/13$ [16].

2.3 Pre-compound deuteron emission

It is supposed that a non-equilibrium deuteron emission in nucleon induced reactions results from: i) the pick-up of nucleons with energy below the Fermi energy after the formation of the (2p,1h) initial exciton state, ii) coalescence of two excited nucleons with energies above E_F, iii) knock-out of a "pre-formed" deuteron, and iv) a direct process resulting in deuteron formation and escape. The non-equilibrium deuteron spectrum is calculated as a sum of different components

$$\frac{d\sigma}{d\varepsilon_d} = \frac{d\sigma^{PU}}{d\varepsilon_d} + \frac{d\sigma^{KO}}{d\varepsilon_d} + \frac{d\sigma^{D}}{d\varepsilon_d} \quad , \qquad \text{(xx)}$$

where the first term relates to pick-up and coalescence after the formation of the (2p,1h) exciton state, the second component describes the contribution of the deuteron knock-out and the last term relates to the direct process.

The exciton level density is calculated following Běták, Dobeš [17] taking into account the finite depth of the nuclear potential well

$$\omega(p,h,E) = g^p \tilde{} \sum_{k=0} (-1)^k \Theta(E - k E_F) \frac{(E - k E_F)^{n-1}}{p!h!(n-1)!} \qquad \text{(xx)}$$

where E is the excitation energy, E_F is the Fermi energy, g and $\tilde{}$ are the single particle level densities for particles and holes, respectively, $\Theta(x)$ is the Heaviside function, $\Theta = 0$ for $x < 0$ and $\Theta = 1$ for $x > 0$.

The exciton coalescence pick-up model [11] is used for the calculation of the

$d\sigma^{P\text{-}U,C}/d\varepsilon_d$ spectrum component [18]

$$\frac{d\sigma^{PU}}{d\varepsilon_d}=\sigma_{non}\sum_{n=n_0}\sum_{k+m=2}F_{k,m}(\varepsilon_d+Q_d)\,\frac{\omega(p-k,h,U)}{\omega(p,h,E)}\,\frac{\lambda_d^e(\varepsilon_d)}{\lambda_d^e(\varepsilon_d)+\lambda_d^+(\varepsilon_d)}\,g_d D_n\,, \qquad \text{(xx)}$$

where $F_{k,m}$ is the deuteron formation factor equal to the probability that the deuteron is composed of "k" particles above the Fermi level and "m" particles below; ε_d is the channel emission energy corresponding to the deuteron emission; λ_d^e is the deuteron emission rate; λ_d^+ is the intranuclear transition rate for the absorption of the deuteron in the nucleus; g_d is the density of single particle states for the deuteron.

The form factors for deuteron formation, $F_{k,m}$ were calculated in Ref.[11] for the effective nuclear radius with a *dR* parameter value equal to 1 fm. The original values [11] are approximated and used as follows

$$F_{1,1}(\varepsilon)=\begin{cases}-1.409\cdot10^{-2}\varepsilon+0.6 & \text{for } \varepsilon\le30\,\text{MeV}\\ 1.377\cdot10^{-4}\varepsilon^2-1.807\cdot10^{-2}\varepsilon+0.5946 & \text{for } 30<\varepsilon\le65\,\text{MeV}\\ 0 & \text{for } \varepsilon>65\,\text{MeV}\end{cases}, \qquad (25)$$

$$F_{2,0}(\varepsilon)=0.6-F_{1,1}(\varepsilon) \qquad (26)$$

In analogy with α-particle emission the knock-out component of the pre-compound deuteron emission spectrum is written as follows

$$\frac{d\sigma^{KO}}{d\varepsilon_d}=\sigma_{non}\sum_{n=n_0}\Phi_d(E_0)\,\frac{g}{g_d\,p}\,\frac{\omega(p-1,h,U)}{\omega(p,h,E)}\,\frac{\lambda_d^e(\varepsilon_d)}{\lambda_d^e(\varepsilon_d)+\lambda_d^+(\varepsilon_d)}\,g_d D(n)\,, \qquad (27)$$

where the factor Φ_d describes the initial number of excited deuteron clusters in the nucleus

$$\Phi_d = 2\,F_d(E_0), \qquad (28)$$

where F_d is the probability of interaction of the incident particle with the "pre-formed" deuteron resulting in its excitation in the nucleus; and the factor of two reflects the normalization on the number of particles in the initial exciton state n_0.

The general expression for F_d [19] is

$$F_d=\frac{\phi\,\sigma_{xd}(E_0)}{\frac{Z'}{A'}\,\sigma_{xp}(E_0)+\frac{(A'-Z')}{A'}\,\sigma_{xn}(E_0)+\phi\,\sigma_{xd}(E_0)}\,, \qquad (29)$$

where "*x*" refers to the initial proton or neutron, σ_{xd}, σ_{xp} and σ_{xn} are the cross-sections of the elastic interaction of projectile with deuteron, proton and neutron, respectively, corrected for a Pauli principle, φ is the number of "pre-formed" deuterons in the nucleus, *Z'* and *A'* are the number of protons and nucleons in the nucleus corrected for a number of clustered deuterons.

The direct pick-up process corresponds to the pick-up of a nucleon without formation of a (2p,1h) exciton configuration. A rigorous description of this process can be done only outside of pre-equilibrium models. However, mathematical expressions obtained formally using the pre-compound exciton model [19,20] are useful for the phenomenological and qualitative description of direct nucleon pick-up.

According to Ref.[18], the direct component of the deuteron spectrum is

$$\frac{d\sigma^D}{d\varepsilon_d} = \sigma_{non}\ \frac{\omega^*(U)}{\omega(1p,0h,E)}\ \frac{\lambda_d^e(\varepsilon_d)}{\lambda_d^e(\varepsilon_d)+\lambda_d^+(\varepsilon_d)}\ g_d\ , \qquad (33)$$

where the final level density $\omega^*(U)$ is approximated by $\omega(0p,1h,U)\cdot\gamma/g_d$ [18]. See details in Ref.[9] or in the code text.

Formal consideration of the finite depth of the nuclear potential well shows that Eq.(33) can contribute only in the highest energy part of the deuteron emission spectrum, as has been mentioned above. In this case the calculated part of the spectrum is a rectangular step with width equal to E_F. To improve the agreement of calculations and the measured deuteron spectra, the direct component of the spectrum was rewritten in the following form [19]

$$\frac{d\sigma^D}{d\varepsilon_d} = \sigma_{non}\ \alpha_1\ \exp\left(-\frac{(E-\alpha_2 E_F)^2}{2(\alpha_3 E_F)^2}\right)\frac{\lambda_d^e(\varepsilon_d)}{\lambda_d^e(\varepsilon_d)+\lambda_d^+(\varepsilon_d)}\ g_d\ , \qquad (34)$$

where α_1, α_2, and α_3 are parameters and E_F is the effective value of the Fermi energy.

The values of α_i are obtained from analysis of experimental deuteron spectra. The global parameterization of α_i parameters is hardly possible.

Model parameters were obtained from the comparison of calculations with available experimental data. The change in values of different parameters results to different energetic dependencies of calculated deuteron spectrum. In most cases such change cannot be represented by a simple redefinition of other model parameters.

3. Changes in the program text

A module providing calculations of pre-equilibrium nucleon and light cluster distributions using GDH was implemented in the TALYS-1.74 code. The module consists of a number of primary subprograms of ALICE/ASH code [9], the ALICE/ASH subprograms modified for an appropriate integration in TALYS, and subroutines written to provide an interface between TALYS and modified ALICE/ASH modules.

The value of the TALYS input variable *preeqmode* equal to five is reserved for GDH calculations. A brief description of changes of TAYLS and ALICE/ASH subprograms and the list of modified and new routines is given below.

3.1 Changes in TALYS subprograms

The following TALYS-1.74 subroutines were modified in the present work

checkvalue
exciton
exciton2
input3
preeq
preeqcomplex

The modification concerns an addition of a number of instructions allowing the calculations with the new value of the *preeqmode* parameter equal to five. The main GDH module **gdh0** is called in the subroutine **preeq**.

3.2 Changes in ALICE/ASH subprograms

The list of modified ALICE/ASH subroutines is follows

gdhadist
gdhangel
gdhangl
gdhbinde
gdhex1ex2

gdhgamma

gdhlymas

gdhmain

gdhmfp

gdhnucmfp

gdhover

gdhparap

gdhshaft

gdhsigi

gdhtlj

gdhtreed

gdhybrid

alph05

ddirec

deut05

iwamoa

iwamod

The modification of subprograms, which name begins with "**gdh**" and original name follows the abbreviation, concerns mainly their formal integration in TALYS. The subroutines **alph05**, **ddirec**, **deut05**, **iwamoa**, and **iwamod** were altered to provide an agreement of experimental data and GDH-TALYS calculations.

An increase of memory load after the implementation of the GDH model in TALYS is about 0.15 %.

4. Example of the input file

A typical example of the input file for calculations applying GDH is given below

```
# GDH model
projectile n
element Fe
mass 56
energy  96.0
preeqmode 5
outspectra  y
```

Calculated energy distributions for emitted proton, deuteron, and α-particles for this task are shown in Figs.2-4. The experimental data are discussed in the next Section.

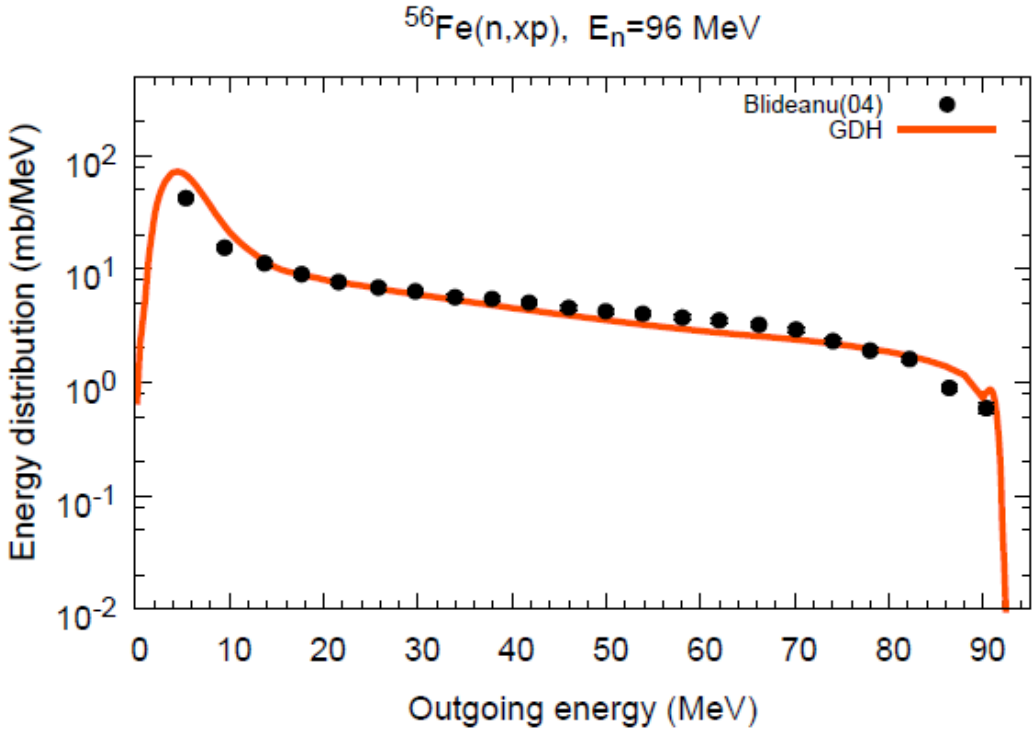

Fig.2 Calculated and measured proton energy distribution for the n+^{56}Fe reaction.

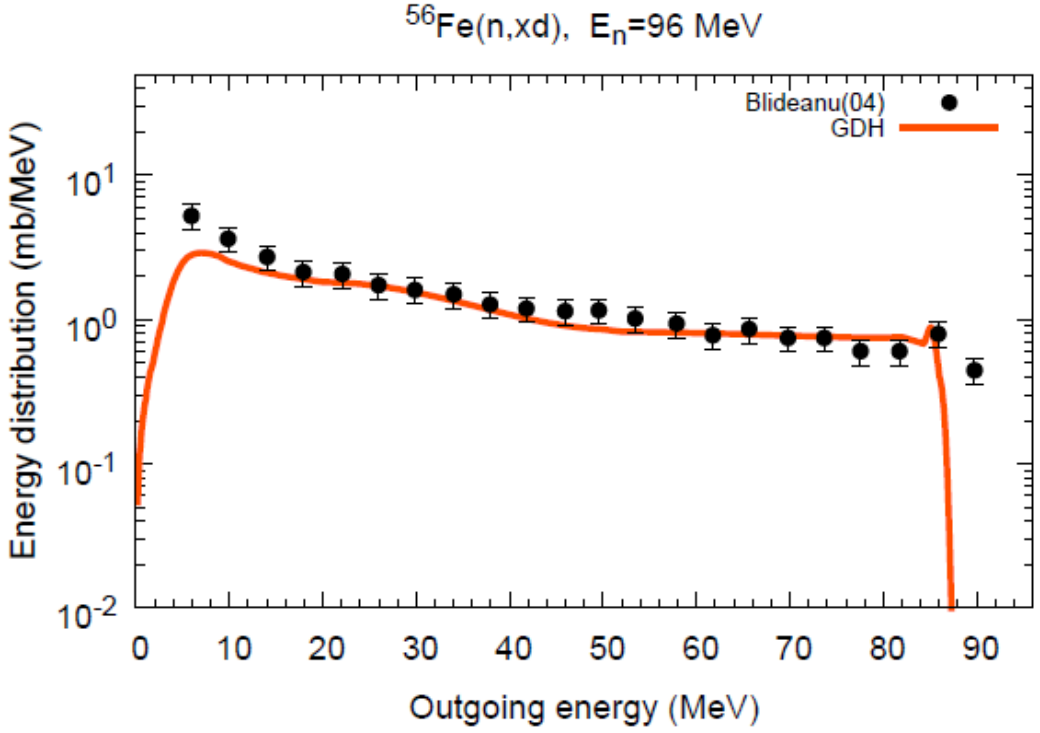

Fig.3 Calculated and measured deuteron energy distribution for the n+^{56}Fe reaction.

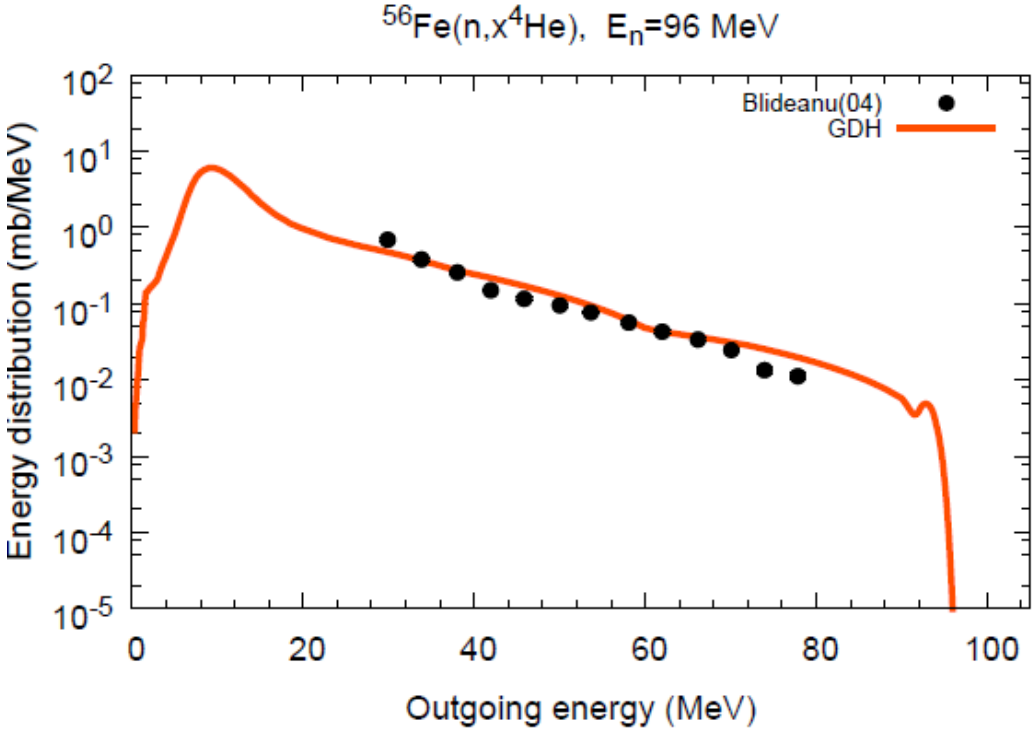

Fig.4 Calculated and measured α-particle energy distribution for the n+^{56}Fe reaction.

5. Comparison of calculations with measured data

Measured energy distributions for emitted neutrons, protons, deuterons, and α-particles in nucleon induced reactions [21-51] were compared with results of calculations using the GDH model and "default" TALYS models.

The figures are given in Appendices A-C.

When comparing the results, it should be borne in mind that "default" calculations use general parameterizations of pre-compound model parameters, while GDH calculations are performed using specific parameters for different targets.

For some neutron induced reactions there is a large discrepancy of calculated and measured values at the high energy tail of spectra. The same disagreement is observed for calculations using the "default" pre-compound model of TALYS. While the TALYS computation of reaction energies is usually correct, the discrepancy is

apparently due to the lack of measurements; the short discussion can be found in Ref.[19].

6. Conclusion

The geometry dependent hybrid model supplemented by phenomenological models for the simulation of non-equilibrium emission of deuterons and α-particles was implemented in the TALYS-1.74 code. Models discussed present an alternative to the pre-compound exciton model of TALYS and can be used for the prediction of cross-sections and secondary particle distribution in nuclear reactions induced by intermediate energy nucleons.

The results of calculations were compared with experimental energy distributions (Appendices A-C).

References

[1] M. Blann, Importance of the nuclear density distribution on pre-equilibrium decay, *Phys. Rev. Lett.,* 28 (1972) 757.

[2] M. Avrigeanu, V. Avrigeanu, STAPRE-H95, NEA Data Bank, IAEA0971, 1996.

[3] A.Yu. Konobeyev, U. Fischer, A.J. Koning, P.E. Pereslavtsev, M. Blann, Implementation of the Geometry Dependent Hybrid Model in TALYS, *J. Korean Phys. Soc.* 59 (2011) 935.

[4] A.J. Koning, S. Hilaire, M. Duijvestijn, TALYS-1.0, Proc. Int. Conf. on Nuclear Data for Science and Engineering, April 22-27, 2007, Nice; for the actual version of the code visit http://www.talys.eu/

[5] M. Blann, H.K. Vonach, Global test of modified precompound decay models, *Phys. Rev.* C28 (1983) 1475.

[6] M. Blann, ALICE-91: Statistical model code system with fission competition, RSIC Code Package PSR-146, 1991.

[7] M. Blann, New precompound decay model, Phys. Rev. C 54 (1996) 1341.

[8] Yu.A. Korovin, A.Yu. Konobeyev, P.E. Pereslavtsev, A.Yu. Stankovsky, C. Broeders, I. Broeders, U. Fischer U., U. von Möllendorff, Evaluated nuclear data files for accelerator driven systems and other intermediate and high-energy applications, *Nucl. Instr. Meth. Phys. Res.* A463 (2001) 544.

[9] C.H.M. Broeders, A.Yu. Konobeyev, A.Yu. Korovin, V.P. Lunev, M. Blann, ALICE/ASH - Pre-compound and evaporation model code system for calculation of excitation functions, energy and angular distributions of emitted particles in nuclear reactions at intermediate energies, Report FZKA 7183 (May, 2006); http://bibliothek.fzk.de/zb/berichte/FZKA7183.pdf

[10] A. Iwamoto A., K. Harada, Mechanism of cluster emission in nucleon-induced preequilibrium reactions*, Phys. Rev.* C 26 (1982) 1821.

[11] K. Sato, A. Iwamoto, K. Harada, Pre-equilibrium emission of light composite particles in the framework of the exciton model *Phys. Rev.* C 28 (1983) 1527.

[12] A.Yu. Konobeyev, V.P. Lunev, Yu.N. Shubin, Pre-equilibrium emission of clusters, *Acta Phys. Slov.* 45 (1995) 705.

[13] P. Obložinský, I. Ribanský, Emission rate of preformed α particles in preequilibrium decay, *Phys. Lett.* 74B (1978) 6.

[14] O.T. Grudzevich, A.V. Zelenetsky, A.B. Pashchenko, KOP code for calculation of cross-section for interaction of neutrons and charged particles with atomic nuclei based on optical model, Report of IPPE, Obninsk, N1802 (1986).

[15] J.R. Huizenga, G. Igo, Theoretical reaction cross sections for alpha particles with an optical model, *Nucl. Phys.* 29 (1962) 462.

[16] A.I. Dityuk, A.Yu. Konobeyev, V.P. Lunev, Yu.N. Shubin, New advanced version of computer code ALICE-IPPE, INDC(CCP)-410 (1998).

[17] E. Běták, J. Dobeš, The finite depth of the nuclear potential well in the exciton model of preequilibrium decay, *Z. Phys.* A 279 (1976) 319.

[18] A.Yu. Konobeyev, Yu.A. Korovin, Calculation of deuteron spectra for nucleon induced reactions on the basis of the hybrid exciton model taking into account direct processes, *Kerntechnik* 61 (1996) 45.

[19] C.H.M. Broeders, A.Yu. Konobeyev, Phenomenological model for non-equilibrium deuteron emission in nucleon induced reactions", *Kerntechnik*, 70 (2005) 260.

[20] C. Kalbach, The Griffin model, complex particles and direct nuclear reactions, *Z. Phys.* A 283 (1977) 401.

[21] F.B. Bateman, R.C. Haight, M.B. Chadwick, S.M. Sterbenz, S.M. Grimes, H. Vonach, Light charged-particle production from neutron bombardment of silicon up to 60 MeV: Role of level densities and isospin, *Phys. Rev.* C60 (1999) 064609.

[22] S. Benck, I. Slypen, J.P. Meulders, V. Corcalciuc, M.B. Chadwick, P.G. Young, A.J. Koning, Light charged particle production in neutron-induced reactions on aluminium at En=28.5-62.7 MeV, *Phys. Rev.* C58 (1998) 1558.

[23] S. Benck, I. Slypen, J.P. Meulders, V. Corcalciuc, Experimental cross sections for light-charged particle production induced by neutrons with energies between 28 and 63 MeV incident energies on oxygen, *At. Data Nucl. Data Tables* 72 (1999) 1.

[24] S. Benck, I. Slypen, J.P. Meulders, V. Corcalciuc, Secondary light charged particle emission from the interaction of 25- to 65-MeV neutrons on silicon, *Nucl. Sci. Eng.* 141 (2002) 55.

[25] F.E. Bertrand, R.W. Peelle, Tabulated cross sections for hydrogen and helium particles produced by 62 MeV protons on 89-Y, ORNL-4450, 1969.

[26] F.E. Bertrand, R.W. Peelle, Tabulated cross sections for hydrogen and helium particles produced by 62 MeV and 29 MeV protons on 27-Al, ORNL-4455, 1969.

[27] F.E. Bertrand, R.W. Peelle, Tabulated cross sections for hydrogen and helium particles produced by 61 MeV protons on 56-Fe, ORNL-4456, 1969.

[28] F.E. Bertrand,R.W. Peelle, Tabulated cross sections for hydrogen and helium particles produced by 62 and 29 MeV protons on 197-Au. ORNL-4460, 1969.

[29] F.E. Bertrand,R.W. Peelle, Tabulated cross sections for hydrogen and helium particles produced by 62, 39 and 29 MeV protons on 54-Fe, ORNL-4469, 1970.

[30] F.E. Bertrand,R.W. Peelle, Tabulated Cross Sections For Hydrogen and Helium Particles Produced by 62 and 29 MeV Protons on 120-Sn, ORNL-4471, 1970.

[31] F.E. Bertrand, R.W. Peelle, Tabulated cross sections for hydrogen and helium particles produced by 62 and 39 MeV protons on 209-Bi, ORNL-4638, 1971.

[32] F.E. Bertrand, R.W. Peelle, Complete hydrogen and helium particle spectra from 30- to 60-MeV proton bombardment of nuclei with A=12 to 209 and comparison with intranuclear cascade, *Phys. Rev.* C8 (1973) 1045; ORNL-4799, 1973.

[33] M. Blann,R.R. Doering, A. Galonsky, D.M. Patterson, F.E. Serr, Preequilibrium analysis of (p,n) spectra on various targets at proton energies of 25 to 45 MeV, *Nucl. Phys.* A257 (1976) 15.

[34] V. Blideanu, F.R. Lecolley, J.F. Lecolley, T. Lefort, N. Marie, A. Atac, G. Ban, B. Bergenwall, J. Blomgren, S. Dangtip, K. Elmgren, Ph. Eudes, Y. Foucher, A. Guertin, F. Haddad, A. Hildebrand, C. Johansson, O. Jonsson, M. Kerveno, T. Kirchner, J. Klug, Ch. Le Brun, C. Lebrun, M. Louvel, P. Nadel-Turonski, L. Nilsson, N. Olsson, S. Pomp, A.V. Prokofiev, P.-U. Renberg, G. Riviere, I. Slypen, L. Stuttge, U. Tippawan, M. Oesterlund, Nucleon-induced reactions at intermediate energies: New data at 96 MeV and theoretical status, *Phys. Rev.* C70 (2004) 014607.

[35] P.Demetriou, Ch.Dufauquez, Y.El.Masri, A.J.Koning, Light charged-particle production from proton and alpha induced reactions on Si-nat at energies from 25 to 65-MeV. A theoretical analysis, *Phys. Rev.* C72 (2005) 034607.

[36] A.Duisebayev, K.M.Ismailov, I.Boztosun, Inclusive spectra of (p,xp) and (p,xd) reactions on 90,92-Zr and 92-Mo nuclei at Ep=30.3 MeV, *Phys. Rev.* C67 (2003) 044608.

[37] A.M. Ferrero, E. Gadioli, E. Gadioli Erba, I. Lori, N. Molho, L. Zetta, Alpha emission in proton induced reactions, Z. Phys. A293 (1979) 123; INFN/BE-78/6, 1978.

[38] A.Guertin, N.Marie, S.Auduc, V.Blideanu, Th.Delbar, P.Eudes, Y.Foucher, F.Haddad, T.Kirchner, Ch.Le Brun, C.Lebrun, F.R.Lecolley, J.F.Lecolley, X.Ledoux, F.Lefebvres, T.Lefort, M.Louvel, A.Ninane, Y.Patin, Ph.Pras, G.Riviere, C.Varignon, Neutron and light charged particle productions in proton induced reactions on Pb-208 at 62.9-MeV, *Eur. Phys. J.* A23 (2005) 49.

[39] A.M. Kalend, B.D. Anderson, A.R. Baldwin, R. Madey, J.W. Watson, C.C. Chang, H.D. Holmgren, R.W. Koontz, J.R. Wu, H. Machner, Energy and angular distributions of neutrons from 90 MeV and 140 MeV alpha-particle bombardment of nuclei, *Phys. Rev.* C28 (1983) 105.

[40] M. Kerveno, F. Haddad, Ph. Eudes, T. Kirchner, C. Lebrun, I. Slypen, J.P. Meulders, C. Le Brun, F.R. Lecolley, J.F. Lecolley, M. Louvel, F. Lefebvre, S. Hilaire, A.J. Koning, Hydrogen isotope double differential production cross sections induced by 62.7 MeV neutrons on a lead target, *Phys. Rev.* C66 (2002) 014601.

[41] Z. Lewandowski, E. Loeffler, R. Wagner, H.H. Mueller, W. Reichart, P. Schober, E. Gadioli, E. Gadioli Erba, Proton-Induced Alpha- And Tritium-Emission at 72 MeV, Lewandowski, E. Loeffler, R. Wagner, H.H. Mueller, W. Reichart, P. Schober, E. Gadioli, E. Gadioli Erba, Proton-Induced Alpha- And Tritium-Emission at 72 MeV, *Lett. Nuovo Cim.* 28 (1980) 15.

[42] N.Marie, A.Guertin, S.Auduc, V.Blideanu, Th.Delbar, P.Eudes, Y.Foucher, F.Haddad, T.Kirchner, Ch.Le Brun, C.Lebrun, F.R.Lecolley, J.F.Lecolley, X.Ledoux, F.Lefebvres, M.Louvel, A.Ninane, Y.Patin, Ph.Pras, G.Riviere, C.Varignon, Light particle production in 63 MeV proton induced reactions on lead, Worksh. Nucl. Data for Transmutation, Darmstadt, 2003.

[43] N. Nica, S. Benck, E. Raeymackers, I. Slypen, J.P. Meulders, V. Corcalciuc, Light charged particle emission induced by fast neutrons (25 to 65 MeV) on Co-59, *J. Phys.* G28 (2002) 2823.

[44] E. Raeymackers, S. Benck, N. Nica, I. Slypen, J.P. Meulders, V. Corcalciuc, A.J. Koning, Light Charged Particle Emission in fast neutron (25 - 65 MeV) induced reactions on Bi-209, *Nucl. Phys.* A726 (2003) 210.

[45] W. Scobel, M. Trabandt, M. Blann, B.A. Pohl, B.A. Remington, R.C. Byrd, C.C. Foster, R. Bonetti, C. Chiesa, S.M. Grimes, Preequilibrium (p,n) reaction as a probe for the effective nucleon-nucleon interaction in multistep direct processes *Phys. Rev.* C41, 2010, 1990

[46] I. Slypen, S. Benck, V. Corcalciuc, J.P. Meulders, M.B. Chadwick, C. Dufauquez. Proton and deutron production in neutron-induced reactions on carbon at En=42.5, 62.7, and 72.8 MeV, *At. Data Nucl. Data Tables* 76 (2000) 26.

[47] I. Slypen, N. Nica, A. Koning, E. Raeymackers, S. Benck, J.P. Meulders, V. Corcalciuc, Light charged particle emission induced by fast neutrons with energies between 25 and 65 MeV on iron, *J. Phys.* G30 (2004) 45.

[48] U. Tippawan, S. Pomp, A. Atac, B. Bergenwall, J. Blomgren, S. Dangtip, A. Hildebrand, C. Johansson, J. Klug, P. Mermod, L. Nilsson, M. Osterlund, N. Olsson, K. Elmgren, O. Jonsson, A.V. Prokofiev, P.-U. Renberg, P. Nadel-Turonski, V. Corcalciuc, Y. Watanabe, A.J. Koning, Light-ion production in the interaction of 96 MeV neutrons with silicon, *Phys. Rev.* C69 (2004) 064609.

[49] U. Tippawan, S. Pomp, A .Atac, B. Bergenwall, J. Blomgren, S. Dangtip, A. Hildebrand, C. Johansson, J. Klug, P. Mermod, L. Nilsson, M. Osterlund, N. Olsson, A.V. Prokofiev, P. Nadel-Turonski, V. Corcalciuc, A.J. Koning, Light-ion production in the interaction of 96 MeV neutrons with oxygen, *Phys. Rev.* C73 (2006) 034611.

[50] U. Tippawan, S. Pomp, J. Blomgren, S. Dangtip, C. Gustavsson, J. Klug,P. Nadel-Turonski, L. Nilsson, M. Osterlund, N. Olsson, O. Jonsson, A.V. Prokofiev, P.-U. Renberg, V. Corcalciuc, Y. Watanabe, A.J. Koning, Light-ion production in the interaction of 96 MeV neutrons with carbon, *Phys. Rev.* C79 (2009) 064611.

[51] J.R. Wu, C.C. Chang, H.D. Holmgren, Charge-particle spectra-90 MeV protons on Al-27,Ni-58, Zr-90 and Bi-209, *Phys. Rev.* C19 (1979) 698.

Appendix A

Calculated and experimental nucleon energy distributions

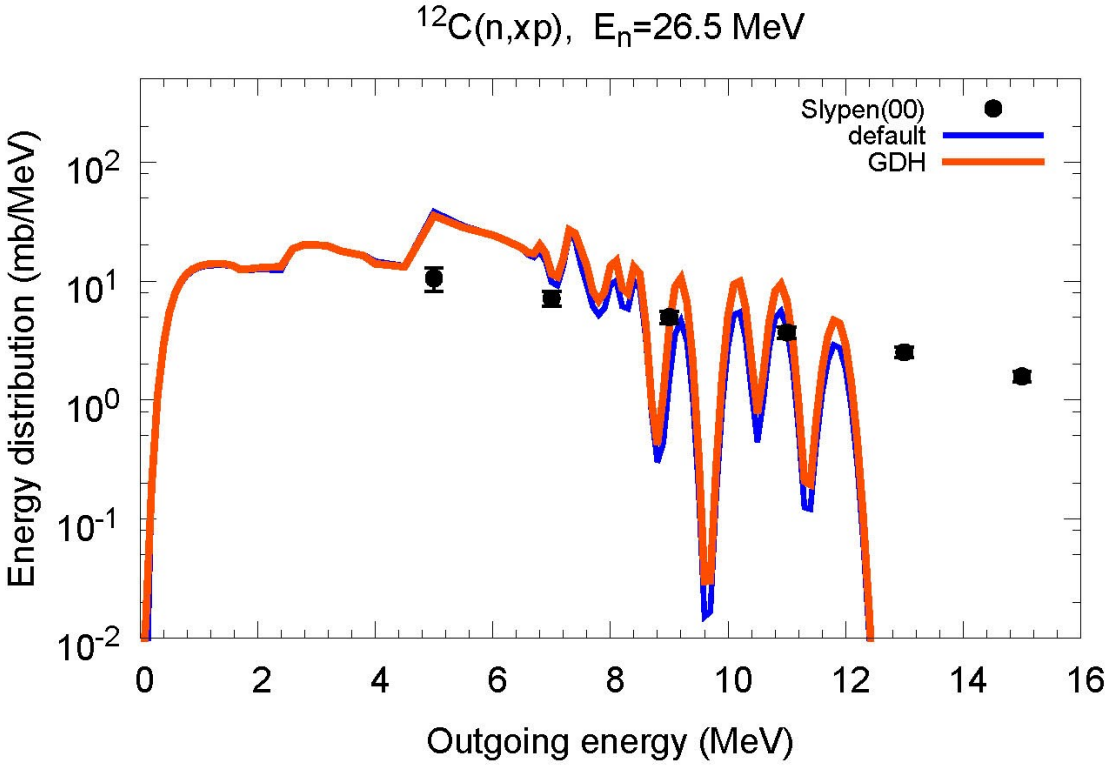
^{12}C(n,xp), E_n=26.5 MeV
Slypen(00)
default
GDH
Energy distribution (mb/MeV)
10^2
10^1
10^0
10^{-1}
10^{-2}
0
2
4
6
8
10
12
14
16
Outgoing energy (MeV)

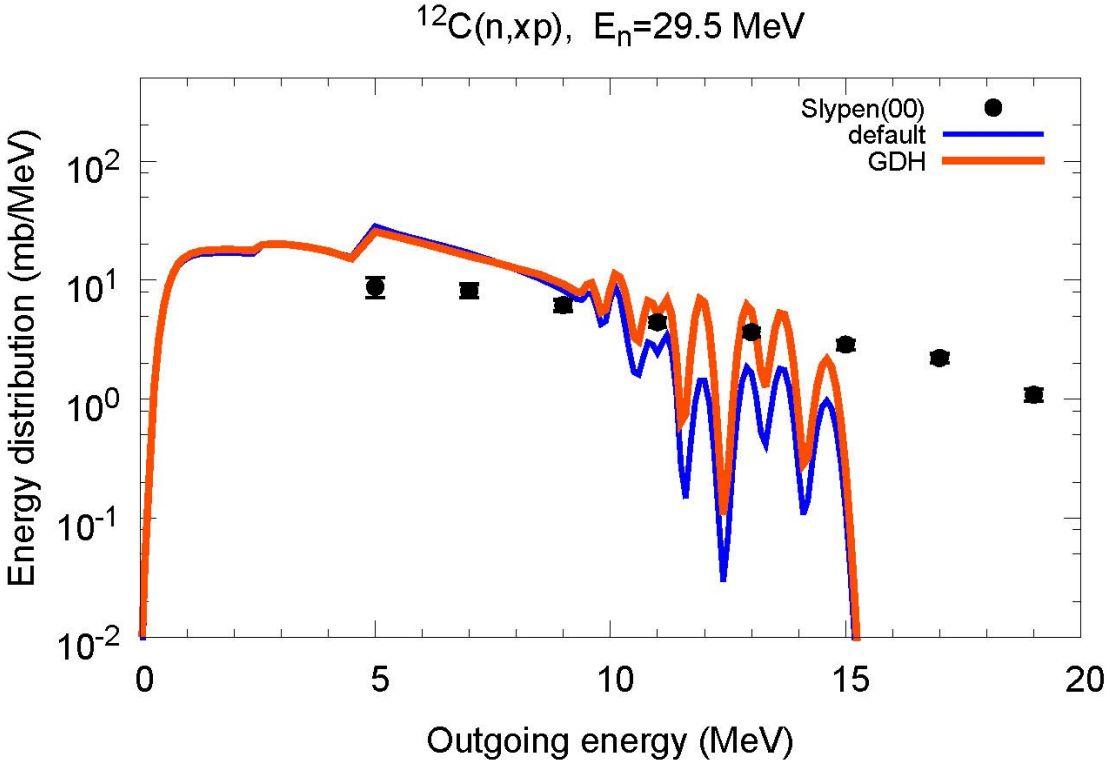
^{12}C(n,xp), E_n=29.5 MeV
Slypen(00)
default
GDH
Energy distribution (mb/MeV)
10^2
10^1
10^0
10^{-1}
10^{-2}
0
5
10
15
20
Outgoing energy (MeV)

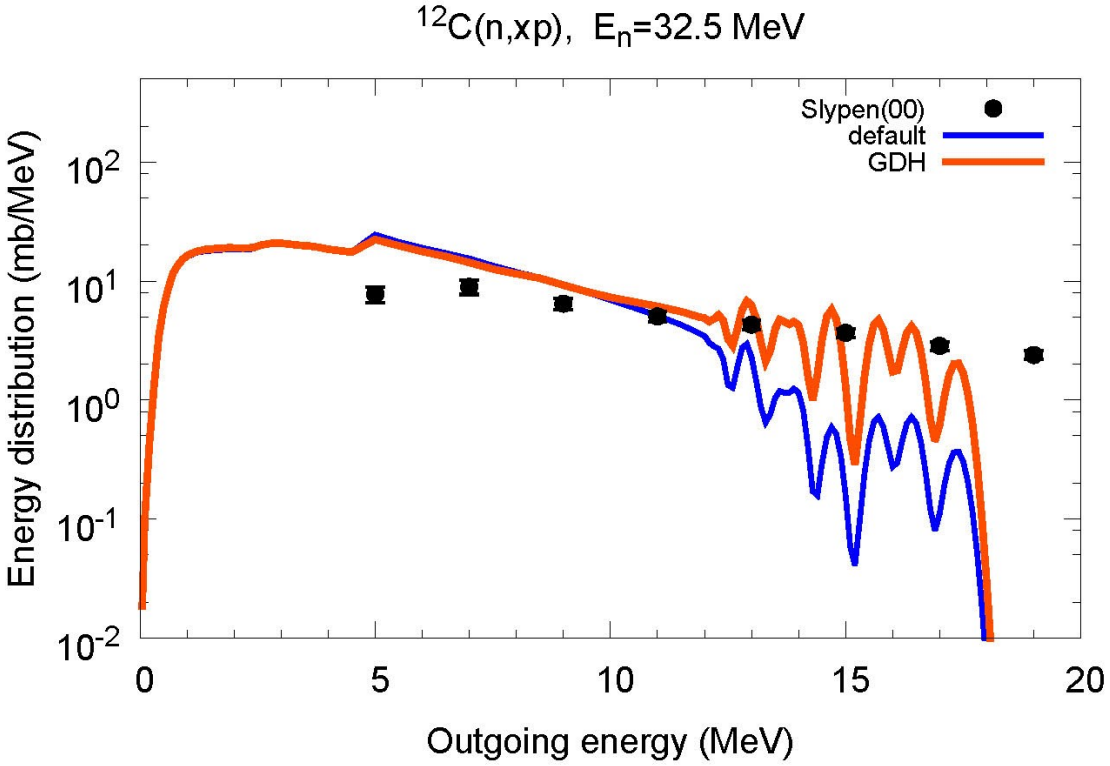
^{12}C(n,xp), E_n=32.5 MeV
Slypen(00)
default
GDH
Energy distribution (mb/MeV)
10^2
10^1
10^0
10^{-1}
10^{-2}
0
5
10
15
20
Outgoing energy (MeV)

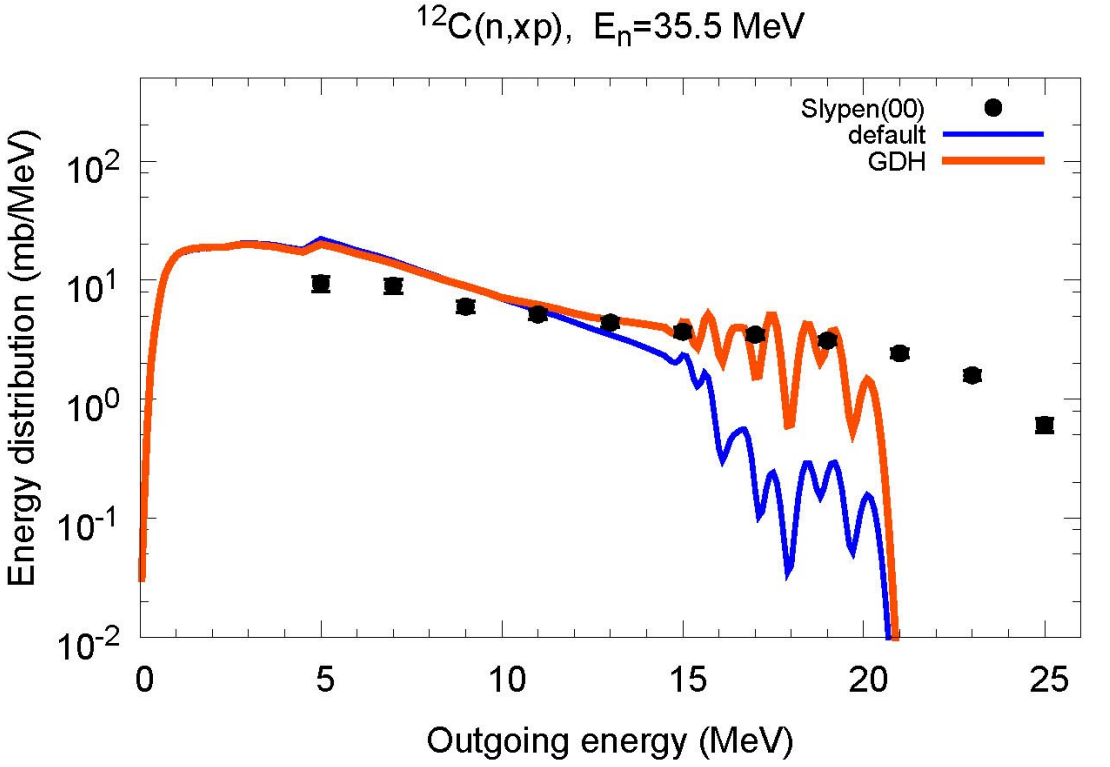
^{12}C(n,xp), E_n=35.5 MeV
Slypen(00)
default
GDH
Energy distribution (mb/MeV)
10^2
10^1
10^0
10^{-1}
10^{-2}
0
5
10
15
20
25
Outgoing energy (MeV)

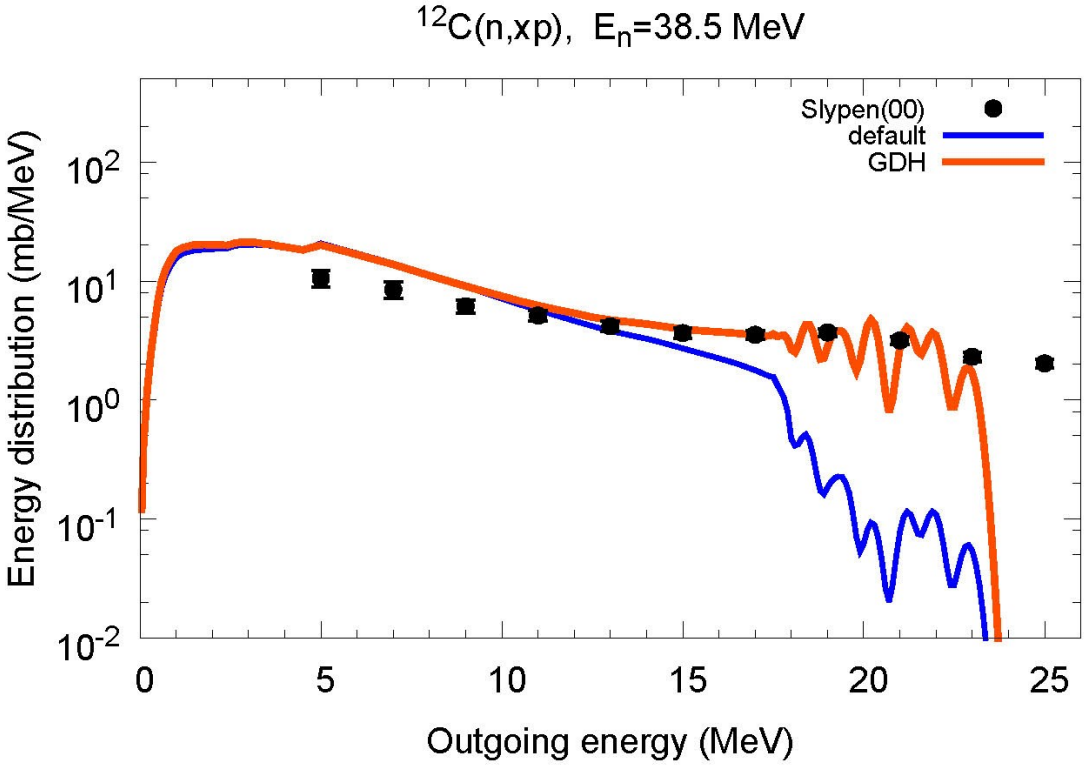
^{12}C(n,xp), E_n=38.5 MeV
Slypen(00)
default
GDH
Energy distribution (mb/MeV)
10^2
10^1
10^0
10^{-1}
10^{-2}
0
5
10
15
20
25
Outgoing energy (MeV)

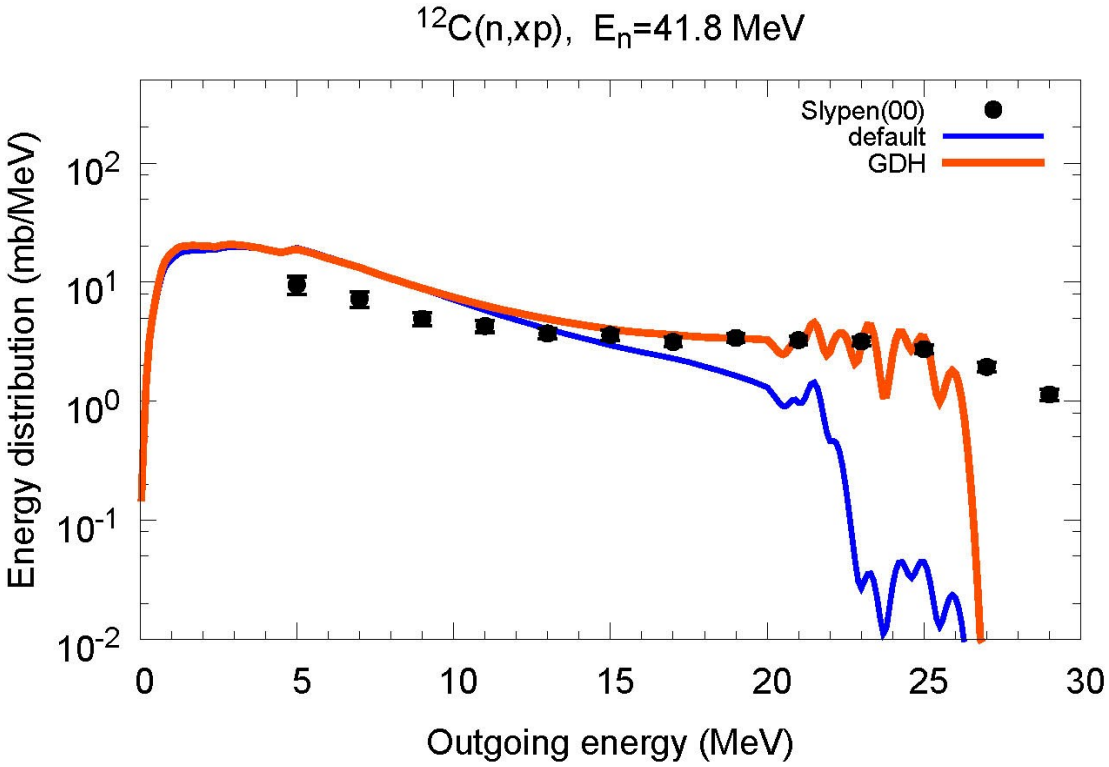
^{12}C(n,xp), E_n=41.8 MeV
Slypen(00)
default
GDH
Energy distribution (mb/MeV)
10^2
10^1
10^0
10^{-1}
10^{-2}
0
5
10
15
20
25
30
Outgoing energy (MeV)

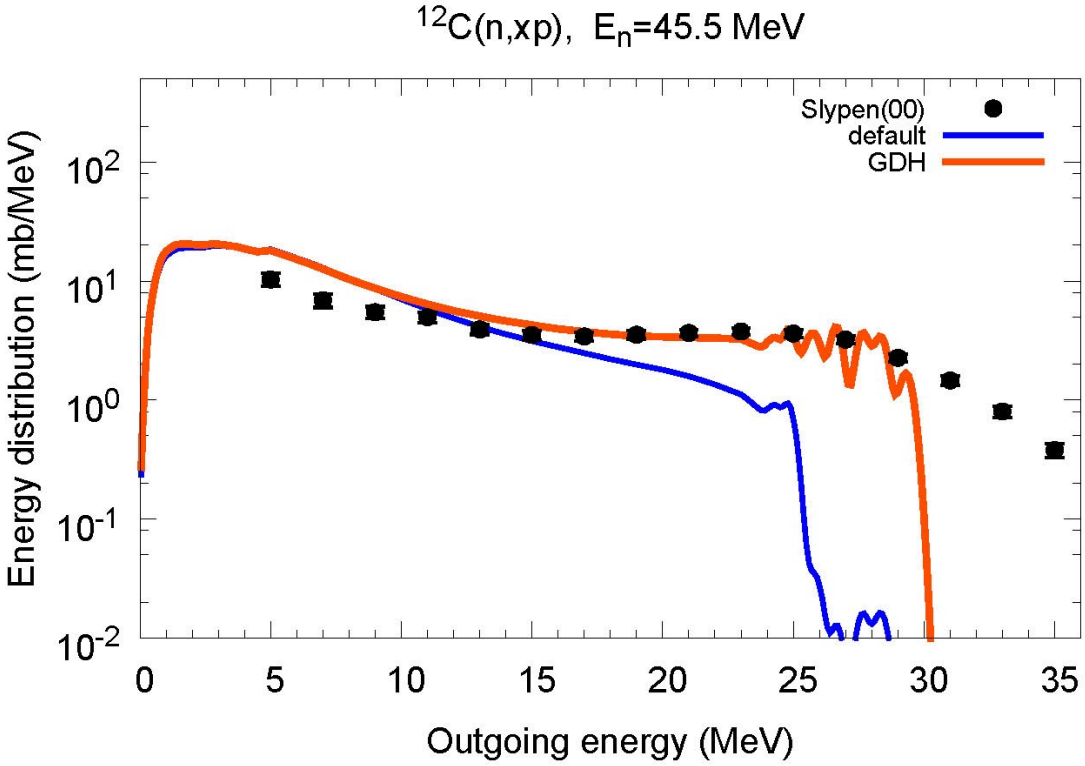
^{12}C(n,xp), E_n=45.5 MeV
Slypen(00)
default
GDH
Energy distribution (mb/MeV)
Outgoing energy (MeV)

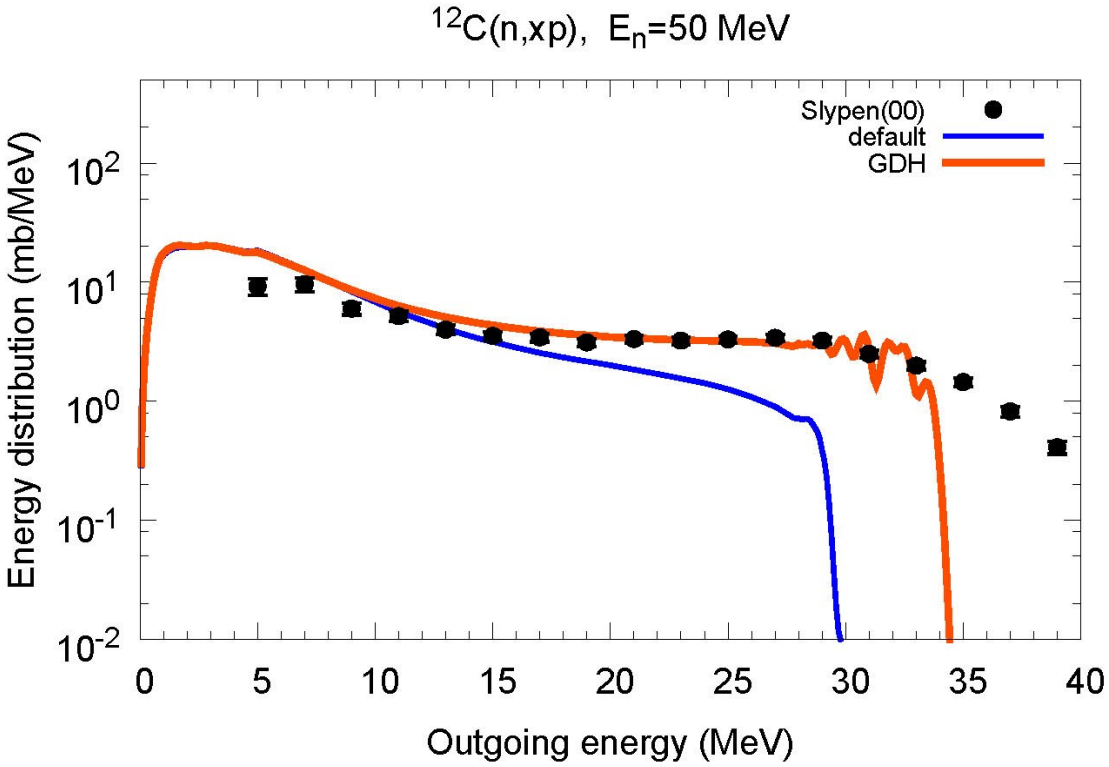
^{12}C(n,xp), E_n=50 MeV
Slypen(00)
default
GDH
Energy distribution (mb/MeV)
Outgoing energy (MeV)

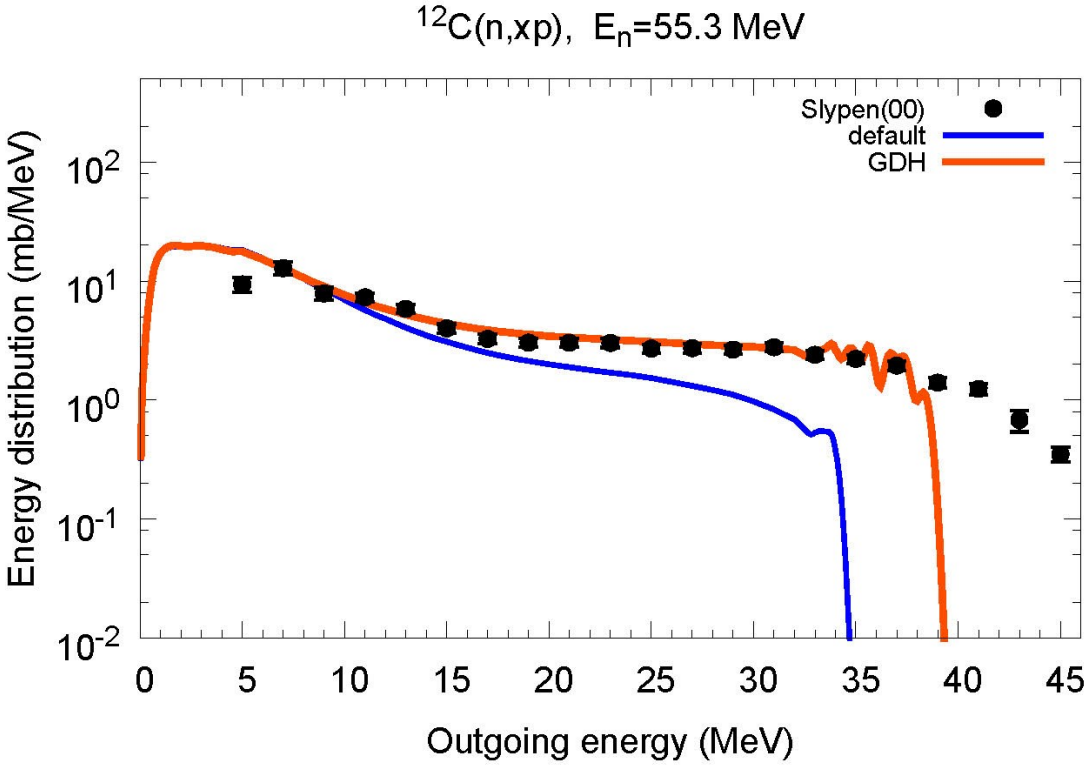
^{12}C(n,xp), E_n=55.3 MeV
Slypen(00)
default
GDH
Energy distribution (mb/MeV)
Outgoing energy (MeV)

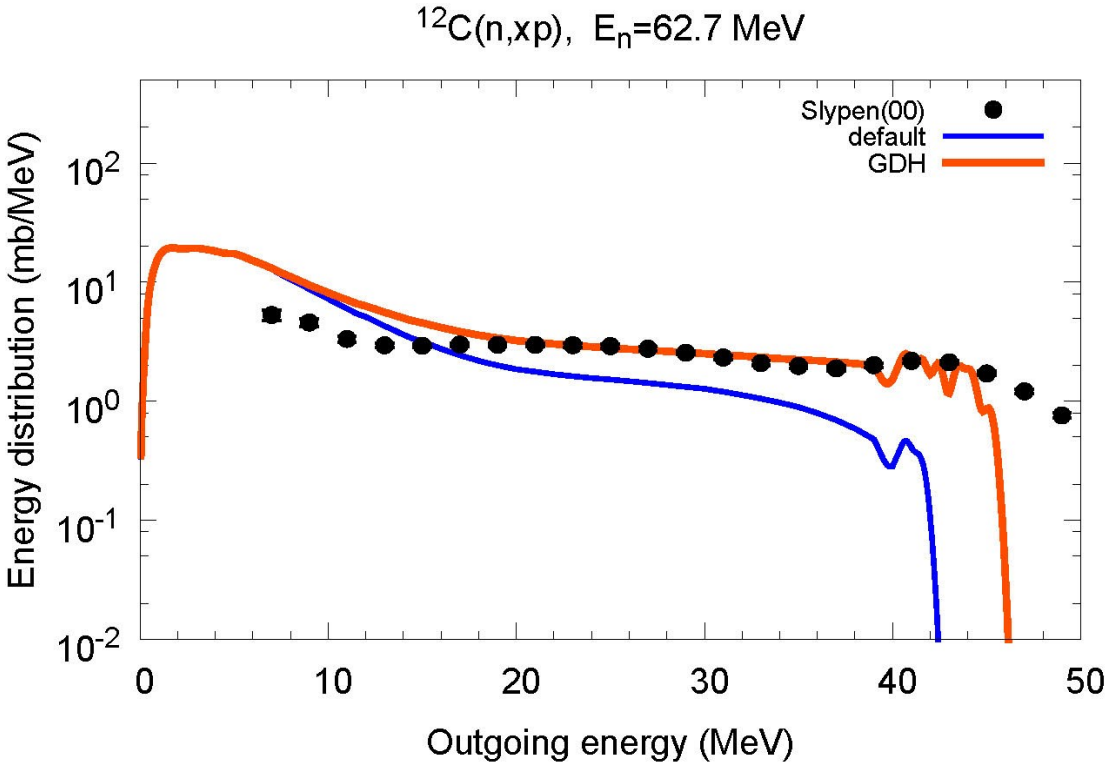
^{12}C(n,xp), E_n=62.7 MeV
Slypen(00)
default
GDH
Energy distribution (mb/MeV)
Outgoing energy (MeV)

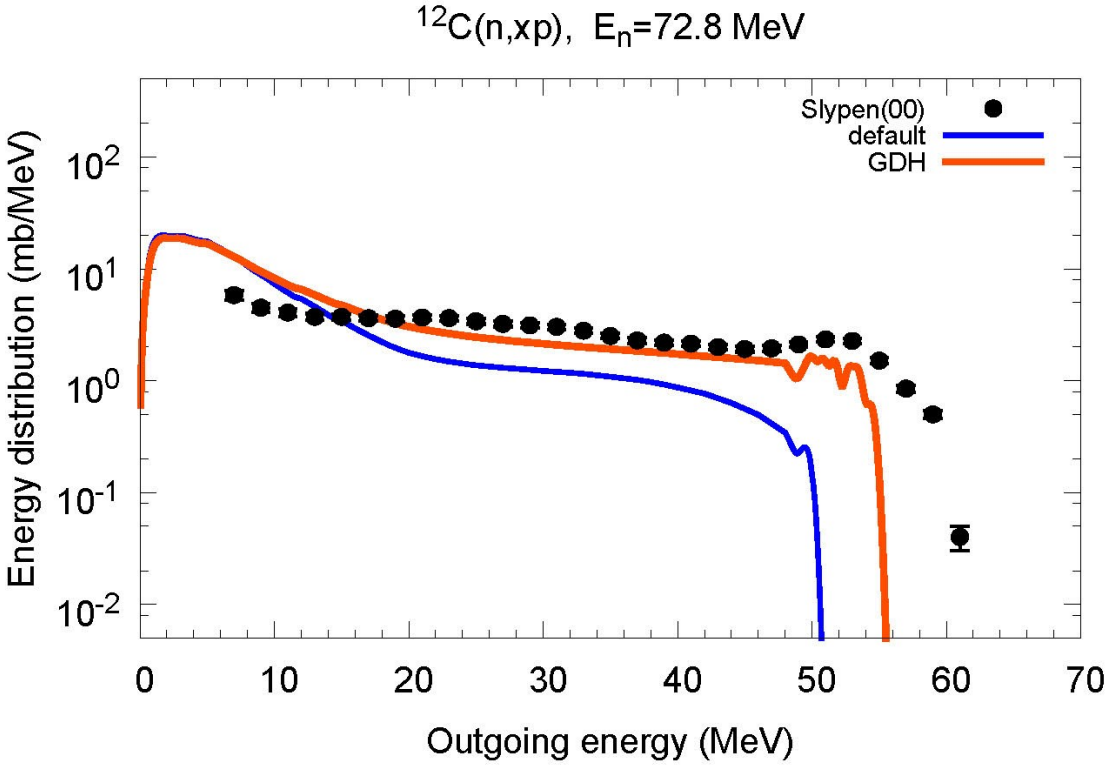
^{12}C(n,xp), E_n=72.8 MeV
Slypen(00)
default
GDH
Energy distribution (mb/MeV)
10^2
10^1
10^0
10^{-1}
10^{-2}
0
10
20
30
40
50
60
70
Outgoing energy (MeV)

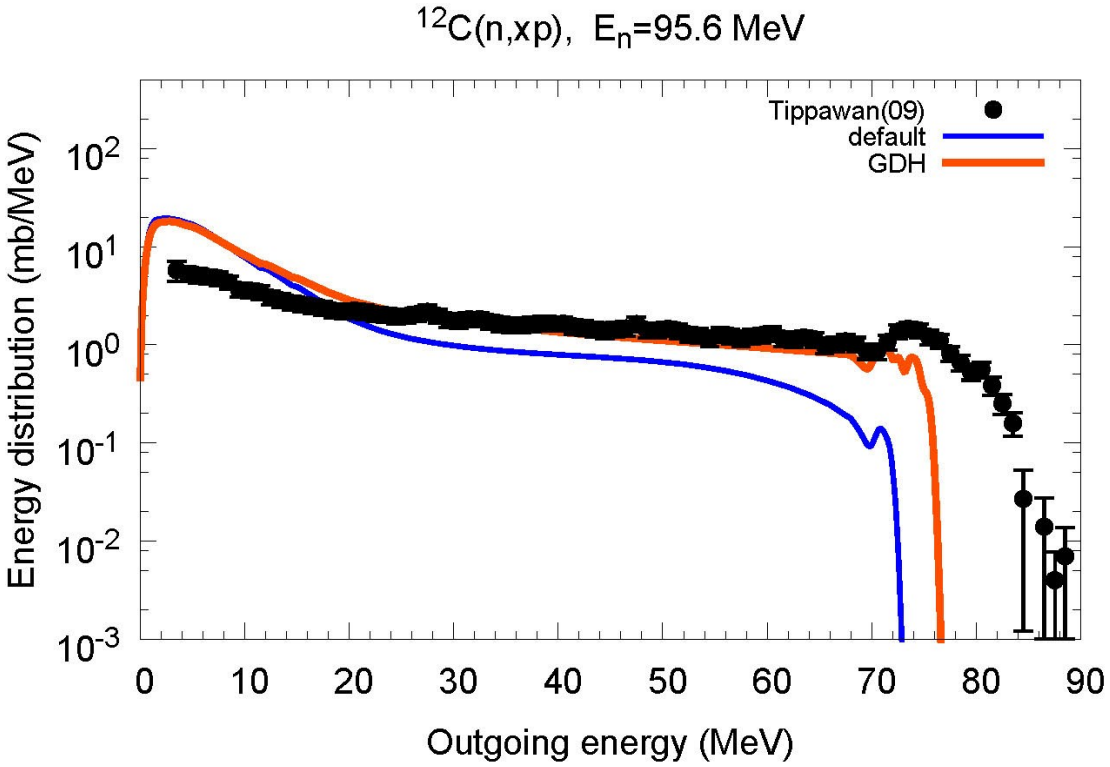
^{12}C(n,xp), E_n=95.6 MeV
Tippawan(09)
default
GDH
Energy distribution (mb/MeV)
10^2
10^1
10^0
10^{-1}
10^{-2}
10^{-3}
0
10
20
30
40
50
60
70
80
90
Outgoing energy (MeV)

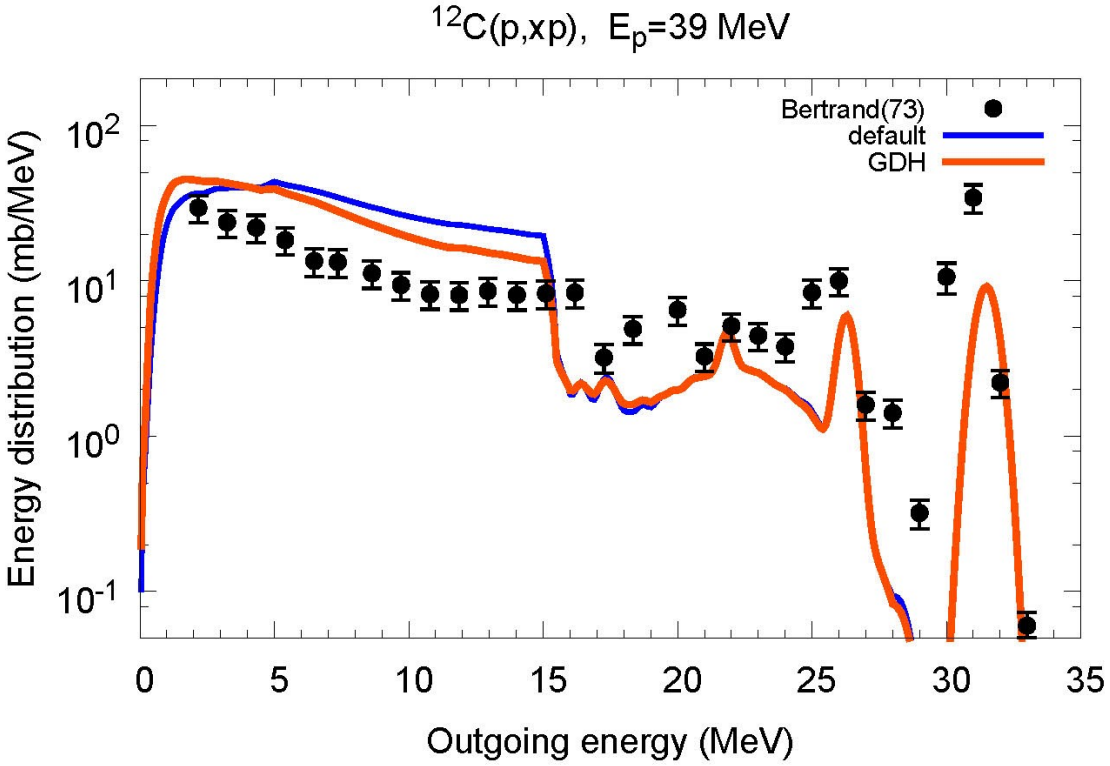
^{12}C(p,xp), E_p=39 MeV
Bertrand(73)
default
GDH
Energy distribution (mb/MeV)
10^2
10^1
10^0
10^{-1}
0
5
10
15
20
25
30
35
Outgoing energy (MeV)

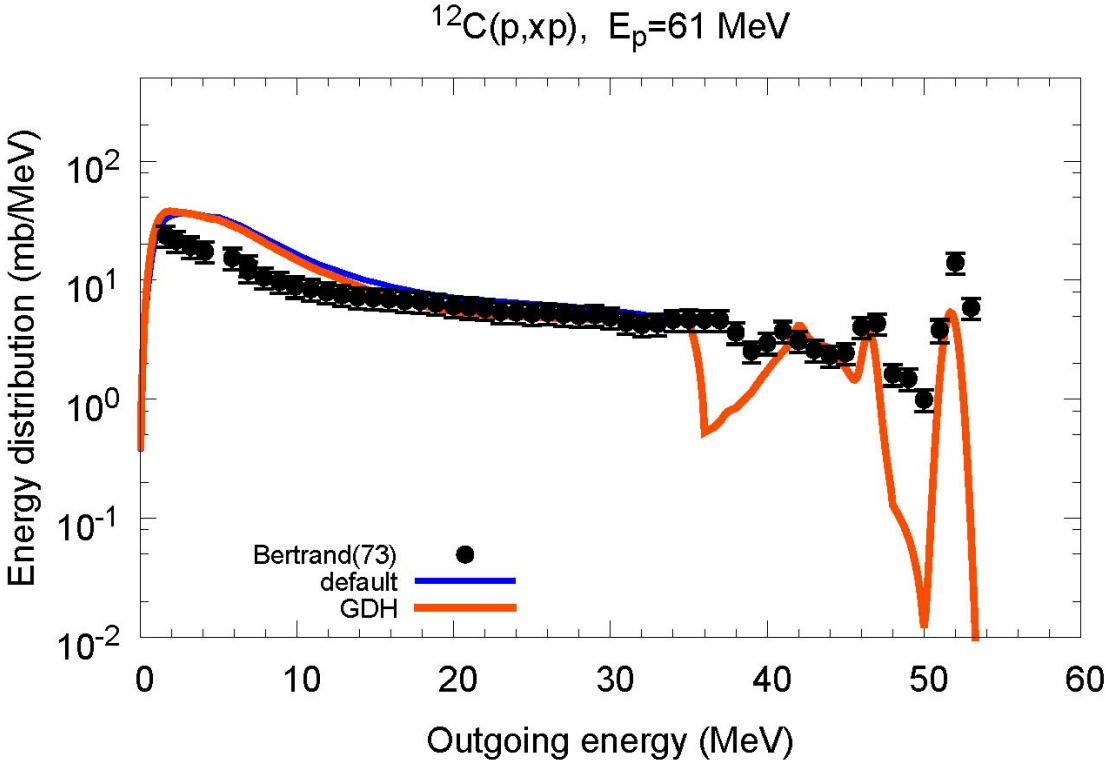
^{12}C(p,xp), E_p=61 MeV
Bertrand(73)
default
GDH
Energy distribution (mb/MeV)
10^2
10^1
10^0
10^{-1}
10^{-2}
0
10
20
30
40
50
60
Outgoing energy (MeV)

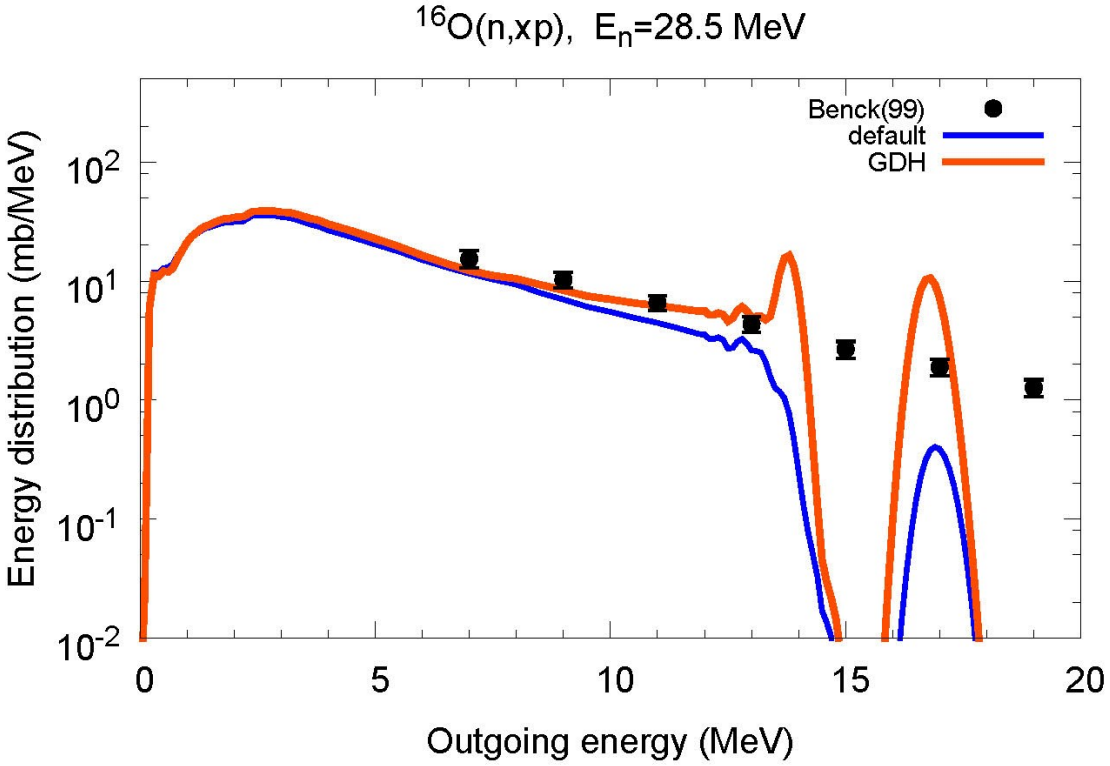
^{16}O(n,xp), E_n=28.5 MeV
Benck(99)
default
GDH
Energy distribution (mb/MeV)
10^2
10^1
10^0
10^{-1}
10^{-2}
0
5
10
15
20
Outgoing energy (MeV)

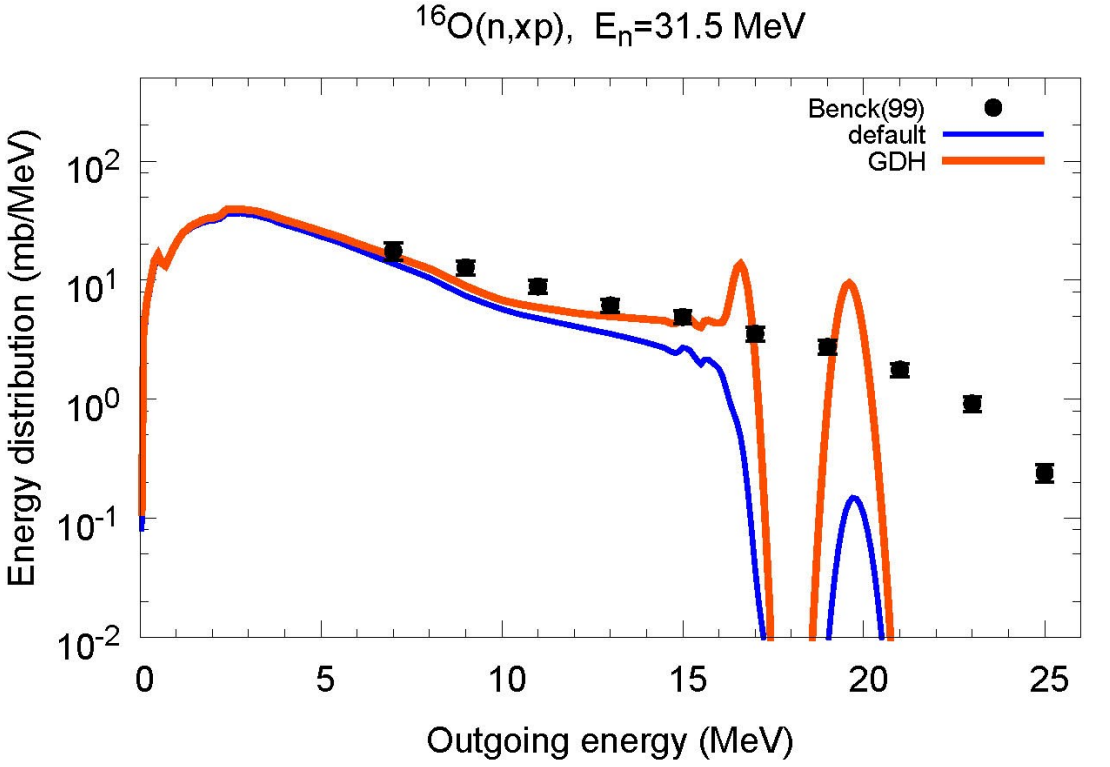
^{16}O(n,xp), E_n=31.5 MeV
Benck(99)
default
GDH
Energy distribution (mb/MeV)
10^2
10^1
10^0
10^{-1}
10^{-2}
0
5
10
15
20
25
Outgoing energy (MeV)

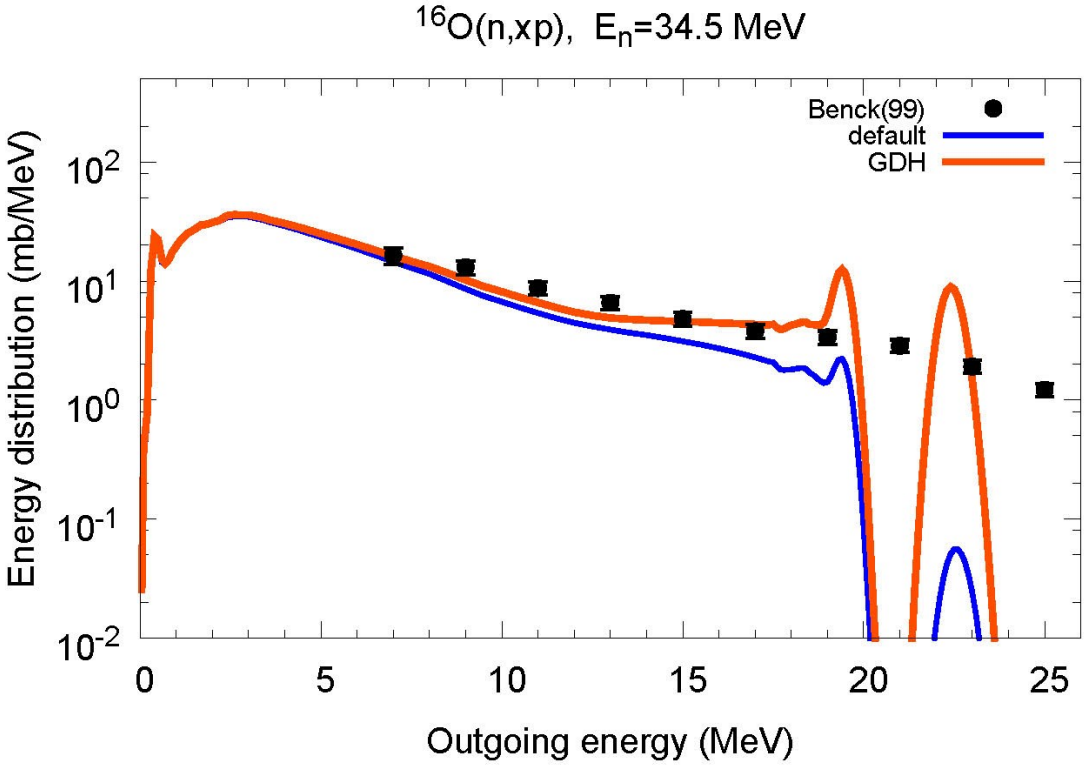
^{16}O(n,xp), E_n=34.5 MeV
Benck(99)
default
GDH
Energy distribution (mb/MeV)
10^2
10^1
10^0
10^{-1}
10^{-2}
0
5
10
15
20
25
Outgoing energy (MeV)

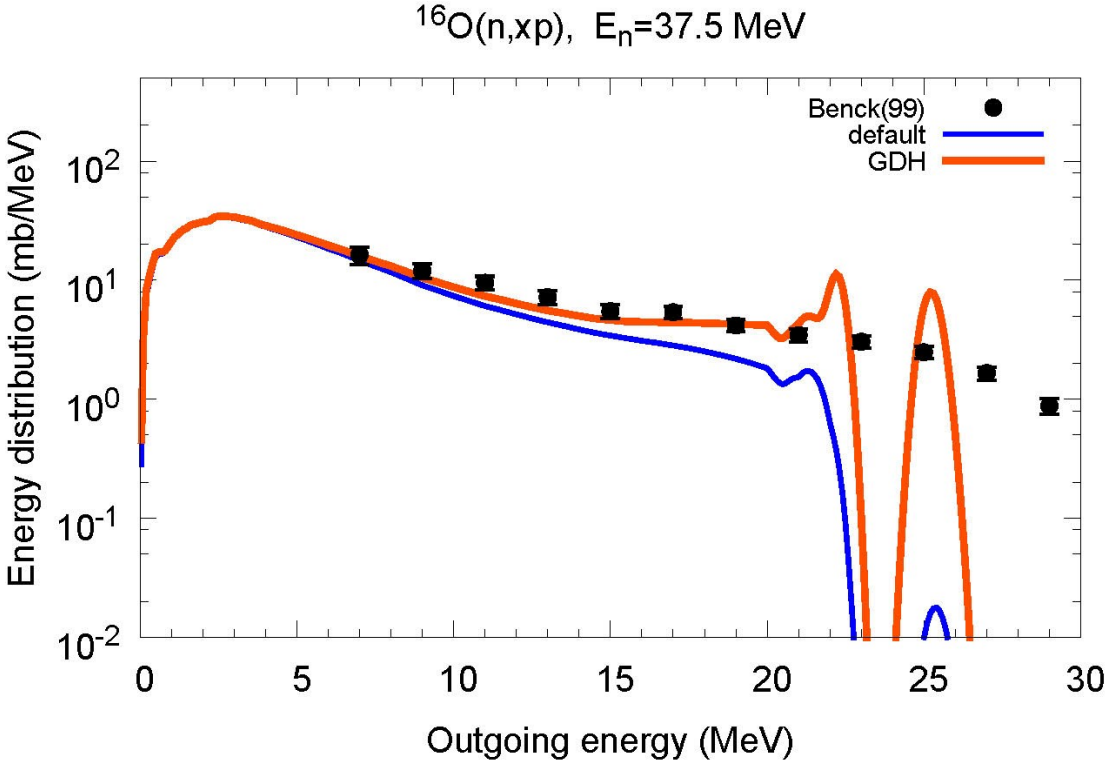
^{16}O(n,xp), E_n=37.5 MeV
Benck(99)
default
GDH
Energy distribution (mb/MeV)
10^2
10^1
10^0
10^{-1}
10^{-2}
0
5
10
15
20
25
30
Outgoing energy (MeV)

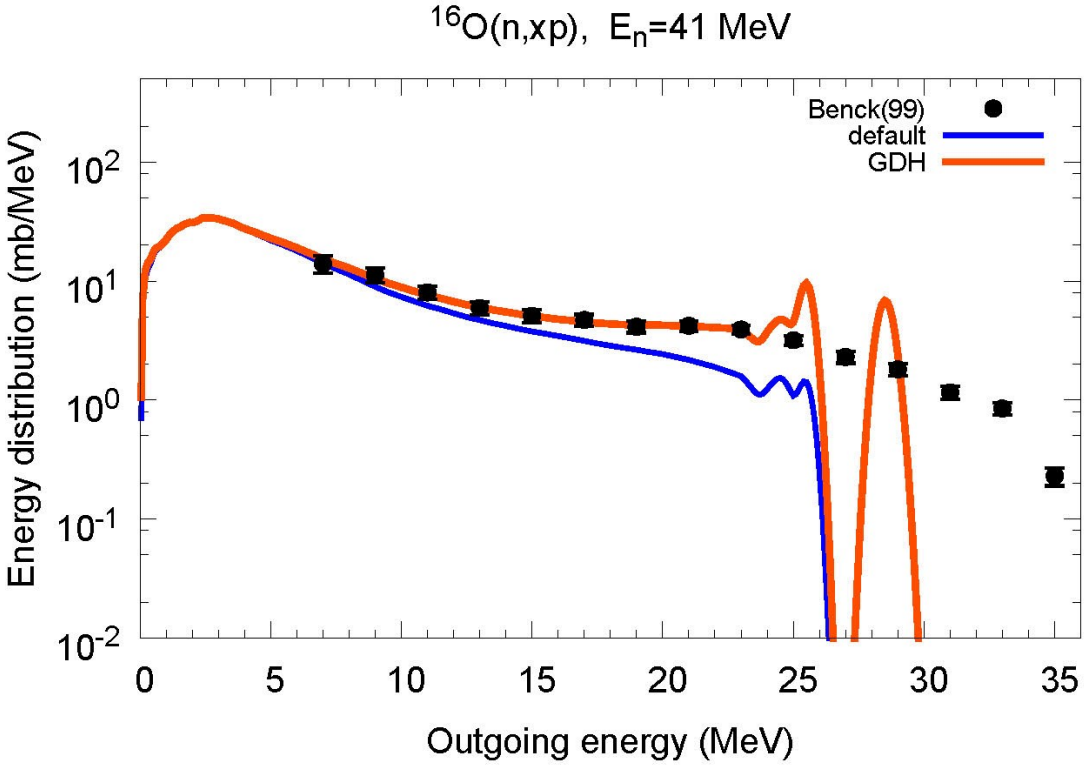
^{16}O(n,xp), E_n=41 MeV
Benck(99)
default
GDH
Energy distribution (mb/MeV)
10^2
10^1
10^0
10^{-1}
10^{-2}
0
5
10
15
20
25
30
35
Outgoing energy (MeV)

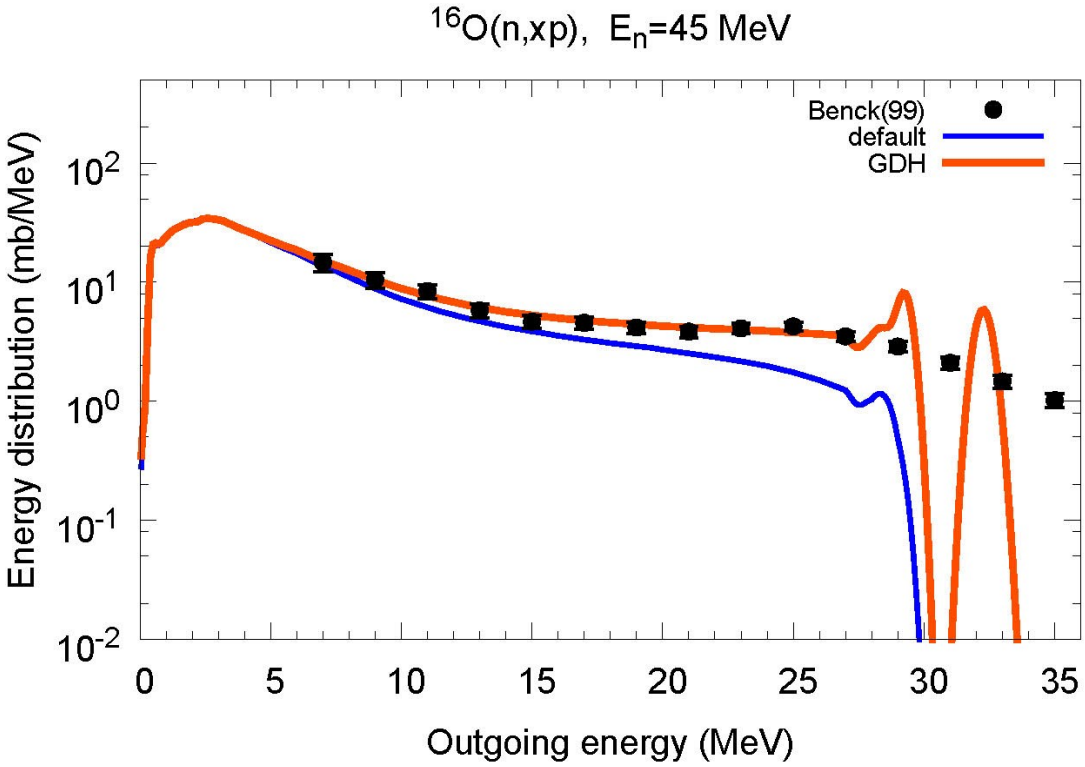
^{16}O(n,xp), E_n=45 MeV
Benck(99)
default
GDH
Energy distribution (mb/MeV)
10^2
10^1
10^0
10^{-1}
10^{-2}
0
5
10
15
20
25
30
35
Outgoing energy (MeV)

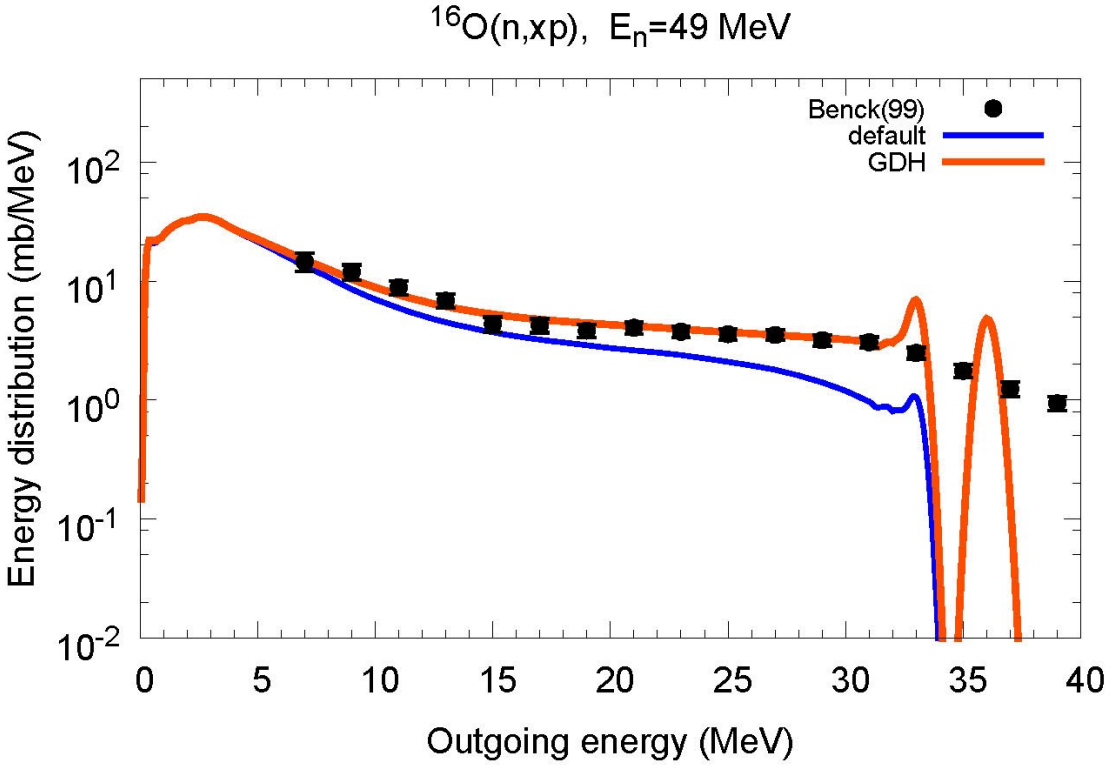
^{16}O(n,xp), E_n=49 MeV
Benck(99)
default
GDH
Energy distribution (mb/MeV)
10^2
10^1
10^0
10^{-1}
10^{-2}
0
5
10
15
20
25
30
35
40
Outgoing energy (MeV)

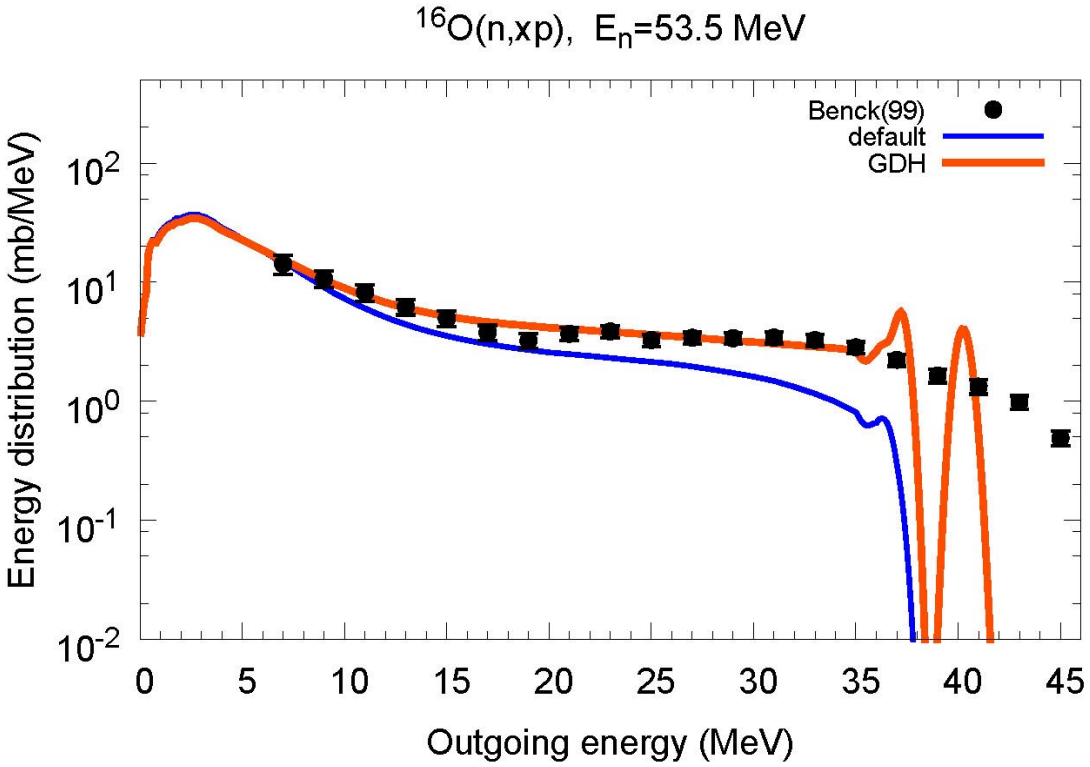
^{16}O(n,xp), E_n=53.5 MeV
Benck(99)
default
GDH
Energy distribution (mb/MeV)
10^2
10^1
10^0
10^{-1}
10^{-2}
0
5
10
15
20
25
30
35
40
45
Outgoing energy (MeV)

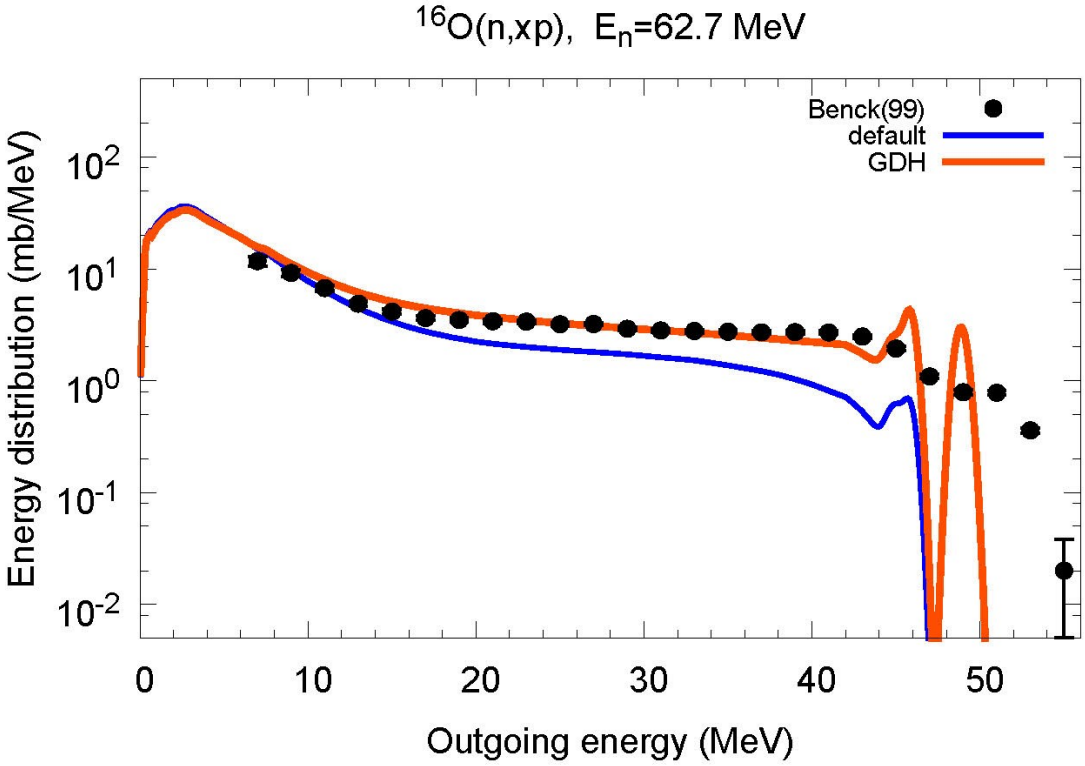
^{16}O(n,xp), E_n=62.7 MeV
Benck(99)
default
GDH
Energy distribution (mb/MeV)
10^2
10^1
10^0
10^{-1}
10^{-2}
0
10
20
30
40
50
Outgoing energy (MeV)

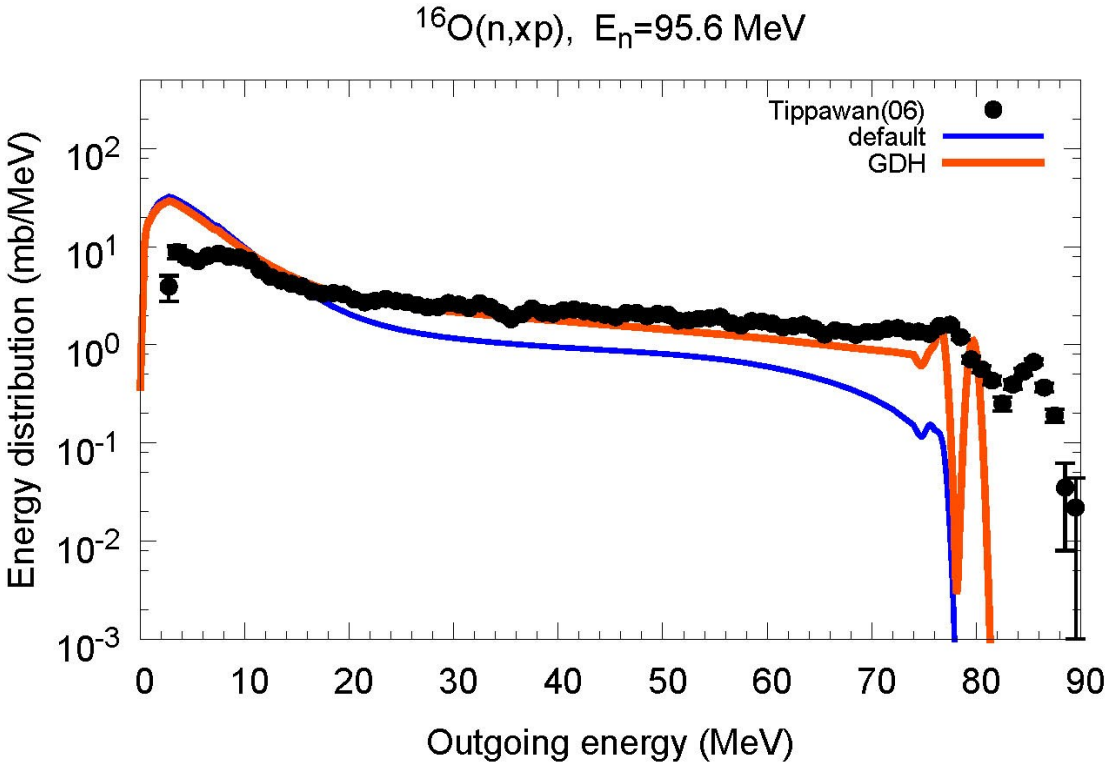
^{16}O(n,xp), E_n=95.6 MeV
Tippawan(06)
default
GDH
Energy distribution (mb/MeV)
10^2
10^1
10^0
10^{-1}
10^{-2}
10^{-3}
0
10
20
30
40
50
60
70
80
90
Outgoing energy (MeV)

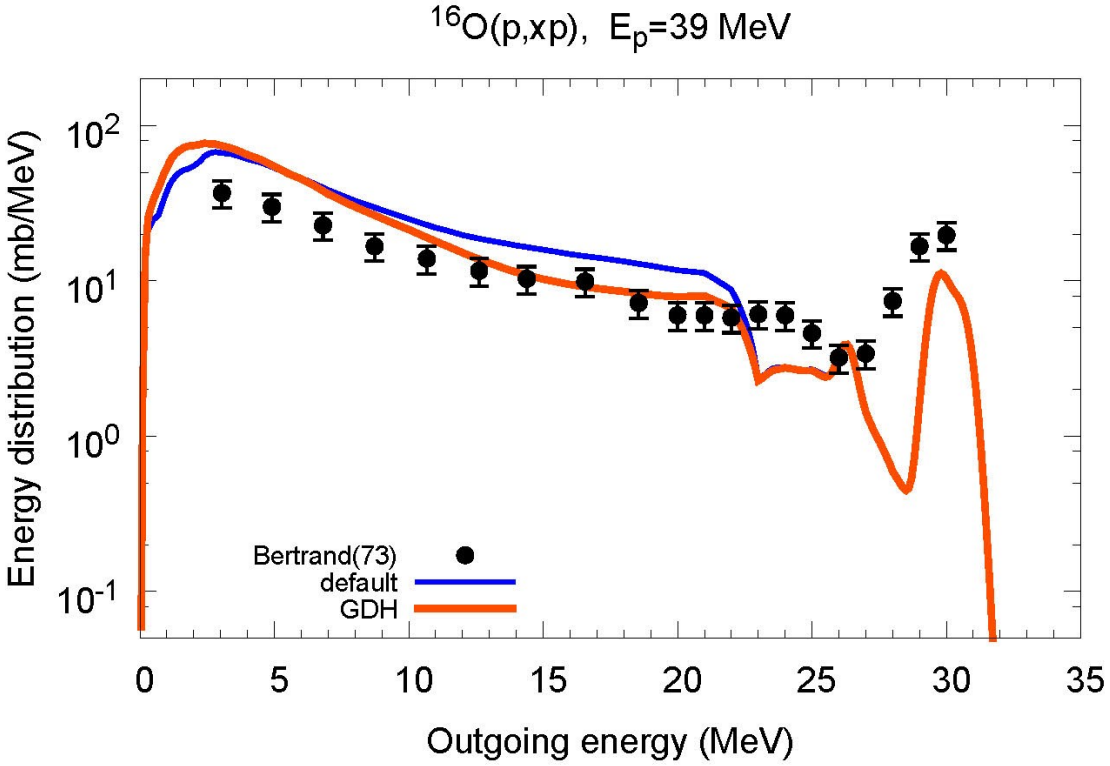
^{16}O(p,xp), E_p=39 MeV
Energy distribution (mb/MeV)
Outgoing energy (MeV)
Bertrand(73)
default
GDH

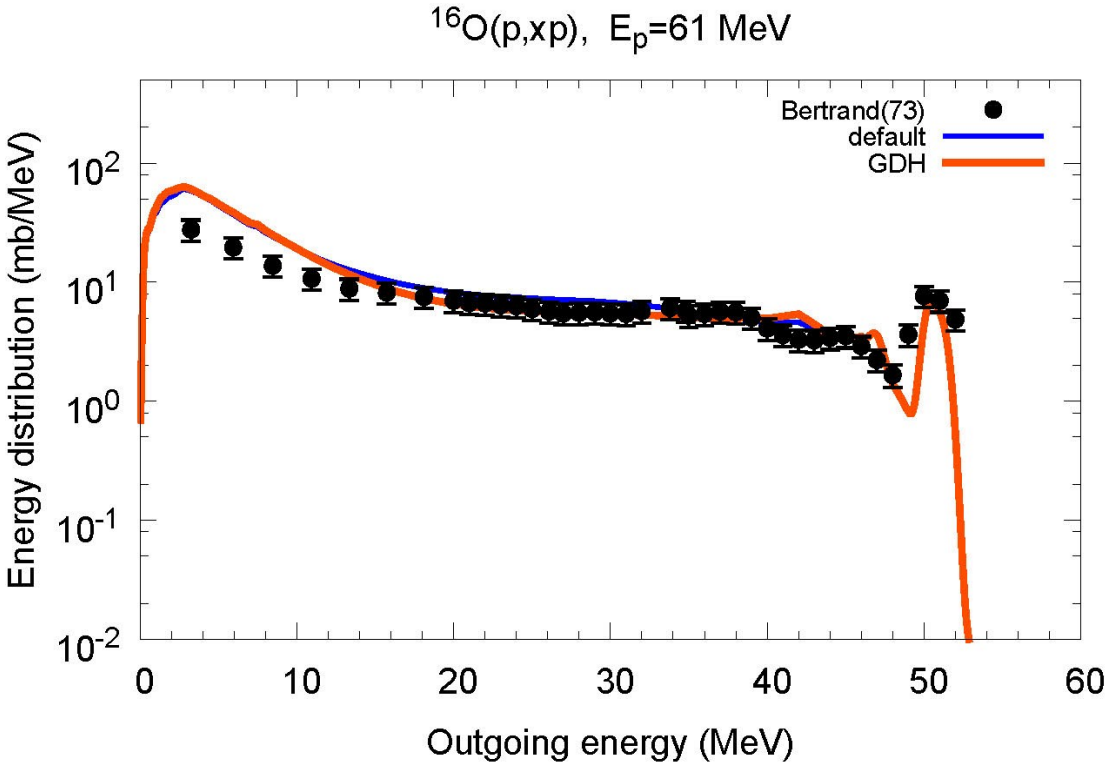
^{16}O(p,xp), E_p=61 MeV
Energy distribution (mb/MeV)
Outgoing energy (MeV)
Bertrand(73)
default
GDH

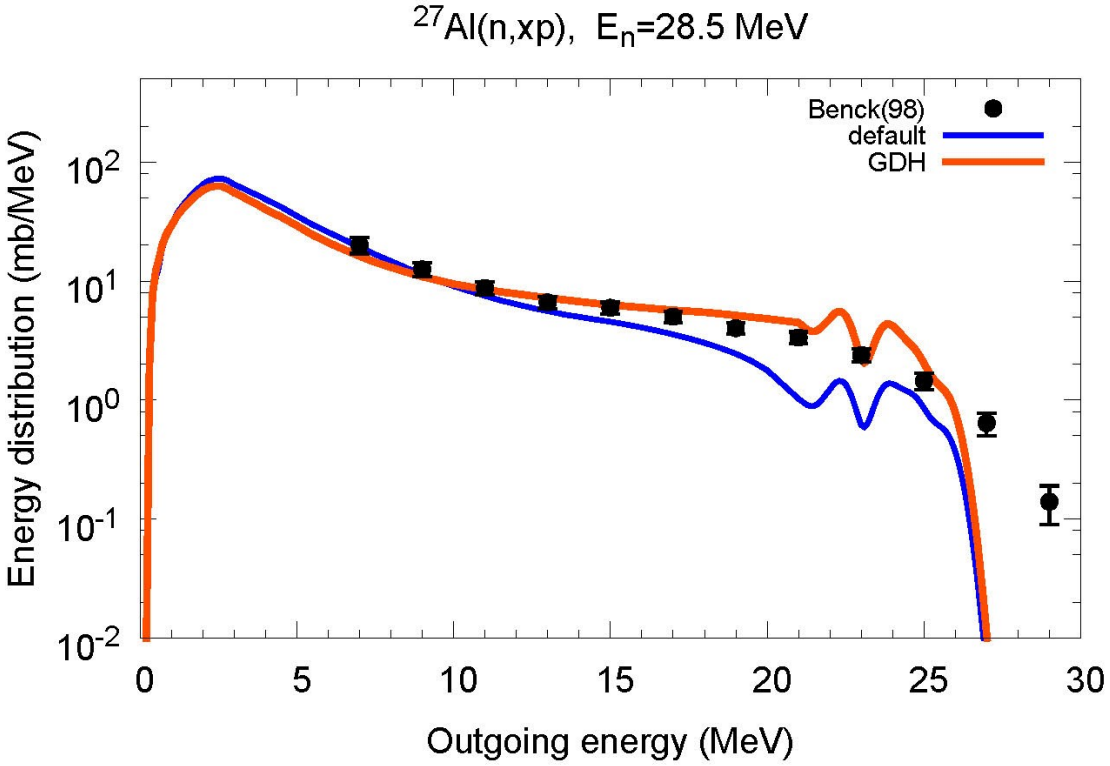
^{27}Al(n,xp), E_n=28.5 MeV
Benck(98)
default
GDH
Energy distribution (mb/MeV)
10^2
10^1
10^0
10^{-1}
10^{-2}
0
5
10
15
20
25
30
Outgoing energy (MeV)

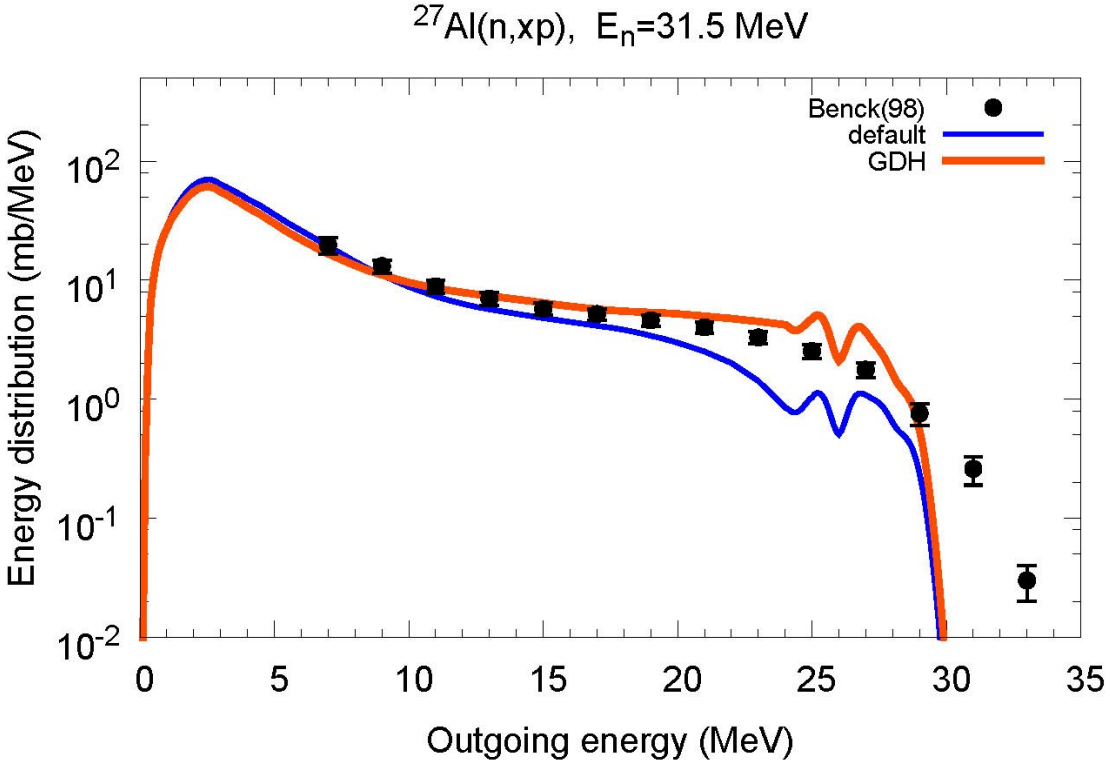
^{27}Al(n,xp), E_n=31.5 MeV
Benck(98)
default
GDH
Energy distribution (mb/MeV)
10^2
10^1
10^0
10^{-1}
10^{-2}
0
5
10
15
20
25
30
35
Outgoing energy (MeV)

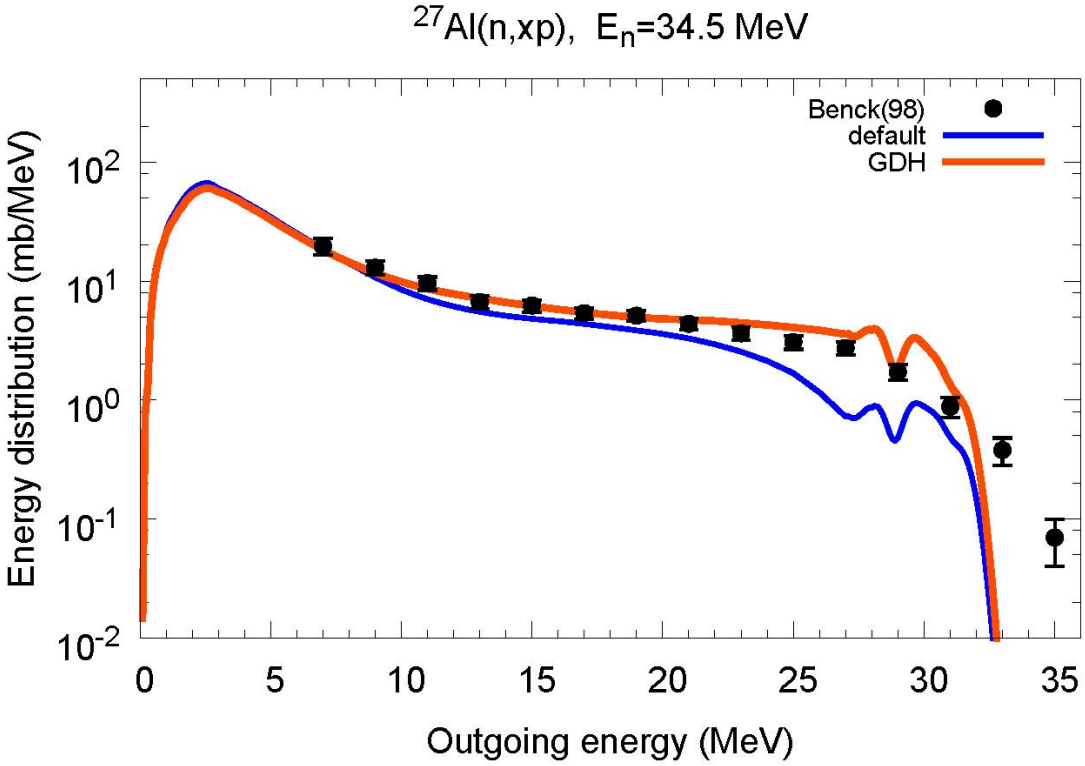
^{27}Al(n,xp), E_n=34.5 MeV
Benck(98)
default
GDH
Energy distribution (mb/MeV)
10^2
10^1
10^0
10^{-1}
10^{-2}
0
5
10
15
20
25
30
35
Outgoing energy (MeV)

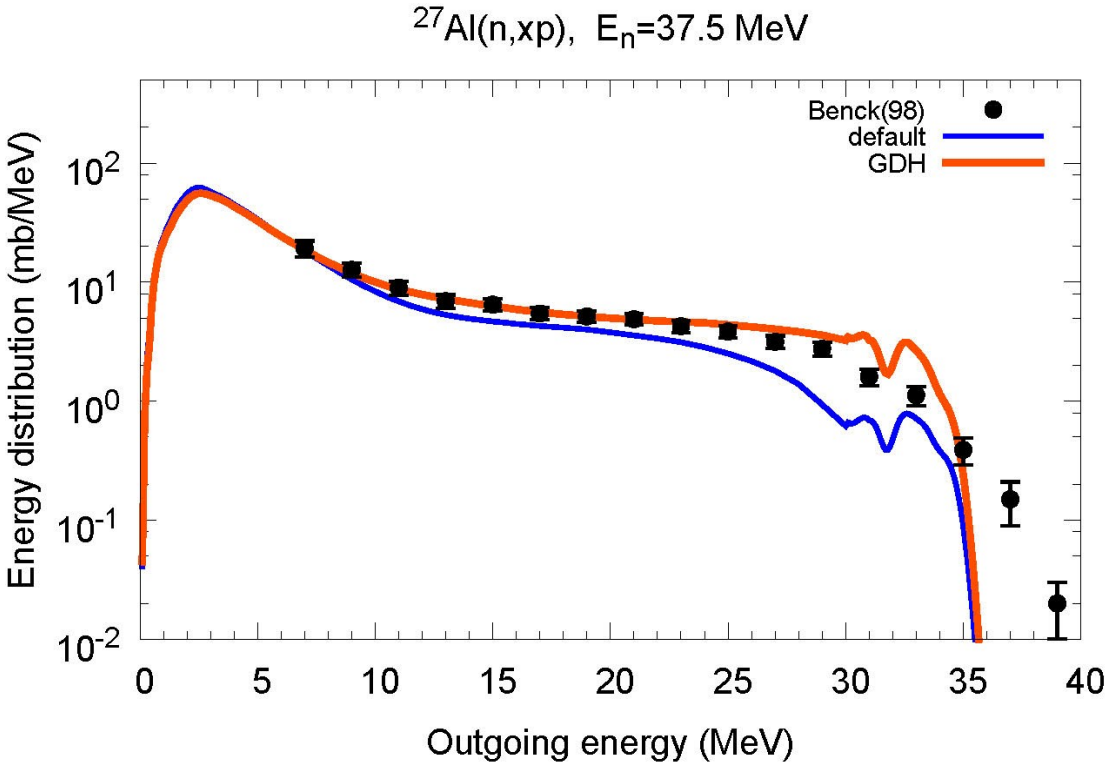
^{27}Al(n,xp), E_n=37.5 MeV
Benck(98)
default
GDH
Energy distribution (mb/MeV)
10^2
10^1
10^0
10^{-1}
10^{-2}
0
5
10
15
20
25
30
35
40
Outgoing energy (MeV)

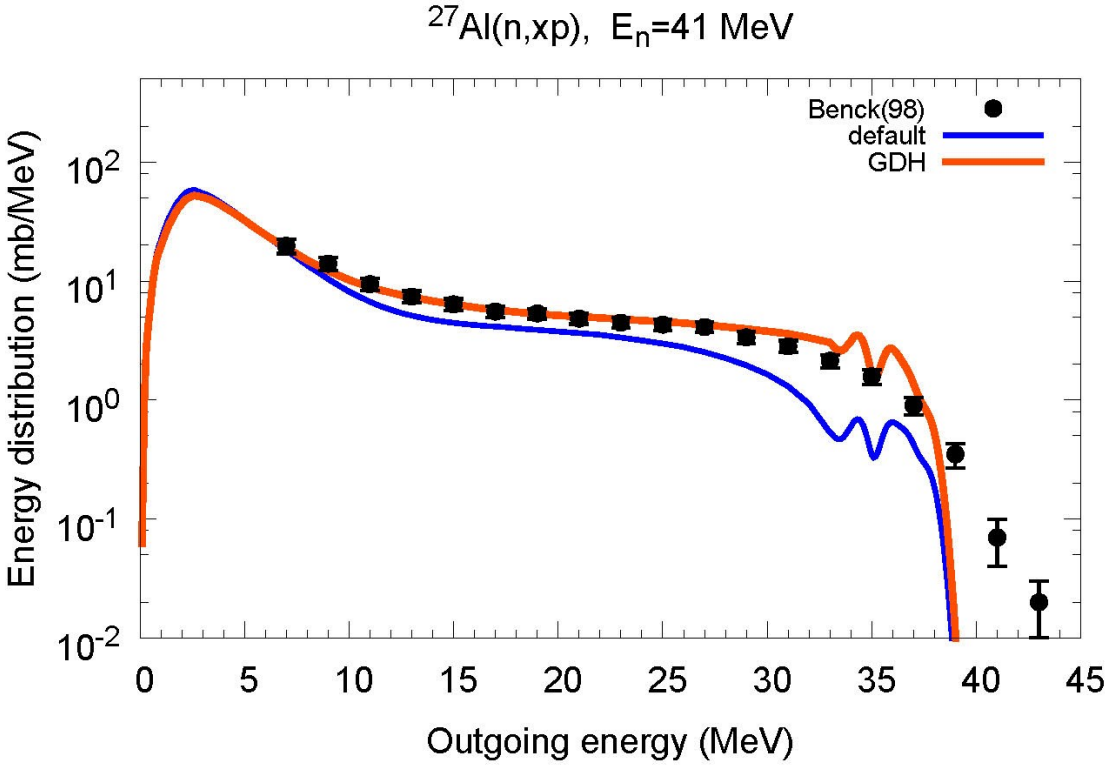
^{27}Al(n,xp), E_n=41 MeV
Benck(98)
default
GDH
Energy distribution (mb/MeV)
10^2
10^1
10^0
10^{-1}
10^{-2}
0
5
10
15
20
25
30
35
40
45
Outgoing energy (MeV)

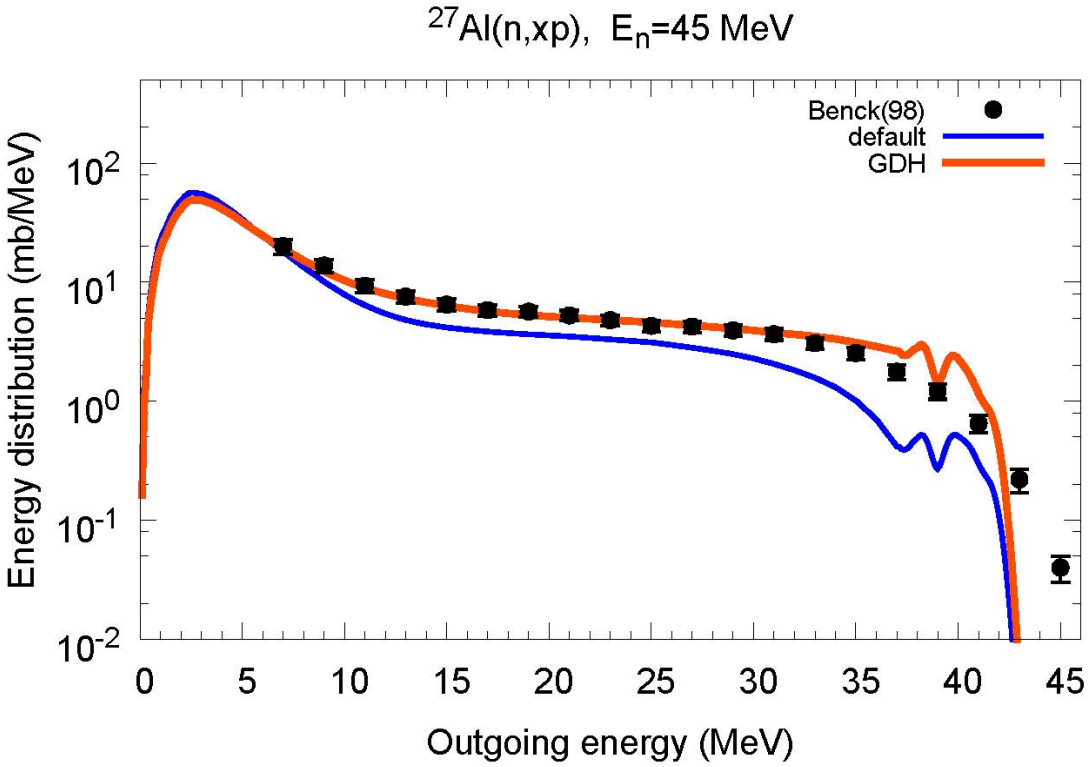
^{27}Al(n,xp), E_n=45 MeV
Benck(98)
default
GDH
Energy distribution (mb/MeV)
10^2
10^1
10^0
10^{-1}
10^{-2}
0
5
10
15
20
25
30
35
40
45
Outgoing energy (MeV)

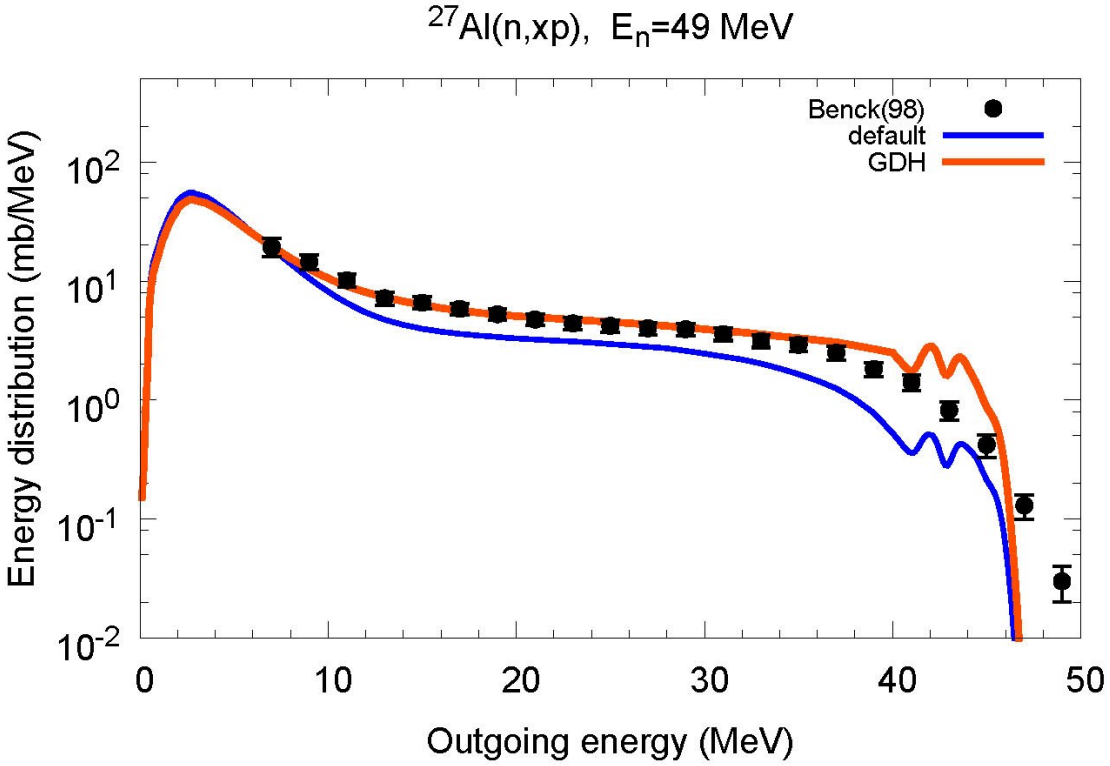
^{27}Al(n,xp), E_n=49 MeV
Benck(98)
default
GDH
Energy distribution (mb/MeV)
10^2
10^1
10^0
10^{-1}
10^{-2}
0
10
20
30
40
50
Outgoing energy (MeV)

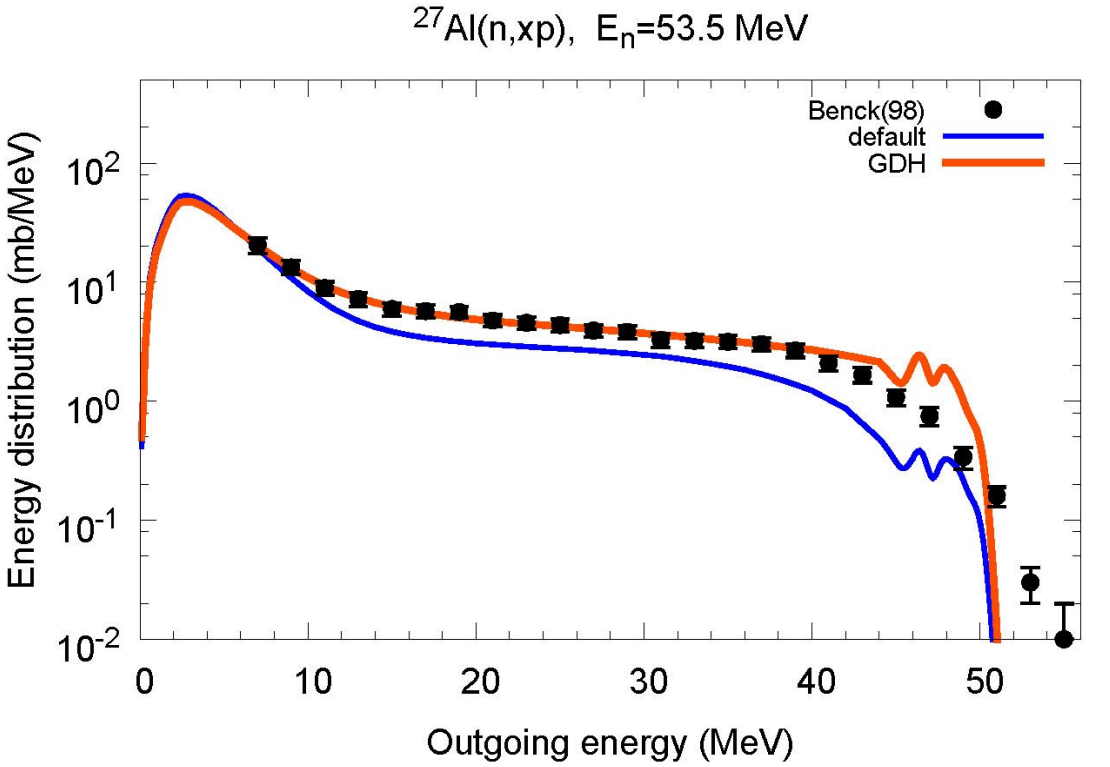
^{27}Al(n,xp), E_n=53.5 MeV
Benck(98)
default
GDH
Energy distribution (mb/MeV)
10^2
10^1
10^0
10^{-1}
10^{-2}
0
10
20
30
40
50
Outgoing energy (MeV)

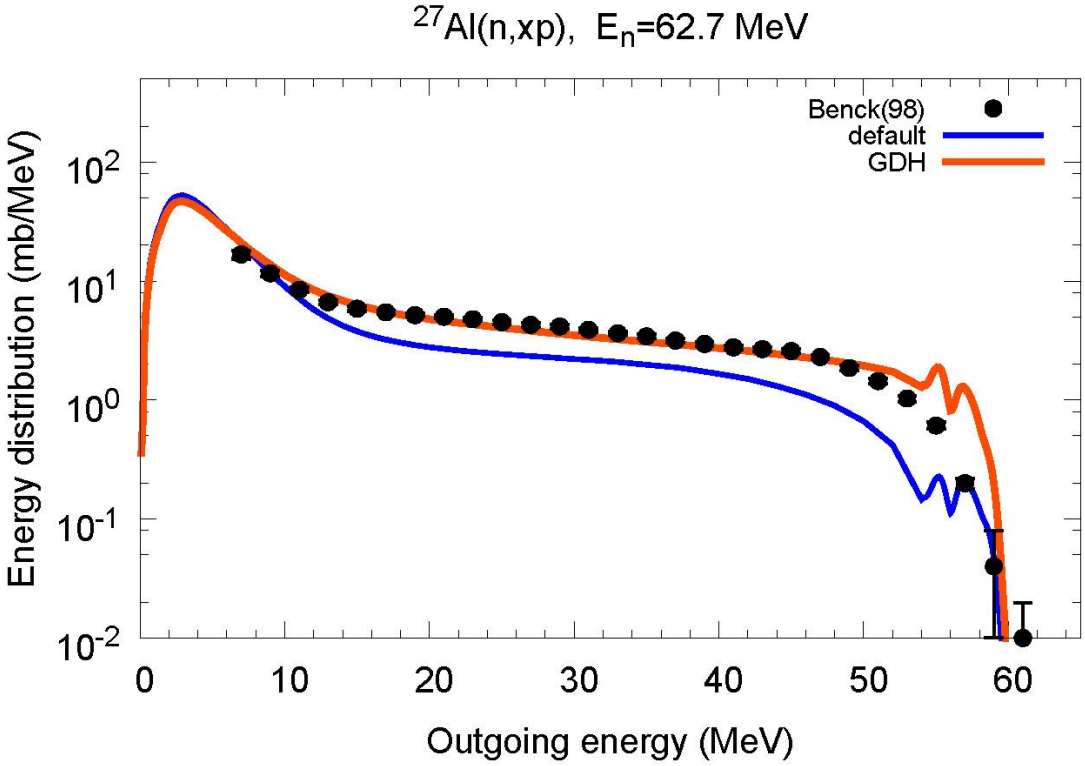
^{27}Al(n,xp), E_n=62.7 MeV
Benck(98)
default
GDH
Energy distribution (mb/MeV)
Outgoing energy (MeV)

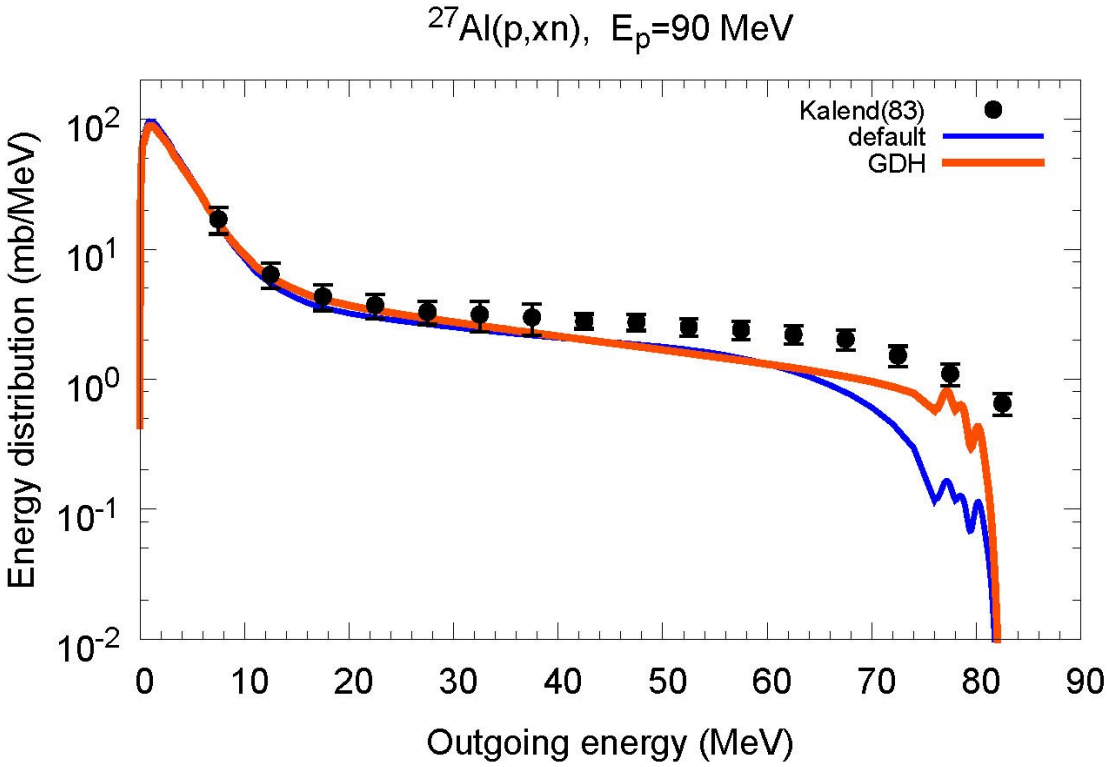
^{27}Al(p,xn), E_p=90 MeV
Kalend(83)
default
GDH
Energy distribution (mb/MeV)
Outgoing energy (MeV)

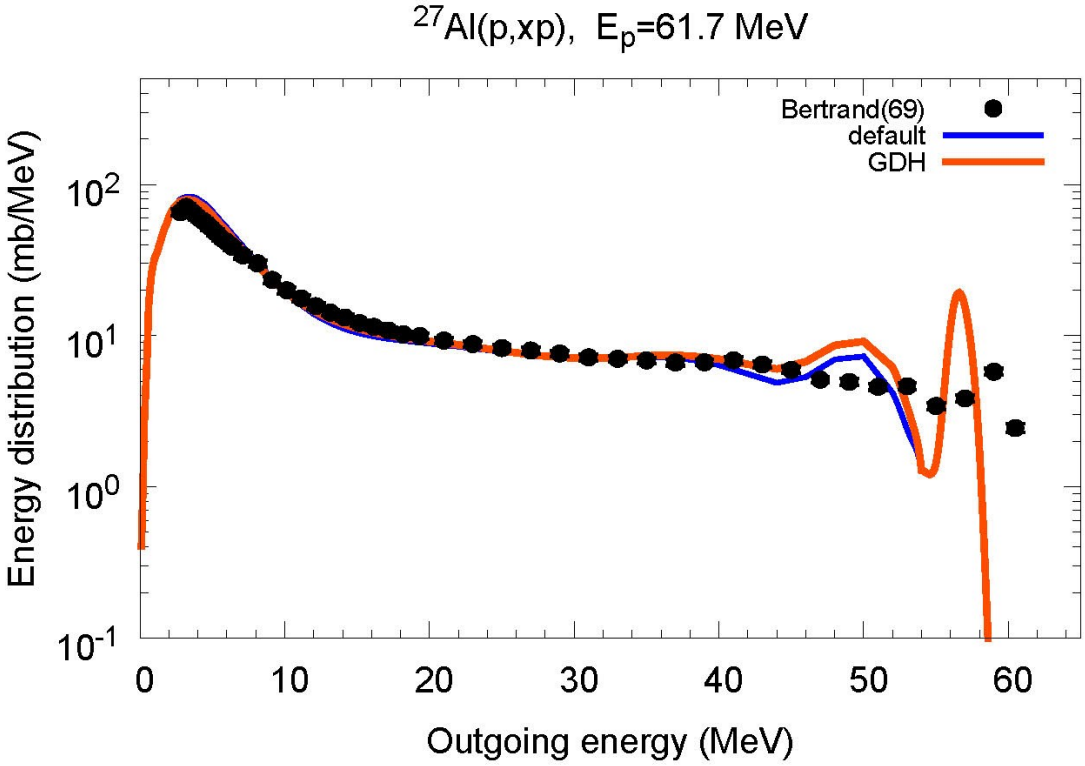
^{27}Al(p,xp), E_p=61.7 MeV
Bertrand(69)
default
GDH
Energy distribution (mb/MeV)
10^2
10^1
10^0
10^{-1}
0
10
20
30
40
50
60
Outgoing energy (MeV)

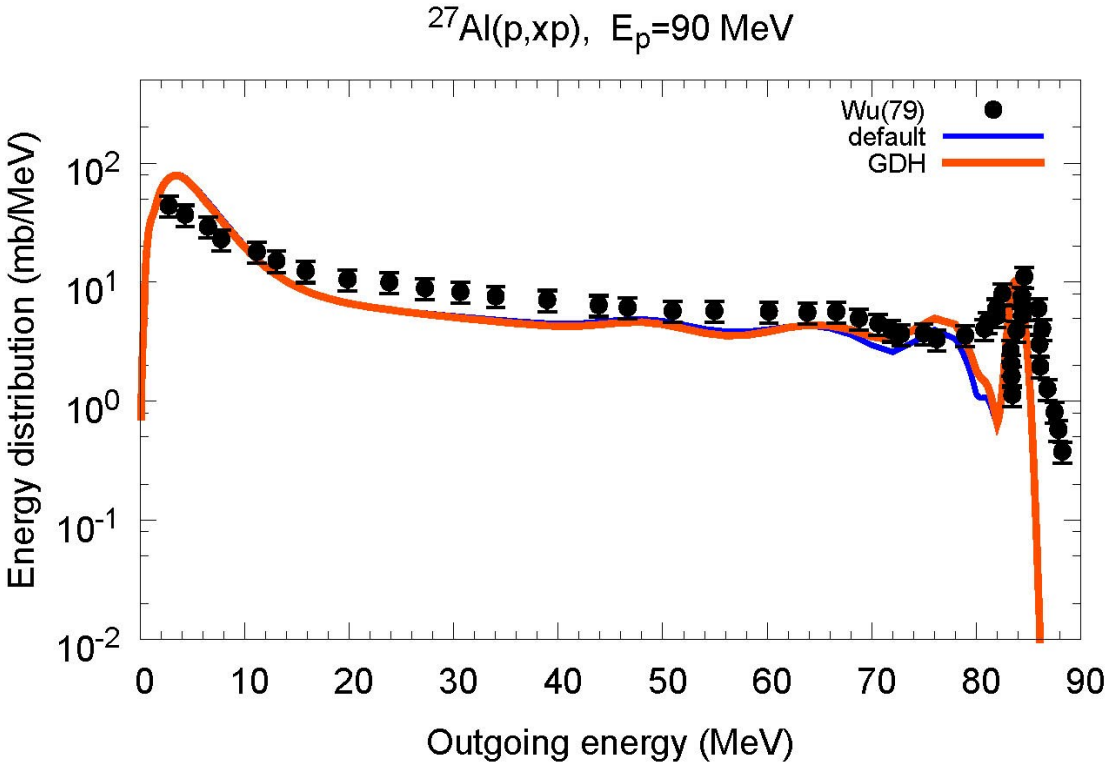
^{27}Al(p,xp), E_p=90 MeV
Wu(79)
default
GDH
Energy distribution (mb/MeV)
10^2
10^1
10^0
10^{-1}
10^{-2}
0
10
20
30
40
50
60
70
80
90
Outgoing energy (MeV)

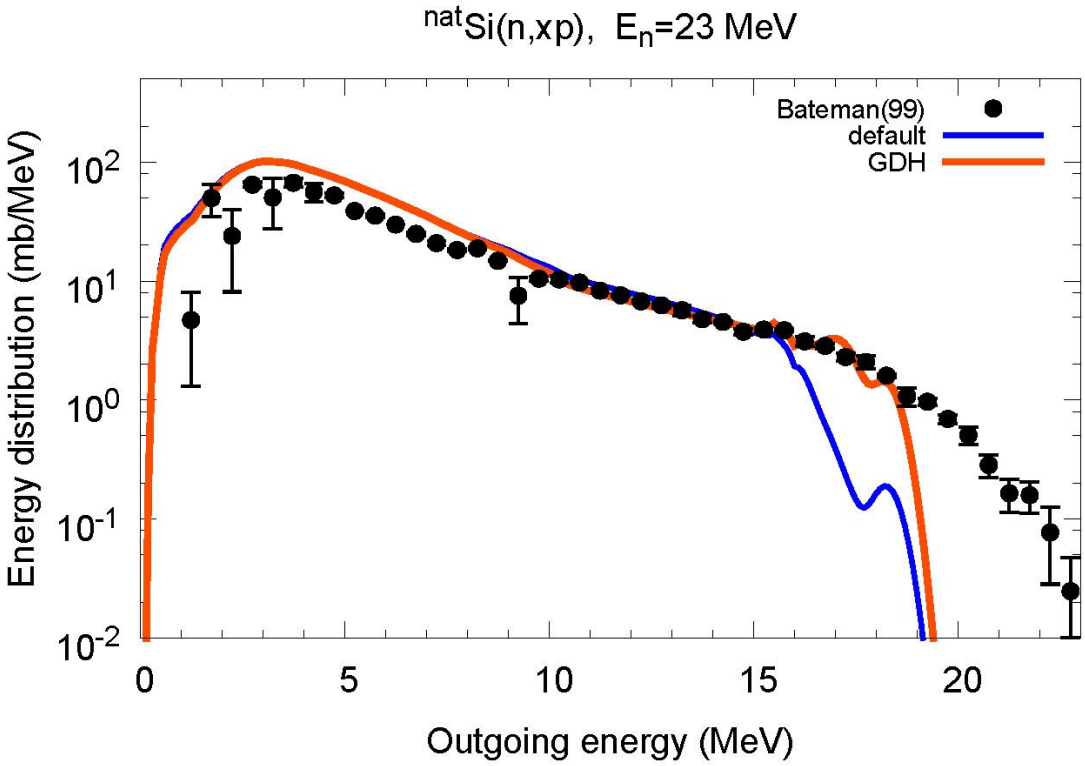
natSi(n,xp), En=23 MeV
Bateman(99)
default
GDH
Energy distribution (mb/MeV)
Outgoing energy (MeV)

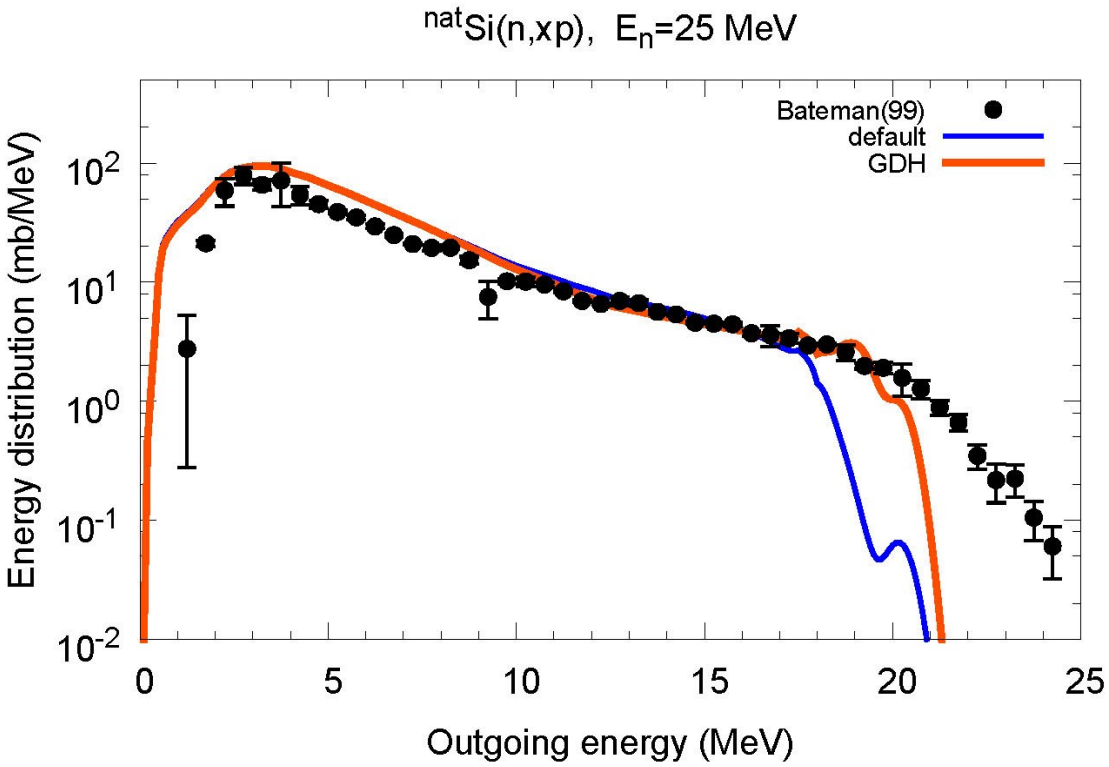
natSi(n,xp), En=25 MeV
Bateman(99)
default
GDH
Energy distribution (mb/MeV)
Outgoing energy (MeV)

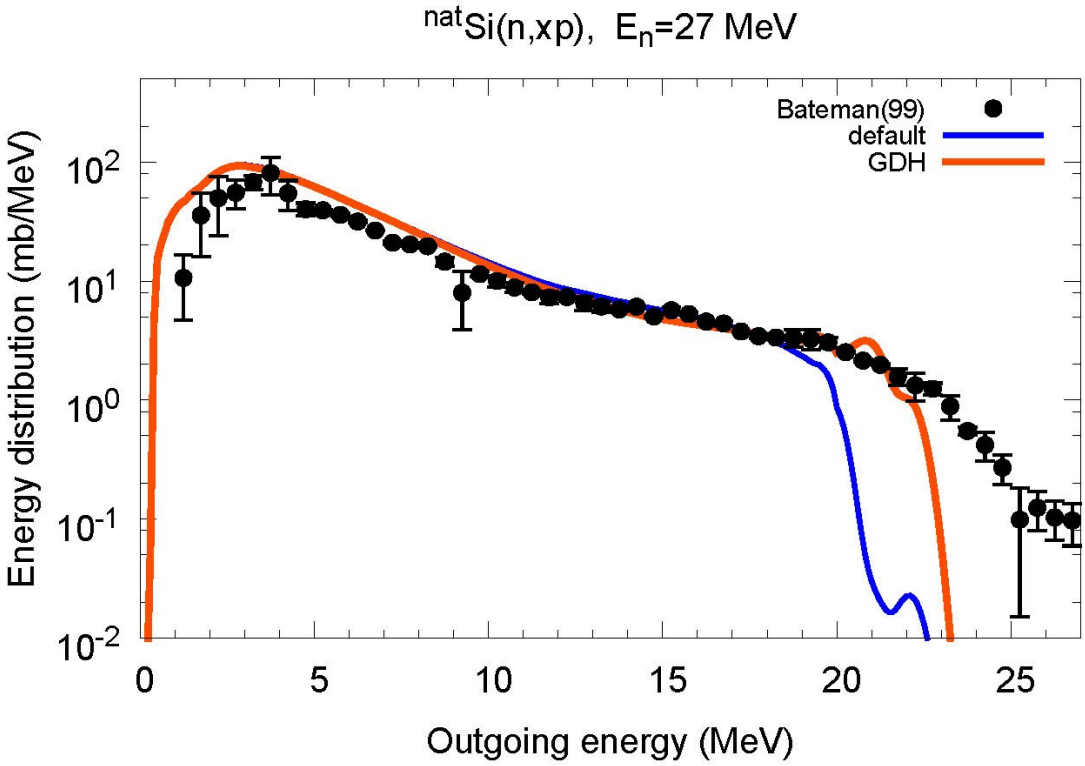
^{nat}Si(n,xp), E_n=27 MeV
Bateman(99)
default
GDH
Energy distribution (mb/MeV)
Outgoing energy (MeV)

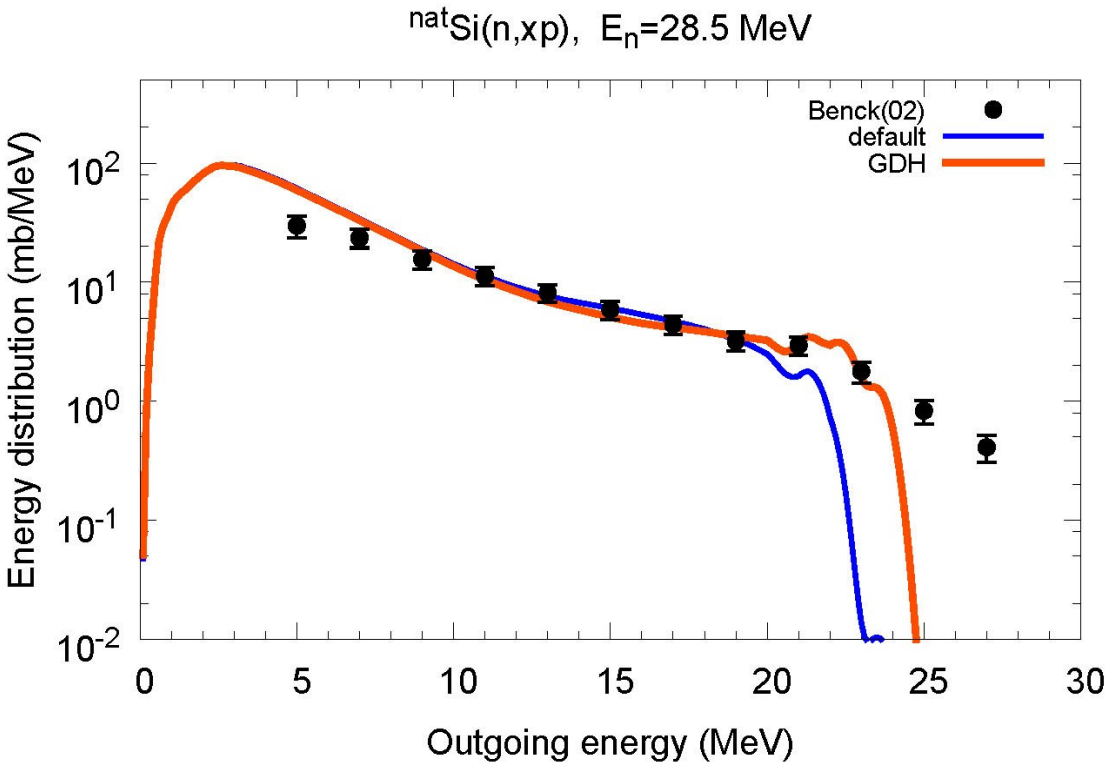
^{nat}Si(n,xp), E_n=28.5 MeV
Benck(02)
default
GDH
Energy distribution (mb/MeV)
Outgoing energy (MeV)

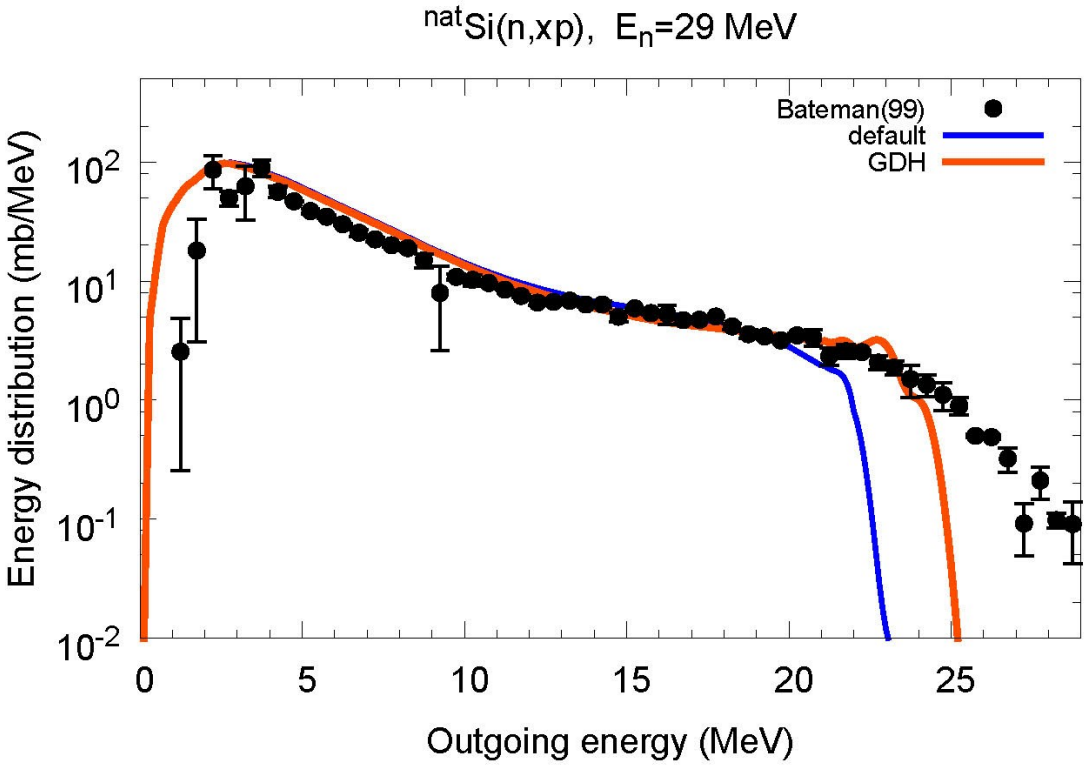
natSi(n,xp), En=29 MeV
Bateman(99)
default
GDH
Energy distribution (mb/MeV)
Outgoing energy (MeV)

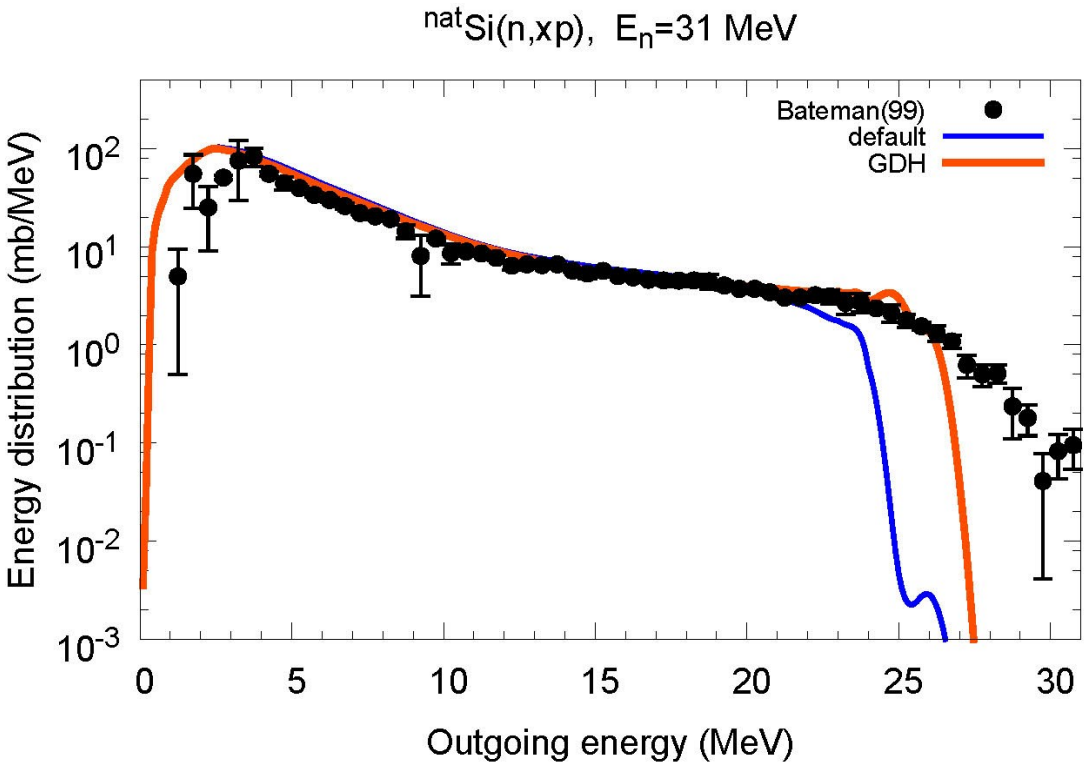
natSi(n,xp), En=31 MeV
Bateman(99)
default
GDH
Energy distribution (mb/MeV)
Outgoing energy (MeV)

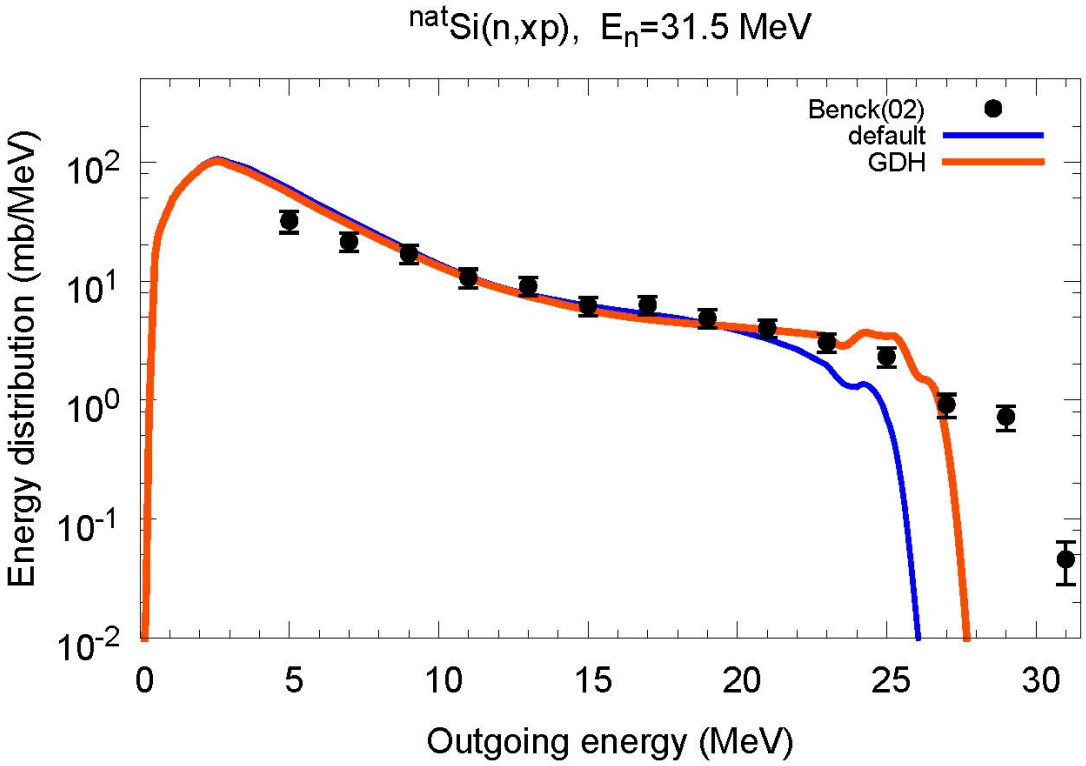
natSi(n,xp), En=31.5 MeV
Benck(02)
default
GDH
Energy distribution (mb/MeV)
Outgoing energy (MeV)

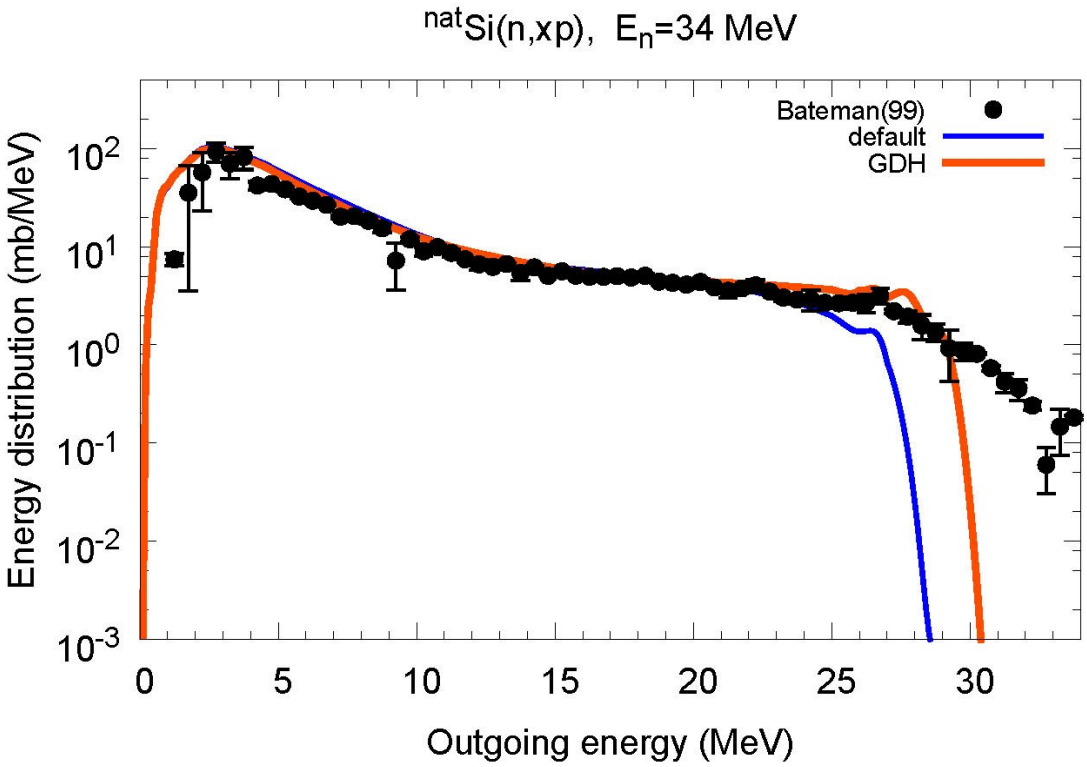
natSi(n,xp), En=34 MeV
Bateman(99)
default
GDH
Energy distribution (mb/MeV)
Outgoing energy (MeV)

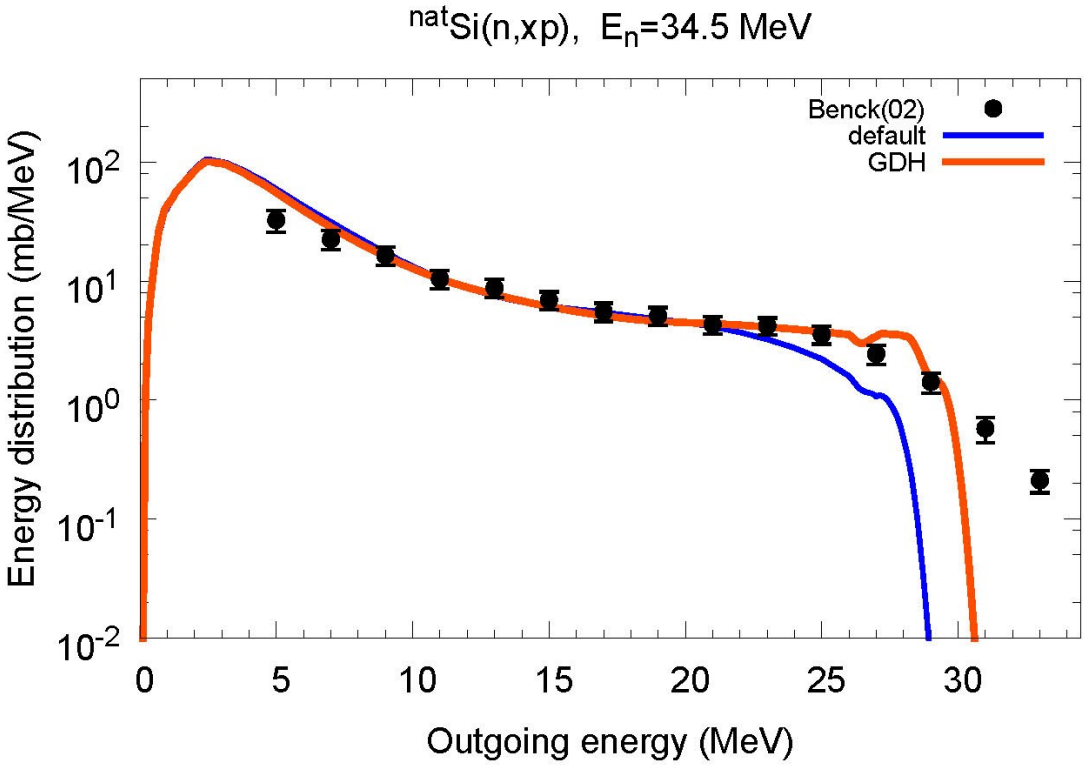
natSi(n,xp), En=34.5 MeV
Benck(02)
default
GDH
Energy distribution (mb/MeV)
Outgoing energy (MeV)

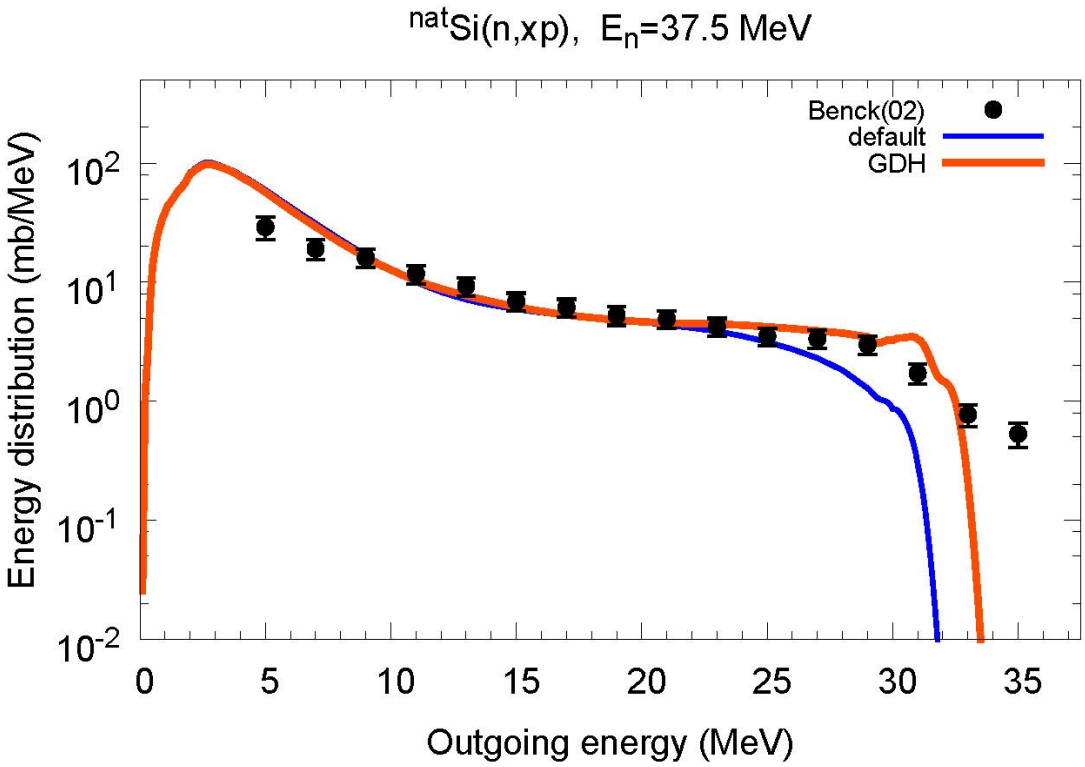
natSi(n,xp), En=37.5 MeV
Benck(02)
default
GDH
Energy distribution (mb/MeV)
Outgoing energy (MeV)

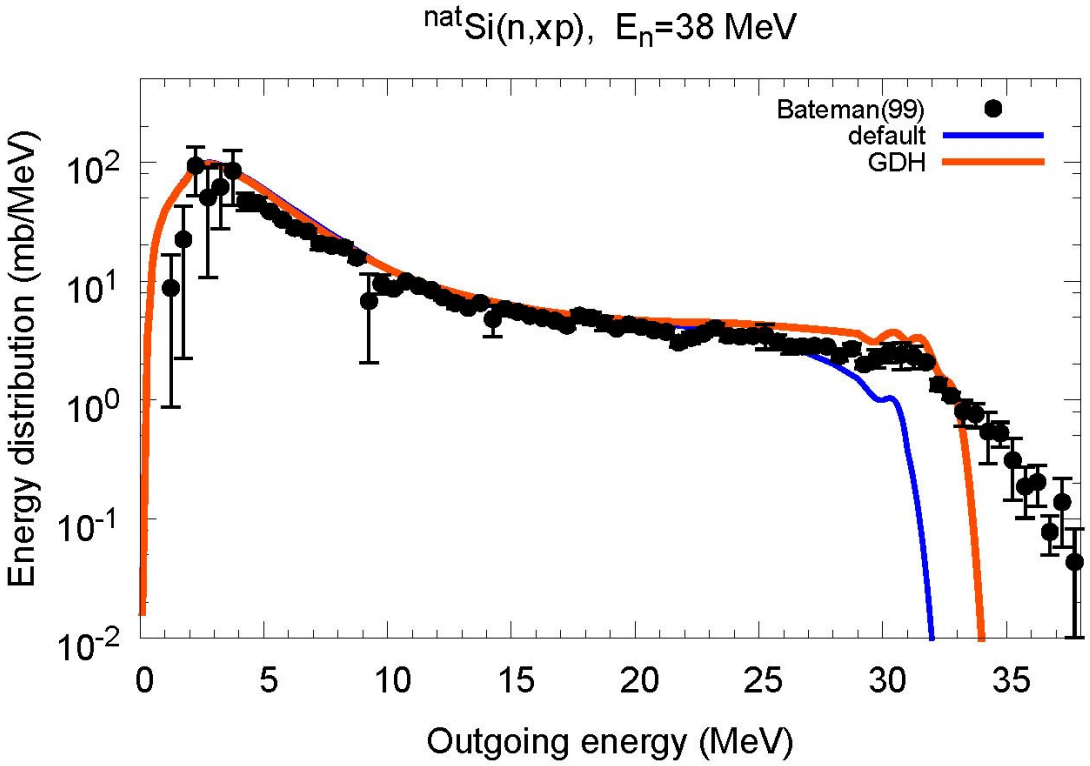
natSi(n,xp), En=38 MeV
Bateman(99)
default
GDH
Energy distribution (mb/MeV)
Outgoing energy (MeV)

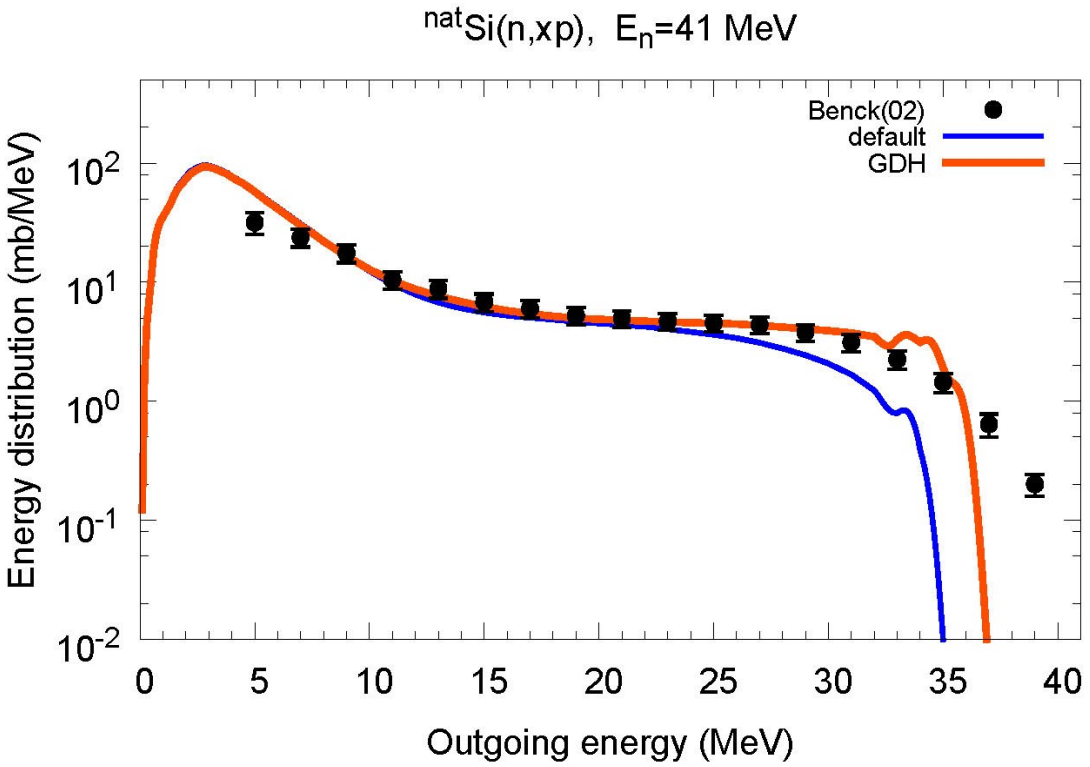
natSi(n,xp), En=41 MeV
Benck(02)
default
GDH
Energy distribution (mb/MeV)
Outgoing energy (MeV)

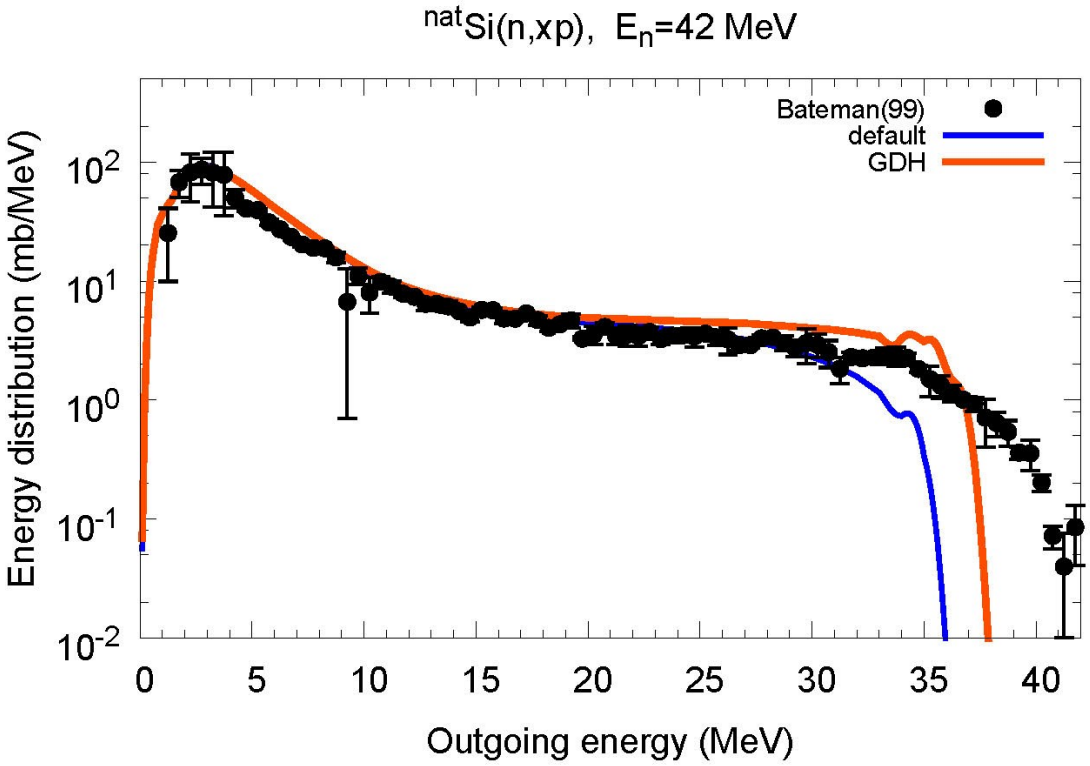
natSi(n,xp), En=42 MeV
Bateman(99)
default
GDH
Energy distribution (mb/MeV)
Outgoing energy (MeV)

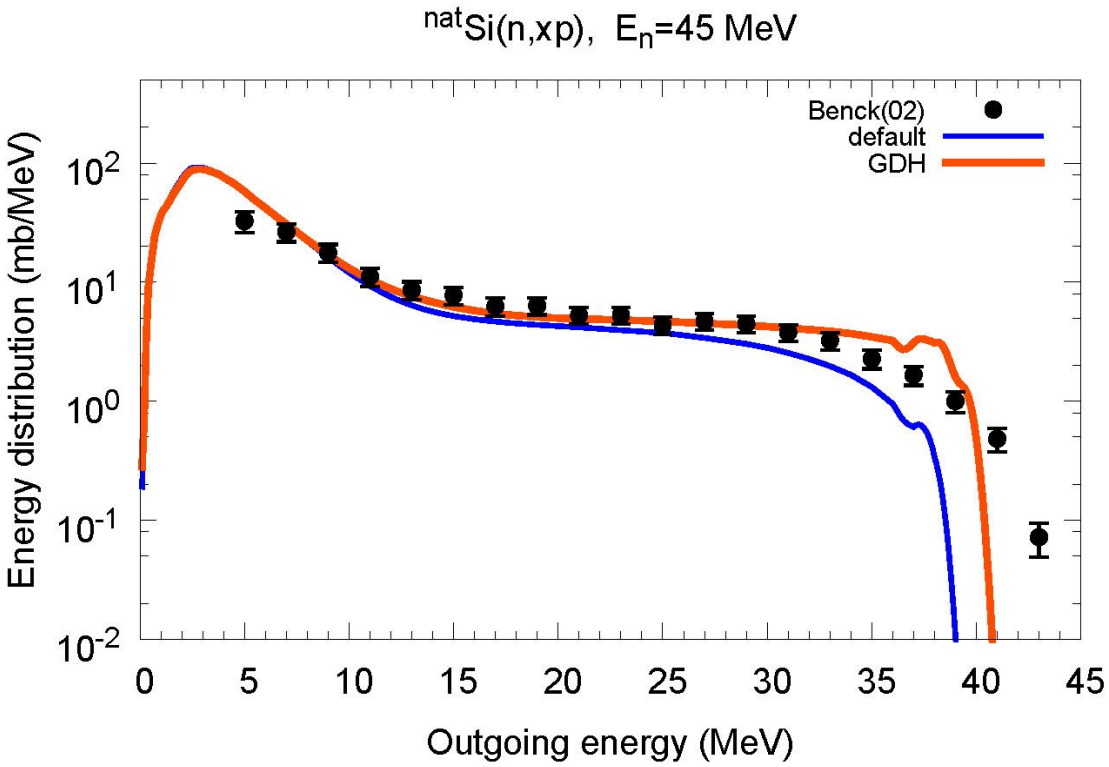
natSi(n,xp), En=45 MeV
Benck(02)
default
GDH
Energy distribution (mb/MeV)
Outgoing energy (MeV)

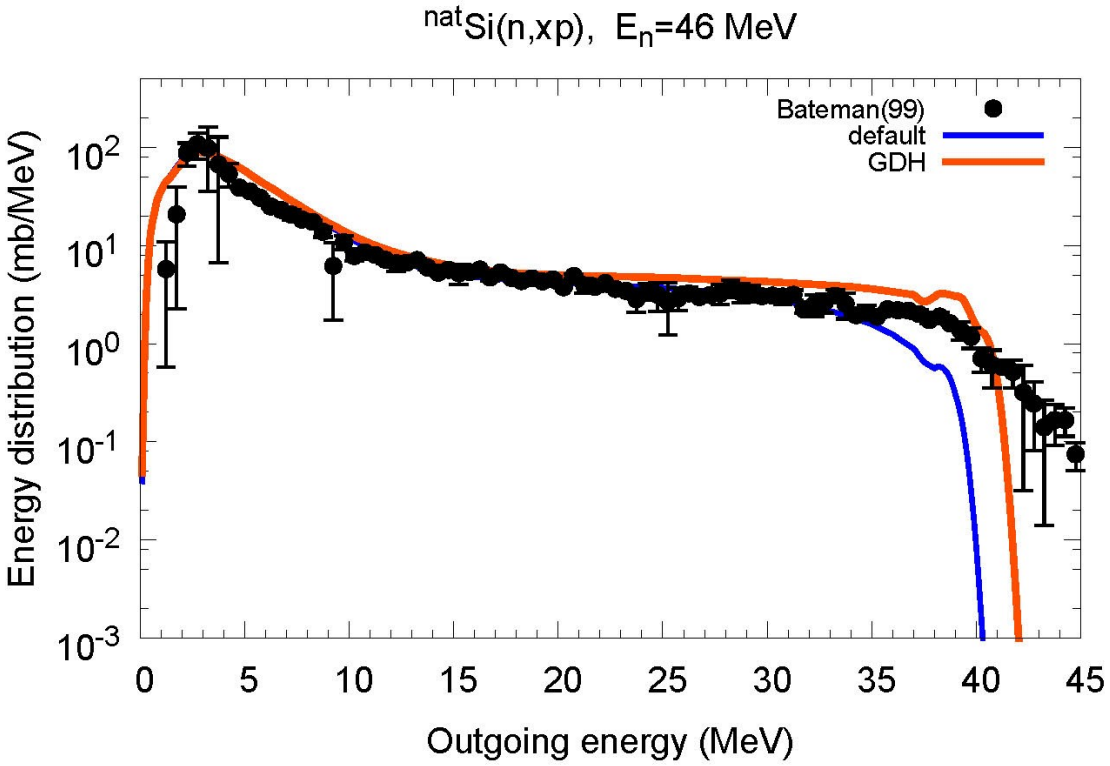
^{nat}Si(n,xp), E_n=46 MeV
Bateman(99)
default
GDH
Energy distribution (mb/MeV)
Outgoing energy (MeV)

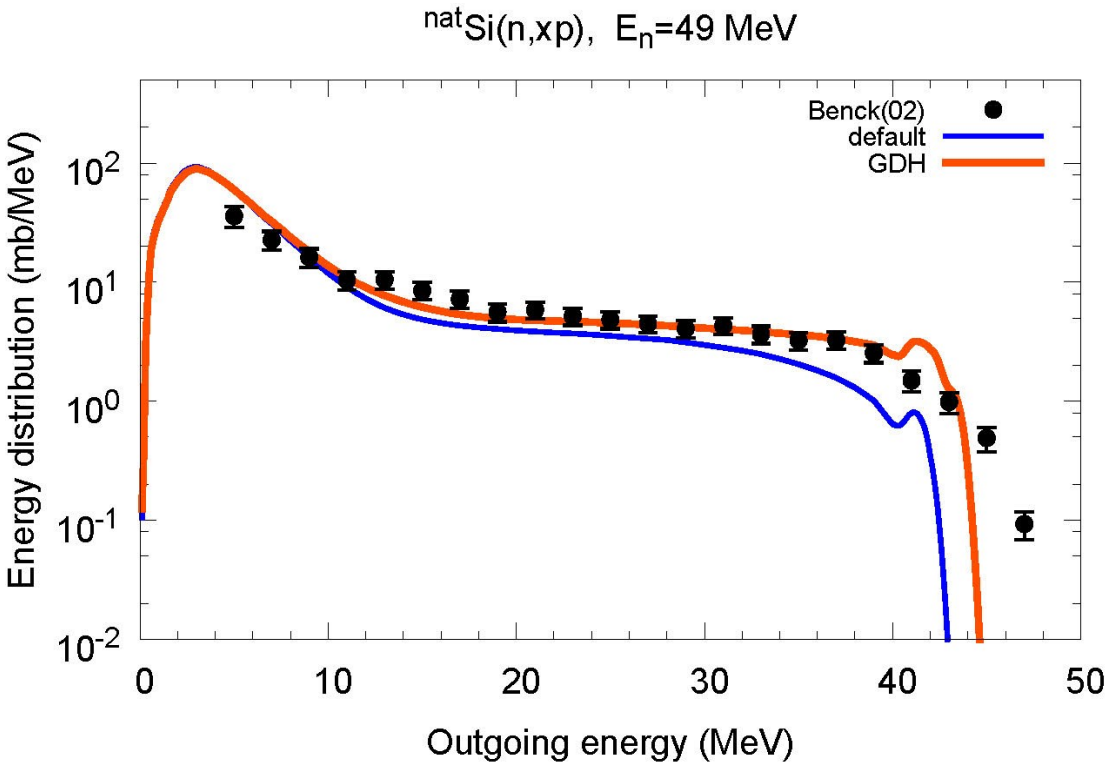
^{nat}Si(n,xp), E_n=49 MeV
Benck(02)
default
GDH
Energy distribution (mb/MeV)
Outgoing energy (MeV)

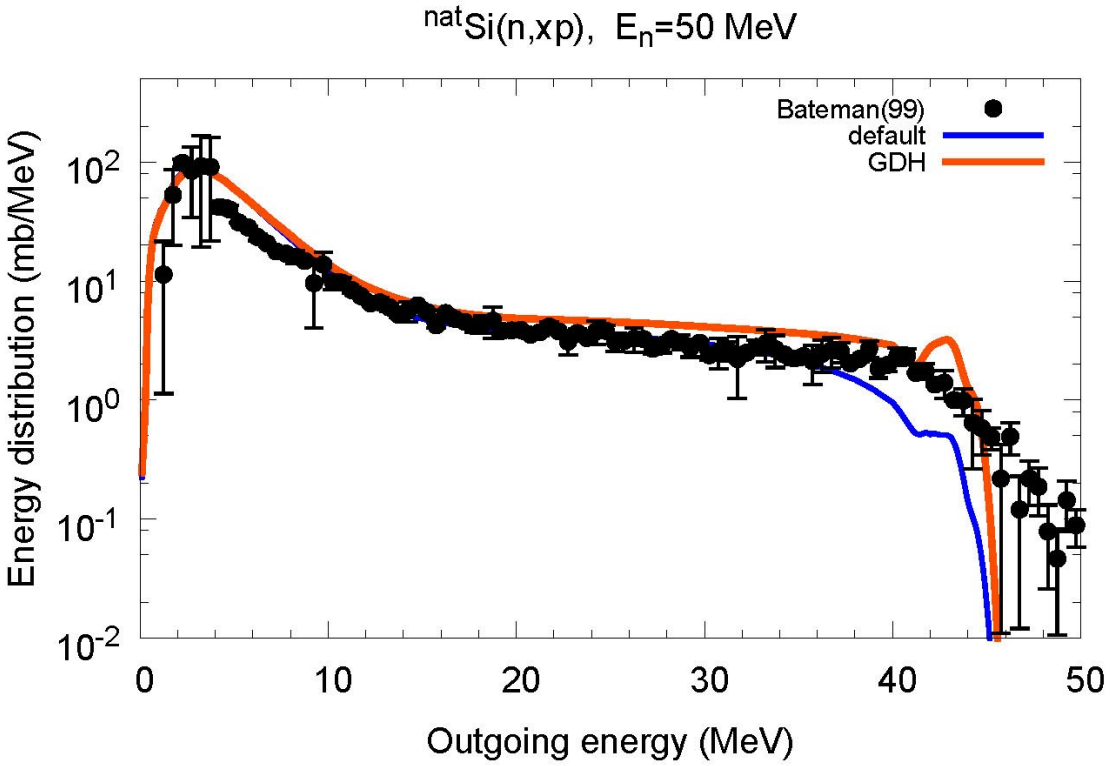
natSi(n,xp), En=50 MeV
Bateman(99)
default
GDH
Energy distribution (mb/MeV)
Outgoing energy (MeV)

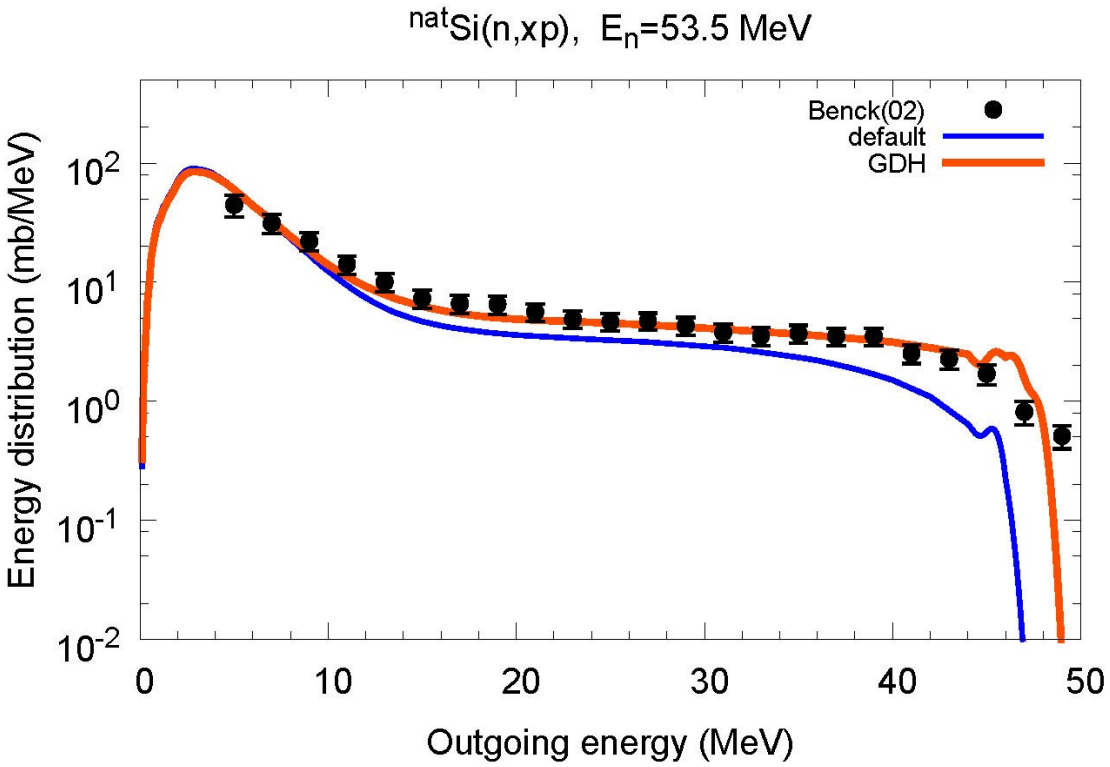
natSi(n,xp), En=53.5 MeV
Benck(02)
default
GDH
Energy distribution (mb/MeV)
Outgoing energy (MeV)

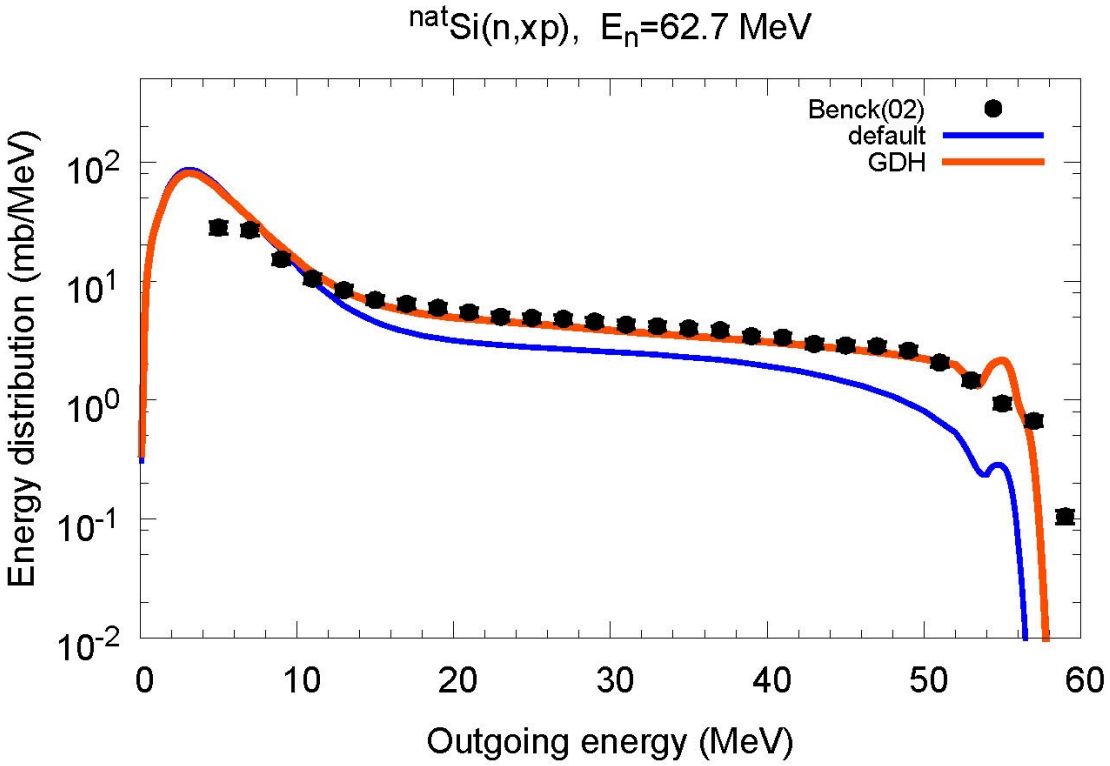
natSi(n,xp), En=62.7 MeV
Benck(02)
default
GDH
Energy distribution (mb/MeV)
Outgoing energy (MeV)

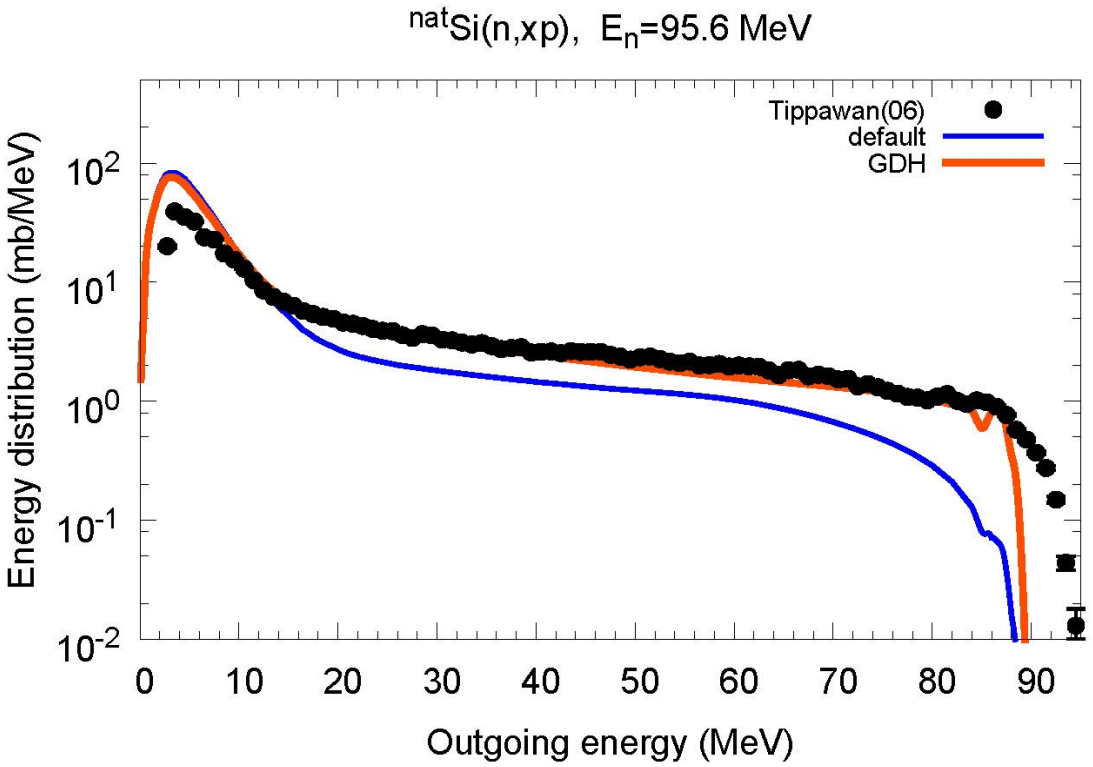
natSi(n,xp), En=95.6 MeV
Tippawan(06)
default
GDH
Energy distribution (mb/MeV)
Outgoing energy (MeV)

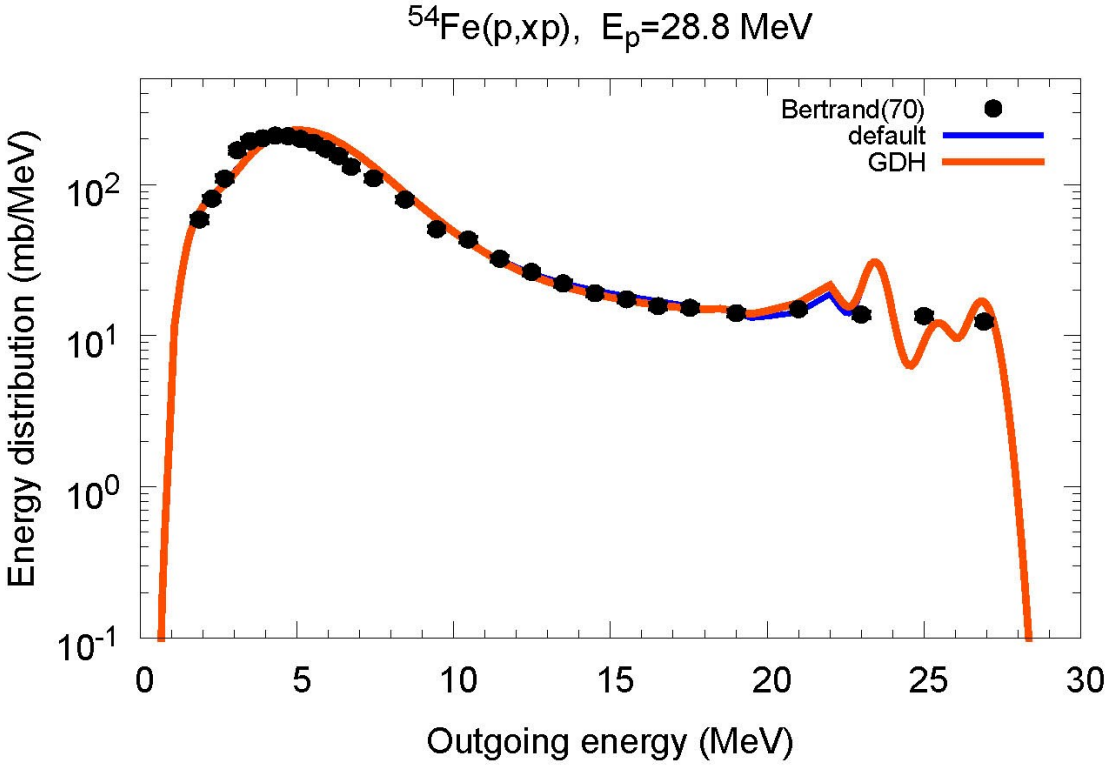
^{54}Fe(p,xp), E_p=28.8 MeV
Bertrand(70)
default
GDH
Energy distribution (mb/MeV)
10^2
10^1
10^0
10^{-1}
0
5
10
15
20
25
30
Outgoing energy (MeV)

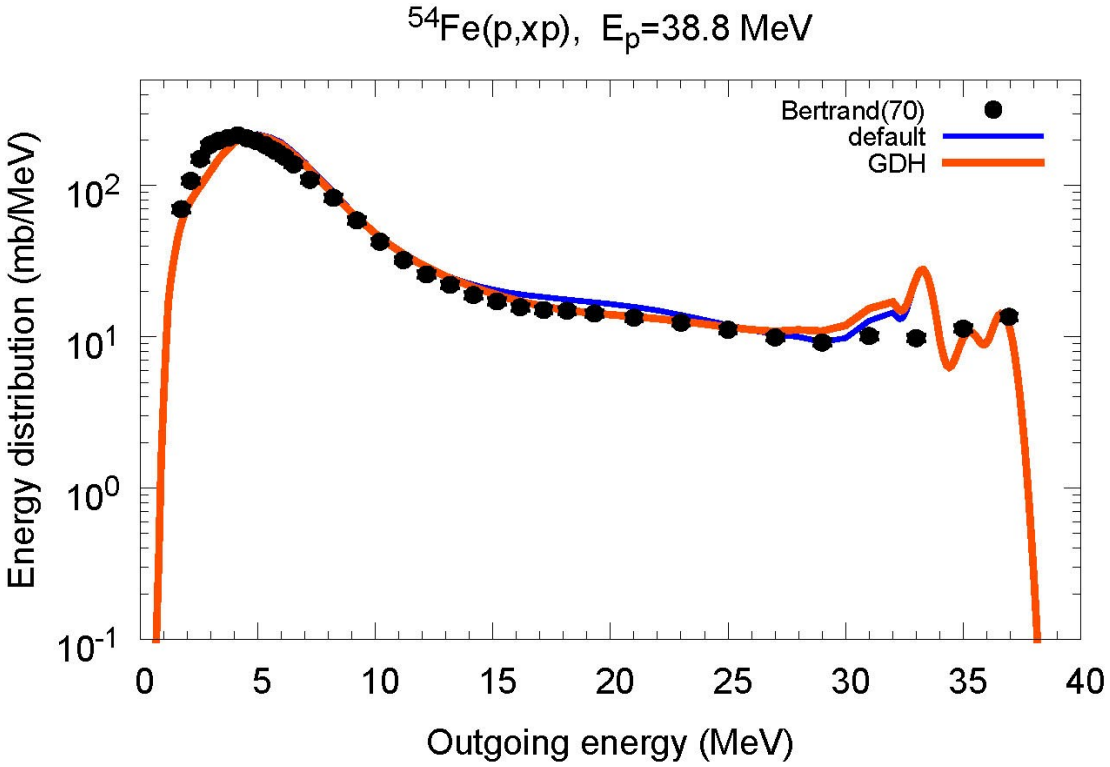
^{54}Fe(p,xp), E_p=38.8 MeV
Bertrand(70)
default
GDH
Energy distribution (mb/MeV)
10^2
10^1
10^0
10^{-1}
0
5
10
15
20
25
30
35
40
Outgoing energy (MeV)

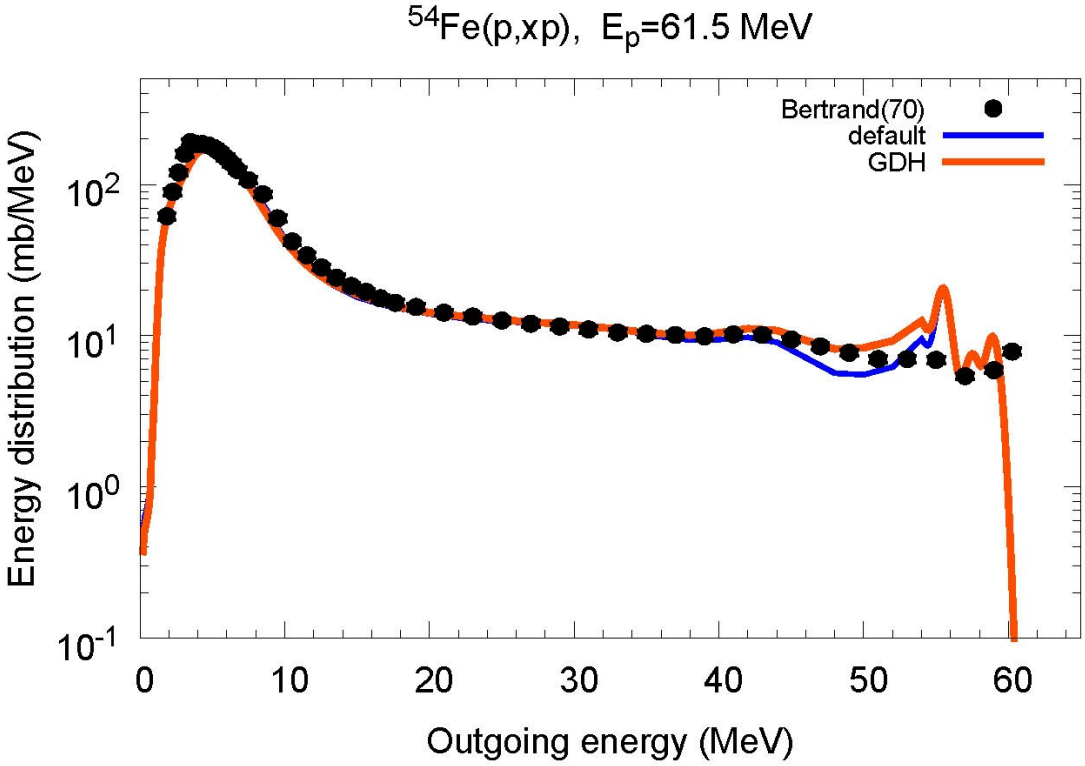
^{54}Fe(p,xp), E_p=61.5 MeV
Bertrand(70)
default
GDH
Energy distribution (mb/MeV)
10^2
10^1
10^0
10^{-1}
0
10
20
30
40
50
60
Outgoing energy (MeV)

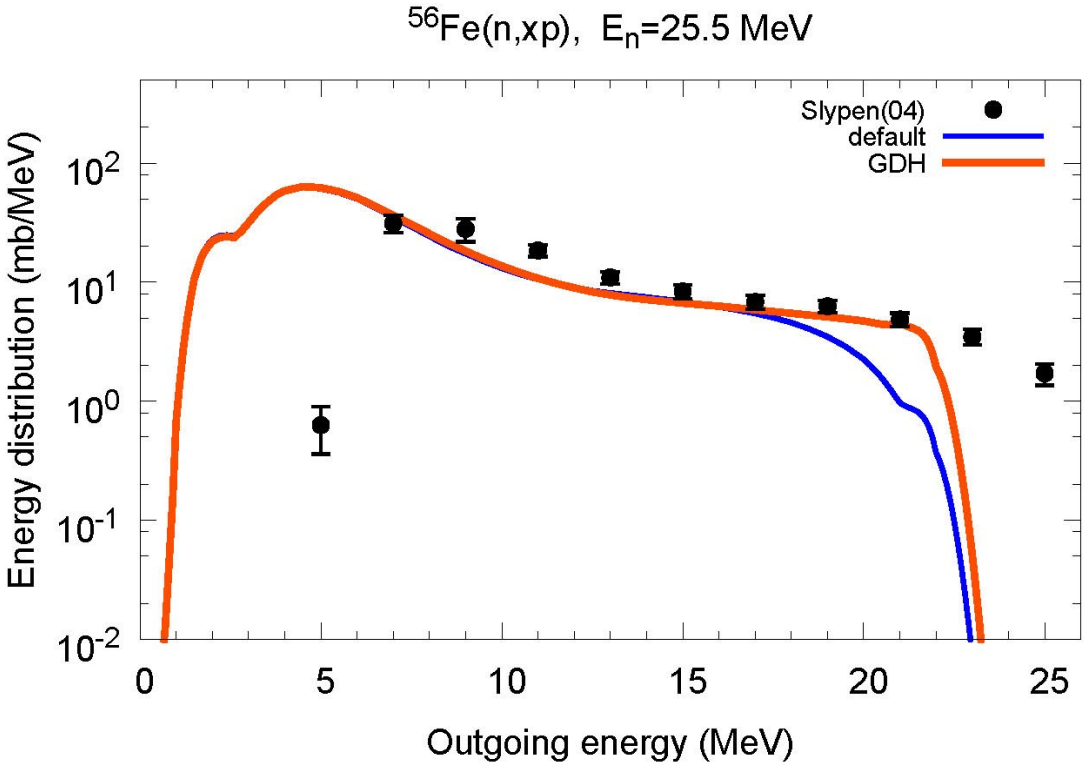
^{56}Fe(n,xp), E_n=25.5 MeV
Slypen(04)
default
GDH
Energy distribution (mb/MeV)
10^2
10^1
10^0
10^{-1}
10^{-2}
0
5
10
15
20
25
Outgoing energy (MeV)

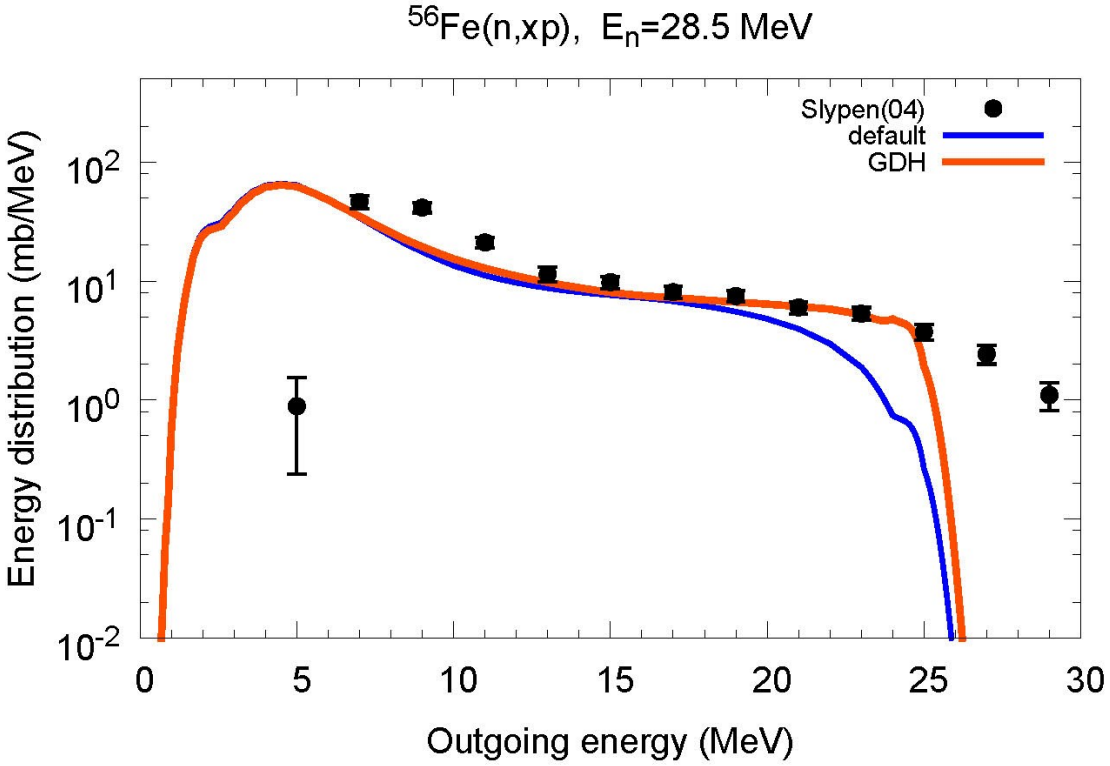
^{56}Fe(n,xp), E_n=28.5 MeV
Slypen(04)
default
GDH
Energy distribution (mb/MeV)
10^2
10^1
10^0
10^{-1}
10^{-2}
0
5
10
15
20
25
30
Outgoing energy (MeV)

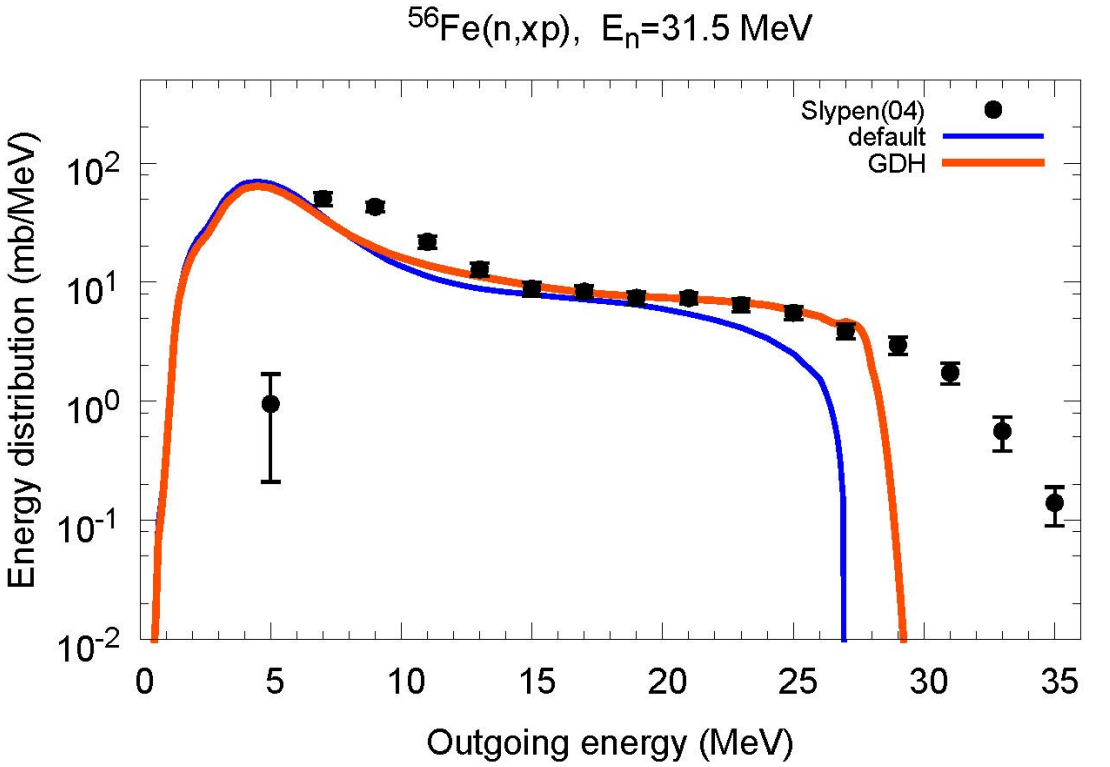
^{56}Fe(n,xp), E_n=31.5 MeV
Slypen(04)
default
GDH
Energy distribution (mb/MeV)
10^2
10^1
10^0
10^{-1}
10^{-2}
0
5
10
15
20
25
30
35
Outgoing energy (MeV)

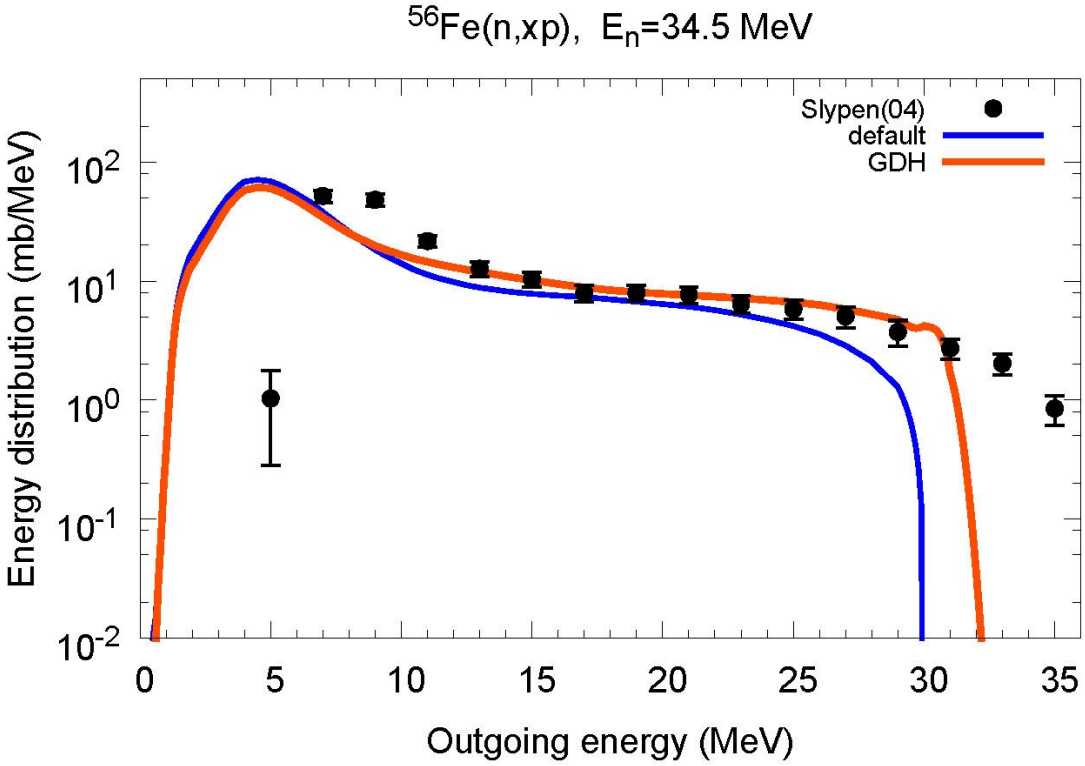
^{56}Fe(n,xp), E_n=34.5 MeV
Slypen(04)
default
GDH
Energy distribution (mb/MeV)
Outgoing energy (MeV)

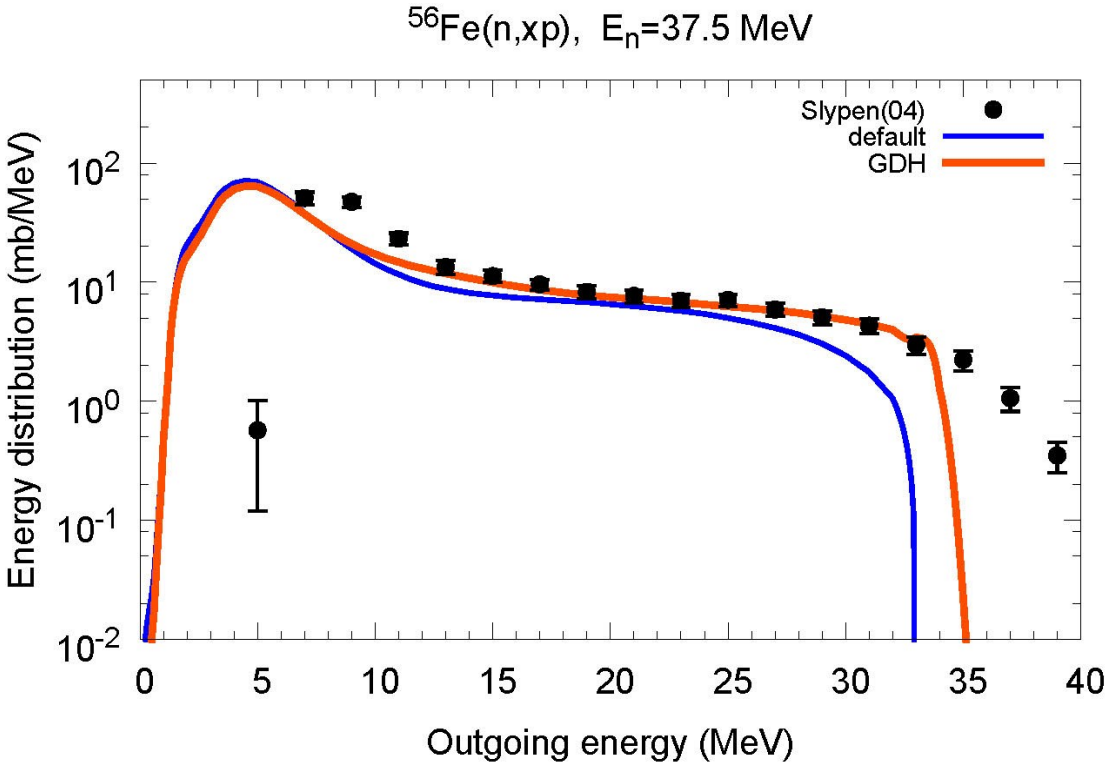
^{56}Fe(n,xp), E_n=37.5 MeV
Slypen(04)
default
GDH
Energy distribution (mb/MeV)
Outgoing energy (MeV)

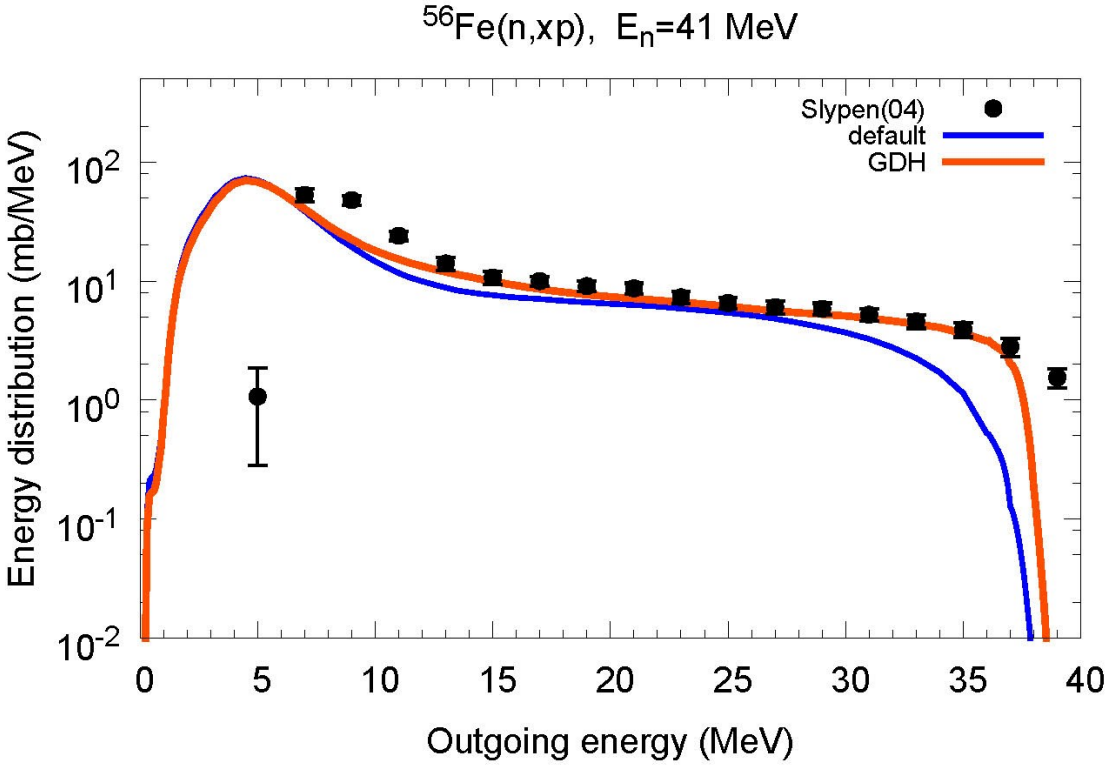
^{56}Fe(n,xp), E_n=41 MeV
Slypen(04)
default
GDH
Energy distribution (mb/MeV)
Outgoing energy (MeV)

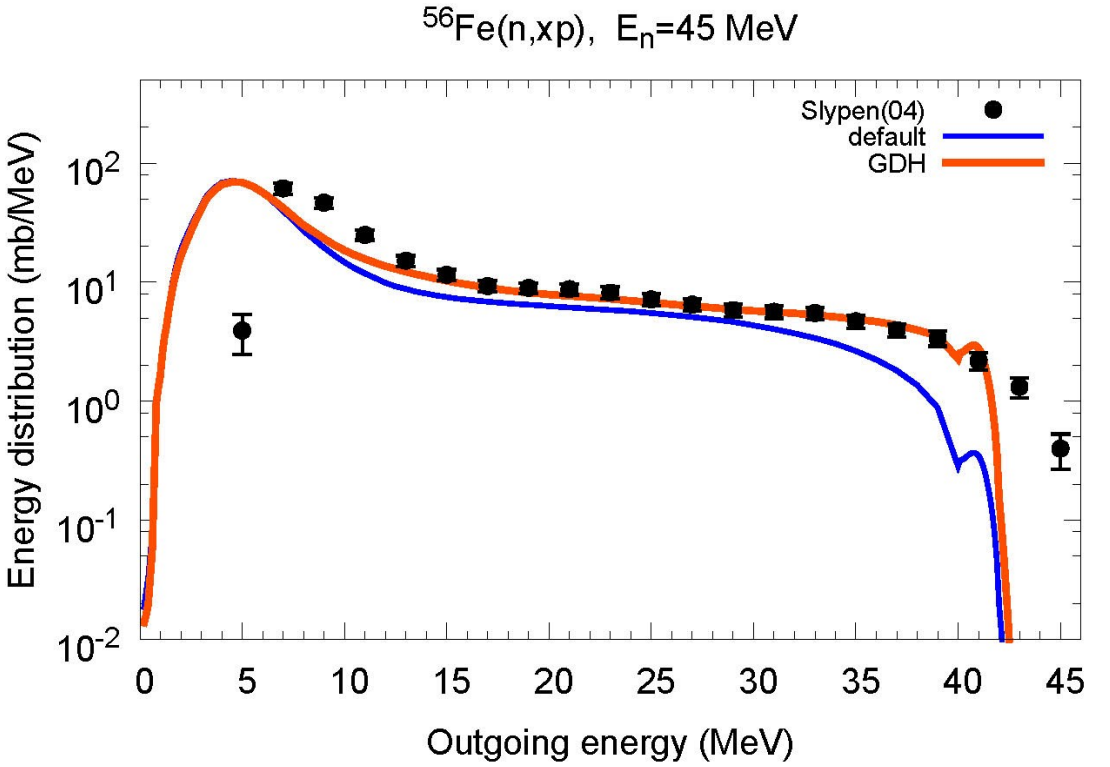
^{56}Fe(n,xp), E_n=45 MeV
Slypen(04)
default
GDH
Energy distribution (mb/MeV)
Outgoing energy (MeV)

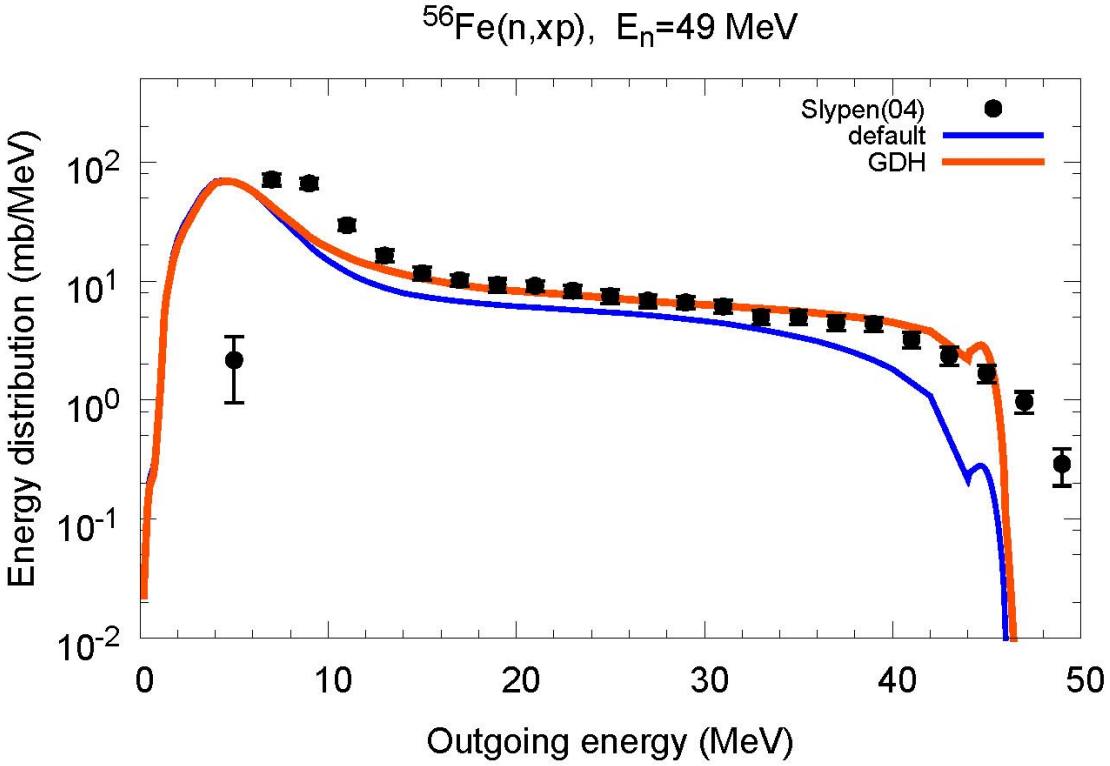
^{56}Fe(n,xp), E_n=49 MeV
Slypen(04)
default
GDH
Energy distribution (mb/MeV)
10^2
10^1
10^0
10^{-1}
10^{-2}
0
10
20
30
40
50
Outgoing energy (MeV)

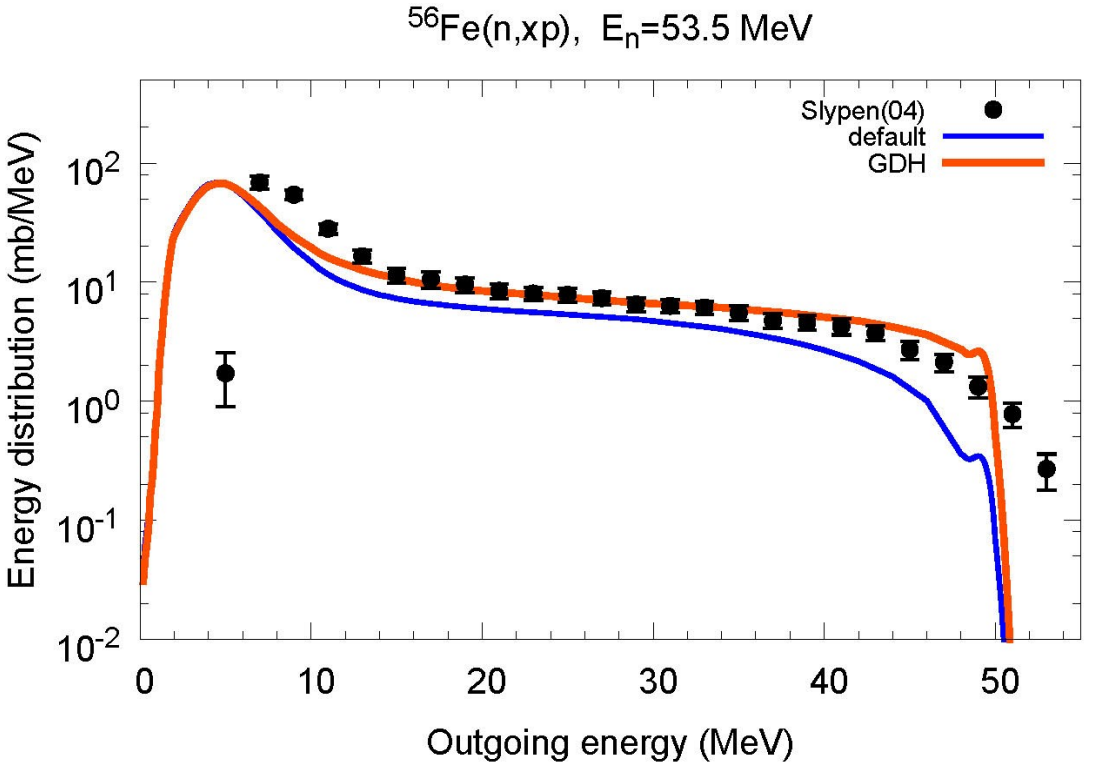
^{56}Fe(n,xp), E_n=53.5 MeV
Slypen(04)
default
GDH
Energy distribution (mb/MeV)
10^2
10^1
10^0
10^{-1}
10^{-2}
0
10
20
30
40
50
Outgoing energy (MeV)

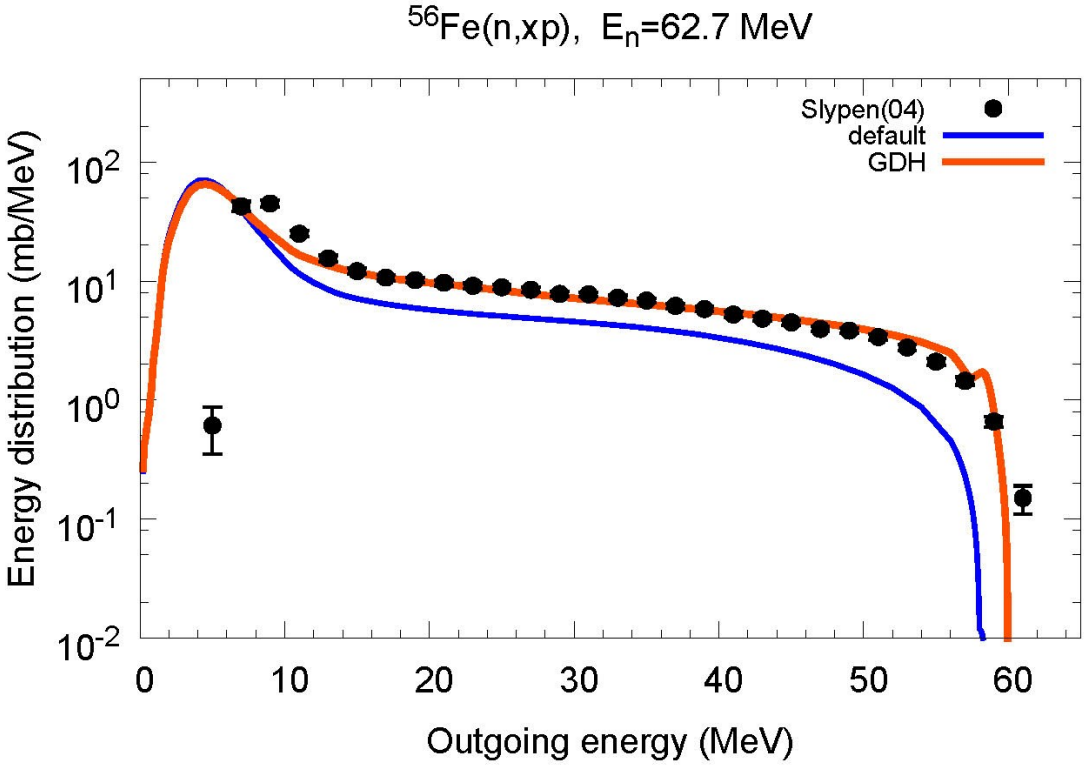
^{56}Fe(n,xp), E_n=62.7 MeV
Slypen(04)
default
GDH
Energy distribution (mb/MeV)
10^2
10^1
10^0
10^{-1}
10^{-2}
0
10
20
30
40
50
60
Outgoing energy (MeV)

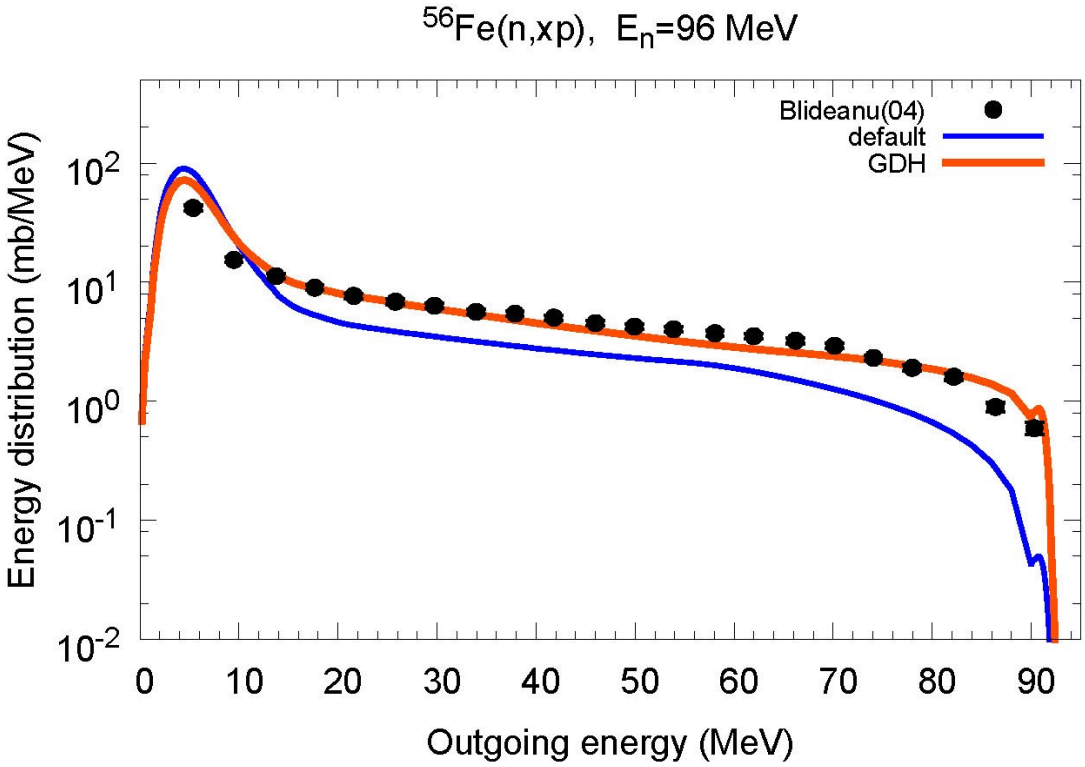
^{56}Fe(n,xp), E_n=96 MeV
Blideanu(04)
default
GDH
Energy distribution (mb/MeV)
10^2
10^1
10^0
10^{-1}
10^{-2}
0
10
20
30
40
50
60
70
80
90
Outgoing energy (MeV)

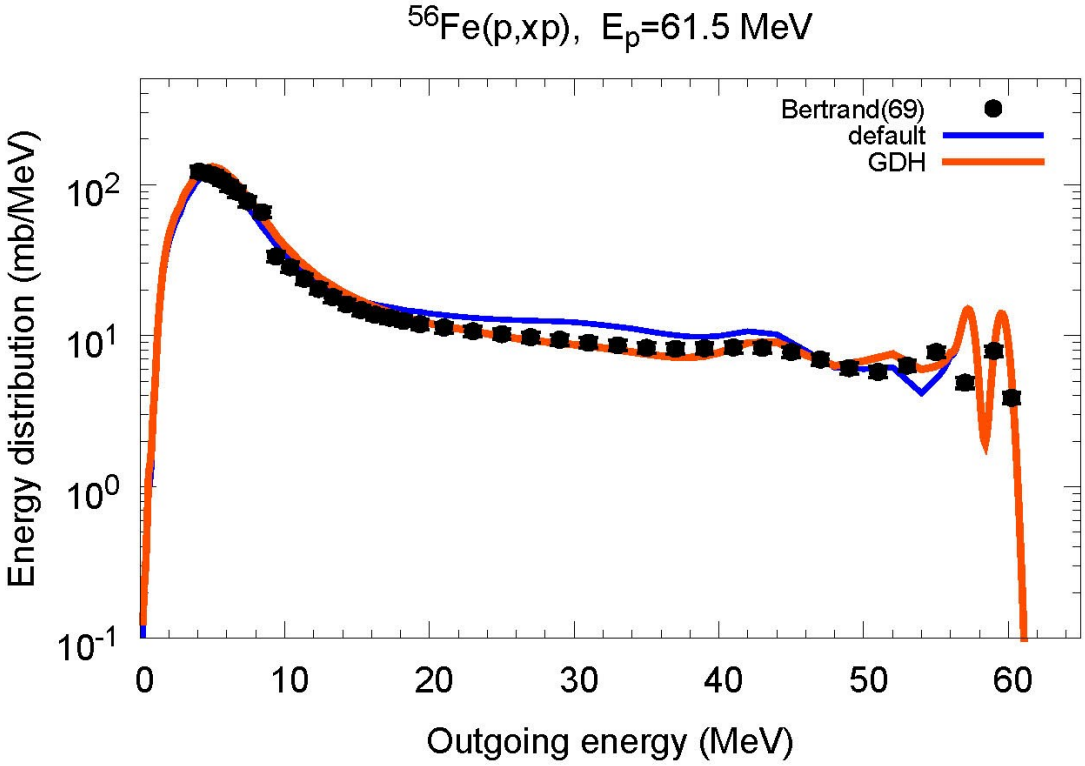
^{56}Fe(p,xp), E_p=61.5 MeV
Bertrand(69)
default
GDH
Energy distribution (mb/MeV)
10^2
10^1
10^0
10^{-1}
0
10
20
30
40
50
60
Outgoing energy (MeV)

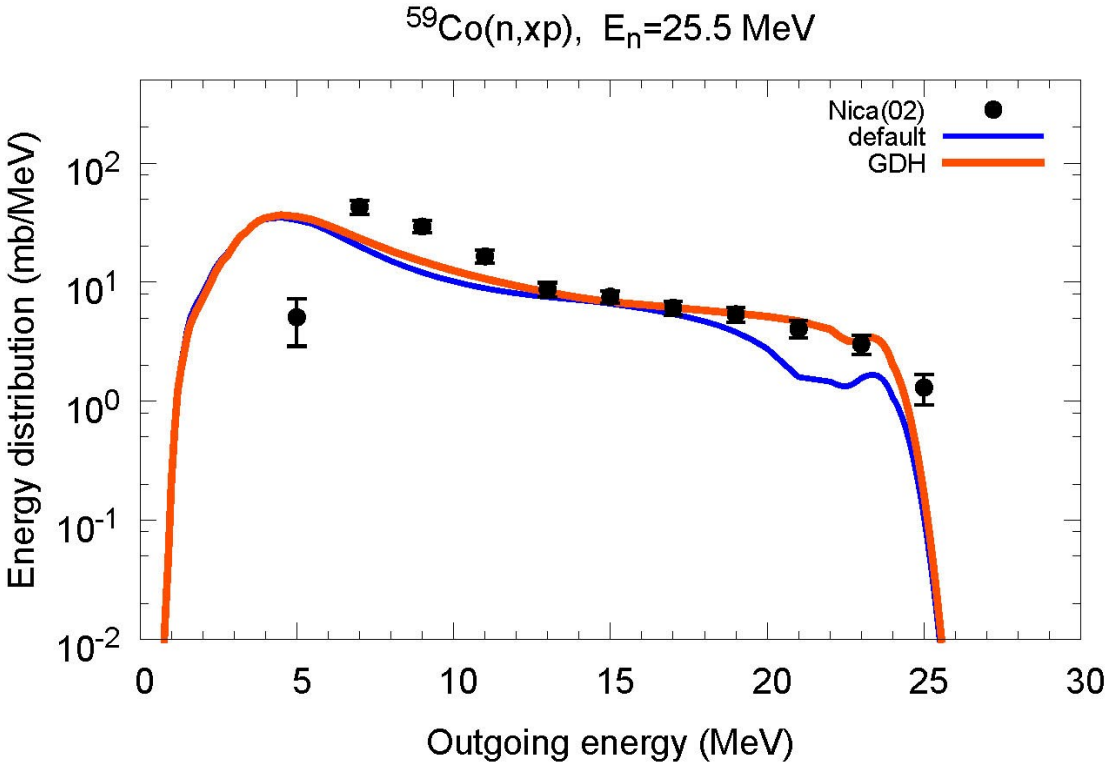
^{59}Co(n,xp), E_n=25.5 MeV
Nica(02)
default
GDH
Energy distribution (mb/MeV)
10^2
10^1
10^0
10^{-1}
10^{-2}
0
5
10
15
20
25
30
Outgoing energy (MeV)

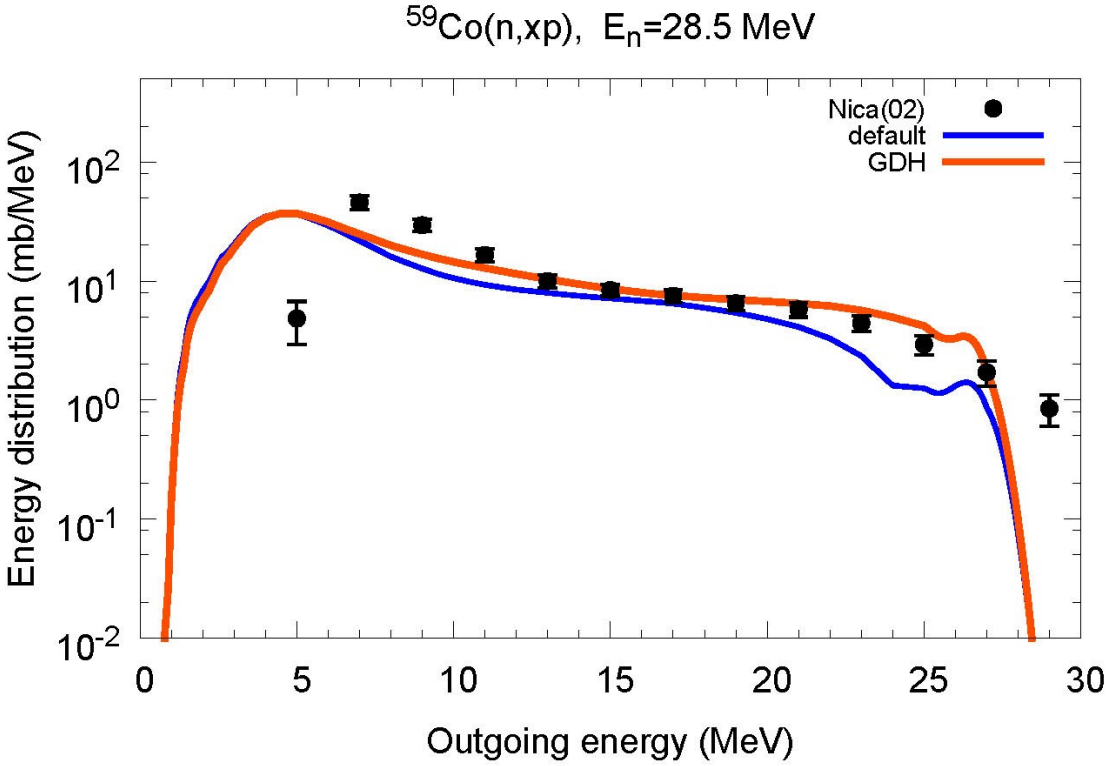
59Co(n,xp), En=28.5 MeV
Nica(02)
default
GDH
Energy distribution (mb/MeV)
Outgoing energy (MeV)

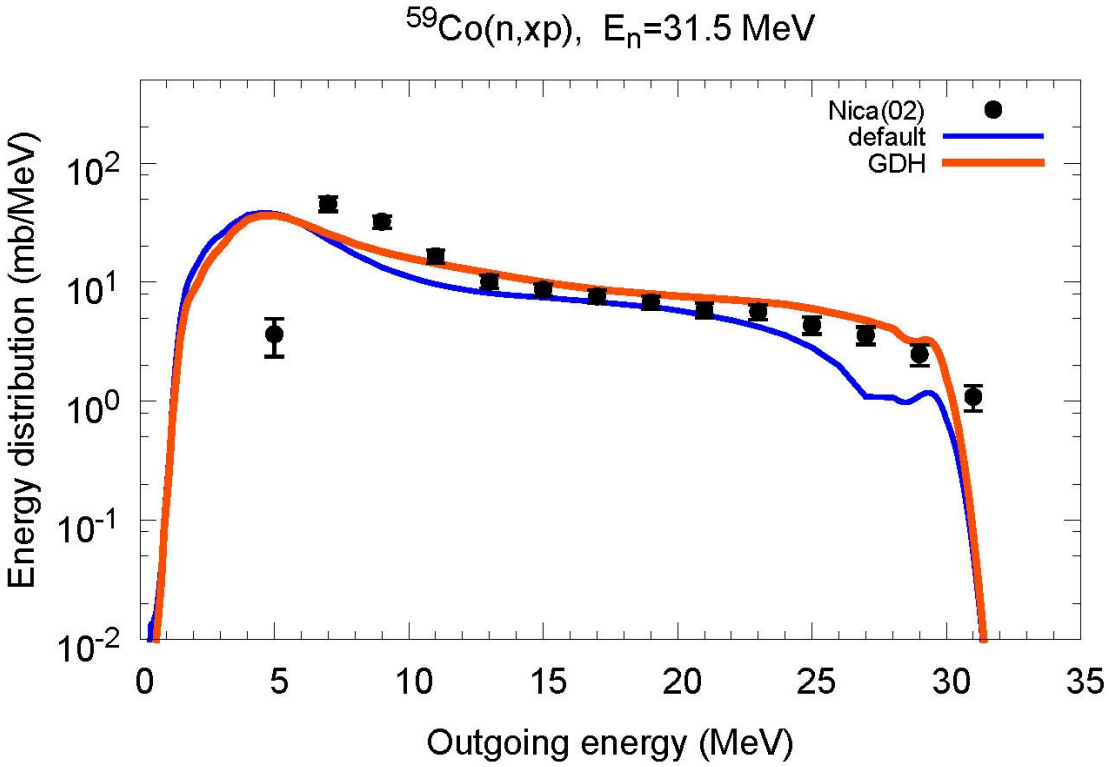
59Co(n,xp), En=31.5 MeV
Nica(02)
default
GDH
Energy distribution (mb/MeV)
Outgoing energy (MeV)

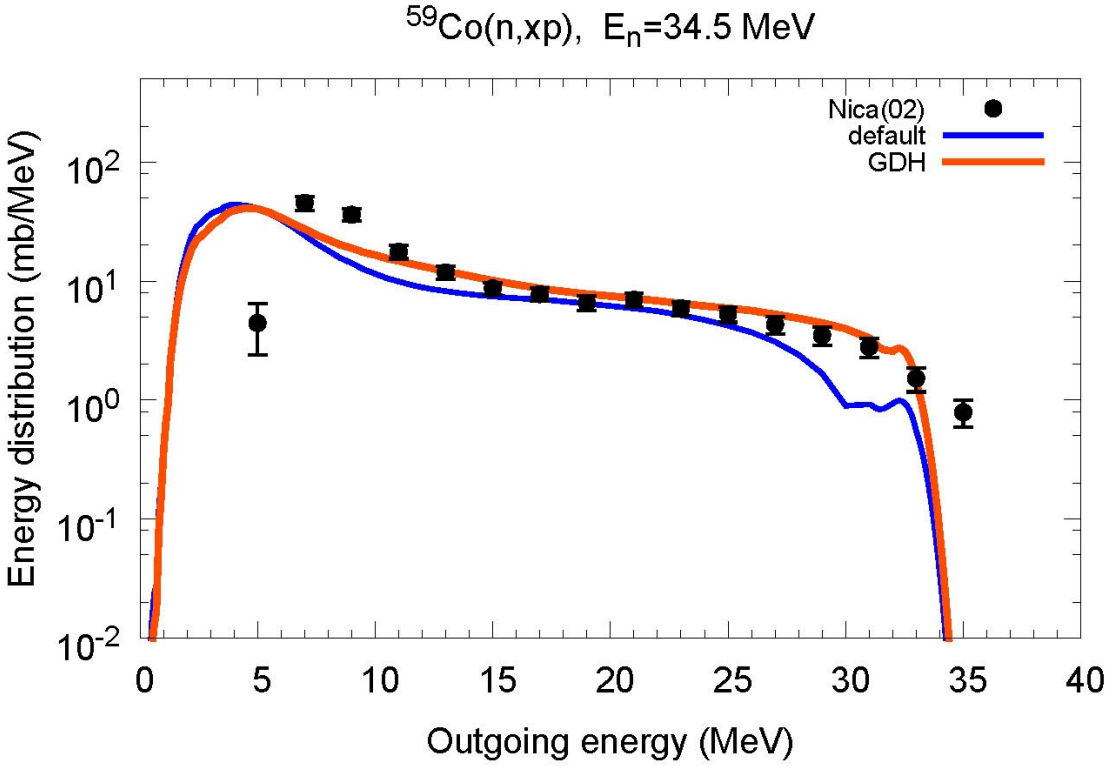
59Co(n,xp), En=34.5 MeV
Nica(02)
default
GDH
Energy distribution (mb/MeV)
Outgoing energy (MeV)

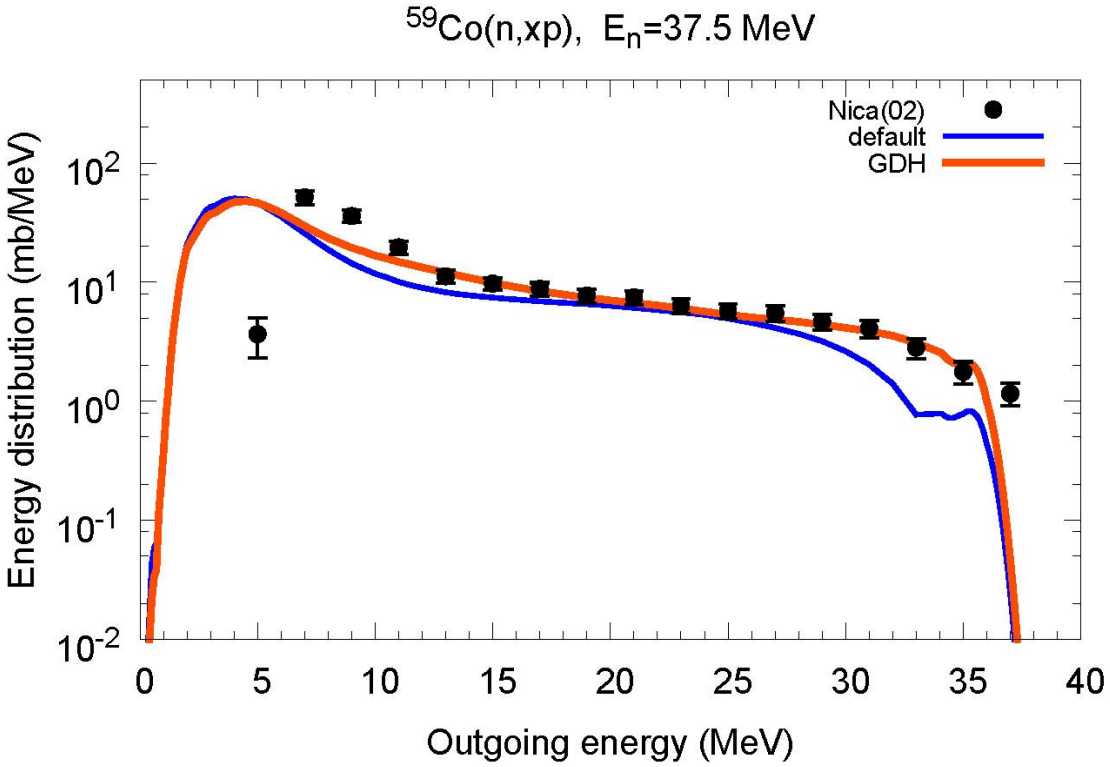
59Co(n,xp), En=37.5 MeV
Nica(02)
default
GDH
Energy distribution (mb/MeV)
Outgoing energy (MeV)

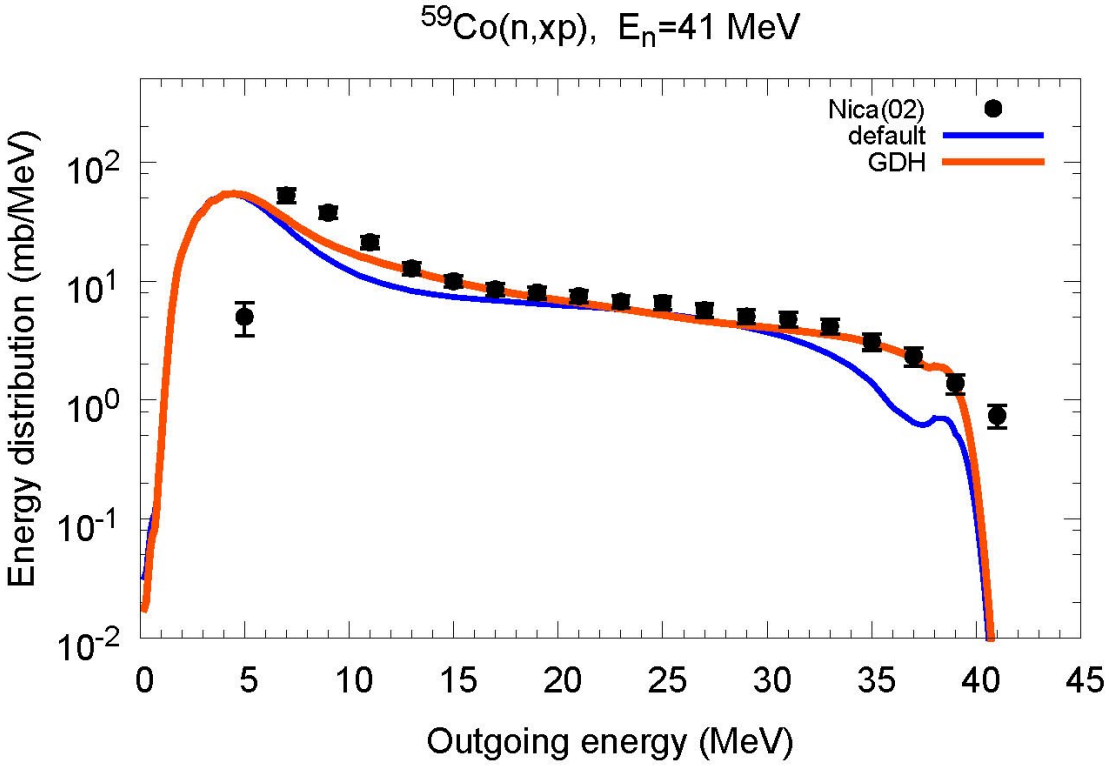
59Co(n,xp), En=41 MeV
Nica(02)
default
GDH
Energy distribution (mb/MeV)
Outgoing energy (MeV)

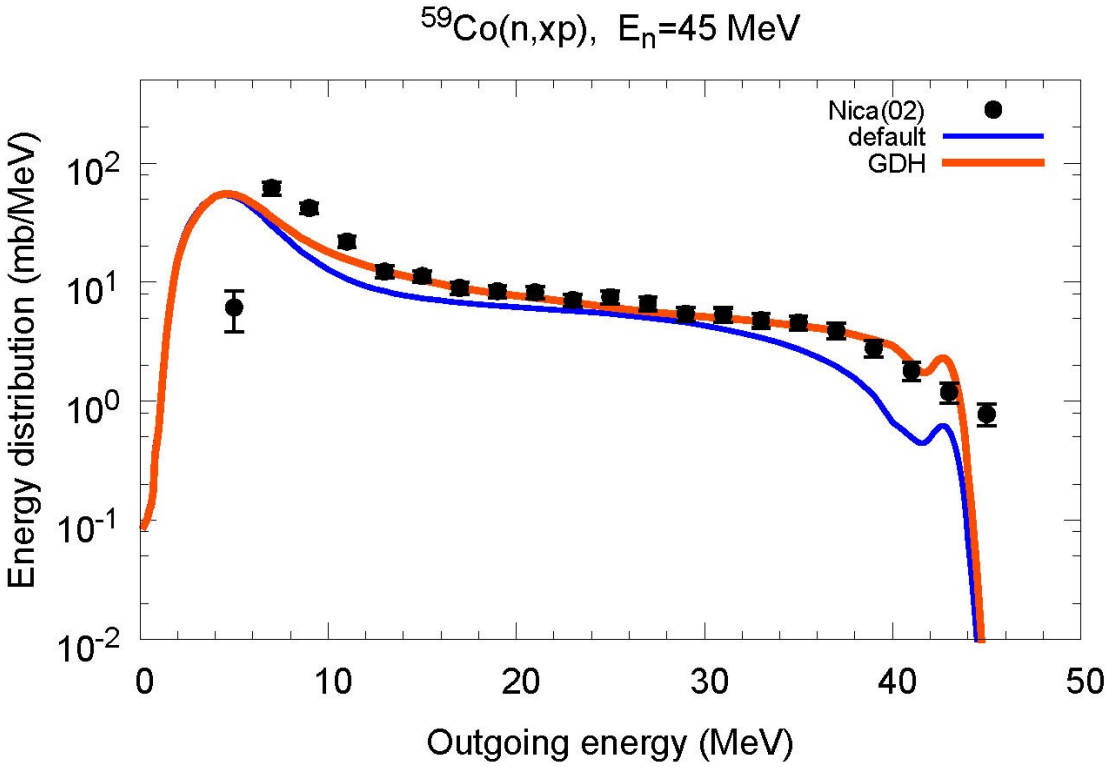
59Co(n,xp), En=45 MeV
Nica(02)
default
GDH
Energy distribution (mb/MeV)
Outgoing energy (MeV)

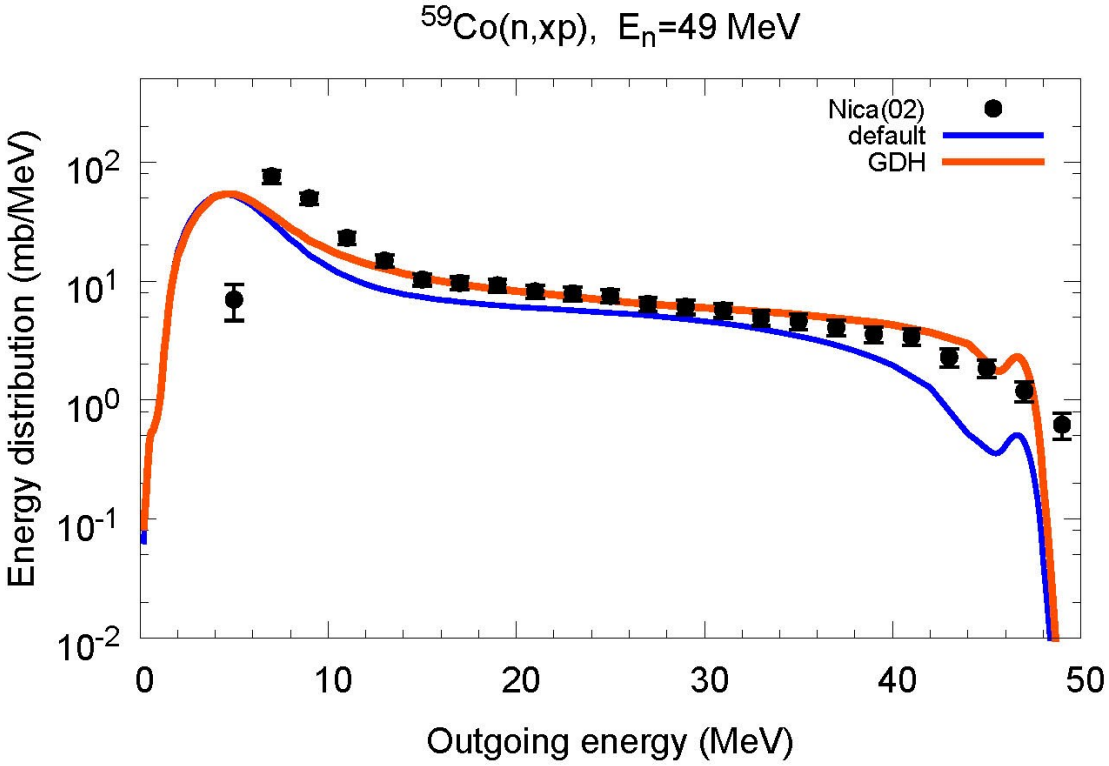
59Co(n,xp), En=49 MeV
Nica(02)
default
GDH
Energy distribution (mb/MeV)
Outgoing energy (MeV)

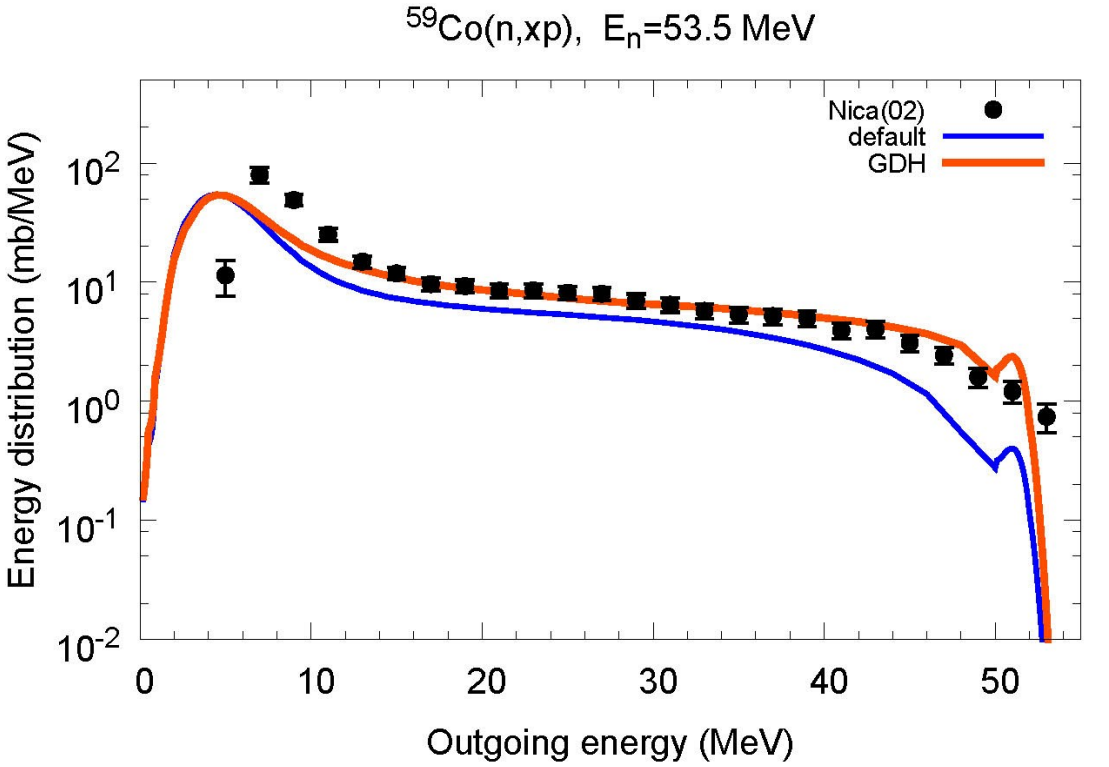
59Co(n,xp), En=53.5 MeV
Nica(02)
default
GDH
Energy distribution (mb/MeV)
Outgoing energy (MeV)

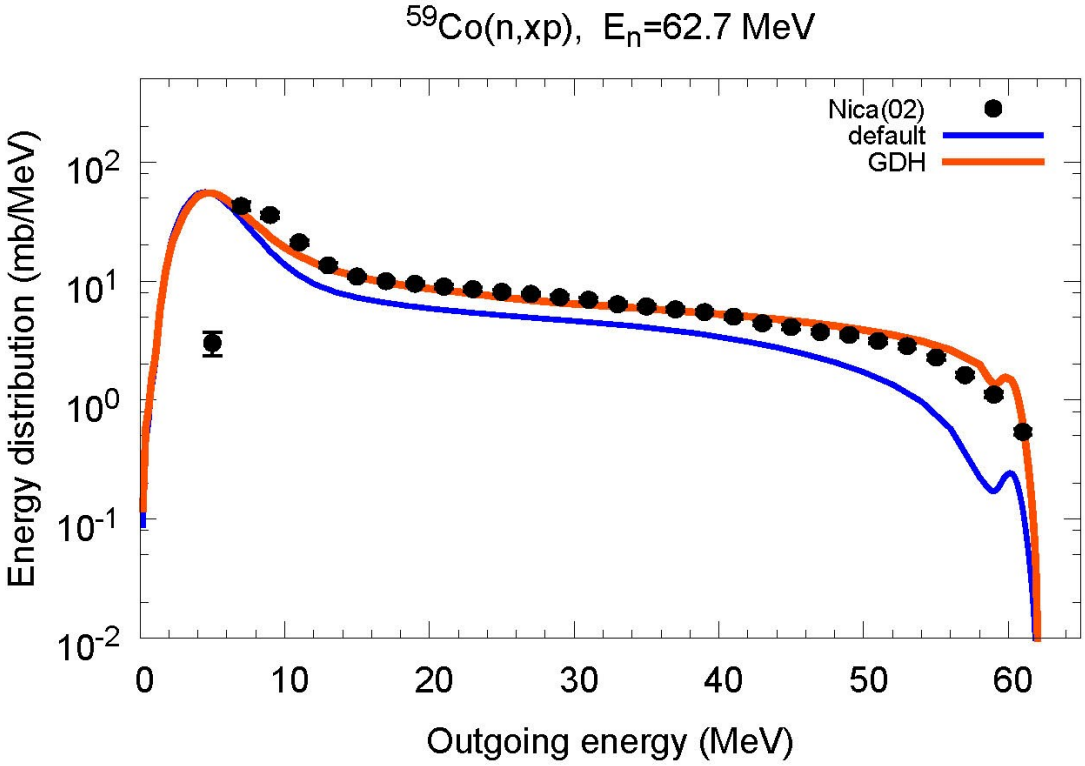
^{59}Co(n,xp), E_n=62.7 MeV
Nica(02)
default
GDH
Energy distribution (mb/MeV)
Outgoing energy (MeV)

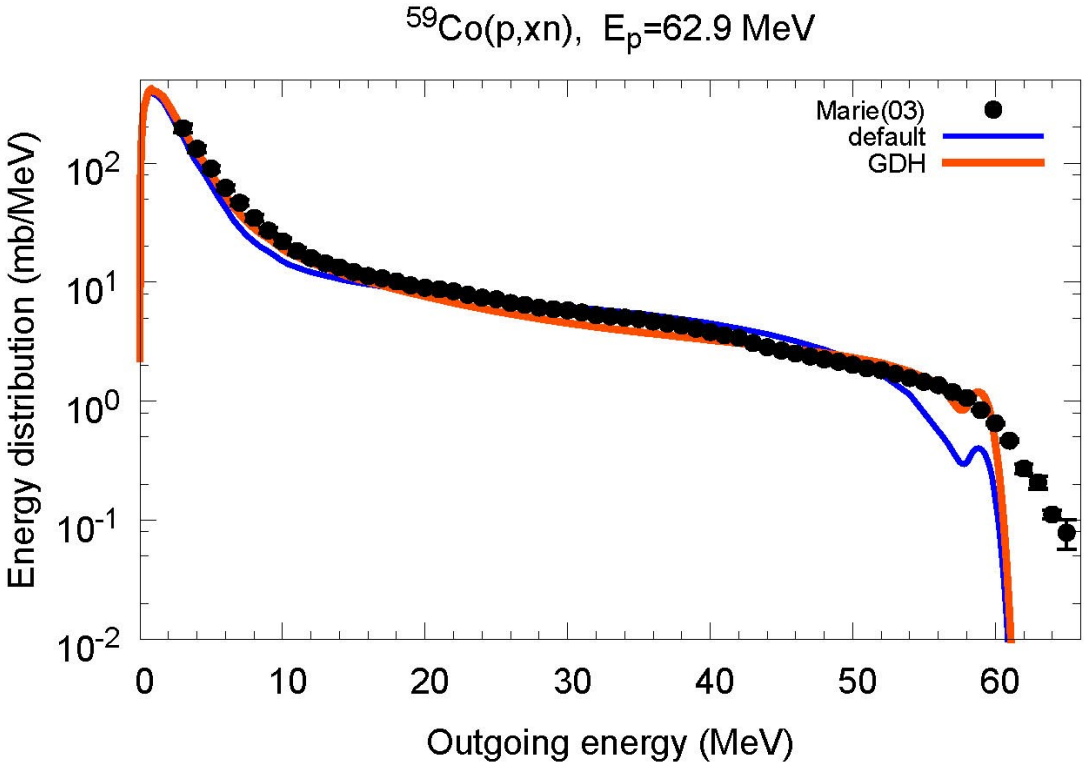
^{59}Co(p,xn), E_p=62.9 MeV
Marie(03)
default
GDH
Energy distribution (mb/MeV)
Outgoing energy (MeV)

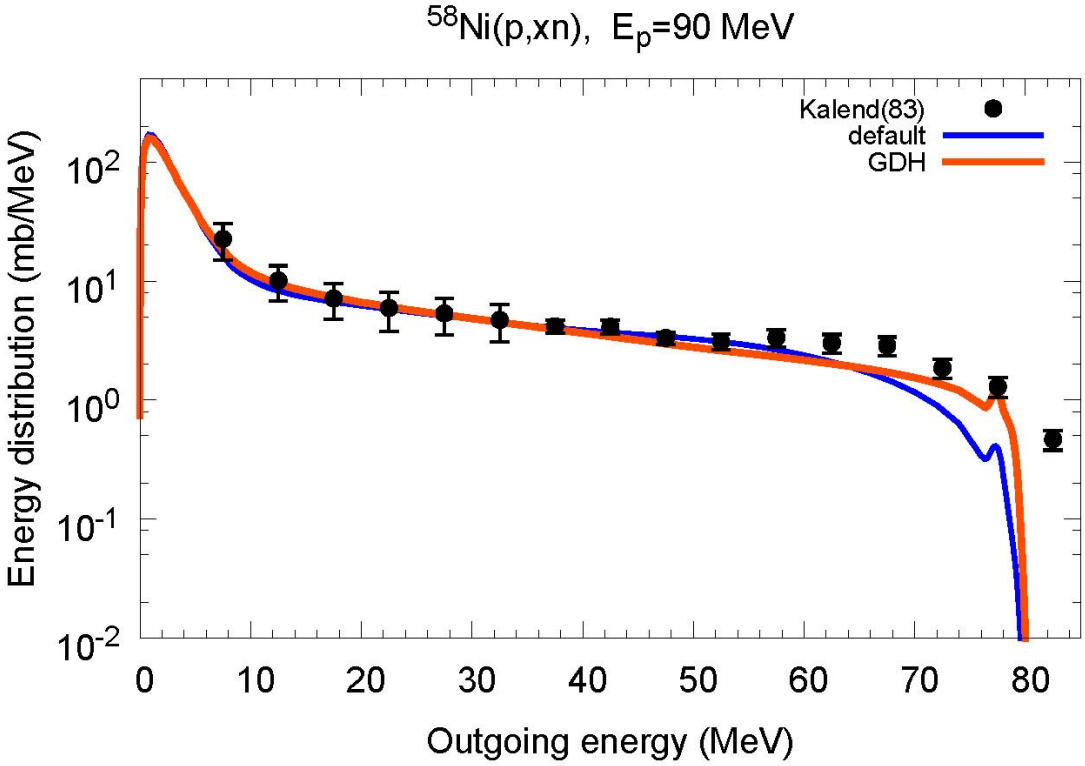
^{58}Ni(p,xn), E_p=90 MeV
Kalend(83)
default
GDH
Energy distribution (mb/MeV)
10^2
10^1
10^0
10^{-1}
10^{-2}
0
10
20
30
40
50
60
70
80
Outgoing energy (MeV)

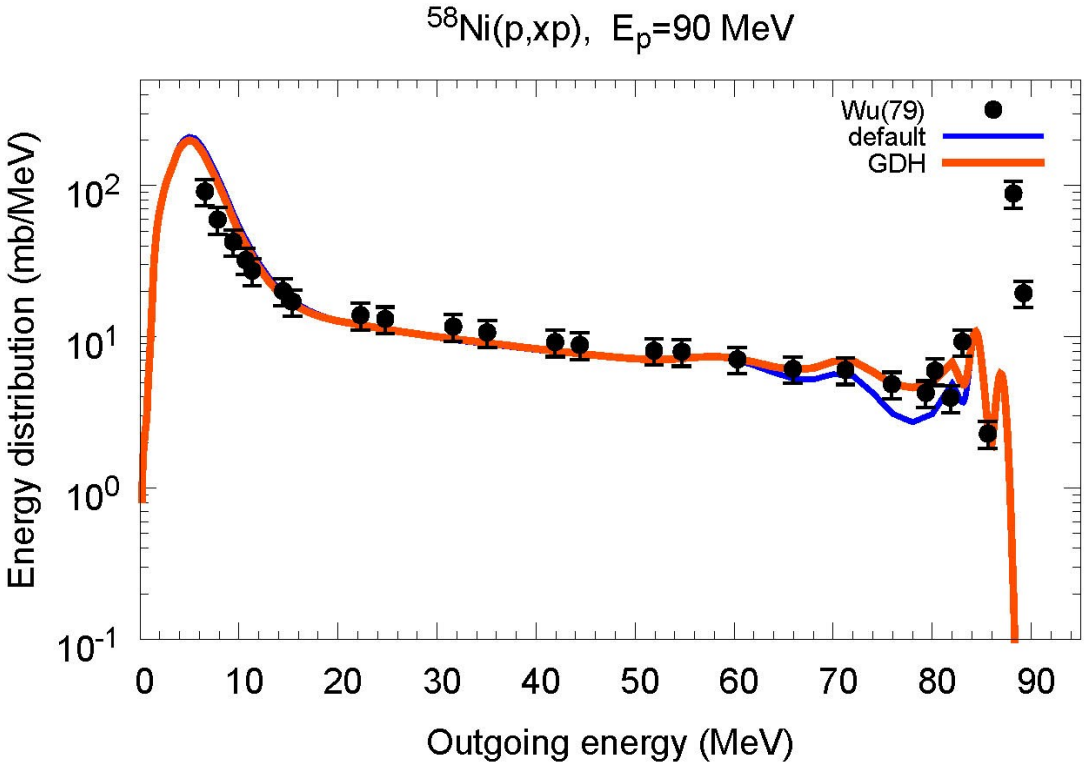
^{58}Ni(p,xp), E_p=90 MeV
Wu(79)
default
GDH
Energy distribution (mb/MeV)
10^2
10^1
10^0
10^{-1}
0
10
20
30
40
50
60
70
80
90
Outgoing energy (MeV)

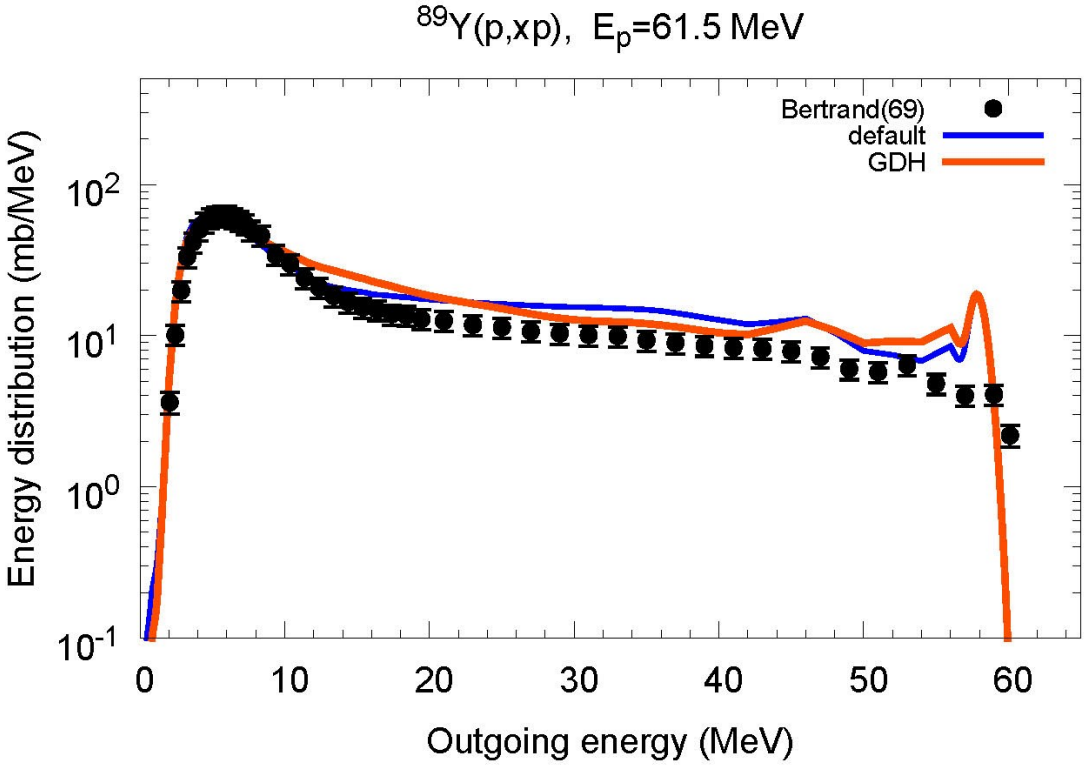
^{89}Y(p,xp), E_p=61.5 MeV
Bertrand(69)
default
GDH
Energy distribution (mb/MeV)
Outgoing energy (MeV)

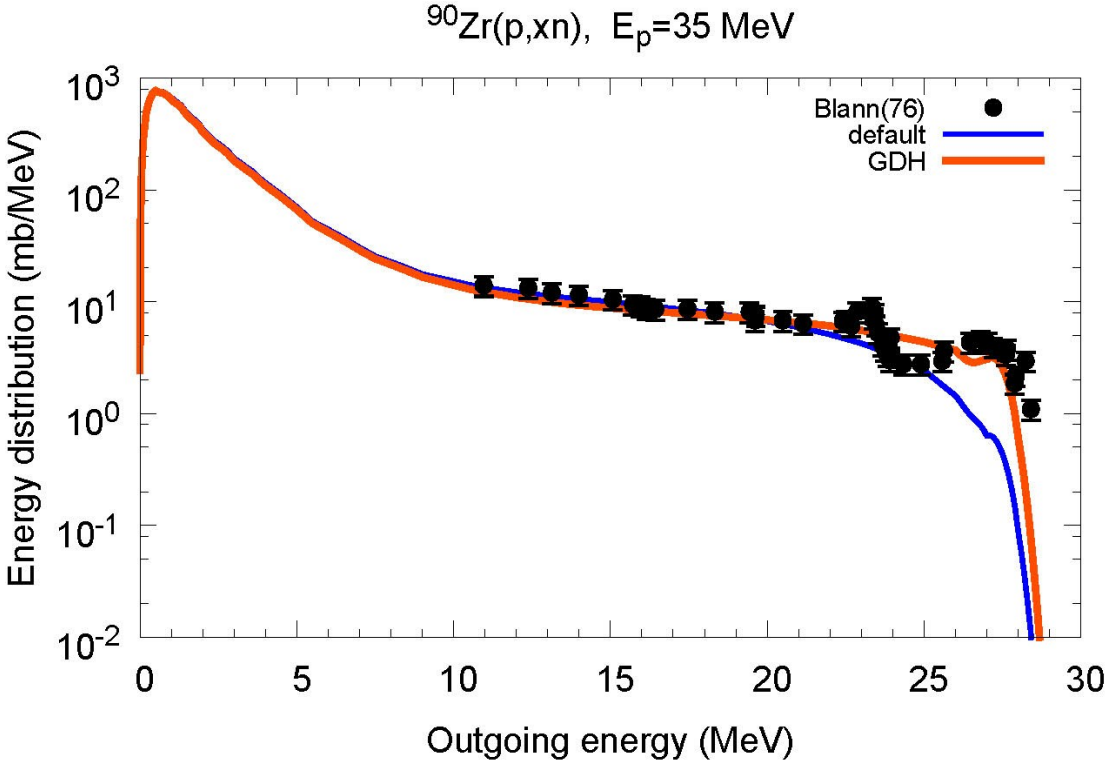
^{90}Zr(p,xn), E_p=35 MeV
Blann(76)
default
GDH
Energy distribution (mb/MeV)
Outgoing energy (MeV)

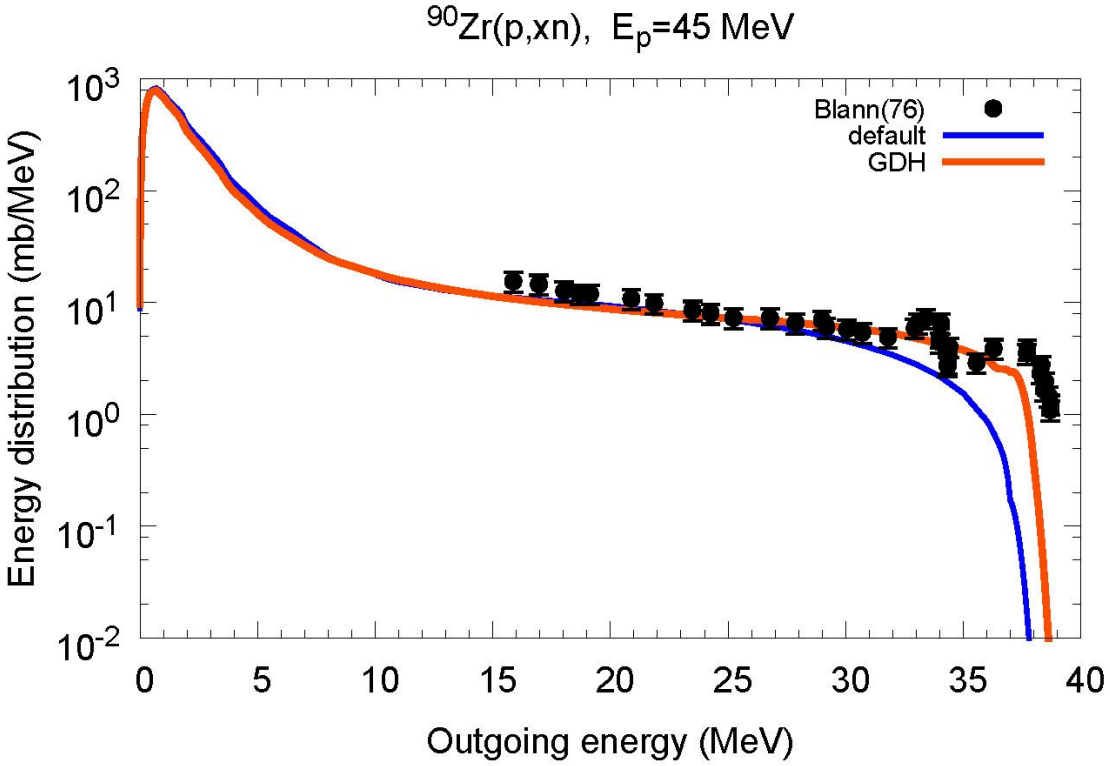
^{90}Zr(p,xn), E_p=45 MeV
Blann(76)
default
GDH
Energy distribution (mb/MeV)
Outgoing energy (MeV)

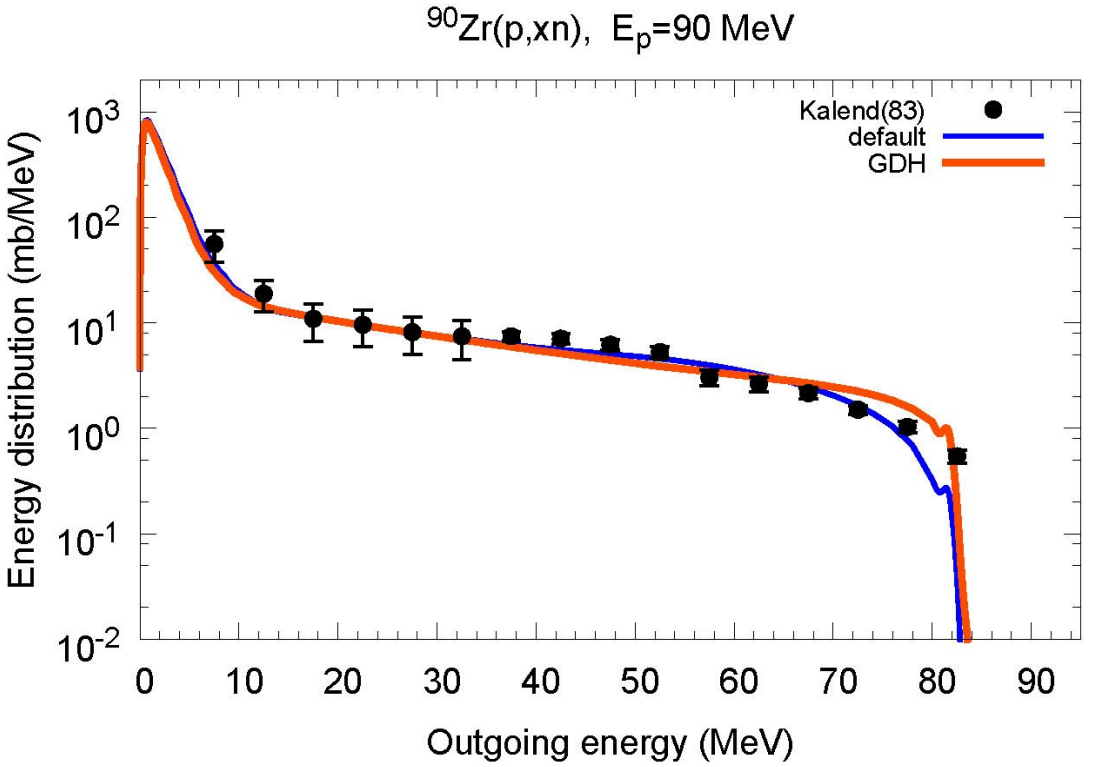
^{90}Zr(p,xn), E_p=90 MeV
Kalend(83)
default
GDH
Energy distribution (mb/MeV)
Outgoing energy (MeV)

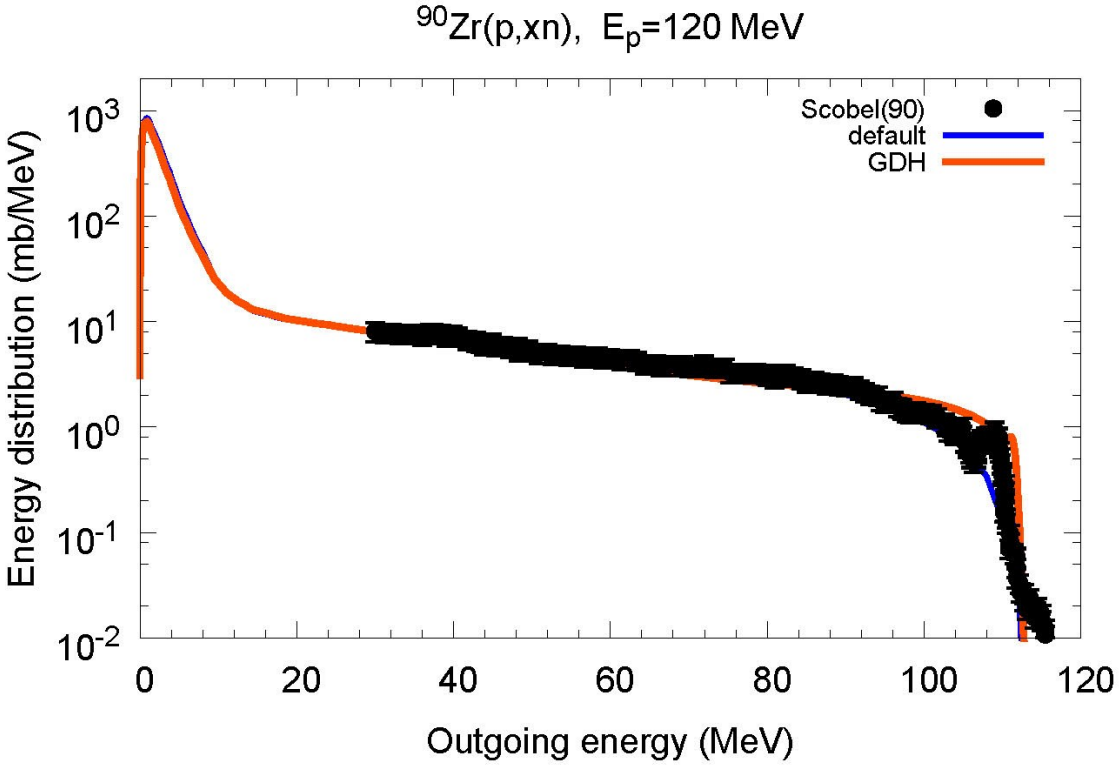
^{90}Zr(p,xn), E_p=120 MeV
Scobel(90)
default
GDH
Energy distribution (mb/MeV)
10^3
10^2
10^1
10^0
10^{-1}
10^{-2}
0
20
40
60
80
100
120
Outgoing energy (MeV)

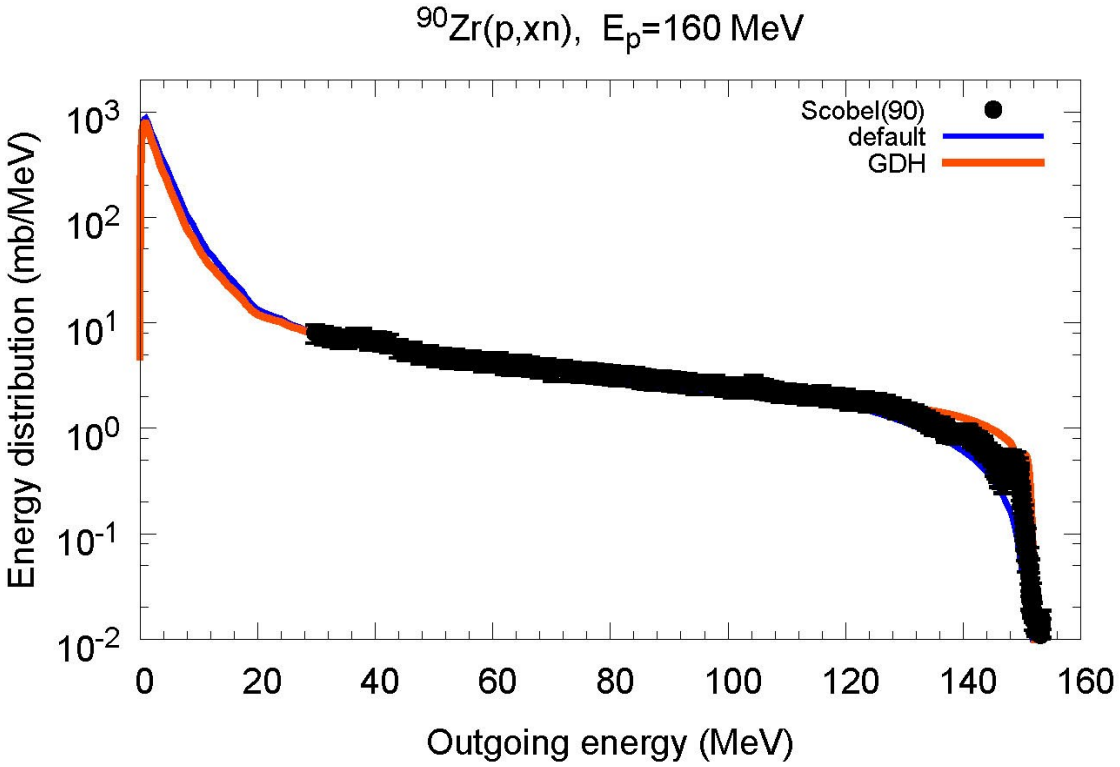
^{90}Zr(p,xn), E_p=160 MeV
Scobel(90)
default
GDH
Energy distribution (mb/MeV)
10^3
10^2
10^1
10^0
10^{-1}
10^{-2}
0
20
40
60
80
100
120
140
160
Outgoing energy (MeV)

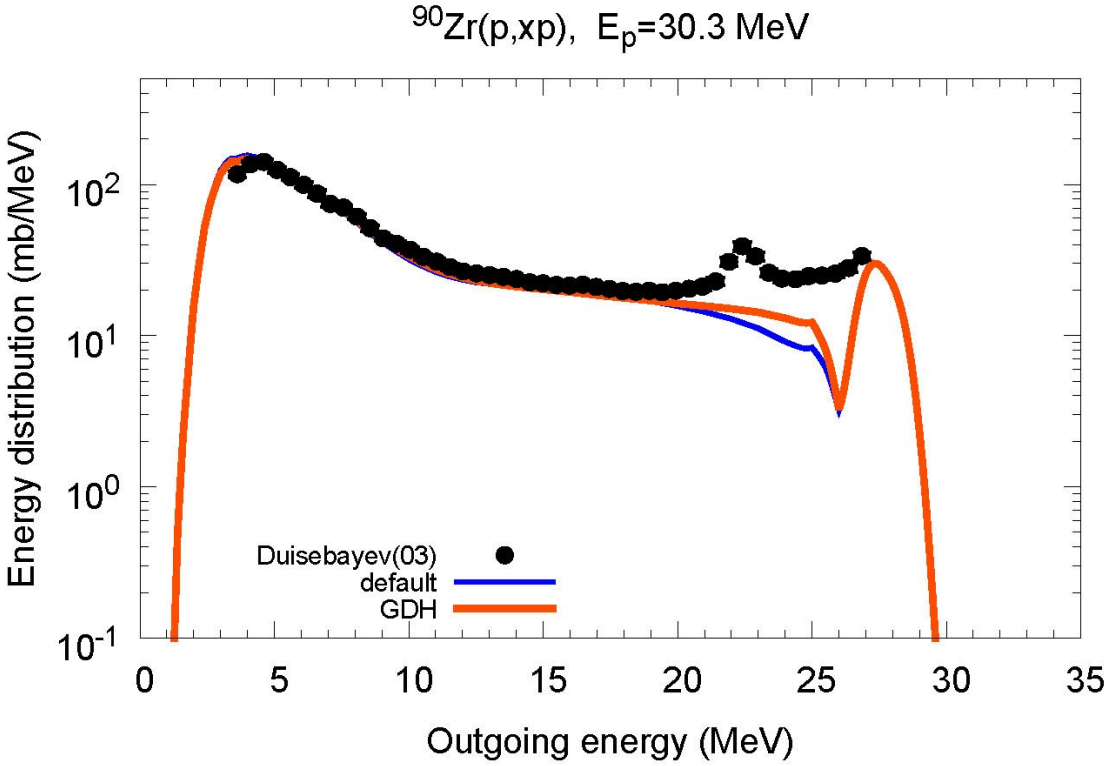
^{90}Zr(p,xp), E_p=30.3 MeV
Energy distribution (mb/MeV)
Outgoing energy (MeV)
Duisebayev(03)
default
GDH

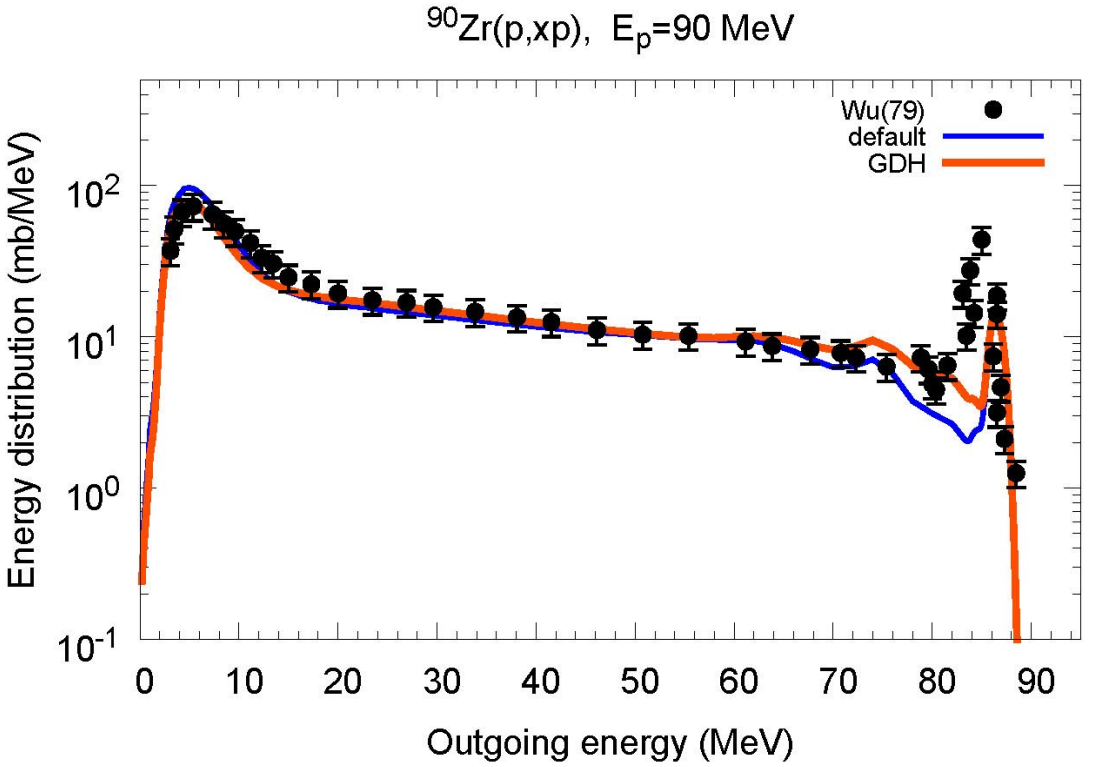
^{90}Zr(p,xp), E_p=90 MeV
Energy distribution (mb/MeV)
Outgoing energy (MeV)
Wu(79)
default
GDH

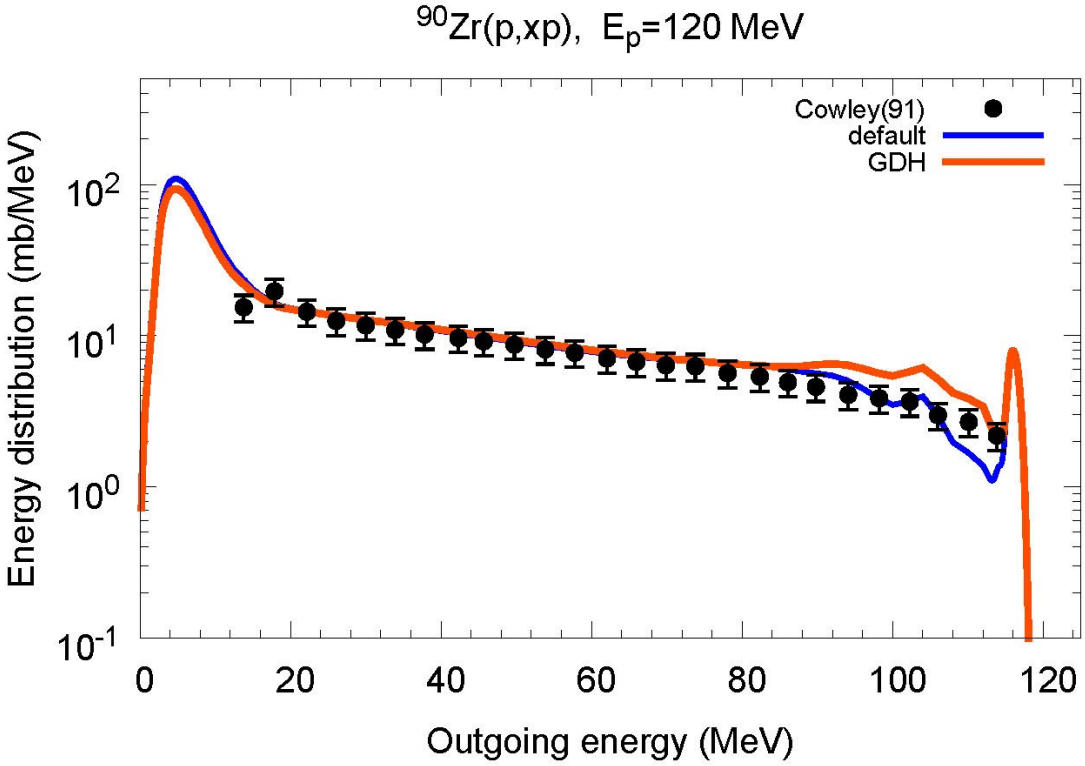
^{90}Zr(p,xp), E_p=120 MeV
Cowley(91)
default
GDH
Energy distribution (mb/MeV)
10^2
10^1
10^0
10^{-1}
0
20
40
60
80
100
120
Outgoing energy (MeV)

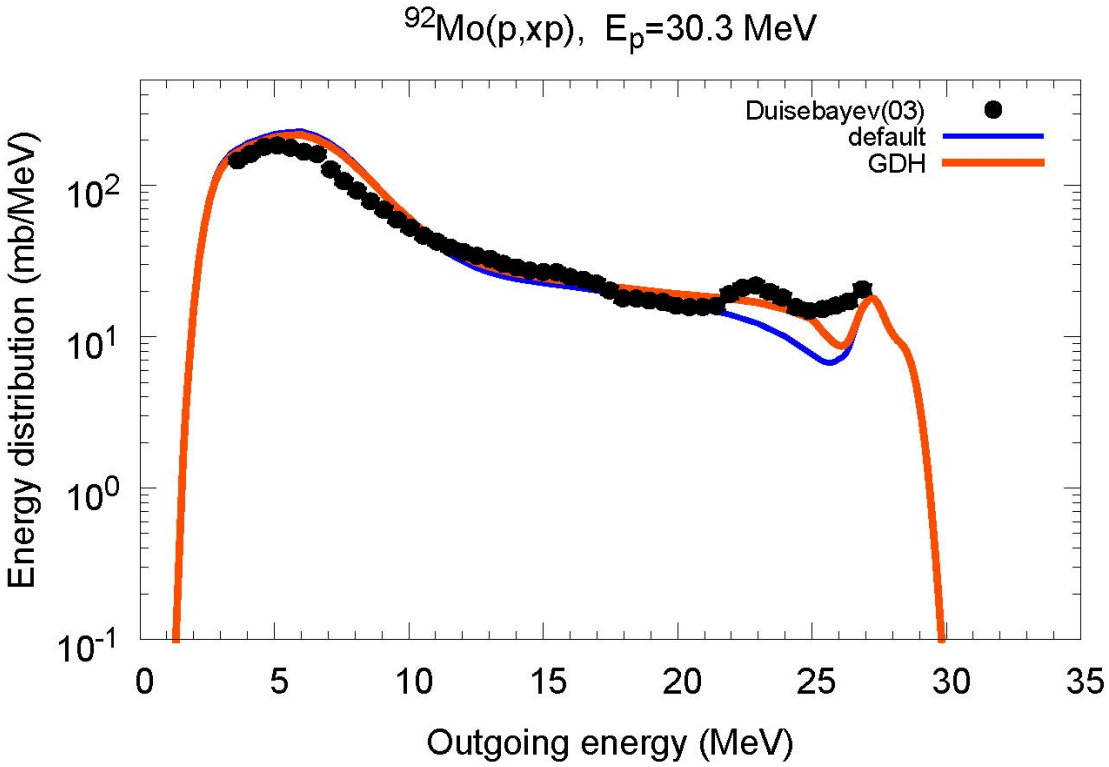
^{92}Mo(p,xp), E_p=30.3 MeV
Duisebayev(03)
default
GDH
Energy distribution (mb/MeV)
10^2
10^1
10^0
10^{-1}
0
5
10
15
20
25
30
35
Outgoing energy (MeV)

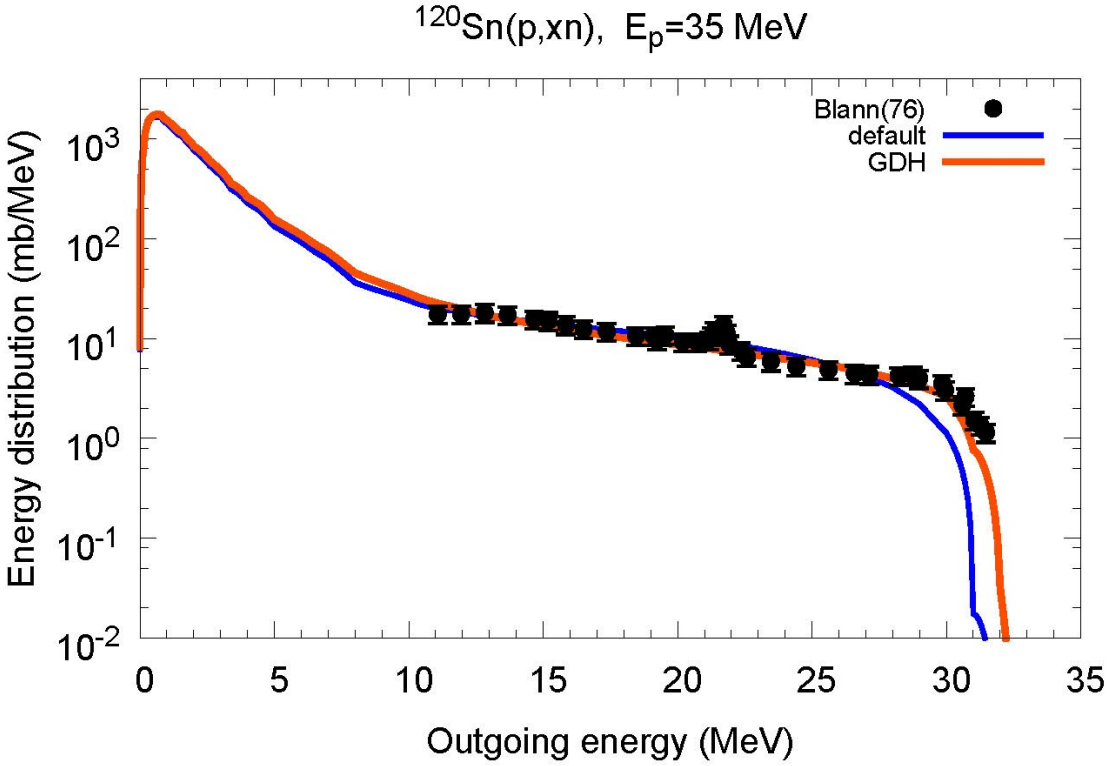
^{120}Sn(p,xn), E_p=35 MeV
Blann(76)
default
GDH
Energy distribution (mb/MeV)
10^3
10^2
10^1
10^0
10^{-1}
10^{-2}
0
5
10
15
20
25
30
35
Outgoing energy (MeV)

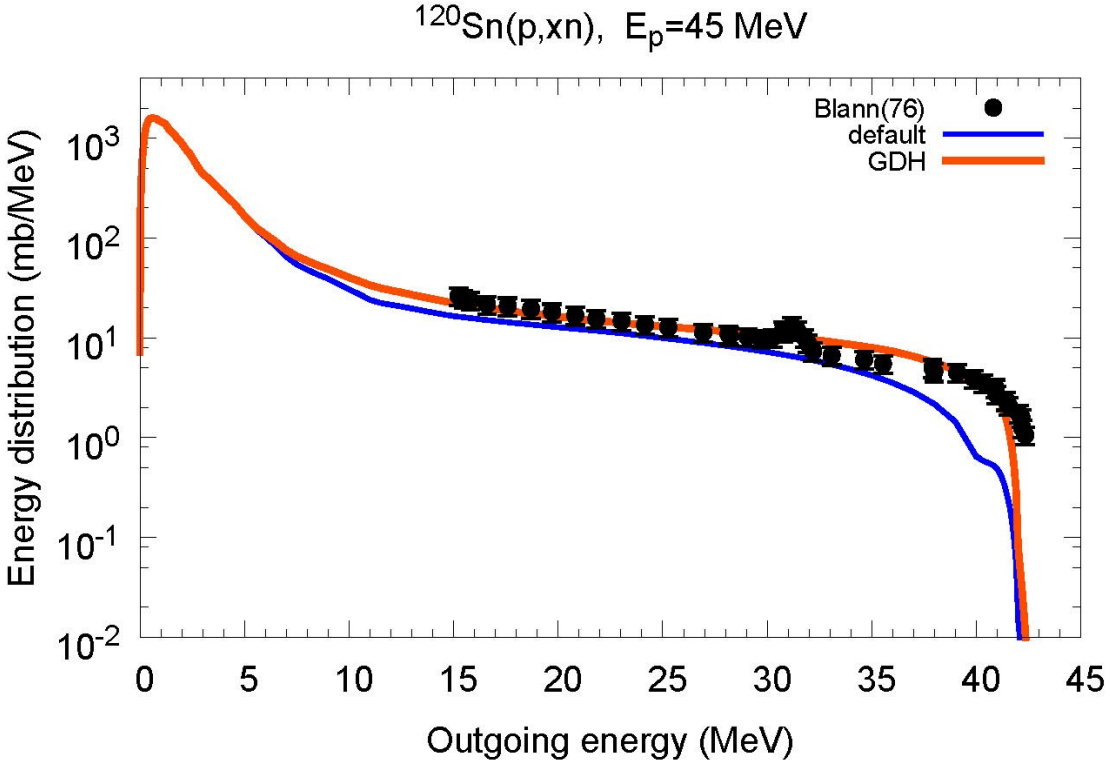
^{120}Sn(p,xn), E_p=45 MeV
Blann(76)
default
GDH
Energy distribution (mb/MeV)
10^3
10^2
10^1
10^0
10^{-1}
10^{-2}
0
5
10
15
20
25
30
35
40
45
Outgoing energy (MeV)

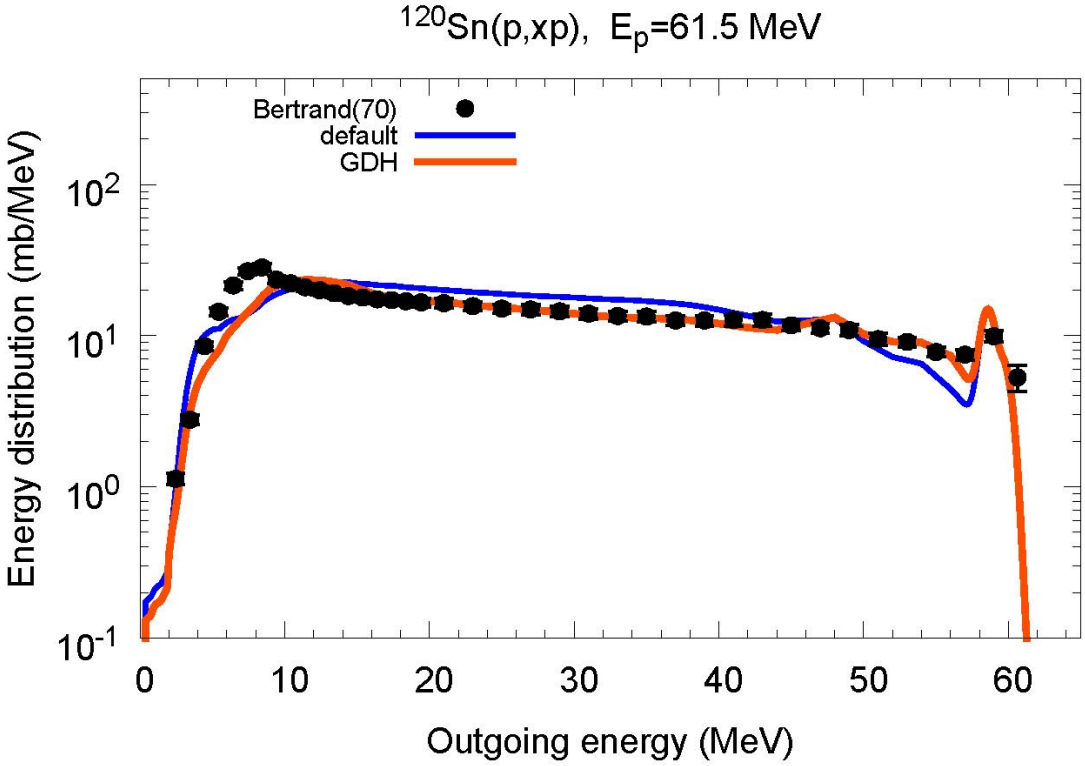
^{120}Sn(p,xp), E_p=61.5 MeV
Bertrand(70)
default
GDH
Energy distribution (mb/MeV)
10^2
10^1
10^0
10^{-1}
0
10
20
30
40
50
60
Outgoing energy (MeV)

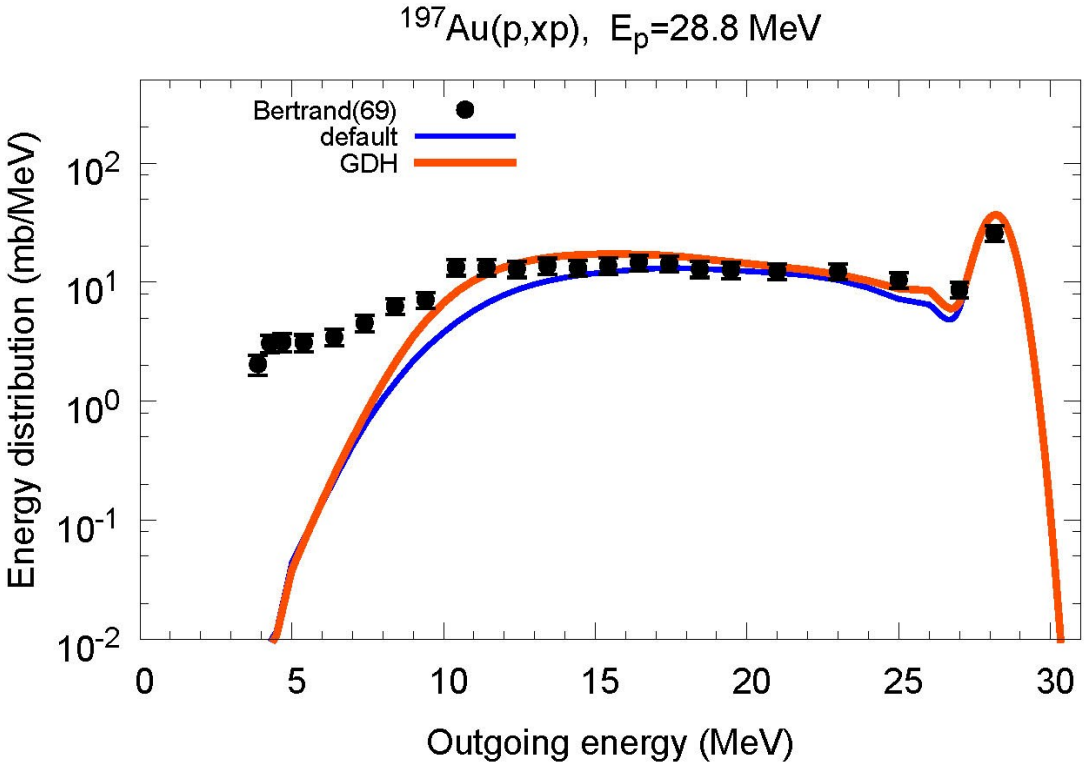
^{197}Au(p,xp), E_p=28.8 MeV
Bertrand(69)
default
GDH
Energy distribution (mb/MeV)
10^2
10^1
10^0
10^{-1}
10^{-2}
0
5
10
15
20
25
30
Outgoing energy (MeV)

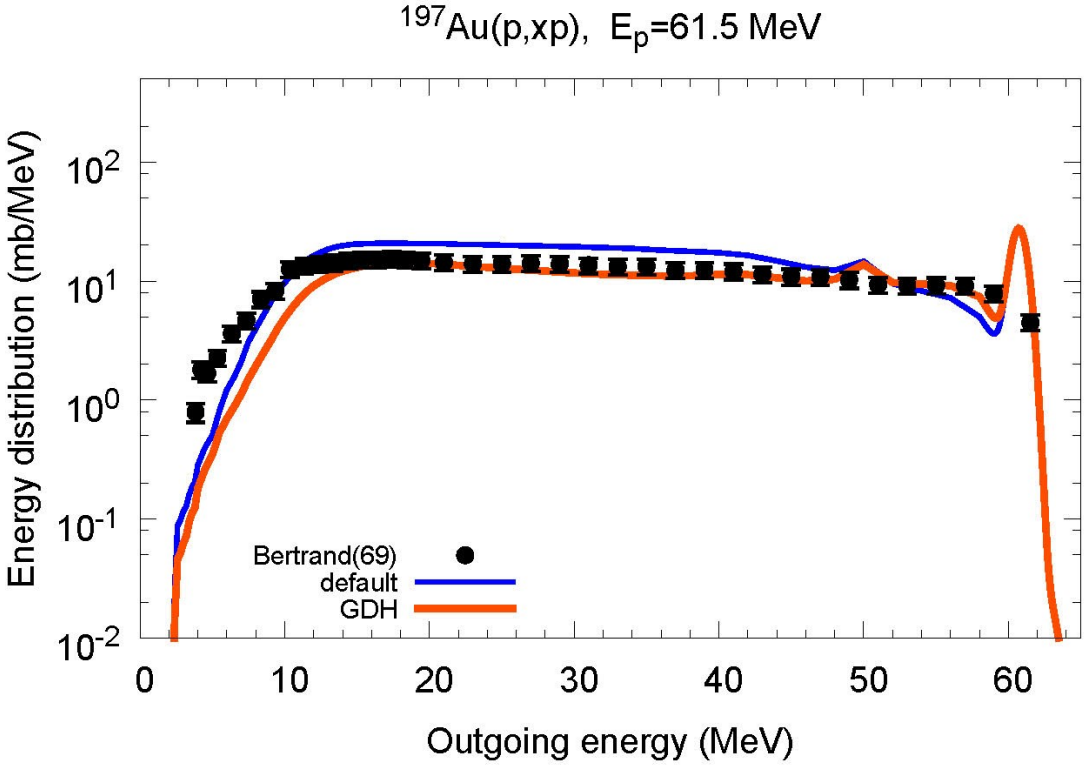
^{197}Au(p,xp), E_p=61.5 MeV
Energy distribution (mb/MeV)
Outgoing energy (MeV)
Bertrand(69)
default
GDH

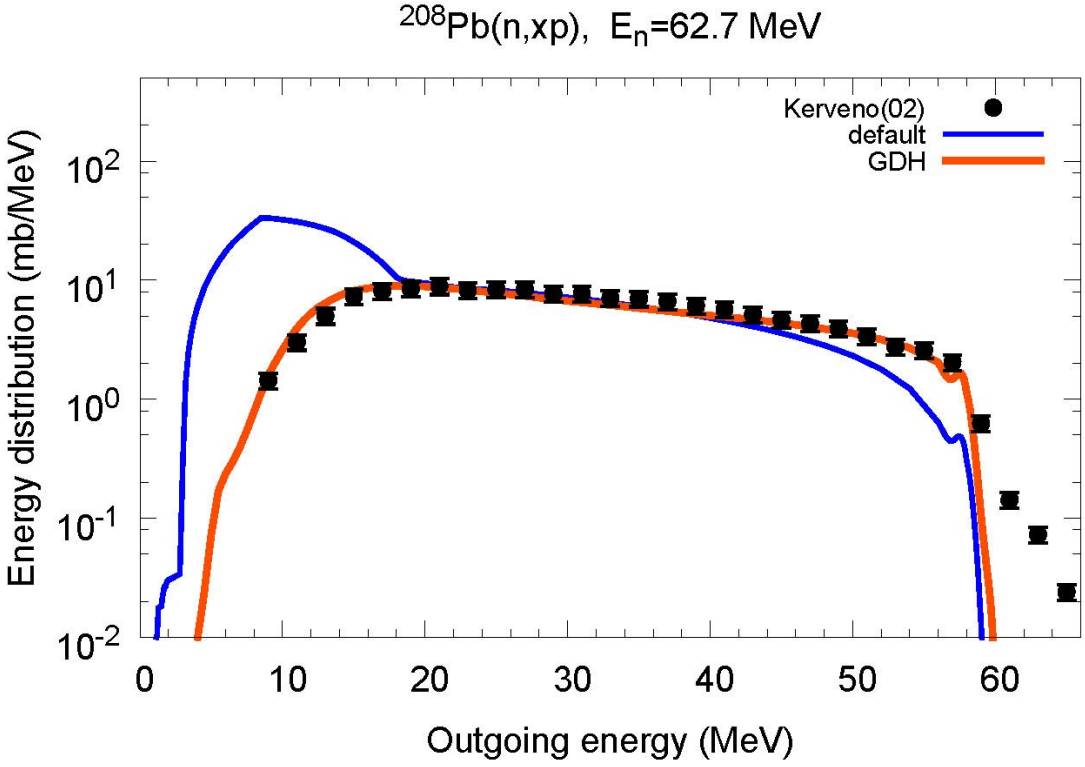
^{208}Pb(n,xp), E_n=62.7 MeV
Energy distribution (mb/MeV)
Outgoing energy (MeV)
Kerveno(02)
default
GDH

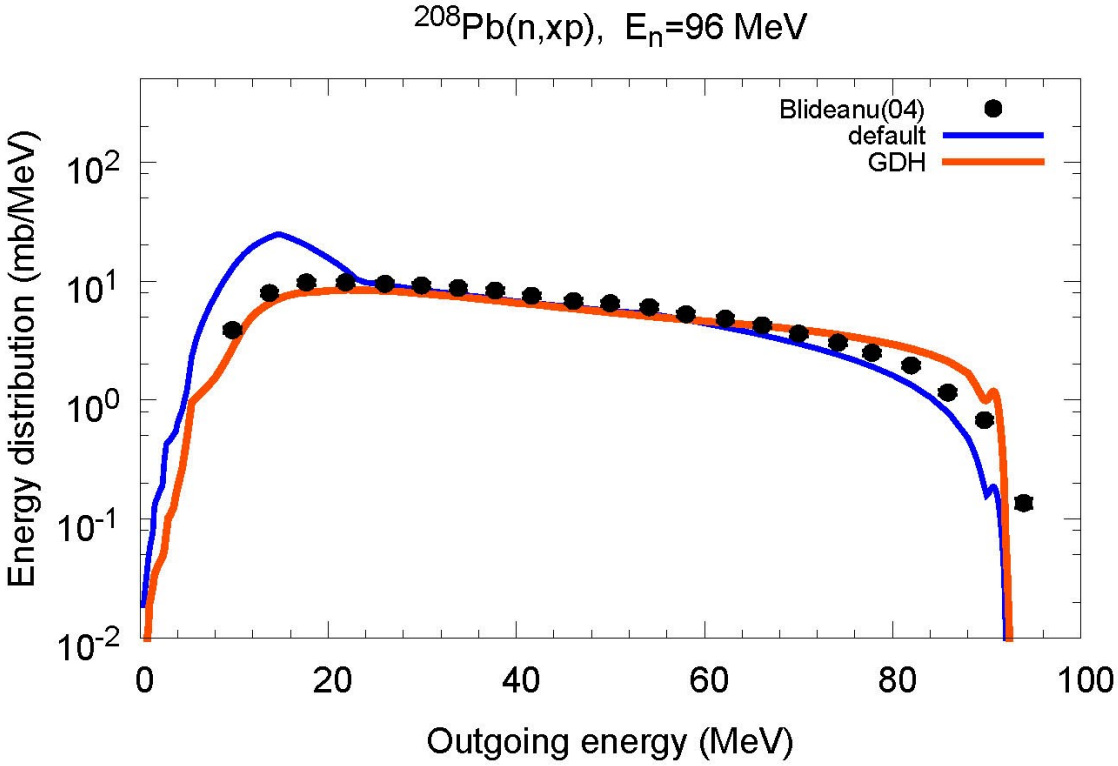
^{208}Pb(n,xp), E_n=96 MeV
Blideanu(04)
default
GDH
Energy distribution (mb/MeV)
10^2
10^1
10^0
10^{-1}
10^{-2}
0
20
40
60
80
100
Outgoing energy (MeV)

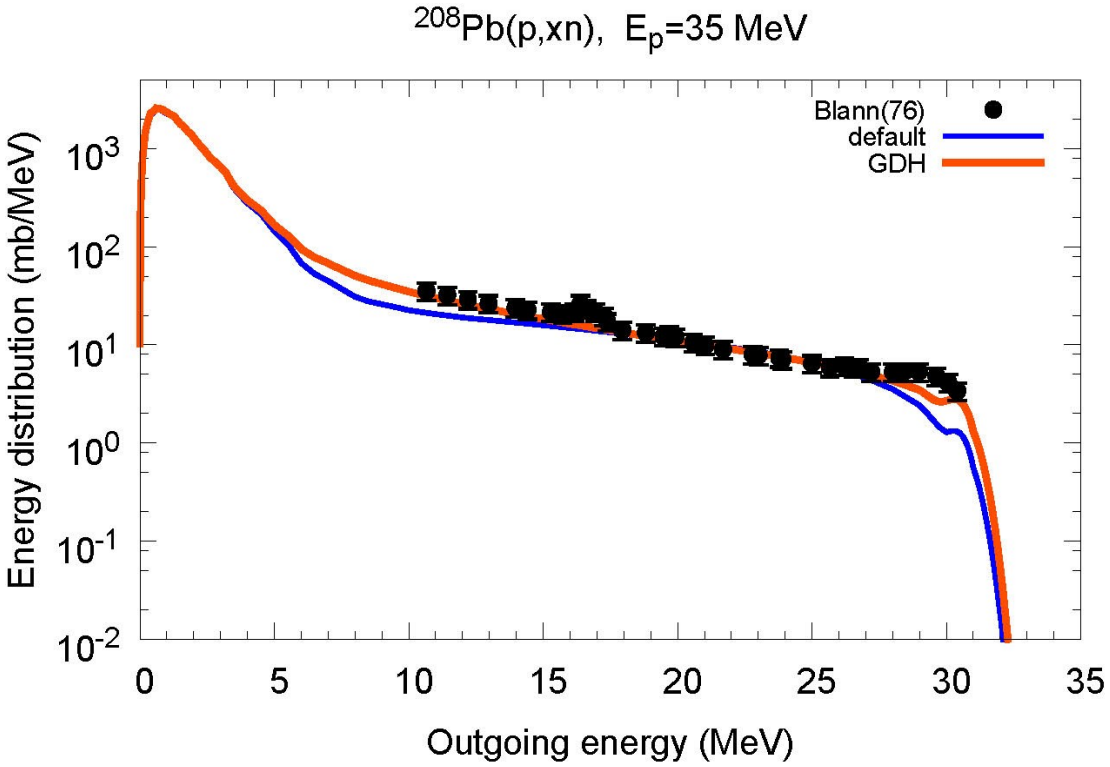
^{208}Pb(p,xn), E_p=35 MeV
Blann(76)
default
GDH
Energy distribution (mb/MeV)
10^3
10^2
10^1
10^0
10^{-1}
10^{-2}
0
5
10
15
20
25
30
35
Outgoing energy (MeV)

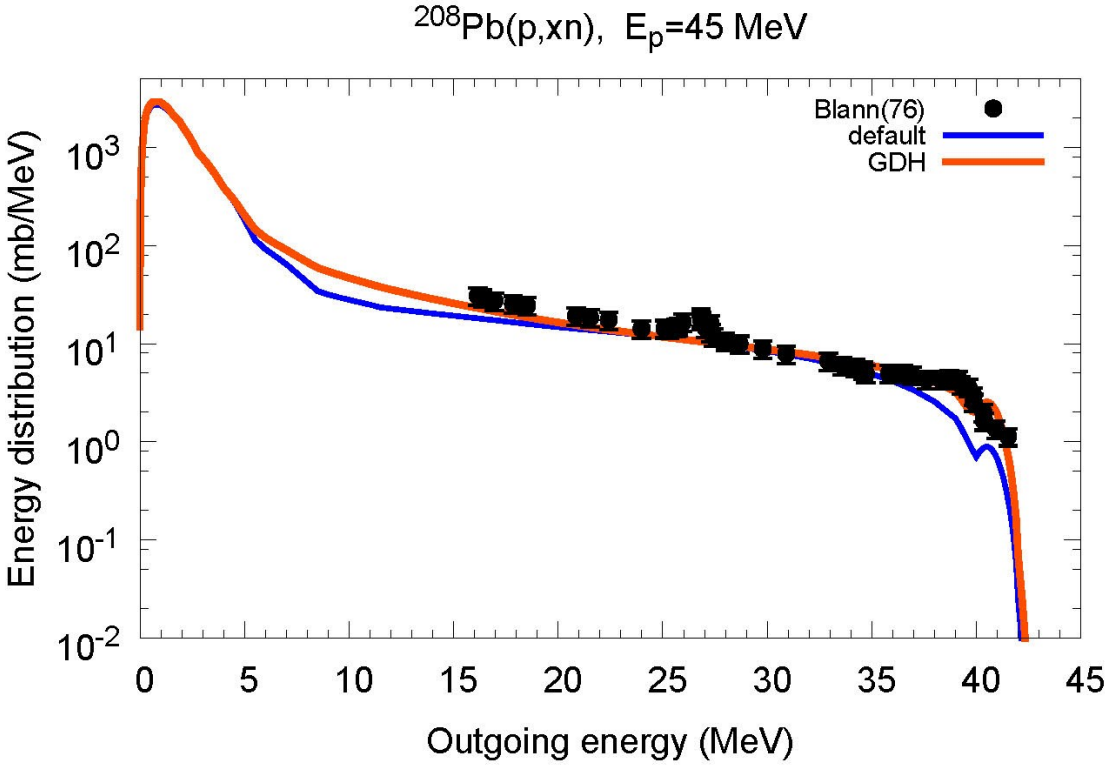
^{208}Pb(p,xn), E_p=45 MeV
Blann(76)
default
GDH
Energy distribution (mb/MeV)
10^3
10^2
10^1
10^0
10^{-1}
10^{-2}
0
5
10
15
20
25
30
35
40
45
Outgoing energy (MeV)

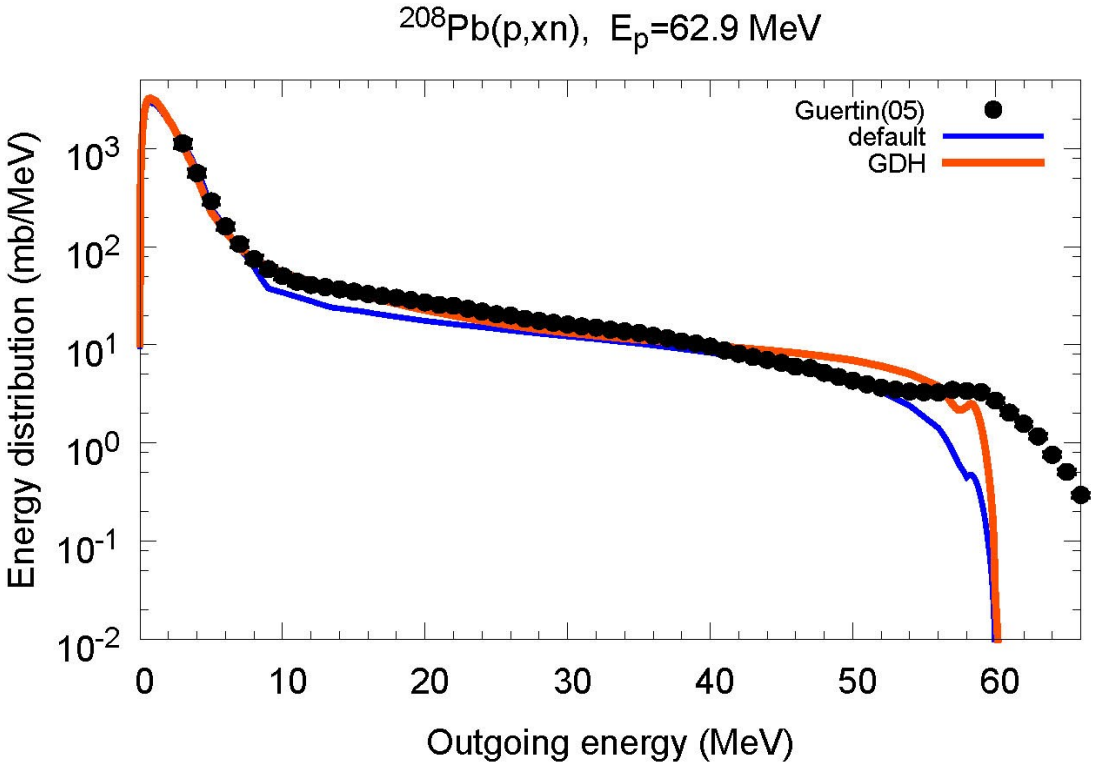
^{208}Pb(p,xn), E_p=62.9 MeV
Guertin(05)
default
GDH
Energy distribution (mb/MeV)
10^3
10^2
10^1
10^0
10^{-1}
10^{-2}
0
10
20
30
40
50
60
Outgoing energy (MeV)

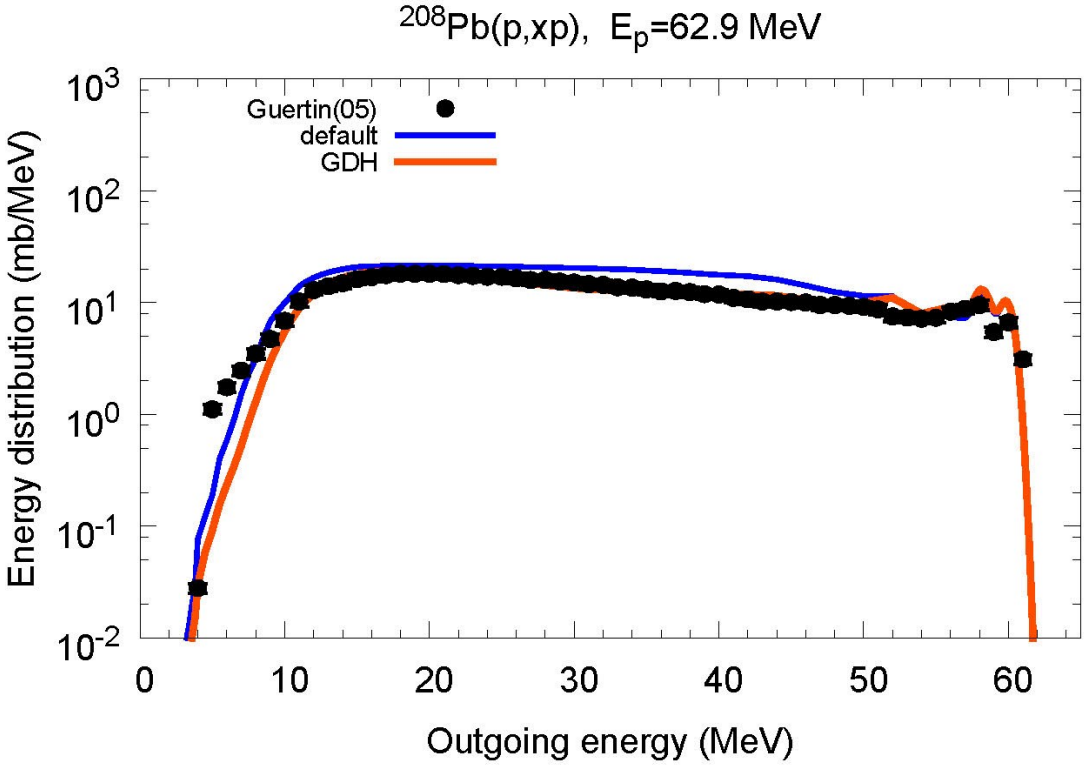
^{208}Pb(p,xp), E_p=62.9 MeV
Guertin(05)
default
GDH
Energy distribution (mb/MeV)
Outgoing energy (MeV)

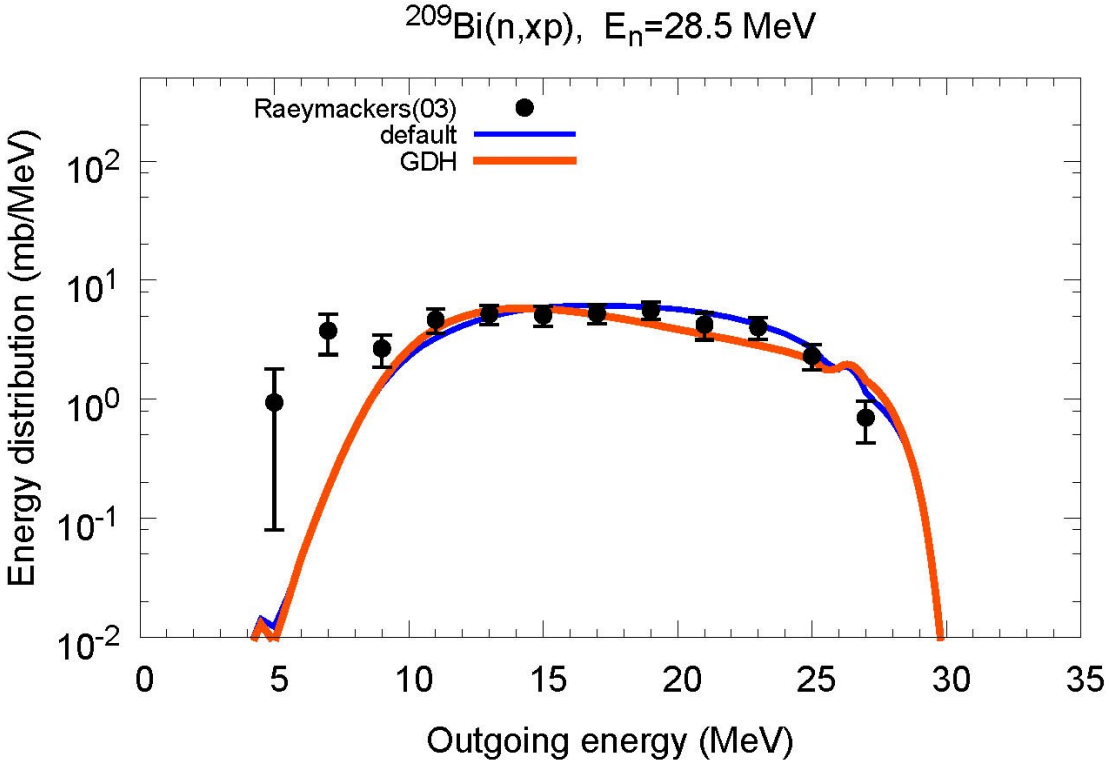
^{209}Bi(n,xp), E_n=28.5 MeV
Raeymackers(03)
default
GDH
Energy distribution (mb/MeV)
Outgoing energy (MeV)

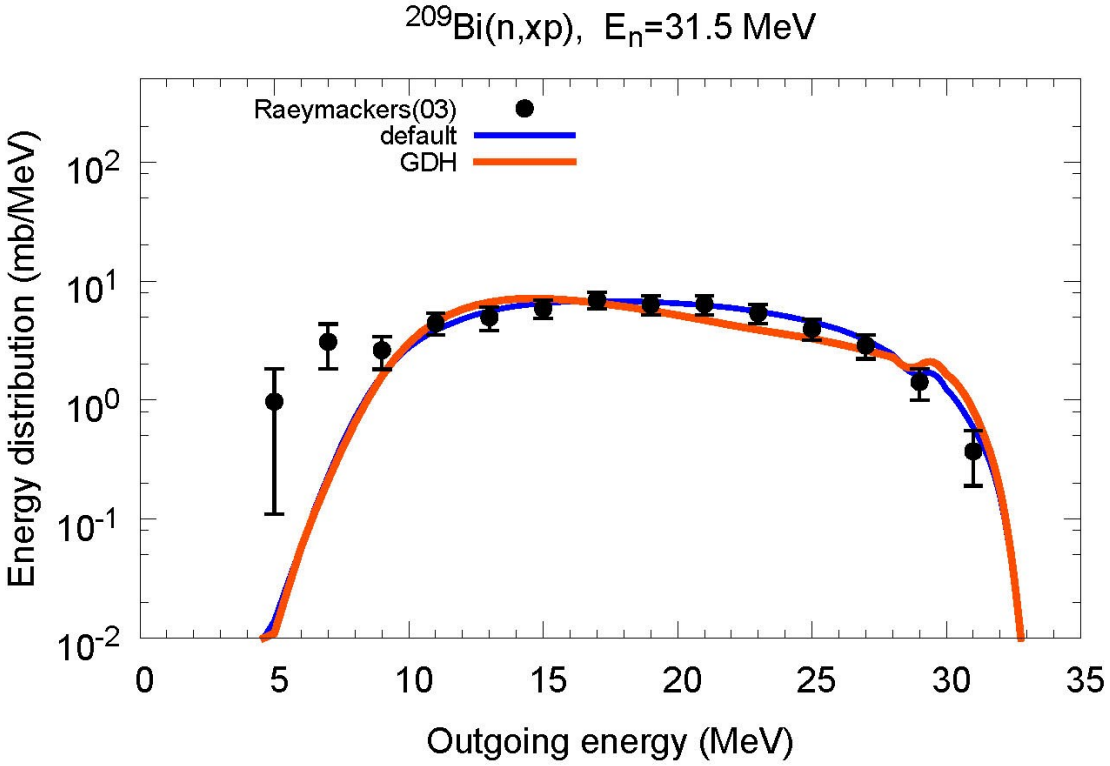
^{209}Bi(n,xp), E_n=31.5 MeV
Raeymackers(03)
default
GDH
Energy distribution (mb/MeV)
Outgoing energy (MeV)

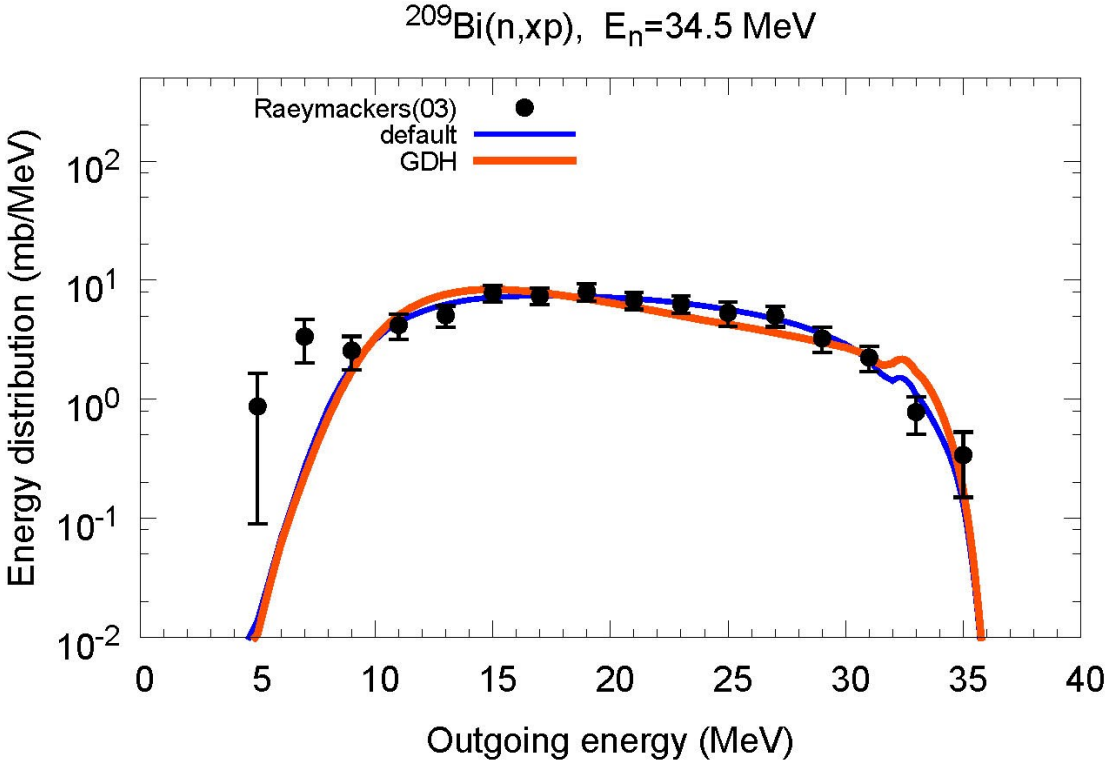
^{209}Bi(n,xp), E_n=34.5 MeV
Raeymackers(03)
default
GDH
Energy distribution (mb/MeV)
Outgoing energy (MeV)

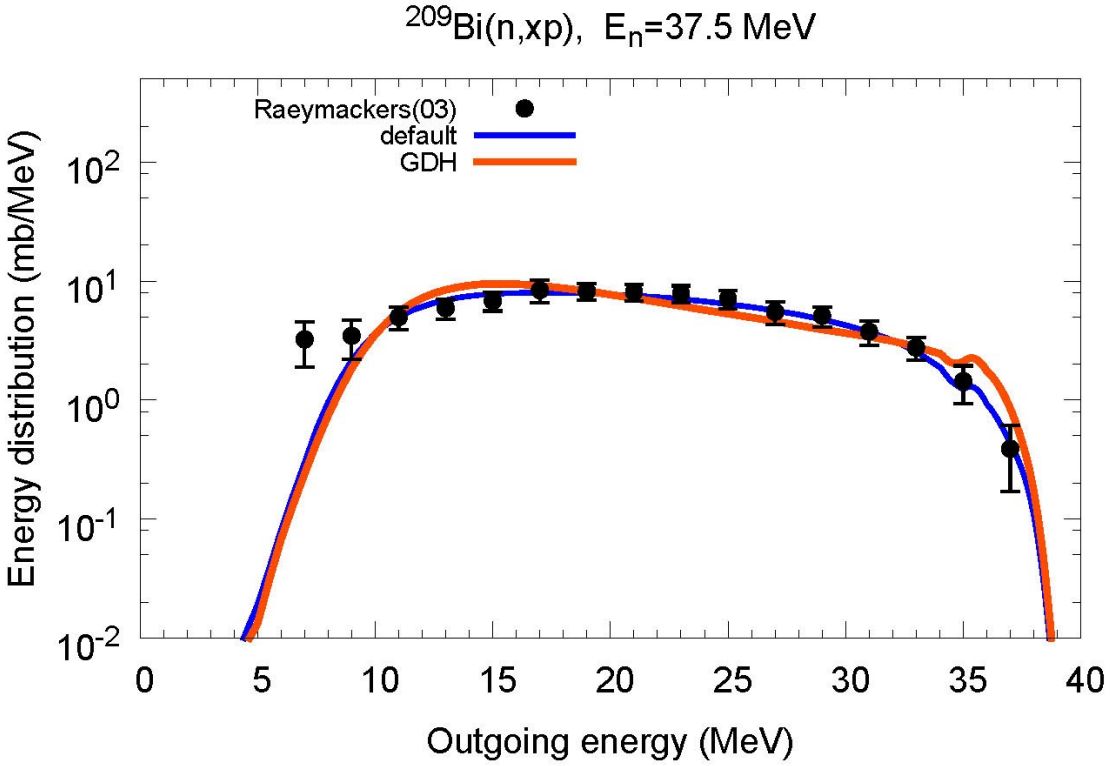
^{209}Bi(n,xp), E_n=37.5 MeV
Raeymackers(03)
default
GDH
Energy distribution (mb/MeV)
10^2
10^1
10^0
10^{-1}
10^{-2}
0
5
10
15
20
25
30
35
40
Outgoing energy (MeV)

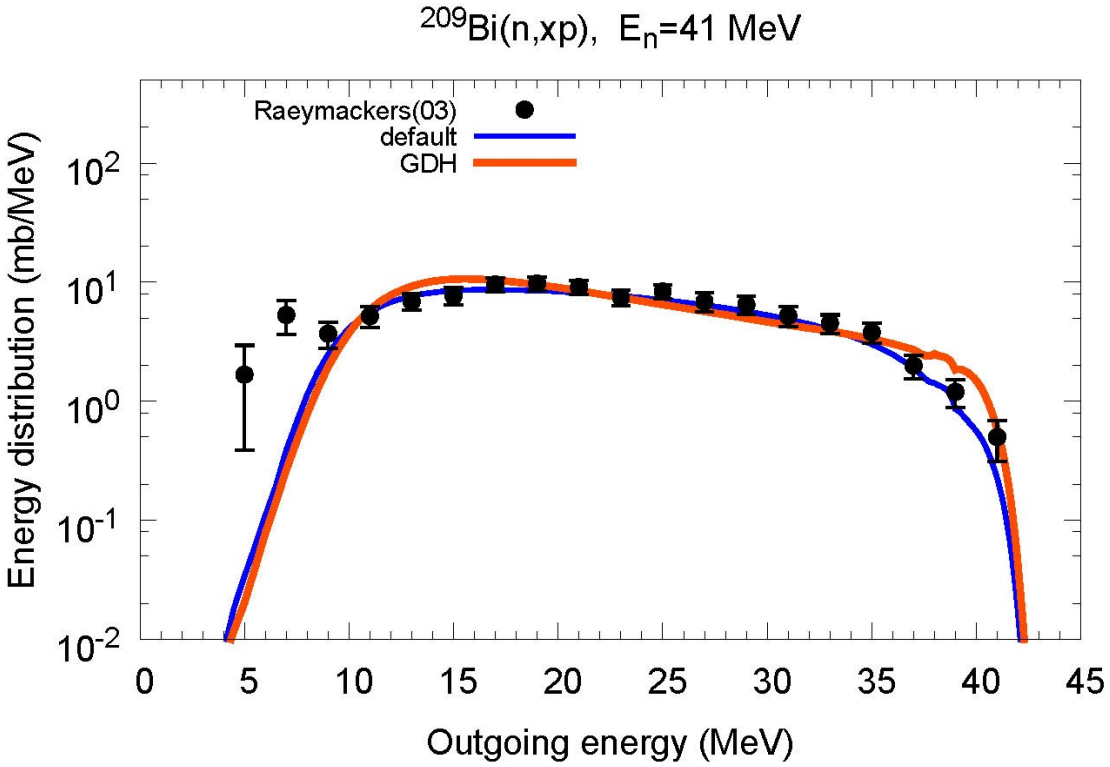
^{209}Bi(n,xp), E_n=41 MeV
Raeymackers(03)
default
GDH
Energy distribution (mb/MeV)
10^2
10^1
10^0
10^{-1}
10^{-2}
0
5
10
15
20
25
30
35
40
45
Outgoing energy (MeV)

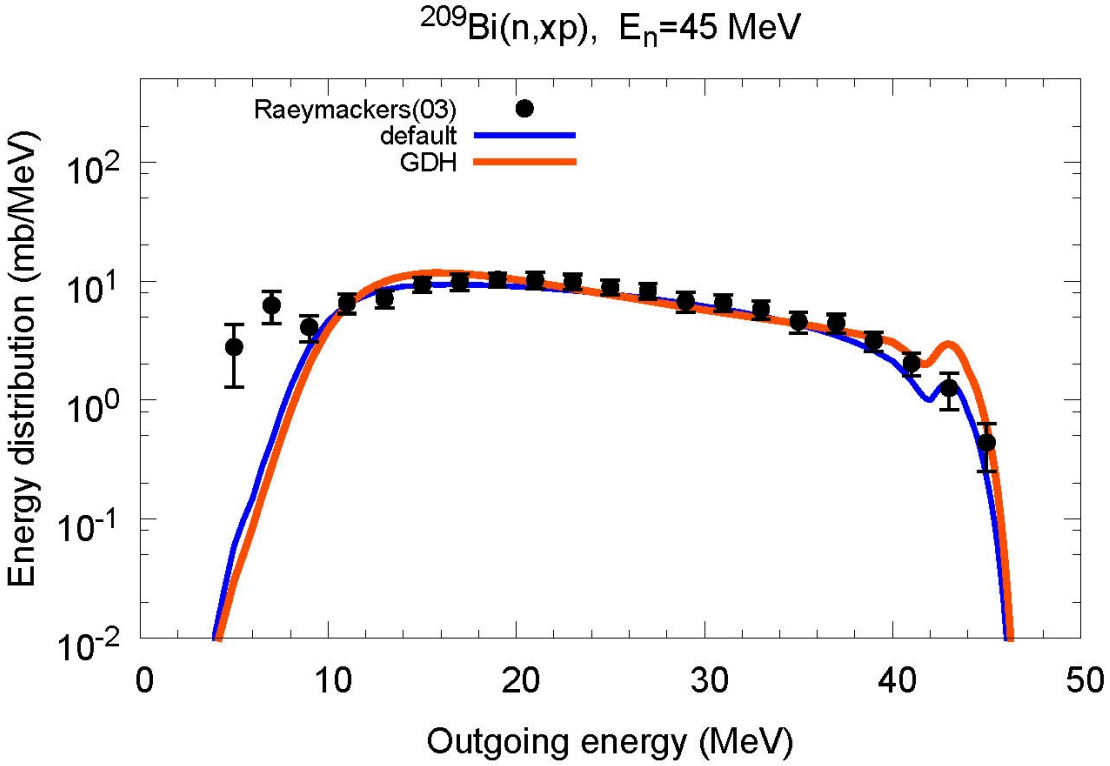
^{209}Bi(n,xp), E_n=45 MeV
Raeymackers(03)
default
GDH
Energy distribution (mb/MeV)
10^2
10^1
10^0
10^{-1}
10^{-2}
0
10
20
30
40
50
Outgoing energy (MeV)

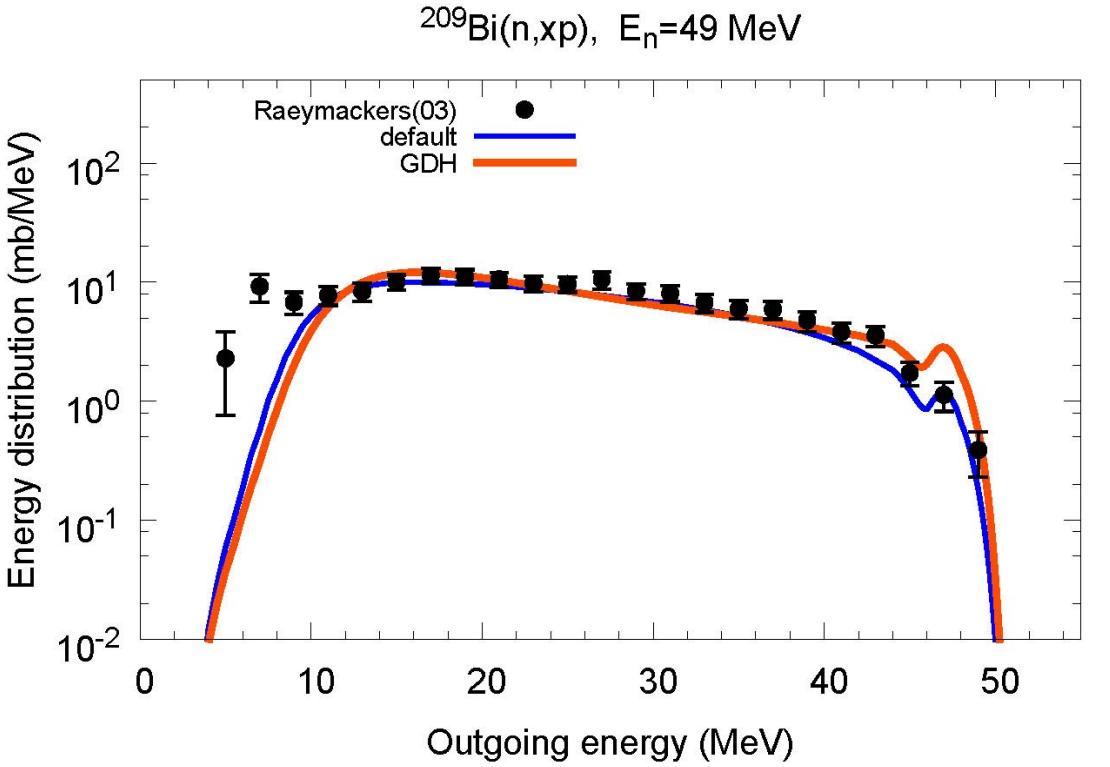
^{209}Bi(n,xp), E_n=49 MeV
Raeymackers(03)
default
GDH
Energy distribution (mb/MeV)
10^2
10^1
10^0
10^{-1}
10^{-2}
0
10
20
30
40
50
Outgoing energy (MeV)

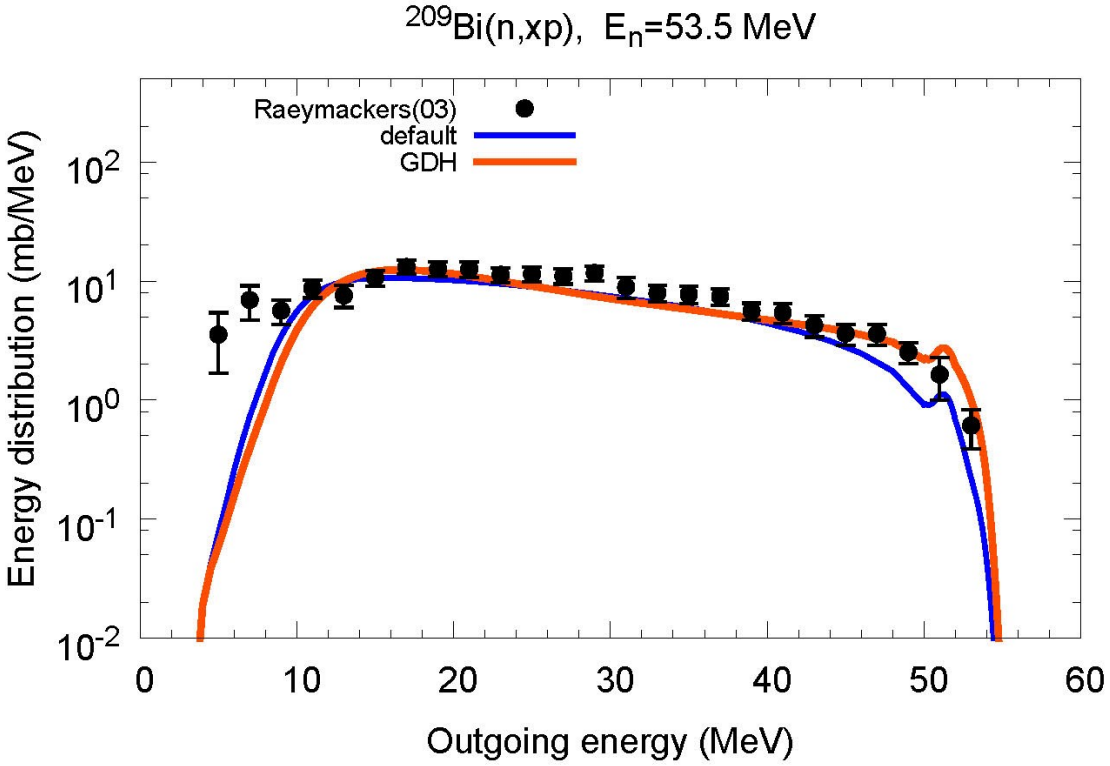
^{209}Bi(n,xp), E_n=53.5 MeV
Raeymackers(03)
default
GDH
Energy distribution (mb/MeV)
10^2
10^1
10^0
10^{-1}
10^{-2}
0
10
20
30
40
50
60
Outgoing energy (MeV)

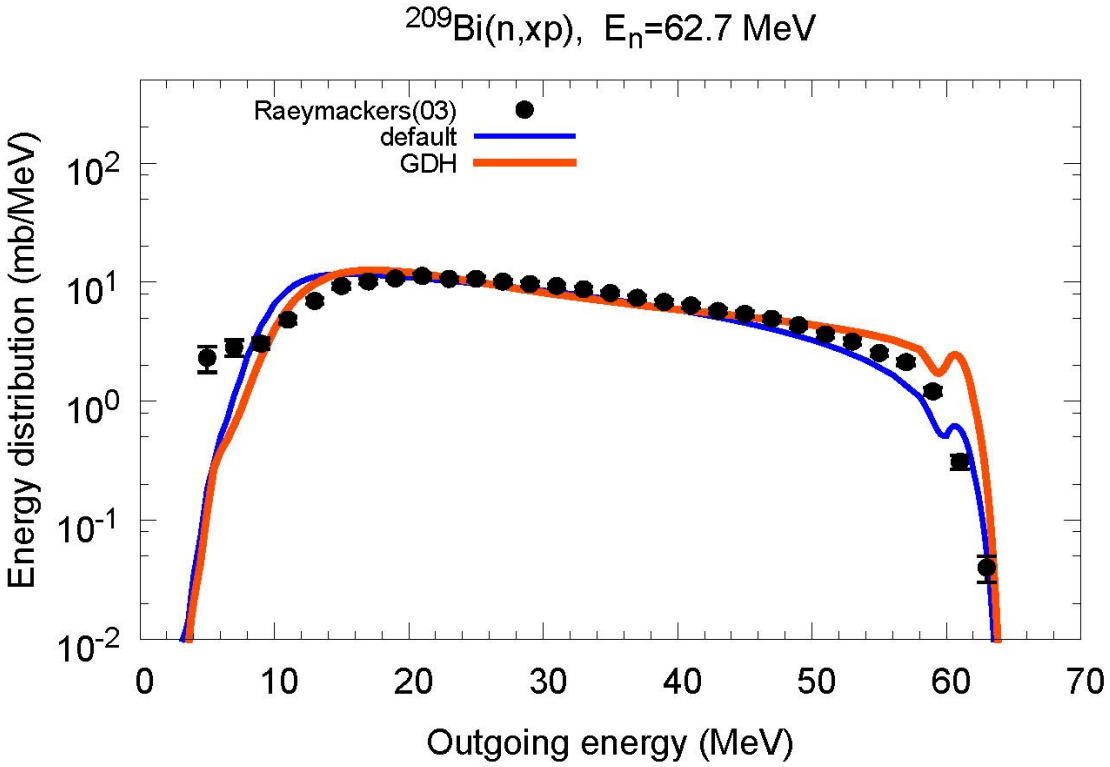
^{209}Bi(n,xp), E_n=62.7 MeV
Raeymackers(03)
default
GDH
Energy distribution (mb/MeV)
10^2
10^1
10^0
10^{-1}
10^{-2}
0
10
20
30
40
50
60
70
Outgoing energy (MeV)

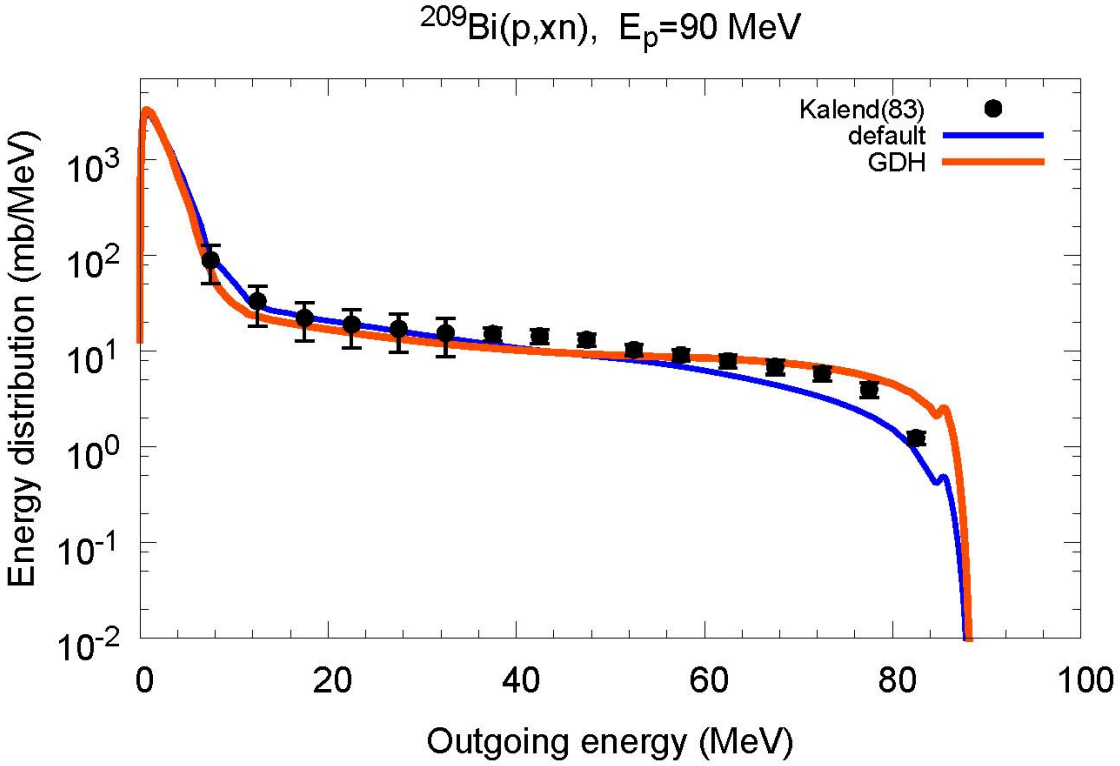
^{209}Bi(p,xn), E_p=90 MeV
Kalend(83)
default
GDH
Energy distribution (mb/MeV)
10^3
10^2
10^1
10^0
10^{-1}
10^{-2}
0
20
40
60
80
100
Outgoing energy (MeV)

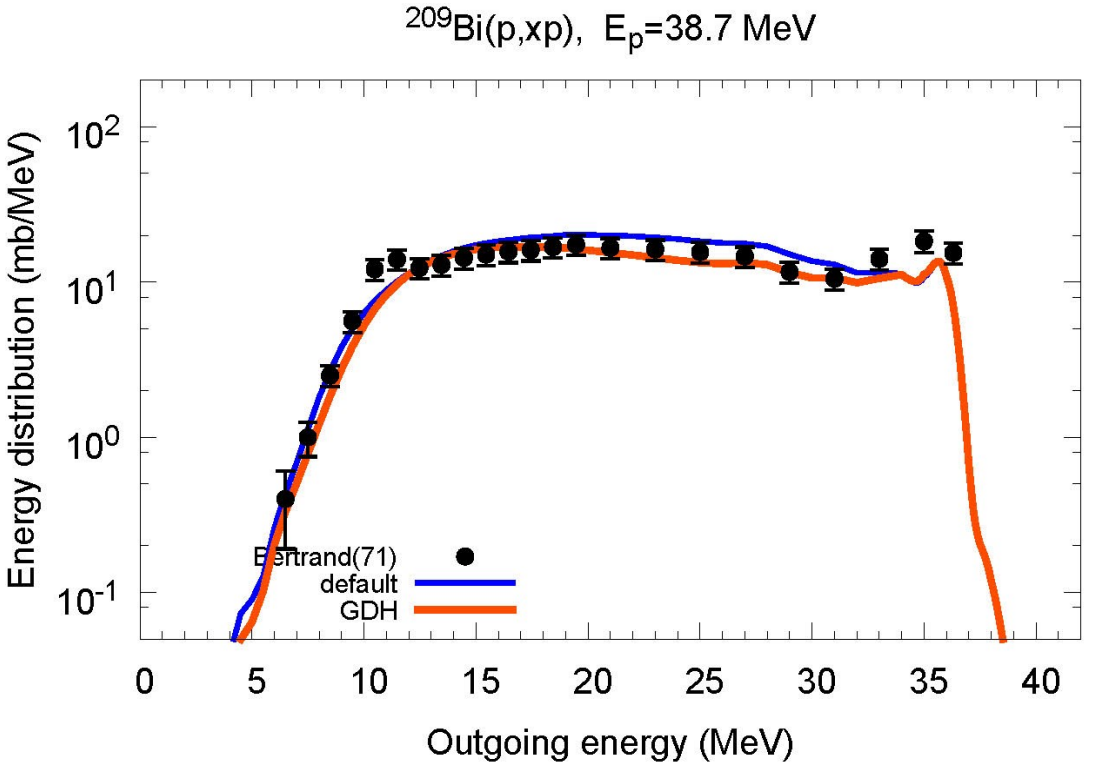
^{209}Bi(p,xp), E_p=38.7 MeV
Bertrand(71)
default
GDH
Energy distribution (mb/MeV)
10^2
10^1
10^0
10^{-1}
0
5
10
15
20
25
30
35
40
Outgoing energy (MeV)

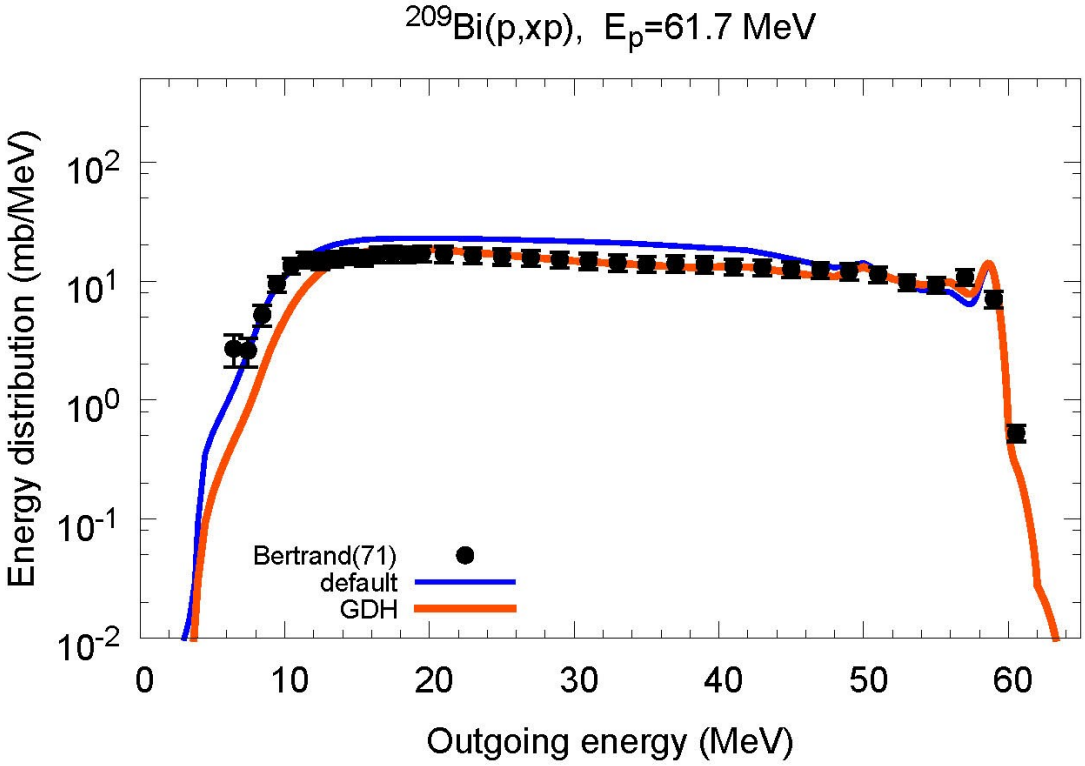
^{209}Bi(p,xp), E_p=61.7 MeV
Energy distribution (mb/MeV)
Outgoing energy (MeV)
Bertrand(71)
default
GDH

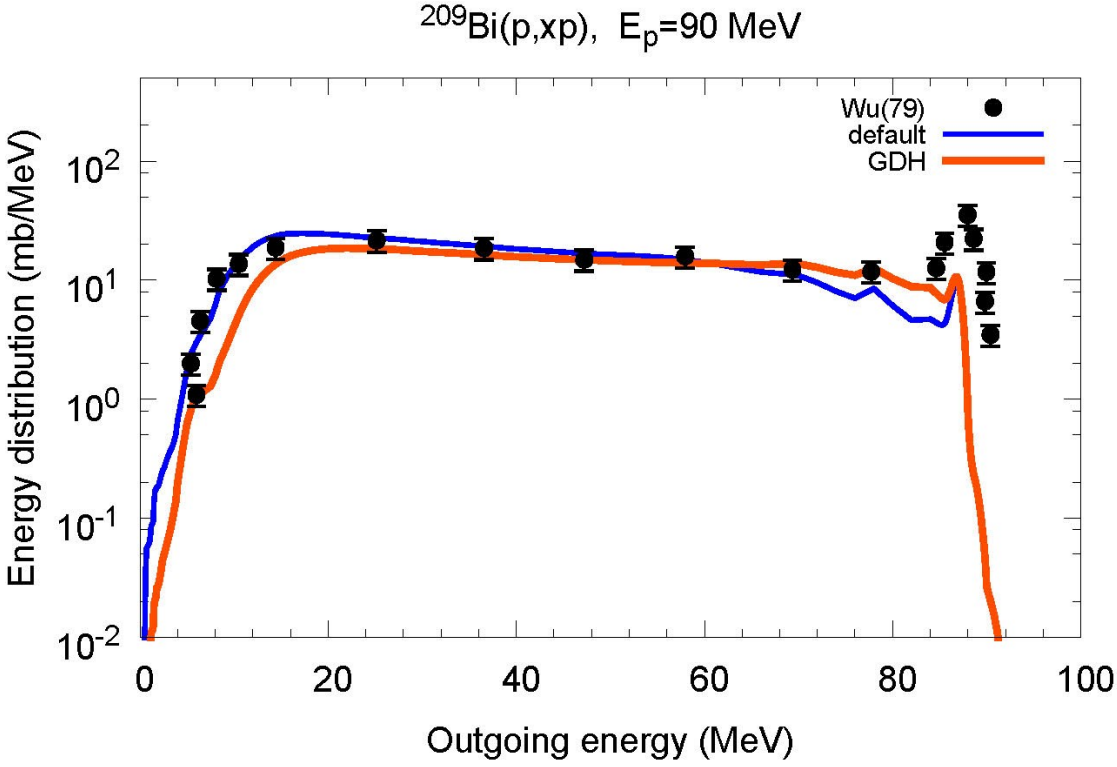
^{209}Bi(p,xp), E_p=90 MeV
Energy distribution (mb/MeV)
Outgoing energy (MeV)
Wu(79)
default
GDH

Appendix B

Calculated and experimental deuteron energy distributions

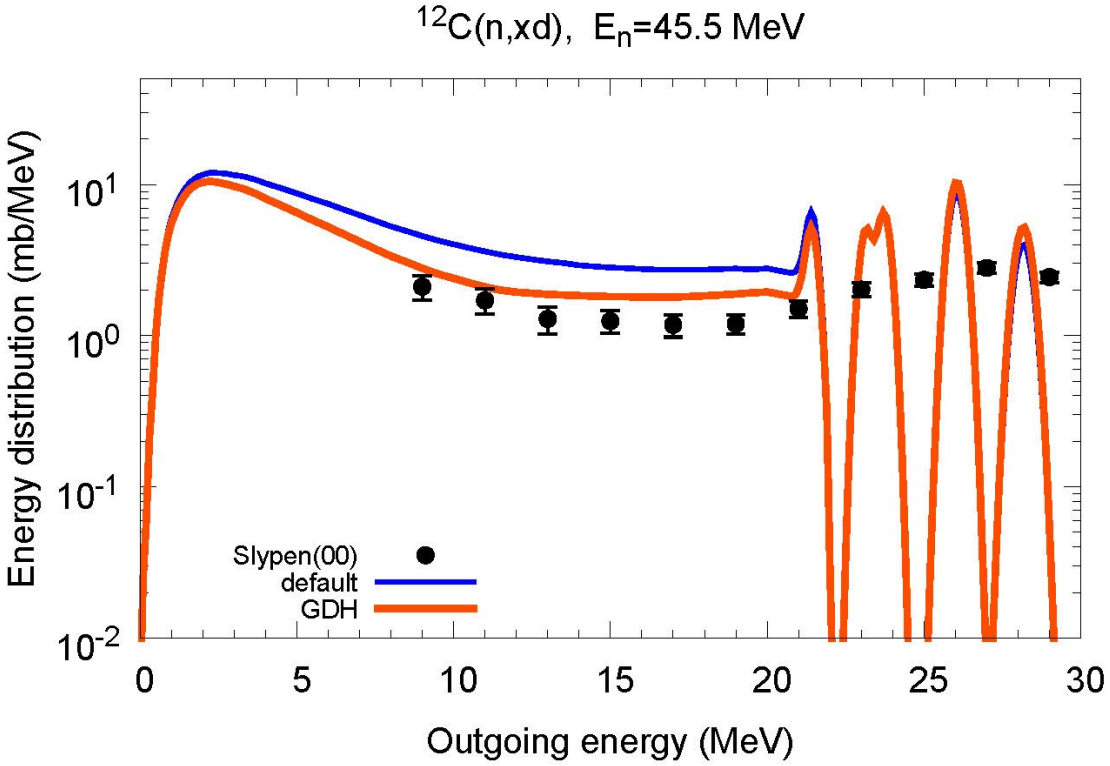
^{12}C(n,xd), E_n=45.5 MeV
Energy distribution (mb/MeV)
10^1
10^0
10^{-1}
10^{-2}
0
5
10
15
20
25
30
Outgoing energy (MeV)
Slypen(00)
default
GDH

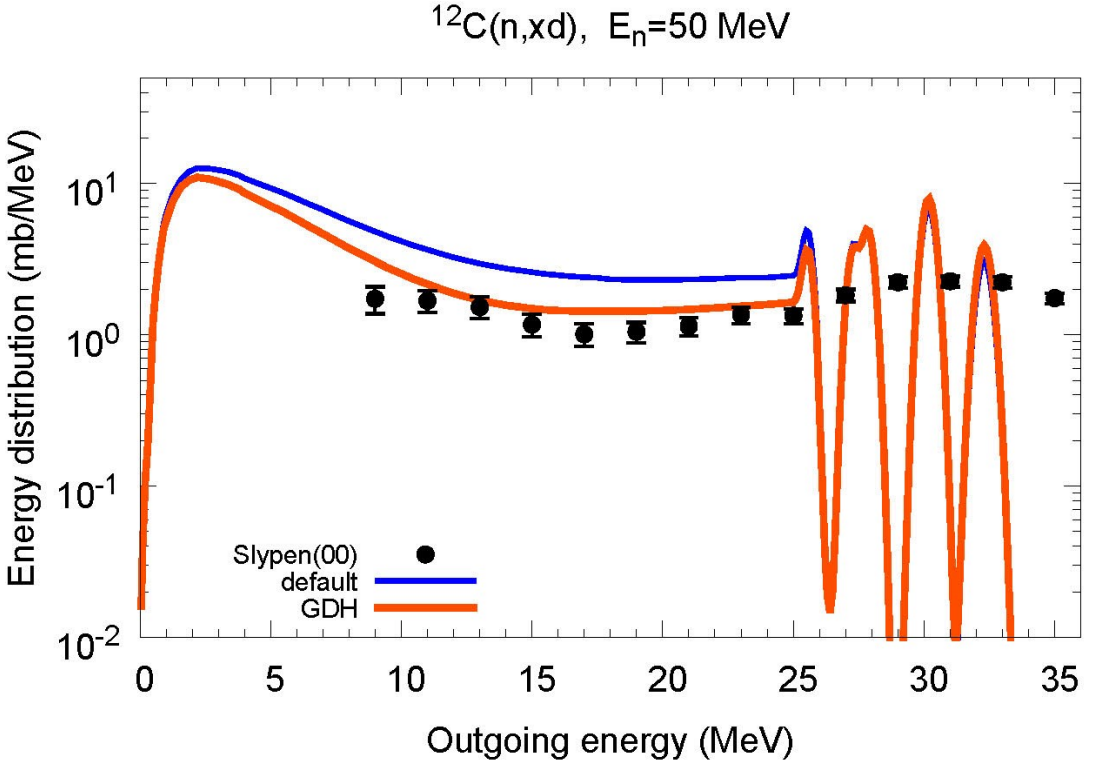
^{12}C(n,xd), E_n=50 MeV
Energy distribution (mb/MeV)
10^1
10^0
10^{-1}
10^{-2}
0
5
10
15
20
25
30
35
Outgoing energy (MeV)
Slypen(00)
default
GDH

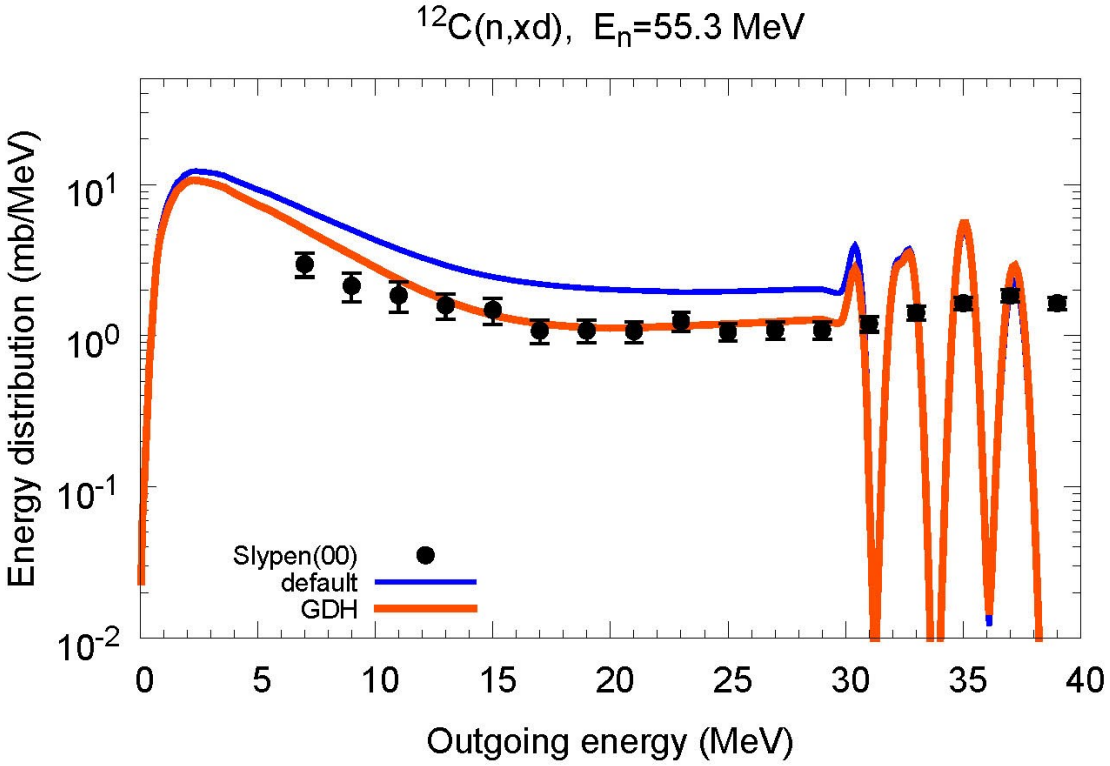
^{12}C(n,xd), E_n=55.3 MeV
Energy distribution (mb/MeV)
Outgoing energy (MeV)
Slypen(00)
default
GDH

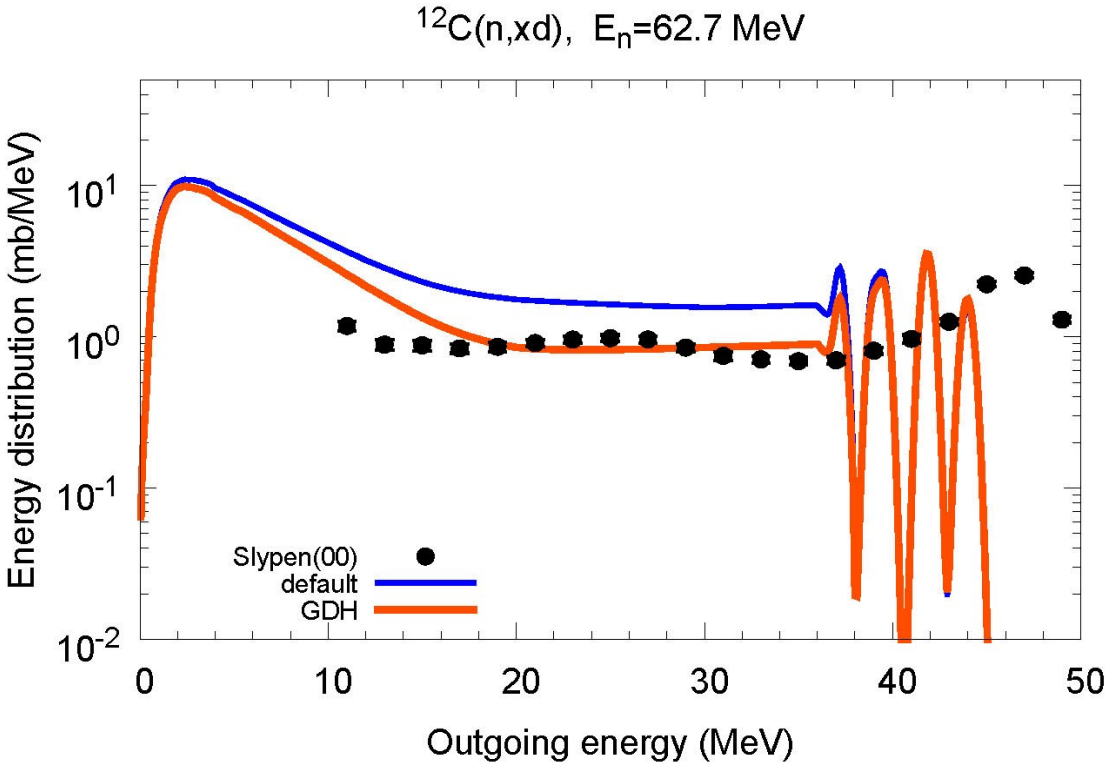
^{12}C(n,xd), E_n=62.7 MeV
Energy distribution (mb/MeV)
Outgoing energy (MeV)
Slypen(00)
default
GDH

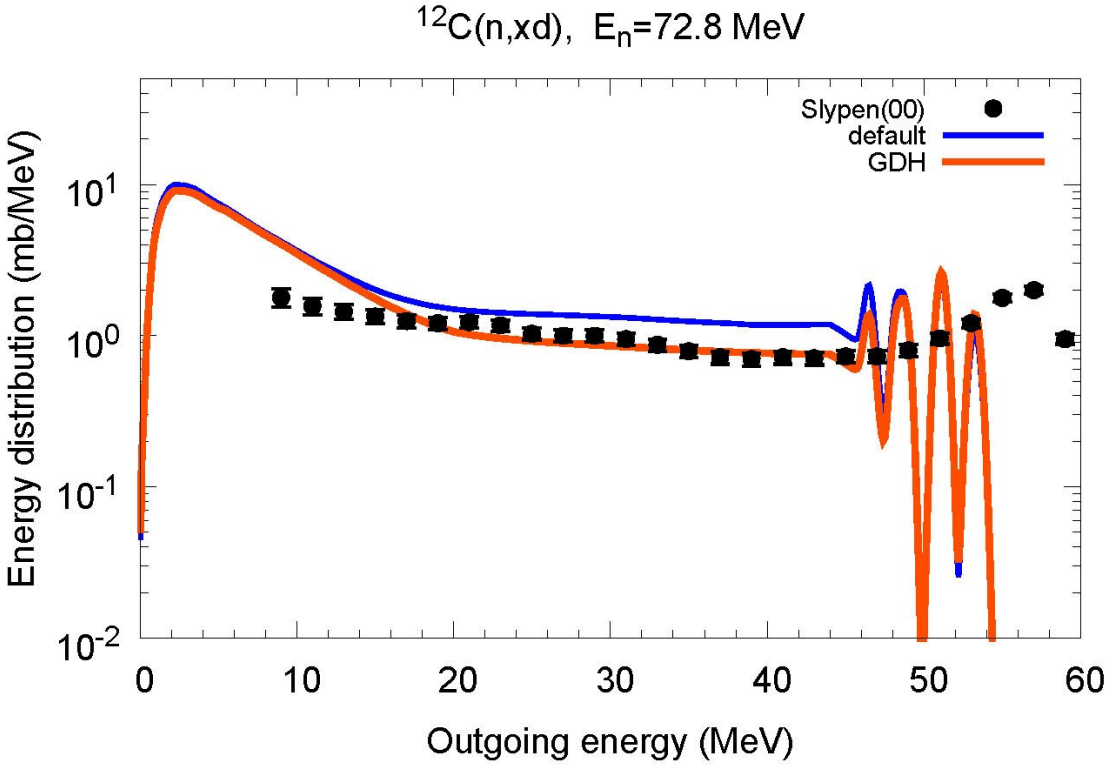
^{12}C(n,xd), E_n=72.8 MeV
Slypen(00)
default
GDH
Energy distribution (mb/MeV)
Outgoing energy (MeV)

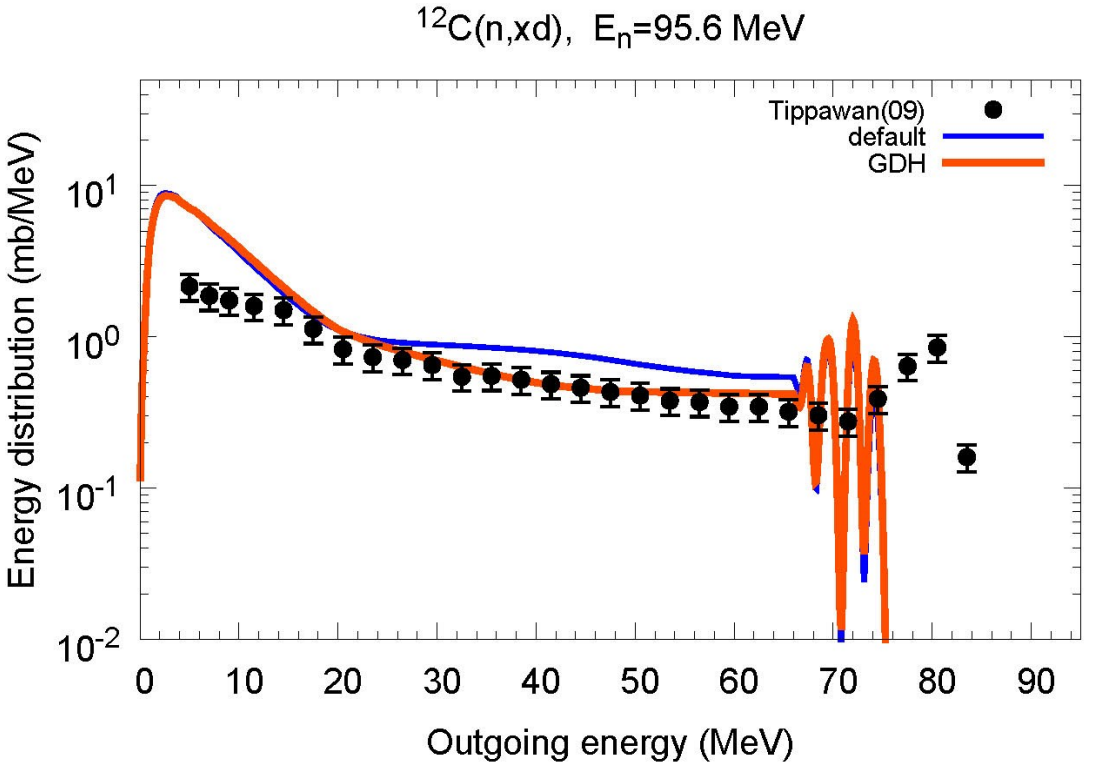
^{12}C(n,xd), E_n=95.6 MeV
Tippawan(09)
default
GDH
Energy distribution (mb/MeV)
Outgoing energy (MeV)

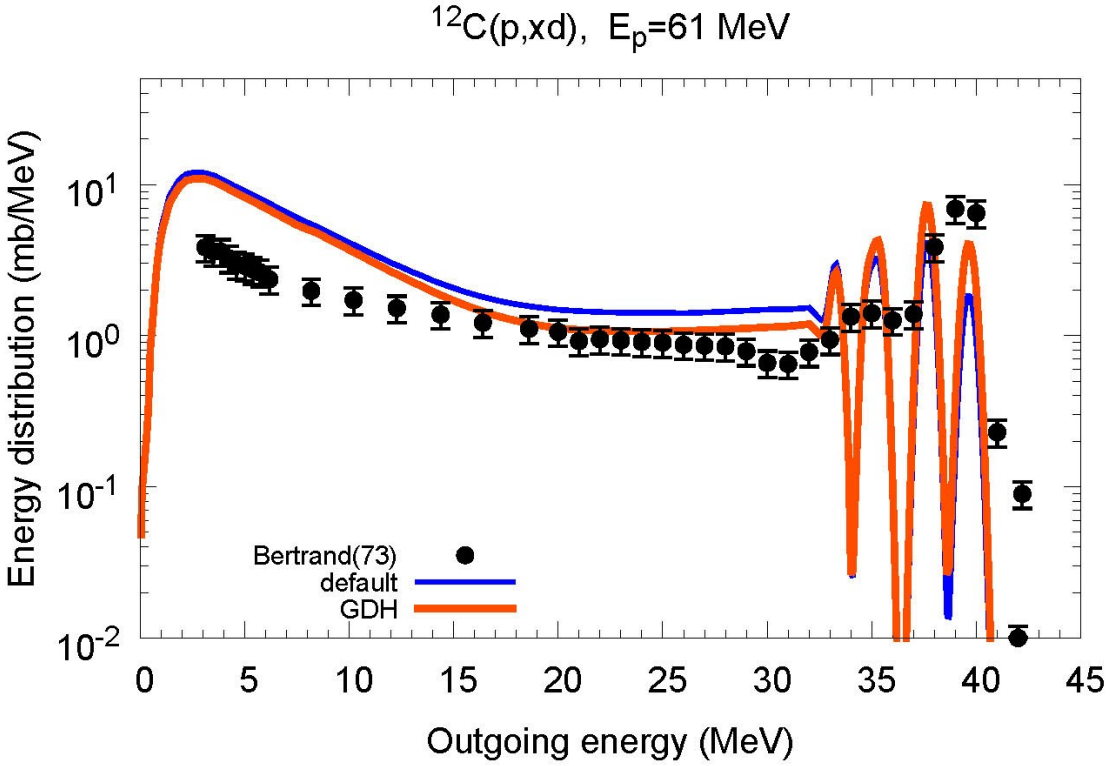
^{12}C(p,xd), E_p=61 MeV
Energy distribution (mb/MeV)
Outgoing energy (MeV)
Bertrand(73)
default
GDH

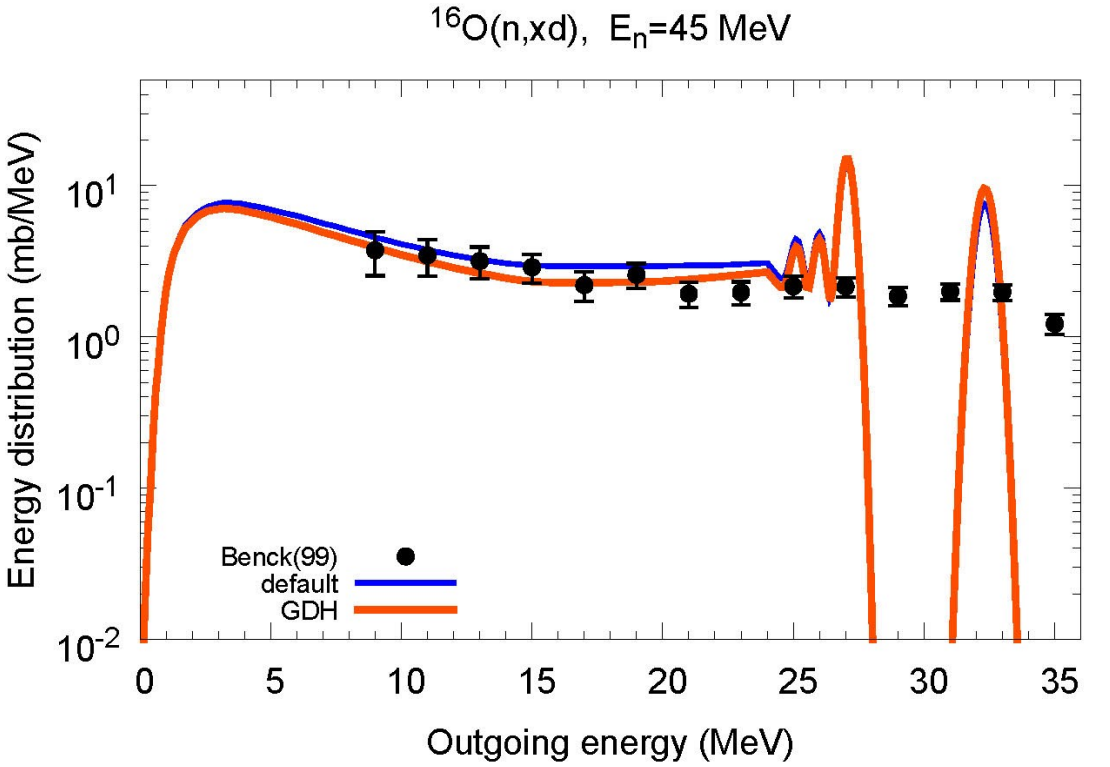
^{16}O(n,xd), E_n=45 MeV
Energy distribution (mb/MeV)
Outgoing energy (MeV)
Benck(99)
default
GDH

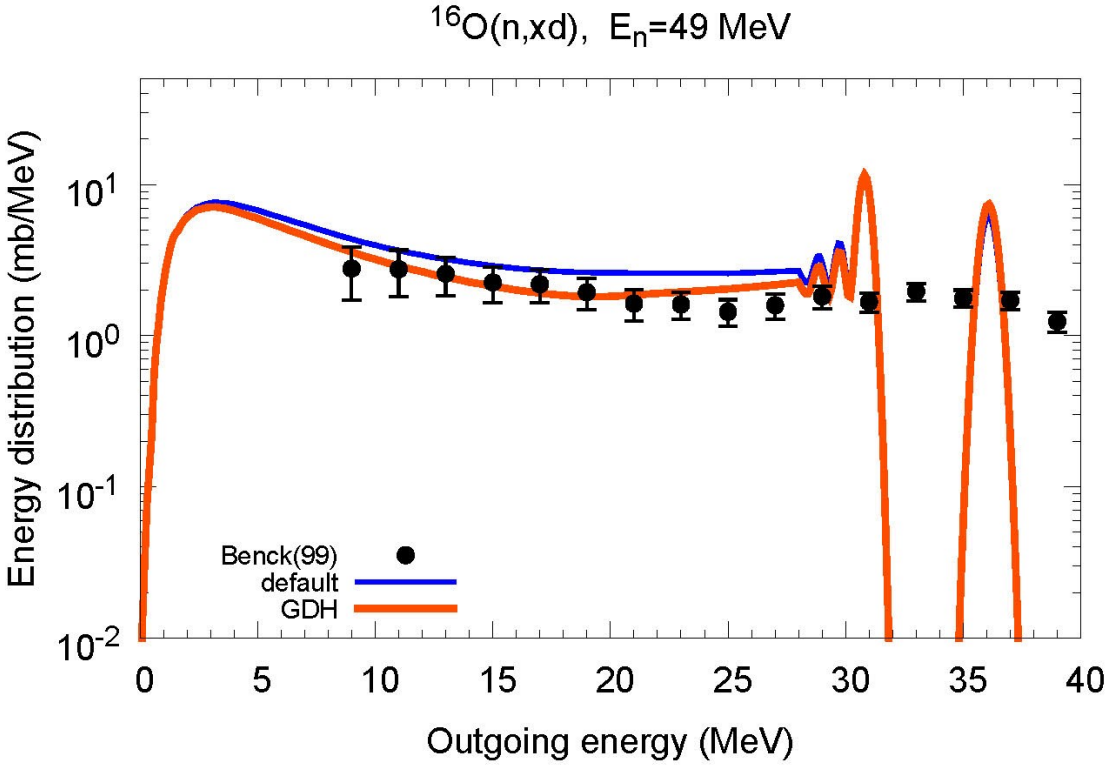
^{16}O(n,xd), E_n=49 MeV
Energy distribution (mb/MeV)
10^1
10^0
10^{-1}
10^{-2}
0
5
10
15
20
25
30
35
40
Outgoing energy (MeV)
Benck(99)
default
GDH

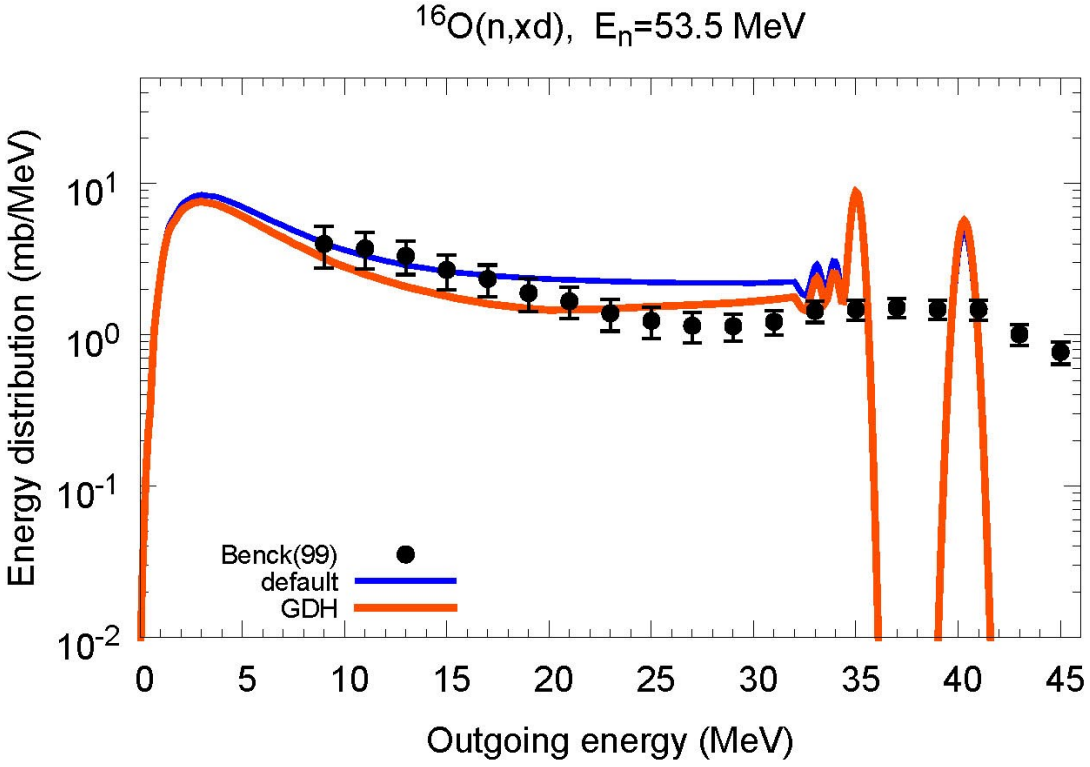
^{16}O(n,xd), E_n=53.5 MeV
Energy distribution (mb/MeV)
10^1
10^0
10^{-1}
10^{-2}
0
5
10
15
20
25
30
35
40
45
Outgoing energy (MeV)
Benck(99)
default
GDH

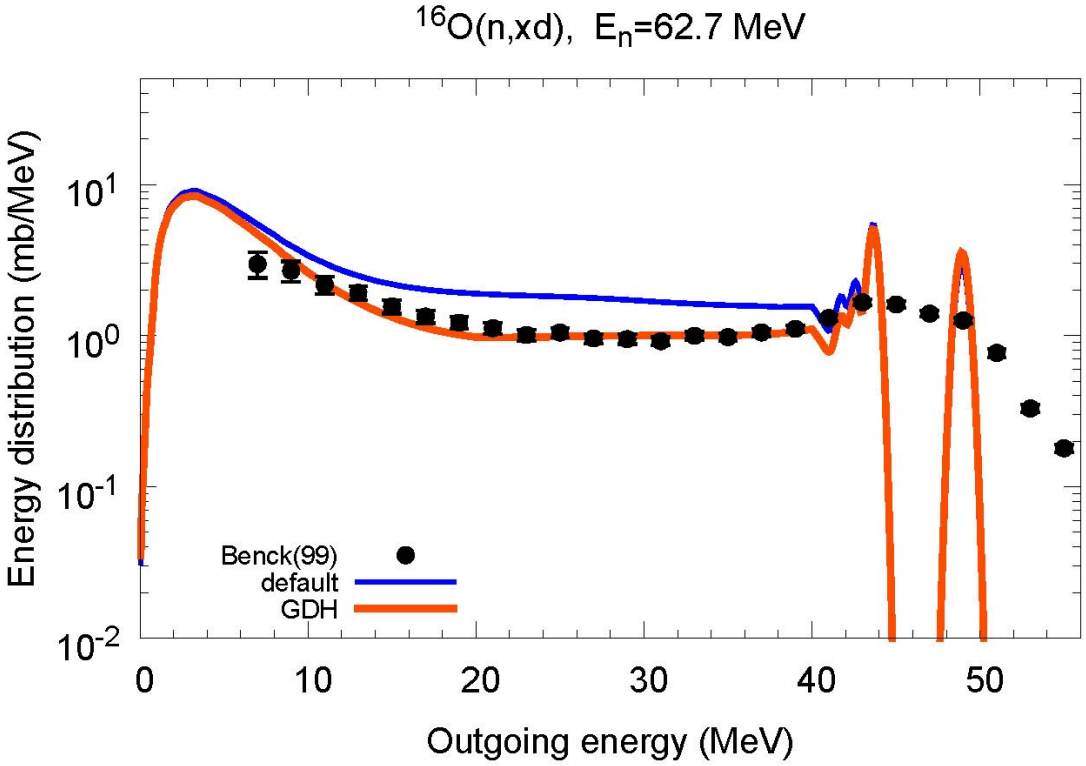
^{16}O(n,xd), E_n=62.7 MeV
Energy distribution (mb/MeV)
Outgoing energy (MeV)
Benck(99)
default
GDH

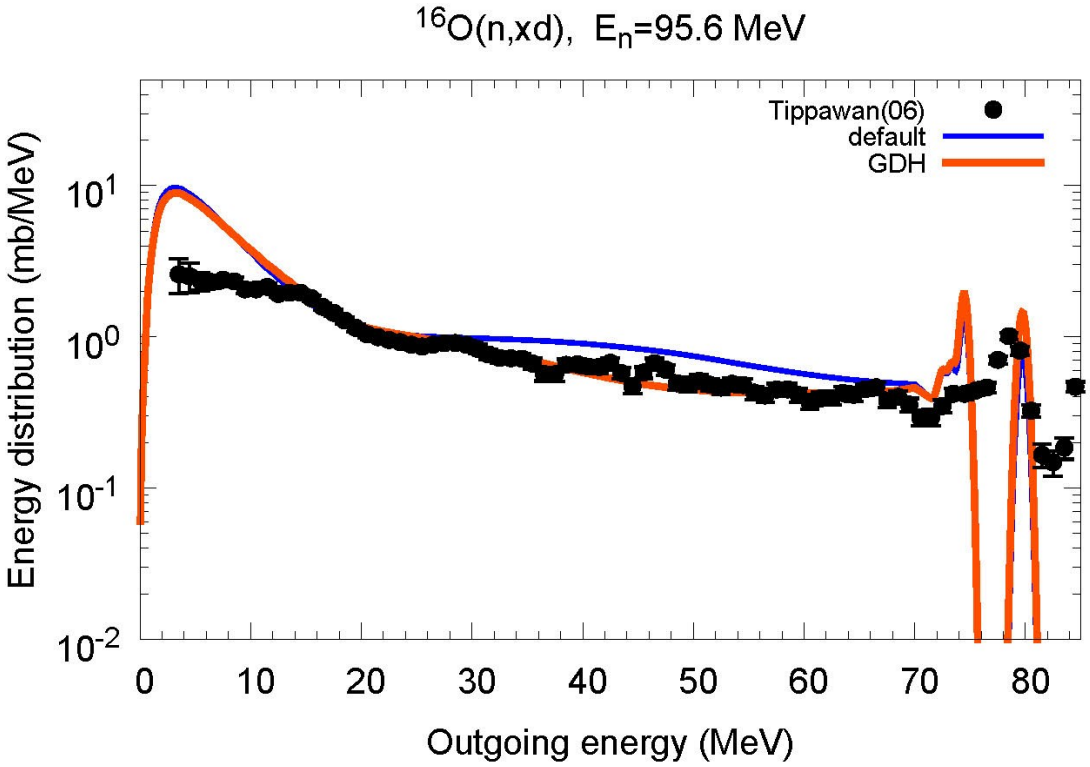
^{16}O(n,xd), E_n=95.6 MeV
Energy distribution (mb/MeV)
Outgoing energy (MeV)
Tippawan(06)
default
GDH

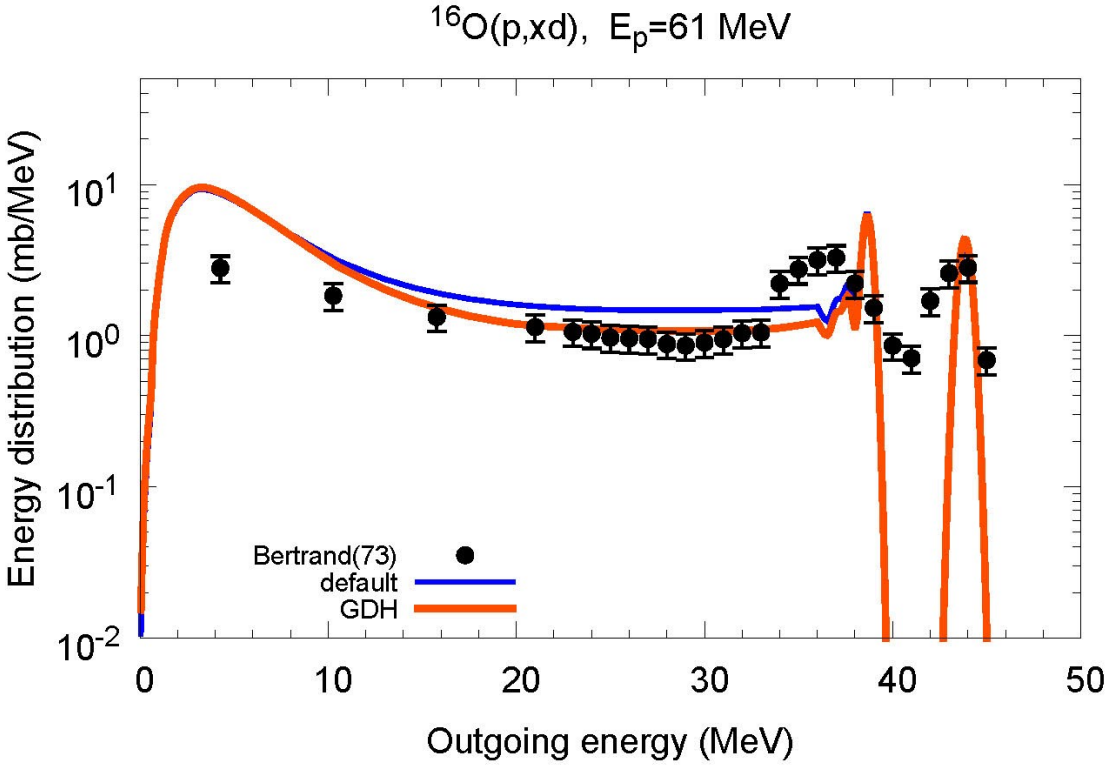
^{16}O(p,xd), E_p=61 MeV
Energy distribution (mb/MeV)
10^1
10^0
10^{-1}
10^{-2}
0
10
20
30
40
50
Outgoing energy (MeV)
Bertrand(73)
default
GDH

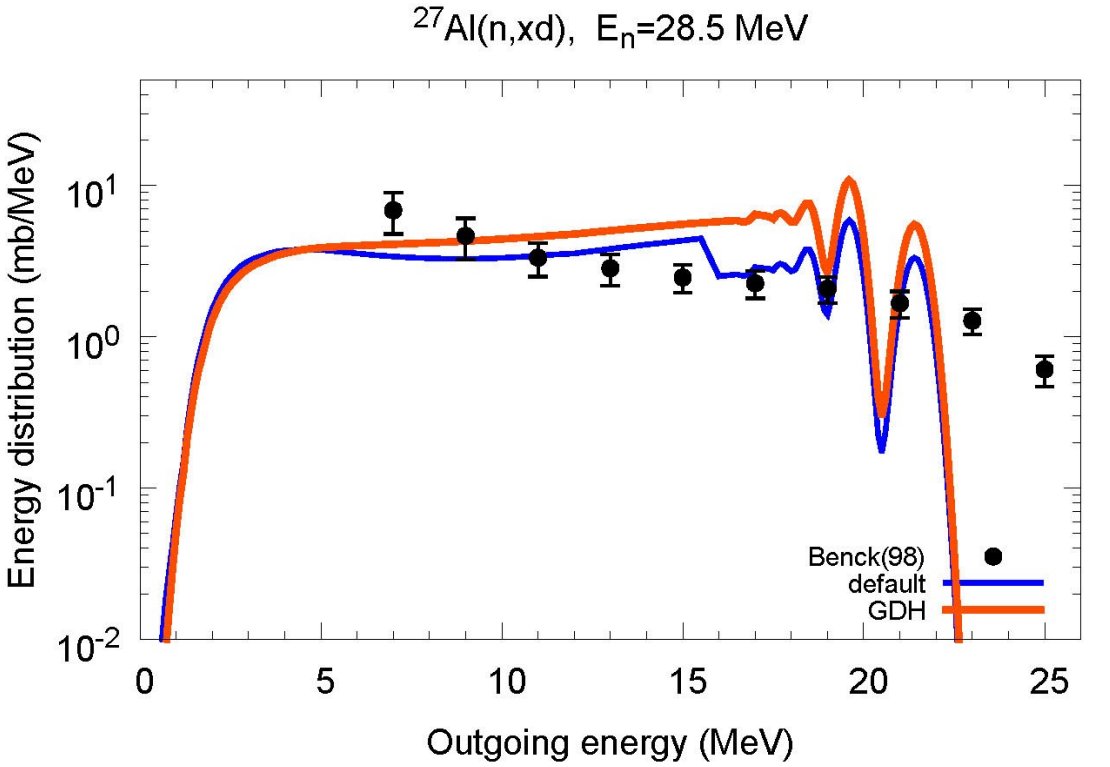
^{27}Al(n,xd), E_n=28.5 MeV
Energy distribution (mb/MeV)
10^1
10^0
10^{-1}
10^{-2}
0
5
10
15
20
25
Outgoing energy (MeV)
Benck(98)
default
GDH

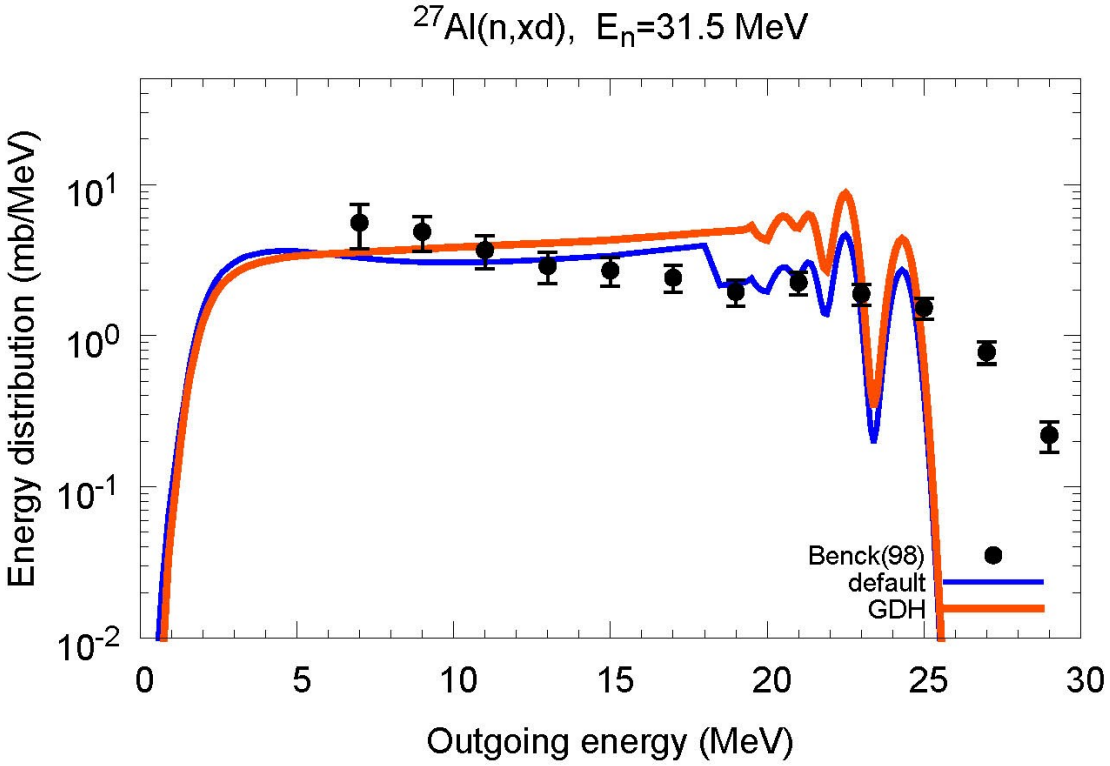
^{27}Al(n,xd), E_n=31.5 MeV
Energy distribution (mb/MeV)
10^1
10^0
10^{-1}
10^{-2}
0
5
10
15
20
25
30
Outgoing energy (MeV)
Benck(98)
default
GDH

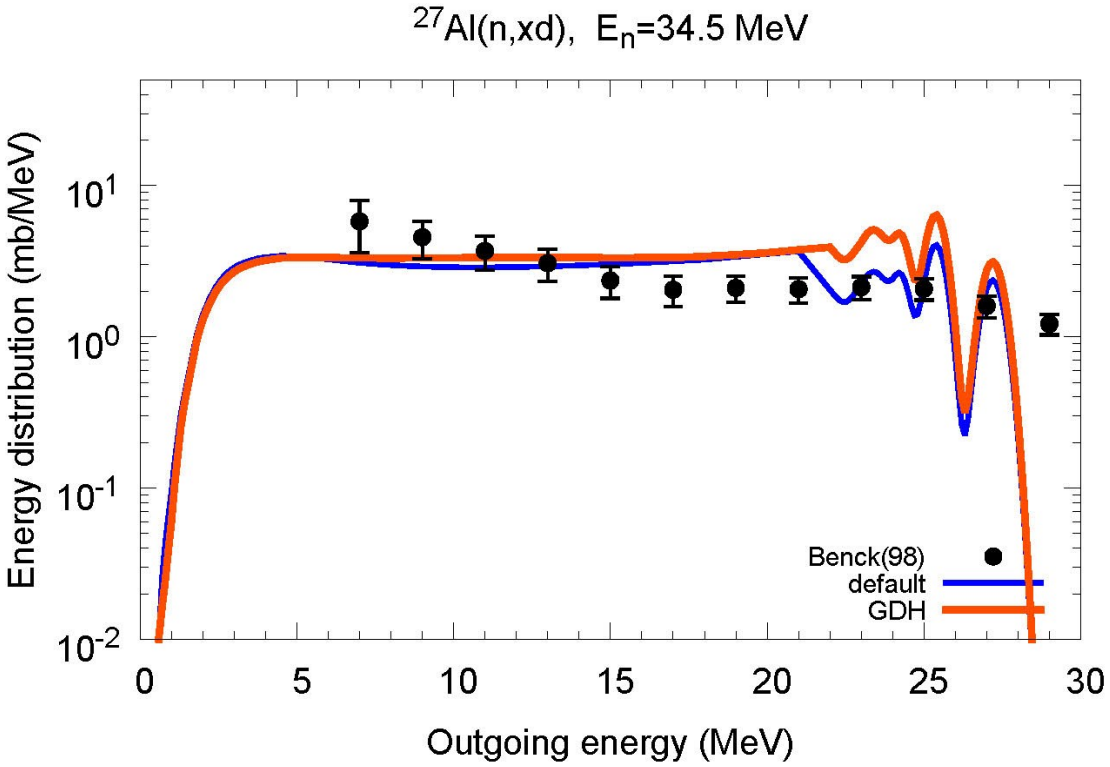
^{27}Al(n,xd), E_n=34.5 MeV
Energy distribution (mb/MeV)
10^1
10^0
10^{-1}
10^{-2}
0
5
10
15
20
25
30
Outgoing energy (MeV)
Benck(98)
default
GDH

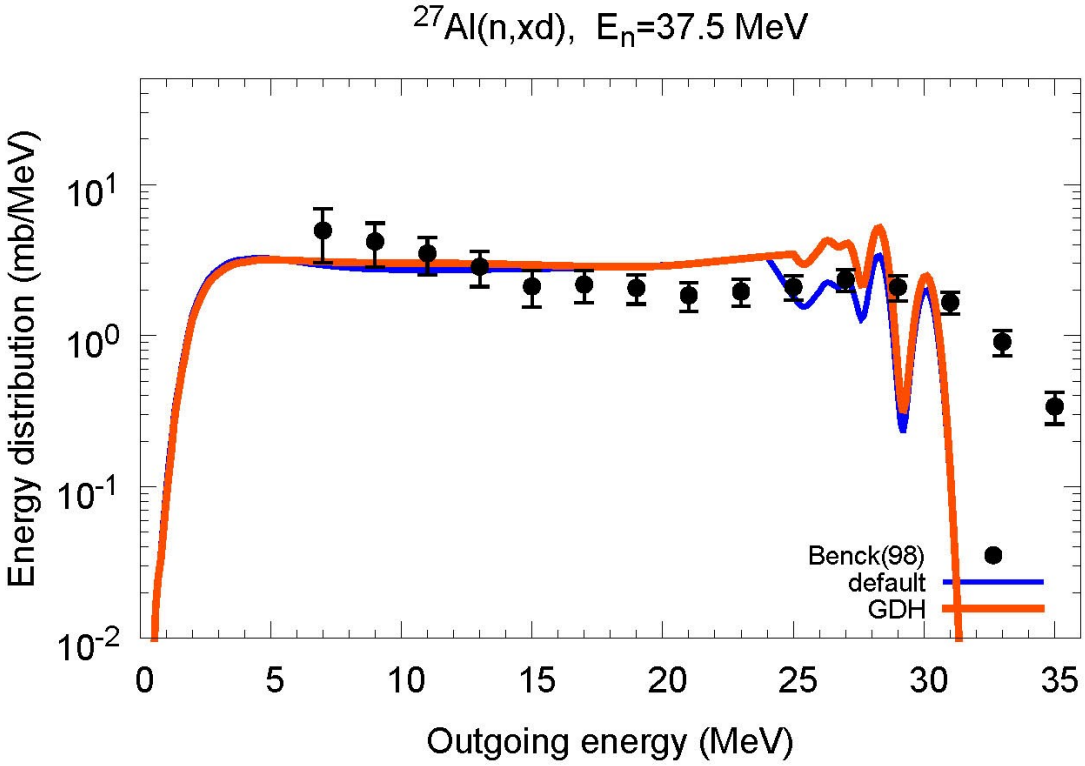
^{27}Al(n,xd), E_n=37.5 MeV
Energy distribution (mb/MeV)
10^1
10^0
10^{-1}
10^{-2}
0
5
10
15
20
25
30
35
Outgoing energy (MeV)
Benck(98)
default
GDH

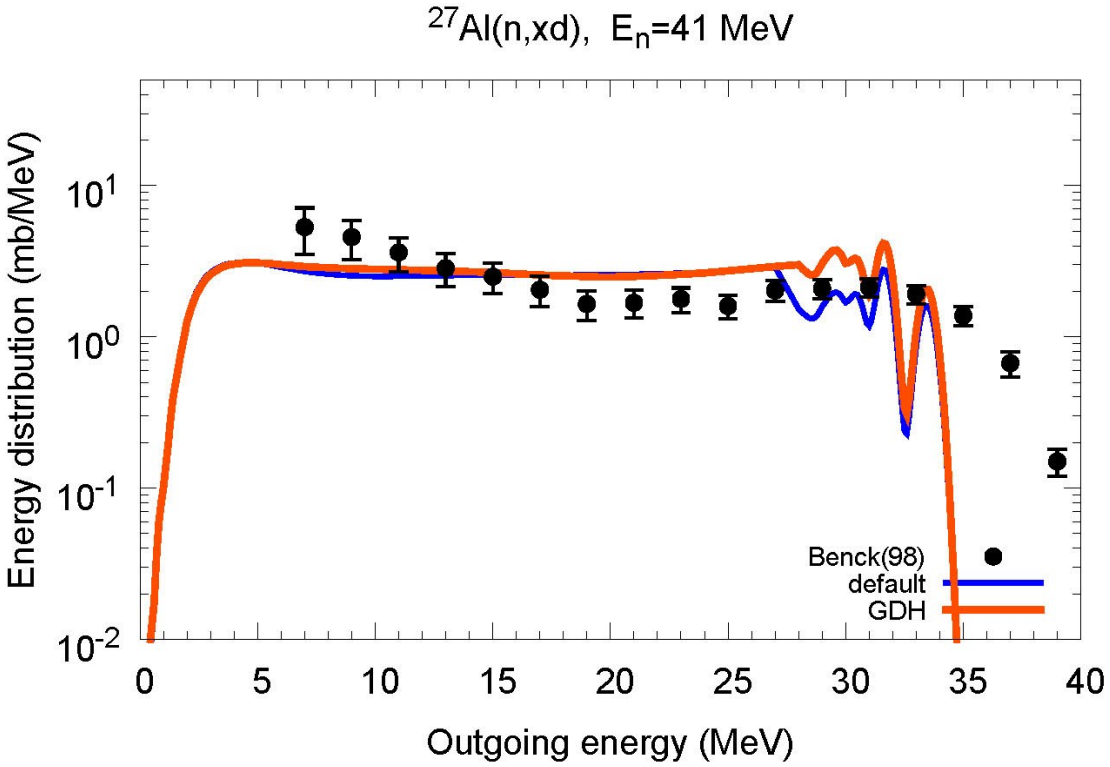
^{27}Al(n,xd), E_n=41 MeV
Energy distribution (mb/MeV)
10^1
10^0
10^{-1}
10^{-2}
0
5
10
15
20
25
30
35
40
Outgoing energy (MeV)
Benck(98)
default
GDH

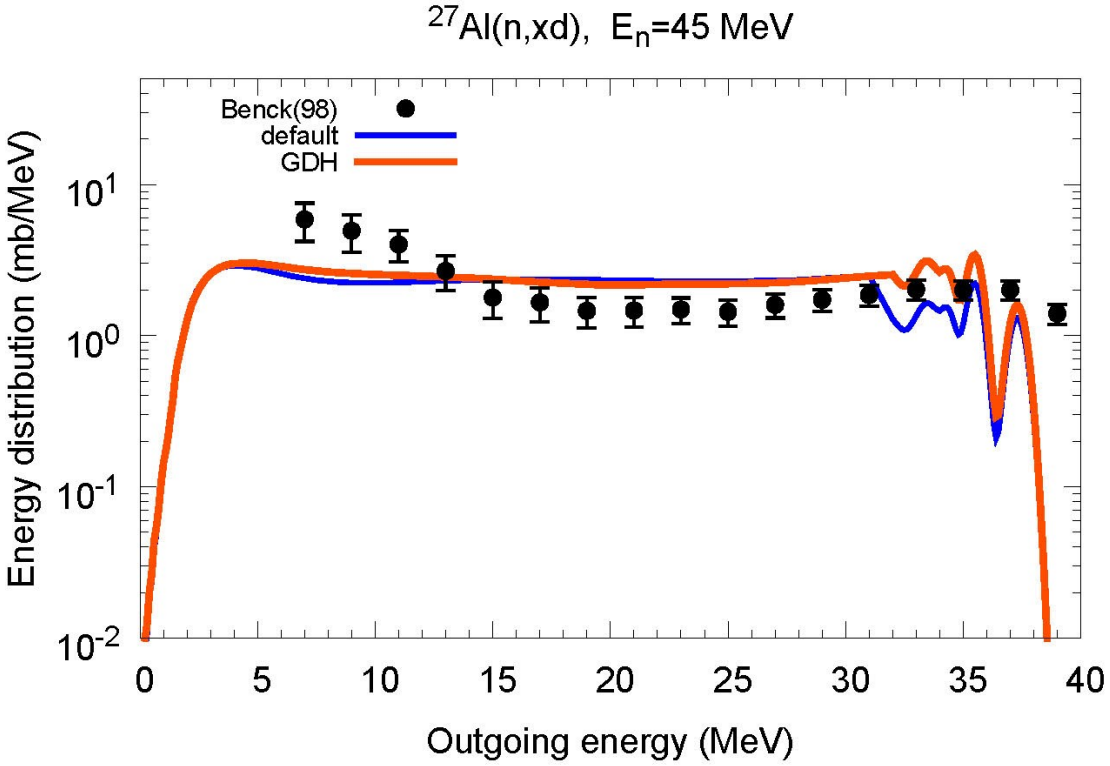
^{27}Al(n,xd), E_n=45 MeV
Benck(98)
default
GDH
Energy distribution (mb/MeV)
10^{1}
10^{0}
10^{-1}
10^{-2}
0
5
10
15
20
25
30
35
40
Outgoing energy (MeV)

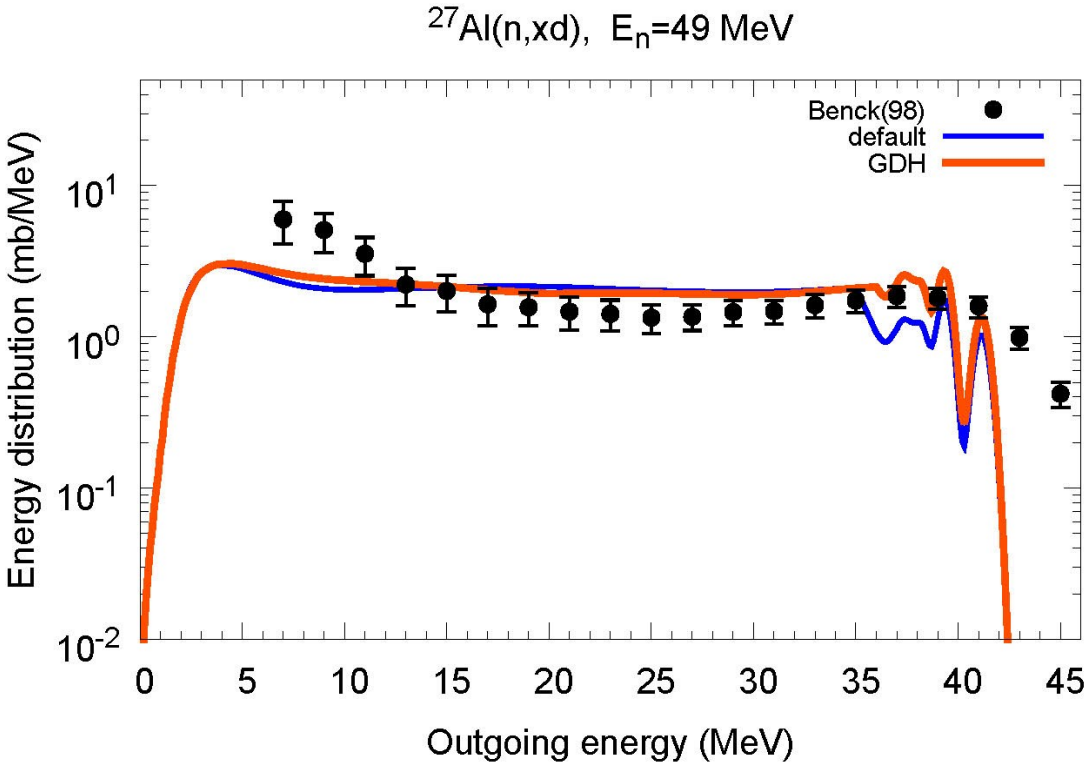
^{27}Al(n,xd), E_n=49 MeV
Benck(98)
default
GDH
Energy distribution (mb/MeV)
10^{1}
10^{0}
10^{-1}
10^{-2}
0
5
10
15
20
25
30
35
40
45
Outgoing energy (MeV)

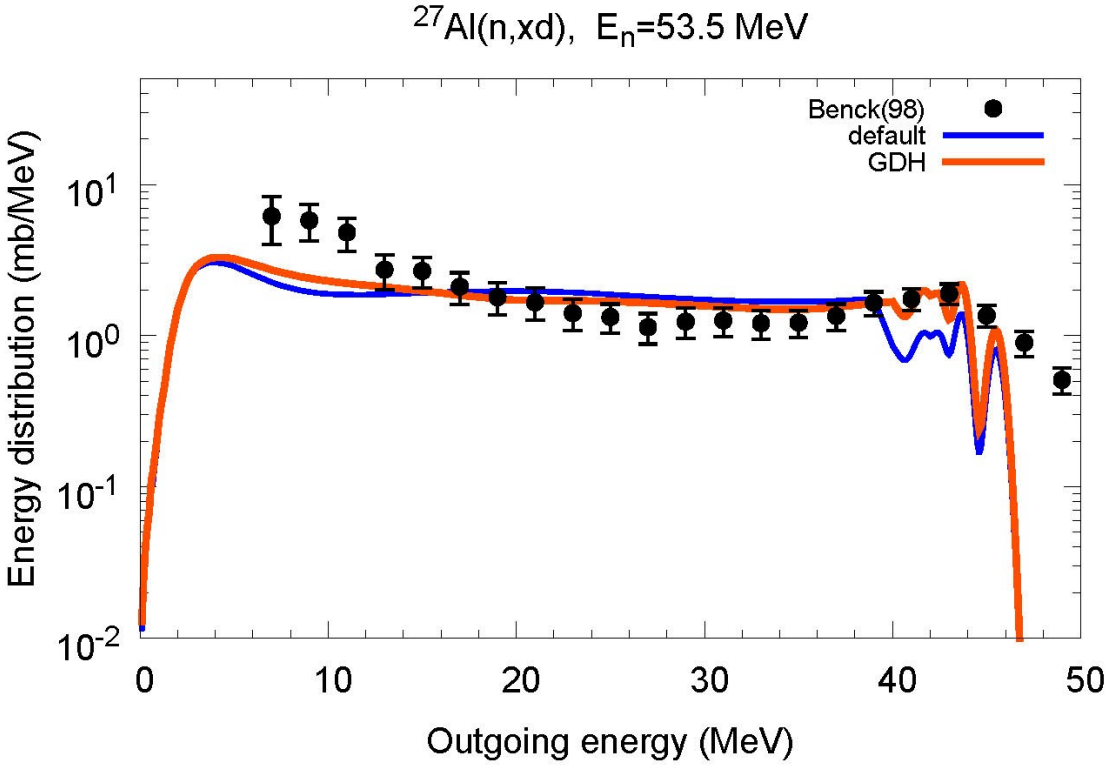
^{27}Al(n,xd), E_n=53.5 MeV
Benck(98)
default
GDH
Energy distribution (mb/MeV)
10^1
10^0
10^{-1}
10^{-2}
0
10
20
30
40
50
Outgoing energy (MeV)

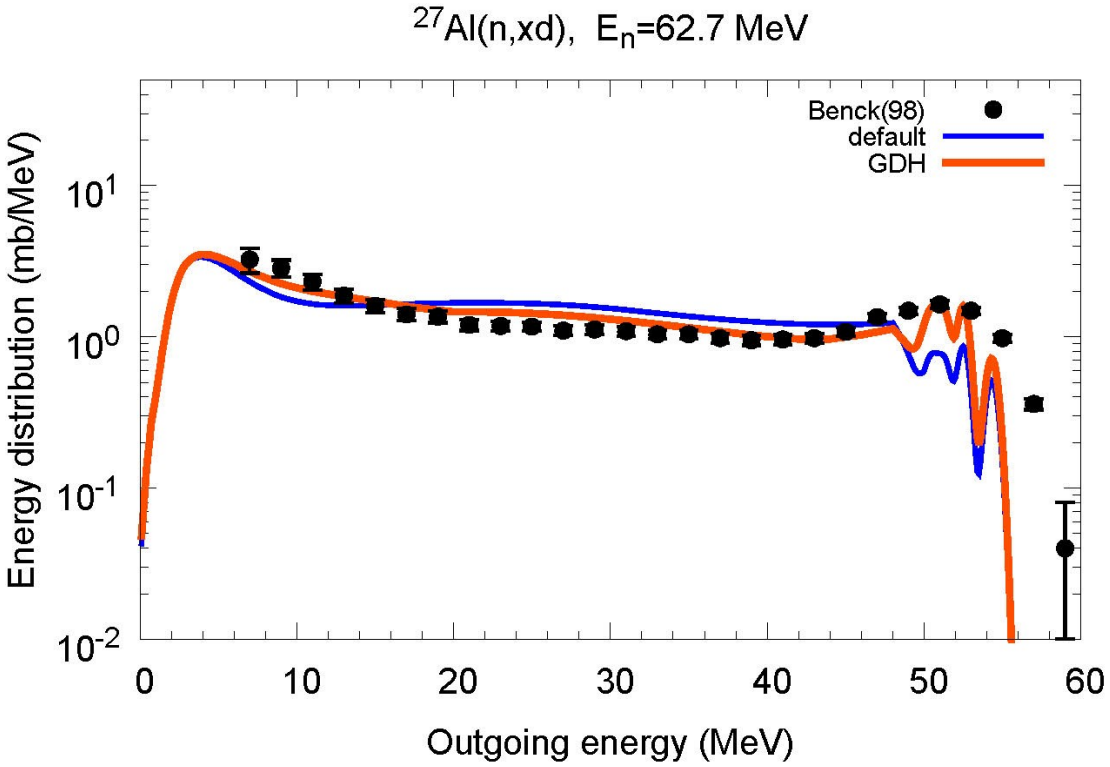
^{27}Al(n,xd), E_n=62.7 MeV
Benck(98)
default
GDH
Energy distribution (mb/MeV)
10^1
10^0
10^{-1}
10^{-2}
0
10
20
30
40
50
60
Outgoing energy (MeV)

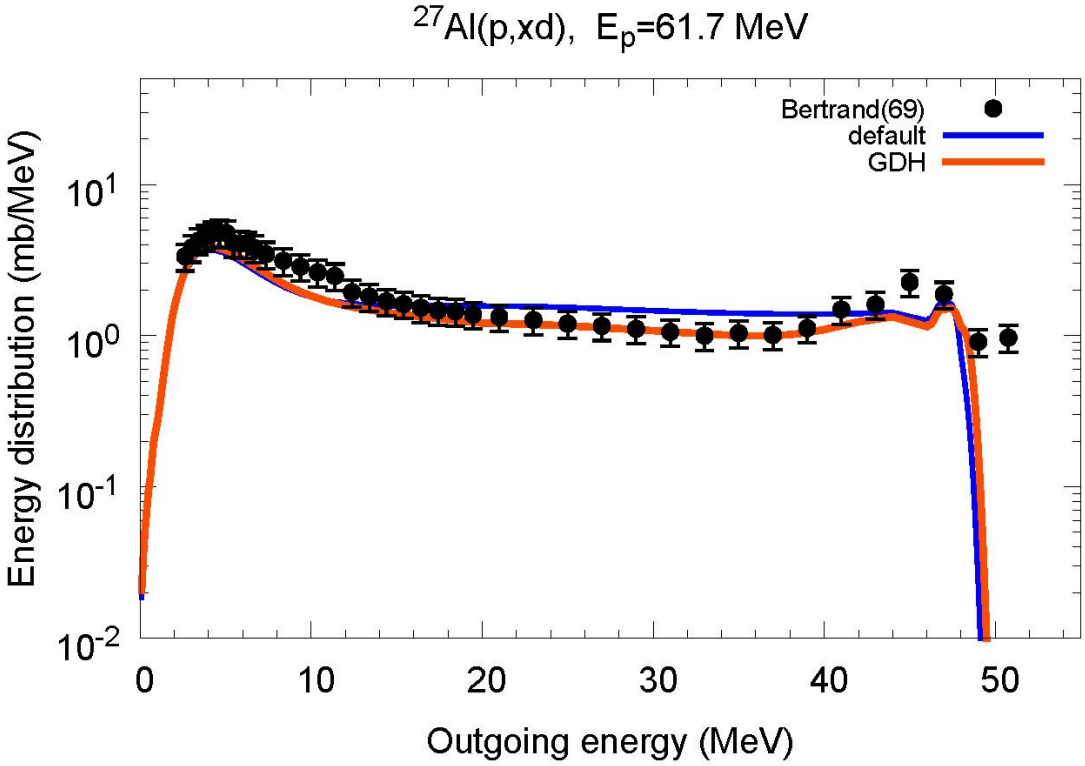
^{27}Al(p,xd), E_p=61.7 MeV
Bertrand(69)
default
GDH
Energy distribution (mb/MeV)
10^{1}
10^{0}
10^{-1}
10^{-2}
0
10
20
30
40
50
Outgoing energy (MeV)

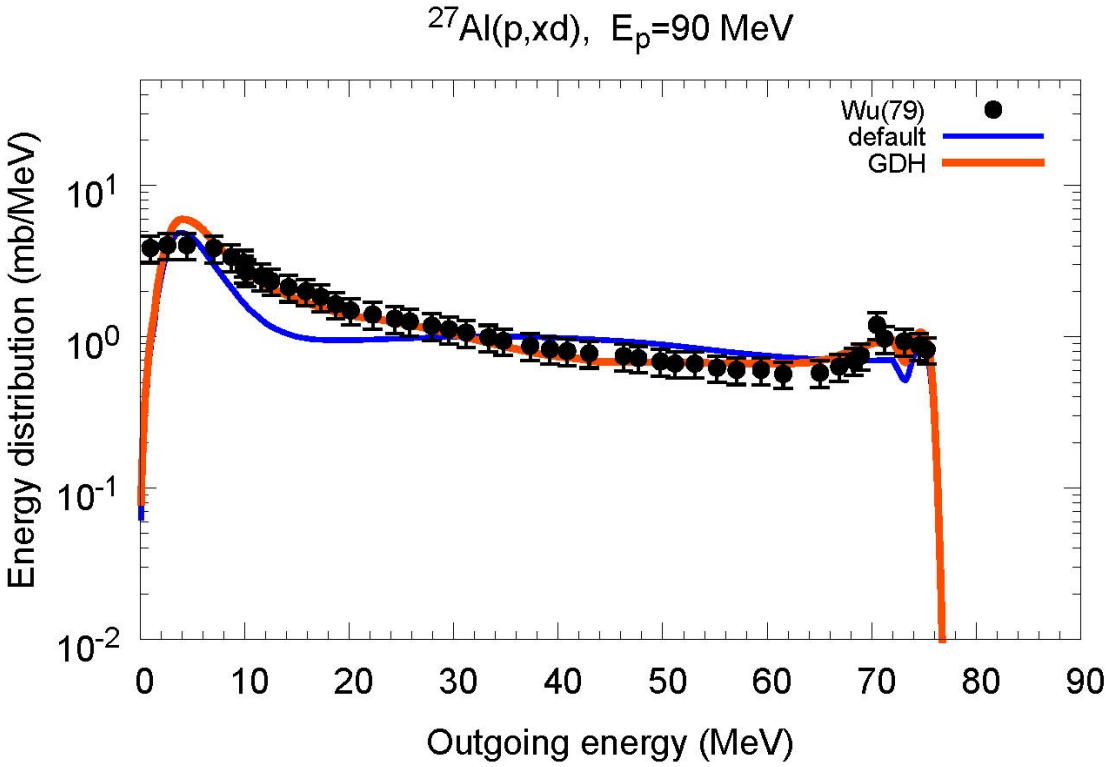
^{27}Al(p,xd), E_p=90 MeV
Wu(79)
default
GDH
Energy distribution (mb/MeV)
10^{1}
10^{0}
10^{-1}
10^{-2}
0
10
20
30
40
50
60
70
80
90
Outgoing energy (MeV)

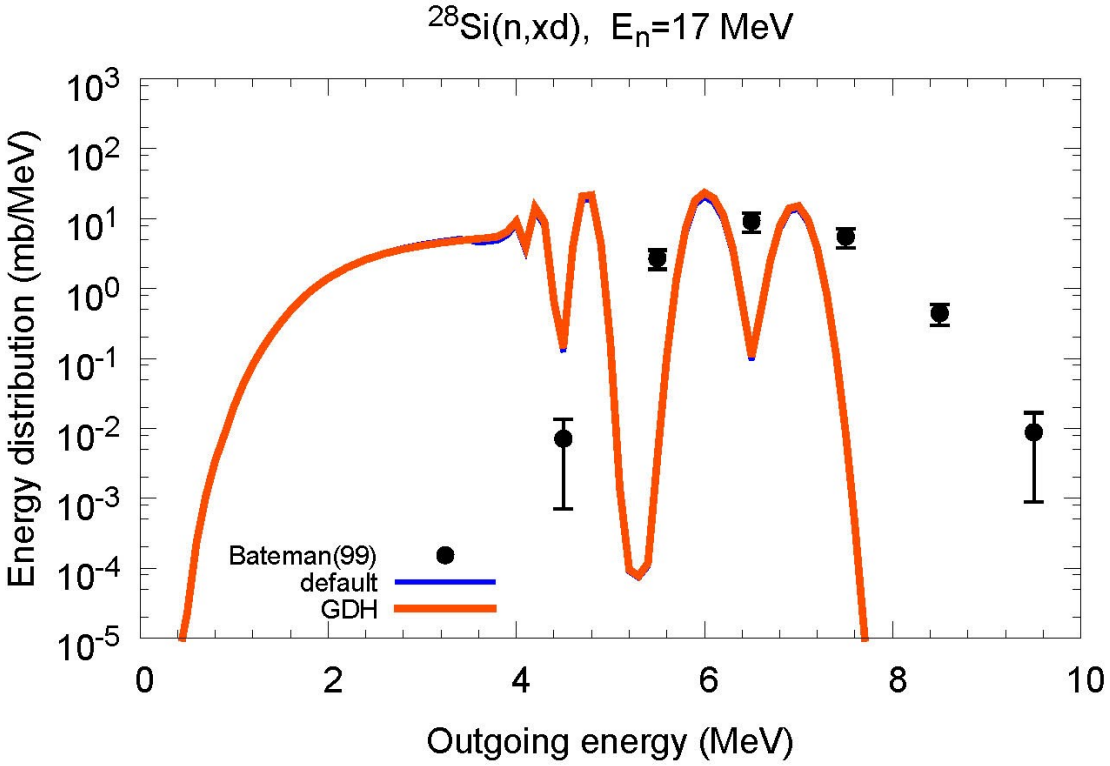
^{28}Si(n,xd), E_n=17 MeV
Energy distribution (mb/MeV)
Outgoing energy (MeV)
Bateman(99)
default
GDH

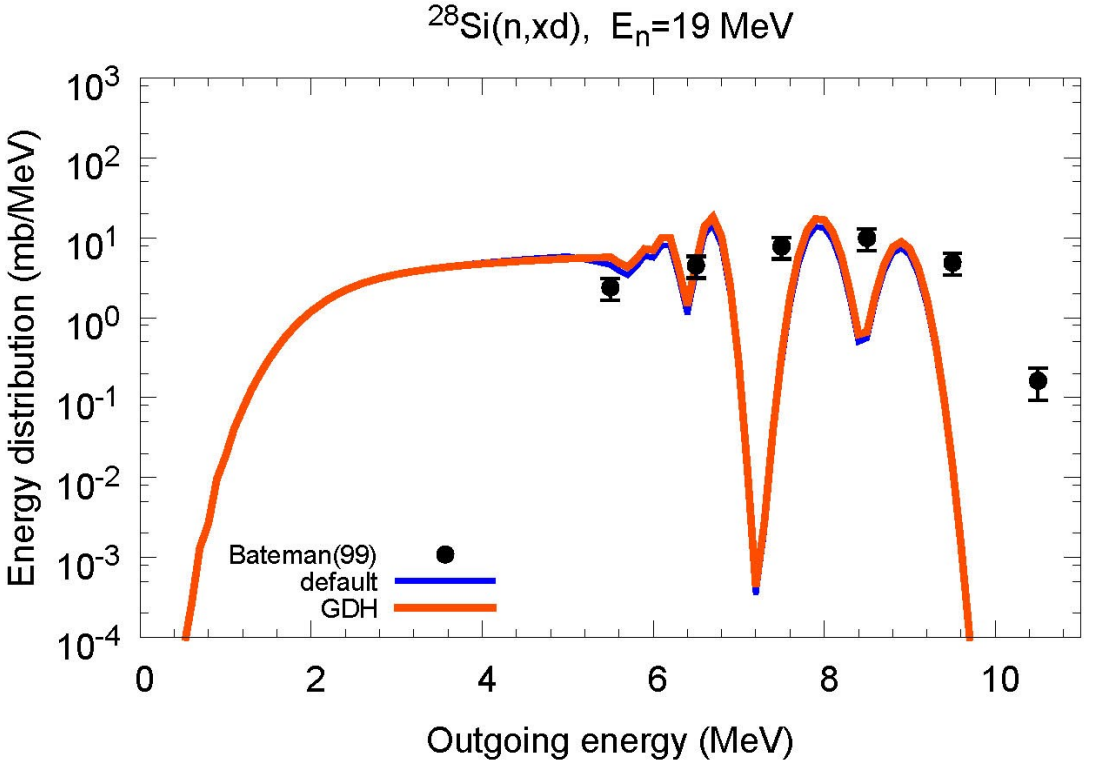
^{28}Si(n,xd), E_n=19 MeV
Energy distribution (mb/MeV)
Outgoing energy (MeV)
Bateman(99)
default
GDH

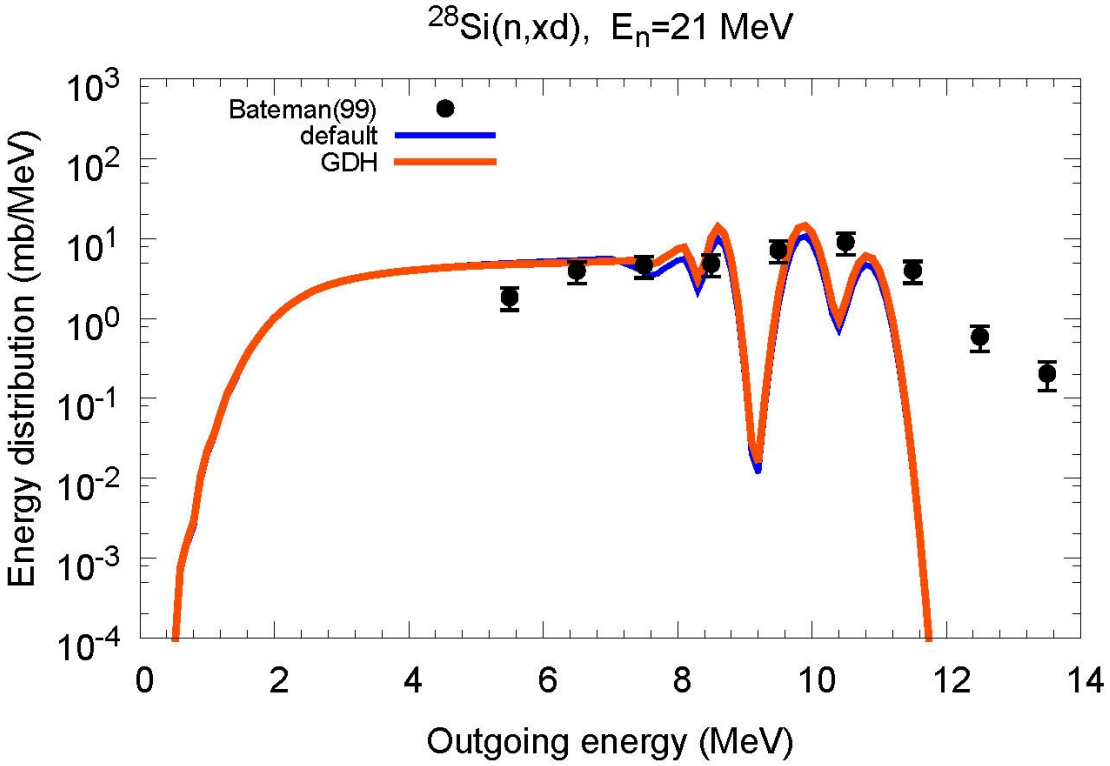
^{28}Si(n,xd), E_n=21 MeV
Bateman(99)
default
GDH
Energy distribution (mb/MeV)
Outgoing energy (MeV)

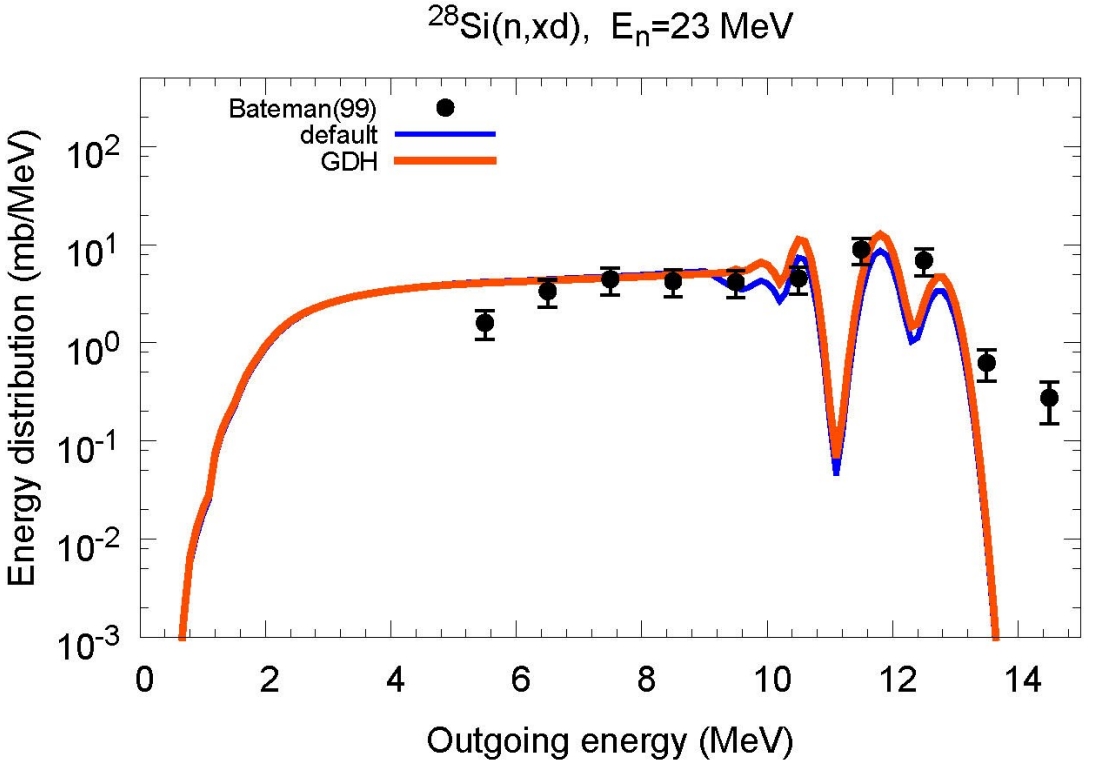
^{28}Si(n,xd), E_n=23 MeV
Bateman(99)
default
GDH
Energy distribution (mb/MeV)
Outgoing energy (MeV)

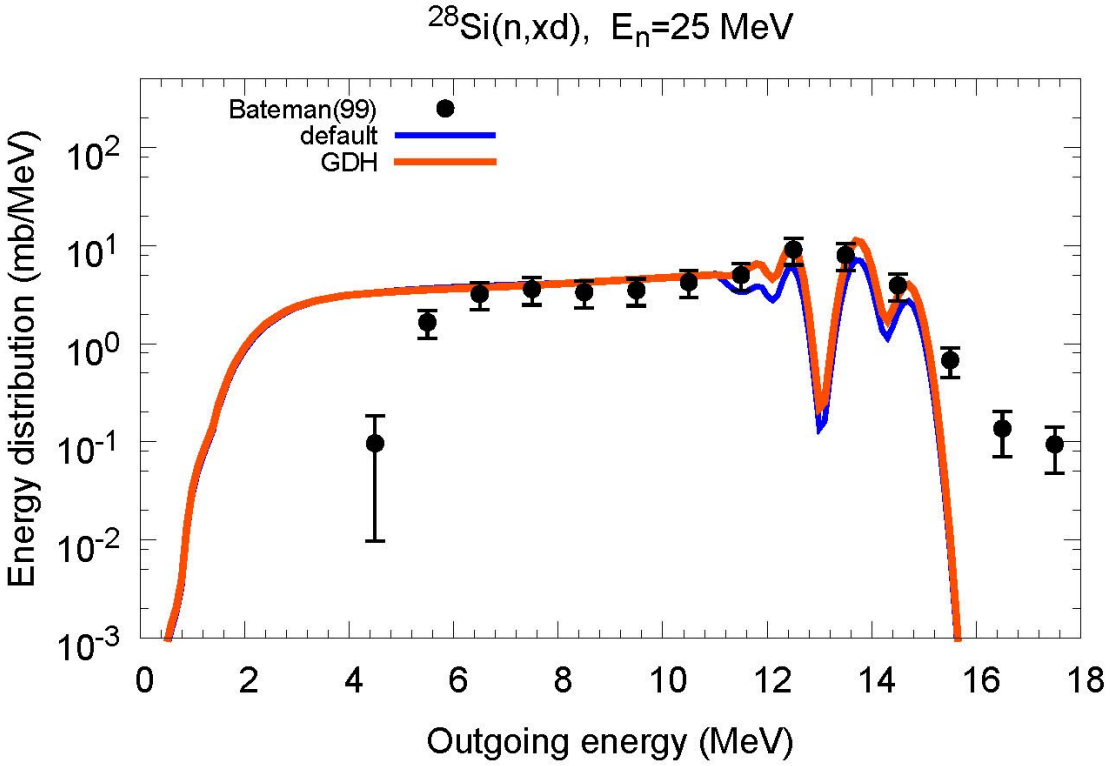
^{28}Si(n,xd), E_n=25 MeV
Bateman(99)
default
GDH
Energy distribution (mb/MeV)
10^{2}
10^{1}
10^{0}
10^{-1}
10^{-2}
10^{-3}
0
2
4
6
8
10
12
14
16
18
Outgoing energy (MeV)

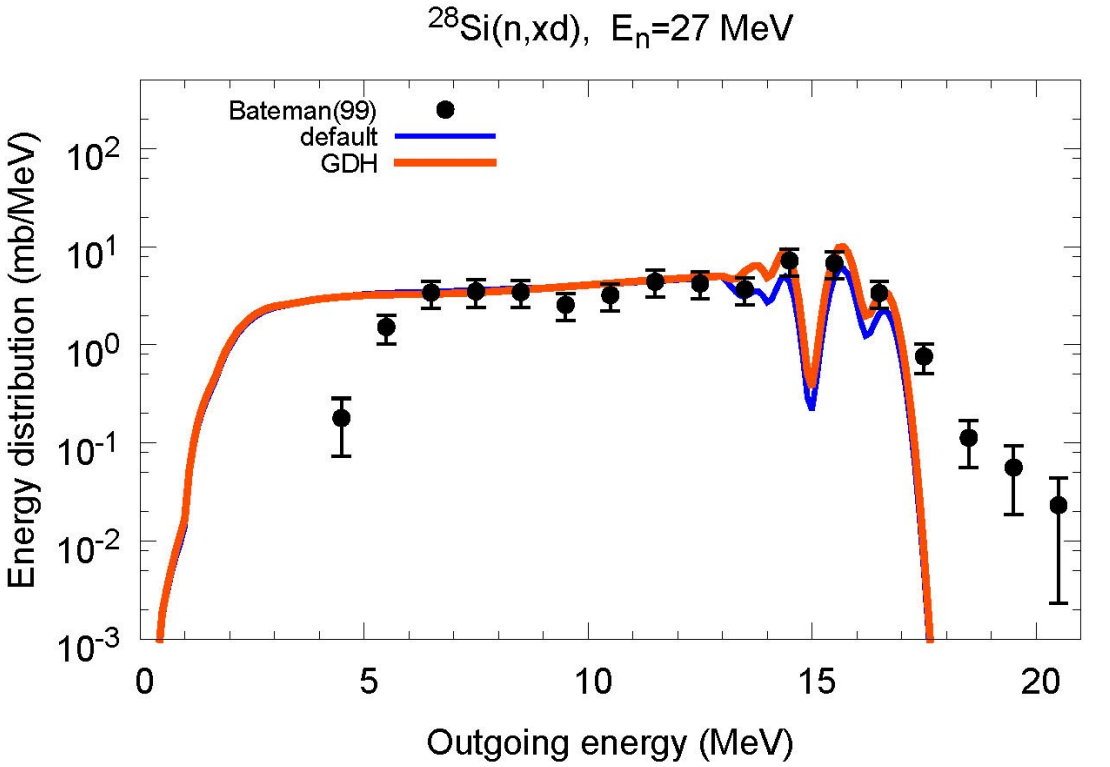
^{28}Si(n,xd), E_n=27 MeV
Bateman(99)
default
GDH
Energy distribution (mb/MeV)
10^{2}
10^{1}
10^{0}
10^{-1}
10^{-2}
10^{-3}
0
5
10
15
20
Outgoing energy (MeV)

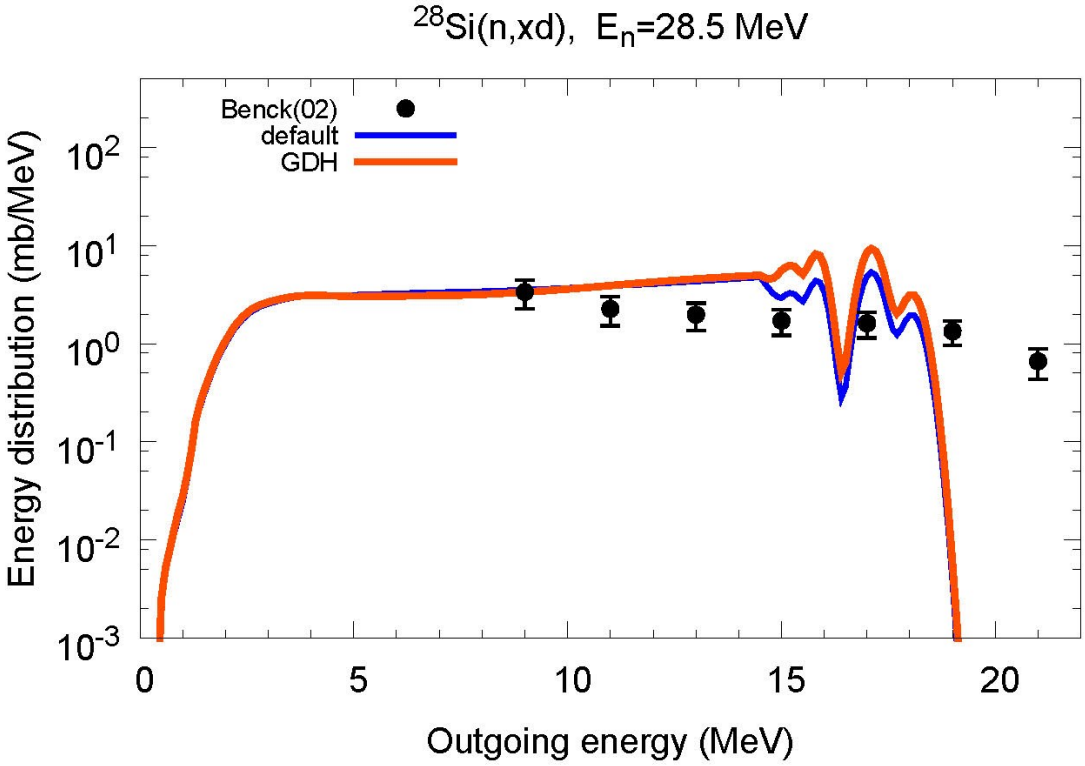
^{28}Si(n,xd), E_n=28.5 MeV
Benck(02)
default
GDH
Energy distribution (mb/MeV)
10^2
10^1
10^0
10^{-1}
10^{-2}
10^{-3}
0
5
10
15
20
Outgoing energy (MeV)

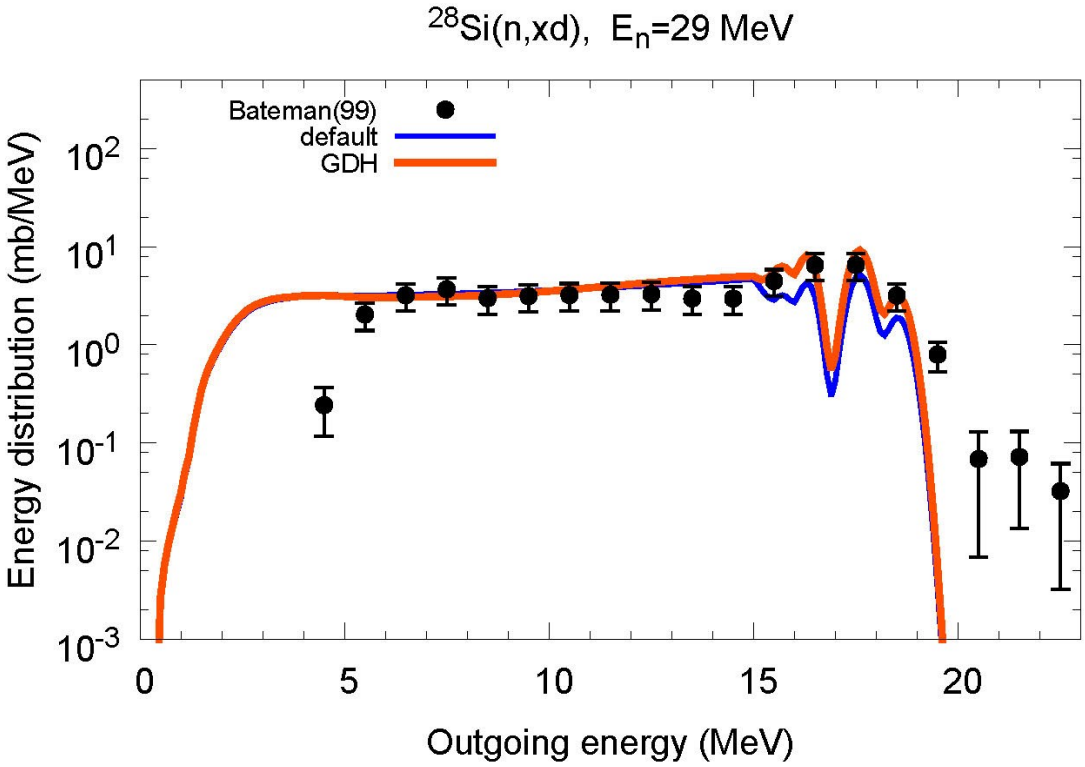
^{28}Si(n,xd), E_n=29 MeV
Bateman(99)
default
GDH
Energy distribution (mb/MeV)
10^2
10^1
10^0
10^{-1}
10^{-2}
10^{-3}
0
5
10
15
20
Outgoing energy (MeV)

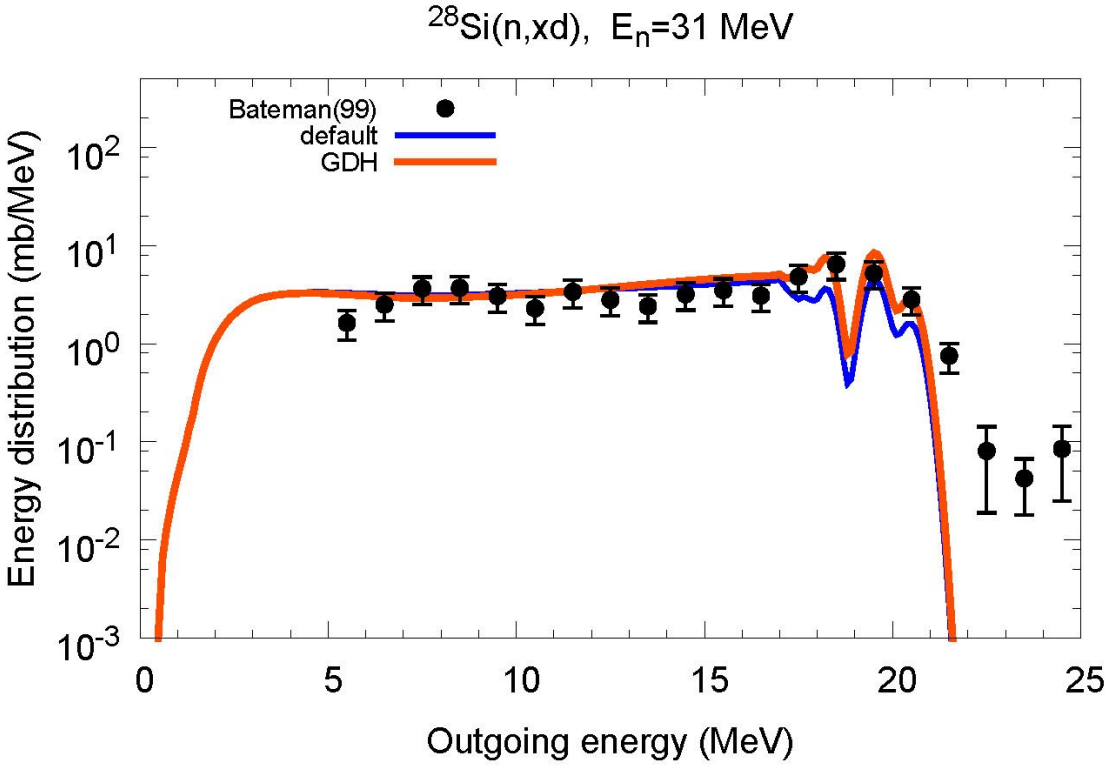
^{28}Si(n,xd), E_n=31 MeV
Bateman(99)
default
GDH
Energy distribution (mb/MeV)
Outgoing energy (MeV)

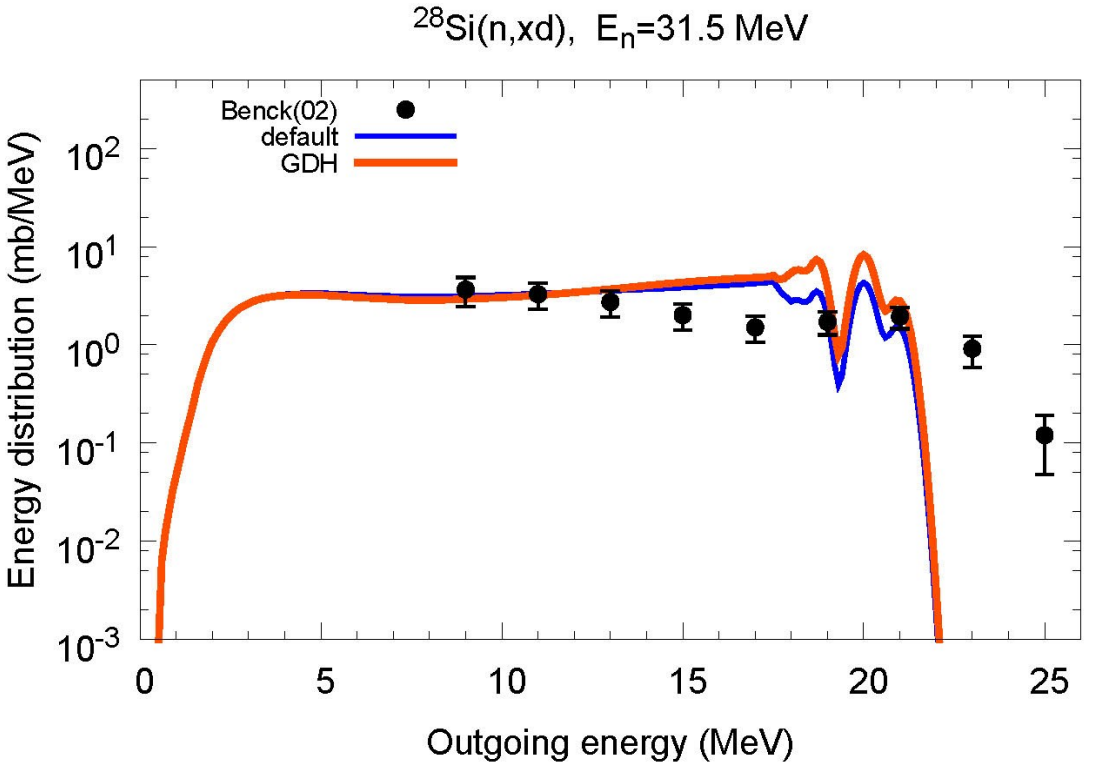
^{28}Si(n,xd), E_n=31.5 MeV
Benck(02)
default
GDH
Energy distribution (mb/MeV)
Outgoing energy (MeV)

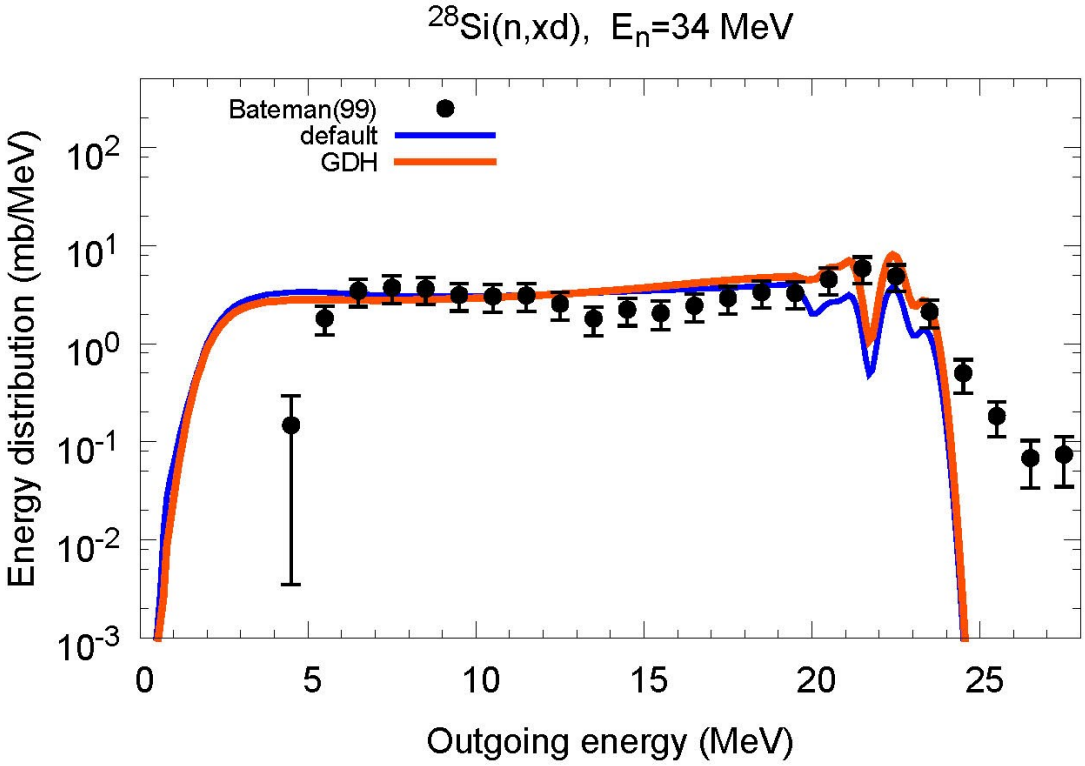
^{28}Si(n,xd), E_n=34 MeV
Bateman(99)
default
GDH
Energy distribution (mb/MeV)
Outgoing energy (MeV)

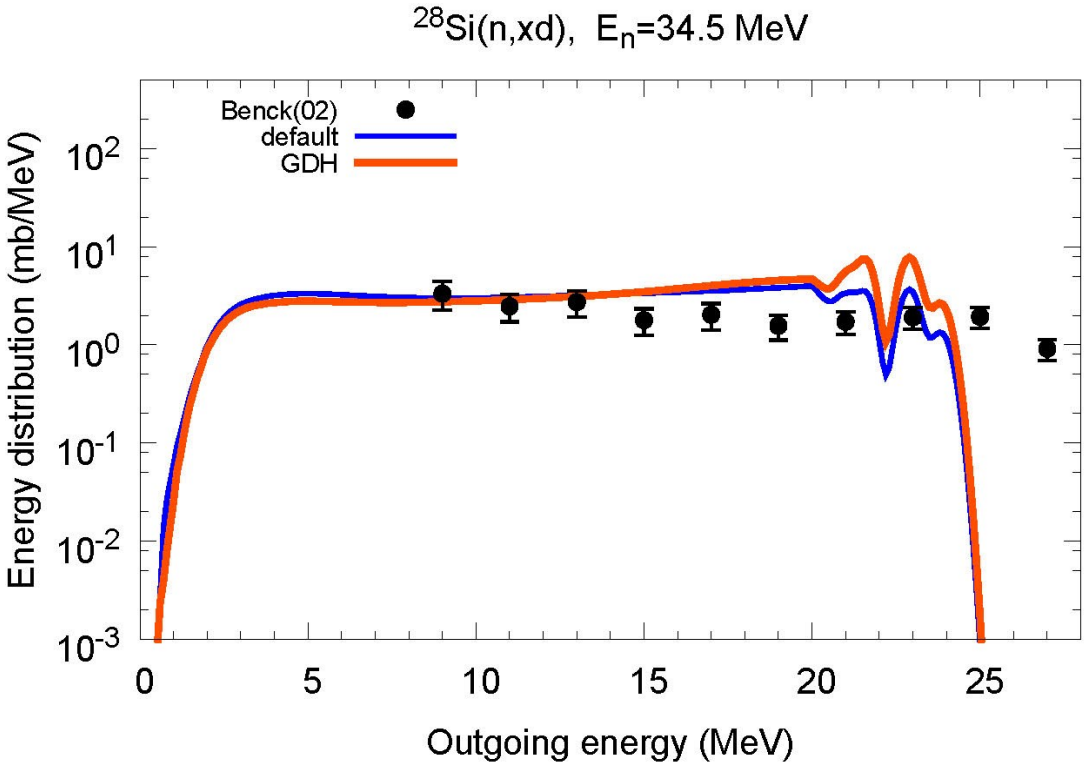
^{28}Si(n,xd), E_n=34.5 MeV
Benck(02)
default
GDH
Energy distribution (mb/MeV)
Outgoing energy (MeV)

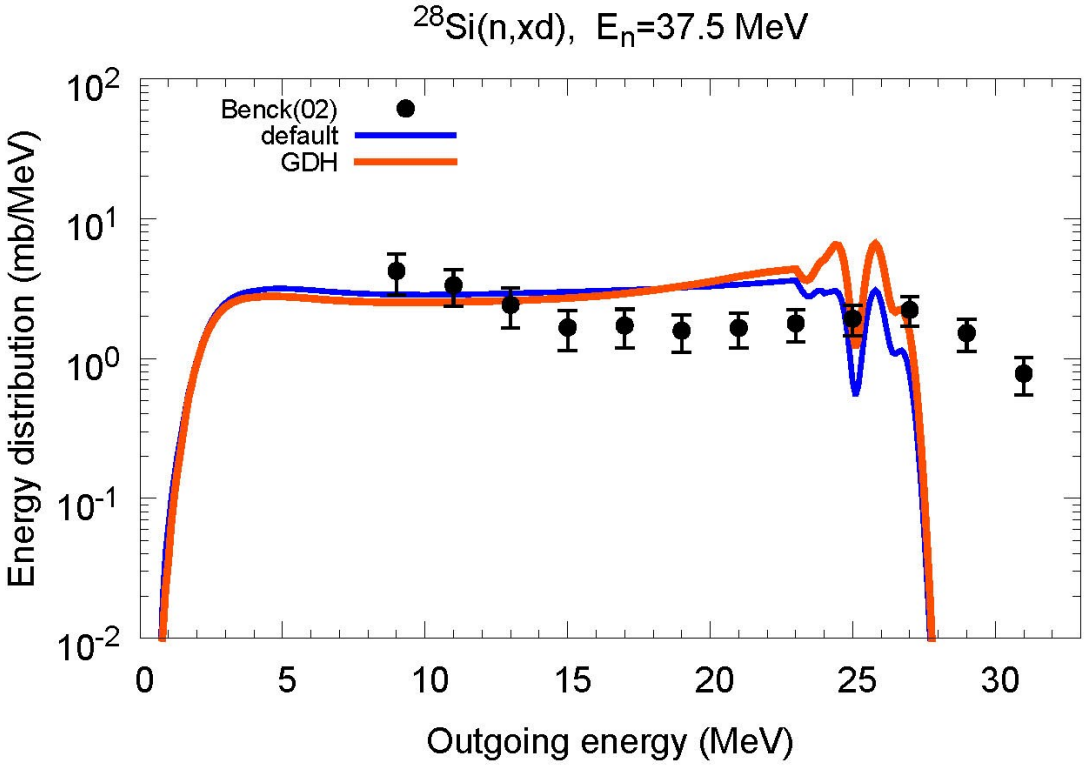
^{28}Si(n,xd), E_n=37.5 MeV
Benck(02)
default
GDH
Energy distribution (mb/MeV)
Outgoing energy (MeV)

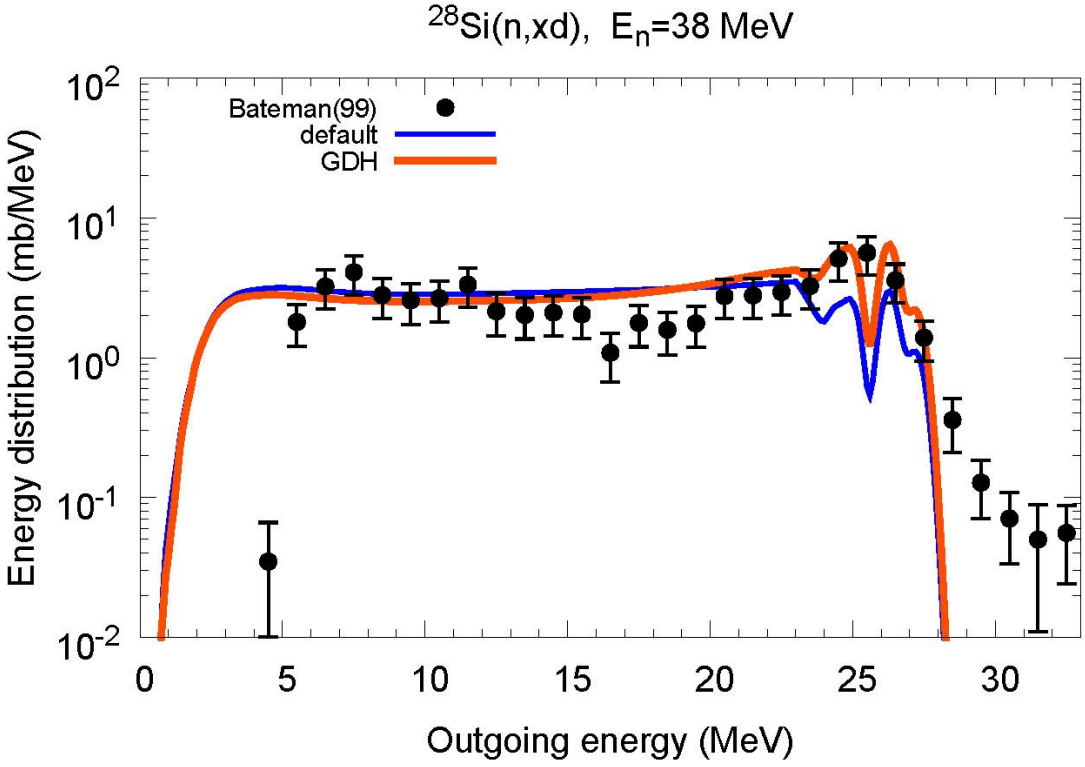
^{28}Si(n,xd), E_n=38 MeV
Bateman(99)
default
GDH
Energy distribution (mb/MeV)
Outgoing energy (MeV)

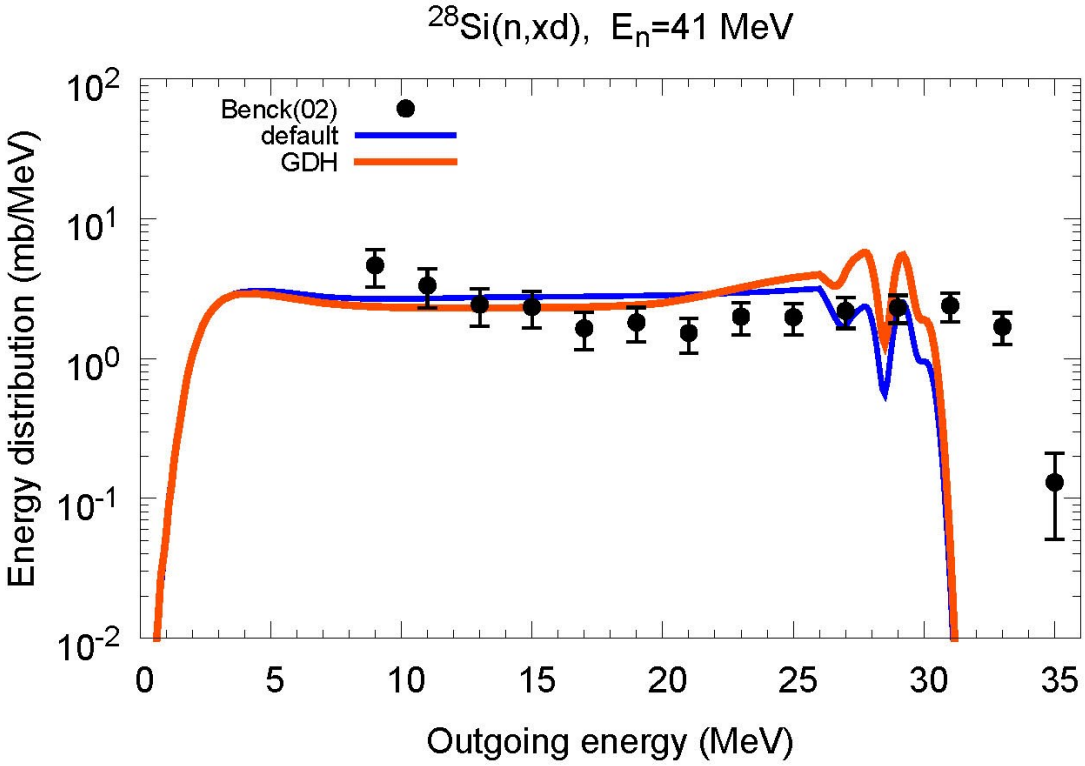
^{28}Si(n,xd), E_n=41 MeV
Benck(02)
default
GDH
Energy distribution (mb/MeV)
Outgoing energy (MeV)

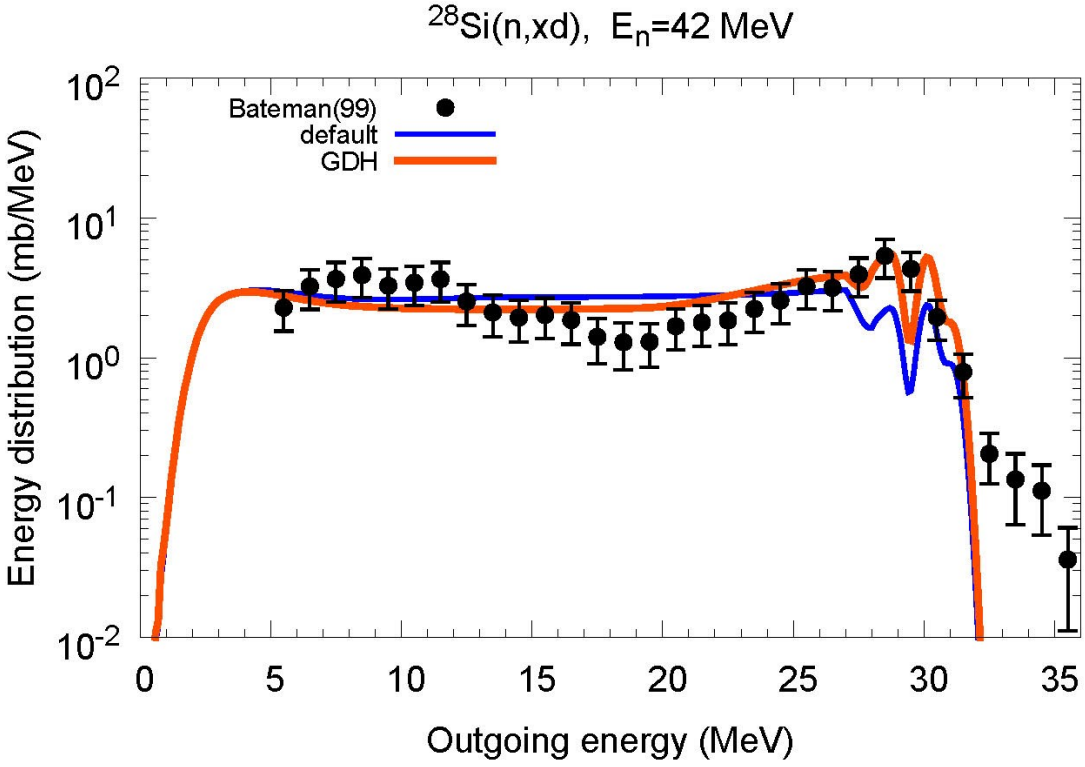
^{28}Si(n,xd), E_n=42 MeV
Bateman(99)
default
GDH
Energy distribution (mb/MeV)
Outgoing energy (MeV)

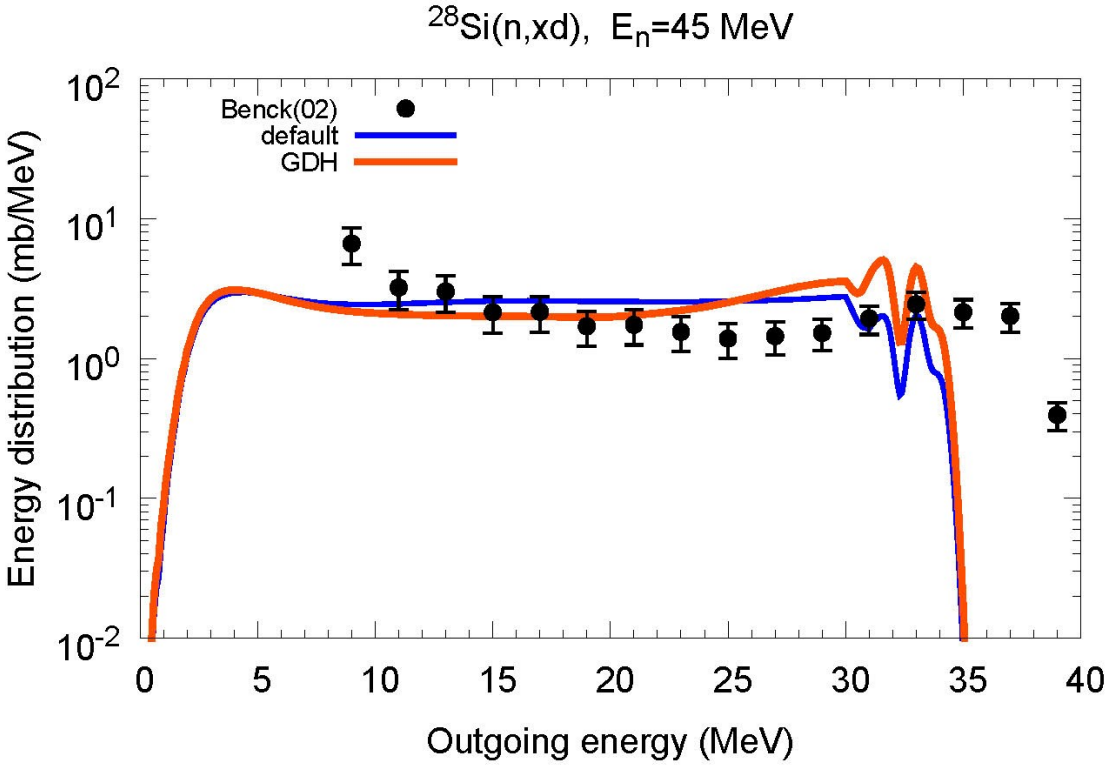
^{28}Si(n,xd), E_n=45 MeV
Benck(02)
default
GDH
Energy distribution (mb/MeV)
Outgoing energy (MeV)

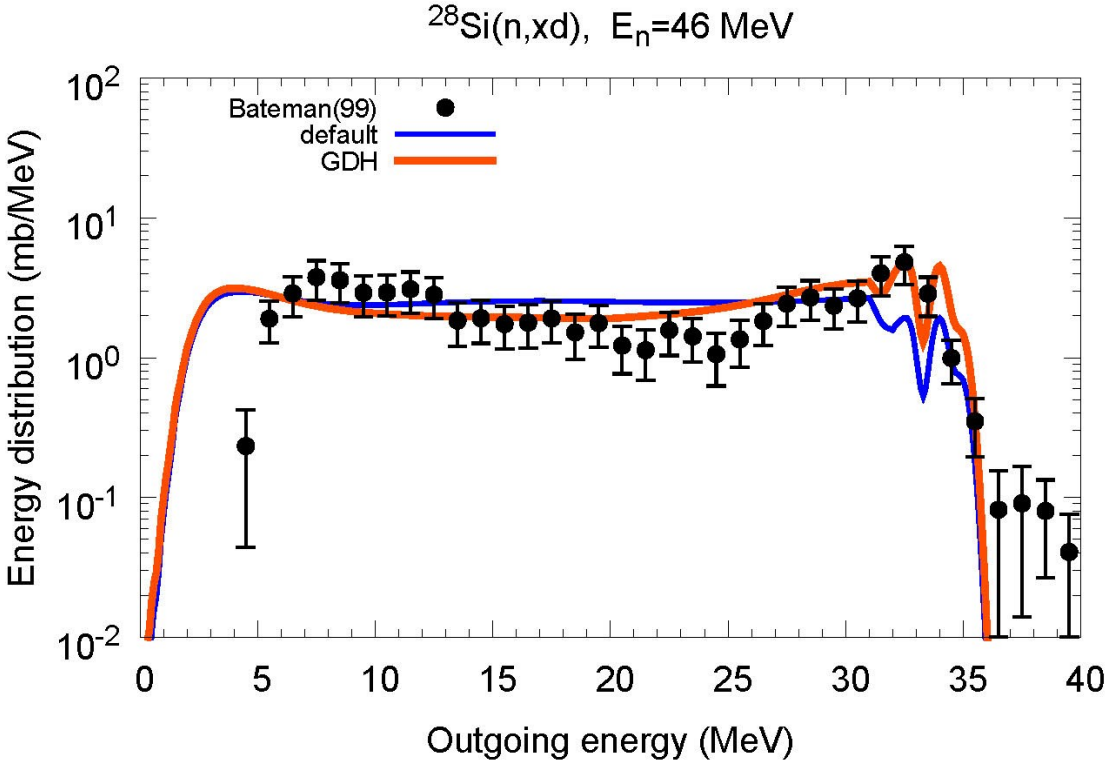
^{28}Si(n,xd), E_n=46 MeV
Bateman(99)
default
GDH
Energy distribution (mb/MeV)
Outgoing energy (MeV)

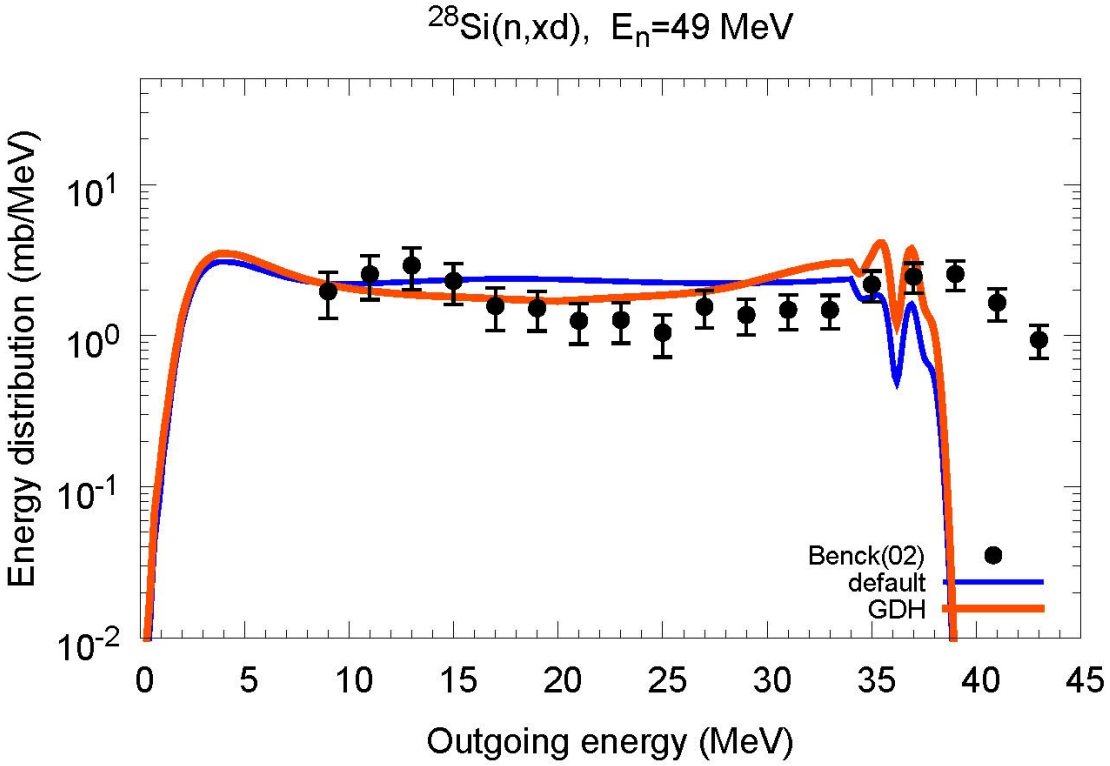
^{28}Si(n,xd), E_n=49 MeV
Energy distribution (mb/MeV)
Outgoing energy (MeV)
Benck(02)
default
GDH

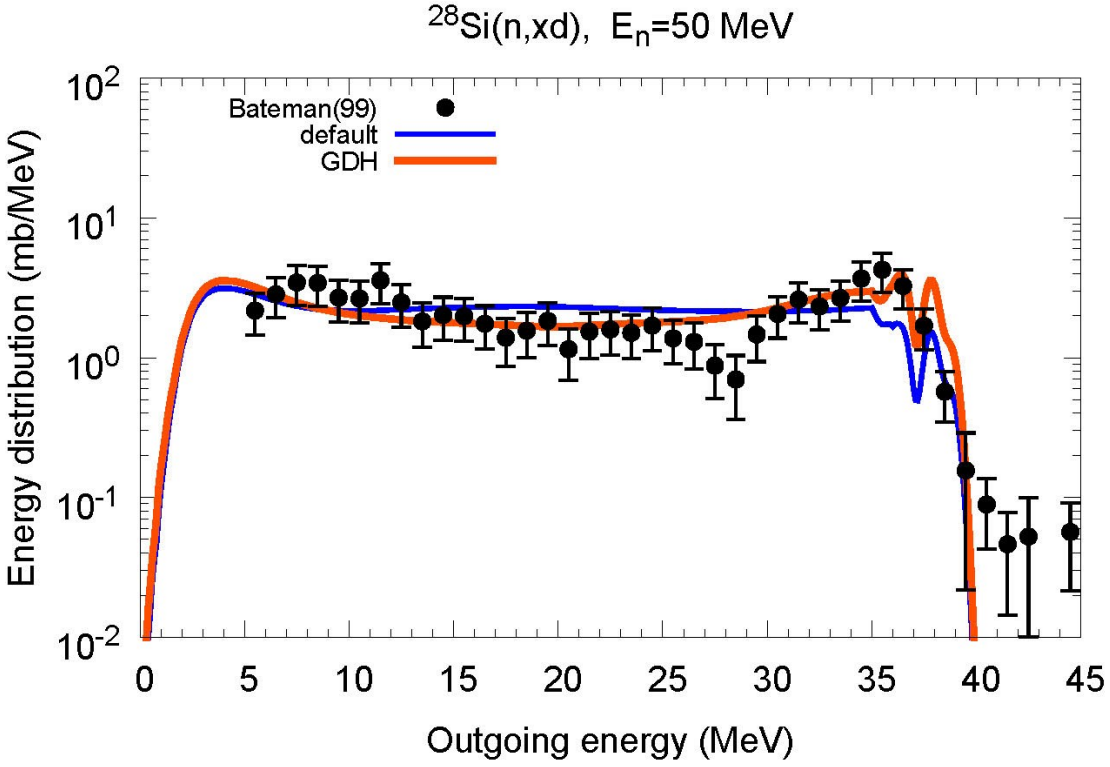
^{28}Si(n,xd), E_n=50 MeV
Energy distribution (mb/MeV)
Outgoing energy (MeV)
Bateman(99)
default
GDH

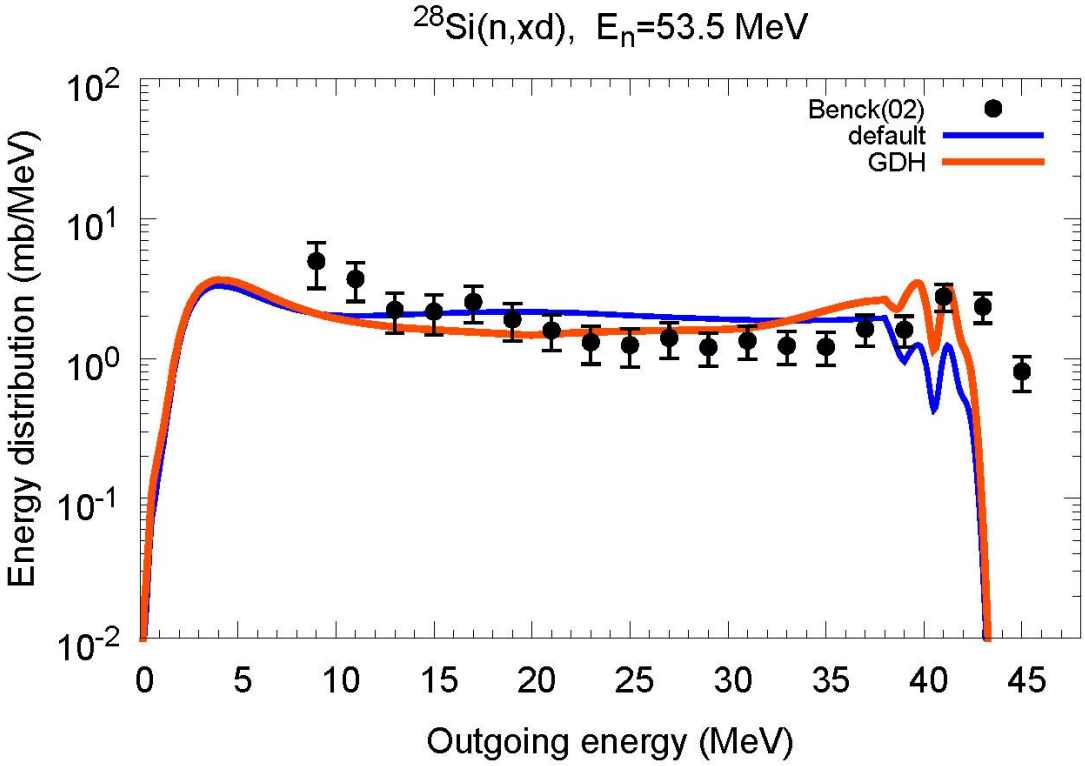
^{28}Si(n,xd), E_n=53.5 MeV
Benck(02)
default
GDH
Energy distribution (mb/MeV)
Outgoing energy (MeV)
10^2
10^1
10^0
10^{-1}
10^{-2}
0
5
10
15
20
25
30
35
40
45

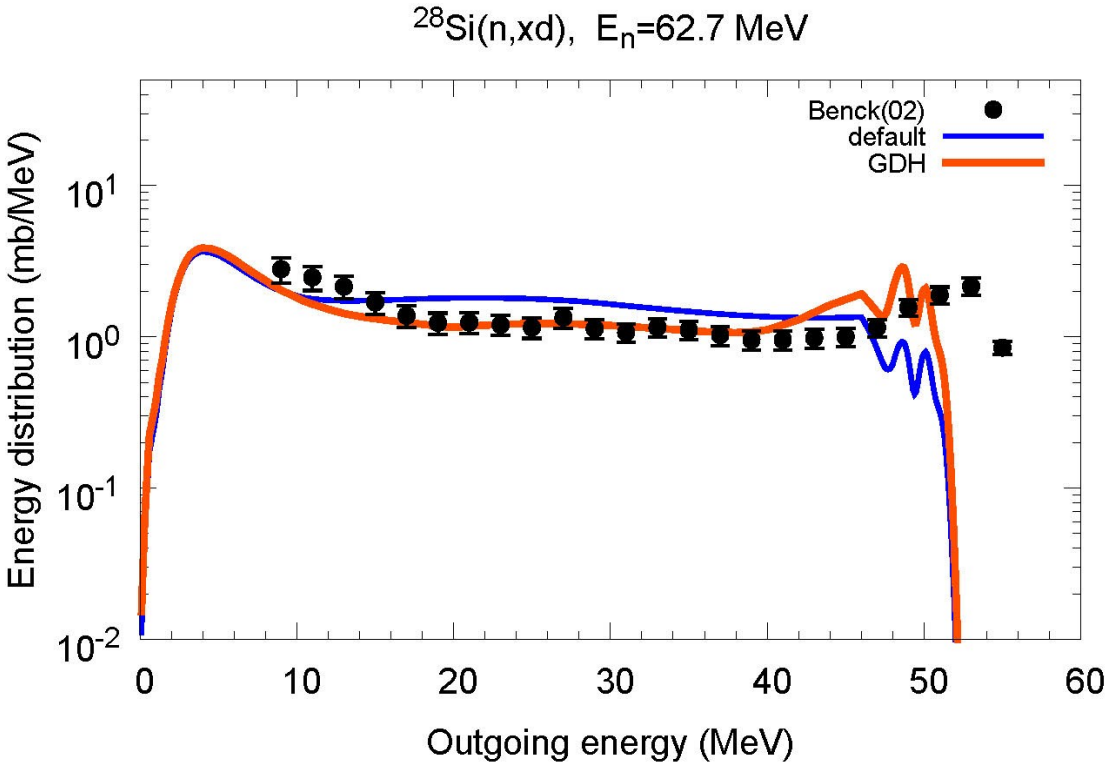
^{28}Si(n,xd), E_n=62.7 MeV
Benck(02)
default
GDH
Energy distribution (mb/MeV)
Outgoing energy (MeV)
10^1
10^0
10^{-1}
10^{-2}
0
10
20
30
40
50
60

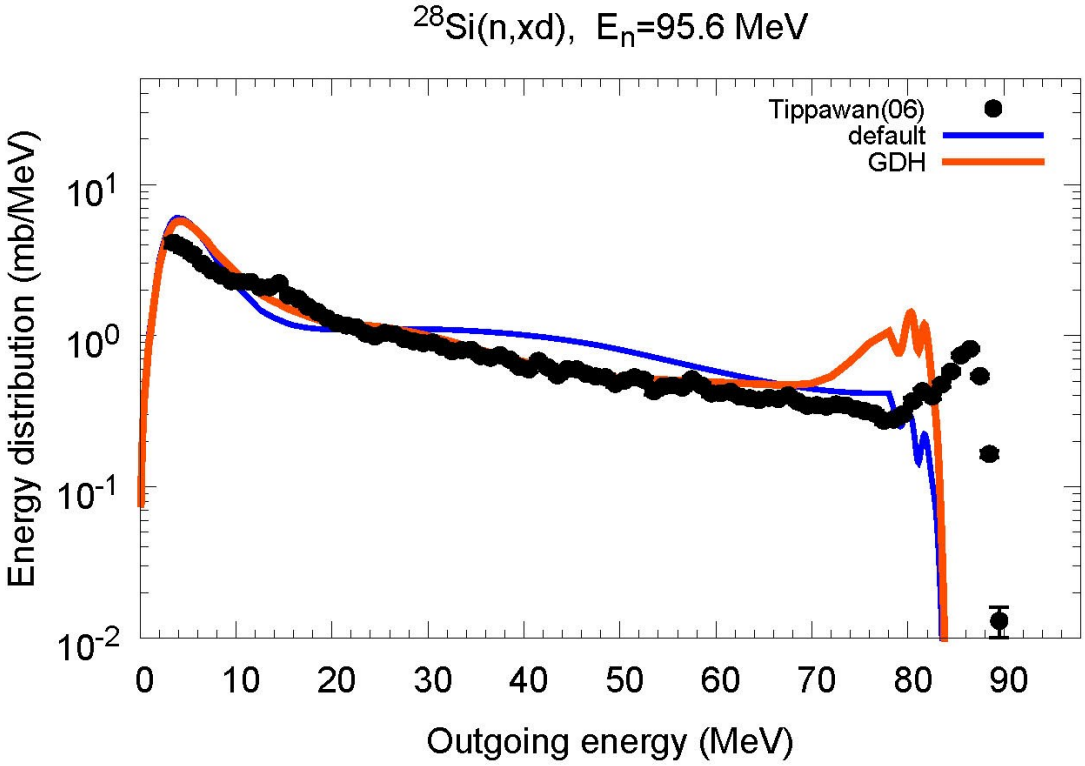
^{28}Si(n,xd), E_n=95.6 MeV
Tippawan(06)
default
GDH
Energy distribution (mb/MeV)
10^1
10^0
10^{-1}
10^{-2}
0
10
20
30
40
50
60
70
80
90
Outgoing energy (MeV)

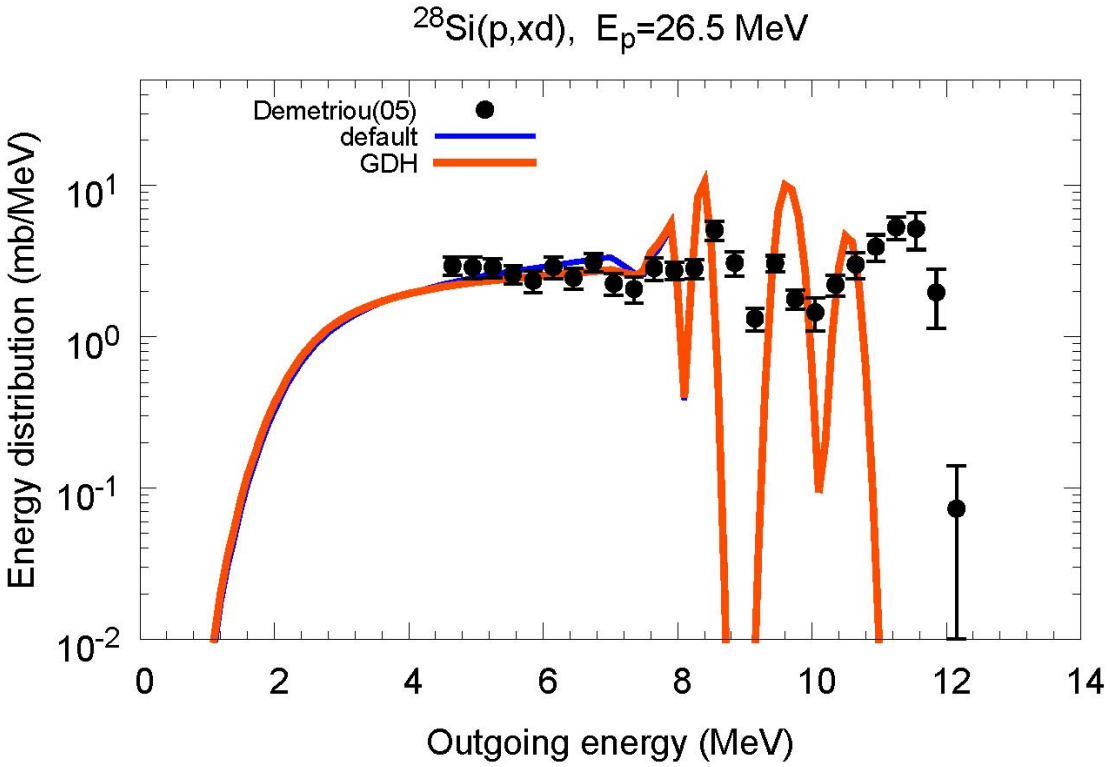
^{28}Si(p,xd), E_p=26.5 MeV
Demetriou(05)
default
GDH
Energy distribution (mb/MeV)
10^1
10^0
10^{-1}
10^{-2}
0
2
4
6
8
10
12
14
Outgoing energy (MeV)

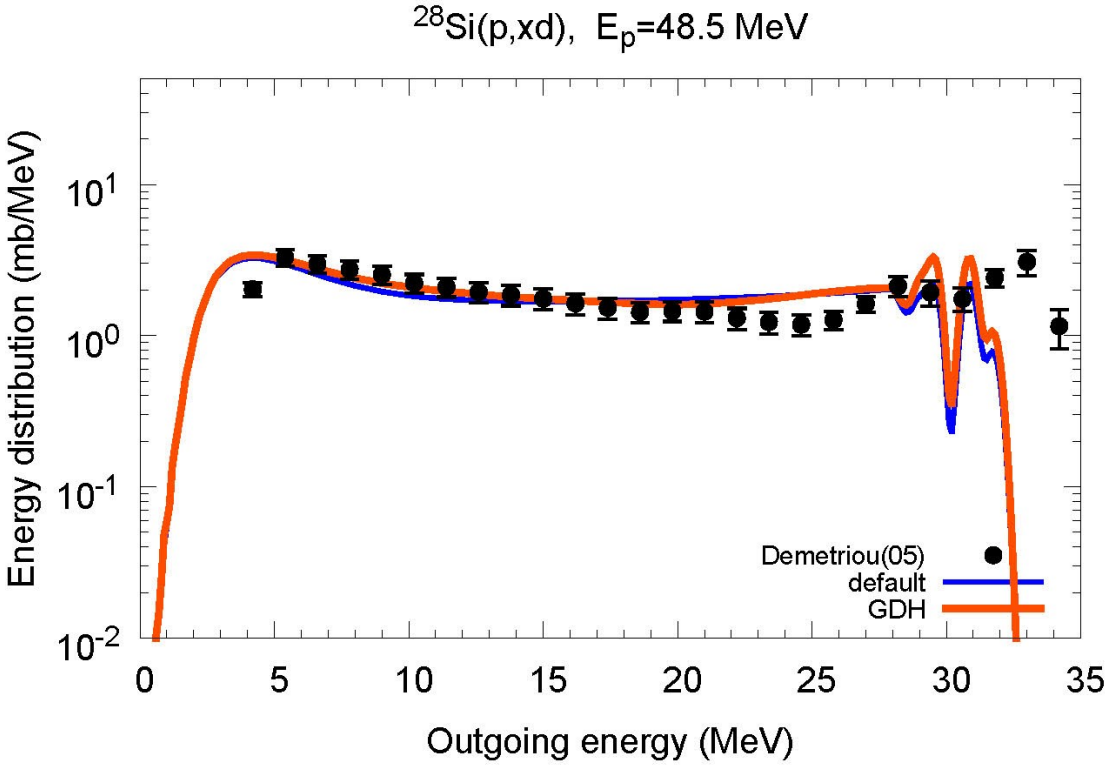
^{28}Si(p,xd), E_p=48.5 MeV
Energy distribution (mb/MeV)
10^1
10^0
10^{-1}
10^{-2}
0
5
10
15
20
25
30
35
Outgoing energy (MeV)
Demetriou(05)
default
GDH

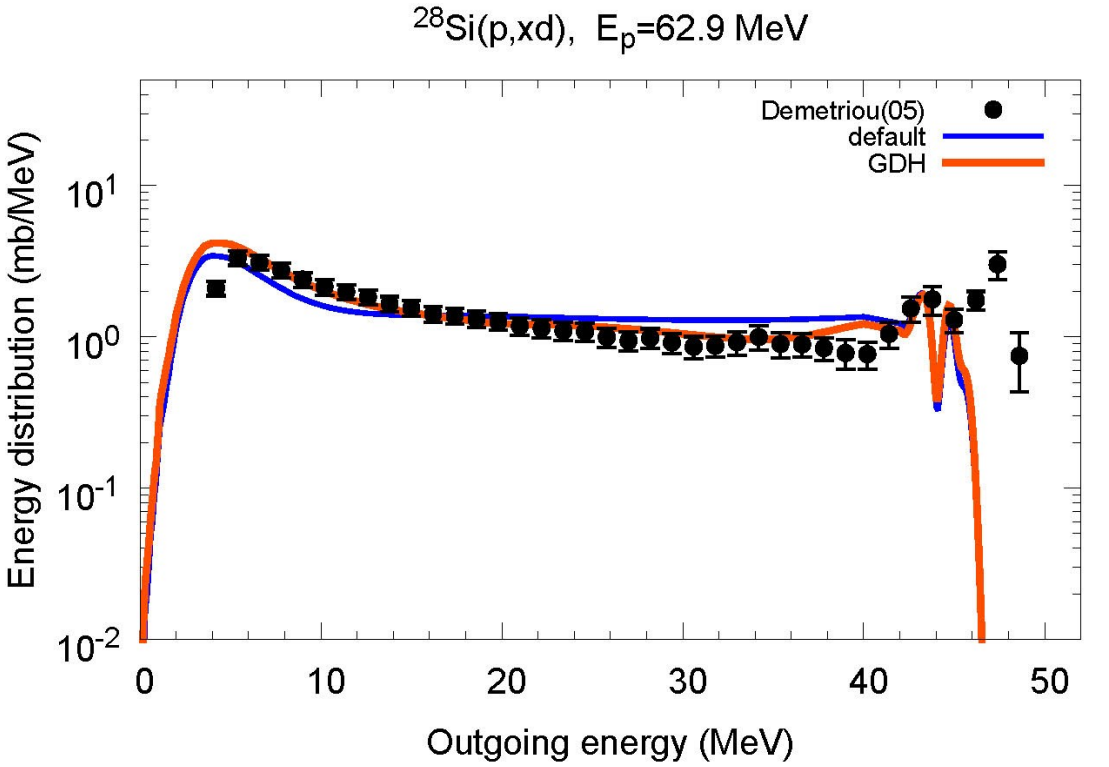
^{28}Si(p,xd), E_p=62.9 MeV
Energy distribution (mb/MeV)
10^1
10^0
10^{-1}
10^{-2}
0
10
20
30
40
50
Outgoing energy (MeV)
Demetriou(05)
default
GDH

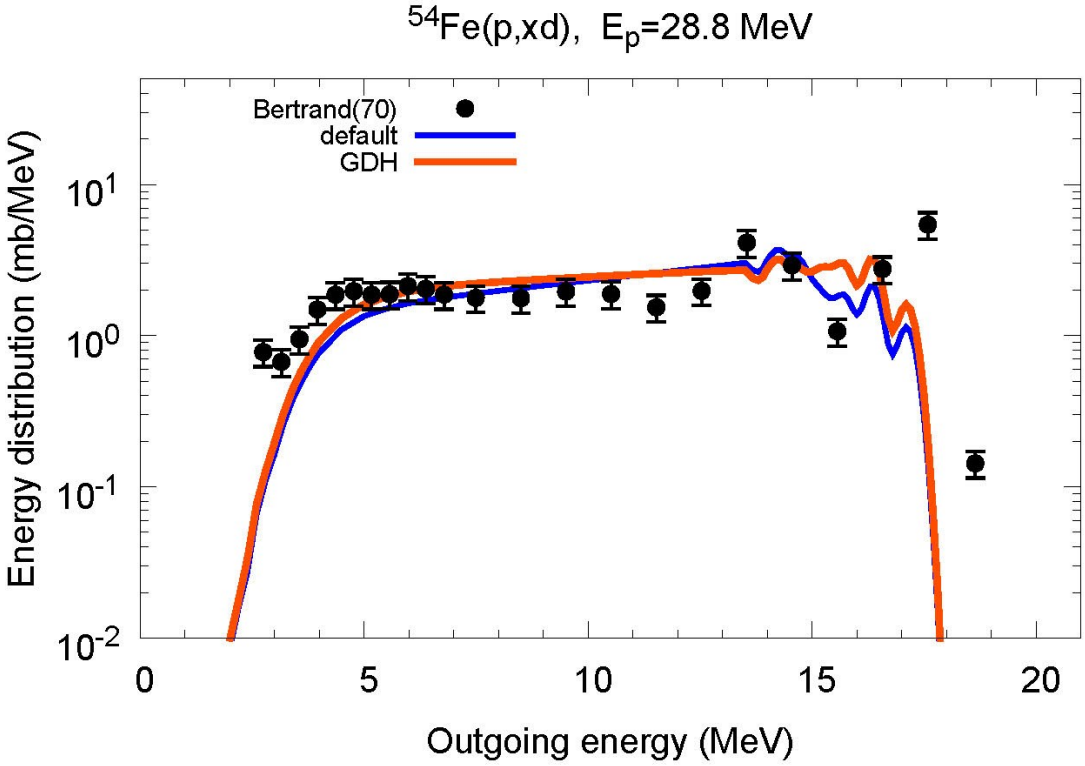
^{54}Fe(p,xd), E_p=28.8 MeV
Bertrand(70)
default
GDH
Energy distribution (mb/MeV)
10^{1}
10^{0}
10^{-1}
10^{-2}
0
5
10
15
20
Outgoing energy (MeV)

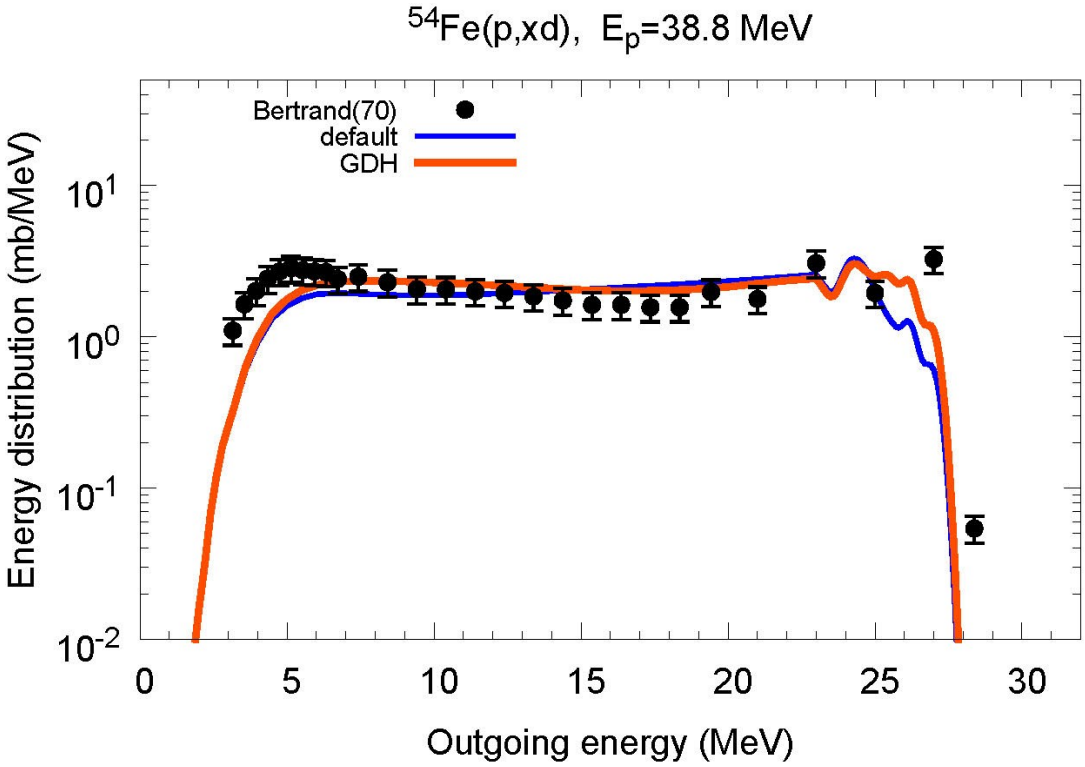
^{54}Fe(p,xd), E_p=38.8 MeV
Bertrand(70)
default
GDH
Energy distribution (mb/MeV)
10^{1}
10^{0}
10^{-1}
10^{-2}
0
5
10
15
20
25
30
Outgoing energy (MeV)

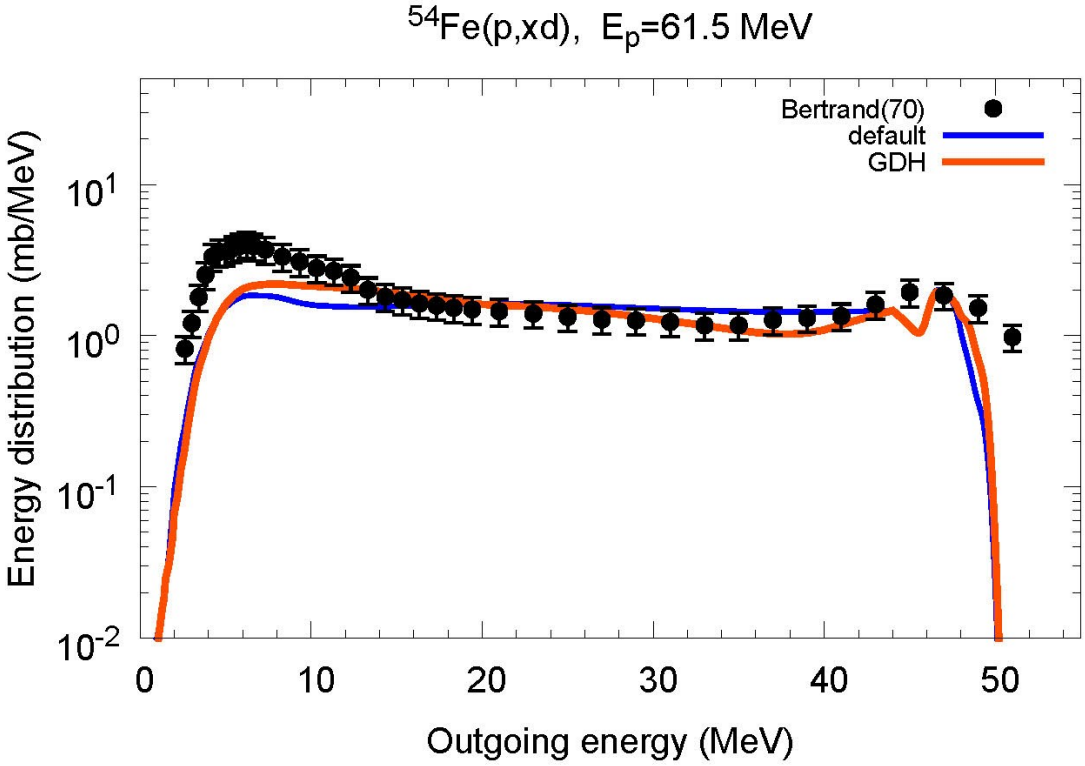
^{54}Fe(p,xd), E_p=61.5 MeV
Bertrand(70)
default
GDH
Energy distribution (mb/MeV)
10^1
10^0
10^{-1}
10^{-2}
0
10
20
30
40
50
Outgoing energy (MeV)

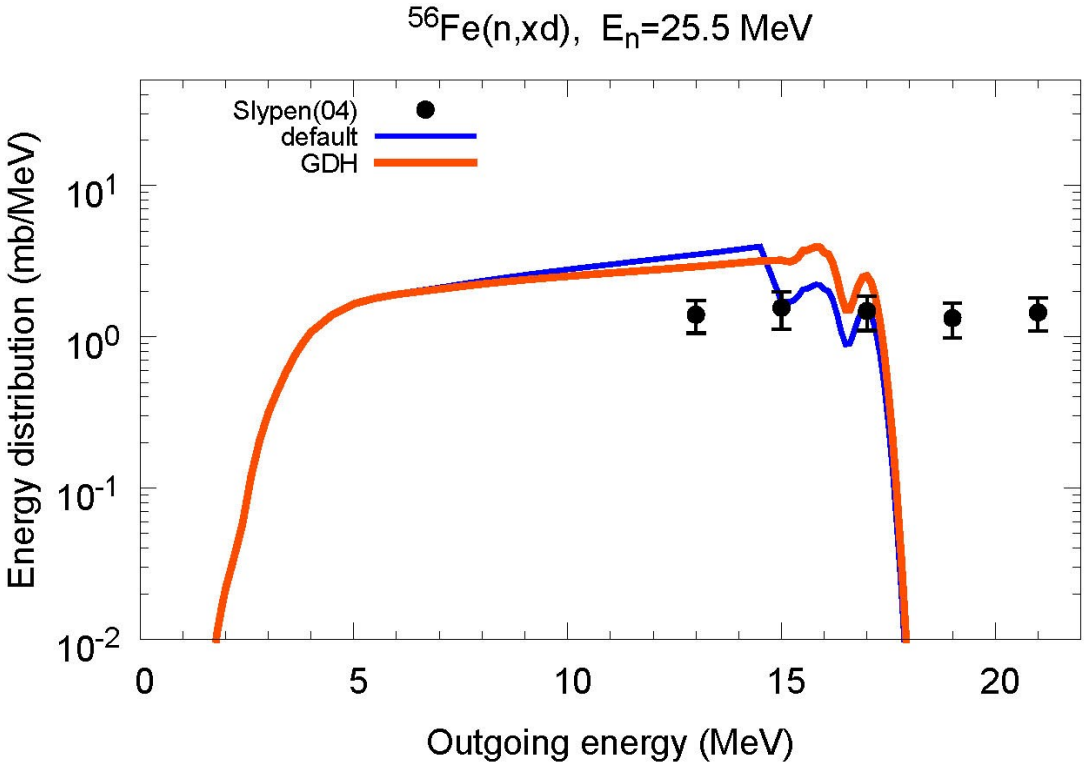
^{56}Fe(n,xd), E_n=25.5 MeV
Slypen(04)
default
GDH
Energy distribution (mb/MeV)
10^1
10^0
10^{-1}
10^{-2}
0
5
10
15
20
Outgoing energy (MeV)

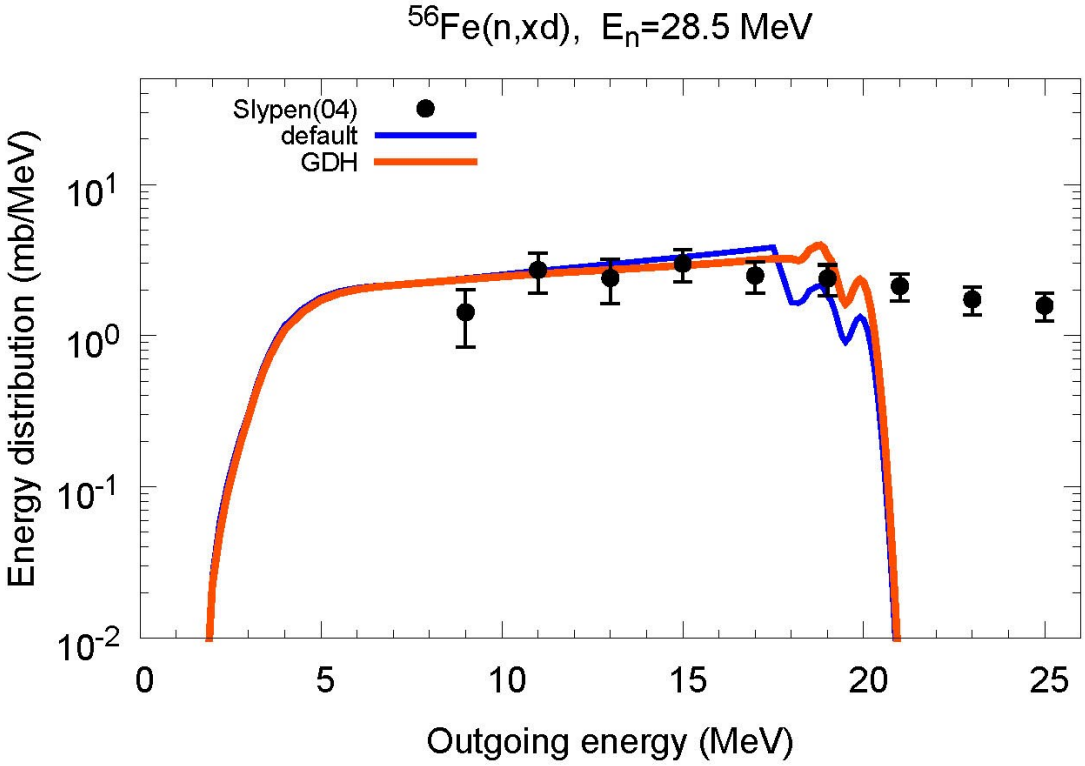
^{56}Fe(n,xd), E_n=28.5 MeV
Slypen(04)
default
GDH
Energy distribution (mb/MeV)
10^{1}
10^{0}
10^{-1}
10^{-2}
0
5
10
15
20
25
Outgoing energy (MeV)

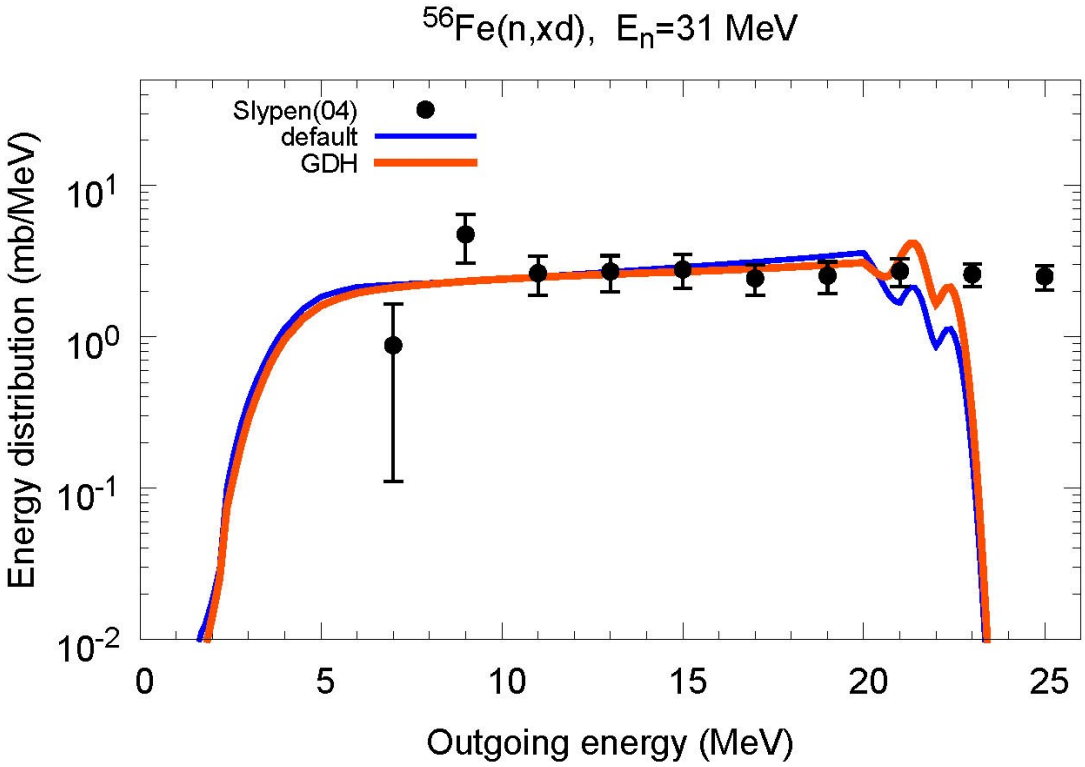
^{56}Fe(n,xd), E_n=31 MeV
Slypen(04)
default
GDH
Energy distribution (mb/MeV)
10^{1}
10^{0}
10^{-1}
10^{-2}
0
5
10
15
20
25
Outgoing energy (MeV)

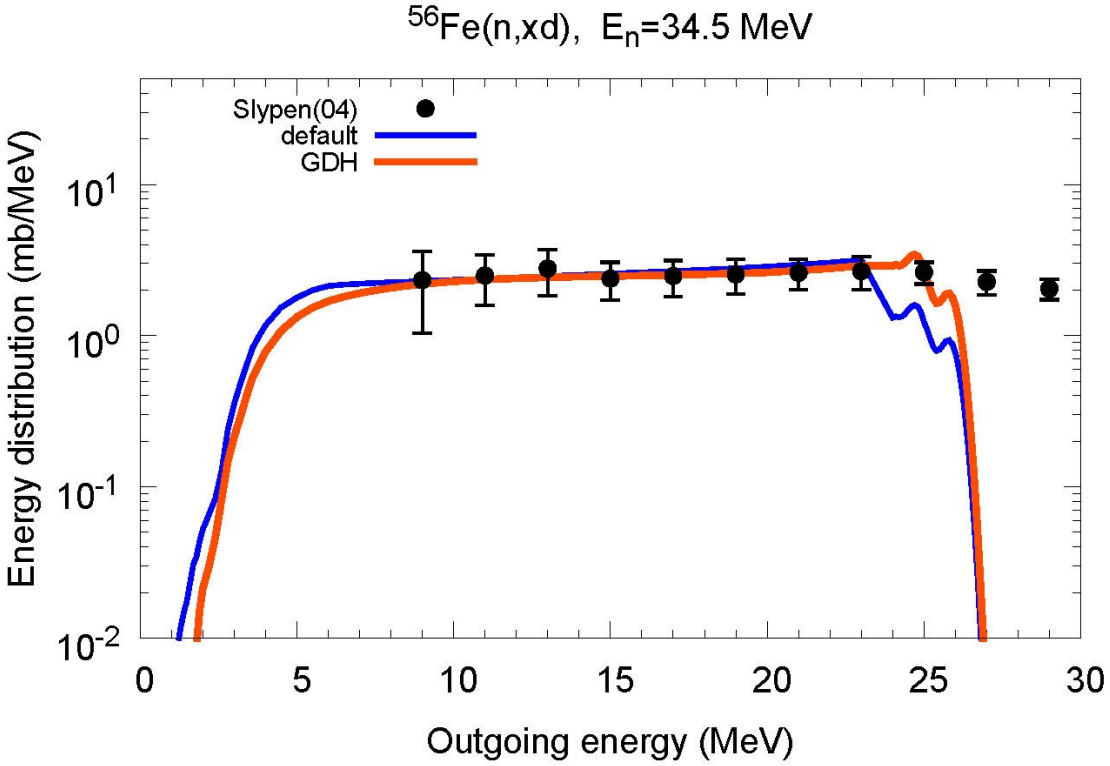
^{56}Fe(n,xd), E_n=34.5 MeV
Slypen(04)
default
GDH
Energy distribution (mb/MeV)
10^{1}
10^{0}
10^{-1}
10^{-2}
0
5
10
15
20
25
30
Outgoing energy (MeV)

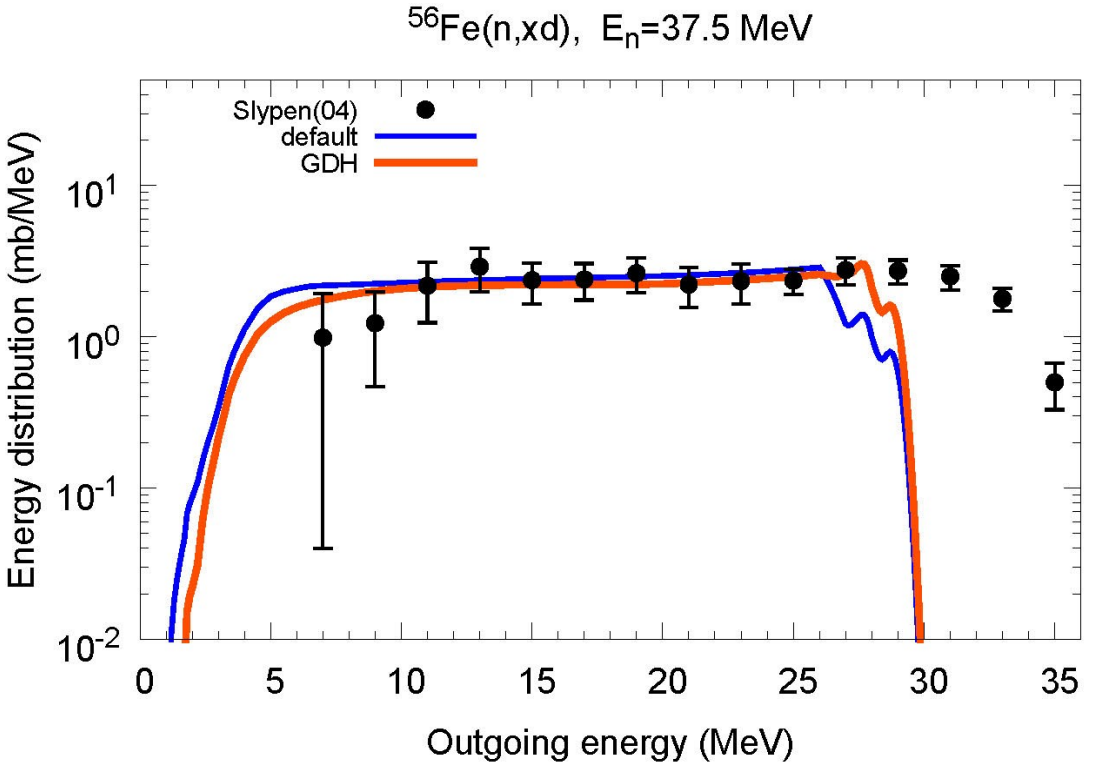
^{56}Fe(n,xd), E_n=37.5 MeV
Slypen(04)
default
GDH
Energy distribution (mb/MeV)
10^{1}
10^{0}
10^{-1}
10^{-2}
0
5
10
15
20
25
30
35
Outgoing energy (MeV)

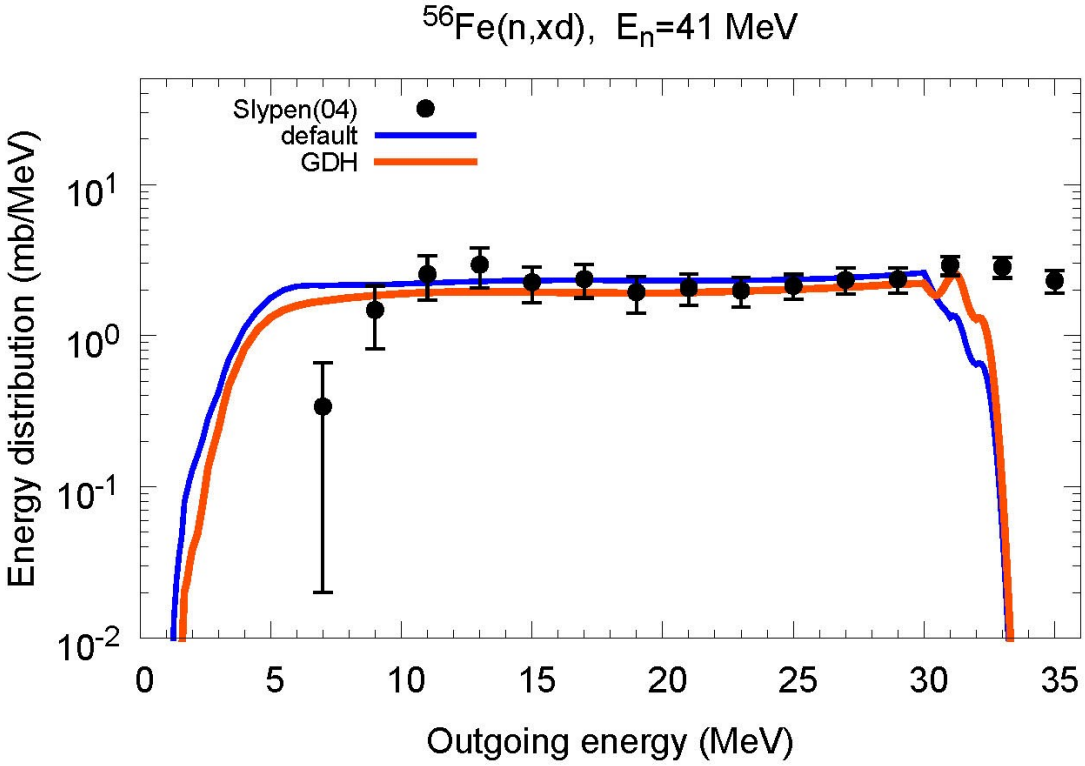
^{56}Fe(n,xd), E_n=41 MeV
Slypen(04)
default
GDH
Energy distribution (mb/MeV)
Outgoing energy (MeV)

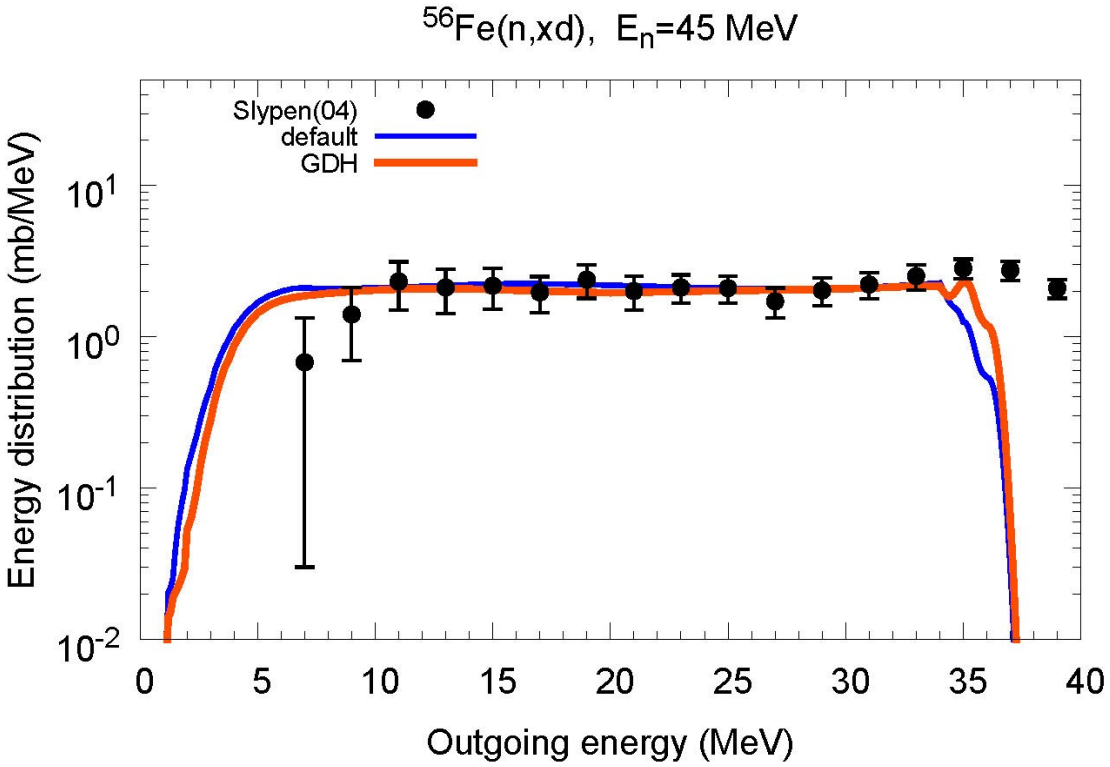
^{56}Fe(n,xd), E_n=45 MeV
Slypen(04)
default
GDH
Energy distribution (mb/MeV)
Outgoing energy (MeV)

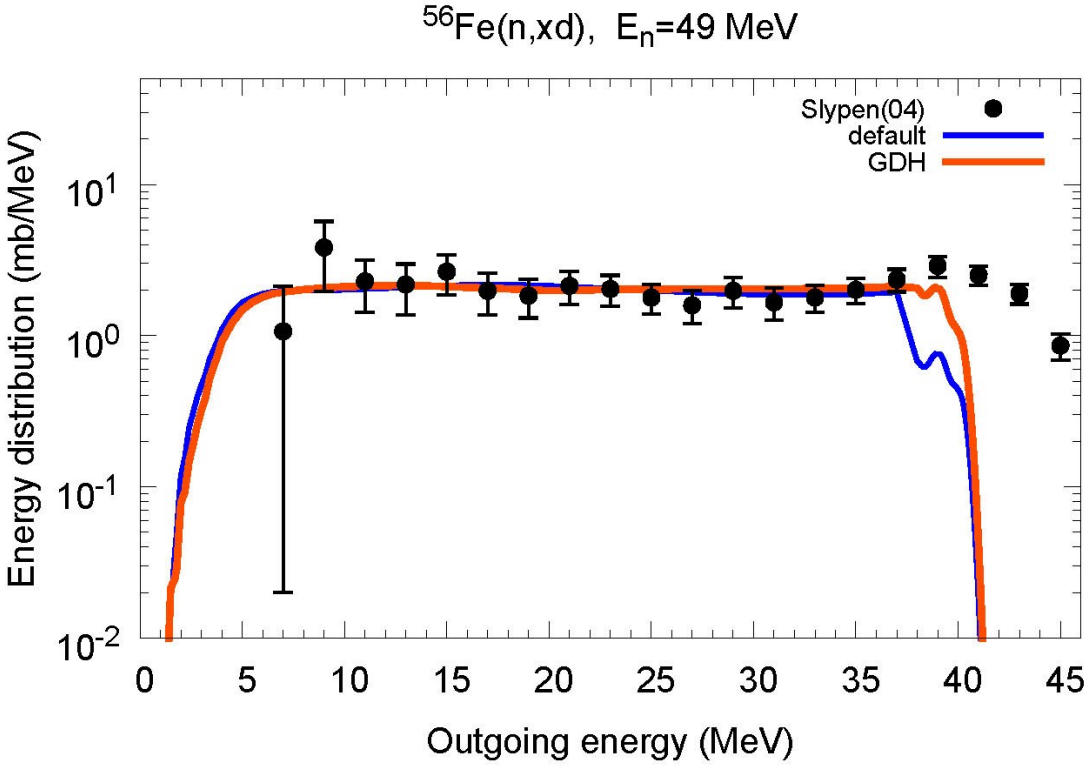
^{56}Fe(n,xd), E_n=49 MeV
Slypen(04)
default
GDH
Energy distribution (mb/MeV)
Outgoing energy (MeV)

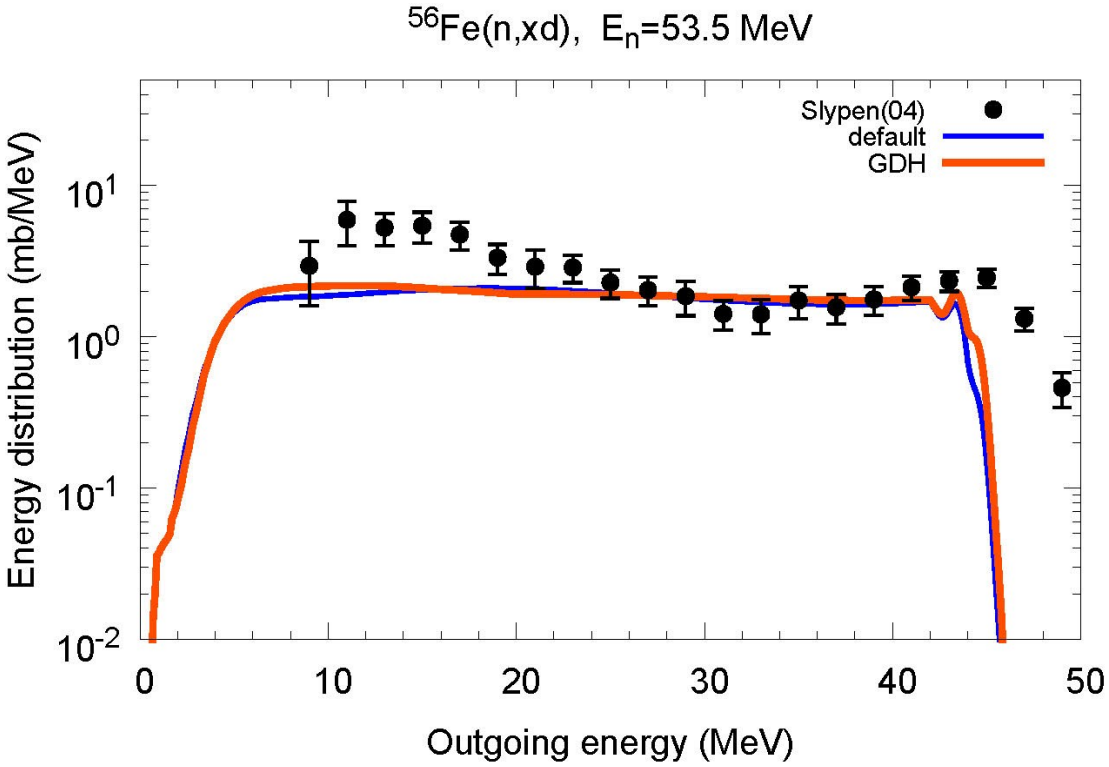
^{56}Fe(n,xd), E_n=53.5 MeV
Slypen(04)
default
GDH
Energy distribution (mb/MeV)
Outgoing energy (MeV)

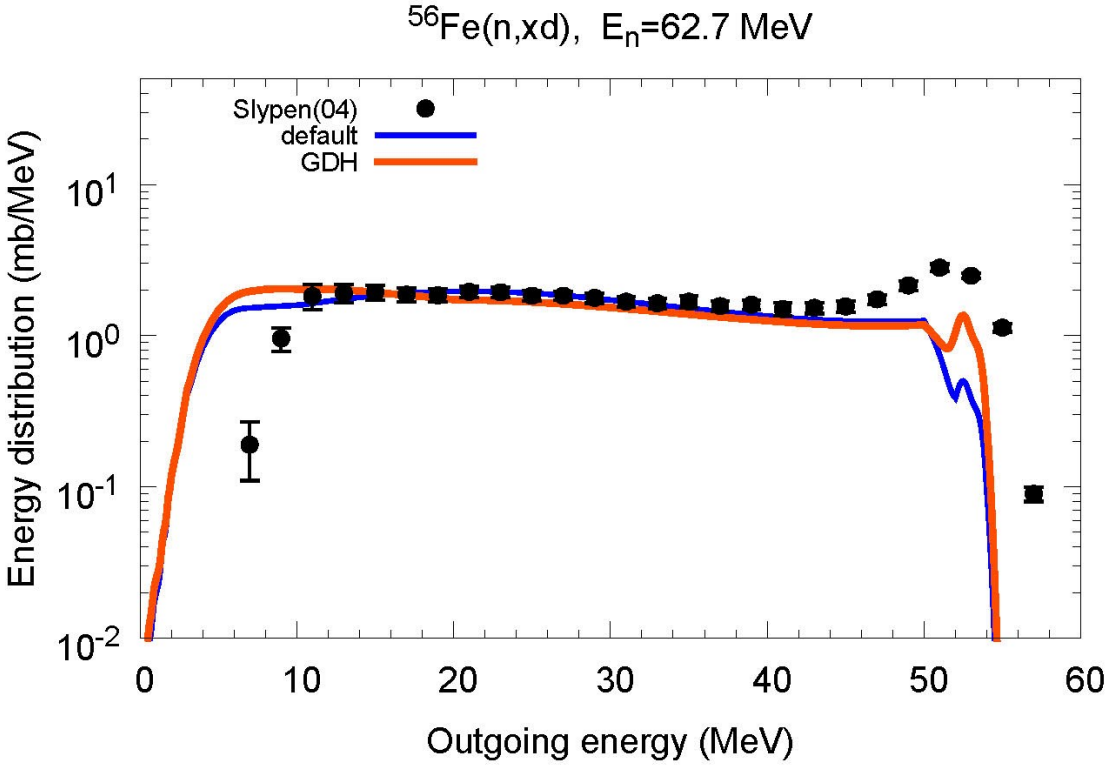
^{56}Fe(n,xd), E_n=62.7 MeV
Slypen(04)
default
GDH
Energy distribution (mb/MeV)
10^{1}
10^{0}
10^{-1}
10^{-2}
0
10
20
30
40
50
60
Outgoing energy (MeV)

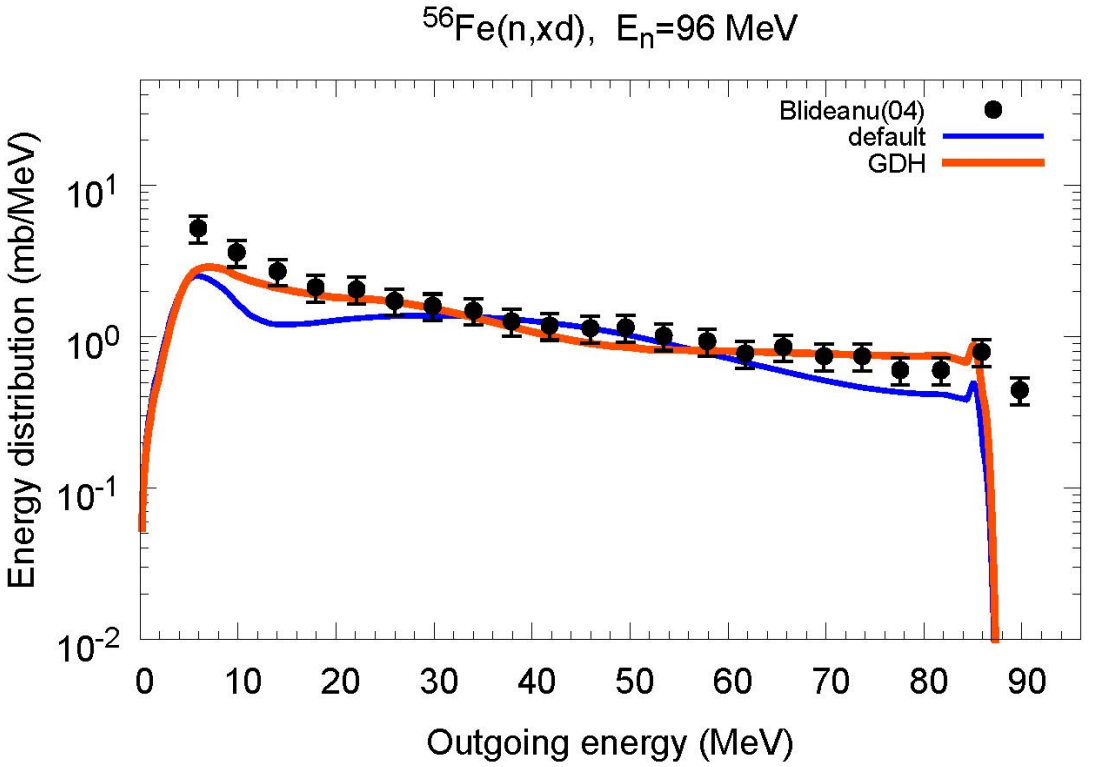
^{56}Fe(n,xd), E_n=96 MeV
Blideanu(04)
default
GDH
Energy distribution (mb/MeV)
10^{1}
10^{0}
10^{-1}
10^{-2}
0
10
20
30
40
50
60
70
80
90
Outgoing energy (MeV)

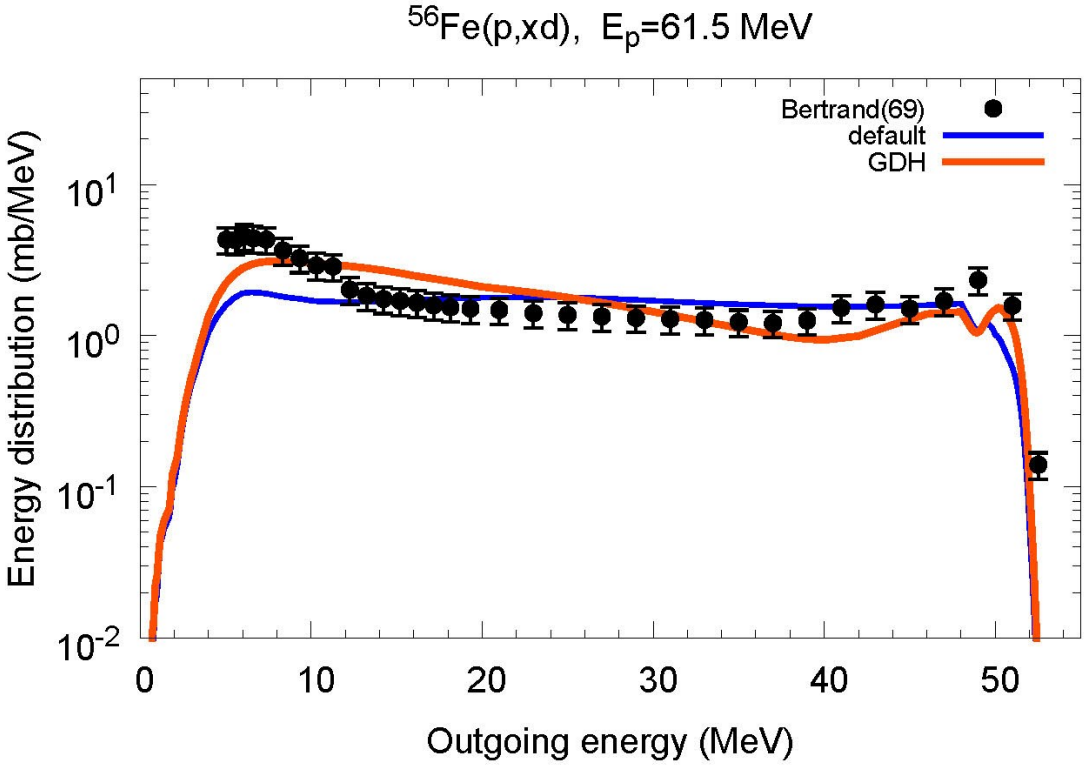
^{56}Fe(p,xd), E_p=61.5 MeV
Bertrand(69)
default
GDH
Energy distribution (mb/MeV)
10^1
10^0
10^{-1}
10^{-2}
0
10
20
30
40
50
Outgoing energy (MeV)

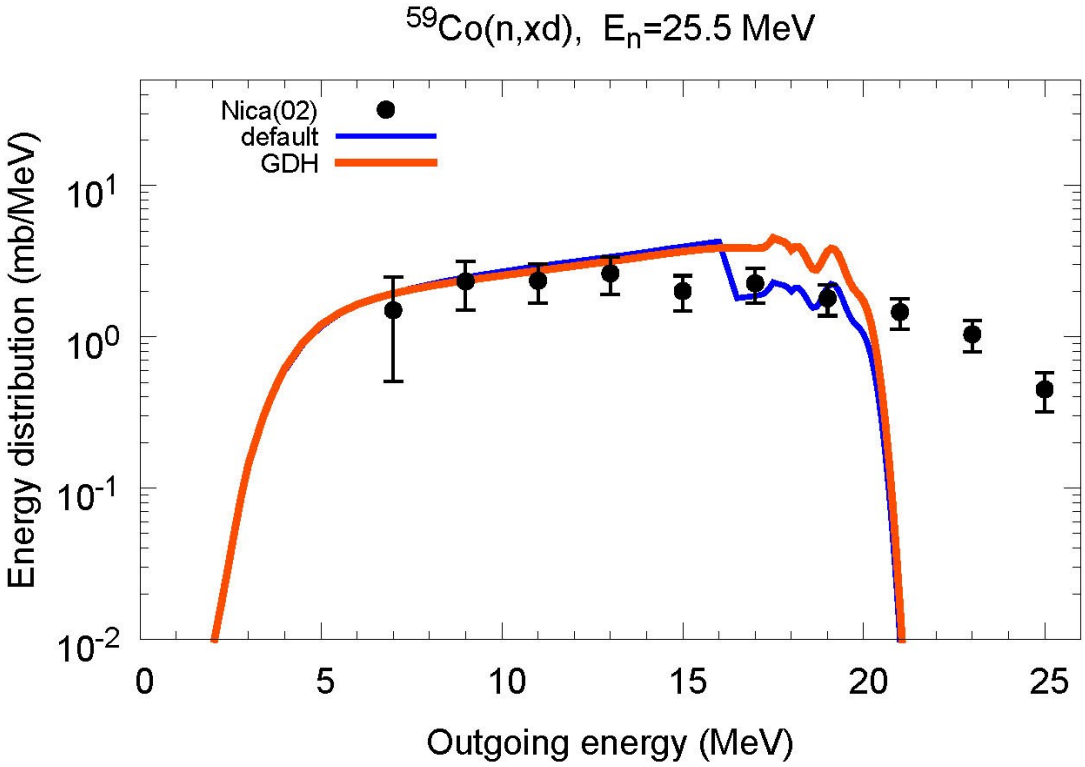
^{59}Co(n,xd), E_n=25.5 MeV
Nica(02)
default
GDH
Energy distribution (mb/MeV)
10^1
10^0
10^{-1}
10^{-2}
0
5
10
15
20
25
Outgoing energy (MeV)

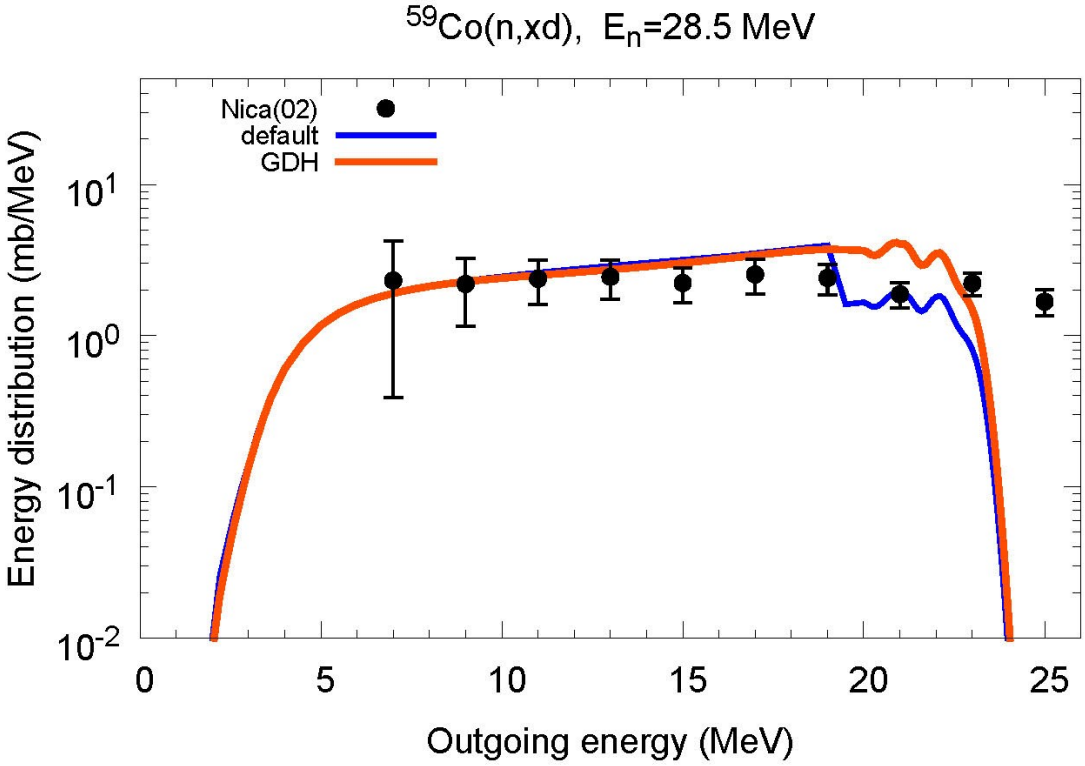
^{59}Co(n,xd), E_n=28.5 MeV
Nica(02)
default
GDH
Energy distribution (mb/MeV)
10^1
10^0
10^{-1}
10^{-2}
0
5
10
15
20
25
Outgoing energy (MeV)

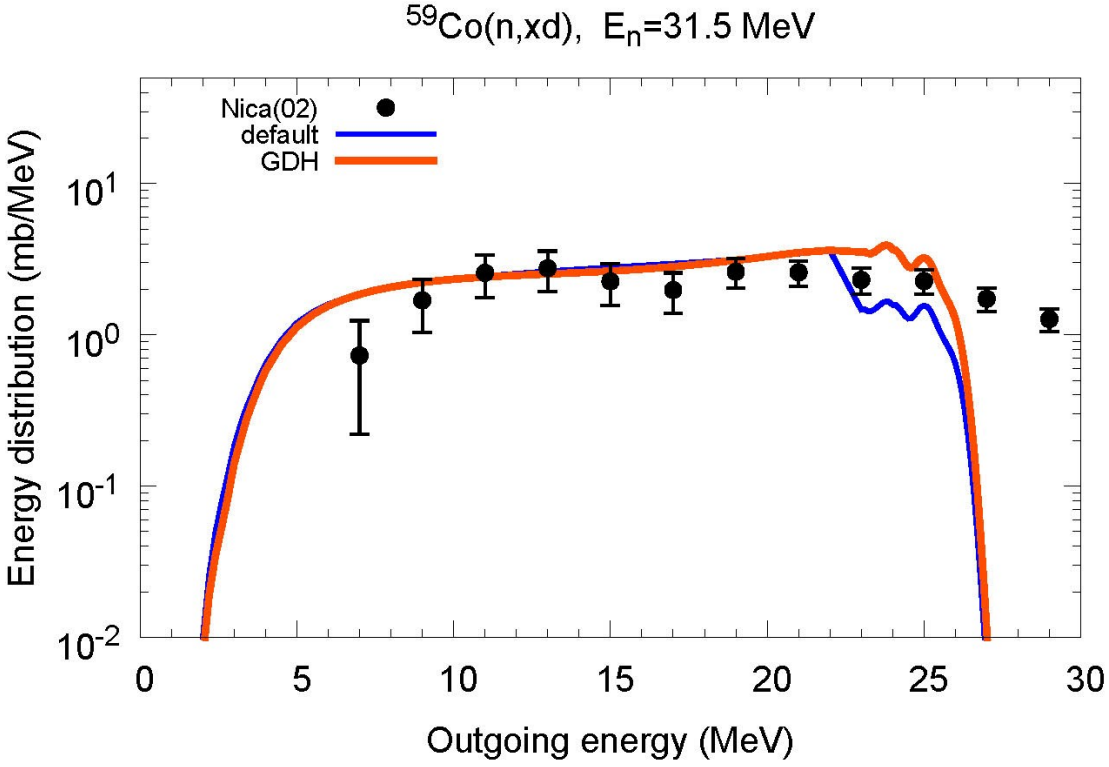
^{59}Co(n,xd), E_n=31.5 MeV
Nica(02)
default
GDH
Energy distribution (mb/MeV)
10^1
10^0
10^{-1}
10^{-2}
0
5
10
15
20
25
30
Outgoing energy (MeV)

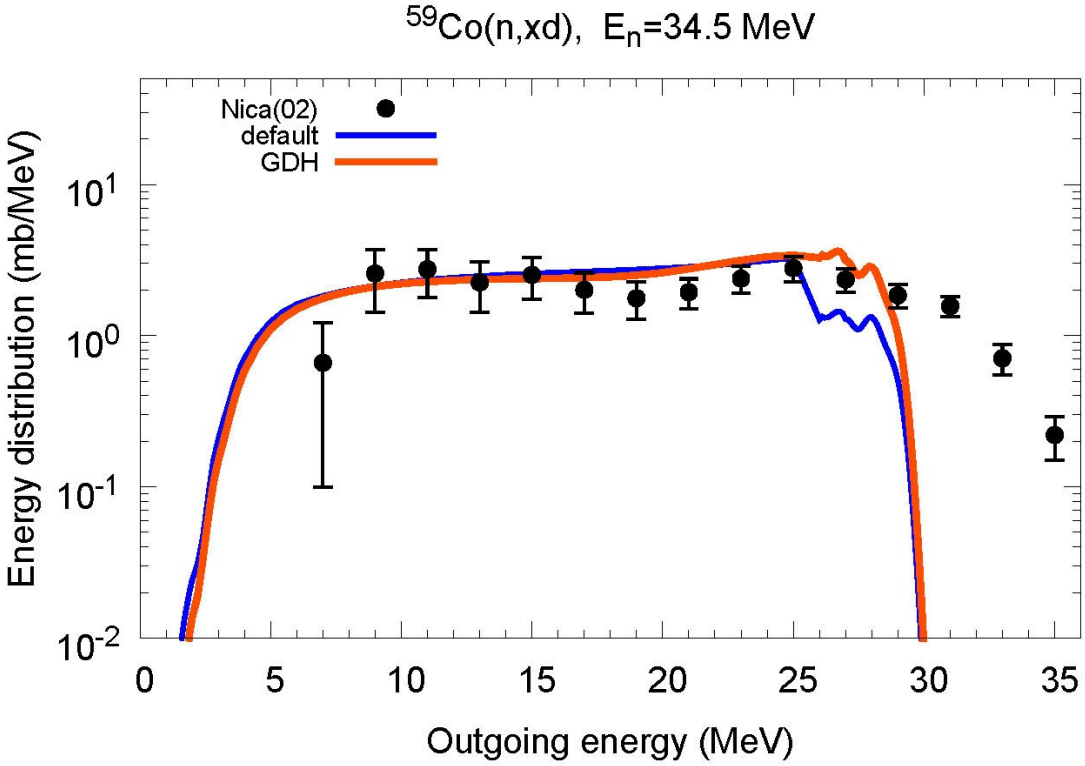
^{59}Co(n,xd), E_n=34.5 MeV
Nica(02)
default
GDH
Energy distribution (mb/MeV)
10^{1}
10^{0}
10^{-1}
10^{-2}
0
5
10
15
20
25
30
35
Outgoing energy (MeV)

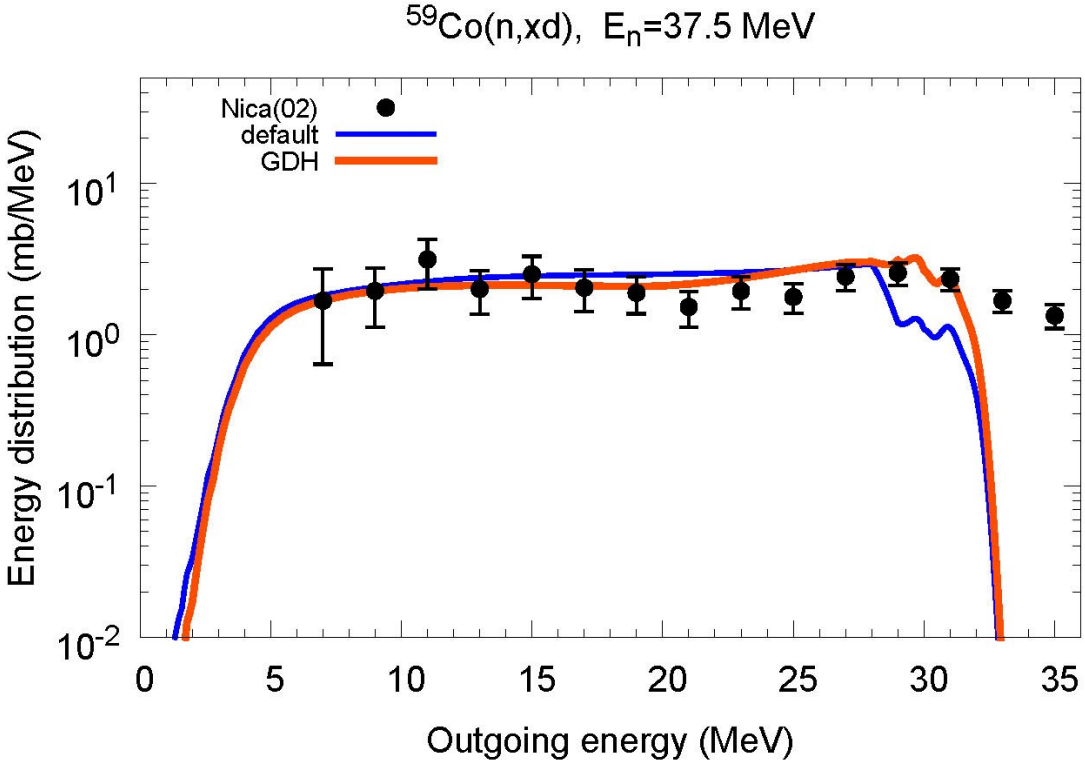
^{59}Co(n,xd), E_n=37.5 MeV
Nica(02)
default
GDH
Energy distribution (mb/MeV)
10^{1}
10^{0}
10^{-1}
10^{-2}
0
5
10
15
20
25
30
35
Outgoing energy (MeV)

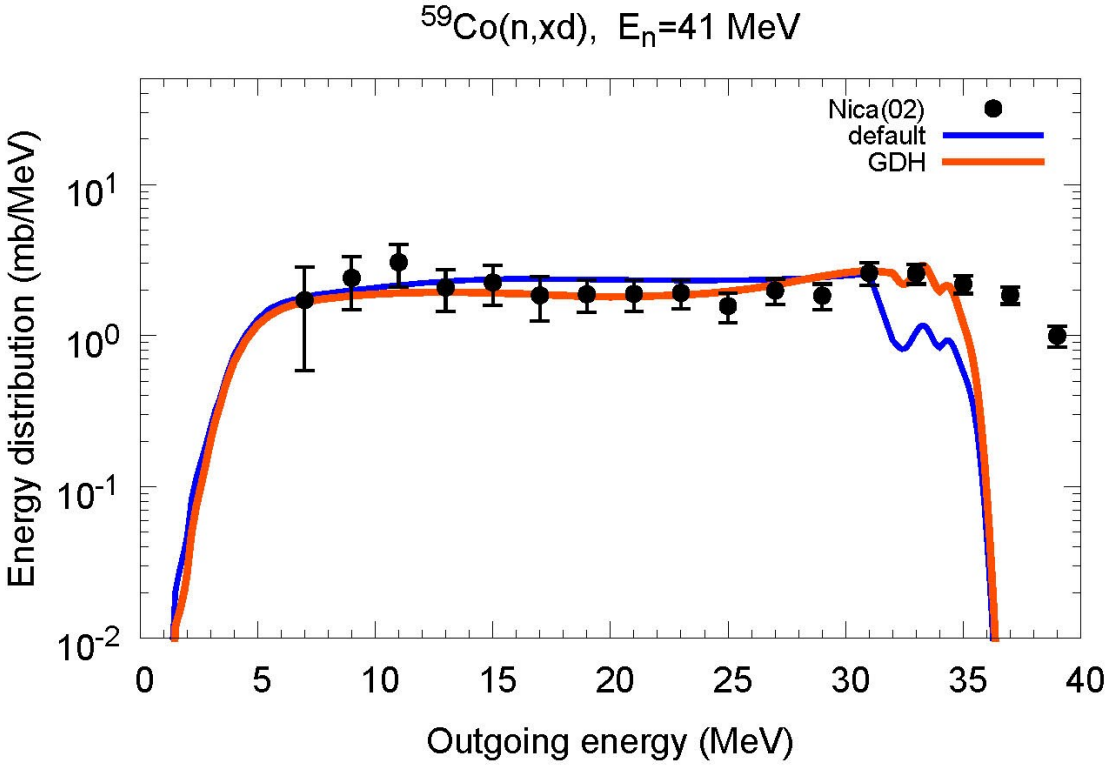
59Co(n,xd), En=41 MeV
Nica(02)
default
GDH
Energy distribution (mb/MeV)
Outgoing energy (MeV)

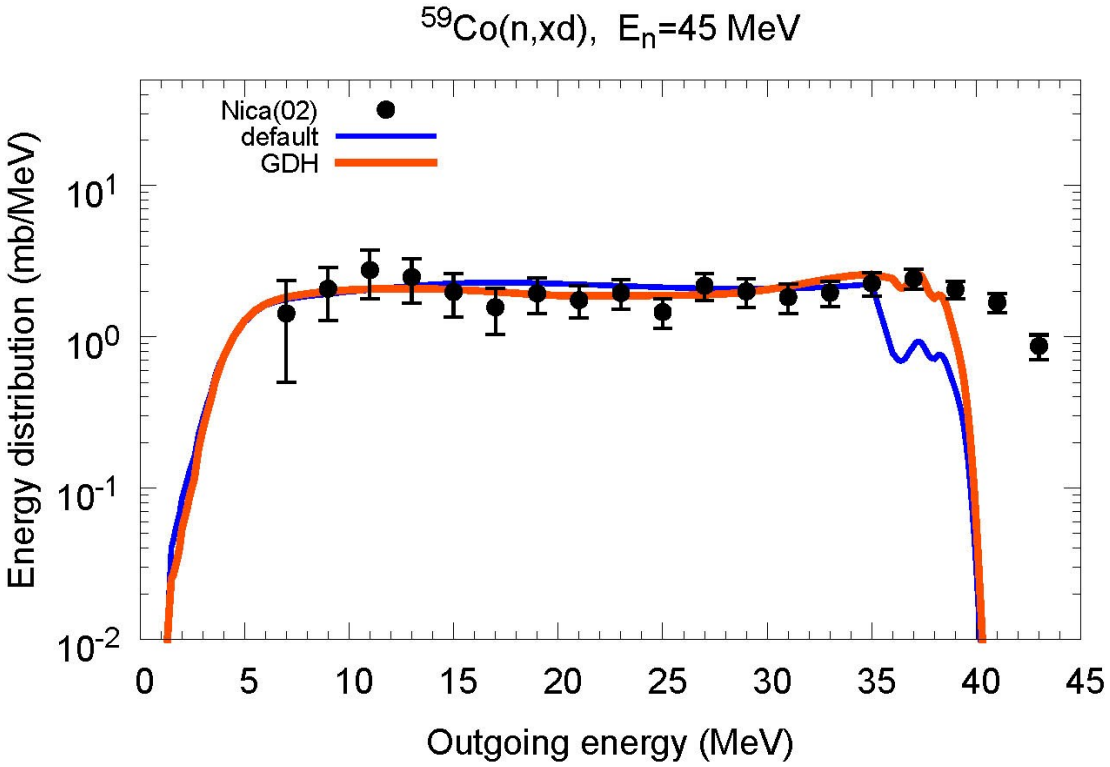
59Co(n,xd), En=45 MeV
Nica(02)
default
GDH
Energy distribution (mb/MeV)
Outgoing energy (MeV)

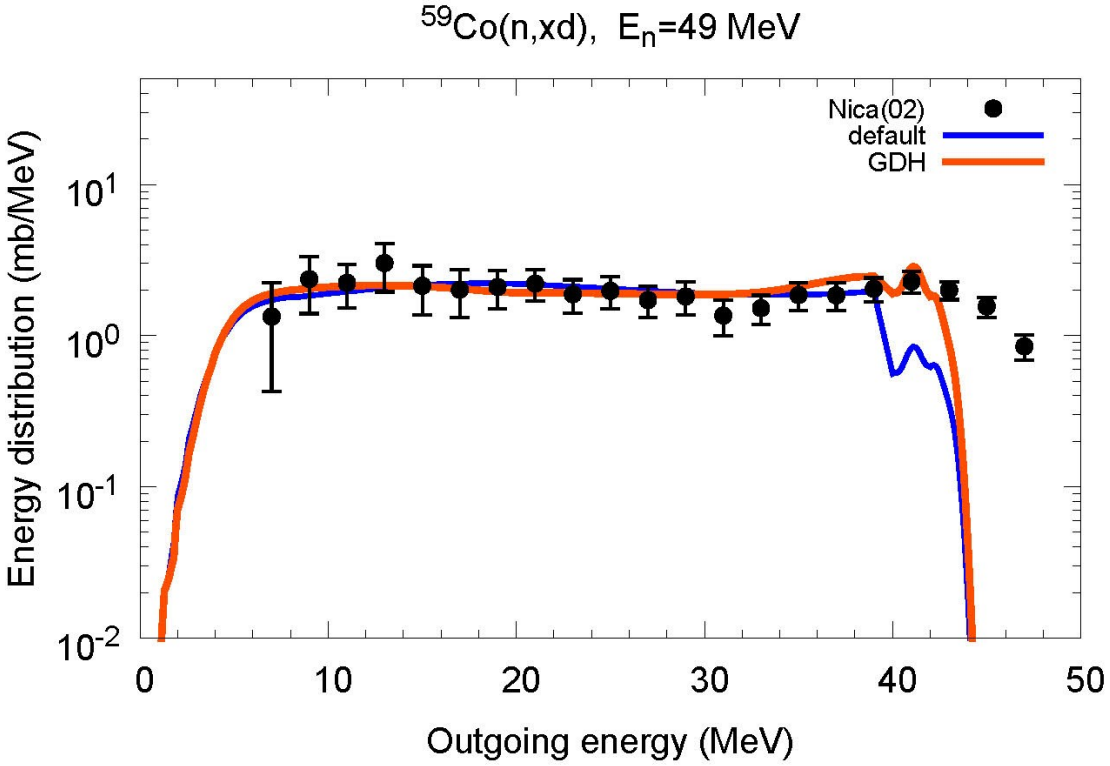
59Co(n,xd), En=49 MeV
Nica(02)
default
GDH
Energy distribution (mb/MeV)
Outgoing energy (MeV)

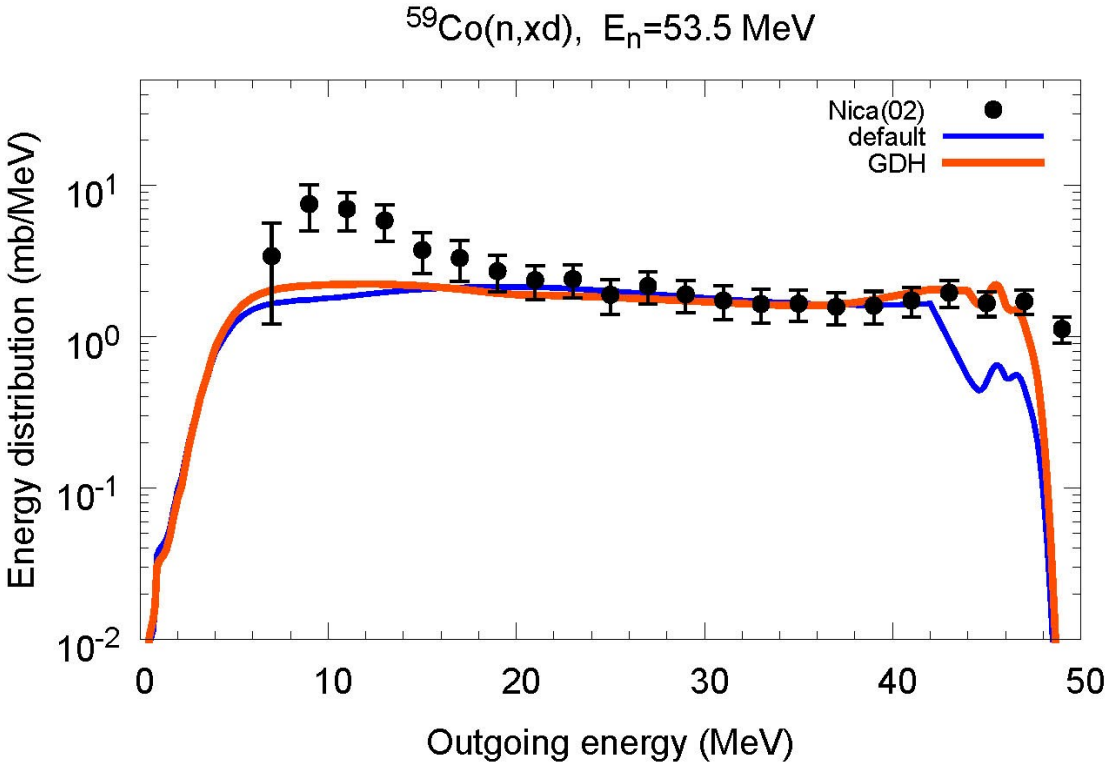
59Co(n,xd), En=53.5 MeV
Nica(02)
default
GDH
Energy distribution (mb/MeV)
Outgoing energy (MeV)

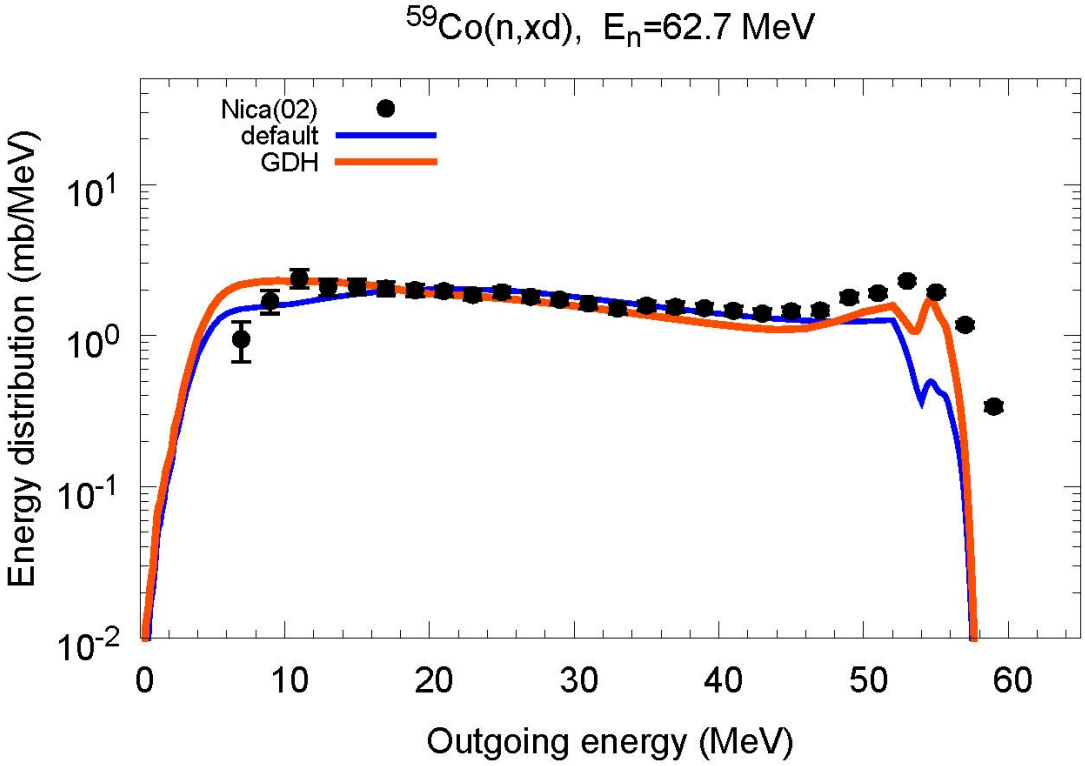
^{59}Co(n,xd), E_n=62.7 MeV
Nica(02)
default
GDH
Energy distribution (mb/MeV)
Outgoing energy (MeV)

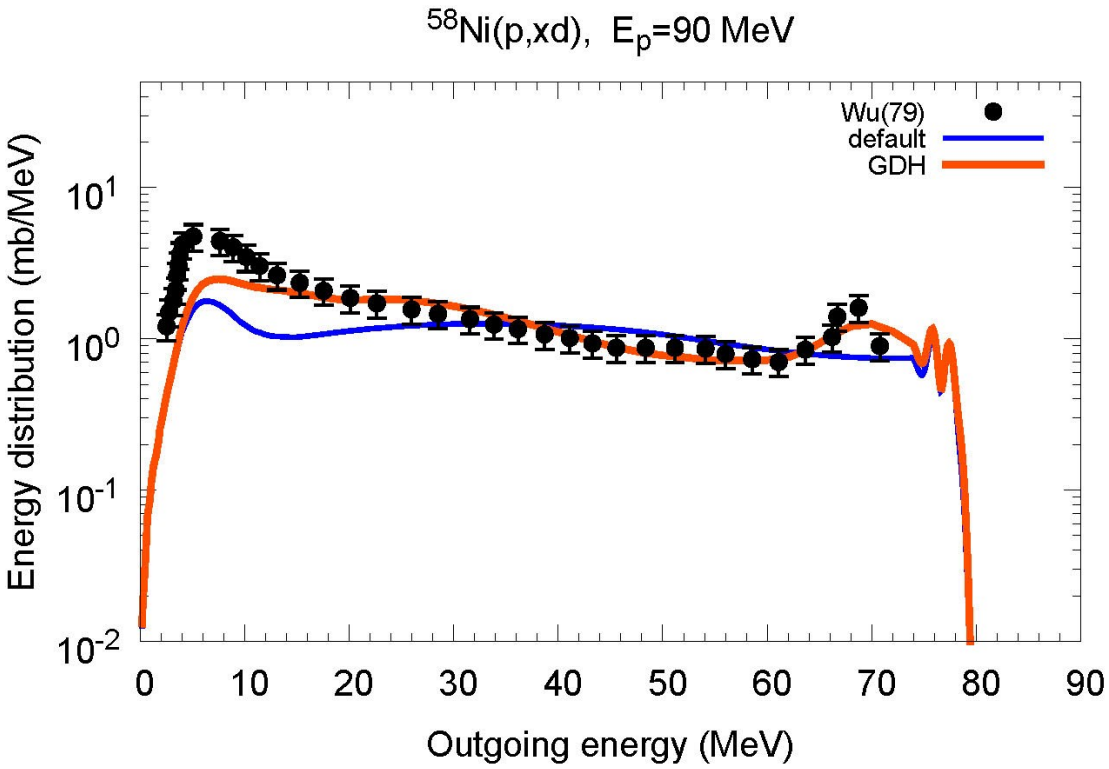
^{58}Ni(p,xd), E_p=90 MeV
Wu(79)
default
GDH
Energy distribution (mb/MeV)
Outgoing energy (MeV)

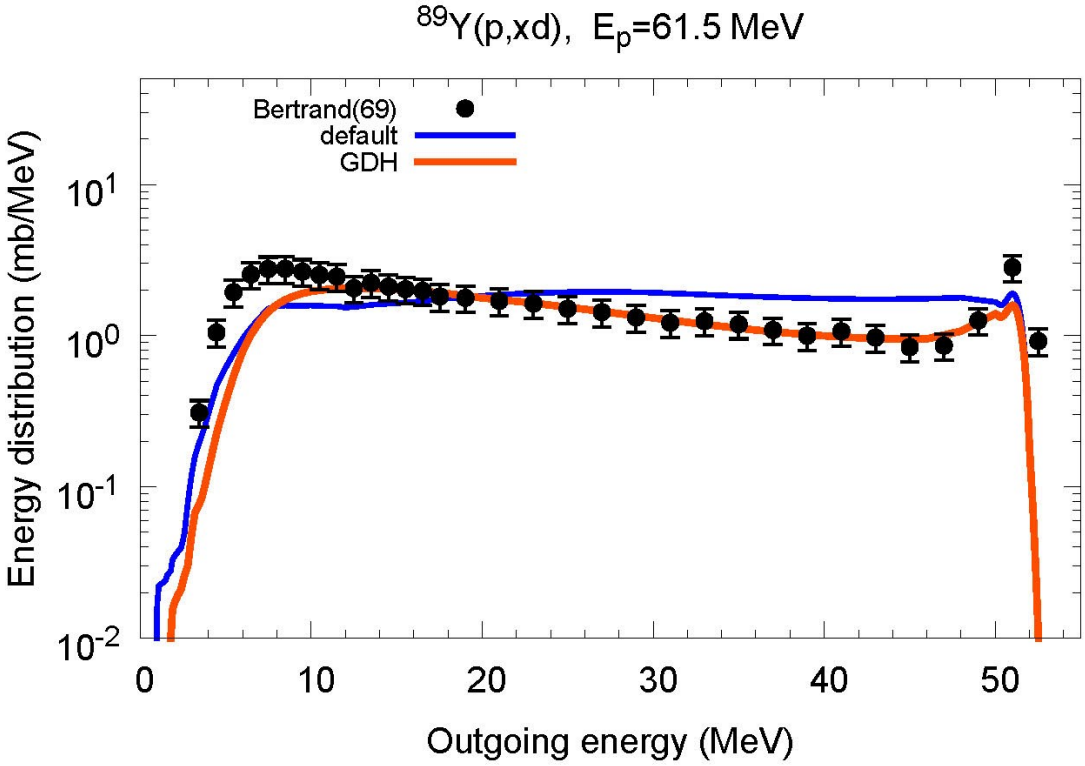
^{89}Y(p,xd), E_p=61.5 MeV
Bertrand(69)
default
GDH
Energy distribution (mb/MeV)
Outgoing energy (MeV)

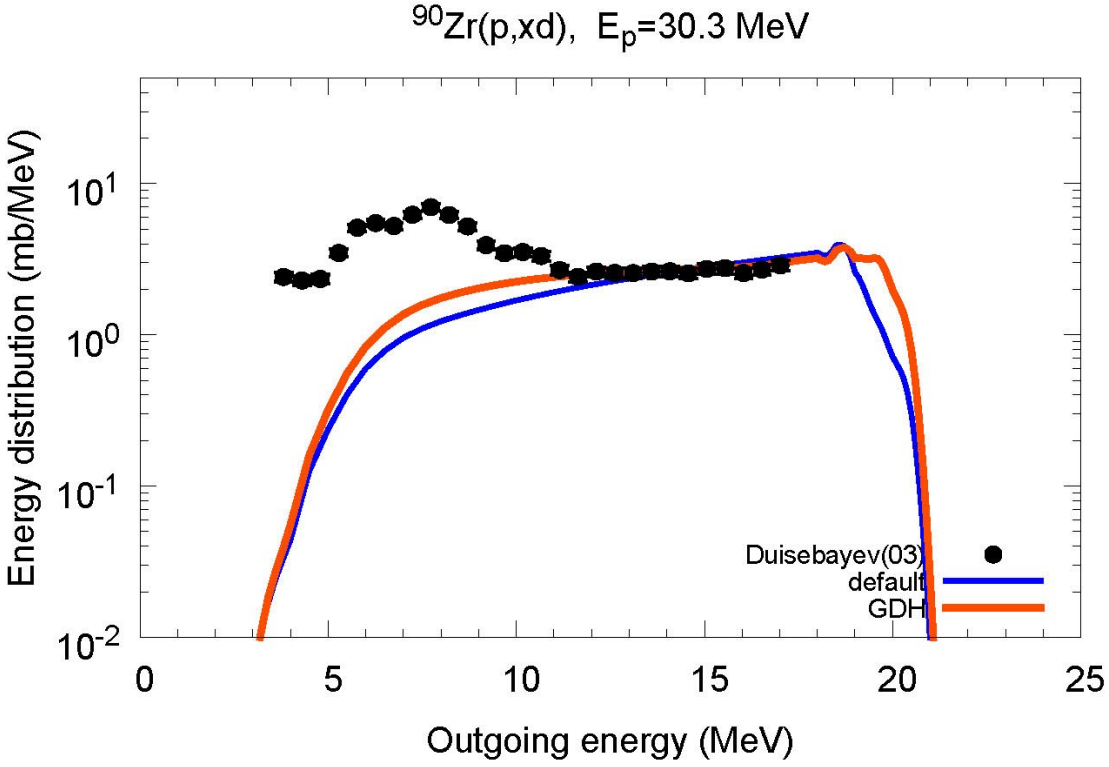
^{90}Zr(p,xd), E_p=30.3 MeV
Duisebayev(03)
default
GDH
Energy distribution (mb/MeV)
Outgoing energy (MeV)

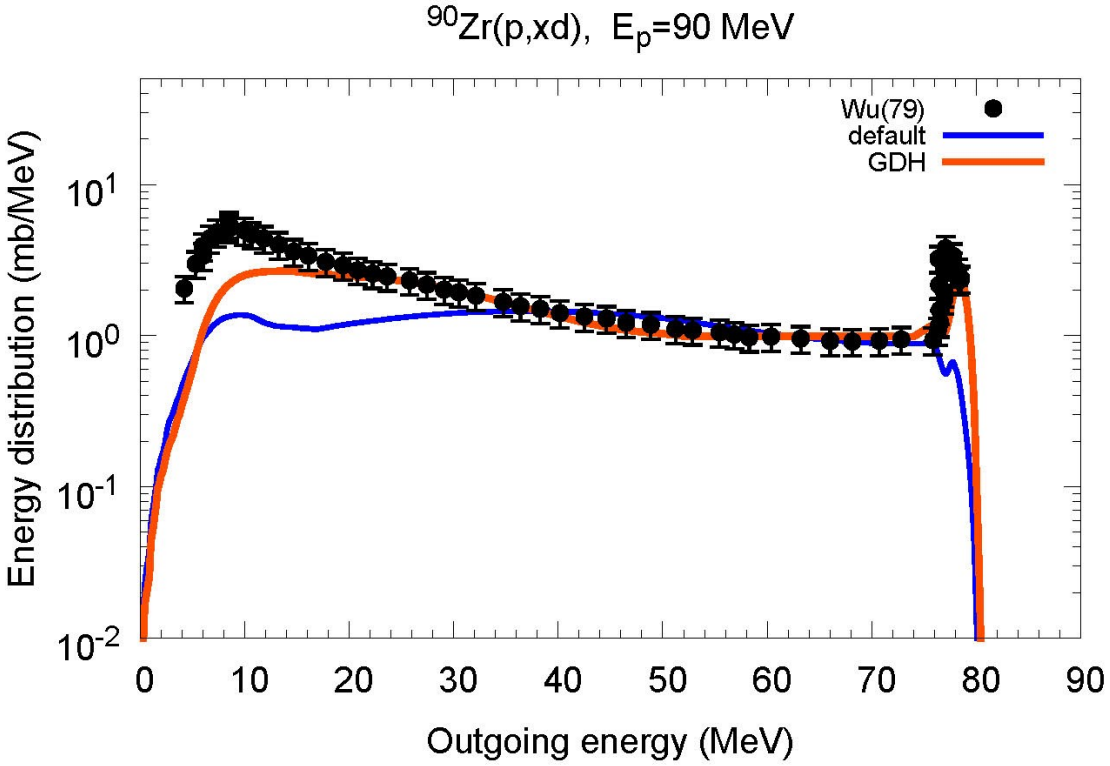
^{90}Zr(p,xd), E_p=90 MeV
Wu(79)
default
GDH
Energy distribution (mb/MeV)
10^{1}
10^{0}
10^{-1}
10^{-2}
0
10
20
30
40
50
60
70
80
90
Outgoing energy (MeV)

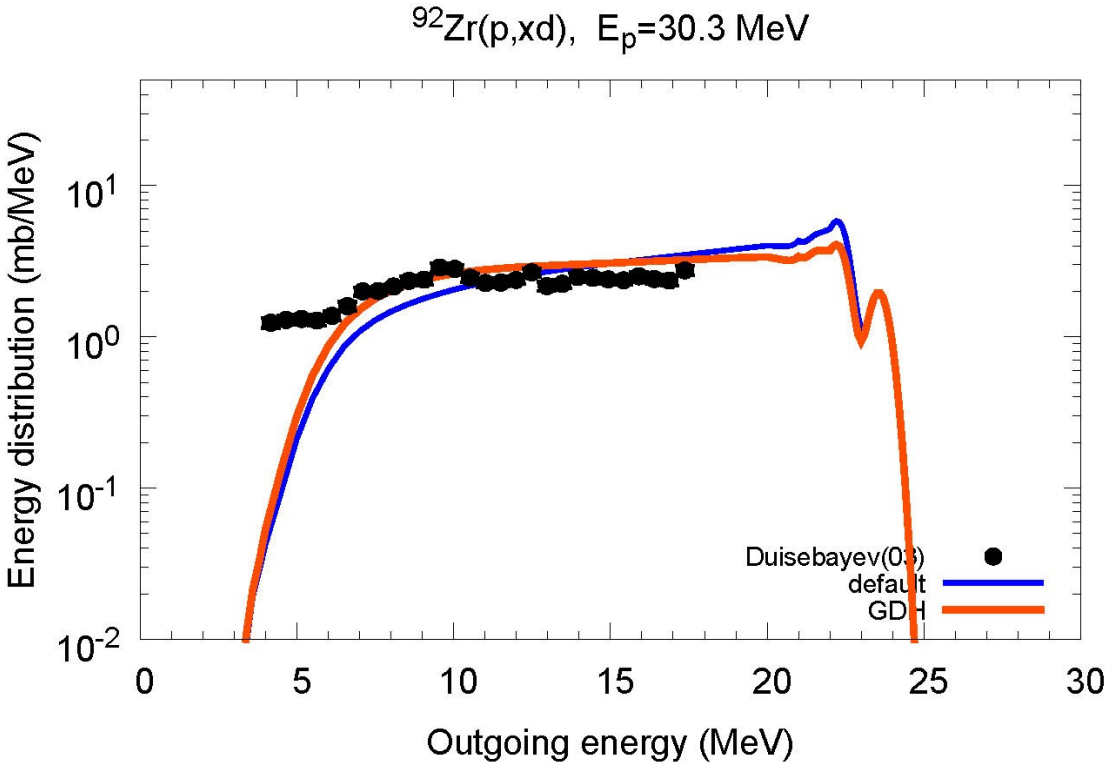
^{92}Zr(p,xd), E_p=30.3 MeV
Duisebayev(08)
default
GDH
Energy distribution (mb/MeV)
10^{1}
10^{0}
10^{-1}
10^{-2}
0
5
10
15
20
25
30
Outgoing energy (MeV)

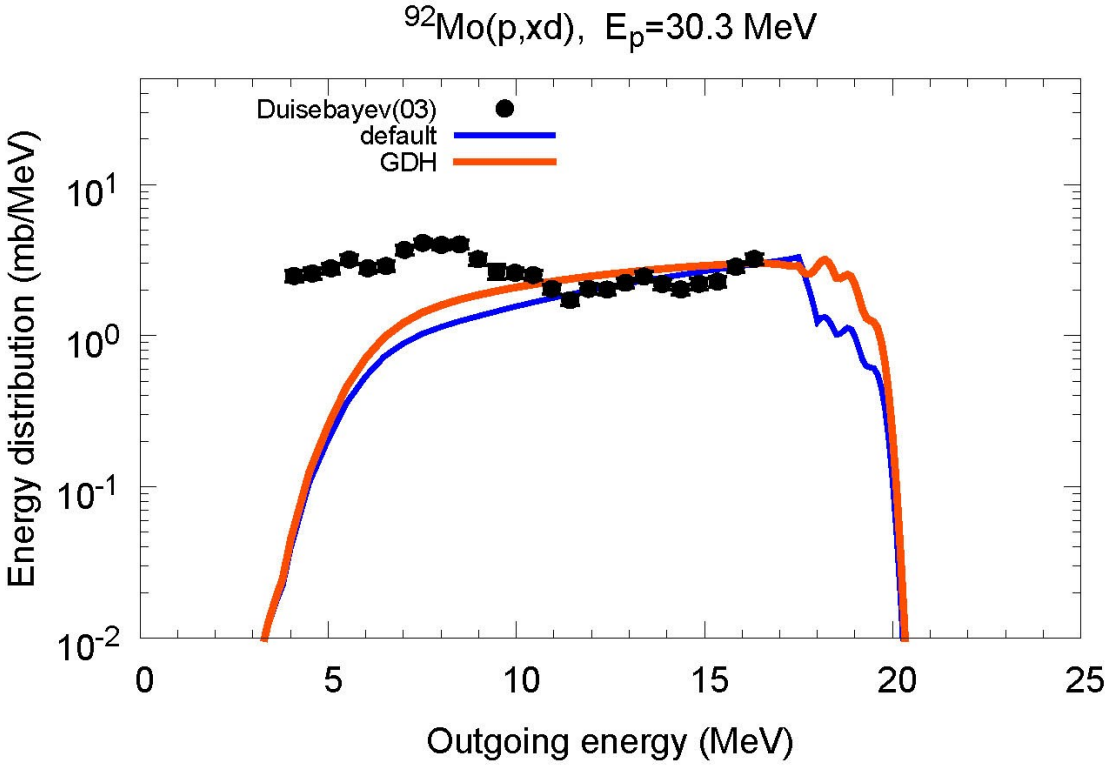
92Mo(p,xd), Ep=30.3 MeV
Duisebayev(03)
default
GDH
Energy distribution (mb/MeV)
Outgoing energy (MeV)

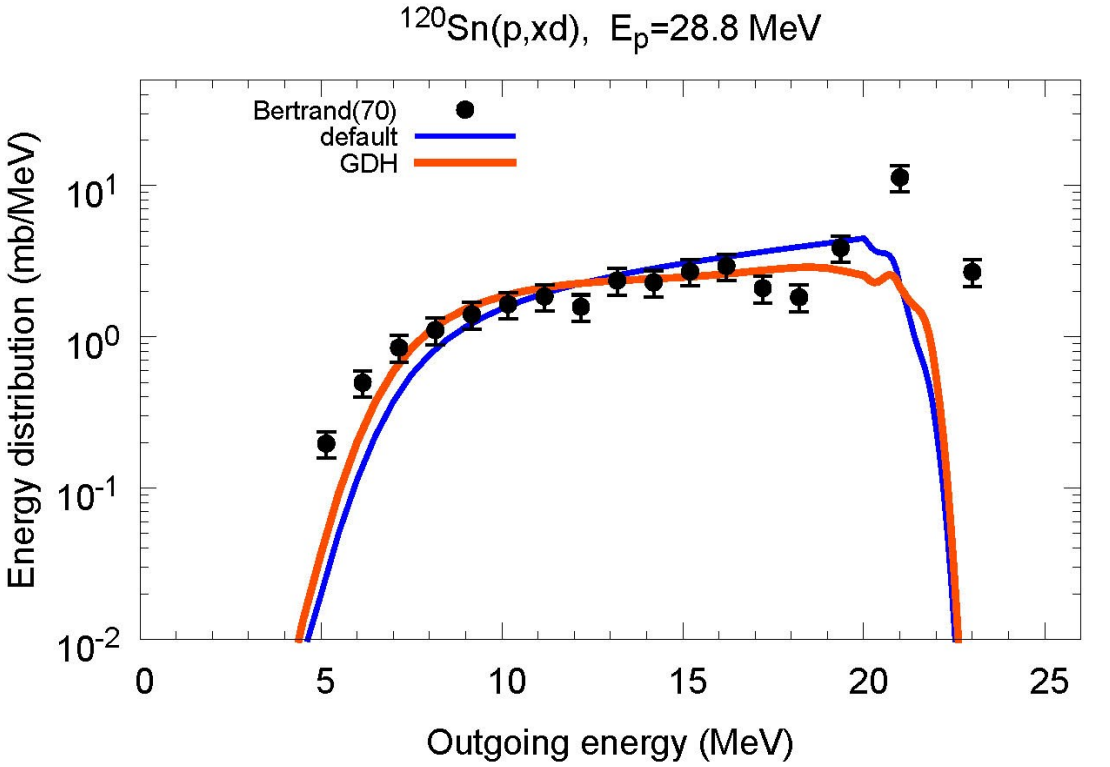
120Sn(p,xd), Ep=28.8 MeV
Bertrand(70)
default
GDH
Energy distribution (mb/MeV)
Outgoing energy (MeV)

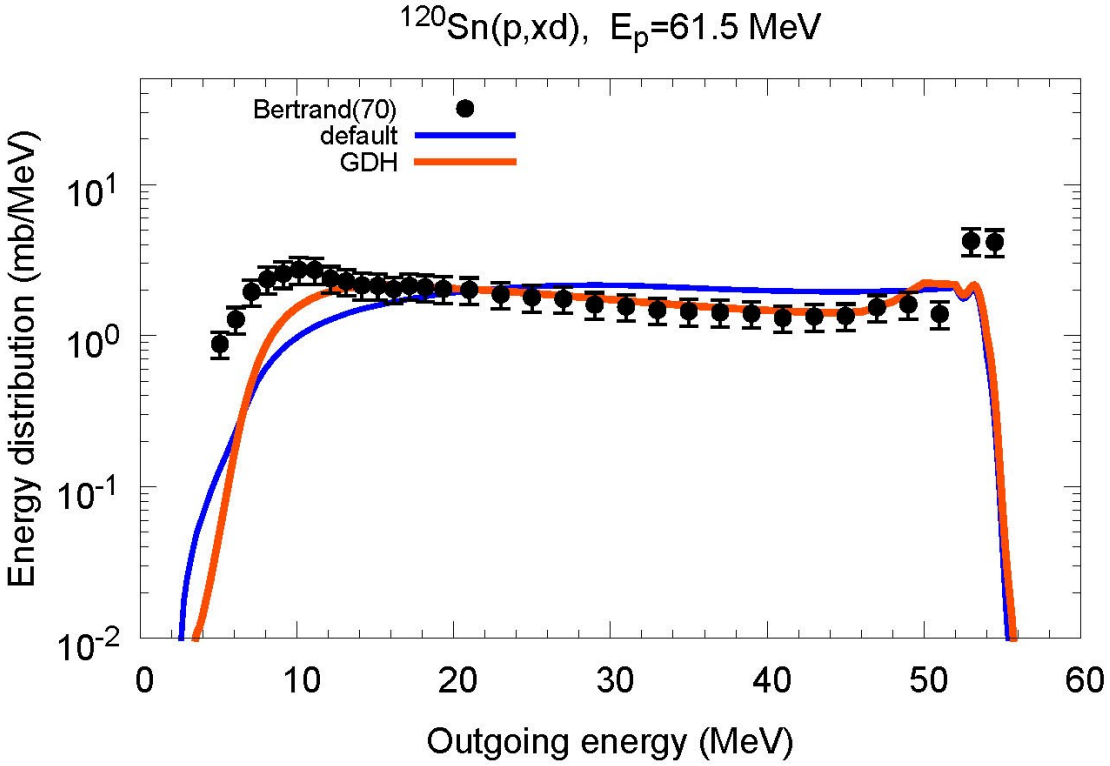
^{120}Sn(p,xd), E_p=61.5 MeV
Bertrand(70)
default
GDH
Energy distribution (mb/MeV)
10^{1}
10^{0}
10^{-1}
10^{-2}
0
10
20
30
40
50
60
Outgoing energy (MeV)

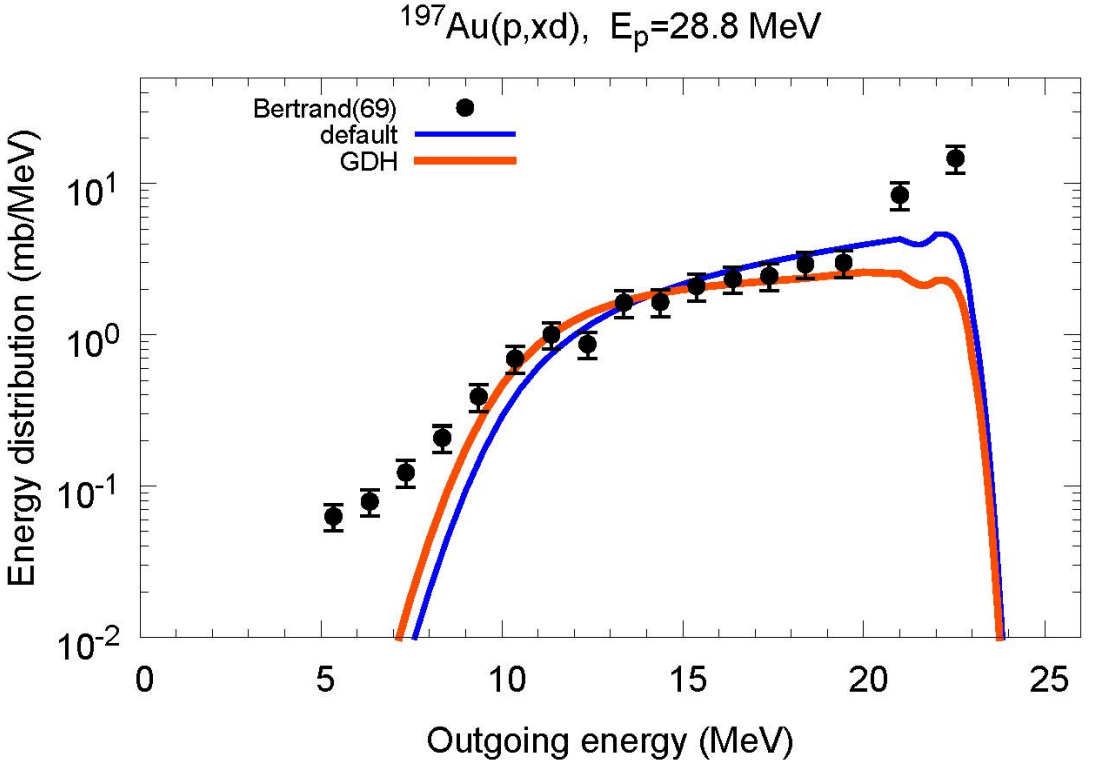
^{197}Au(p,xd), E_p=28.8 MeV
Bertrand(69)
default
GDH
Energy distribution (mb/MeV)
10^{1}
10^{0}
10^{-1}
10^{-2}
0
5
10
15
20
25
Outgoing energy (MeV)

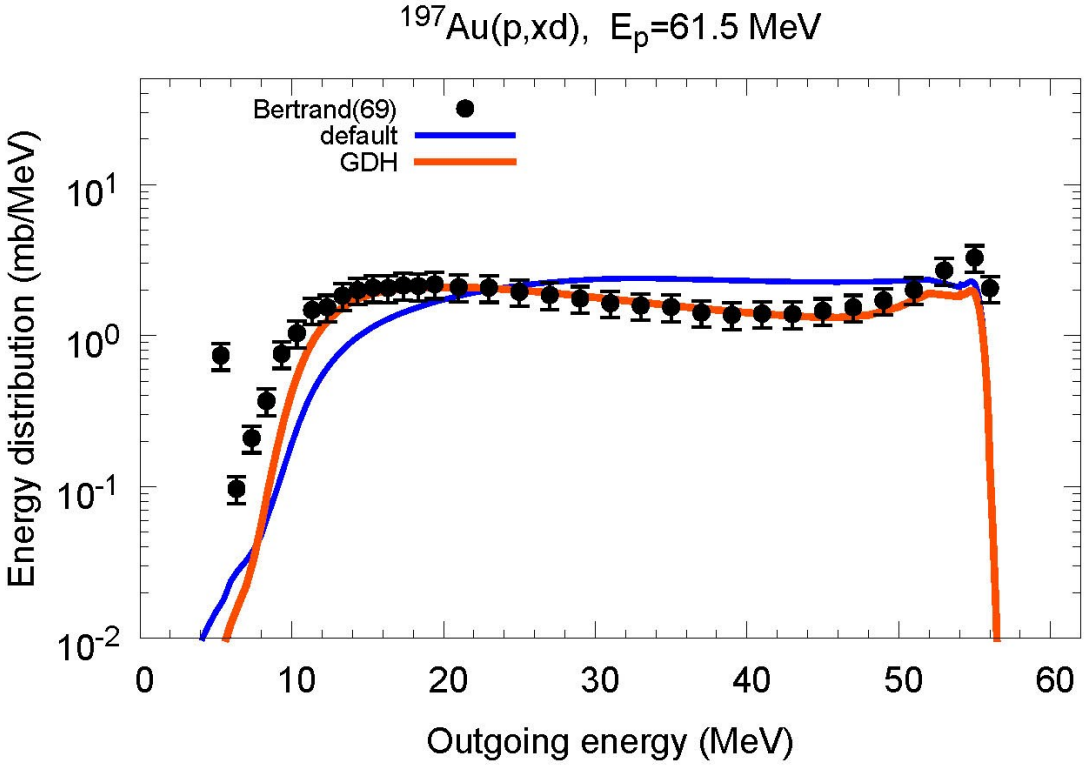
^{197}Au(p,xd), E_p=61.5 MeV
Bertrand(69)
default
GDH
Energy distribution (mb/MeV)
10^1
10^0
10^{-1}
10^{-2}
0
10
20
30
40
50
60
Outgoing energy (MeV)

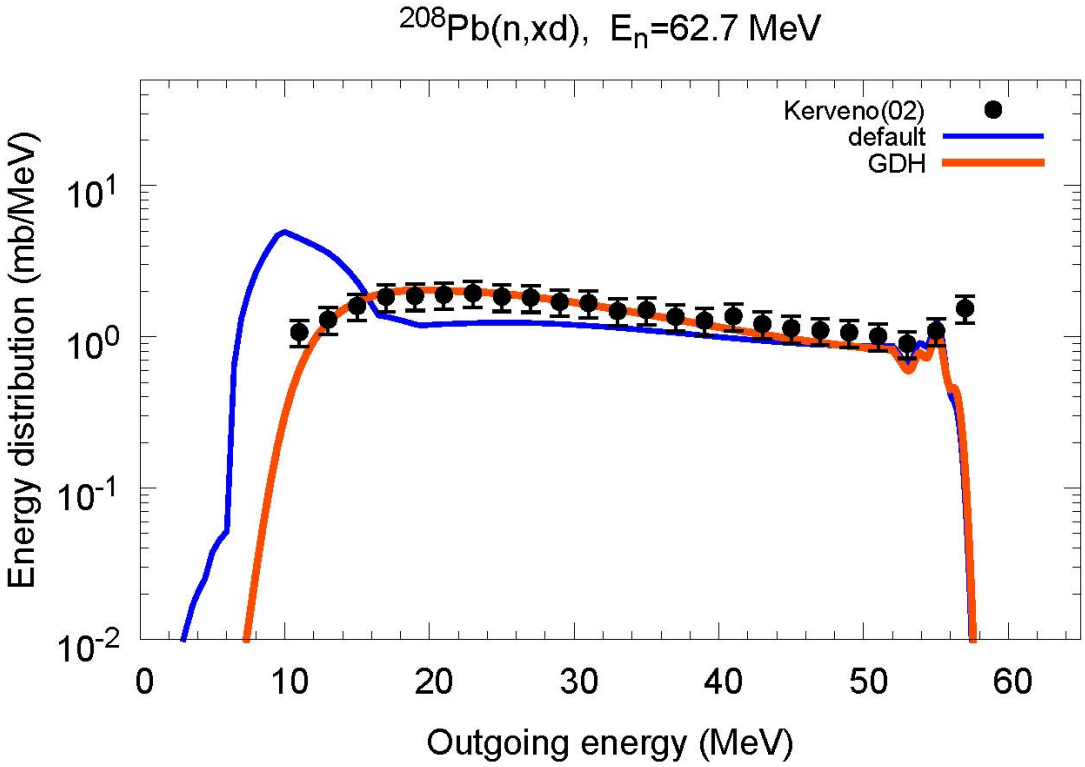
^{208}Pb(n,xd), E_n=62.7 MeV
Kerveno(02)
default
GDH
Energy distribution (mb/MeV)
10^1
10^0
10^{-1}
10^{-2}
0
10
20
30
40
50
60
Outgoing energy (MeV)

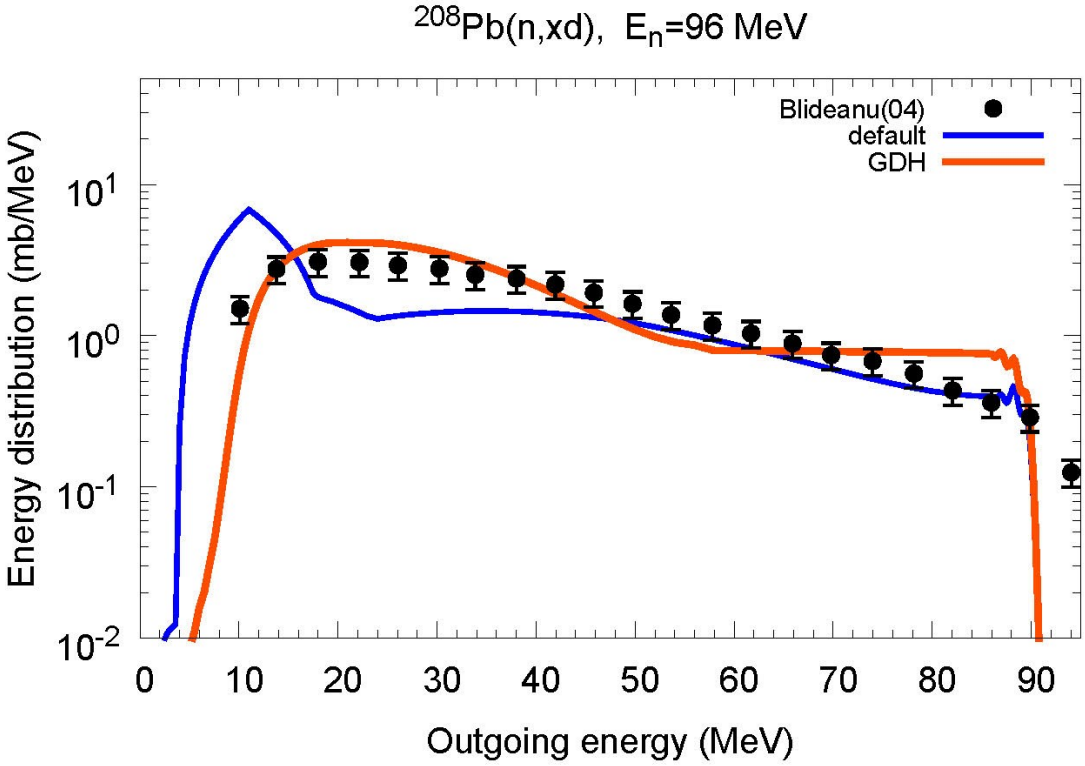
^{208}Pb(n,xd), E_n=96 MeV
Blideanu(04)
default
GDH
Energy distribution (mb/MeV)
10^1
10^0
10^{-1}
10^{-2}
0
10
20
30
40
50
60
70
80
90
Outgoing energy (MeV)

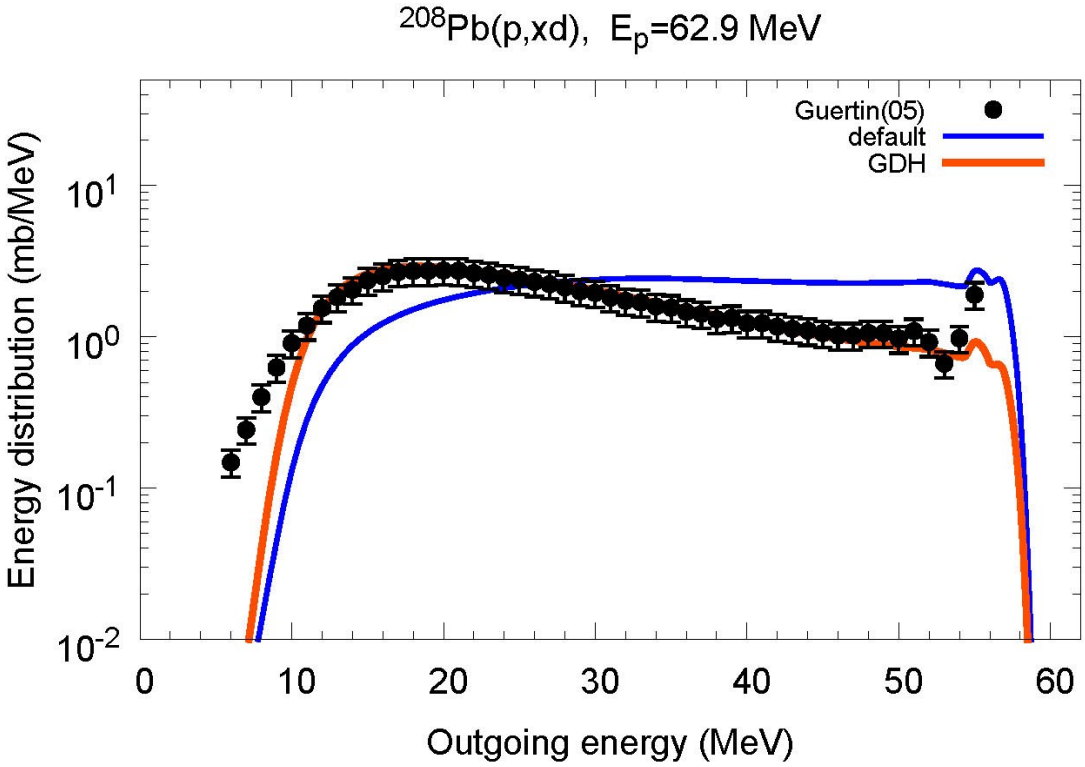
^{208}Pb(p,xd), E_p=62.9 MeV
Guertin(05)
default
GDH
Energy distribution (mb/MeV)
10^1
10^0
10^{-1}
10^{-2}
0
10
20
30
40
50
60
Outgoing energy (MeV)

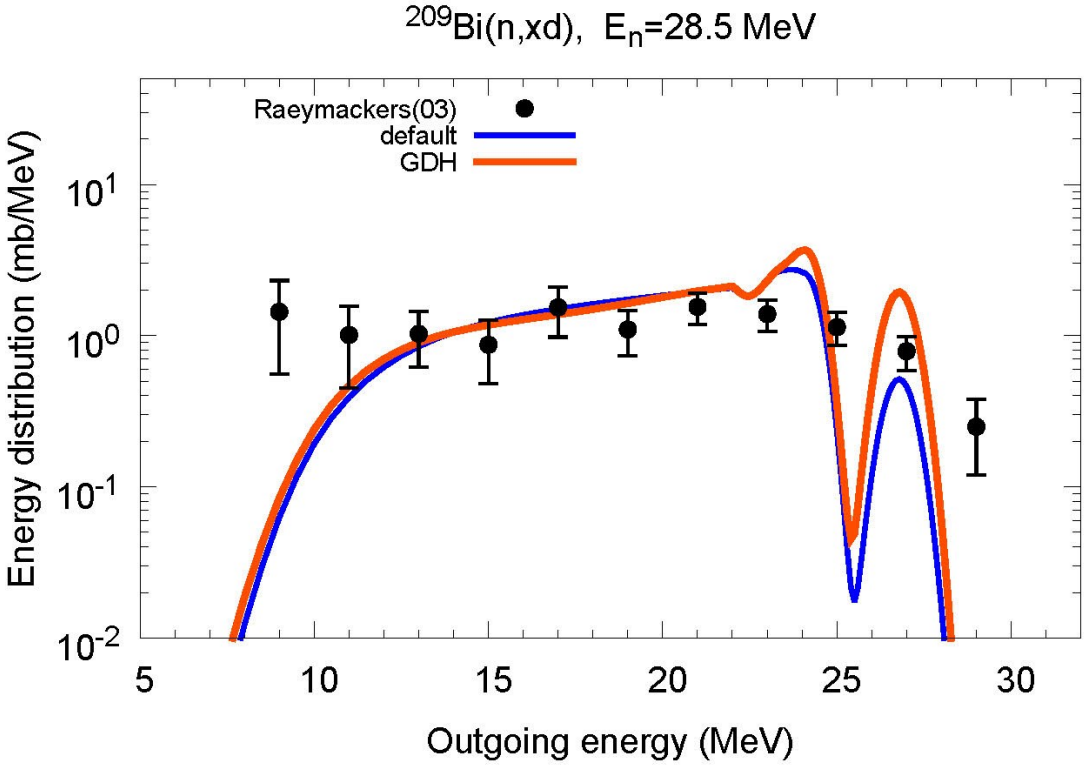
^{209}Bi(n,xd), E_n=28.5 MeV
Raeymackers(03)
default
GDH
Energy distribution (mb/MeV)
10^1
10^0
10^{-1}
10^{-2}
5
10
15
20
25
30
Outgoing energy (MeV)

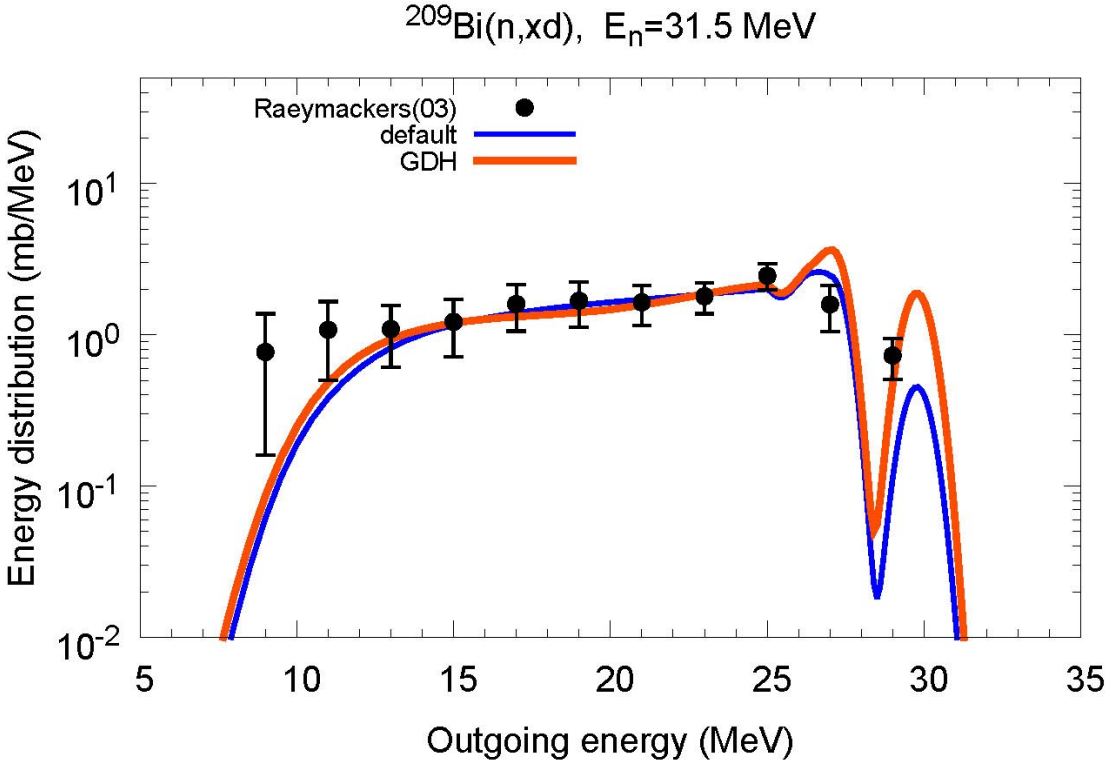
^{209}Bi(n,xd), E_n=31.5 MeV
Raeymackers(03)
default
GDH
Energy distribution (mb/MeV)
10^1
10^0
10^{-1}
10^{-2}
5
10
15
20
25
30
35
Outgoing energy (MeV)

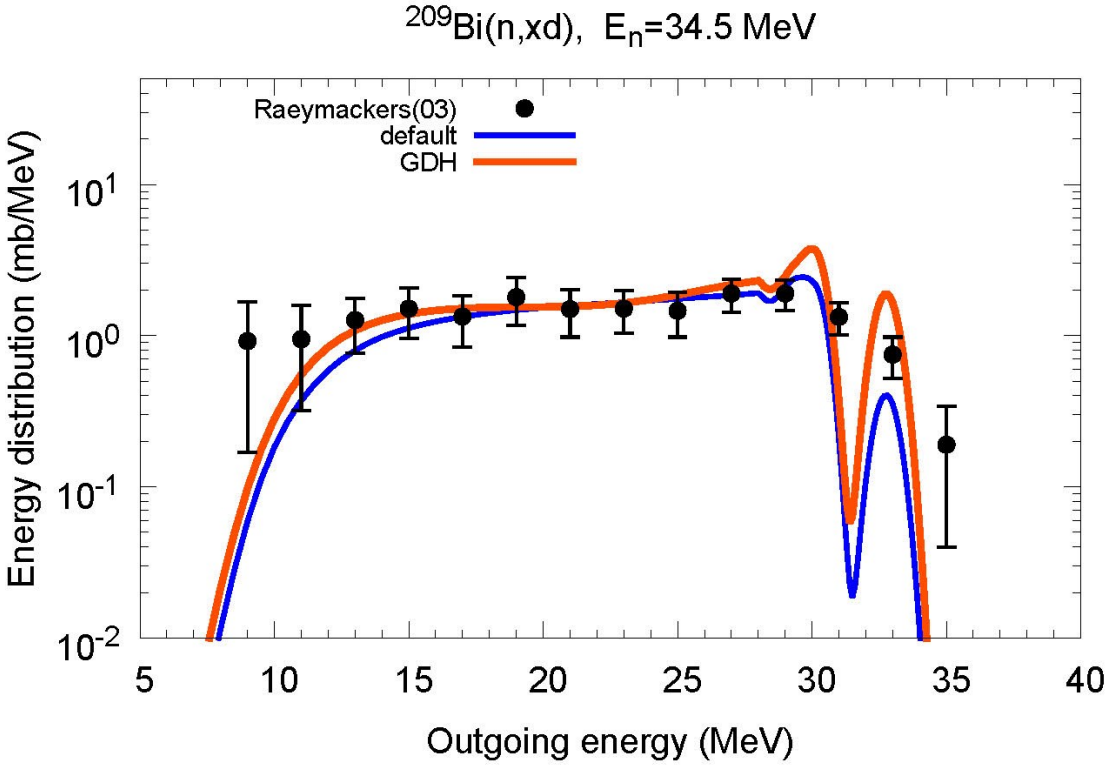
^{209}Bi(n,xd), E_n=34.5 MeV
Raeymackers(03)
default
GDH
Energy distribution (mb/MeV)
10^{1}
10^{0}
10^{-1}
10^{-2}
5
10
15
20
25
30
35
40
Outgoing energy (MeV)

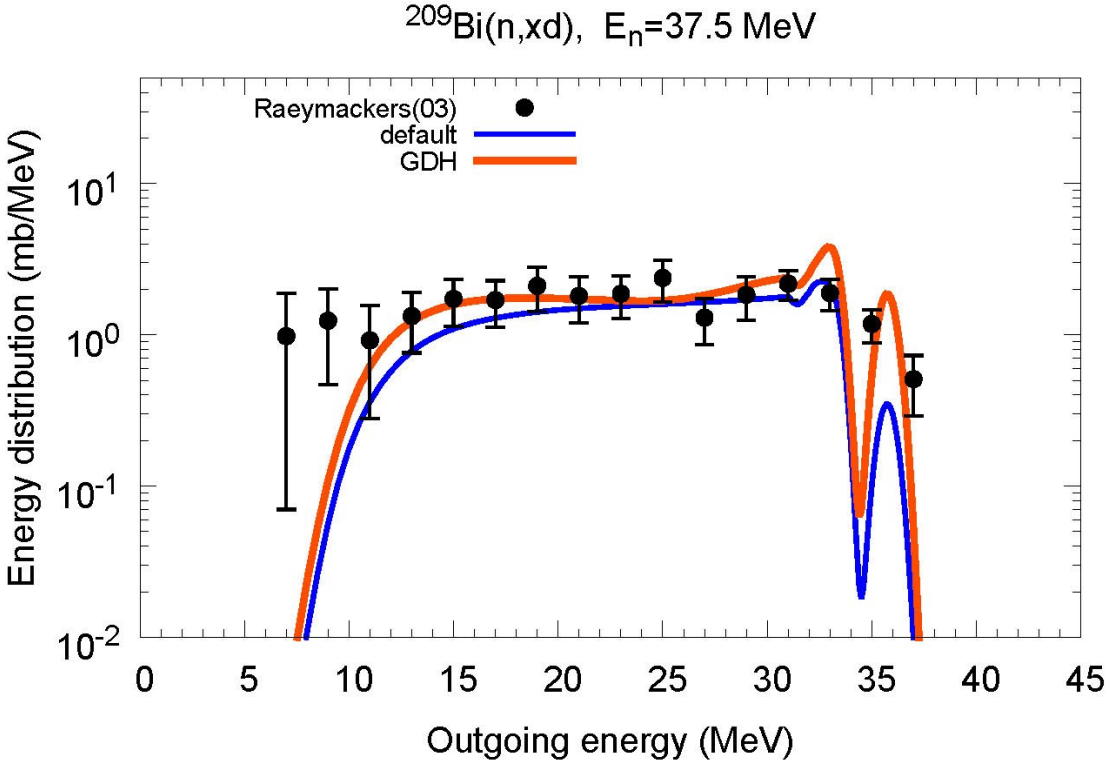
^{209}Bi(n,xd), E_n=37.5 MeV
Raeymackers(03)
default
GDH
Energy distribution (mb/MeV)
10^{1}
10^{0}
10^{-1}
10^{-2}
0
5
10
15
20
25
30
35
40
45
Outgoing energy (MeV)

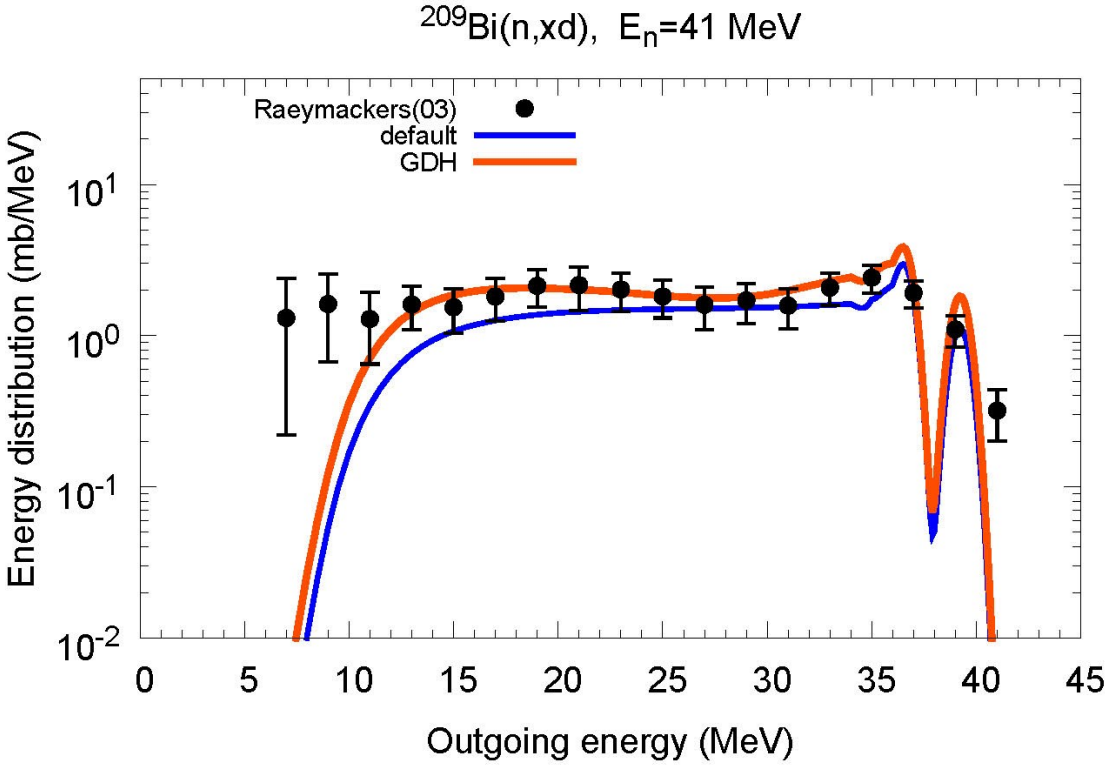
^{209}Bi(n,xd), E_n=41 MeV
Raeymackers(03)
default
GDH
Energy distribution (mb/MeV)
10^{1}
10^{0}
10^{-1}
10^{-2}
0
5
10
15
20
25
30
35
40
45
Outgoing energy (MeV)

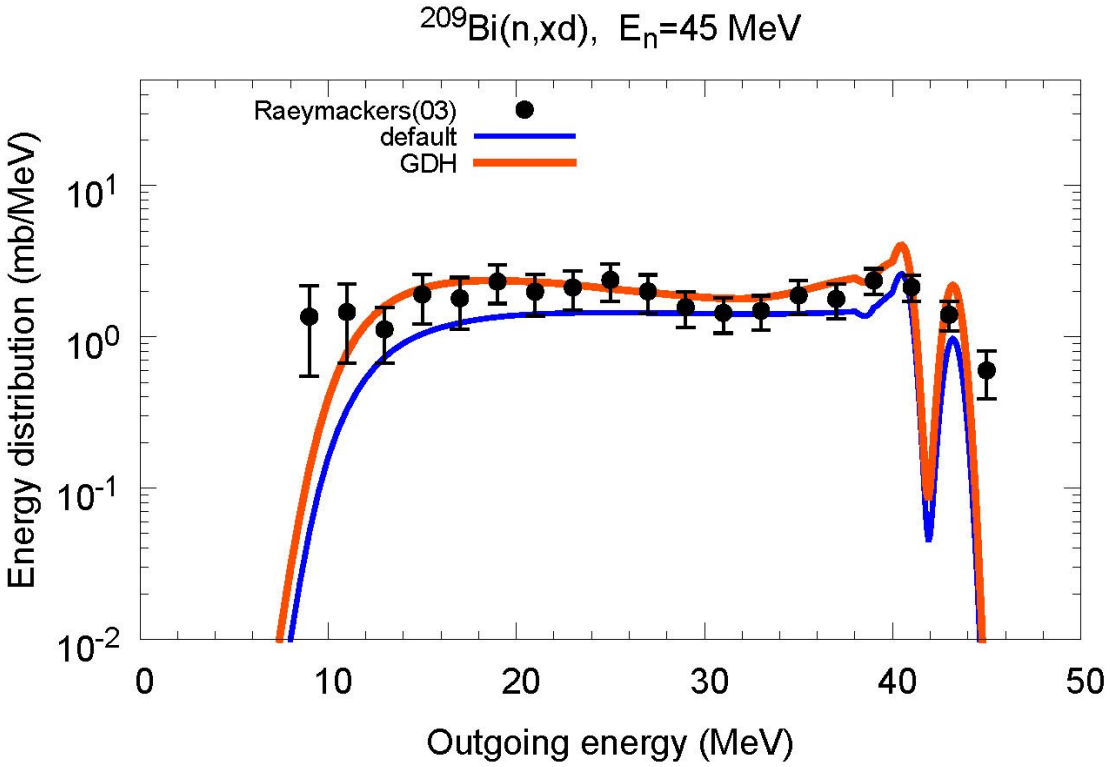
^{209}Bi(n,xd), E_n=45 MeV
Raeymackers(03)
default
GDH
Energy distribution (mb/MeV)
10^{1}
10^{0}
10^{-1}
10^{-2}
0
10
20
30
40
50
Outgoing energy (MeV)

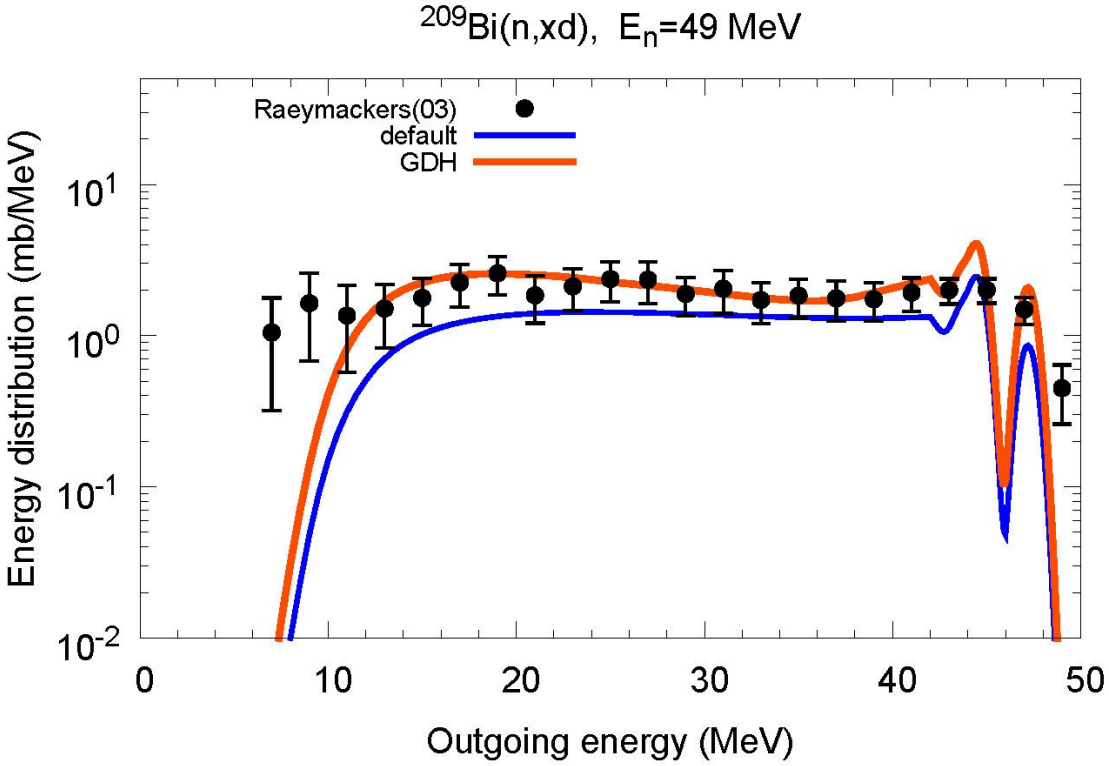
^{209}Bi(n,xd), E_n=49 MeV
Raeymackers(03)
default
GDH
Energy distribution (mb/MeV)
10^{1}
10^{0}
10^{-1}
10^{-2}
0
10
20
30
40
50
Outgoing energy (MeV)

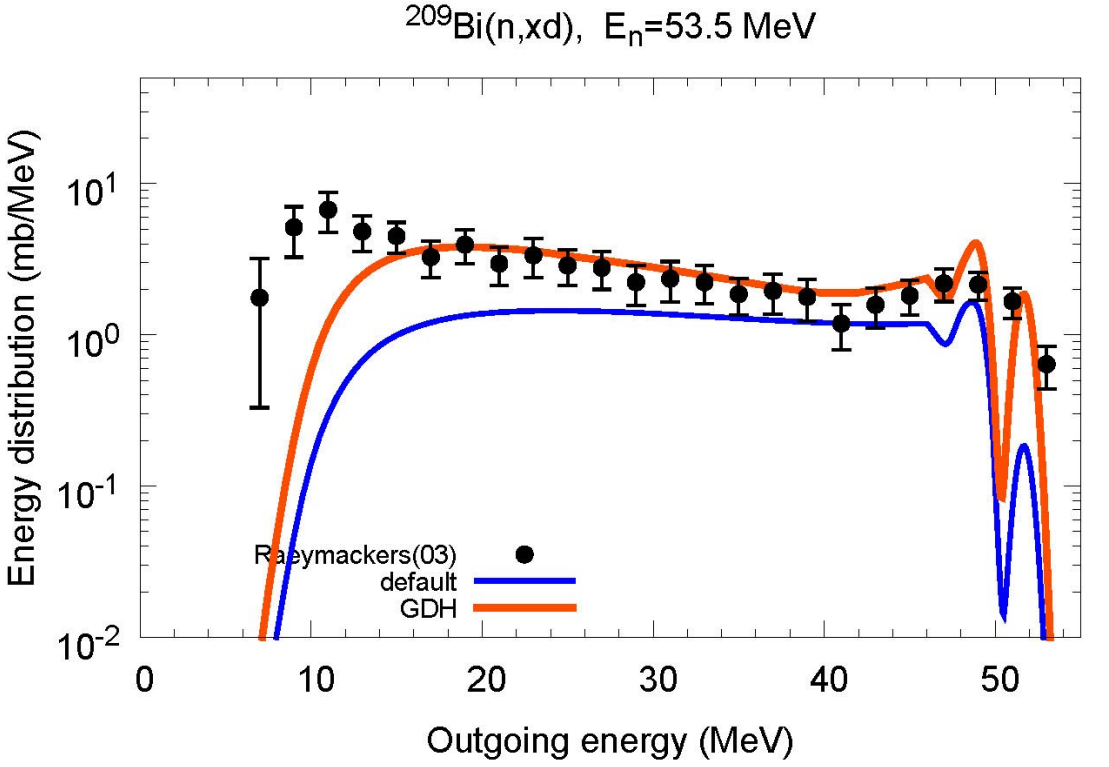
^{209}Bi(n,xd), E_n=53.5 MeV
Raeymackers(03)
default
GDH
Energy distribution (mb/MeV)
10^{1}
10^{0}
10^{-1}
10^{-2}
0
10
20
30
40
50
Outgoing energy (MeV)

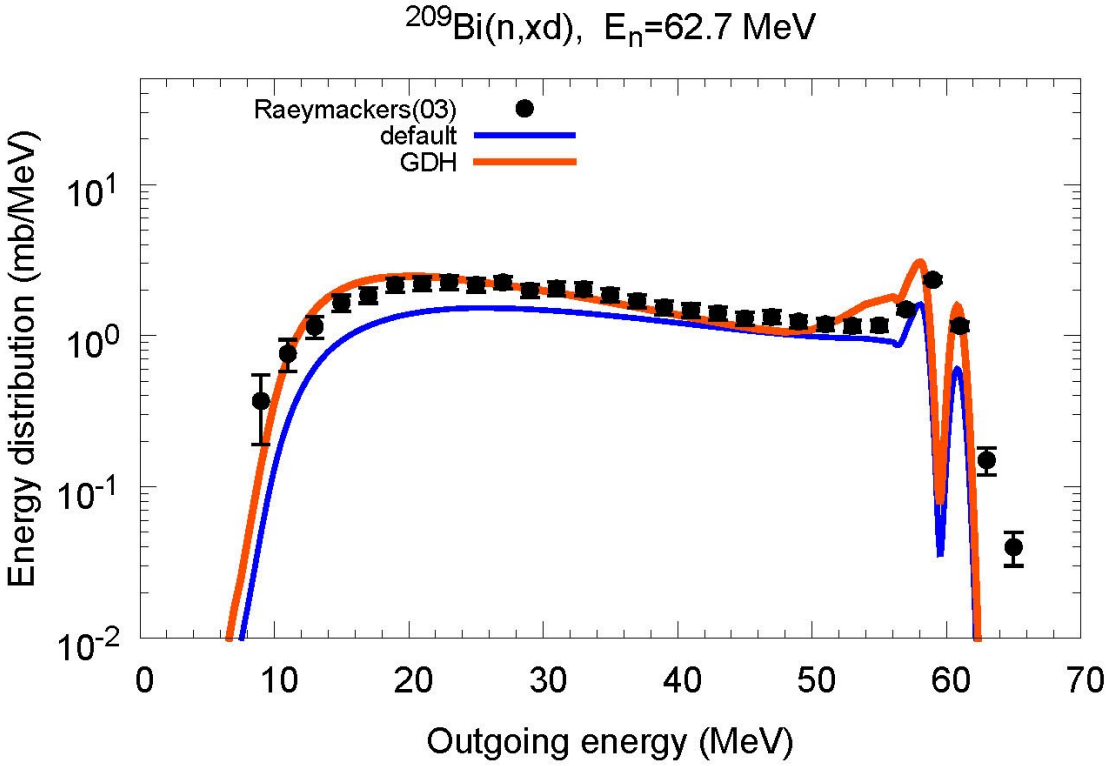
^{209}Bi(n,xd), E_n=62.7 MeV
Raeymackers(03)
default
GDH
Energy distribution (mb/MeV)
Outgoing energy (MeV)

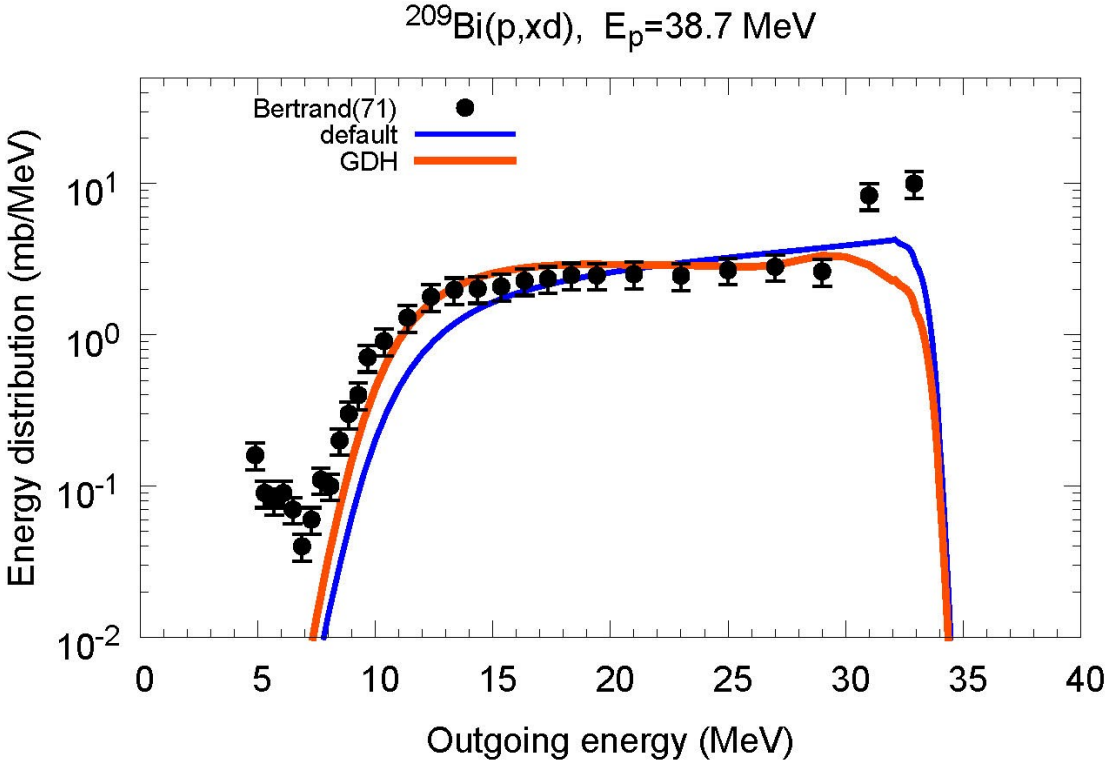
^{209}Bi(p,xd), E_p=38.7 MeV
Bertrand(71)
default
GDH
Energy distribution (mb/MeV)
Outgoing energy (MeV)

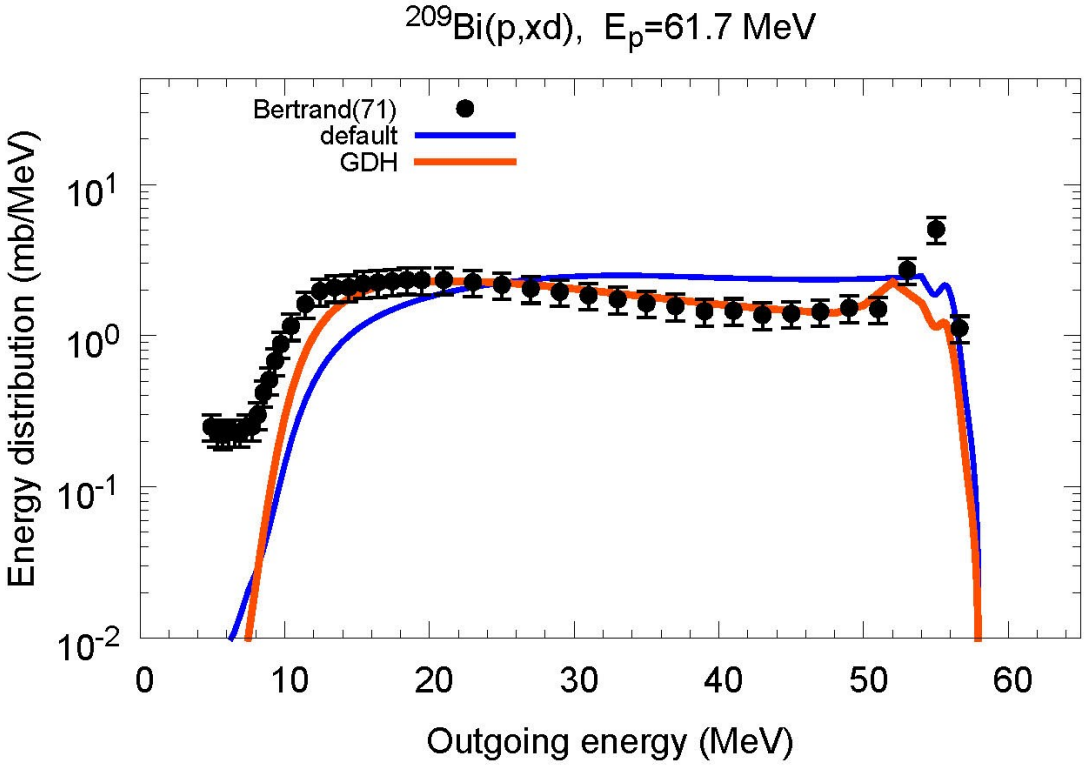
^{209}Bi(p,xd), E_p=61.7 MeV
Bertrand(71)
default
GDH
Energy distribution (mb/MeV)
10^1
10^0
10^{-1}
10^{-2}
0
10
20
30
40
50
60
Outgoing energy (MeV)

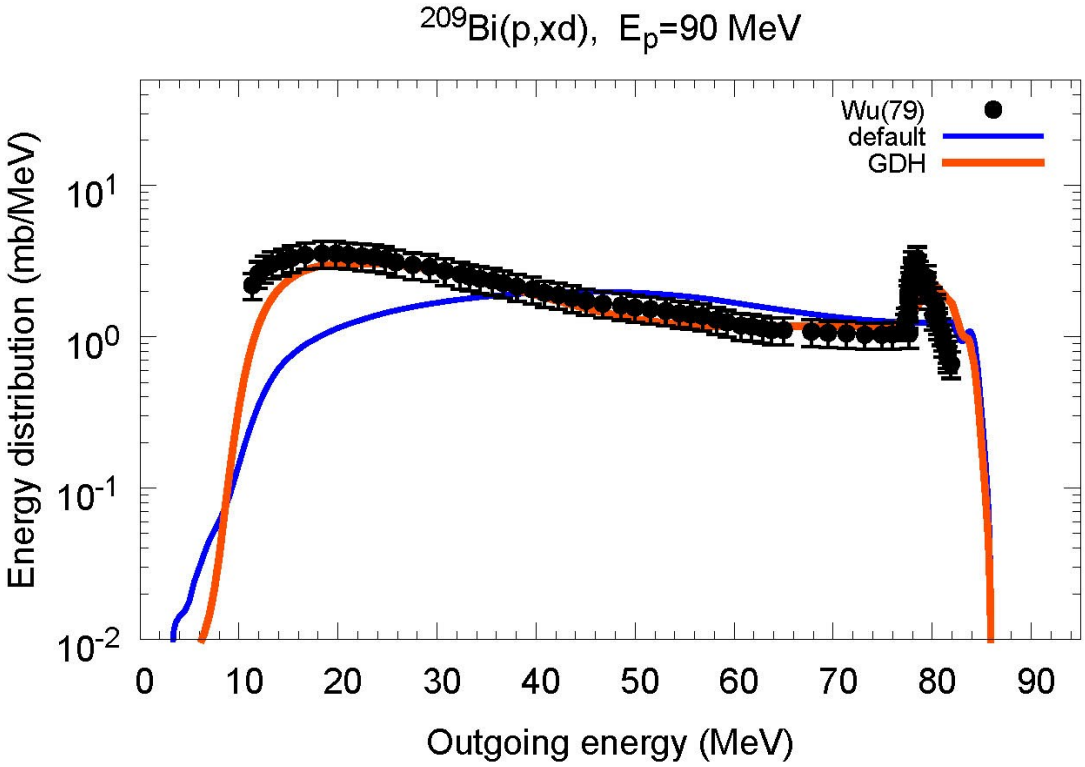
^{209}Bi(p,xd), E_p=90 MeV
Wu(79)
default
GDH
Energy distribution (mb/MeV)
10^1
10^0
10^{-1}
10^{-2}
0
10
20
30
40
50
60
70
80
90
Outgoing energy (MeV)

Appendix C

Calculated and experimental α-particle energy distributions

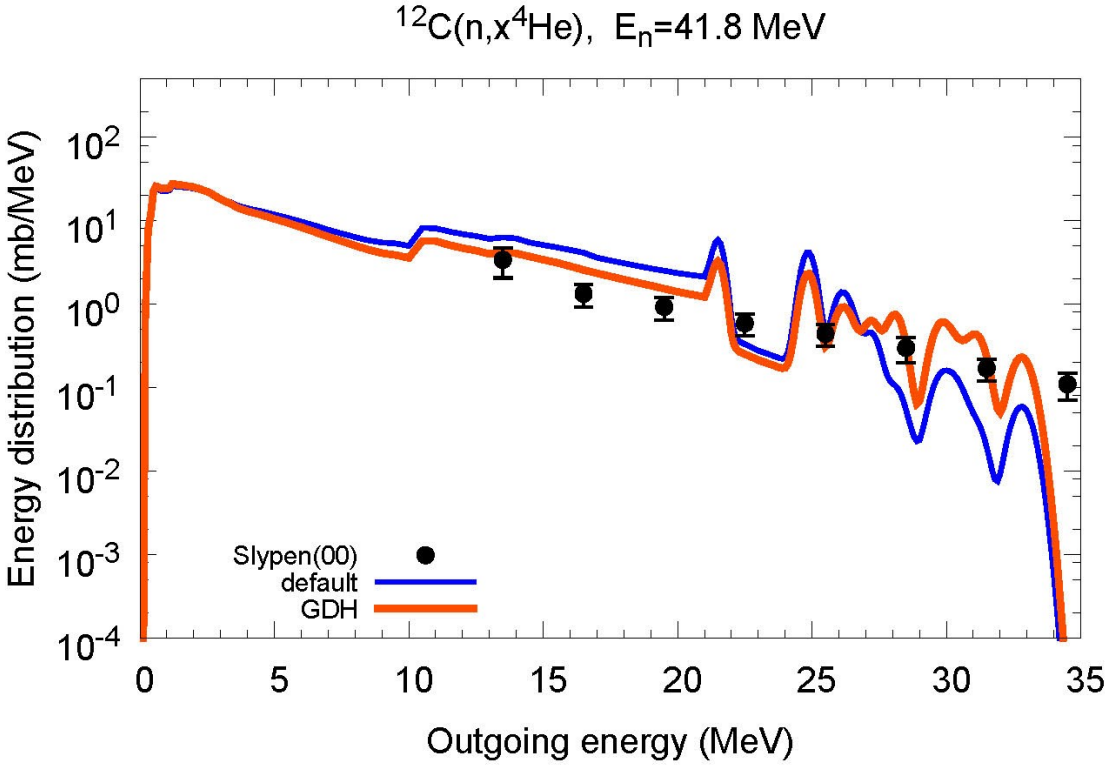
^{12}C(n,x^{4}He), E$_n$=41.8 MeV
Energy distribution (mb/MeV)
Outgoing energy (MeV)
Slypen(00)
default
GDH

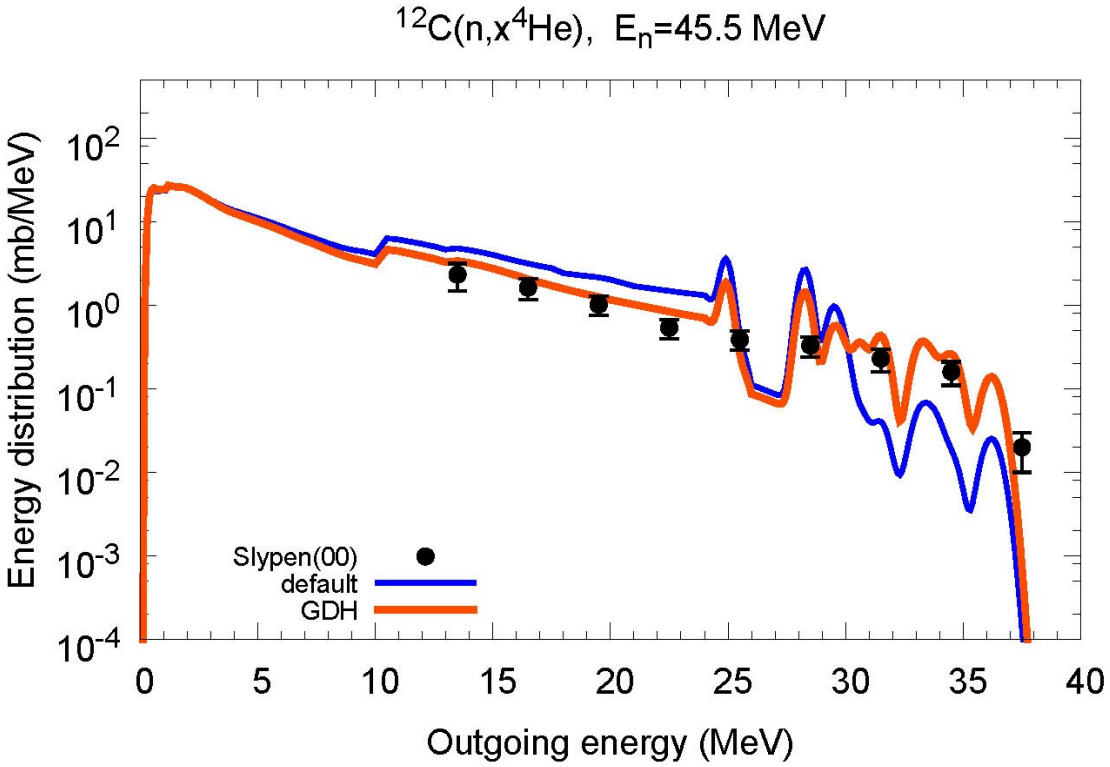
^{12}C(n,x^{4}He), E$_n$=45.5 MeV
Energy distribution (mb/MeV)
Outgoing energy (MeV)
Slypen(00)
default
GDH

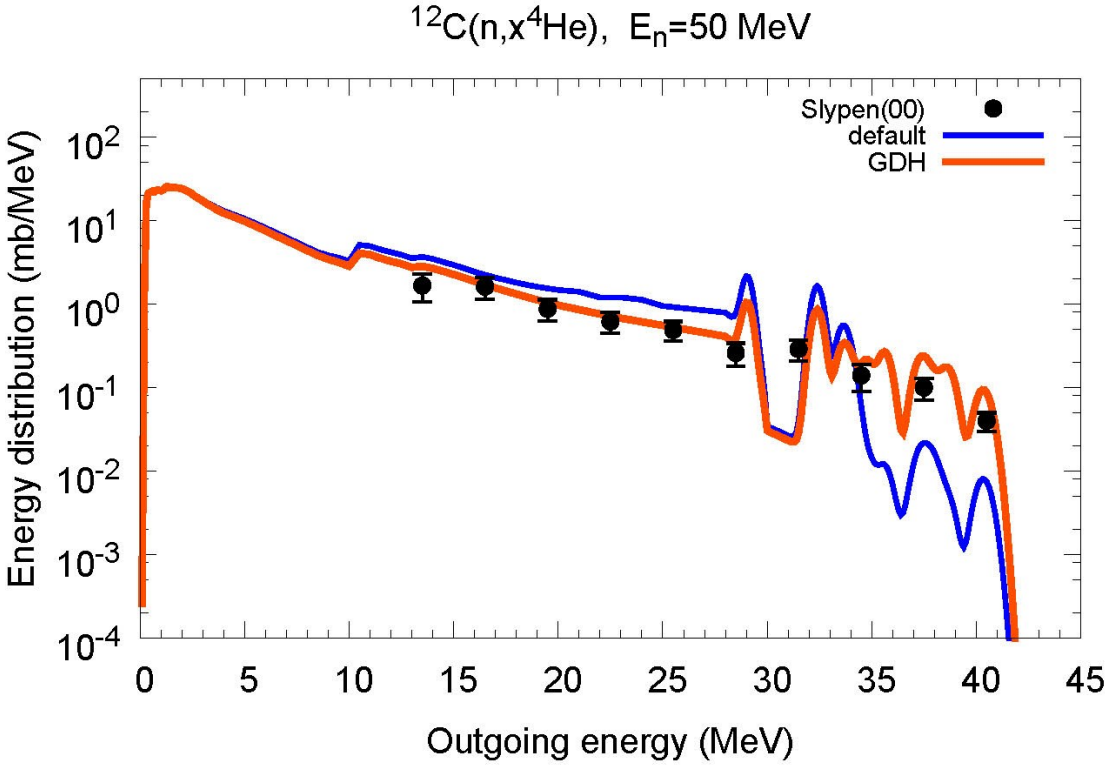
^{12}C(n,x^{4}He), E$_n$=50 MeV
Slypen(00)
default
GDH
Energy distribution (mb/MeV)
Outgoing energy (MeV)

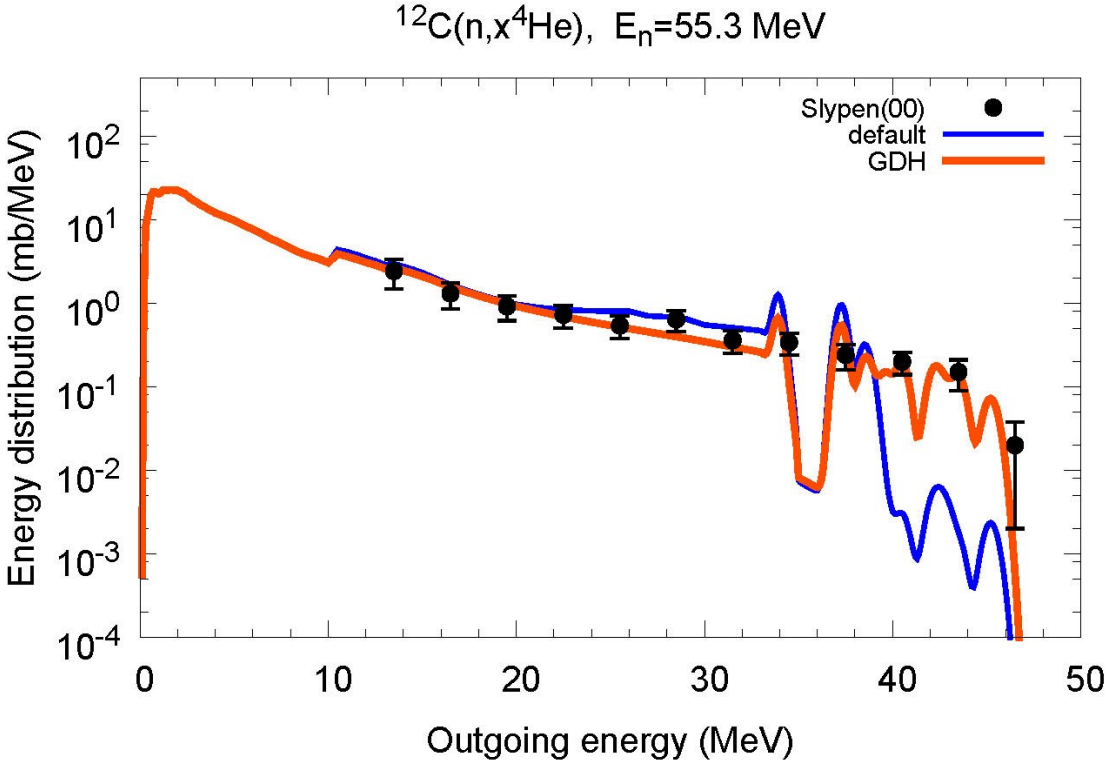
^{12}C(n,x^{4}He), E$_n$=55.3 MeV
Slypen(00)
default
GDH
Energy distribution (mb/MeV)
Outgoing energy (MeV)

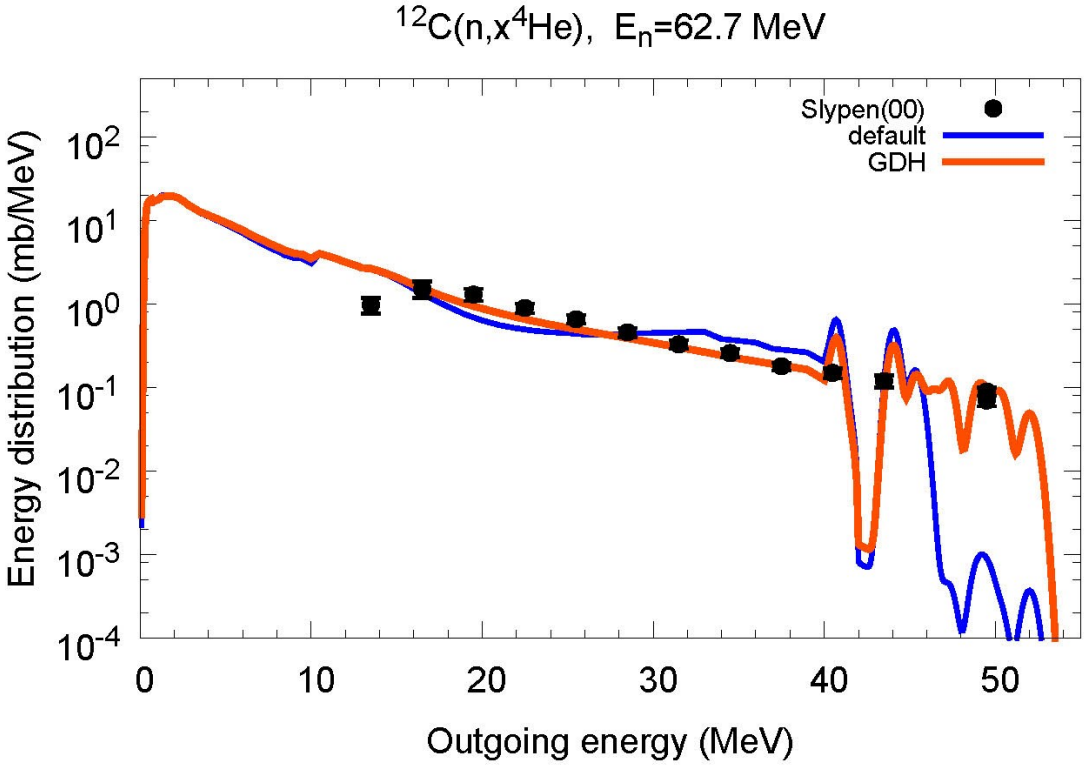
^{12}C(n,x^{4}He), E$_n$=62.7 MeV
Slypen(00)
default
GDH
Energy distribution (mb/MeV)
Outgoing energy (MeV)

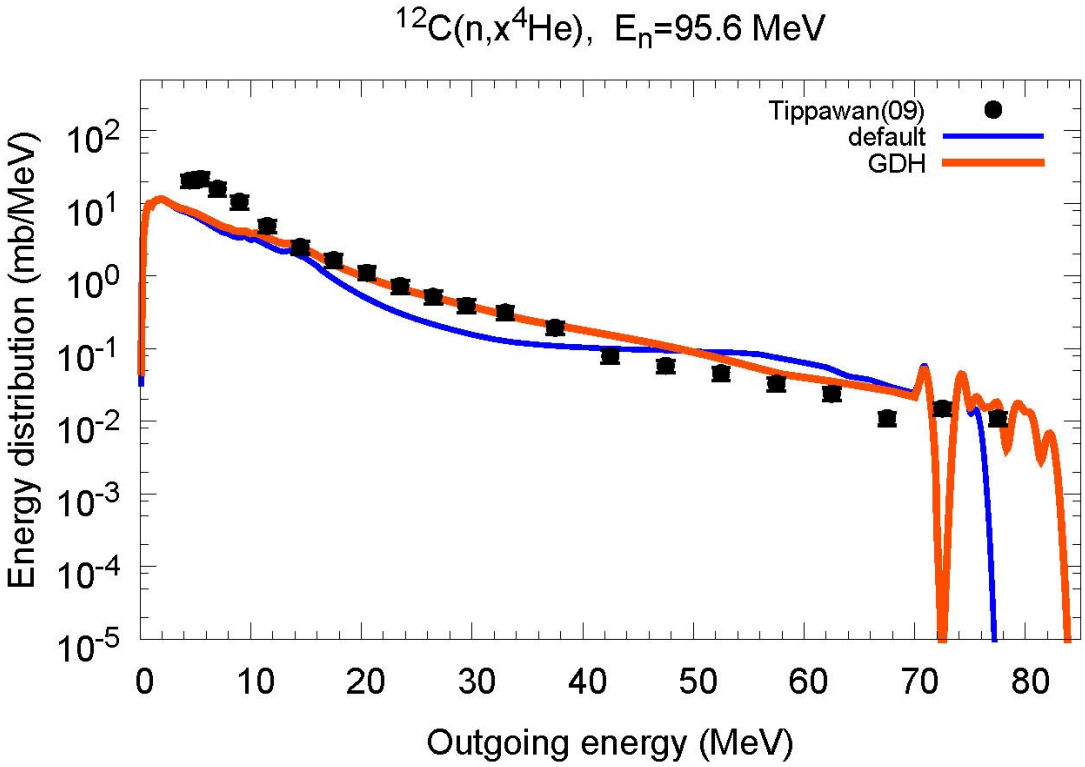
^{12}C(n,x^{4}He), E$_n$=95.6 MeV
Tippawan(09)
default
GDH
Energy distribution (mb/MeV)
Outgoing energy (MeV)

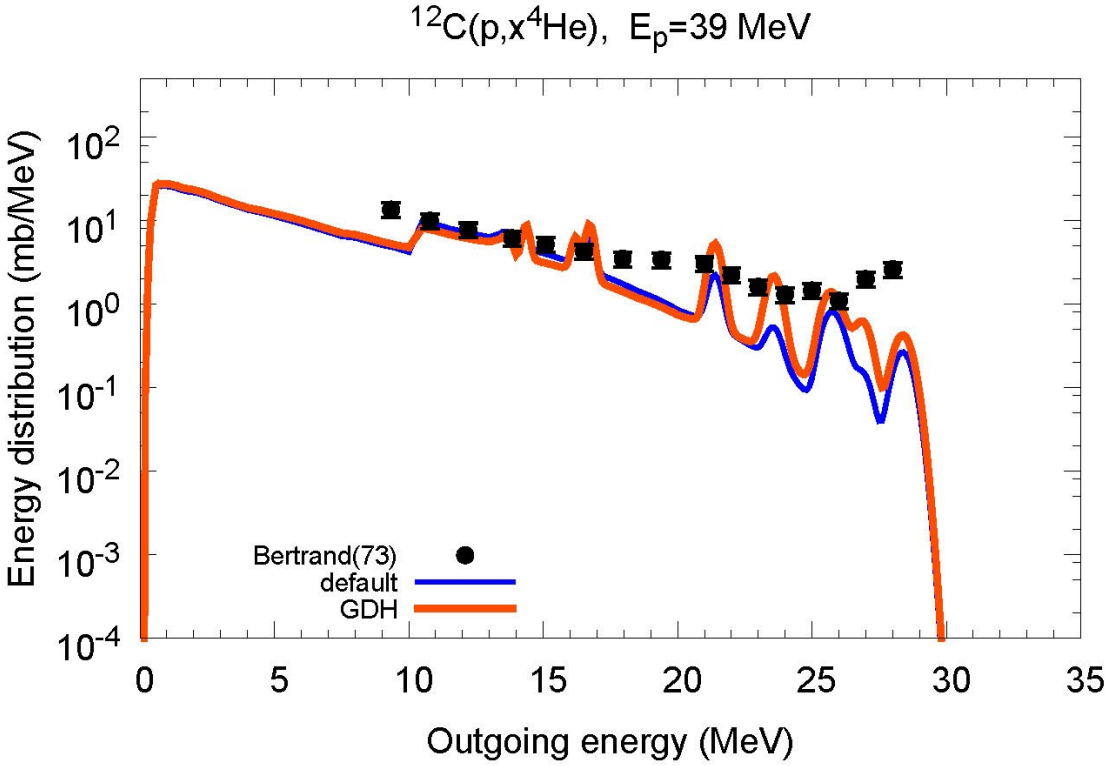
^{12}C(p,x^{4}He), E$_p$=39 MeV
Energy distribution (mb/MeV)
Outgoing energy (MeV)
Bertrand(73)
default
GDH

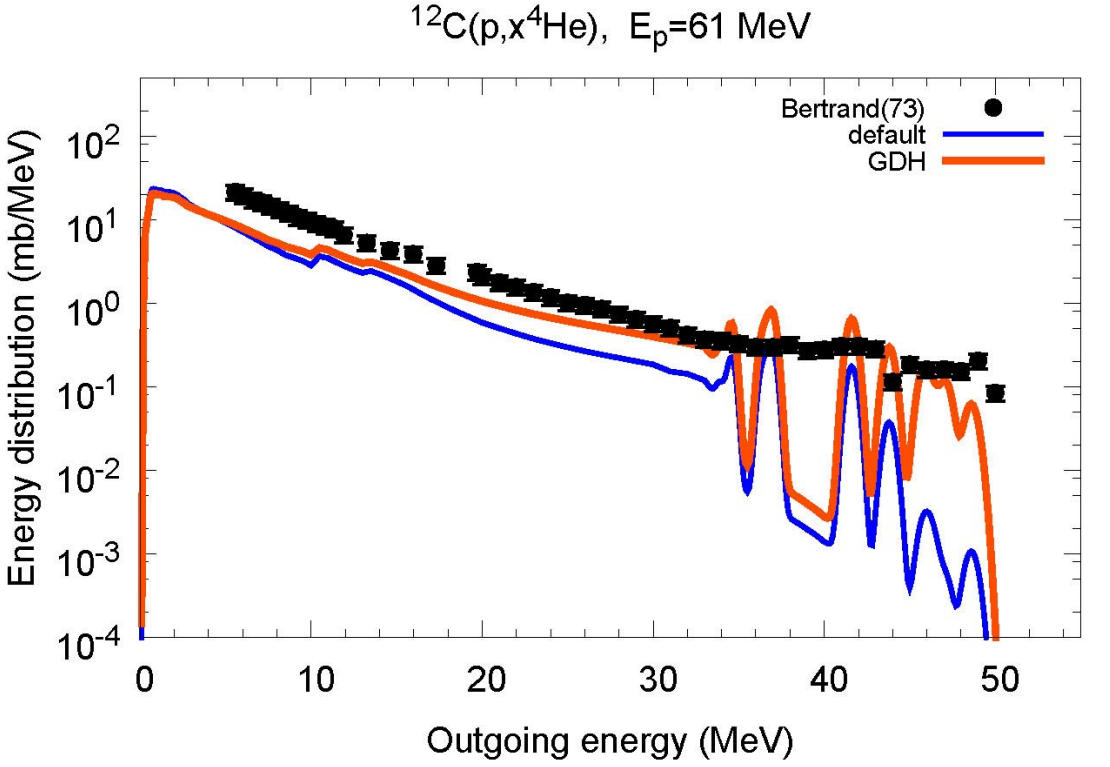
^{12}C(p,x^{4}He), E$_p$=61 MeV
Energy distribution (mb/MeV)
Outgoing energy (MeV)
Bertrand(73)
default
GDH

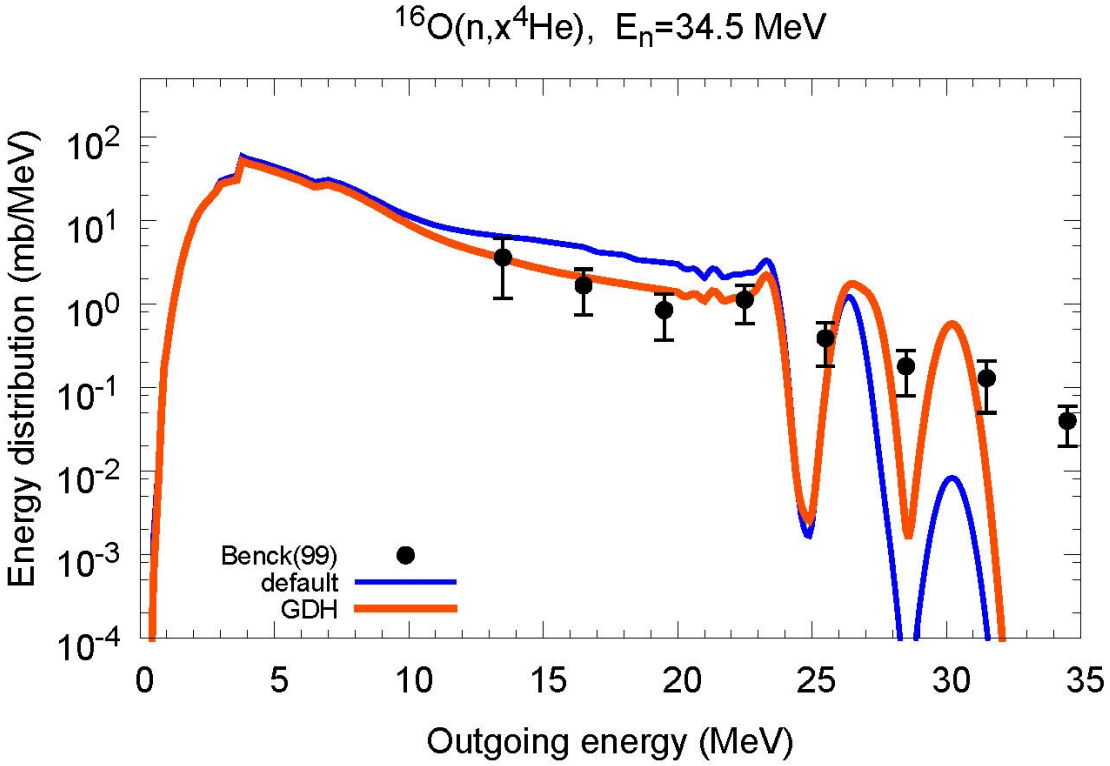
^{16}O(n,x^{4}He), E_n=34.5 MeV
Energy distribution (mb/MeV)
Outgoing energy (MeV)
Benck(99)
default
GDH

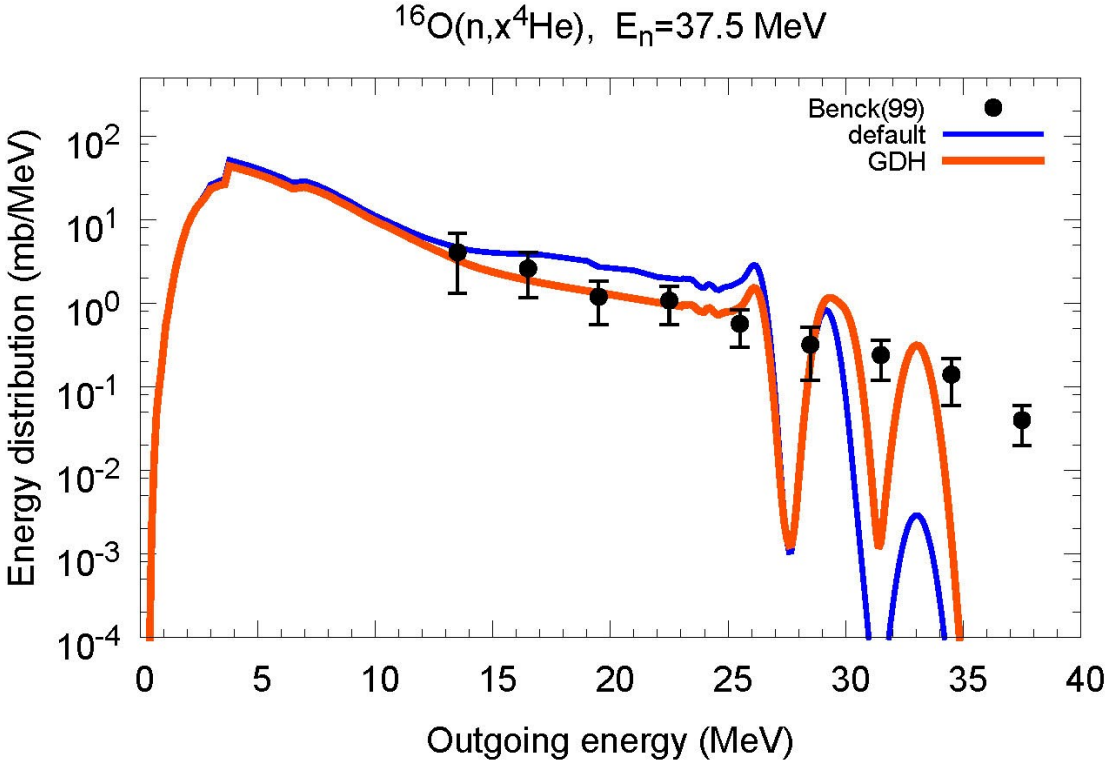
^{16}O(n,x^{4}He), E_n=37.5 MeV
Energy distribution (mb/MeV)
Outgoing energy (MeV)
Benck(99)
default
GDH

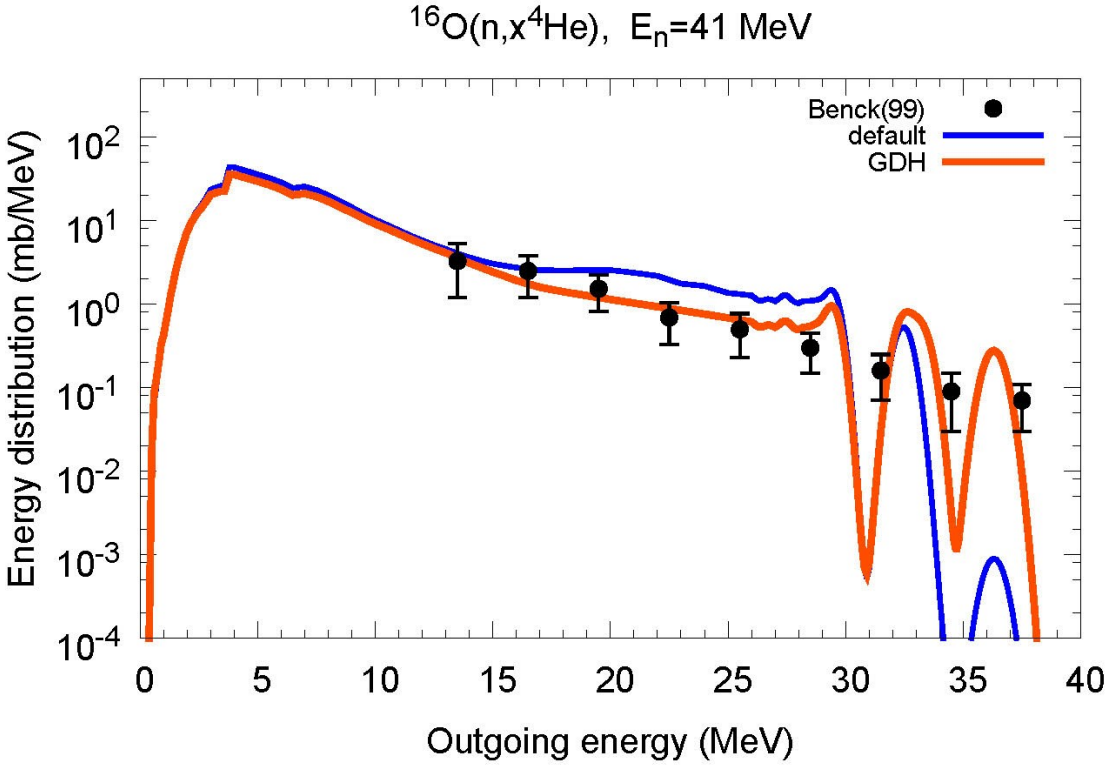
^{16}O(n,x^{4}He), E$_n$=41 MeV
Benck(99)
default
GDH
Energy distribution (mb/MeV)
Outgoing energy (MeV)

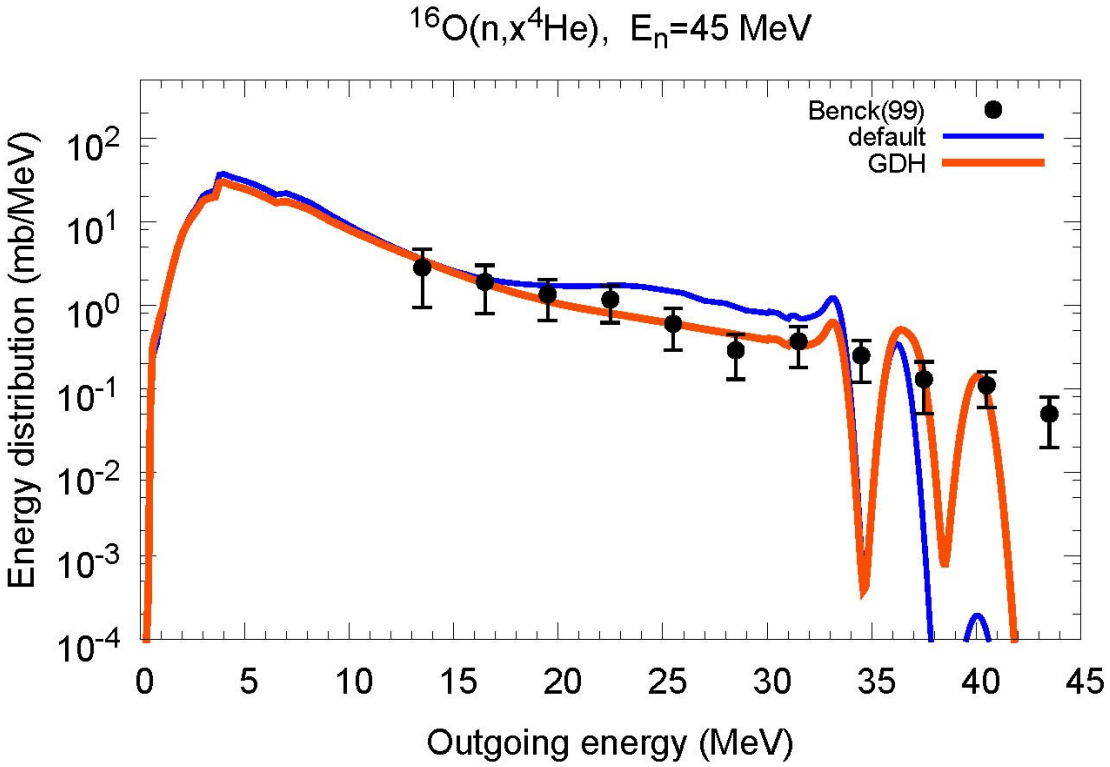
^{16}O(n,x^{4}He), E$_n$=45 MeV
Benck(99)
default
GDH
Energy distribution (mb/MeV)
Outgoing energy (MeV)

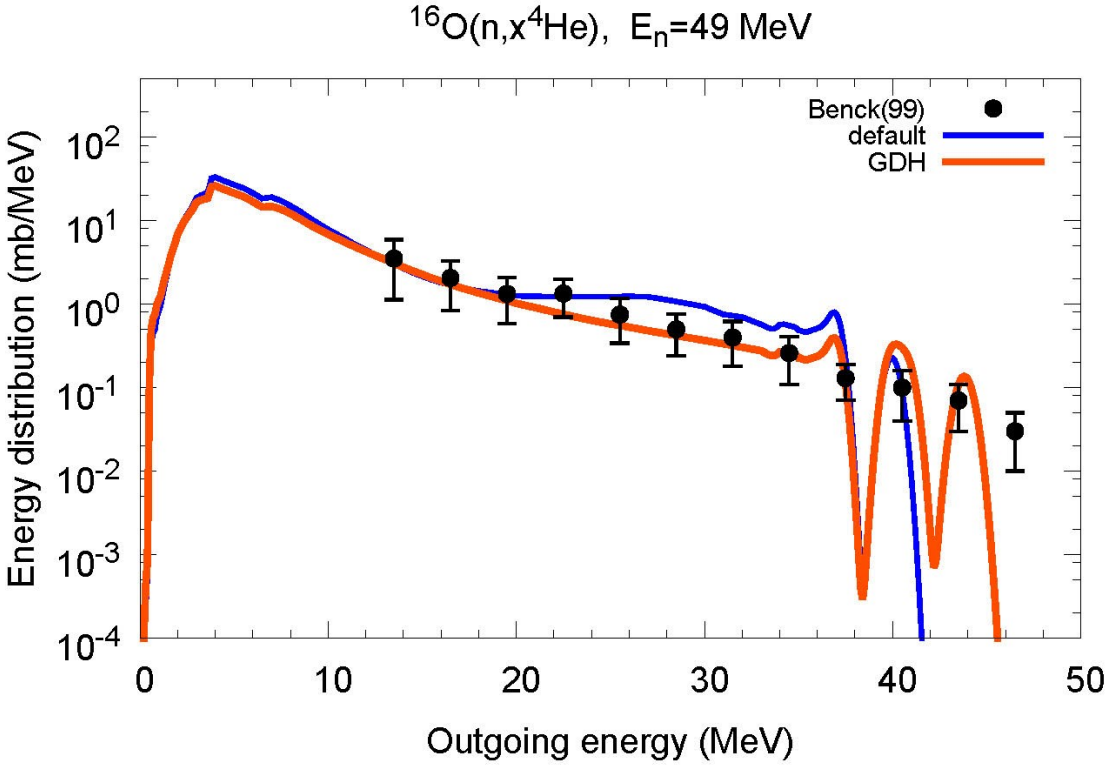
^{16}O(n,x^{4}He), E$_n$=49 MeV
Benck(99)
default
GDH
Energy distribution (mb/MeV)
Outgoing energy (MeV)

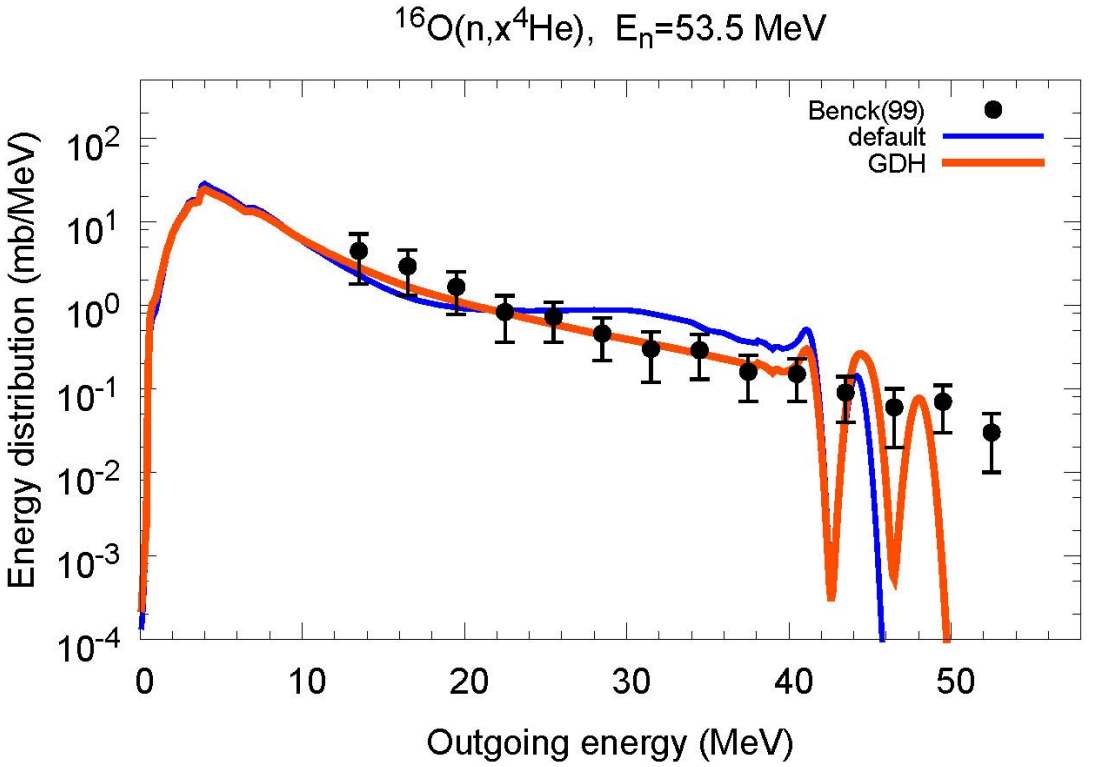
^{16}O(n,x^{4}He), E$_n$=53.5 MeV
Benck(99)
default
GDH
Energy distribution (mb/MeV)
Outgoing energy (MeV)

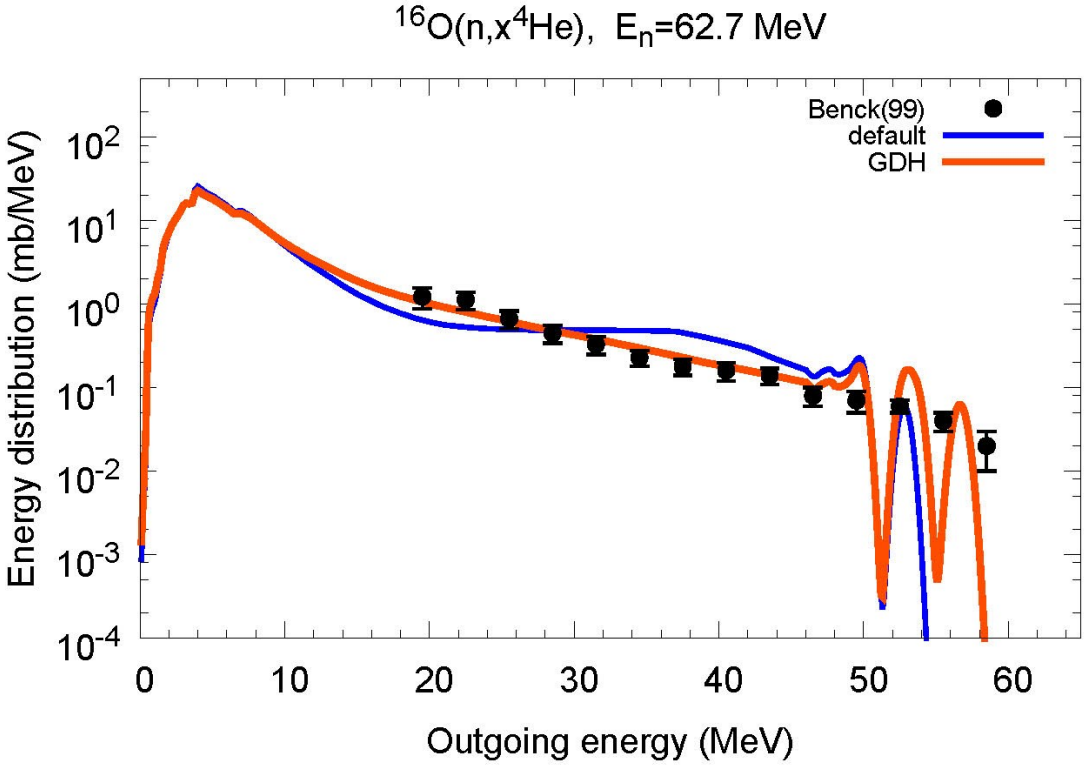
^{16}O(n,x^{4}He), E_n=62.7 MeV
Benck(99)
default
GDH
Energy distribution (mb/MeV)
Outgoing energy (MeV)

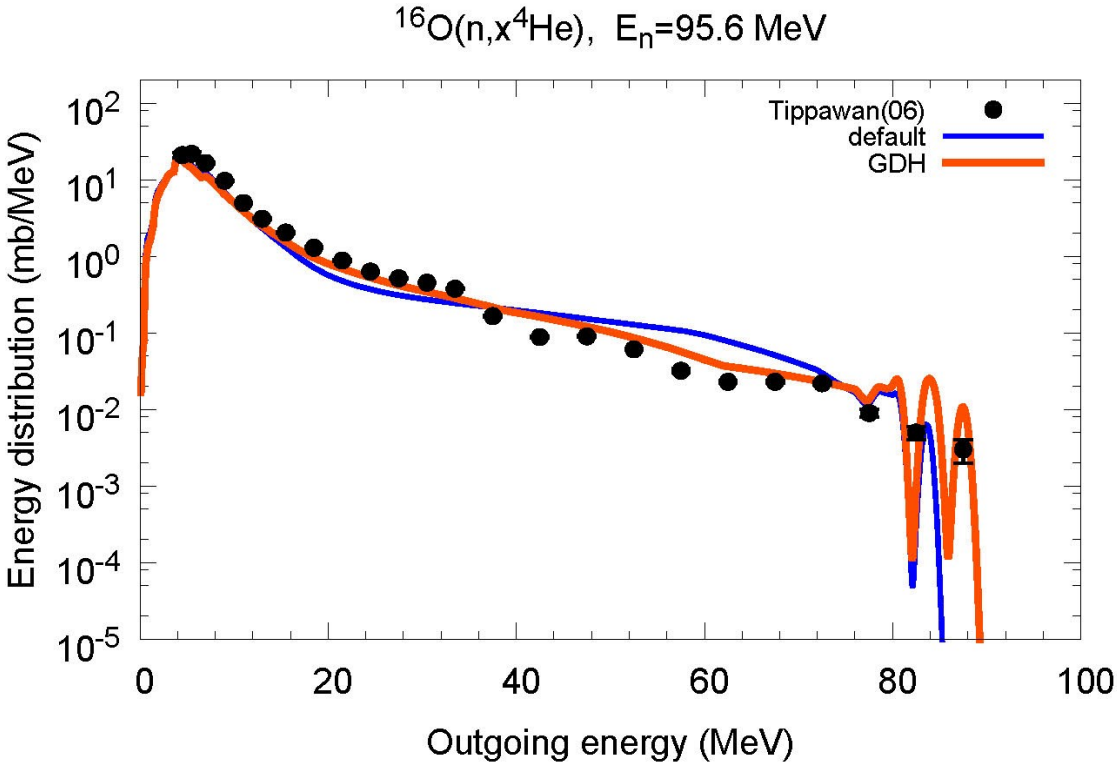
^{16}O(n,x^{4}He), E_n=95.6 MeV
Tippawan(06)
default
GDH
Energy distribution (mb/MeV)
Outgoing energy (MeV)

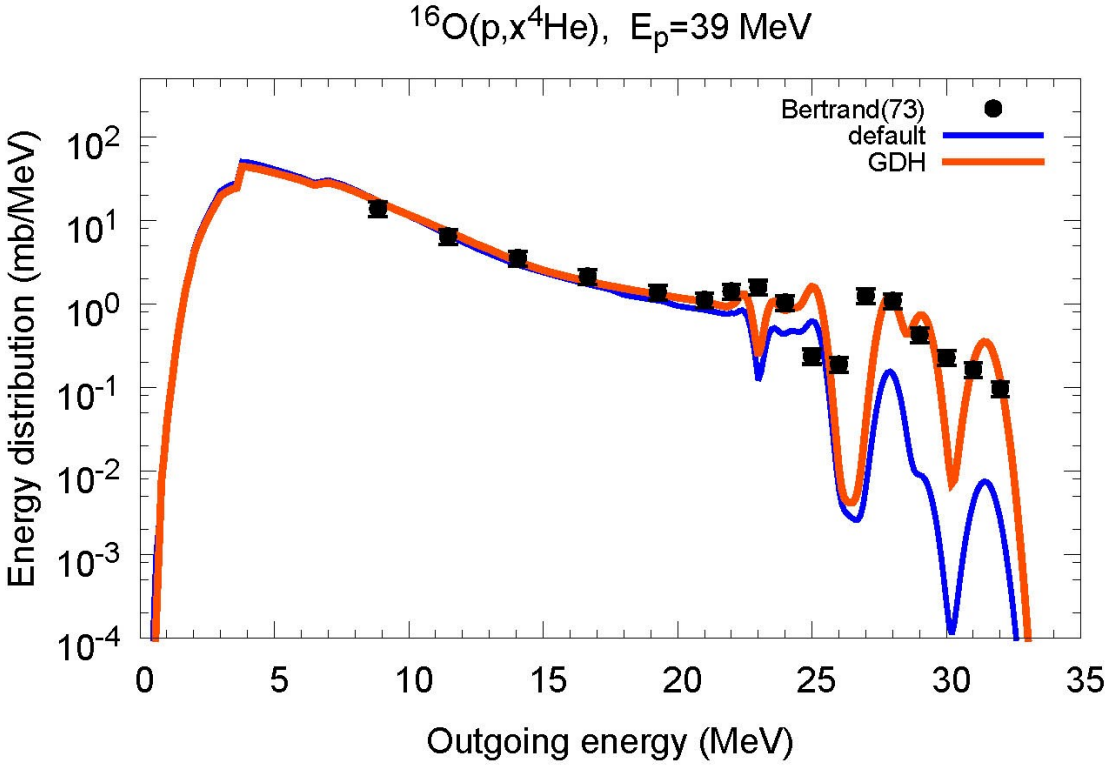
^{16}O(p,x^{4}He), E$_p$=39 MeV
Bertrand(73)
default
GDH
Energy distribution (mb/MeV)
Outgoing energy (MeV)

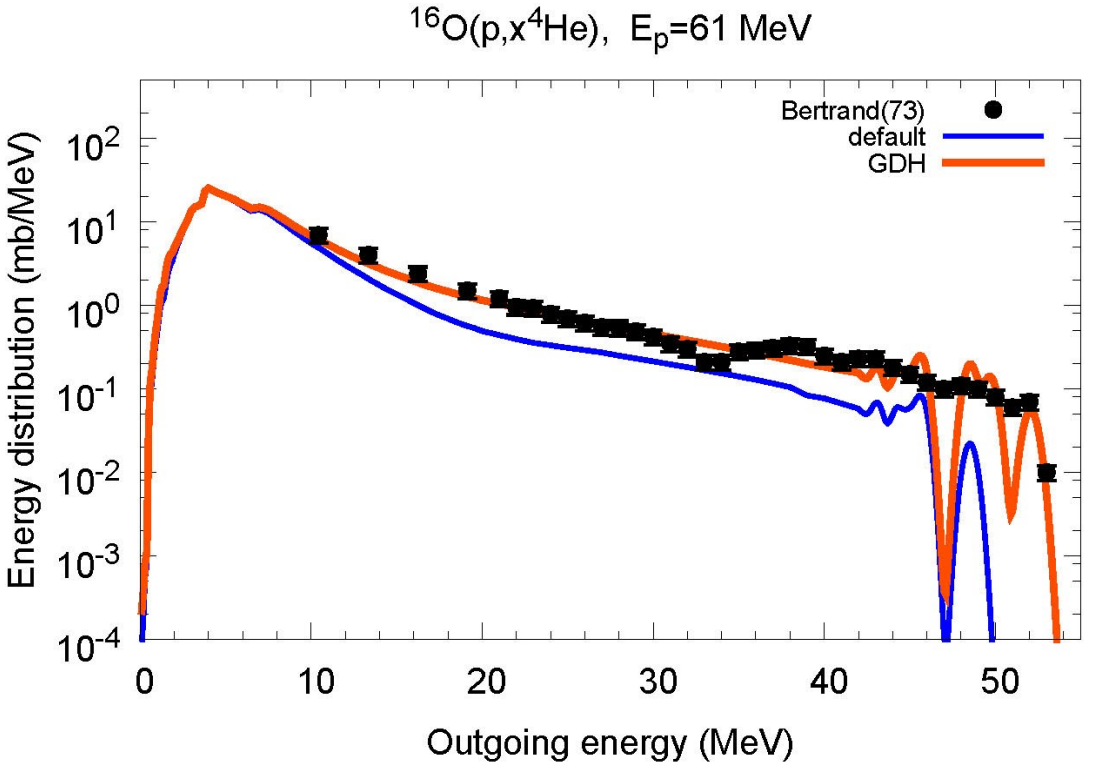
^{16}O(p,x^{4}He), E$_p$=61 MeV
Bertrand(73)
default
GDH
Energy distribution (mb/MeV)
Outgoing energy (MeV)

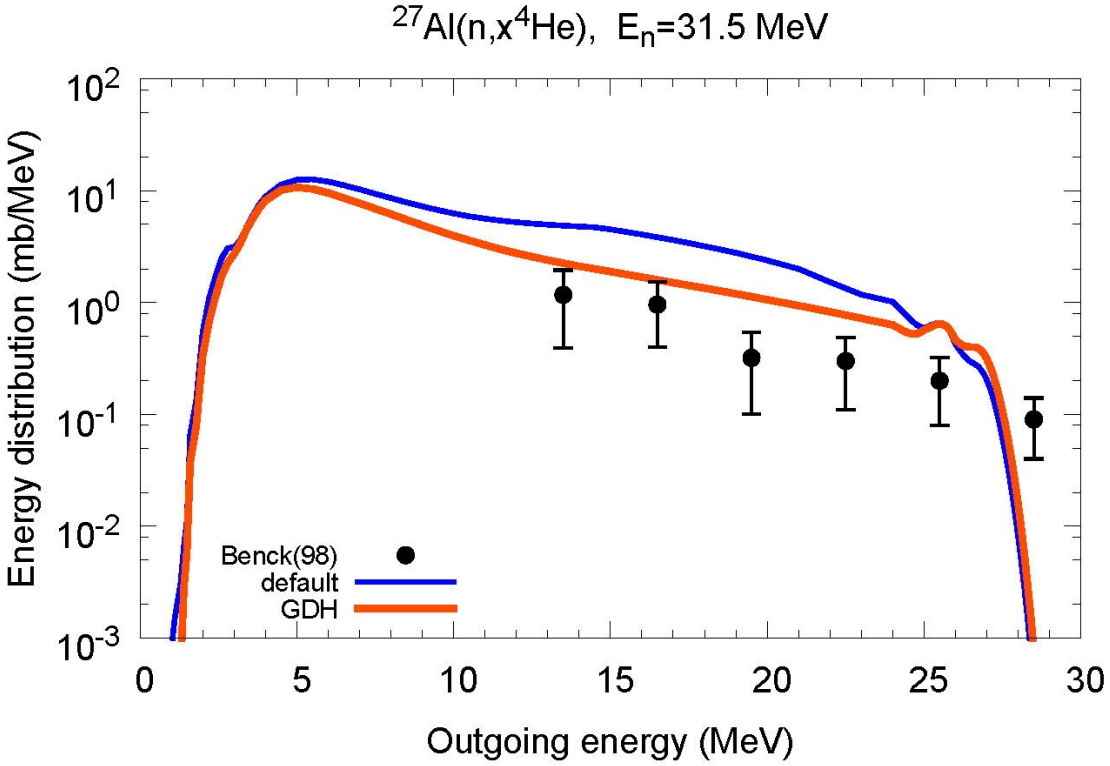
^{27}Al(n,x^{4}He), E_n=31.5 MeV
Energy distribution (mb/MeV)
Outgoing energy (MeV)
Benck(98)
default
GDH

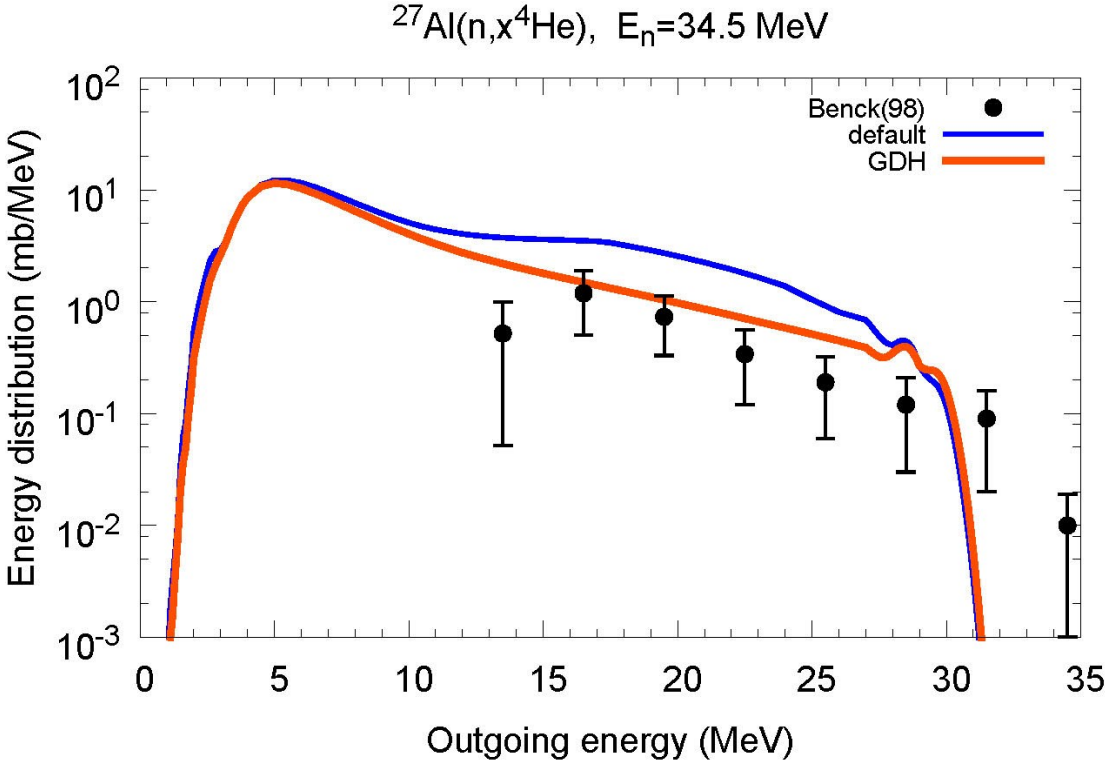
^{27}Al(n,x^{4}He), E_n=34.5 MeV
Energy distribution (mb/MeV)
Outgoing energy (MeV)
Benck(98)
default
GDH

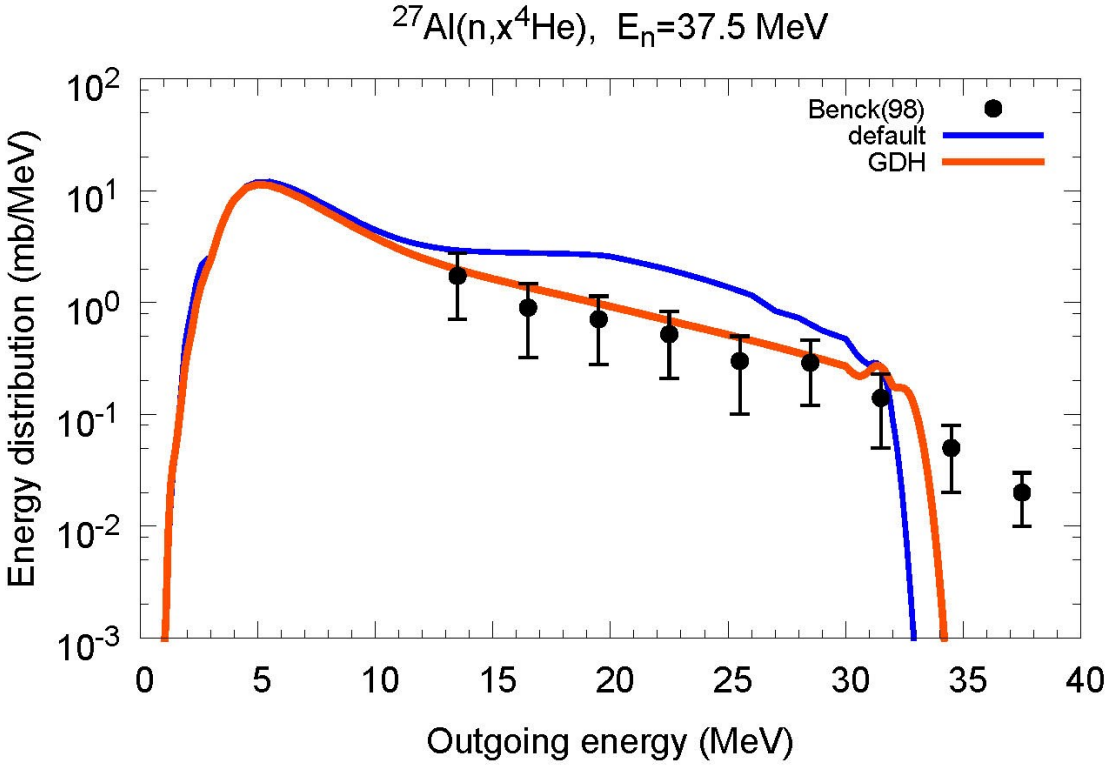
^{27}Al(n,x^{4}He), E_n=37.5 MeV
Benck(98)
default
GDH
Energy distribution (mb/MeV)
Outgoing energy (MeV)
10^{2}
10^{1}
10^{0}
10^{-1}
10^{-2}
10^{-3}
0
5
10
15
20
25
30
35
40

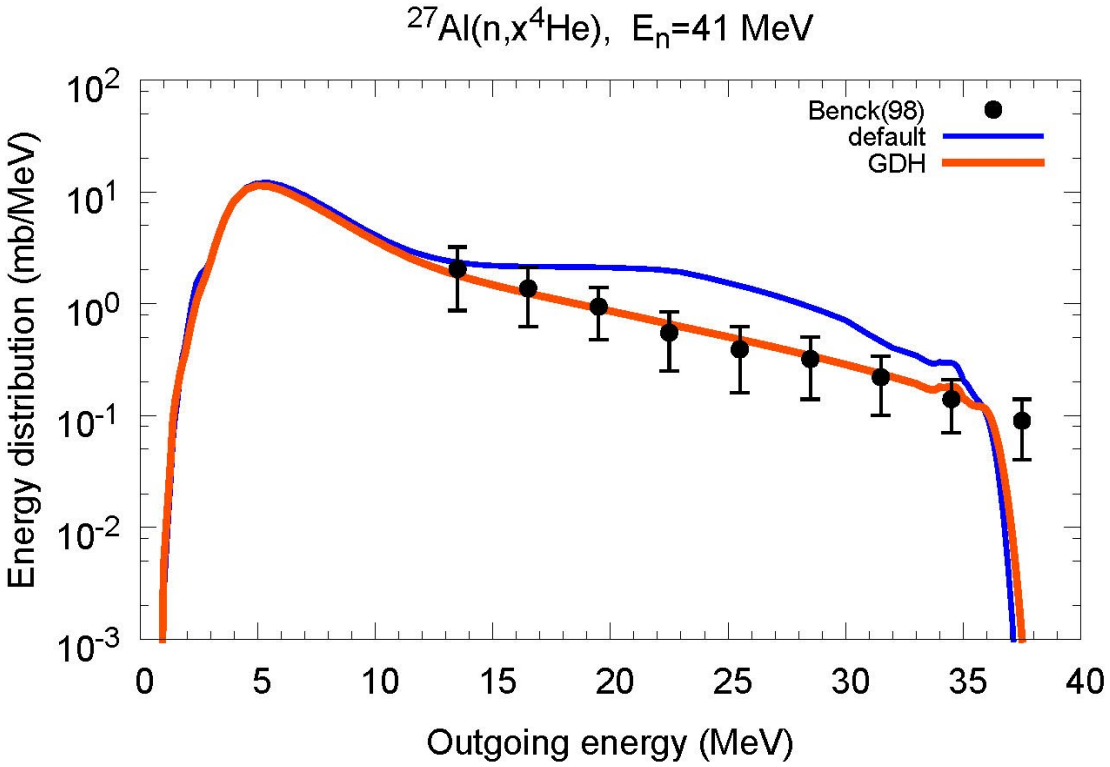
^{27}Al(n,x^{4}He), E_n=41 MeV
Benck(98)
default
GDH
Energy distribution (mb/MeV)
Outgoing energy (MeV)
10^{2}
10^{1}
10^{0}
10^{-1}
10^{-2}
10^{-3}
0
5
10
15
20
25
30
35
40

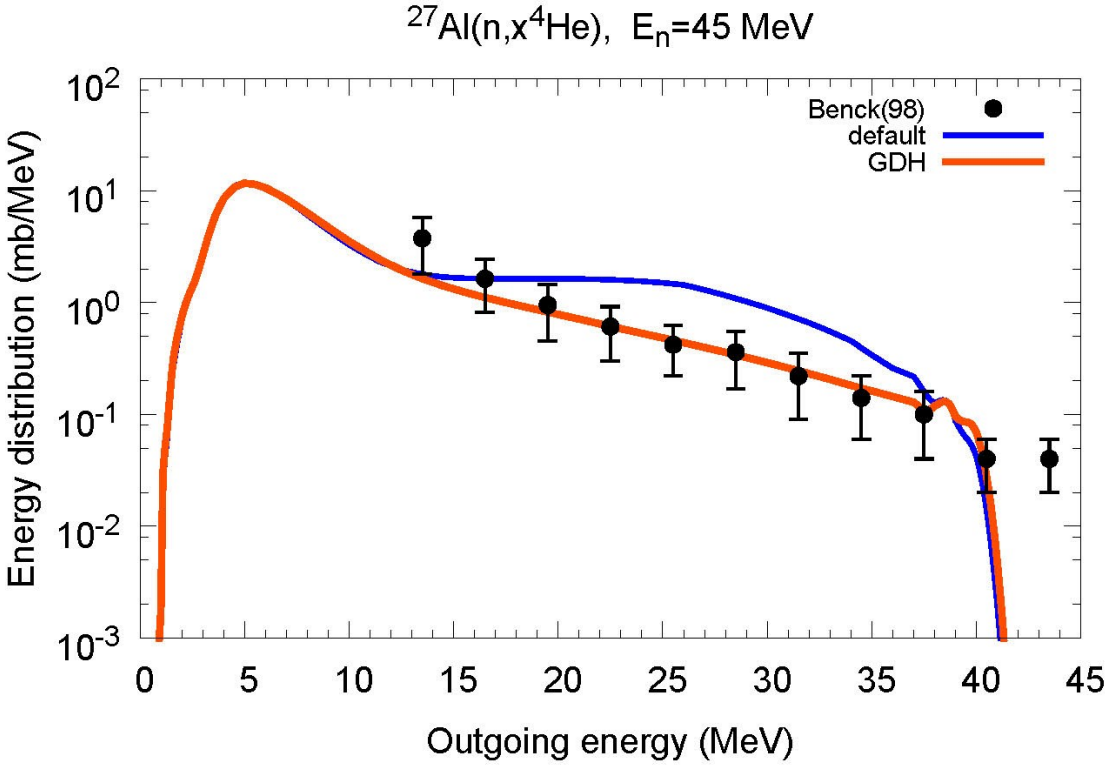
^{27}Al(n,x^{4}He), E_n=45 MeV
Benck(98)
default
GDH
Energy distribution (mb/MeV)
Outgoing energy (MeV)
10^{2}
10^{1}
10^{0}
10^{-1}
10^{-2}
10^{-3}
0
5
10
15
20
25
30
35
40
45

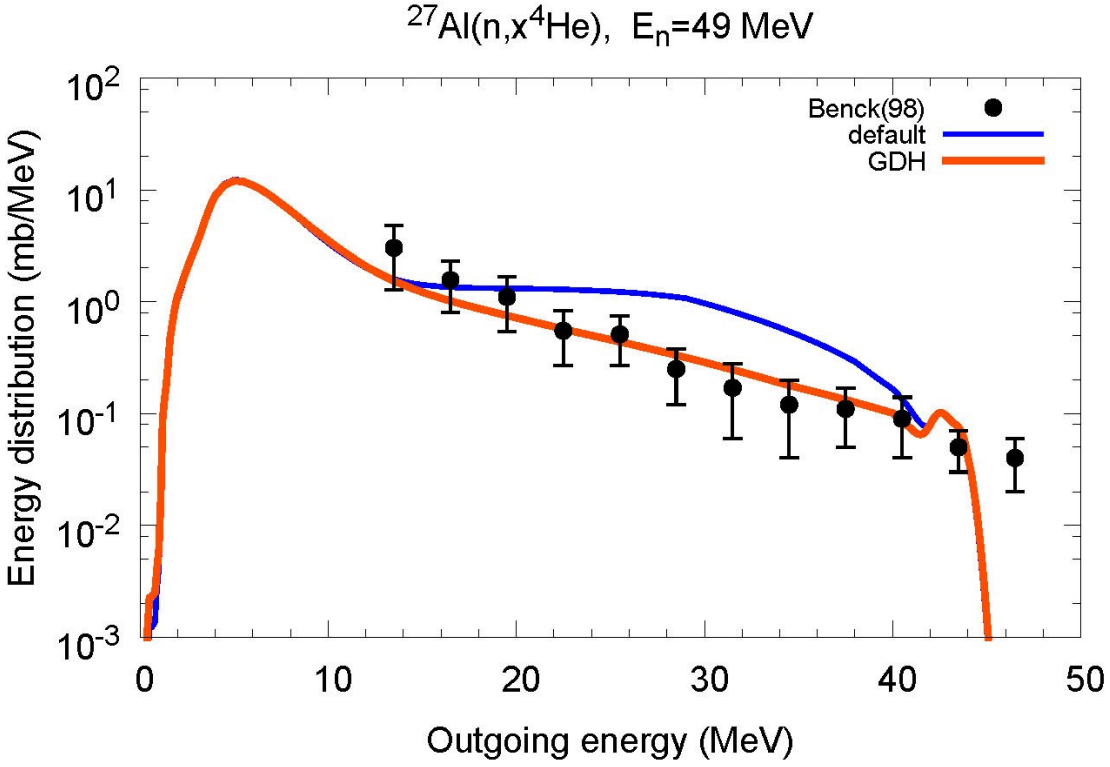
^{27}Al(n,x^{4}He), E_n=49 MeV
Benck(98)
default
GDH
Energy distribution (mb/MeV)
Outgoing energy (MeV)
10^{2}
10^{1}
10^{0}
10^{-1}
10^{-2}
10^{-3}
0
10
20
30
40
50

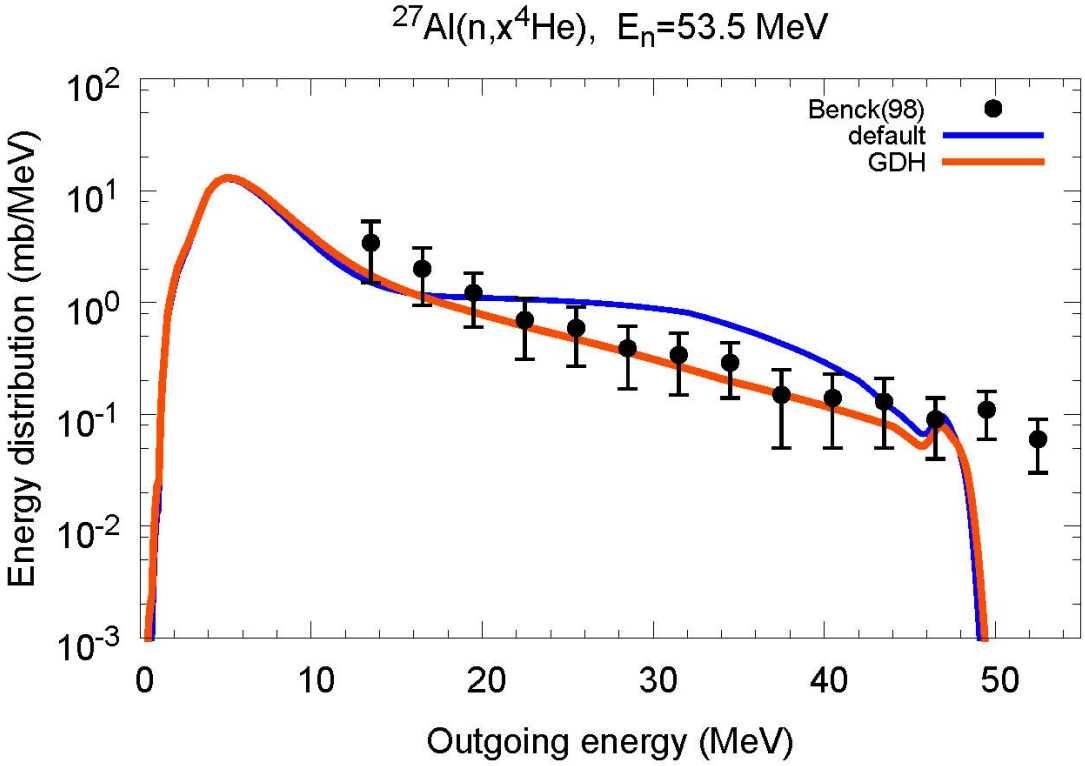
^{27}Al(n,x^{4}He), E_n=53.5 MeV
Benck(98)
default
GDH
Energy distribution (mb/MeV)
Outgoing energy (MeV)
10^{2}
10^{1}
10^{0}
10^{-1}
10^{-2}
10^{-3}
0
10
20
30
40
50

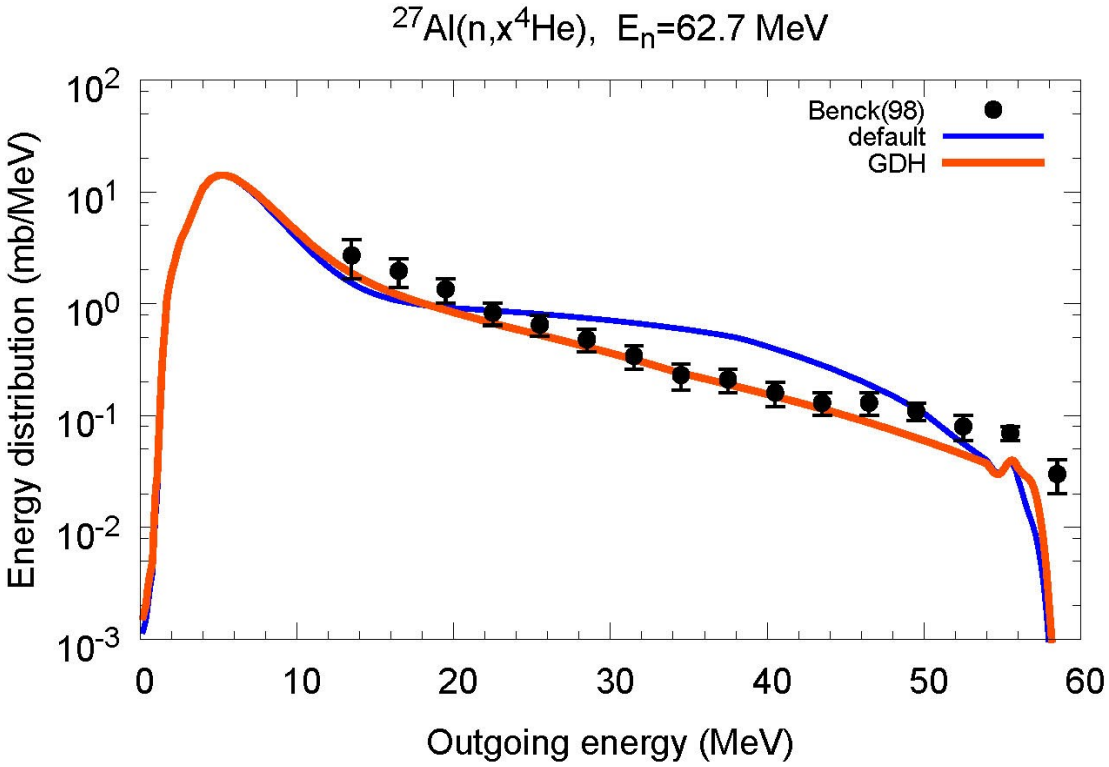
^{27}Al(n,x^{4}He), E_n=62.7 MeV
Benck(98)
default
GDH
Energy distribution (mb/MeV)
Outgoing energy (MeV)
10^{2}
10^{1}
10^{0}
10^{-1}
10^{-2}
10^{-3}
0
10
20
30
40
50
60

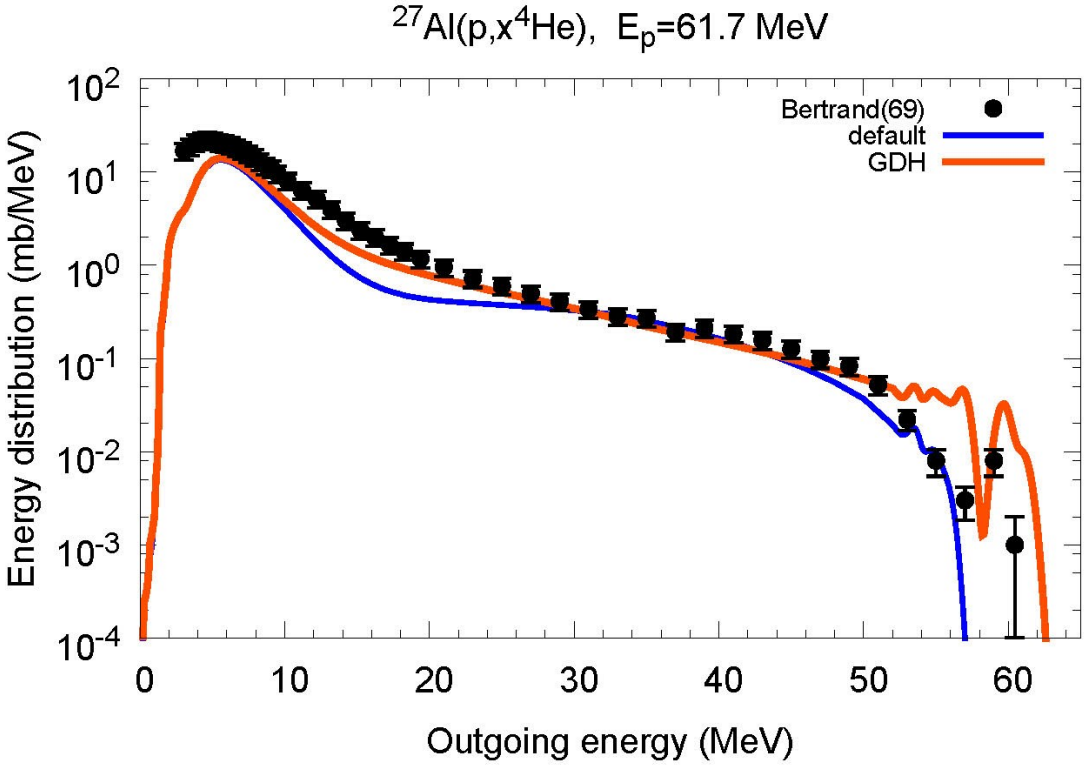
^{27}Al(p,x^{4}He), E$_p$=61.7 MeV
Bertrand(69)
default
GDH
Energy distribution (mb/MeV)
Outgoing energy (MeV)
10^{2}
10^{1}
10^{0}
10^{-1}
10^{-2}
10^{-3}
10^{-4}
0
10
20
30
40
50
60

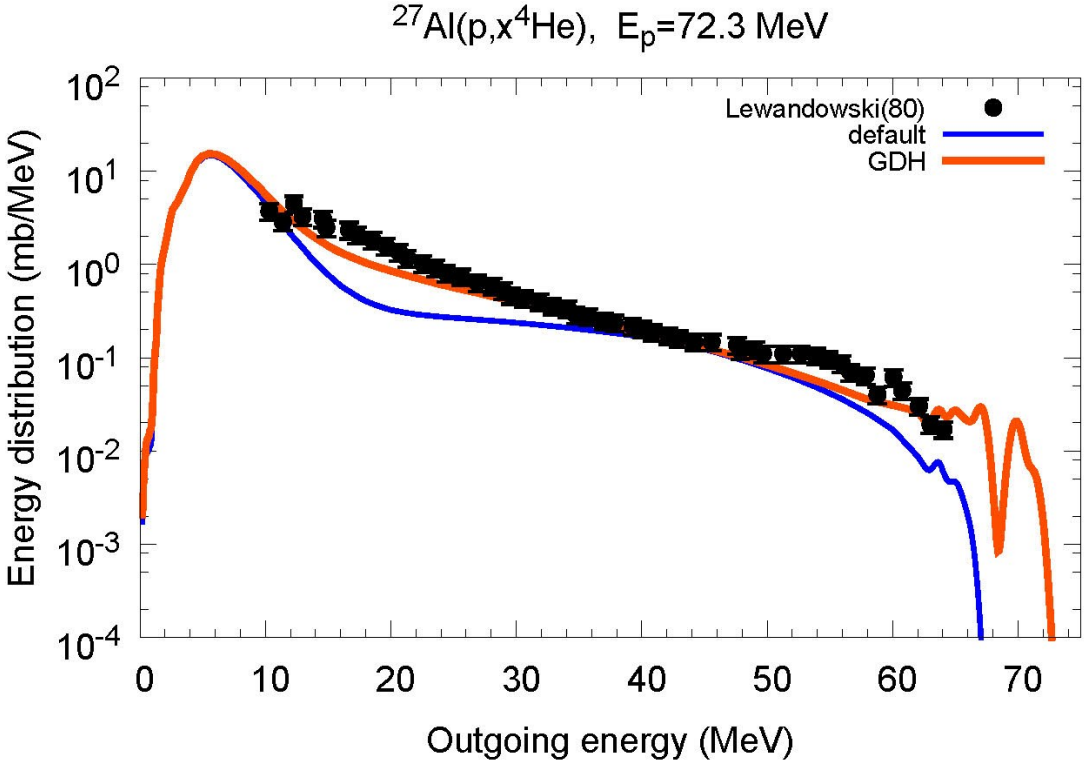
^{27}Al(p,x^{4}He), E$_p$=72.3 MeV
Lewandowski(80)
default
GDH
Energy distribution (mb/MeV)
Outgoing energy (MeV)
10^{2}
10^{1}
10^{0}
10^{-1}
10^{-2}
10^{-3}
10^{-4}
0
10
20
30
40
50
60
70

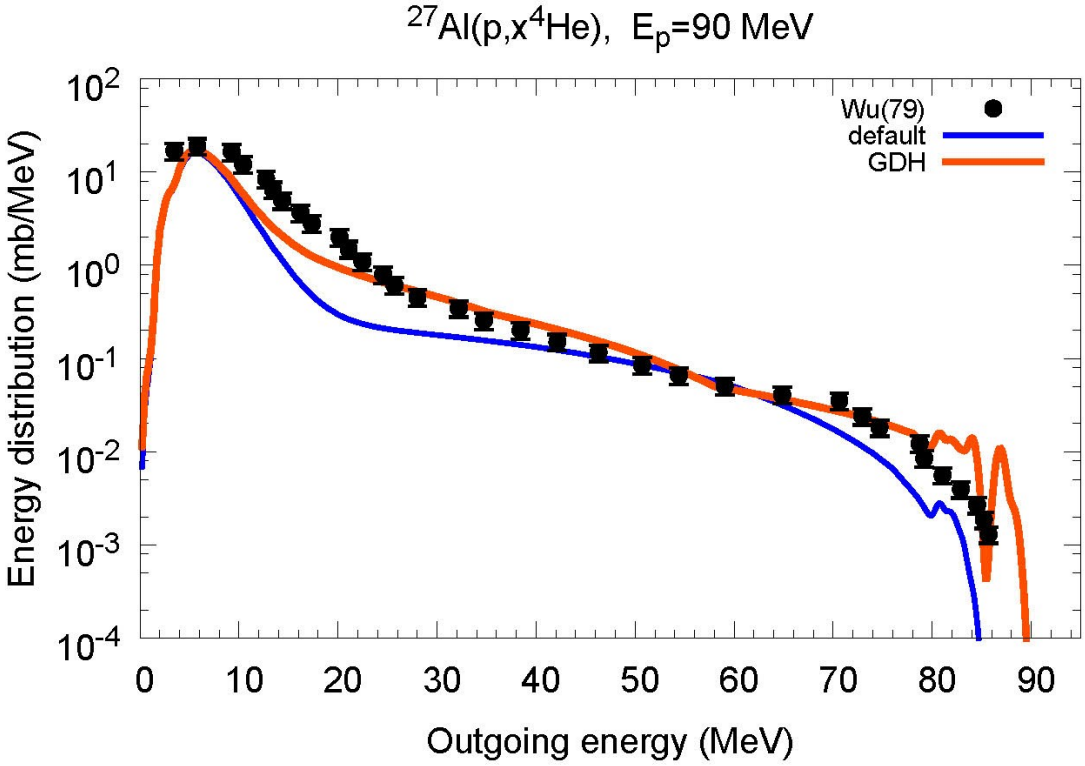
^{27}Al(p,x^{4}He), E$_p$=90 MeV
Energy distribution (mb/MeV)
Outgoing energy (MeV)
Wu(79)
default
GDH

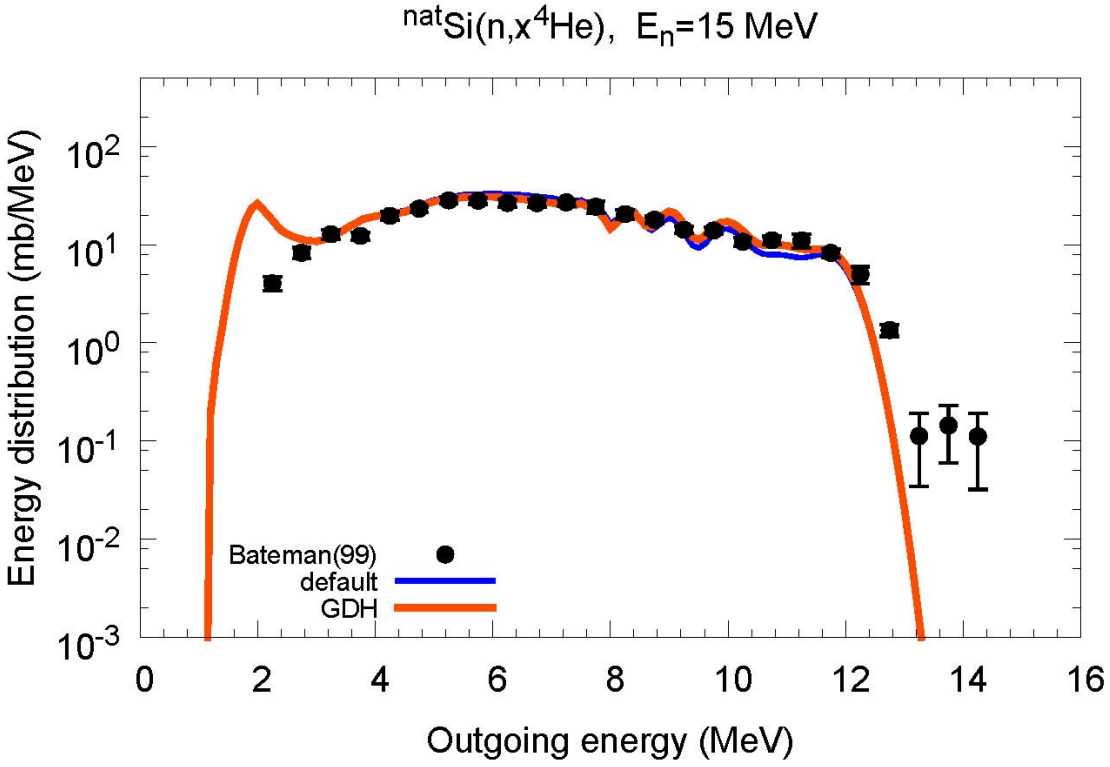
^{nat}Si(n,x^{4}He), E$_n$=15 MeV
Energy distribution (mb/MeV)
Outgoing energy (MeV)
Bateman(99)
default
GDH

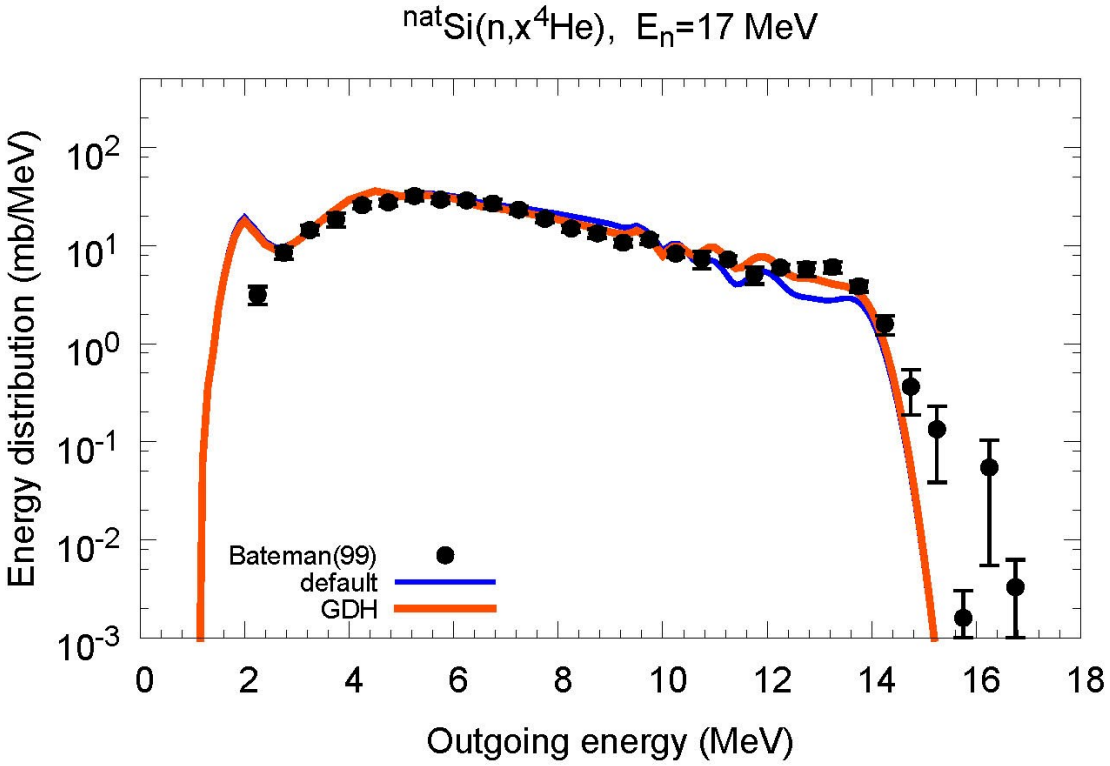
natSi(n,x4He), En=17 MeV
Energy distribution (mb/MeV)
Outgoing energy (MeV)
Bateman(99)
default
GDH

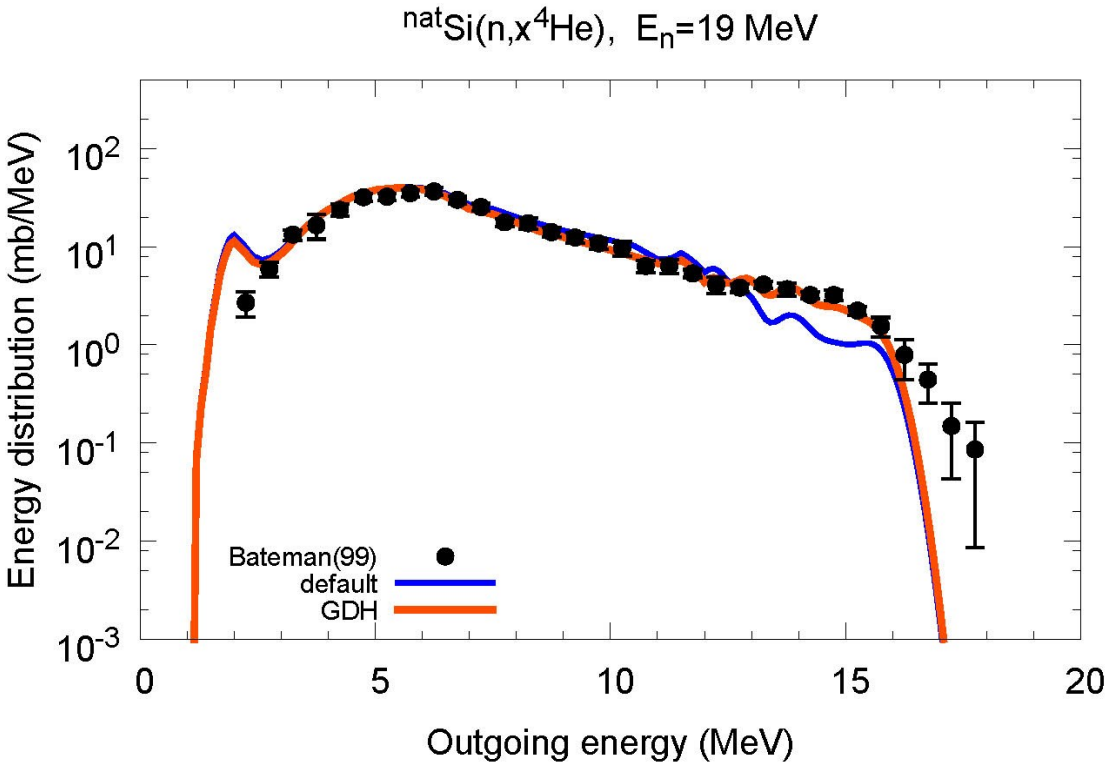
natSi(n,x4He), En=19 MeV
Energy distribution (mb/MeV)
Outgoing energy (MeV)
Bateman(99)
default
GDH

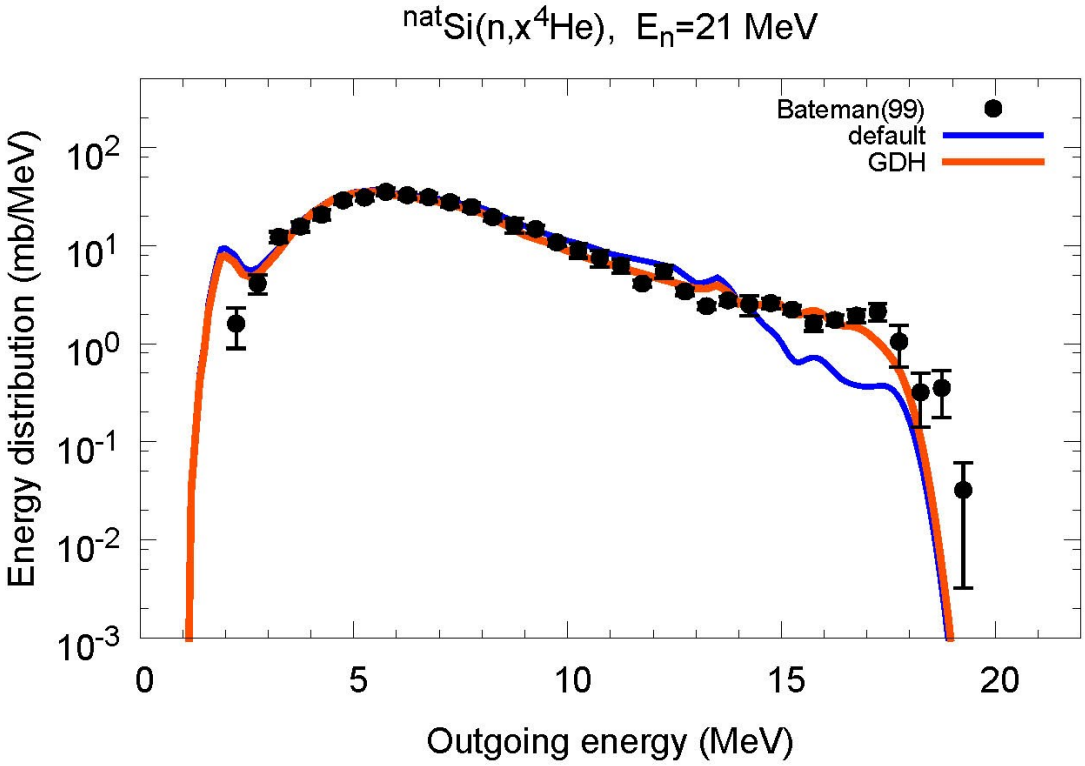
natSi(n,x4He), En=21 MeV
Bateman(99)
default
GDH
Energy distribution (mb/MeV)
Outgoing energy (MeV)

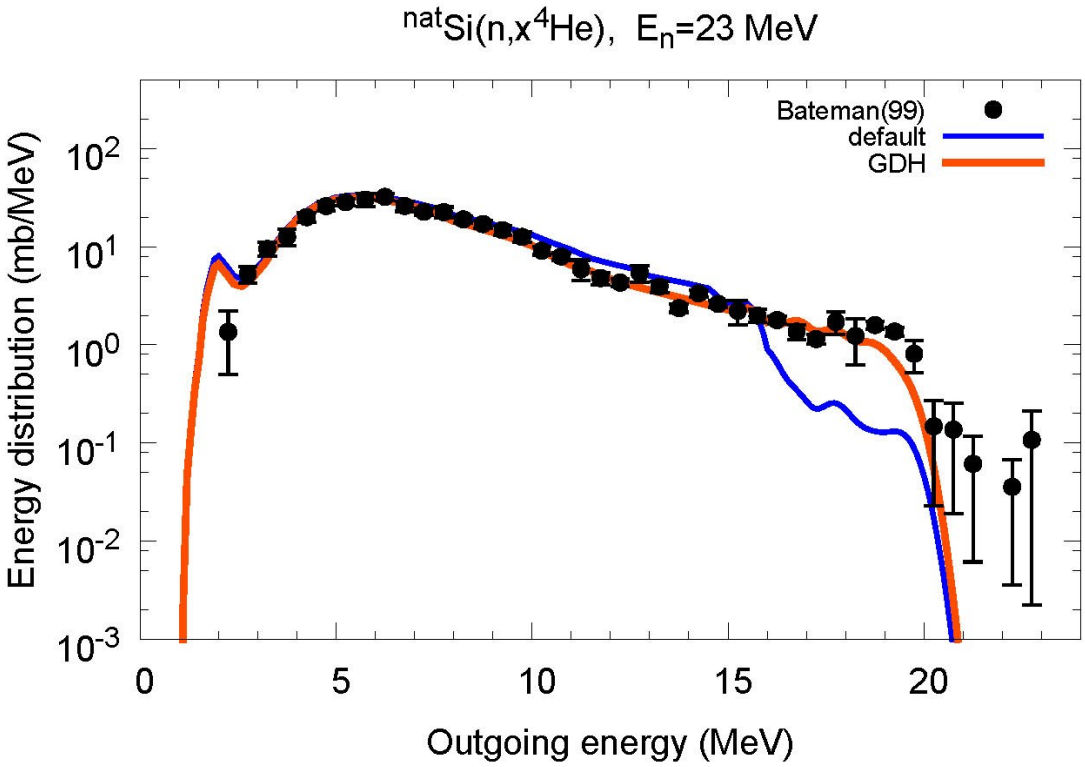
natSi(n,x4He), En=23 MeV
Bateman(99)
default
GDH
Energy distribution (mb/MeV)
Outgoing energy (MeV)

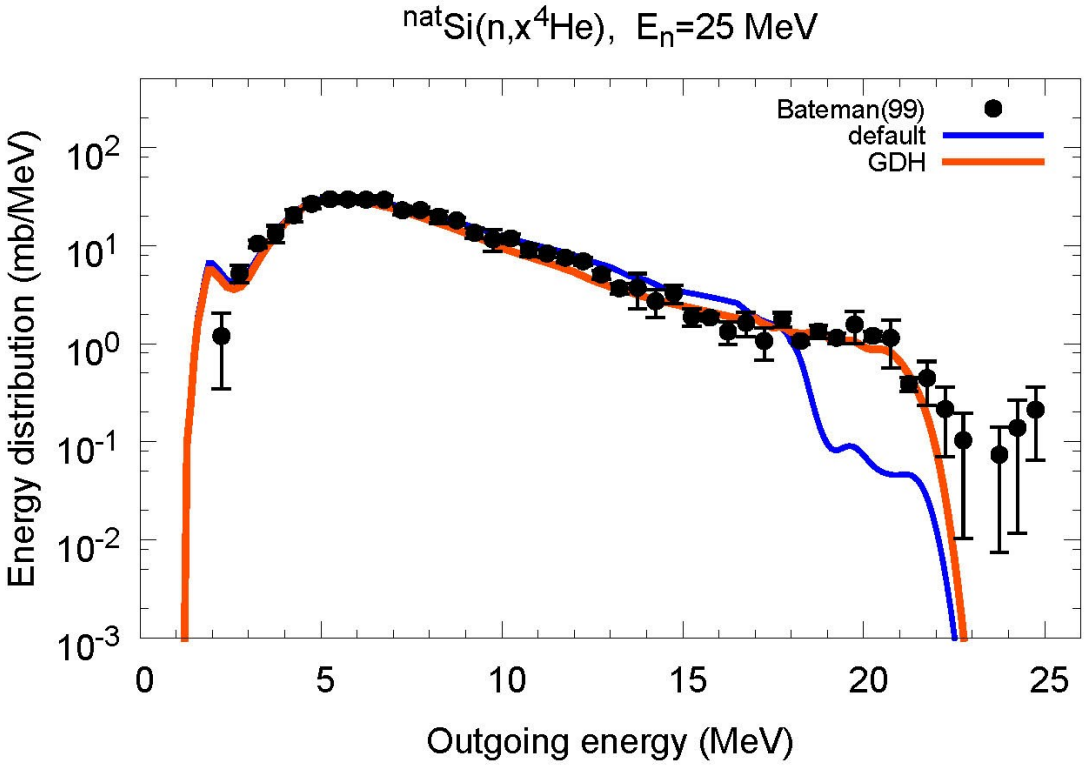
natSi(n,x4He), En=25 MeV
Bateman(99)
default
GDH
Energy distribution (mb/MeV)
Outgoing energy (MeV)

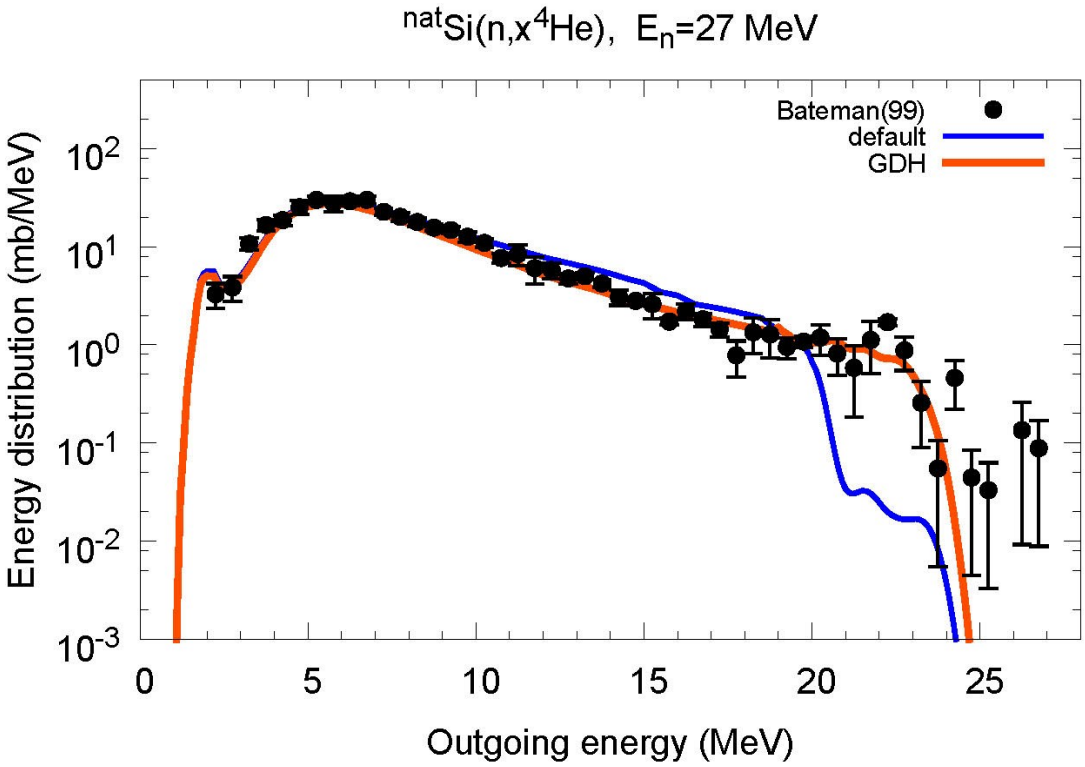
natSi(n,x4He), En=27 MeV
Bateman(99)
default
GDH
Energy distribution (mb/MeV)
Outgoing energy (MeV)

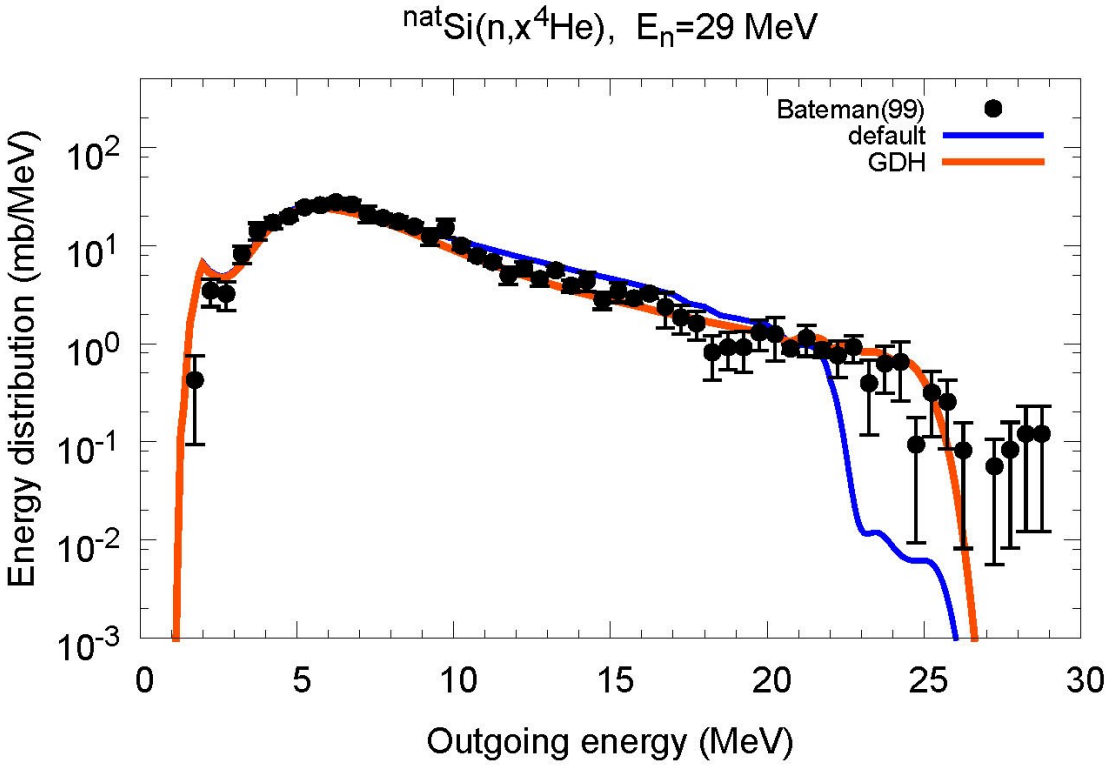
natSi(n,x4He), En=29 MeV
Bateman(99)
default
GDH
Energy distribution (mb/MeV)
Outgoing energy (MeV)

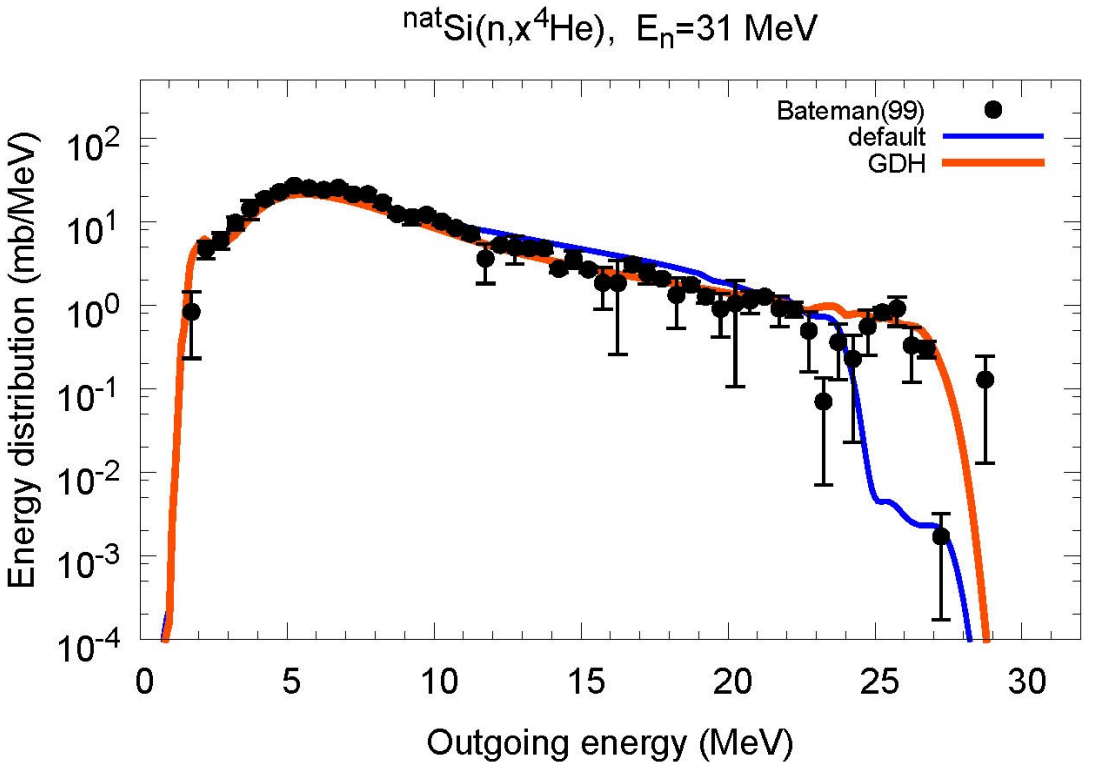
natSi(n,x4He), En=31 MeV
Bateman(99)
default
GDH
Energy distribution (mb/MeV)
Outgoing energy (MeV)

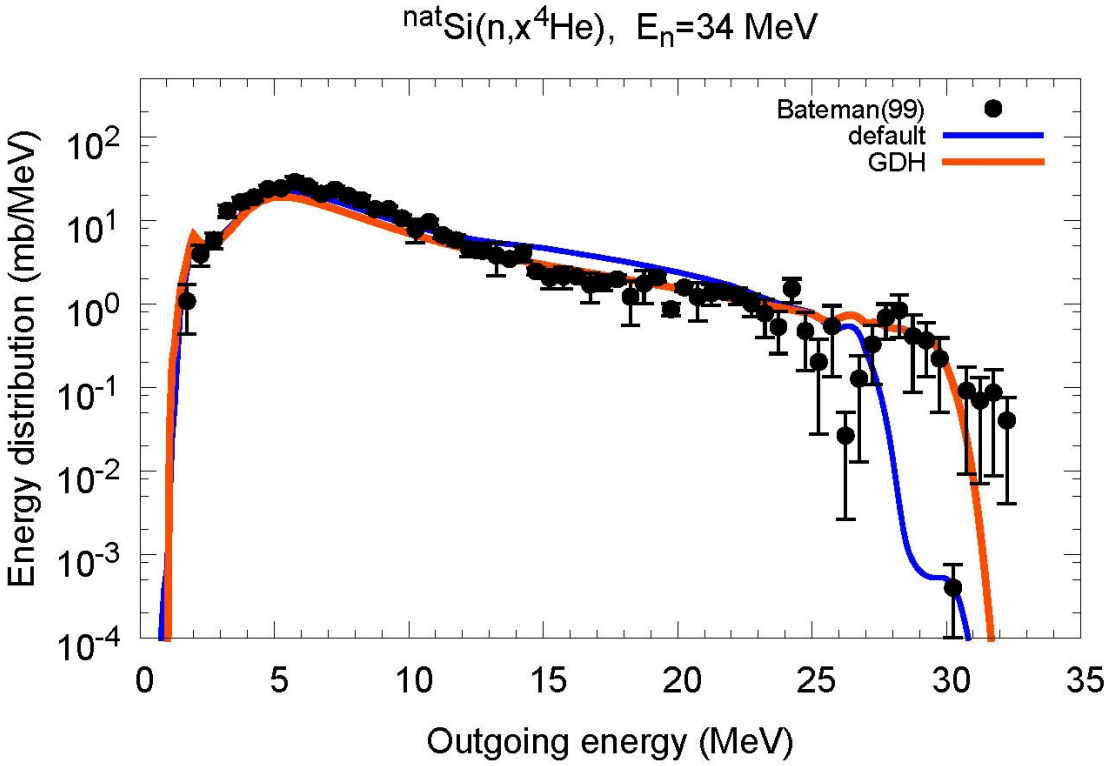
natSi(n,x4He), En=34 MeV
Bateman(99)
default
GDH
Energy distribution (mb/MeV)
Outgoing energy (MeV)

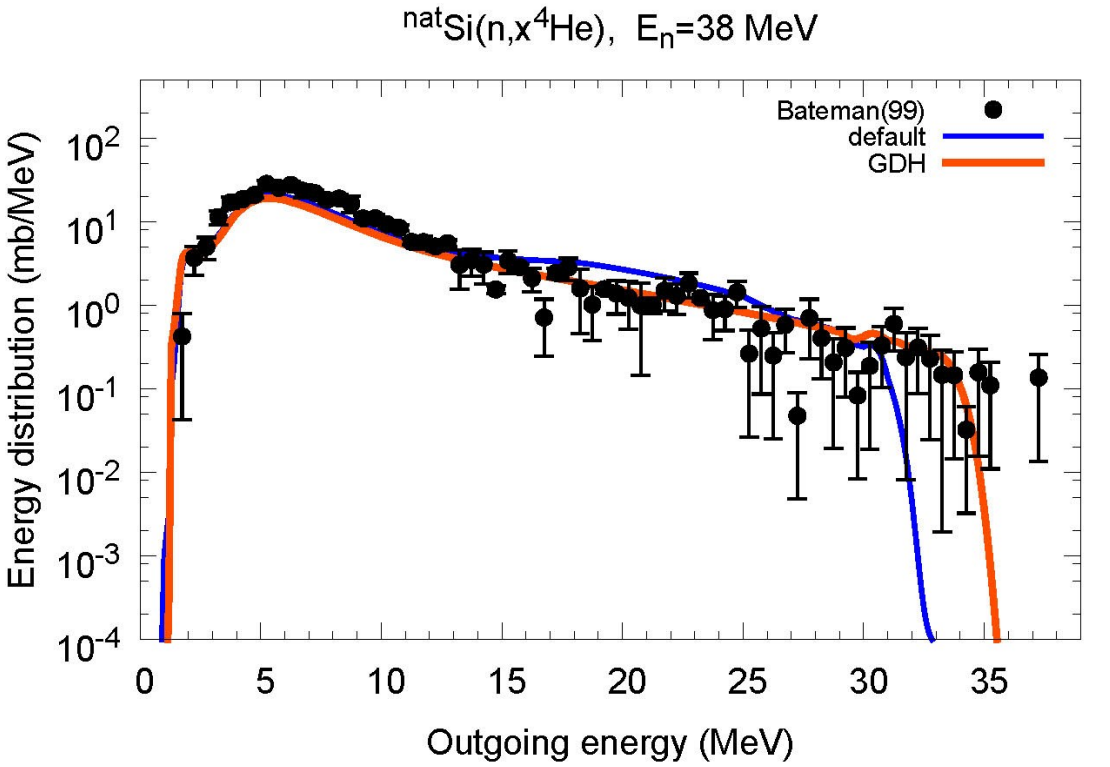
natSi(n,x4He), En=38 MeV
Bateman(99)
default
GDH
Energy distribution (mb/MeV)
Outgoing energy (MeV)

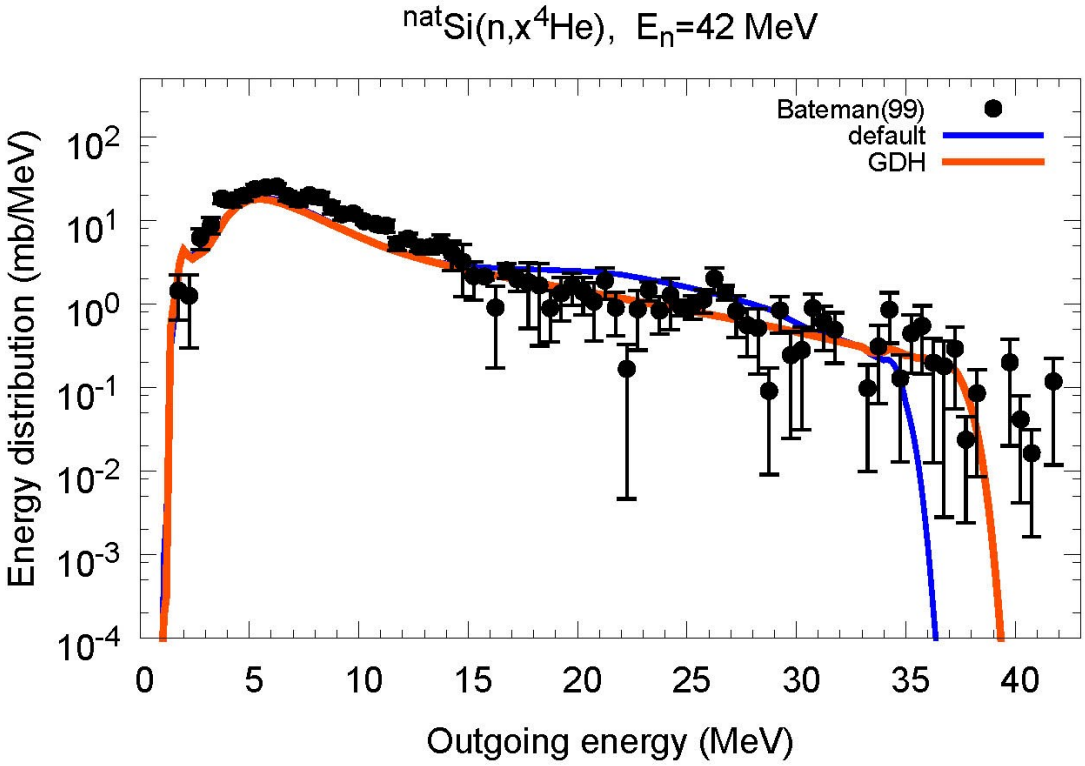
natSi(n,x4He), En=42 MeV
Bateman(99)
default
GDH
Energy distribution (mb/MeV)
Outgoing energy (MeV)

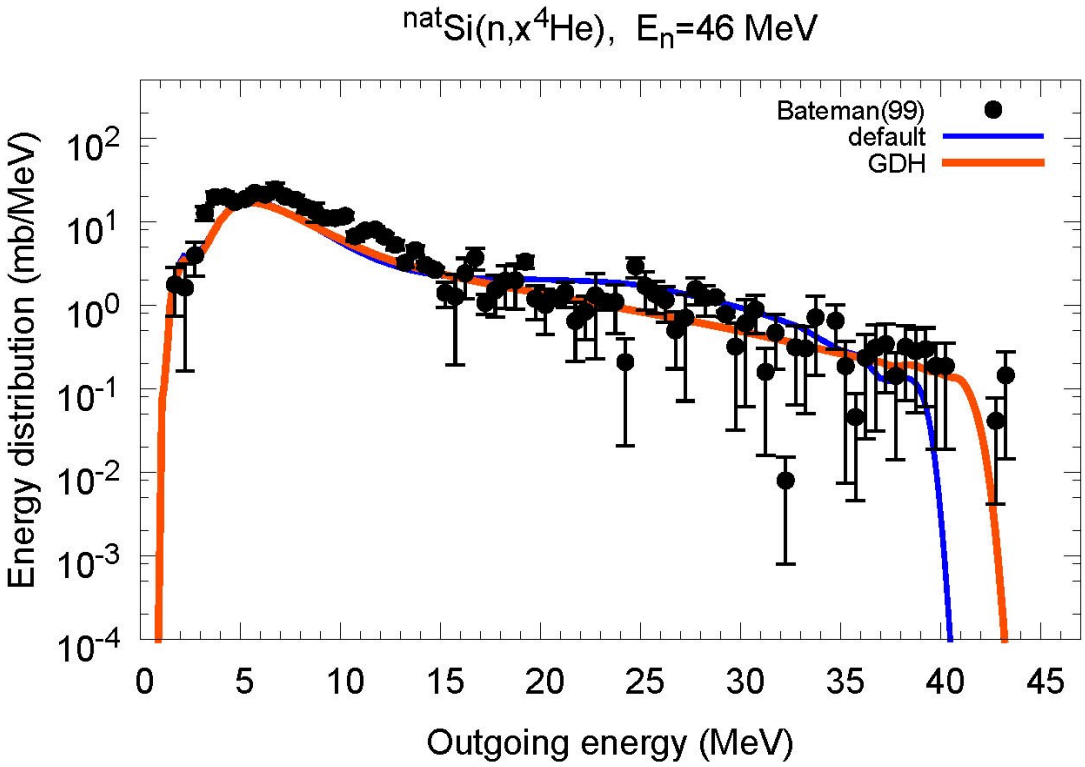
natSi(n,x4He), En=46 MeV
Bateman(99)
default
GDH
Energy distribution (mb/MeV)
Outgoing energy (MeV)

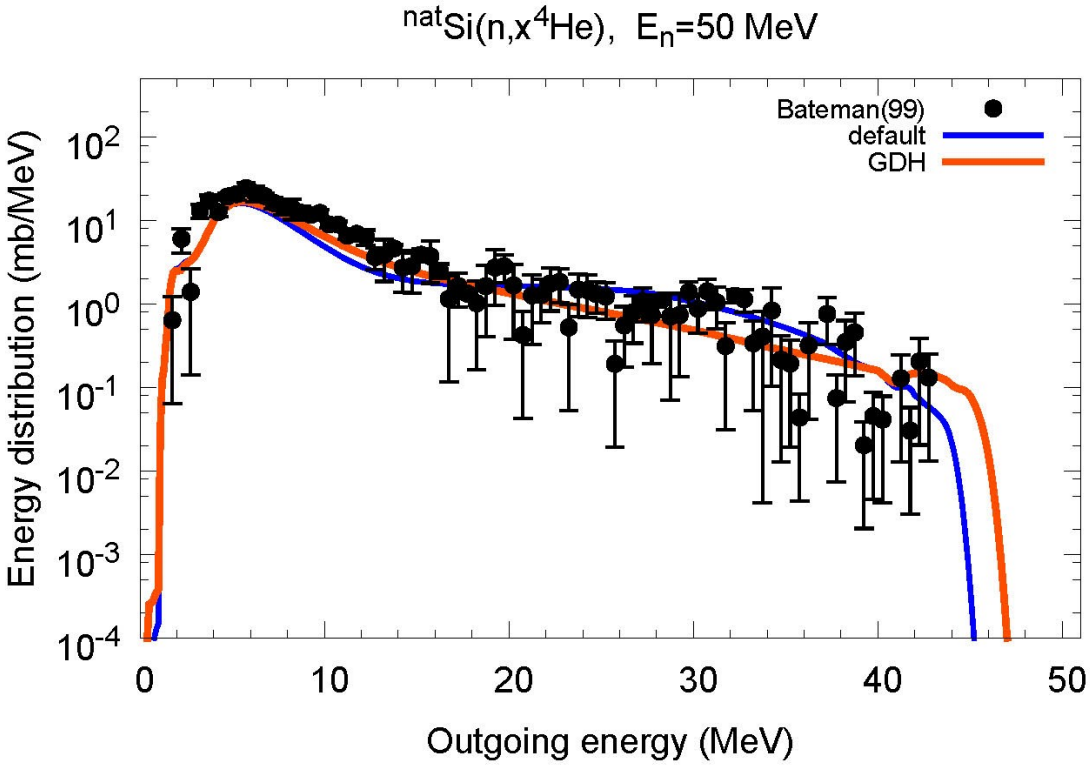
natSi(n,x4He), En=50 MeV
Bateman(99)
default
GDH
Energy distribution (mb/MeV)
Outgoing energy (MeV)

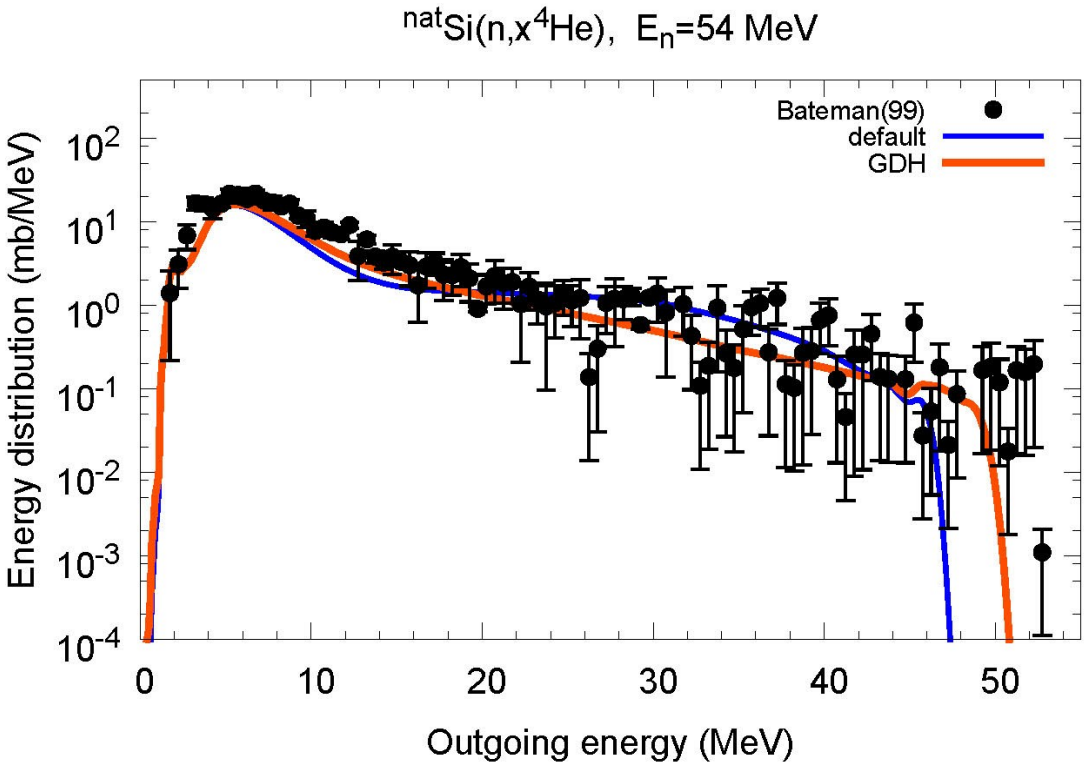
natSi(n,x4He), En=54 MeV
Bateman(99)
default
GDH
Energy distribution (mb/MeV)
Outgoing energy (MeV)

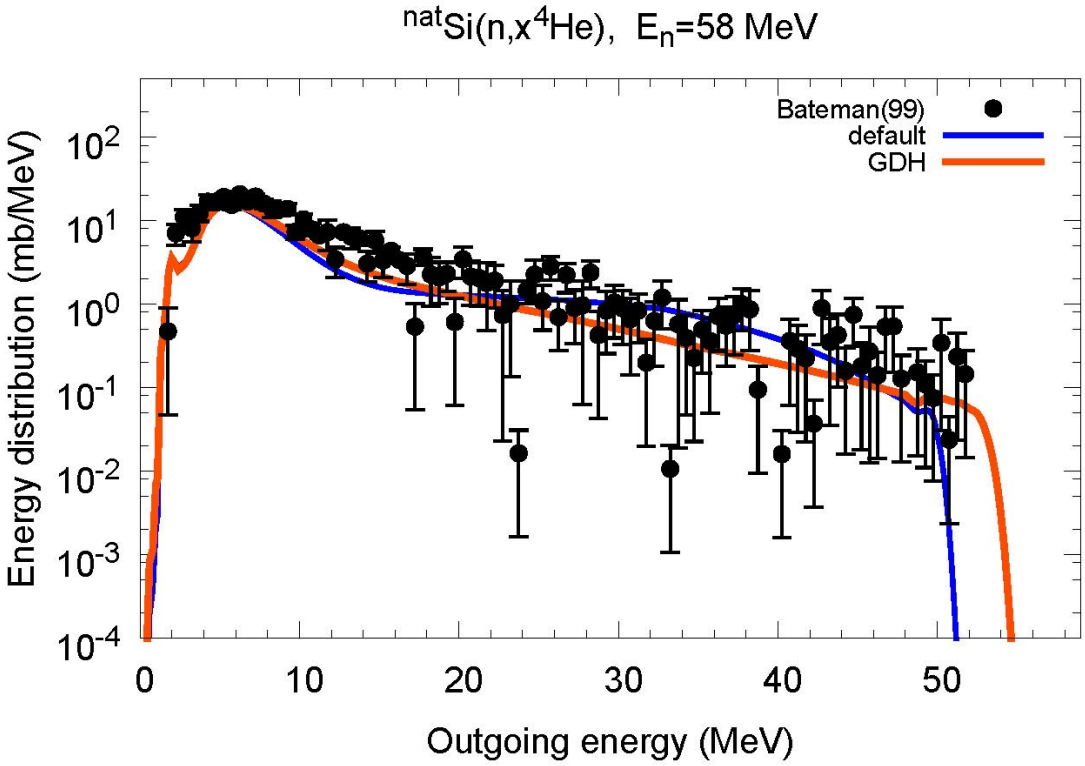
natSi(n,x4He), En=58 MeV
Bateman(99)
default
GDH
Energy distribution (mb/MeV)
Outgoing energy (MeV)

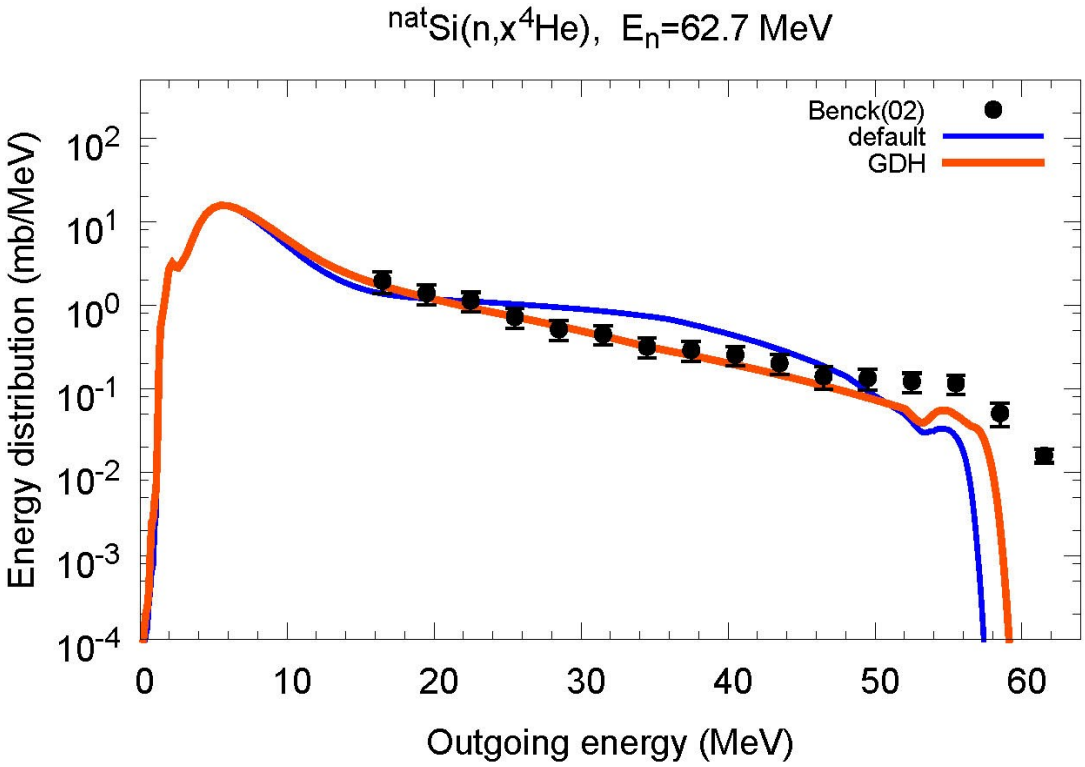
natSi(n,x4He), En=62.7 MeV
Benck(02)
default
GDH
Energy distribution (mb/MeV)
Outgoing energy (MeV)

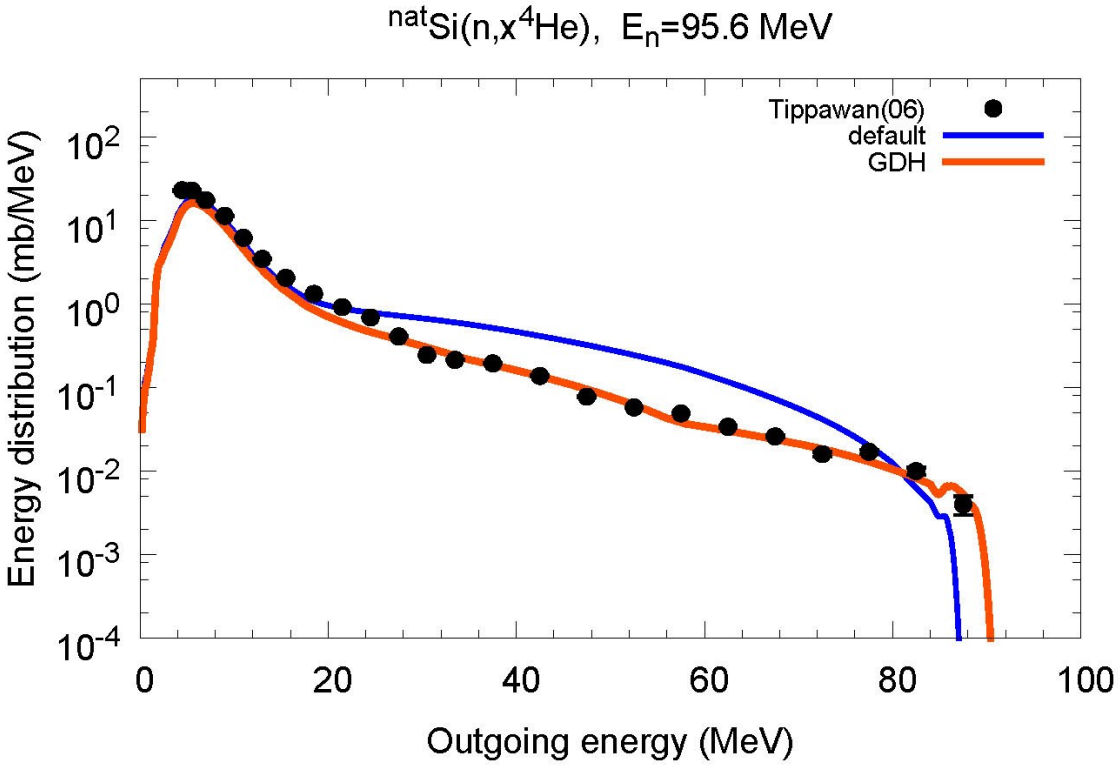
natSi(n,x4He), En=95.6 MeV
Tippawan(06)
default
GDH
Energy distribution (mb/MeV)
Outgoing energy (MeV)

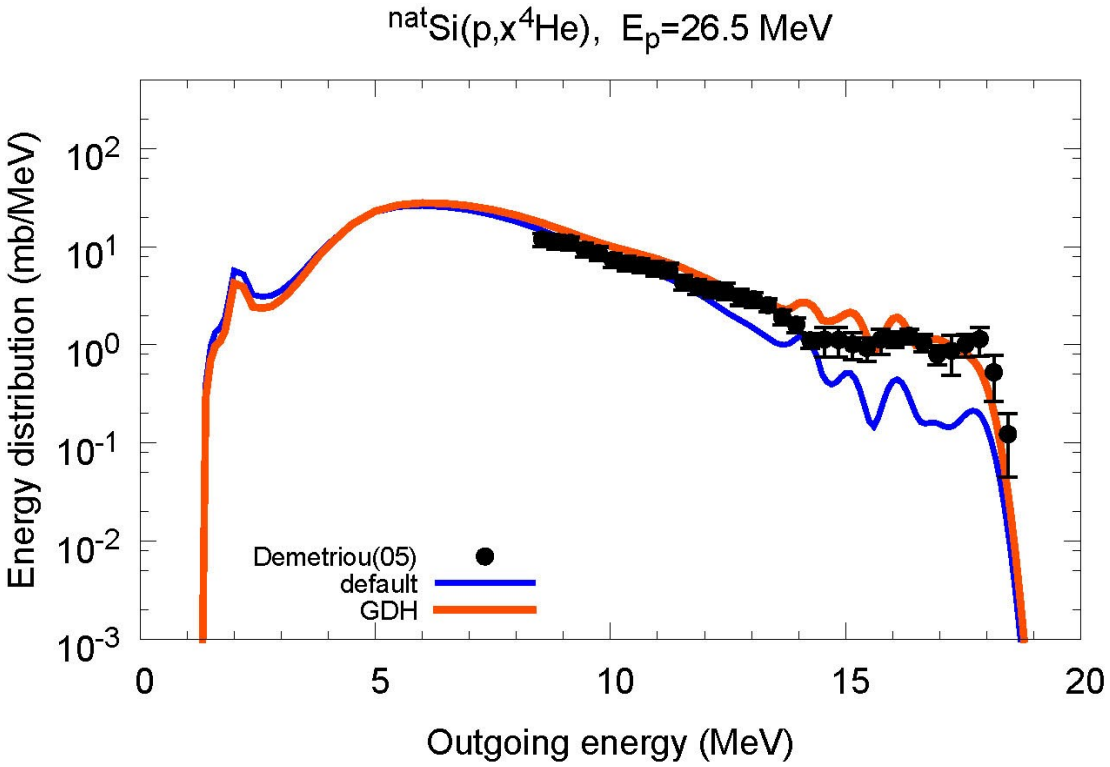
natSi(p,x4He), Ep=26.5 MeV
Demetriou(05)
default
GDH
Energy distribution (mb/MeV)
Outgoing energy (MeV)

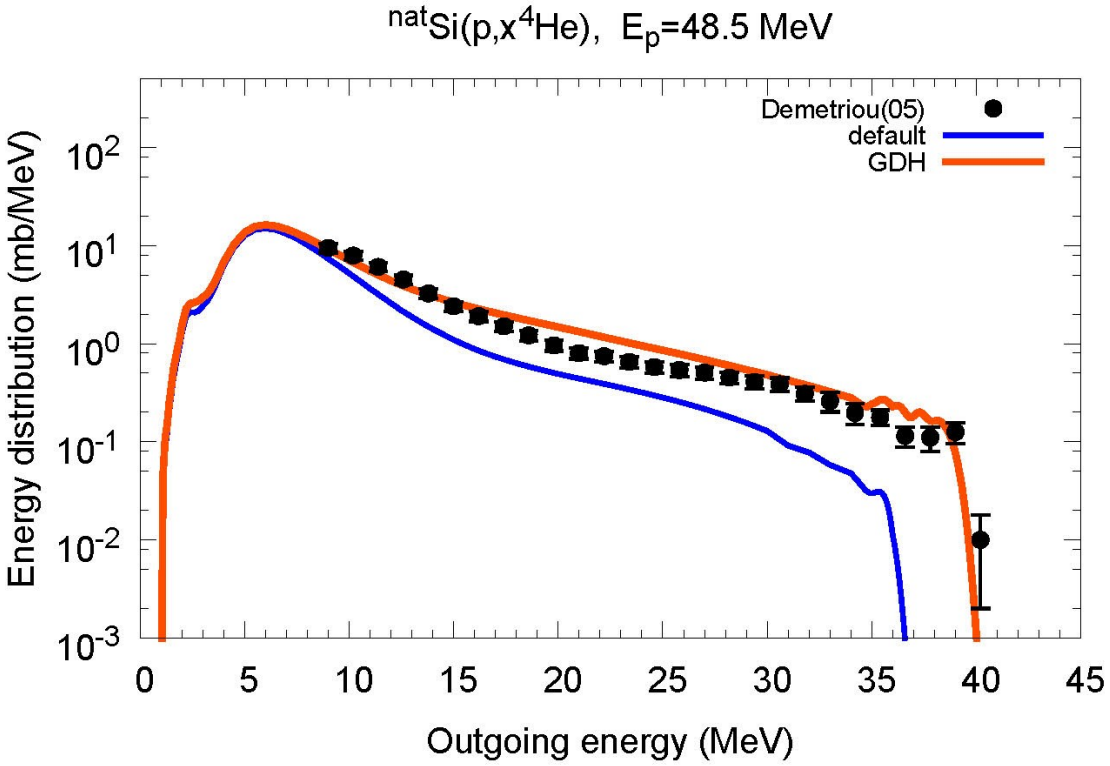
natSi(p,x4He), Ep=48.5 MeV
Demetriou(05)
default
GDH
Energy distribution (mb/MeV)
Outgoing energy (MeV)

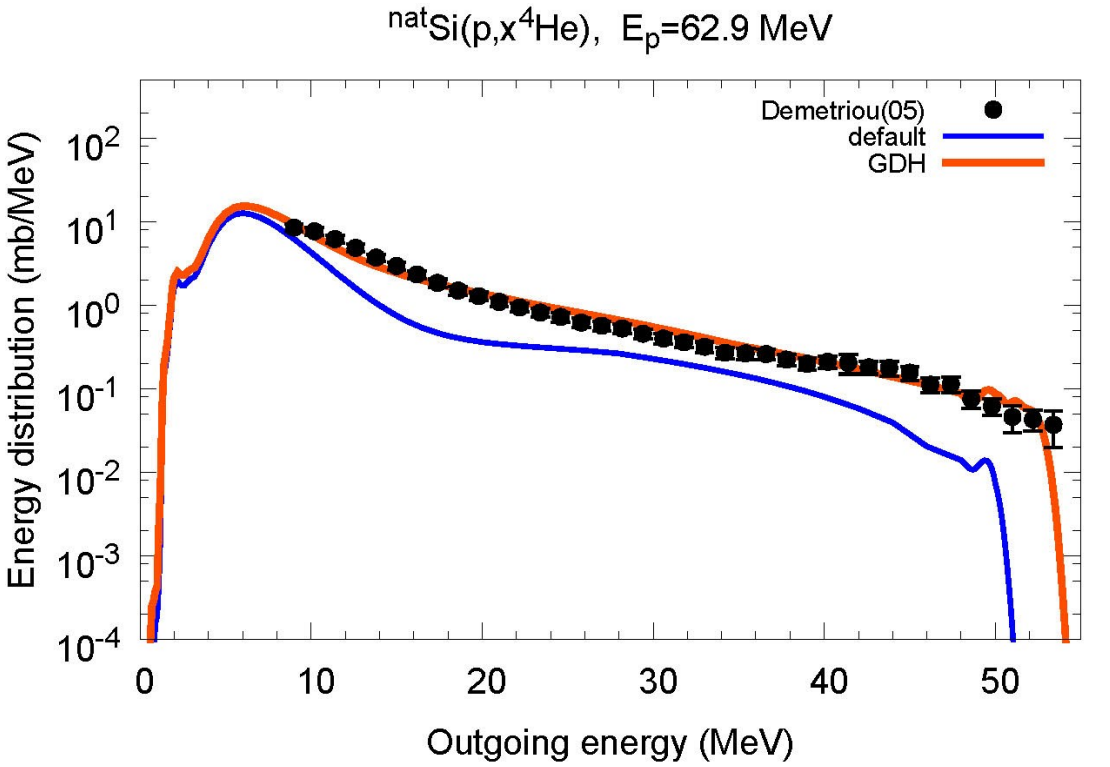
natSi(p,x4He), Ep=62.9 MeV
Demetriou(05)
default
GDH
Energy distribution (mb/MeV)
Outgoing energy (MeV)

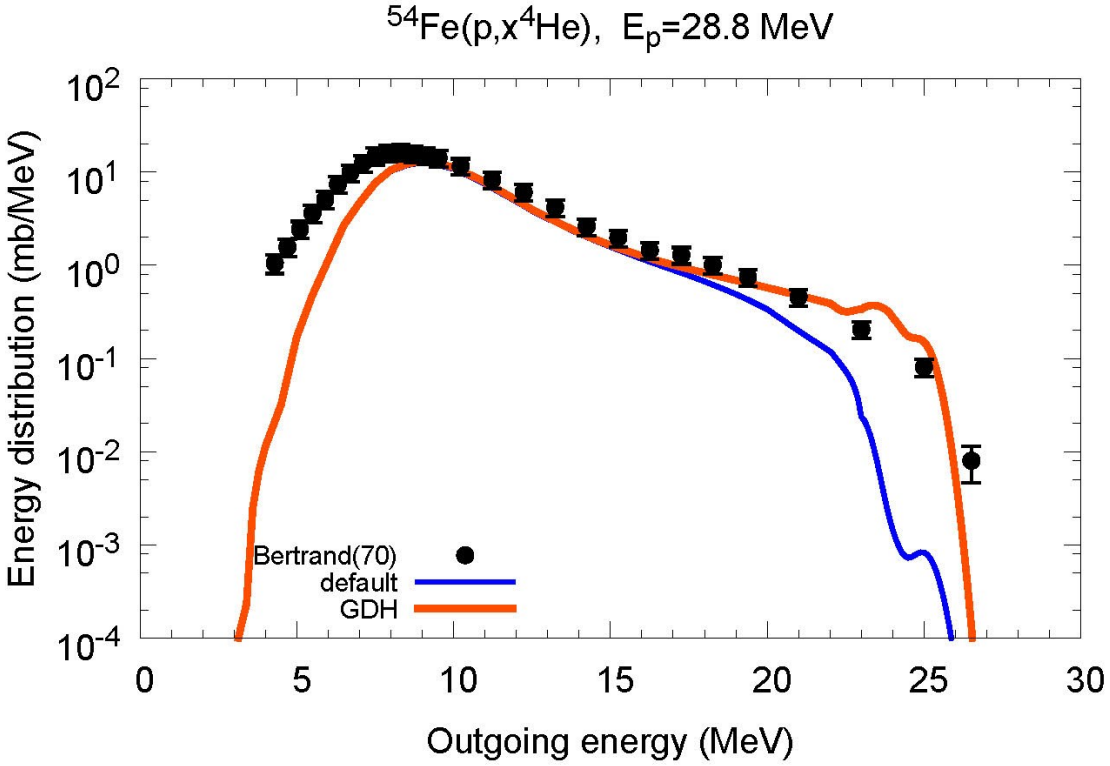
^{54}Fe(p,x^{4}He), E$_p$=28.8 MeV
Energy distribution (mb/MeV)
Outgoing energy (MeV)
Bertrand(70)
default
GDH

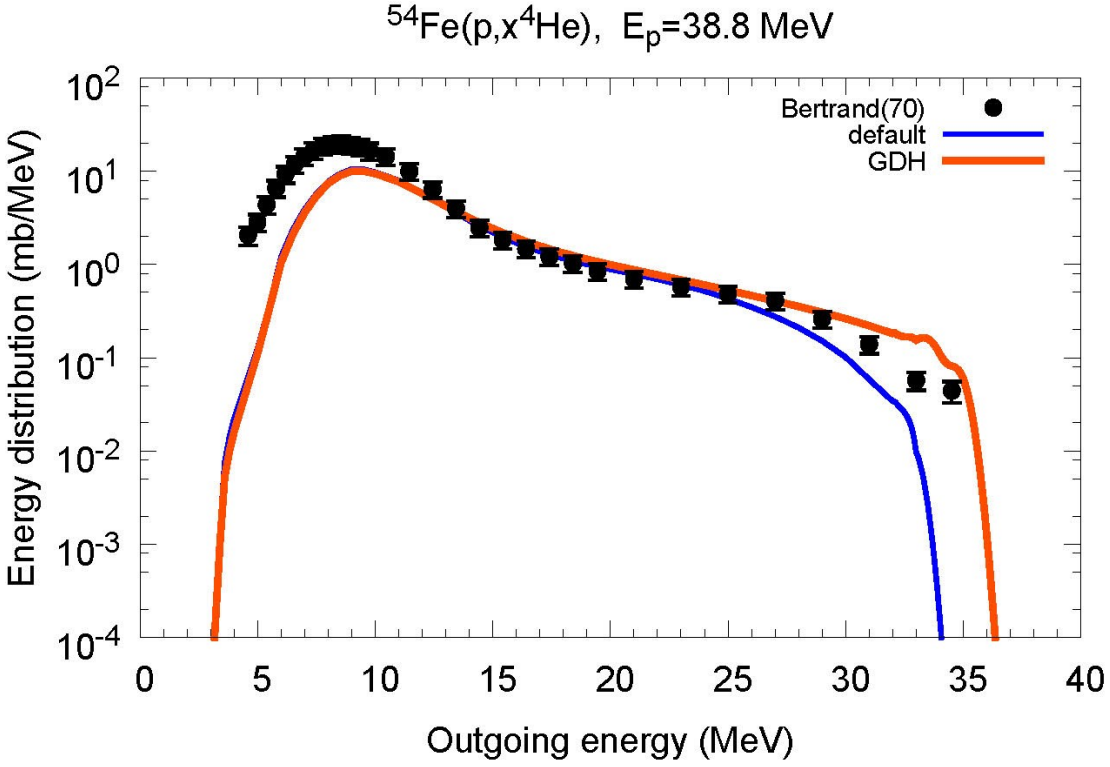
^{54}Fe(p,x^{4}He), E$_p$=38.8 MeV
Energy distribution (mb/MeV)
Outgoing energy (MeV)
Bertrand(70)
default
GDH

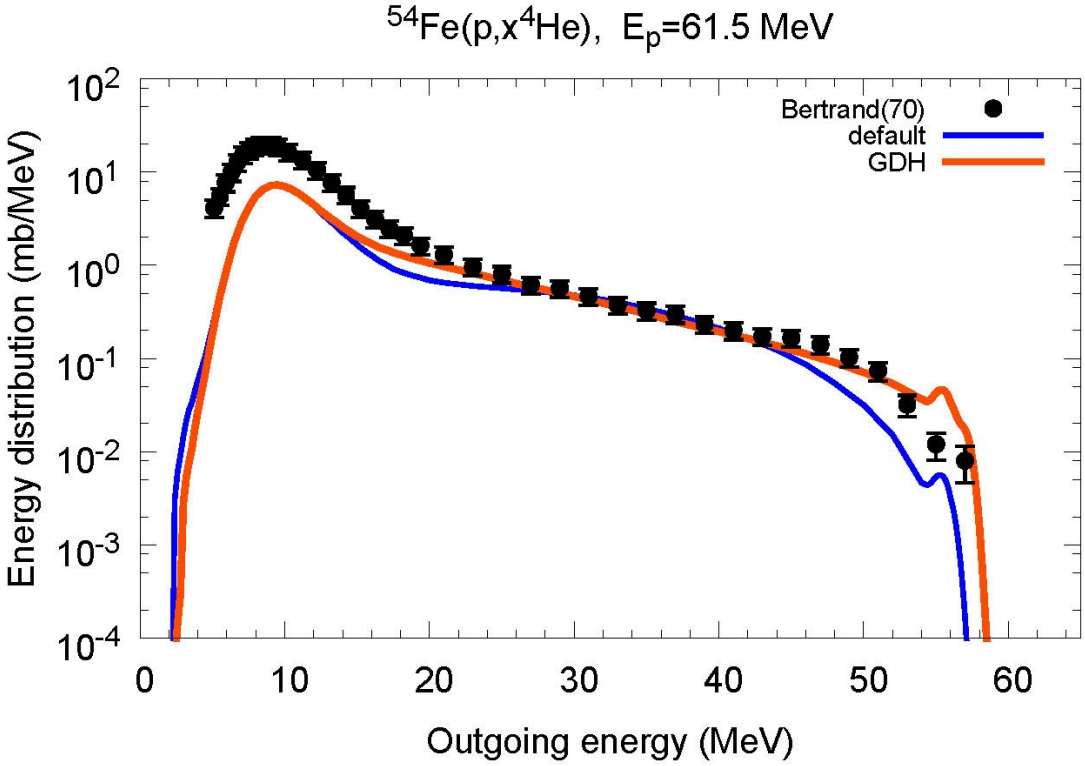
^{54}Fe(p,x^{4}He), E$_p$=61.5 MeV
Bertrand(70)
default
GDH
Energy distribution (mb/MeV)
Outgoing energy (MeV)
10^{2}
10^{1}
10^{0}
10^{-1}
10^{-2}
10^{-3}
10^{-4}
0
10
20
30
40
50
60

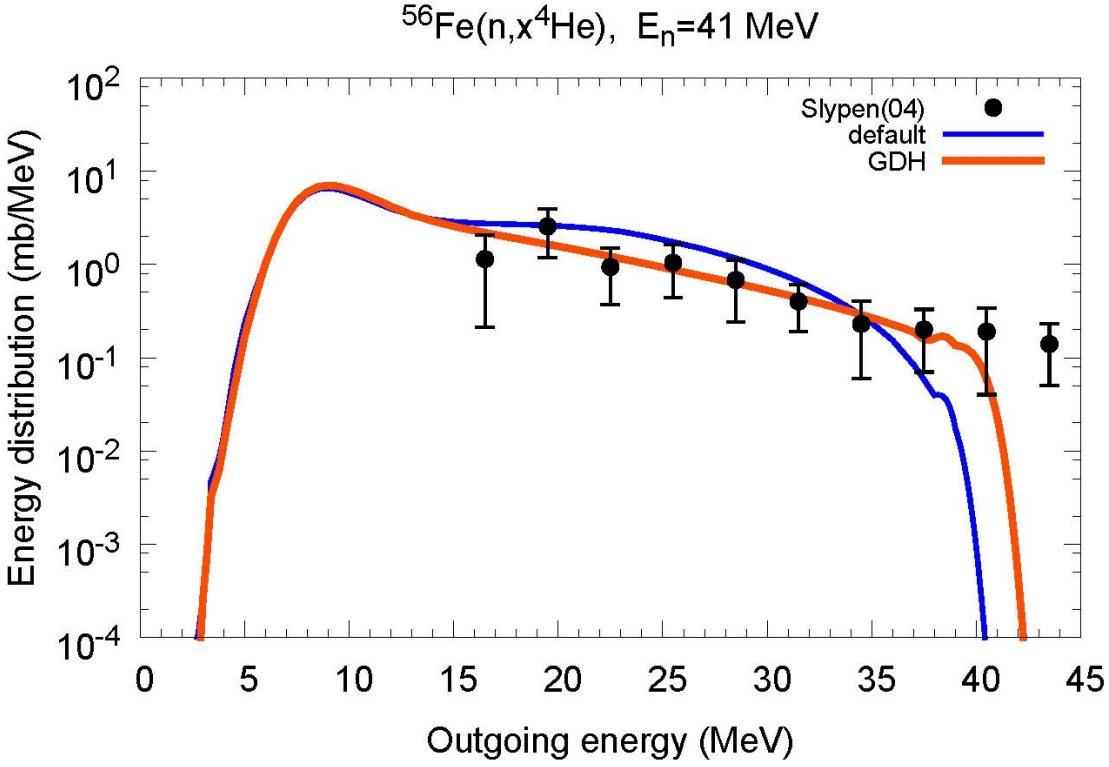
^{56}Fe(n,x^{4}He), E$_n$=41 MeV
Slypen(04)
default
GDH
Energy distribution (mb/MeV)
Outgoing energy (MeV)
10^{2}
10^{1}
10^{0}
10^{-1}
10^{-2}
10^{-3}
10^{-4}
0
5
10
15
20
25
30
35
40
45

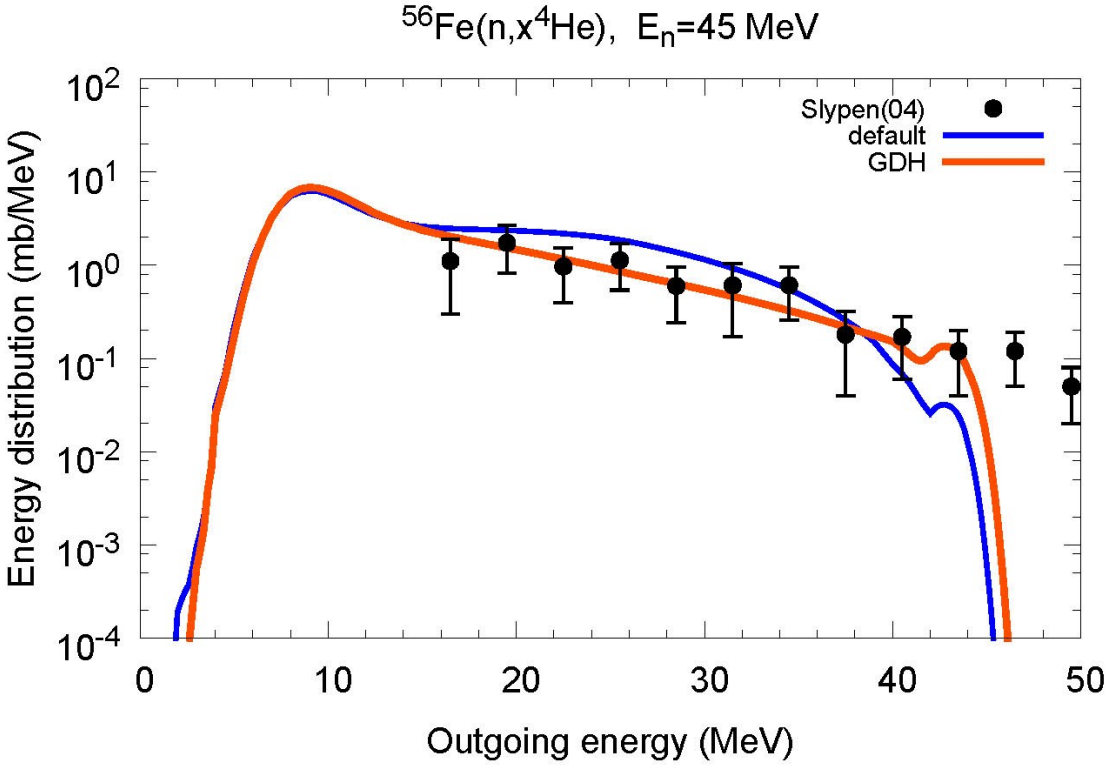
^{56}Fe(n,x^{4}He), E_n=45 MeV
Slypen(04)
default
GDH
Energy distribution (mb/MeV)
Outgoing energy (MeV)
10^{2}
10^{1}
10^{0}
10^{-1}
10^{-2}
10^{-3}
10^{-4}
0
10
20
30
40
50

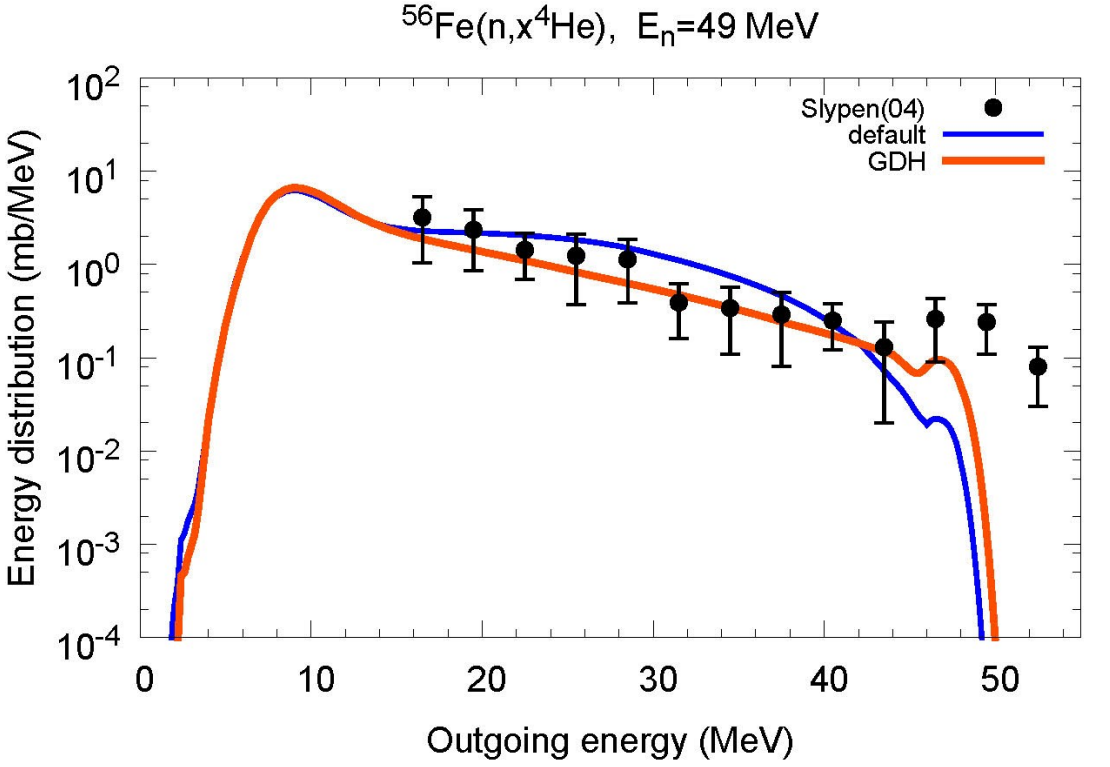
^{56}Fe(n,x^{4}He), E_n=49 MeV
Slypen(04)
default
GDH
Energy distribution (mb/MeV)
Outgoing energy (MeV)
10^{2}
10^{1}
10^{0}
10^{-1}
10^{-2}
10^{-3}
10^{-4}
0
10
20
30
40
50

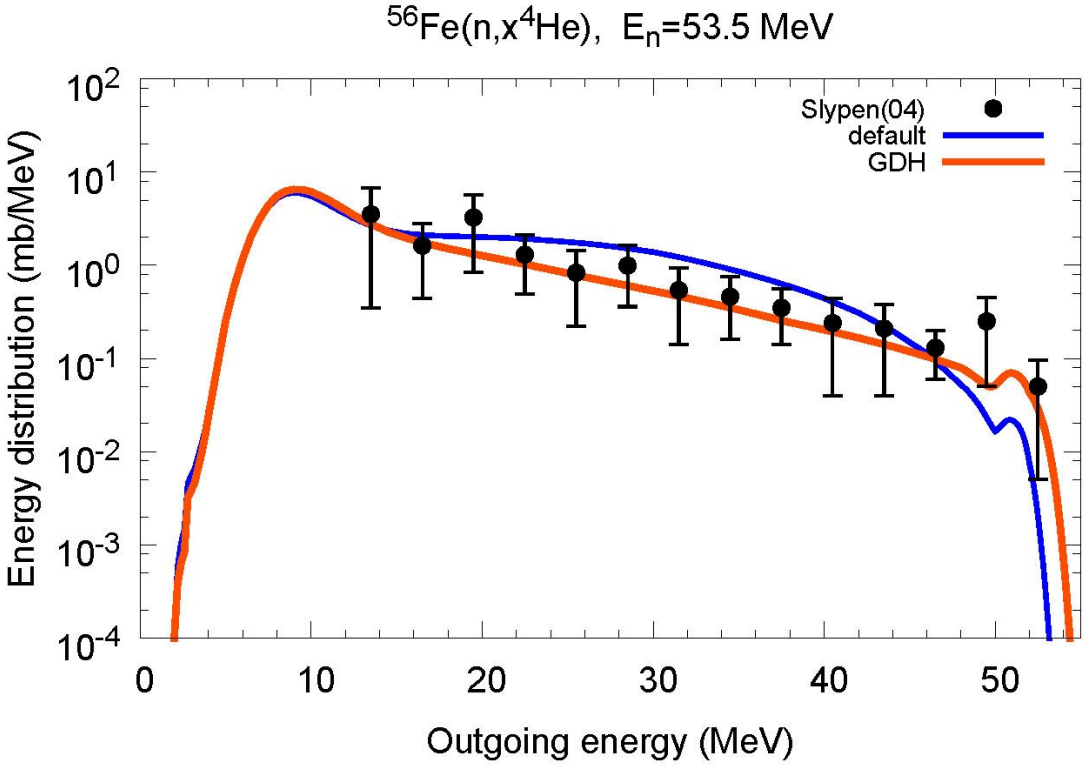
^{56}Fe(n,x^{4}He), E$_n$=53.5 MeV
Slypen(04)
default
GDH
Energy distribution (mb/MeV)
Outgoing energy (MeV)
10^{2}
10^{1}
10^{0}
10^{-1}
10^{-2}
10^{-3}
10^{-4}
0
10
20
30
40
50

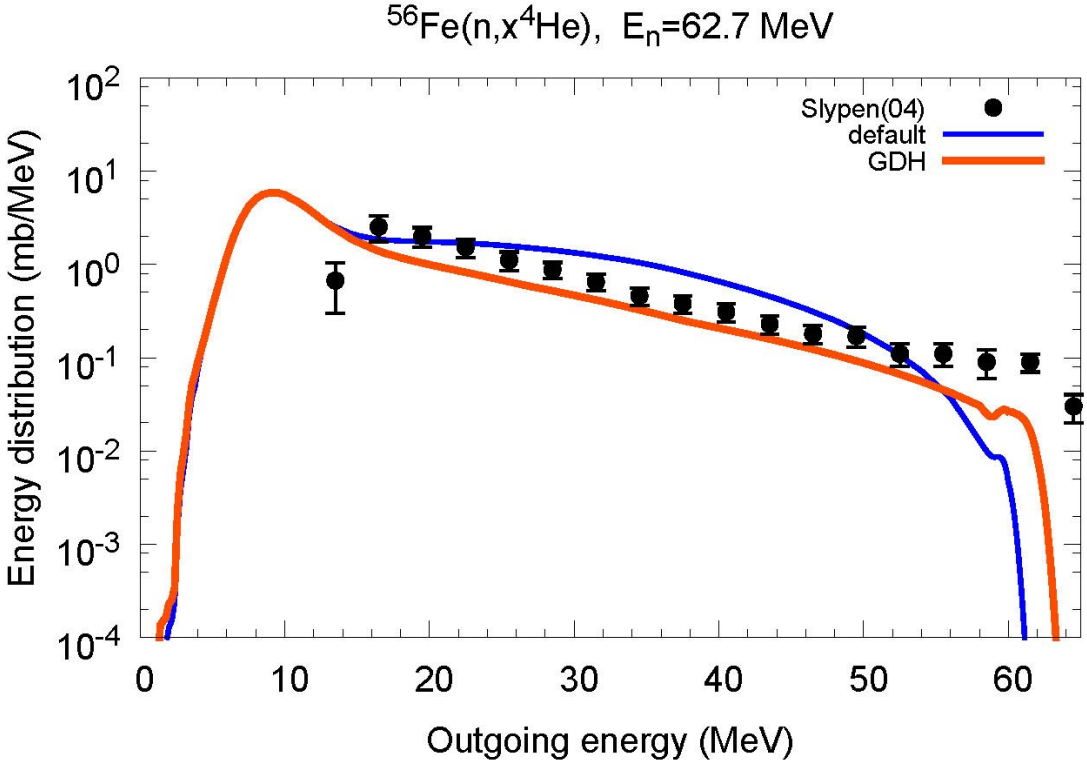
^{56}Fe(n,x^{4}He), E$_n$=62.7 MeV
Slypen(04)
default
GDH
Energy distribution (mb/MeV)
Outgoing energy (MeV)
10^{2}
10^{1}
10^{0}
10^{-1}
10^{-2}
10^{-3}
10^{-4}
0
10
20
30
40
50
60

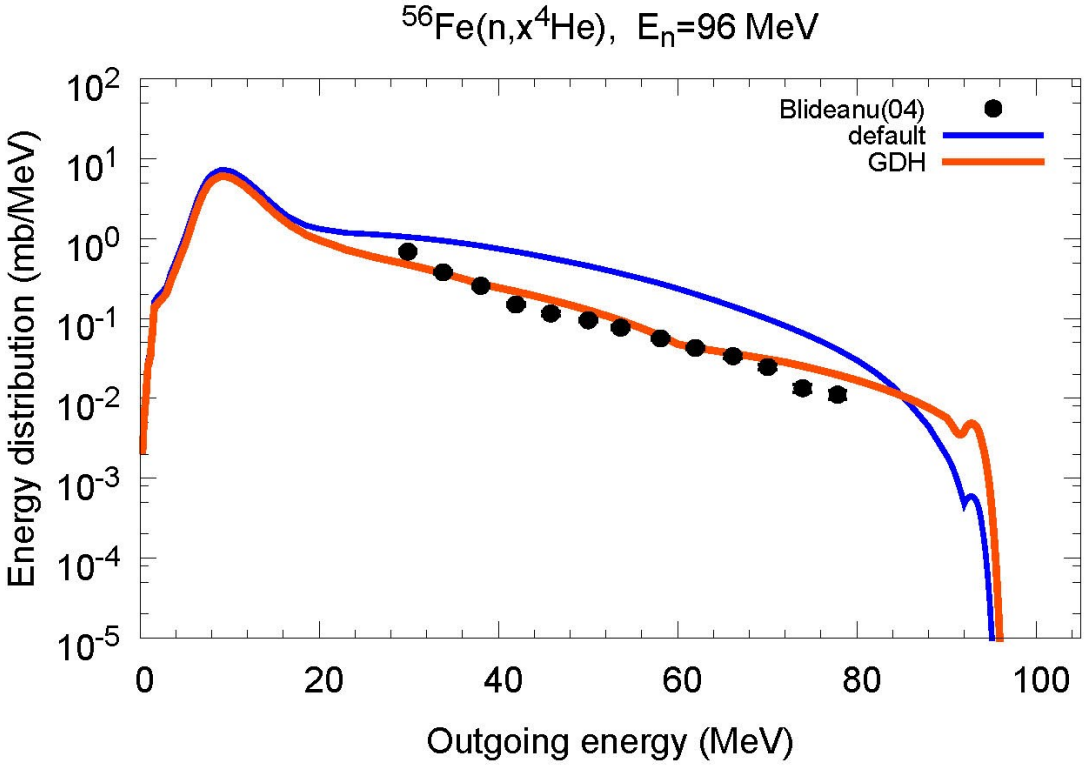
^{56}Fe(n,x^{4}He), E$_n$=96 MeV
Blideanu(04)
default
GDH
Energy distribution (mb/MeV)
Outgoing energy (MeV)

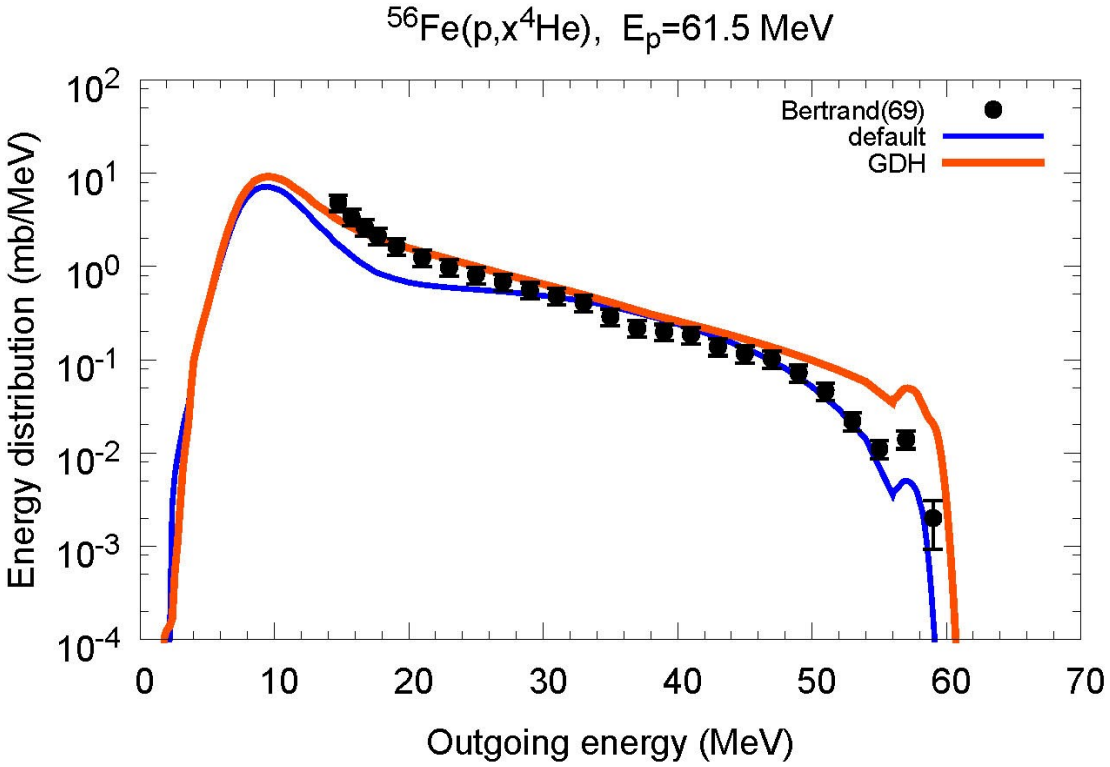
^{56}Fe(p,x^{4}He), E$_p$=61.5 MeV
Bertrand(69)
default
GDH
Energy distribution (mb/MeV)
Outgoing energy (MeV)

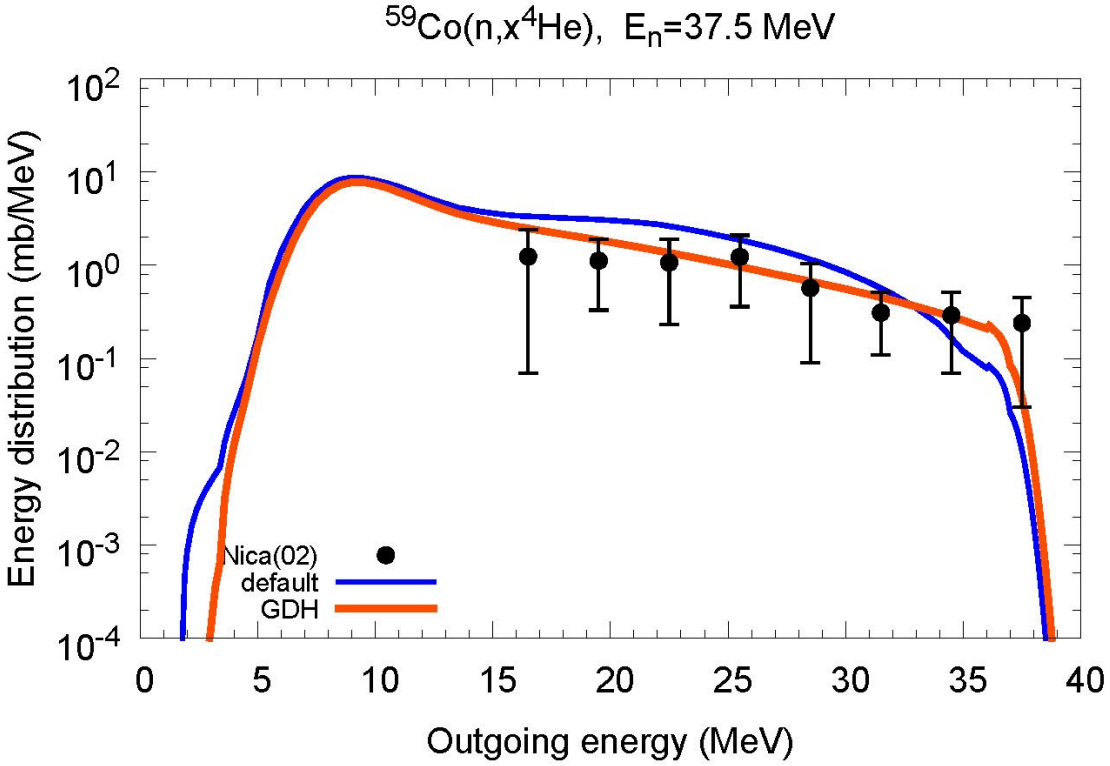
59Co(n,x4He), En=37.5 MeV
Energy distribution (mb/MeV)
Outgoing energy (MeV)
Nica(02)
default
GDH

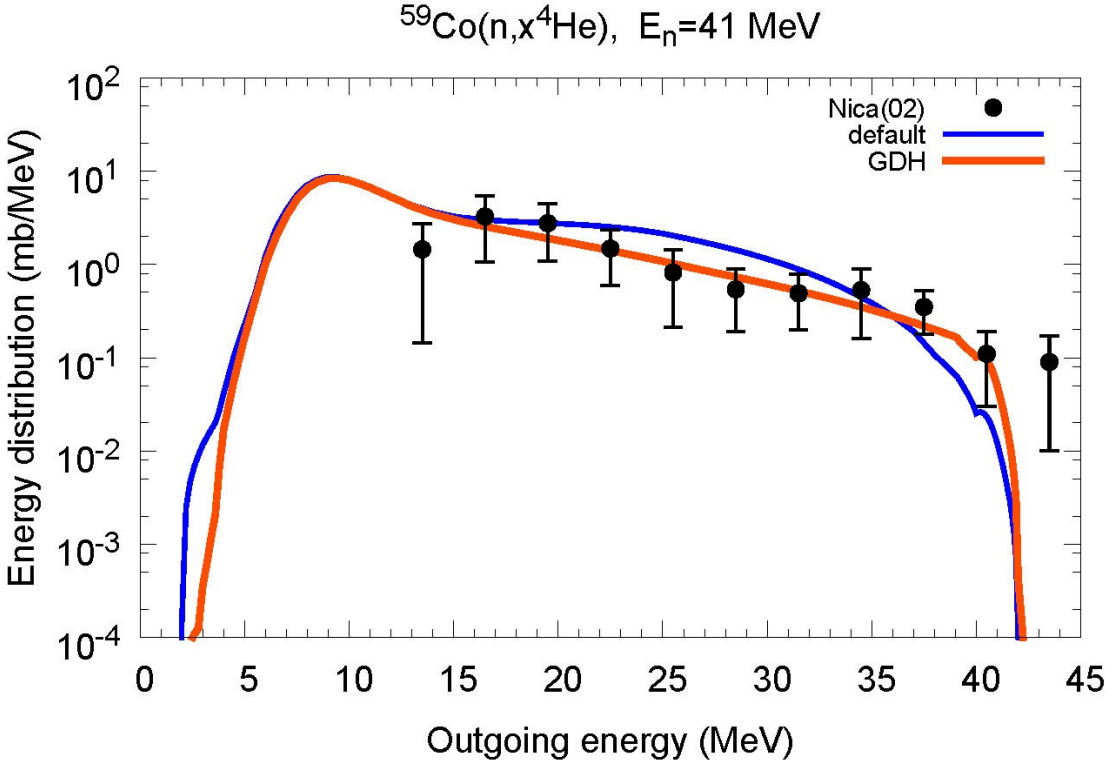
59Co(n,x4He), En=41 MeV
Energy distribution (mb/MeV)
Outgoing energy (MeV)
Nica(02)
default
GDH

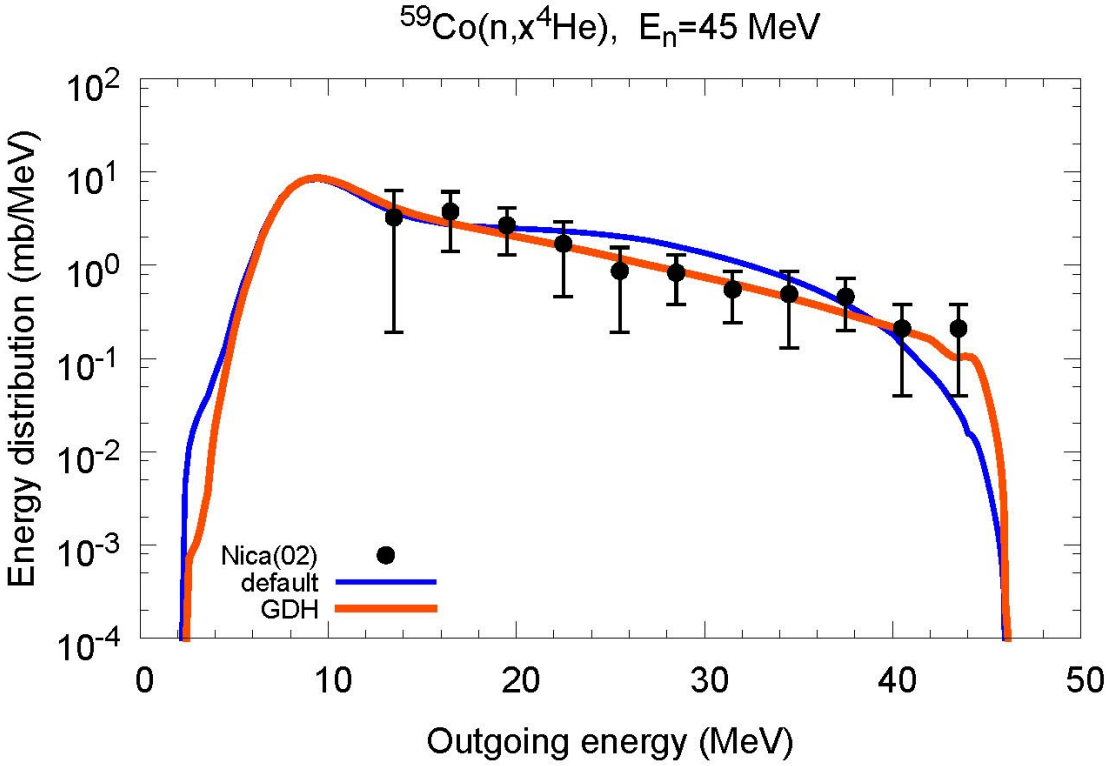
^{59}Co(n,x^{4}He), E_n=45 MeV
Energy distribution (mb/MeV)
Outgoing energy (MeV)
Nica(02)
default
GDH

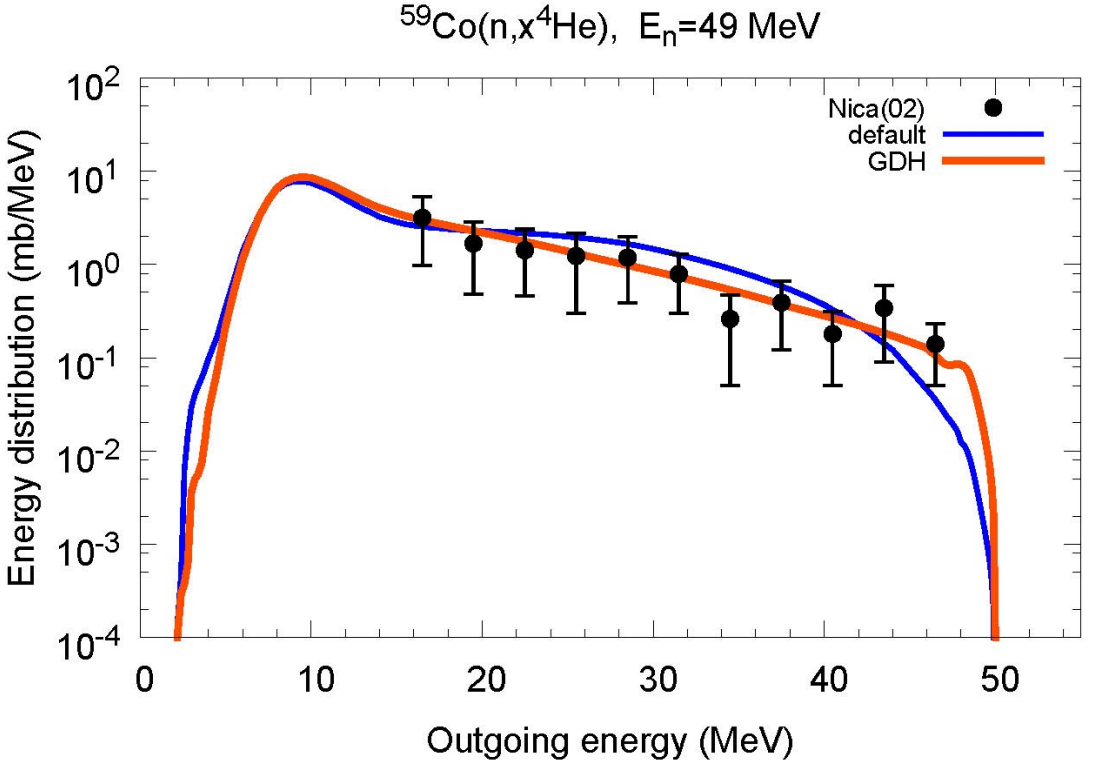
^{59}Co(n,x^{4}He), E_n=49 MeV
Energy distribution (mb/MeV)
Outgoing energy (MeV)
Nica(02)
default
GDH

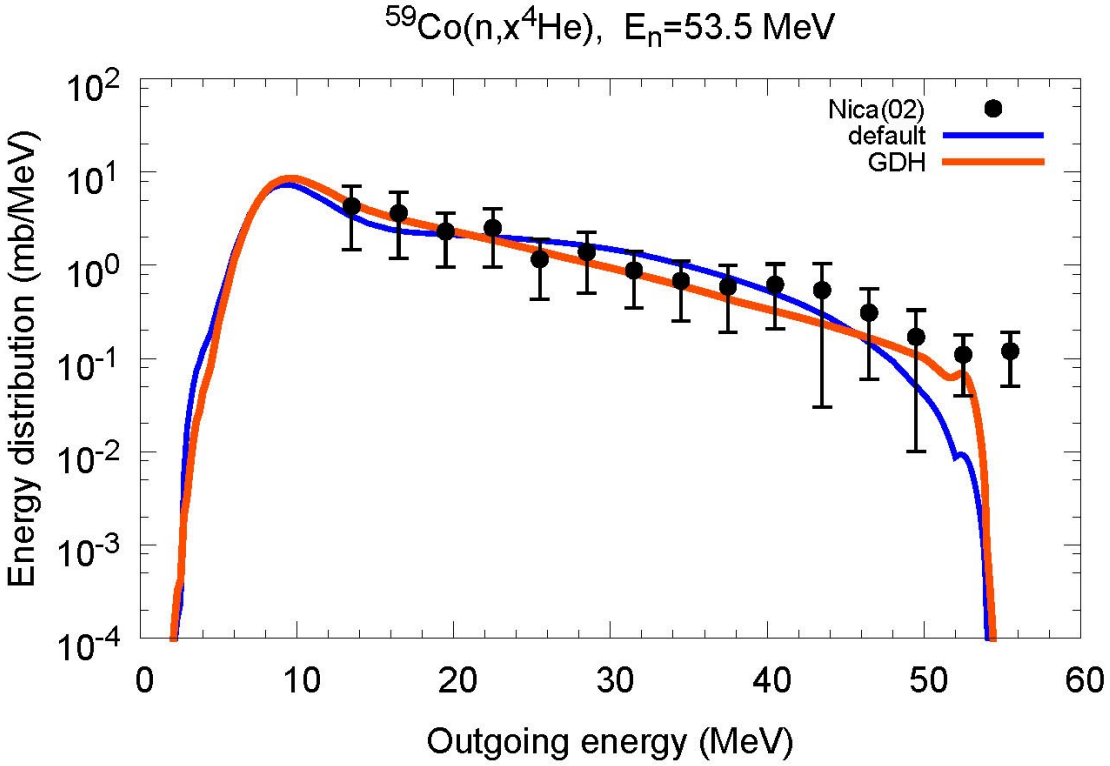
59Co(n,x4He), En=53.5 MeV
Nica(02)
default
GDH
Energy distribution (mb/MeV)
Outgoing energy (MeV)
10^2
10^1
10^0
10^-1
10^-2
10^-3
10^-4
0
10
20
30
40
50
60

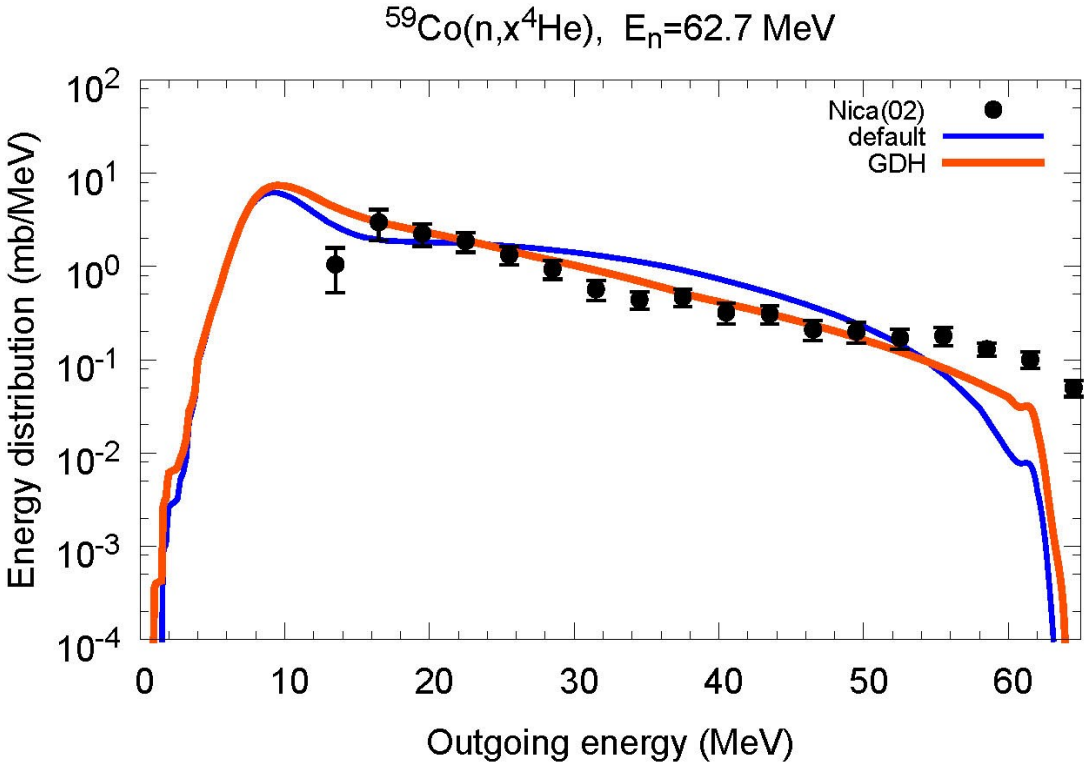
59Co(n,x4He), En=62.7 MeV
Nica(02)
default
GDH
Energy distribution (mb/MeV)
Outgoing energy (MeV)
10^2
10^1
10^0
10^-1
10^-2
10^-3
10^-4
0
10
20
30
40
50
60

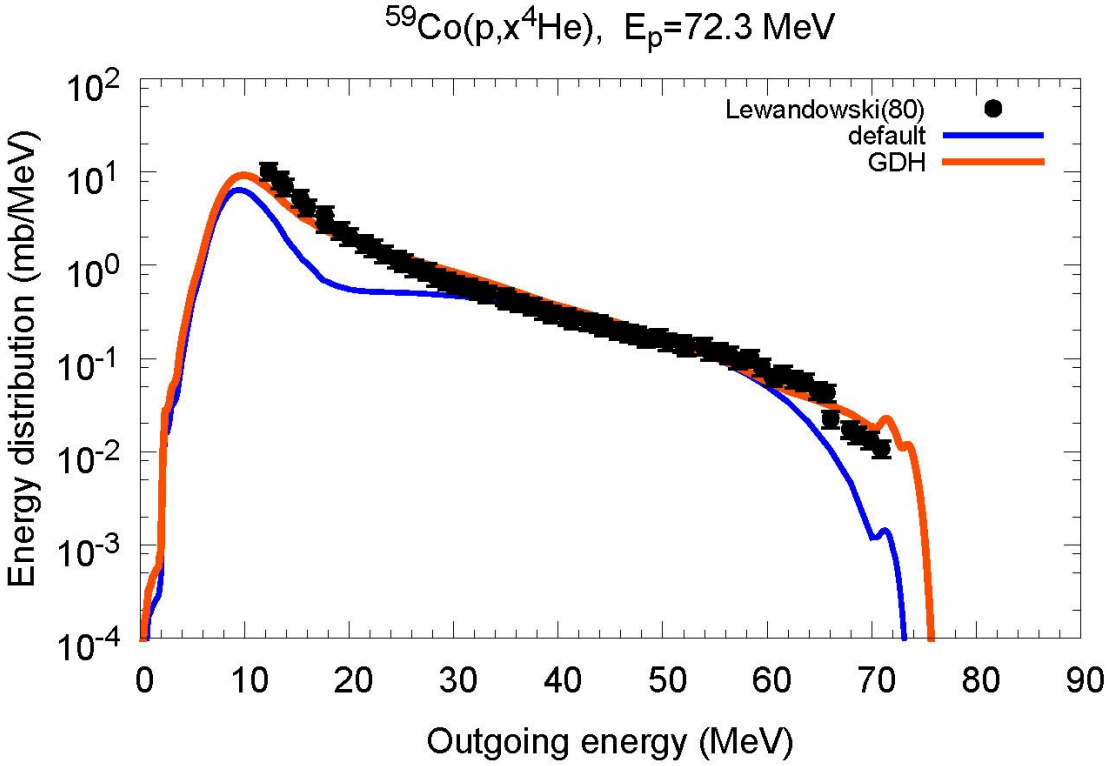
^{59}Co(p,x^{4}He), E$_p$=72.3 MeV
Lewandowski(80)
default
GDH
Energy distribution (mb/MeV)
Outgoing energy (MeV)

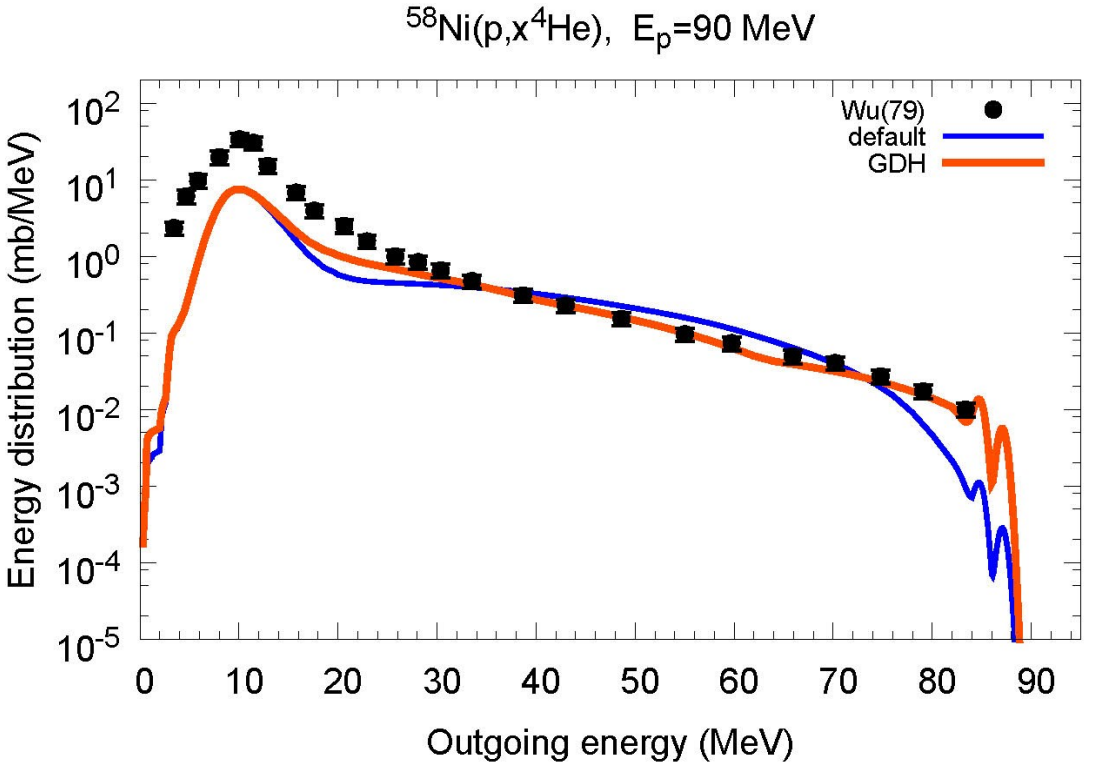
^{58}Ni(p,x^{4}He), E$_p$=90 MeV
Wu(79)
default
GDH
Energy distribution (mb/MeV)
Outgoing energy (MeV)

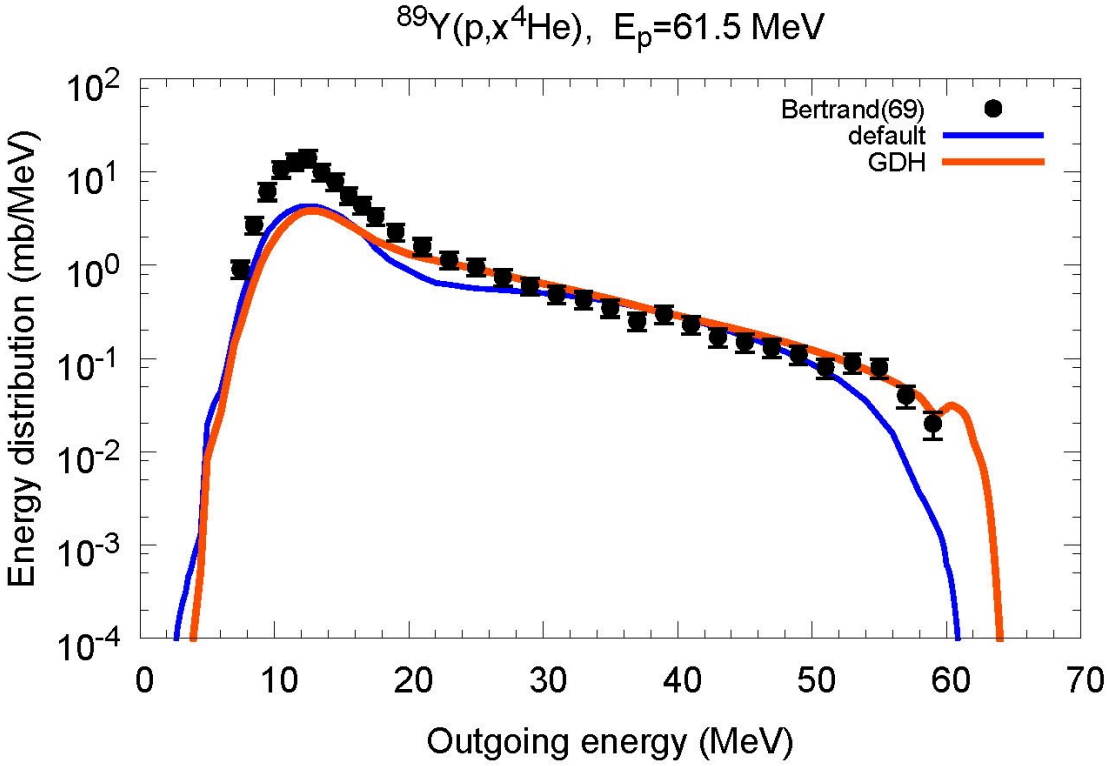
^{89}Y(p,x^{4}He), E$_p$=61.5 MeV
Bertrand(69)
default
GDH
Energy distribution (mb/MeV)
Outgoing energy (MeV)

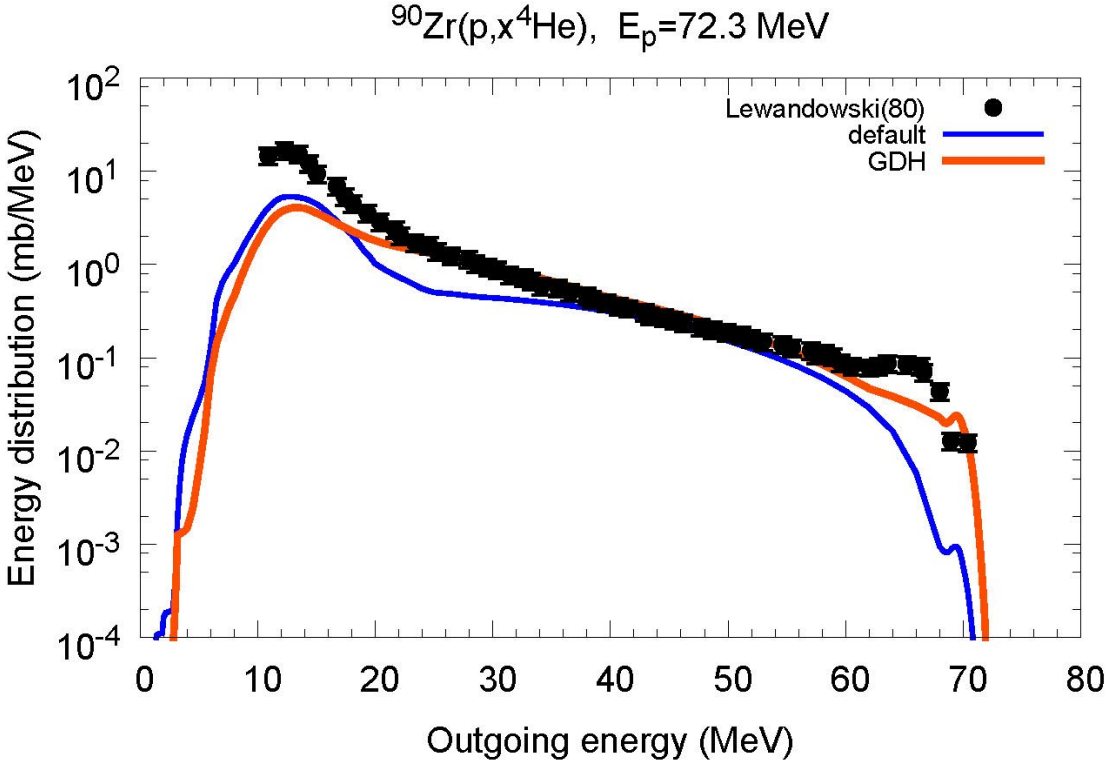
^{90}Zr(p,x^{4}He), E$_p$=72.3 MeV
Lewandowski(80)
default
GDH
Energy distribution (mb/MeV)
Outgoing energy (MeV)

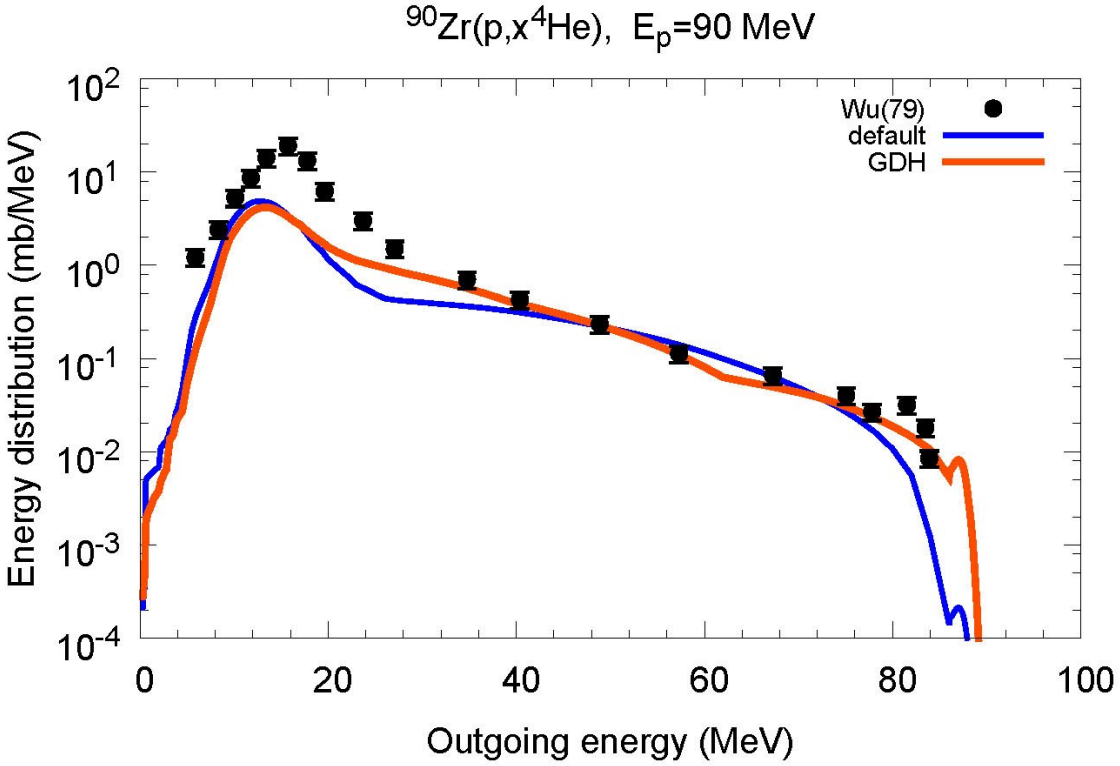
^{90}Zr(p,x^{4}He), E$_p$=90 MeV
Energy distribution (mb/MeV)
Outgoing energy (MeV)
Wu(79)
default
GDH
10^{2}
10^{1}
10^{0}
10^{-1}
10^{-2}
10^{-3}
10^{-4}
0
20
40
60
80
100

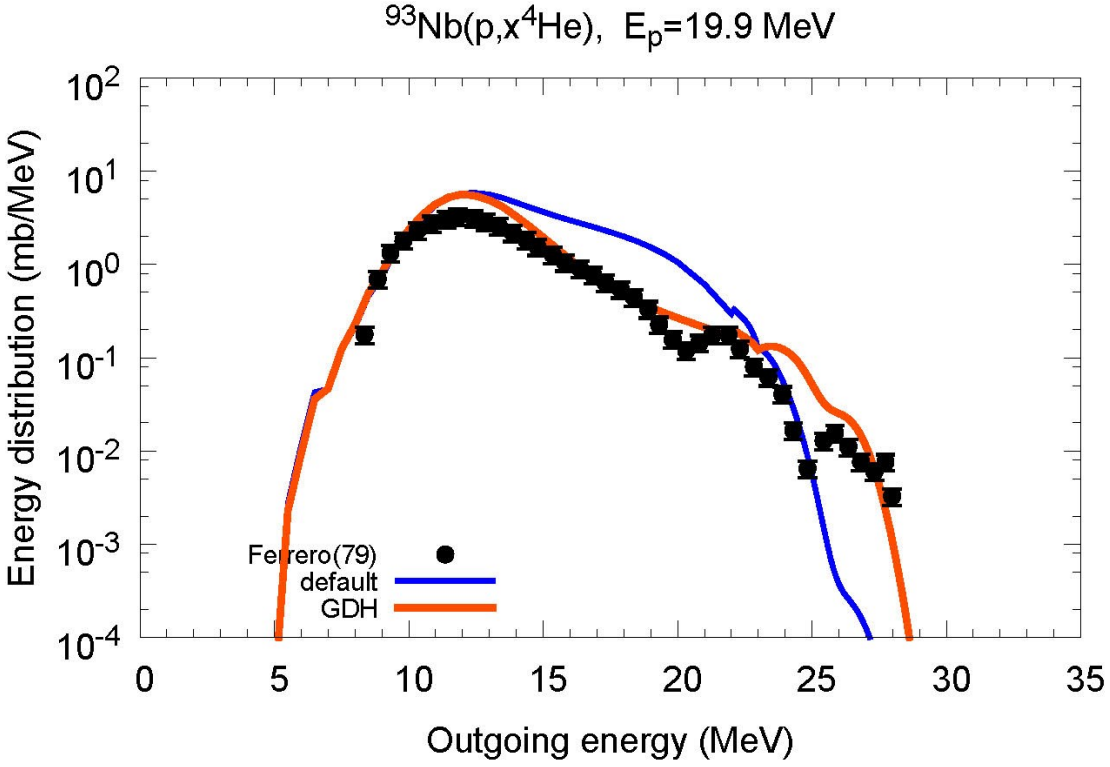
^{93}Nb(p,x^{4}He), E$_p$=19.9 MeV
Energy distribution (mb/MeV)
Outgoing energy (MeV)
Ferrero(79)
default
GDH
10^{2}
10^{1}
10^{0}
10^{-1}
10^{-2}
10^{-3}
10^{-4}
0
5
10
15
20
25
30
35

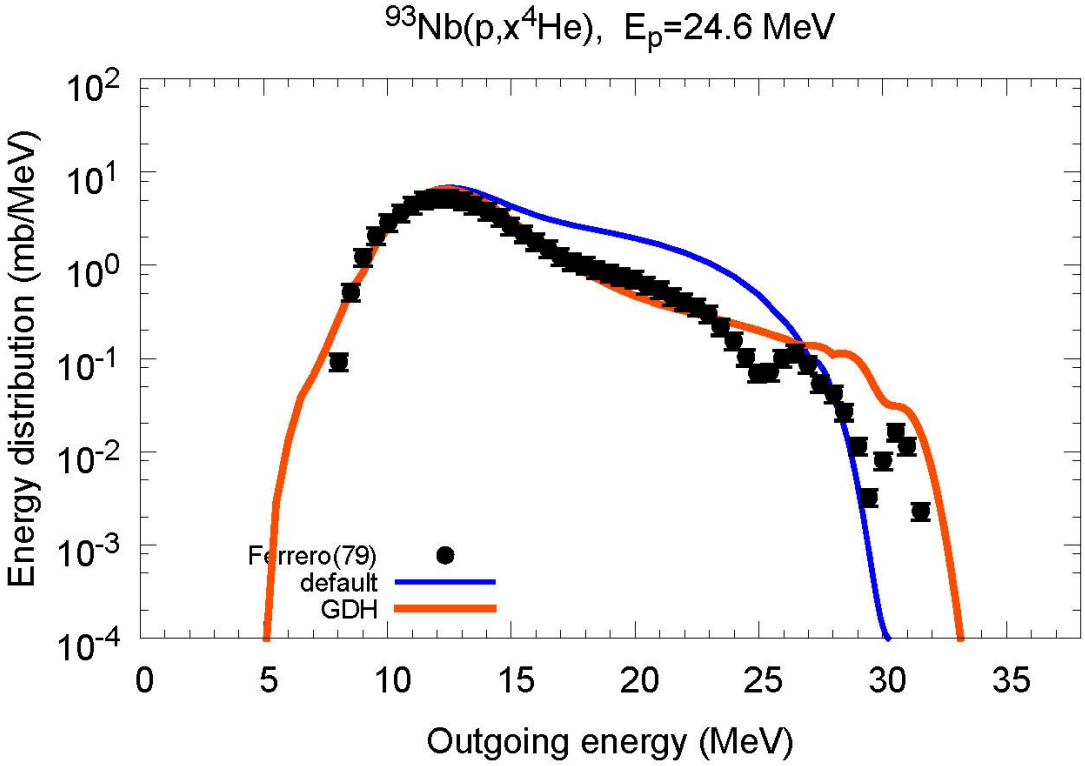
^{93}Nb(p,x^{4}He), E$_p$=24.6 MeV
Energy distribution (mb/MeV)
Outgoing energy (MeV)
Ferrero(79)
default
GDH

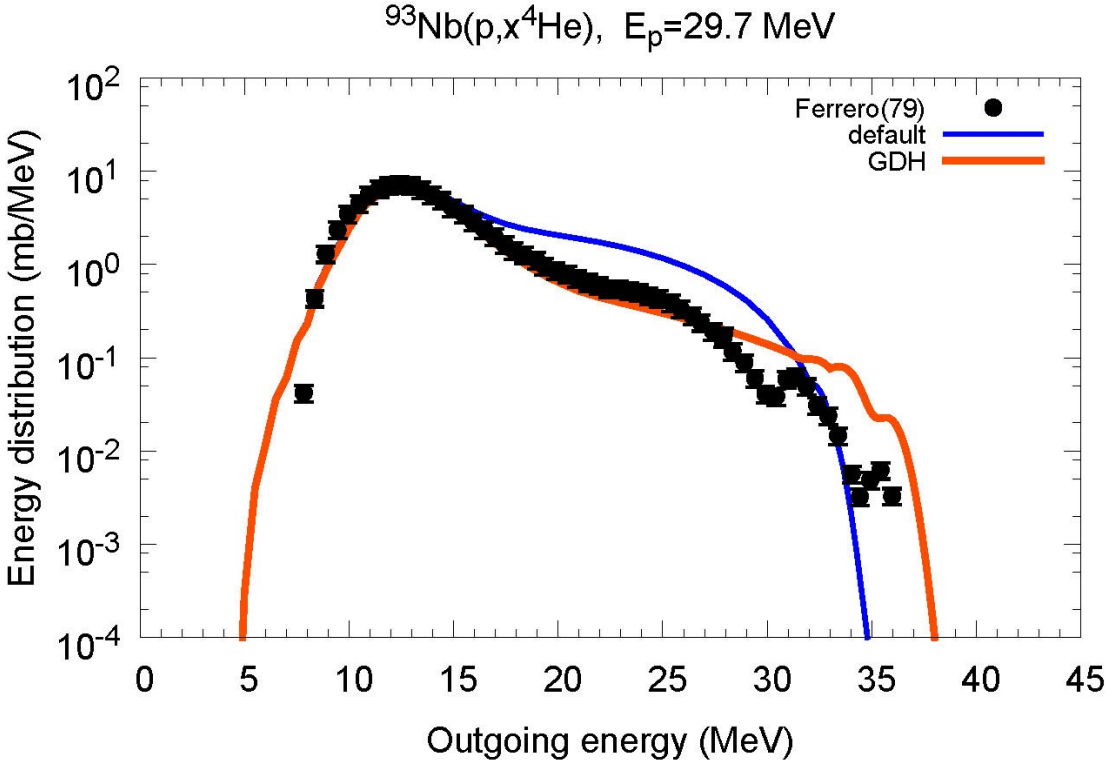
^{93}Nb(p,x^{4}He), E$_p$=29.7 MeV
Energy distribution (mb/MeV)
Outgoing energy (MeV)
Ferrero(79)
default
GDH

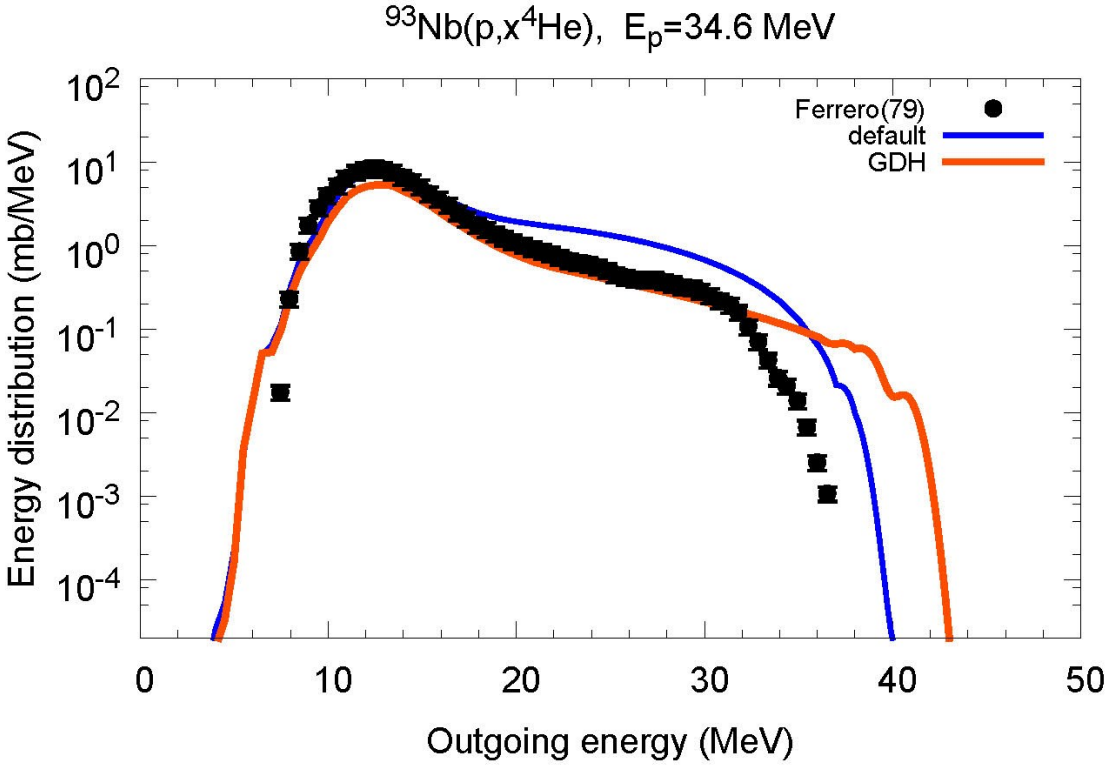
^{93}Nb(p,x^{4}He), E$_p$=34.6 MeV
Ferrero(79)
default
GDH
Energy distribution (mb/MeV)
Outgoing energy (MeV)
10^{2}
10^{1}
10^{0}
10^{-1}
10^{-2}
10^{-3}
10^{-4}
0
10
20
30
40
50

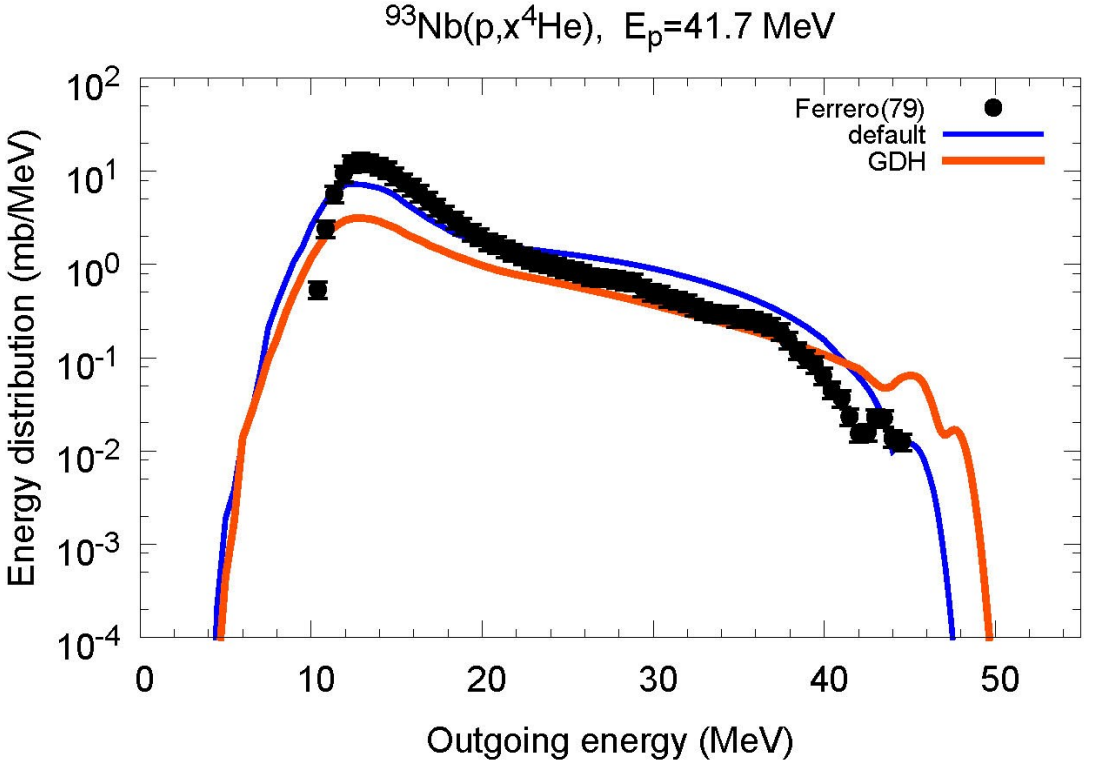
^{93}Nb(p,x^{4}He), E$_p$=41.7 MeV
Ferrero(79)
default
GDH
Energy distribution (mb/MeV)
Outgoing energy (MeV)
10^{2}
10^{1}
10^{0}
10^{-1}
10^{-2}
10^{-3}
10^{-4}
0
10
20
30
40
50

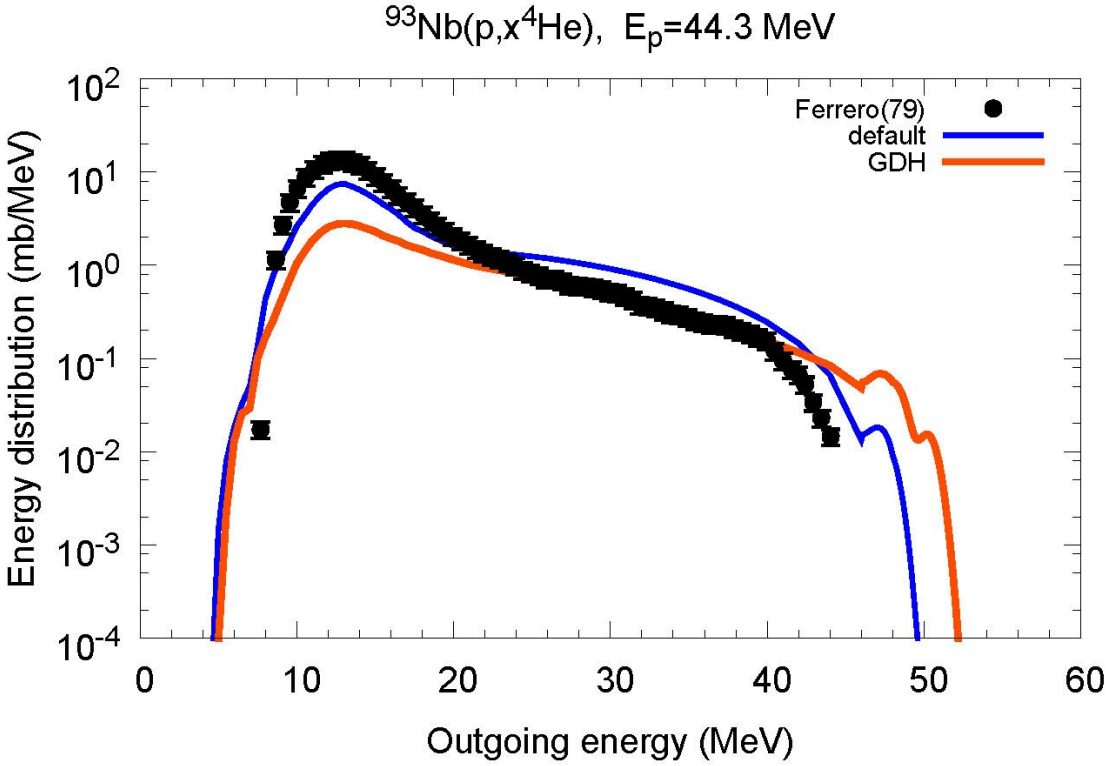
^{93}Nb(p,x^{4}He), E_p=44.3 MeV
Ferrero(79)
default
GDH
Energy distribution (mb/MeV)
Outgoing energy (MeV)
10^{2}
10^{1}
10^{0}
10^{-1}
10^{-2}
10^{-3}
10^{-4}
0
10
20
30
40
50
60

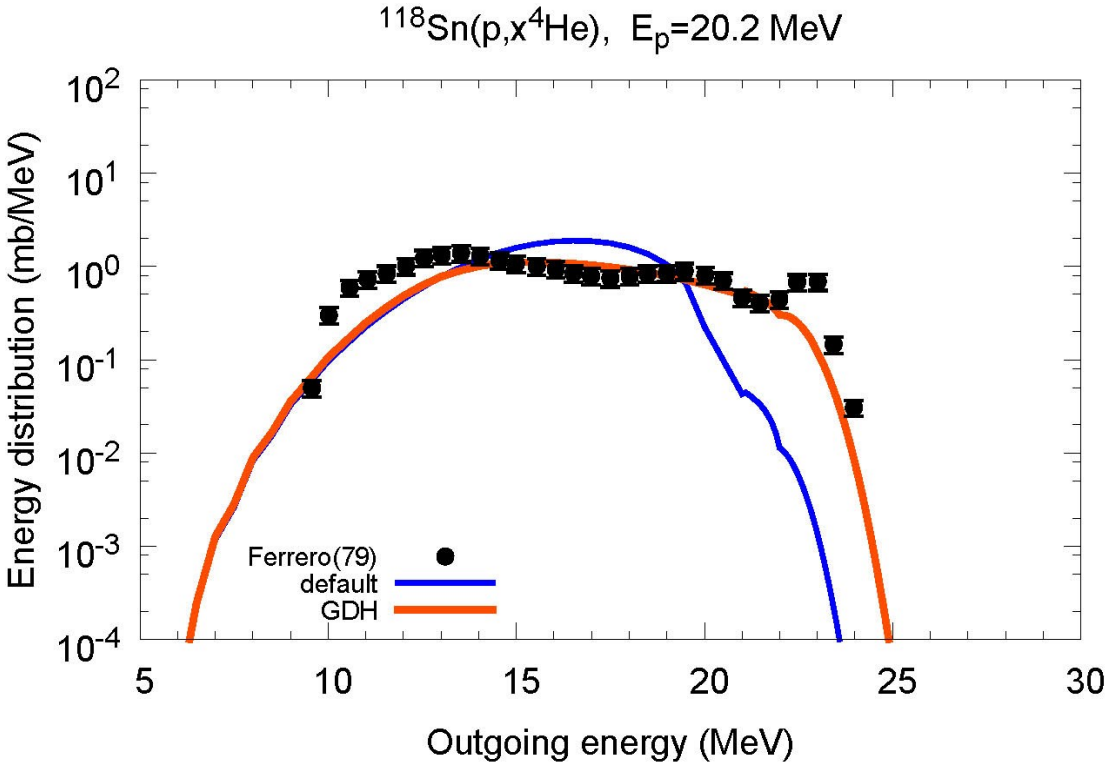
^{118}Sn(p,x^{4}He), E_p=20.2 MeV
Ferrero(79)
default
GDH
Energy distribution (mb/MeV)
Outgoing energy (MeV)
10^{2}
10^{1}
10^{0}
10^{-1}
10^{-2}
10^{-3}
10^{-4}
5
10
15
20
25
30

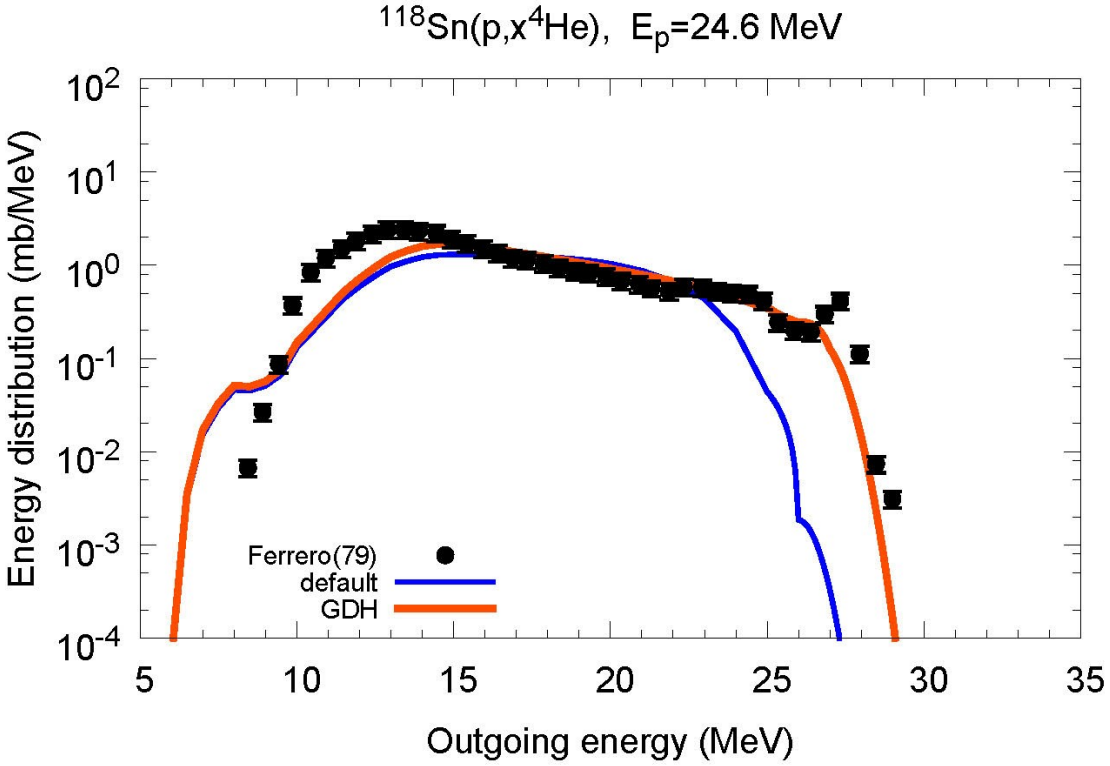
^{118}Sn(p,x^{4}He), E$_p$=24.6 MeV
Energy distribution (mb/MeV)
Outgoing energy (MeV)
Ferrero(79)
default
GDH

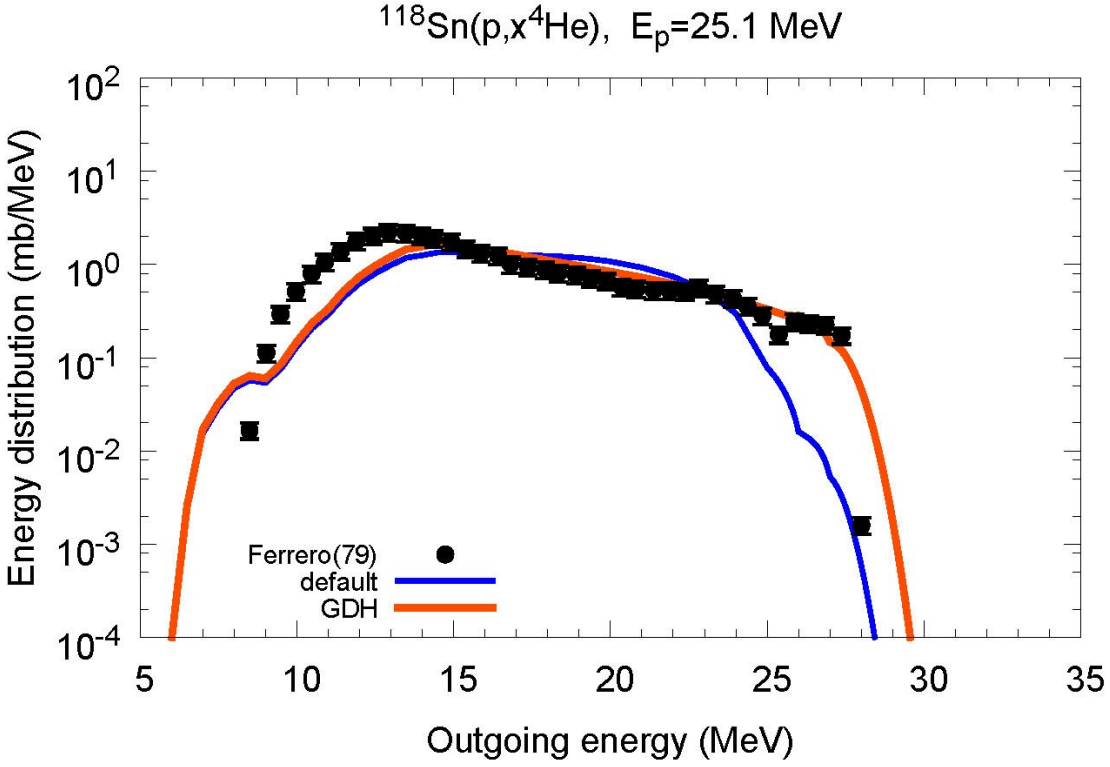
^{118}Sn(p,x^{4}He), E$_p$=25.1 MeV
Energy distribution (mb/MeV)
Outgoing energy (MeV)
Ferrero(79)
default
GDH

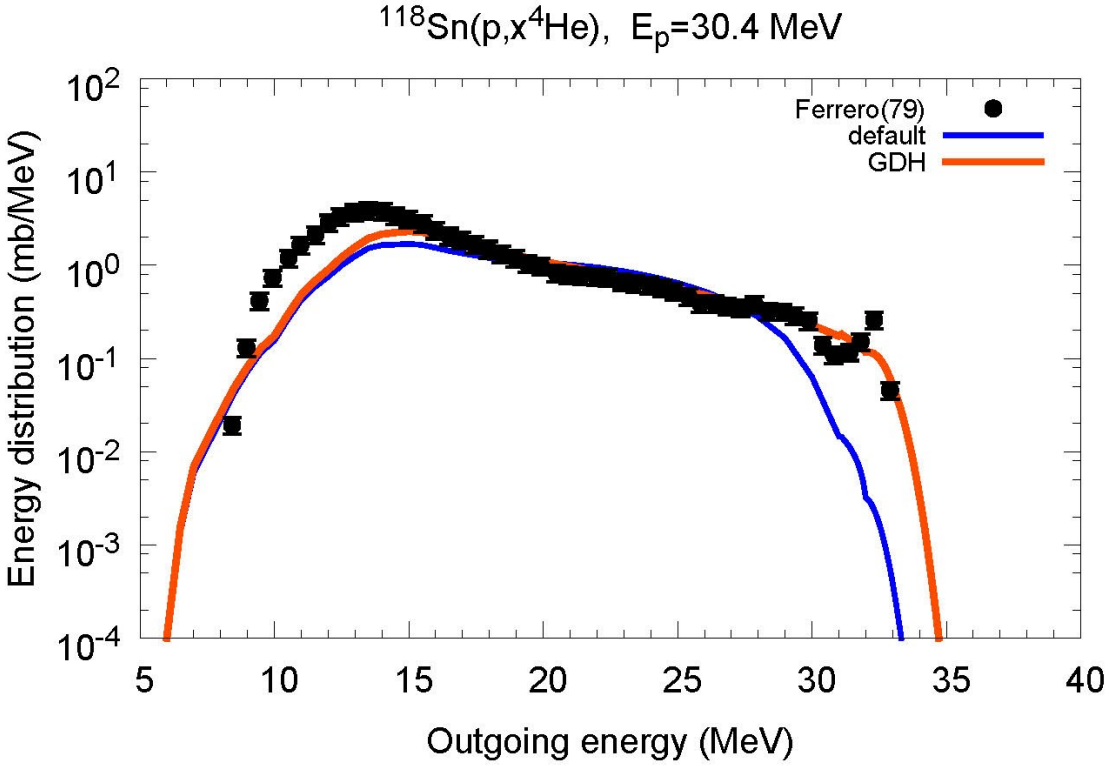
^{118}Sn(p,x^{4}He), E$_p$=30.4 MeV
Ferrero(79)
default
GDH
Energy distribution (mb/MeV)
Outgoing energy (MeV)
10^{2}
10^{1}
10^{0}
10^{-1}
10^{-2}
10^{-3}
10^{-4}
5
10
15
20
25
30
35
40

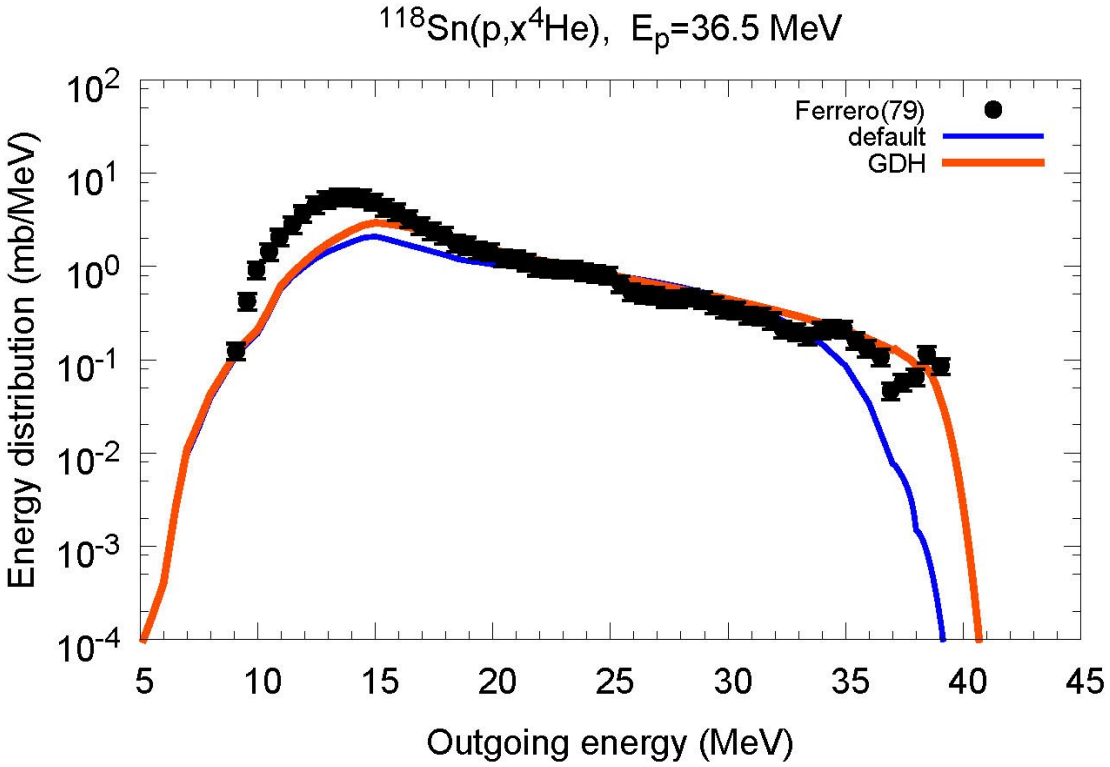
^{118}Sn(p,x^{4}He), E$_p$=36.5 MeV
Ferrero(79)
default
GDH
Energy distribution (mb/MeV)
Outgoing energy (MeV)
10^{2}
10^{1}
10^{0}
10^{-1}
10^{-2}
10^{-3}
10^{-4}
5
10
15
20
25
30
35
40
45

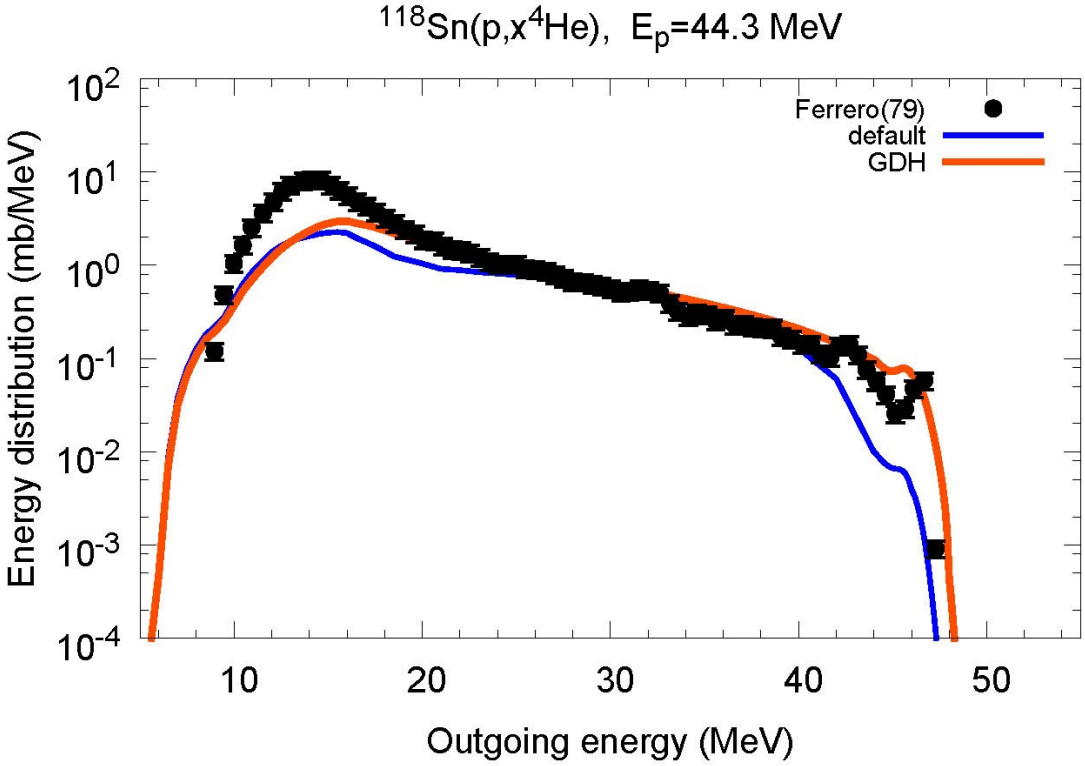
^{118}Sn(p,x^{4}He), E_p=44.3 MeV
Ferrero(79)
default
GDH
Energy distribution (mb/MeV)
Outgoing energy (MeV)

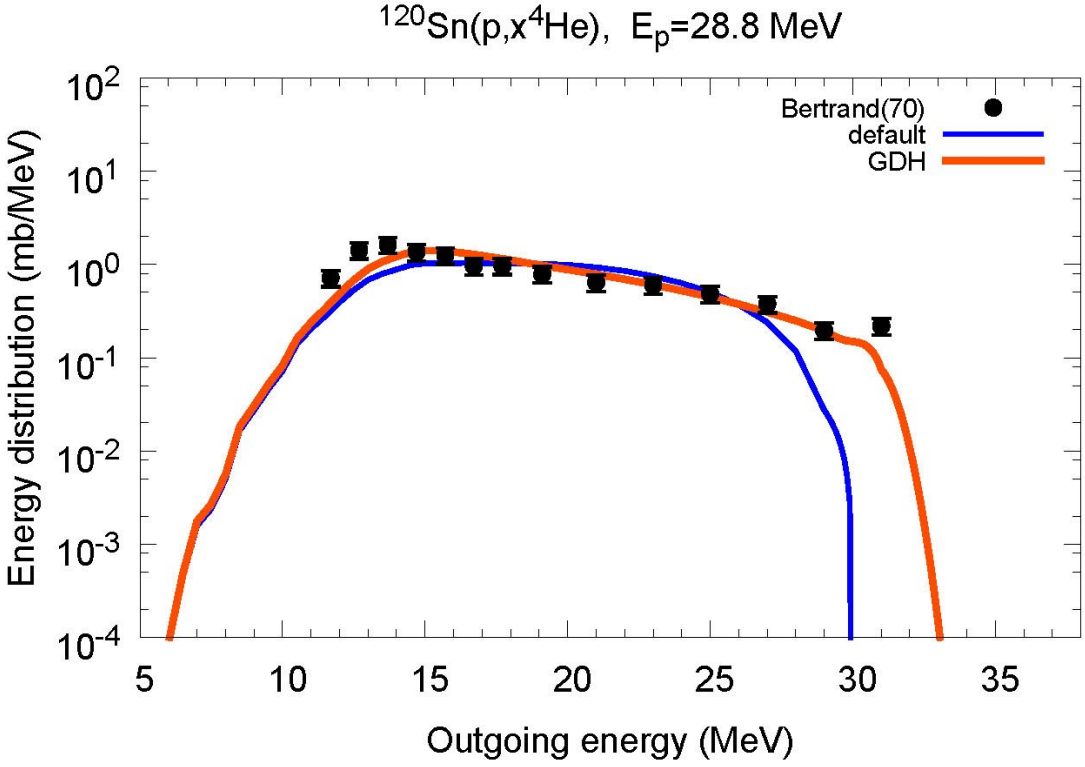
^{120}Sn(p,x^{4}He), E_p=28.8 MeV
Bertrand(70)
default
GDH
Energy distribution (mb/MeV)
Outgoing energy (MeV)

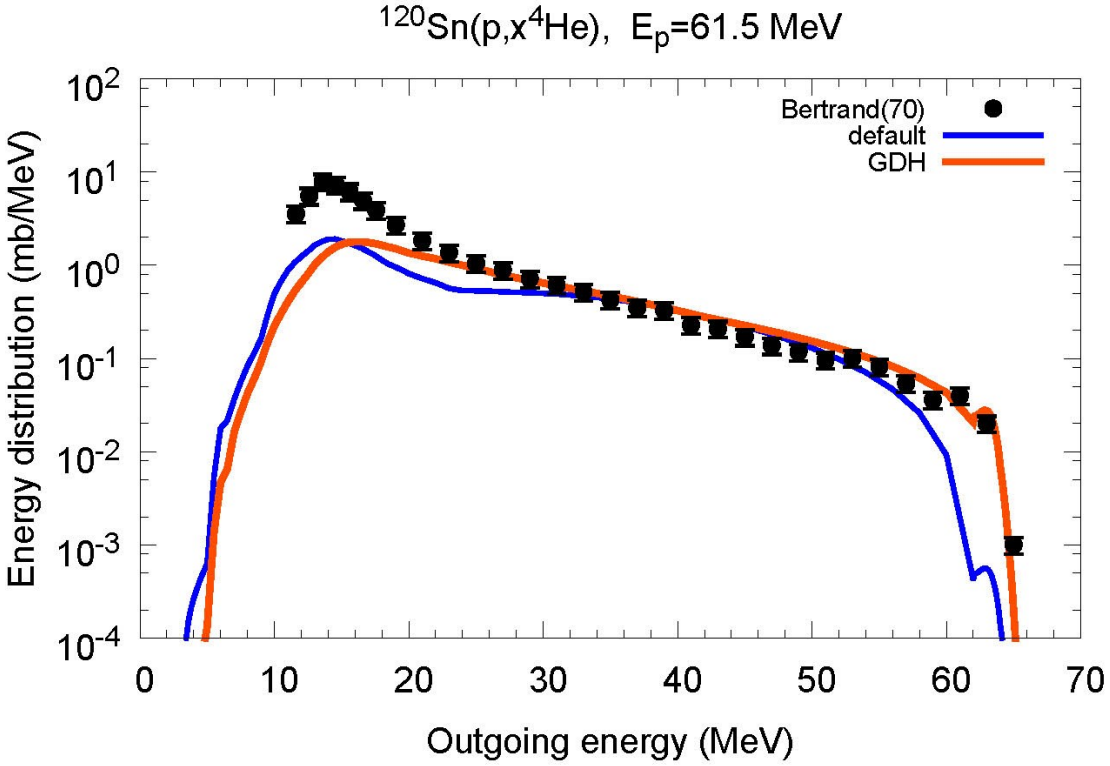
^{120}Sn(p,x^{4}He), E_p=61.5 MeV
Bertrand(70)
default
GDH
Energy distribution (mb/MeV)
Outgoing energy (MeV)

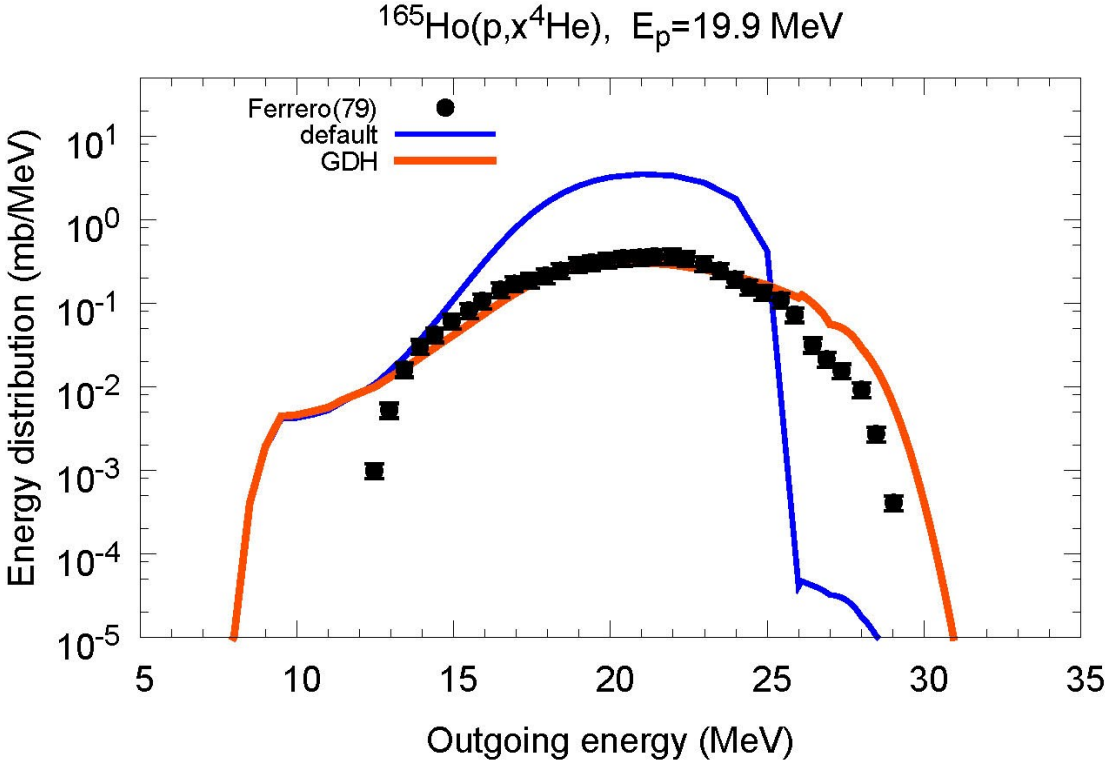
^{165}Ho(p,x^{4}He), E_p=19.9 MeV
Ferrero(79)
default
GDH
Energy distribution (mb/MeV)
Outgoing energy (MeV)

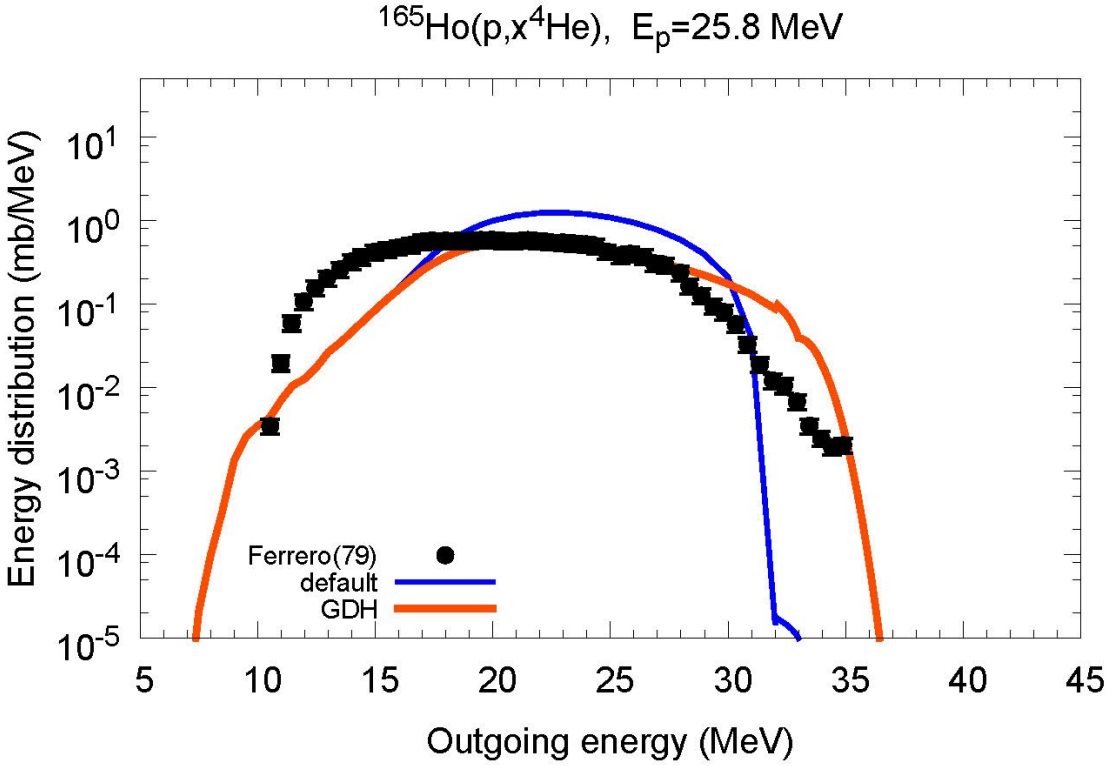
^{165}Ho(p,x^{4}He), E$_p$=25.8 MeV
Energy distribution (mb/MeV)
Outgoing energy (MeV)
Ferrero(79)
default
GDH

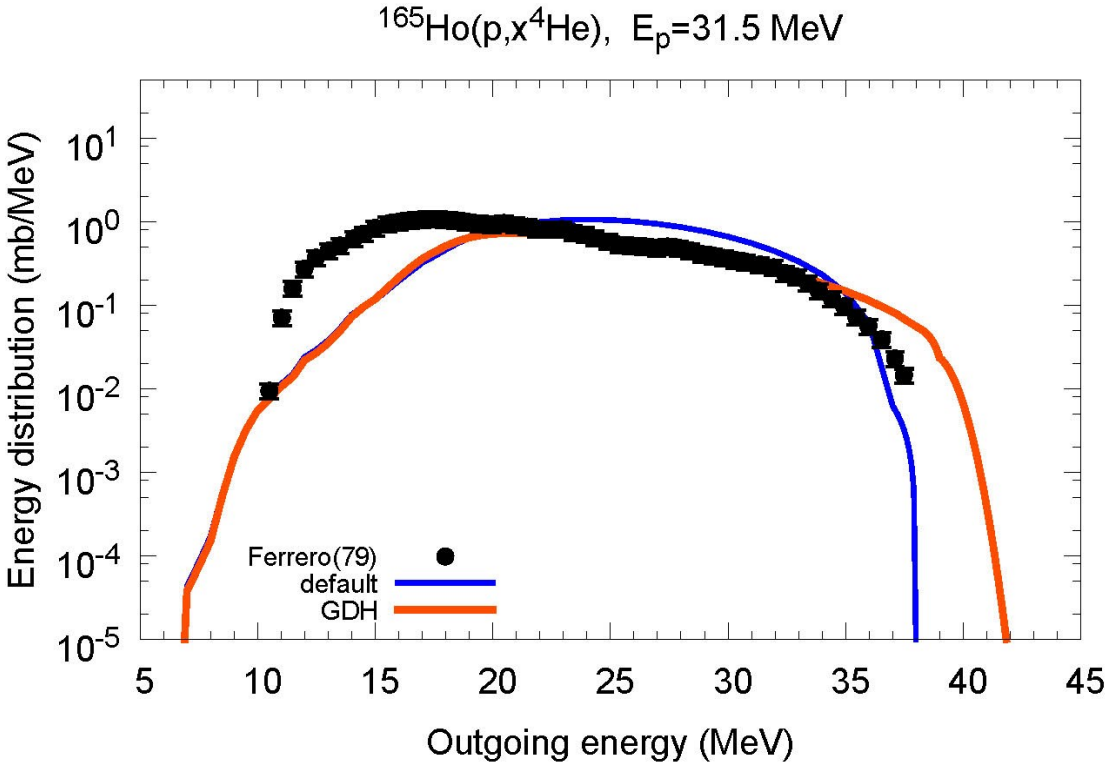
^{165}Ho(p,x^{4}He), E$_p$=31.5 MeV
Energy distribution (mb/MeV)
Outgoing energy (MeV)
Ferrero(79)
default
GDH

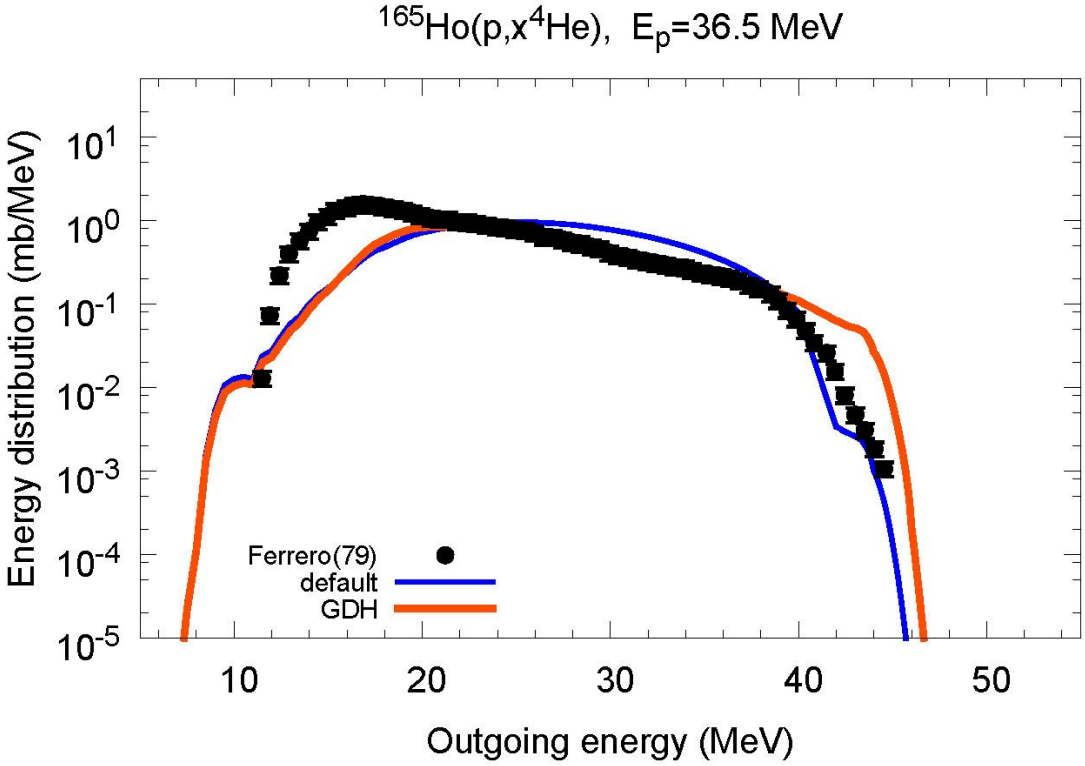
^{165}Ho(p,x^{4}He), E$_p$=36.5 MeV
Energy distribution (mb/MeV)
Outgoing energy (MeV)
Ferrero(79)
default
GDH

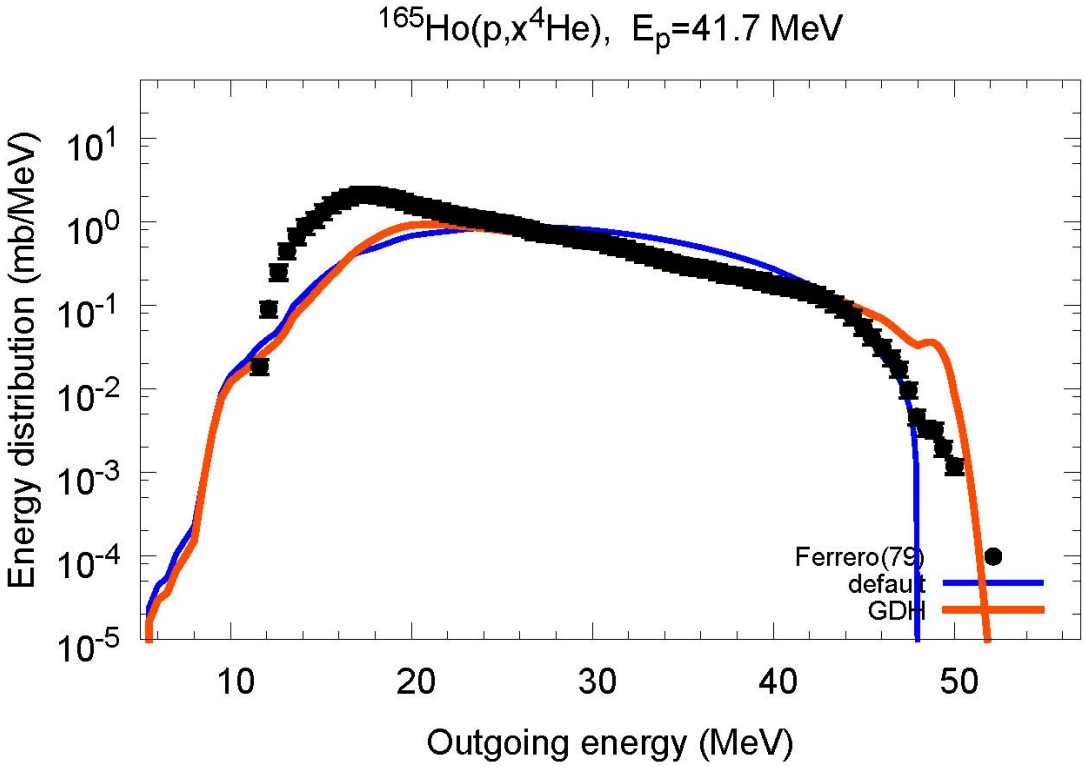
^{165}Ho(p,x^{4}He), E$_p$=41.7 MeV
Energy distribution (mb/MeV)
Outgoing energy (MeV)
Ferrero(79)
default
GDH

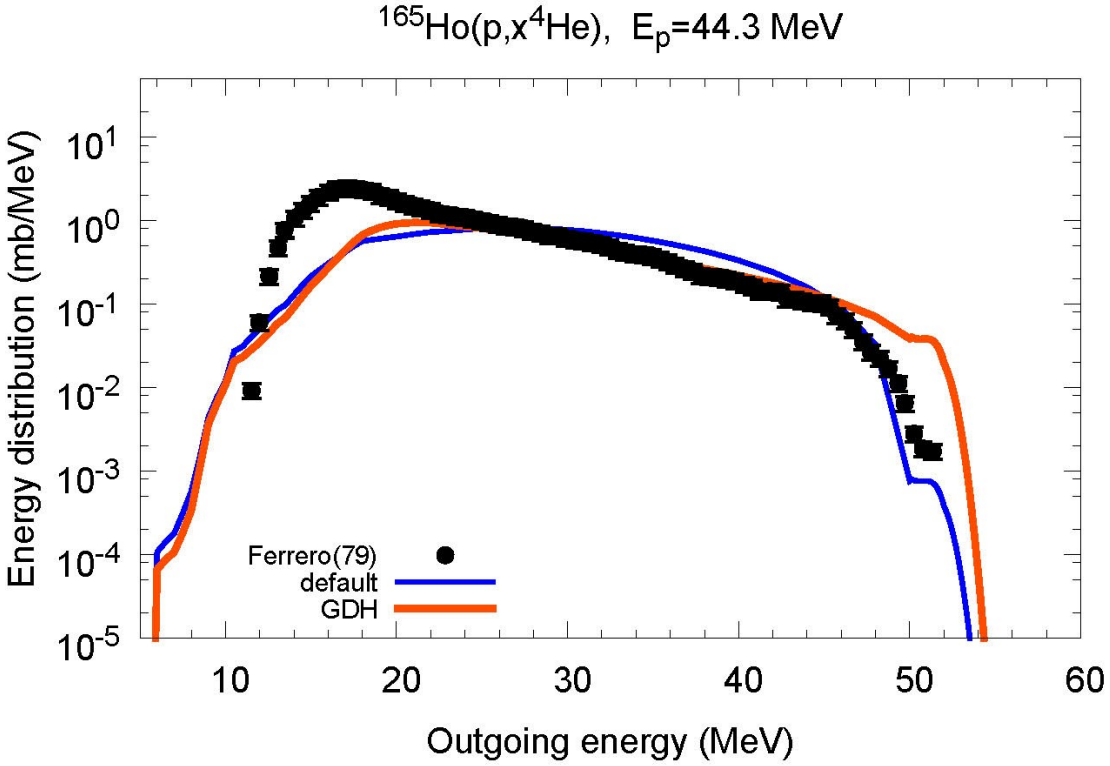
^{165}Ho(p,x^{4}He), E_p=44.3 MeV
Energy distribution (mb/MeV)
Outgoing energy (MeV)
Ferrero(79)
default
GDH

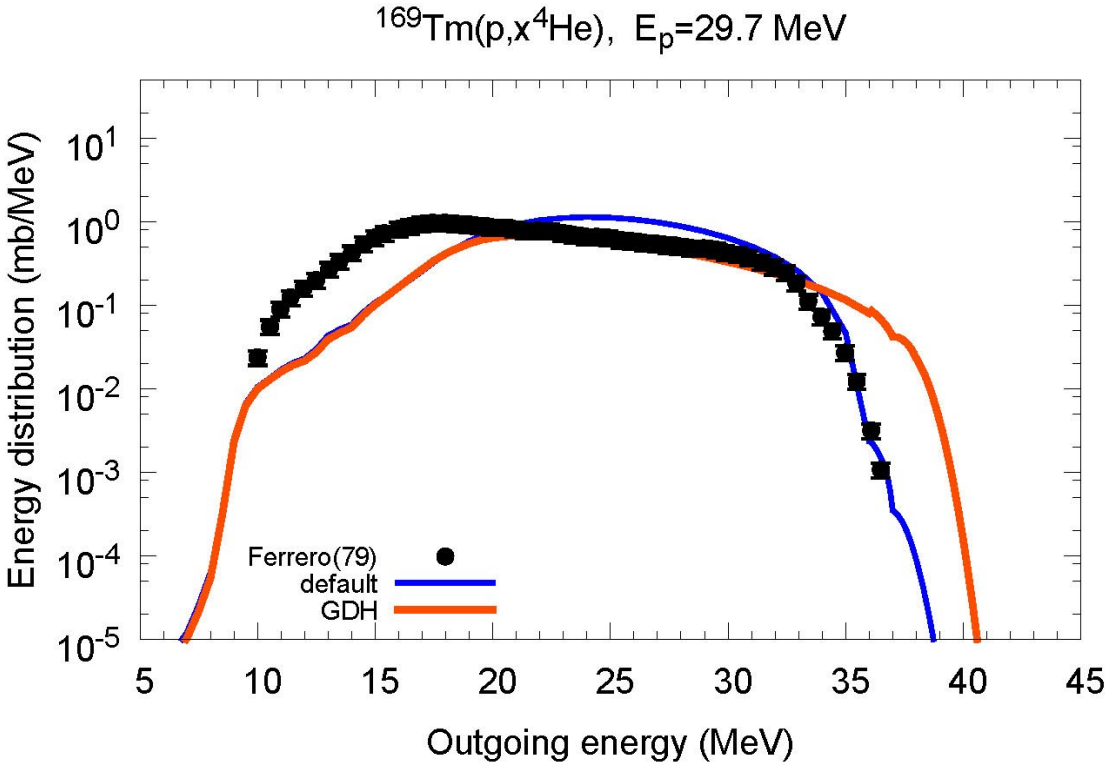
^{169}Tm(p,x^{4}He), E_p=29.7 MeV
Energy distribution (mb/MeV)
Outgoing energy (MeV)
Ferrero(79)
default
GDH

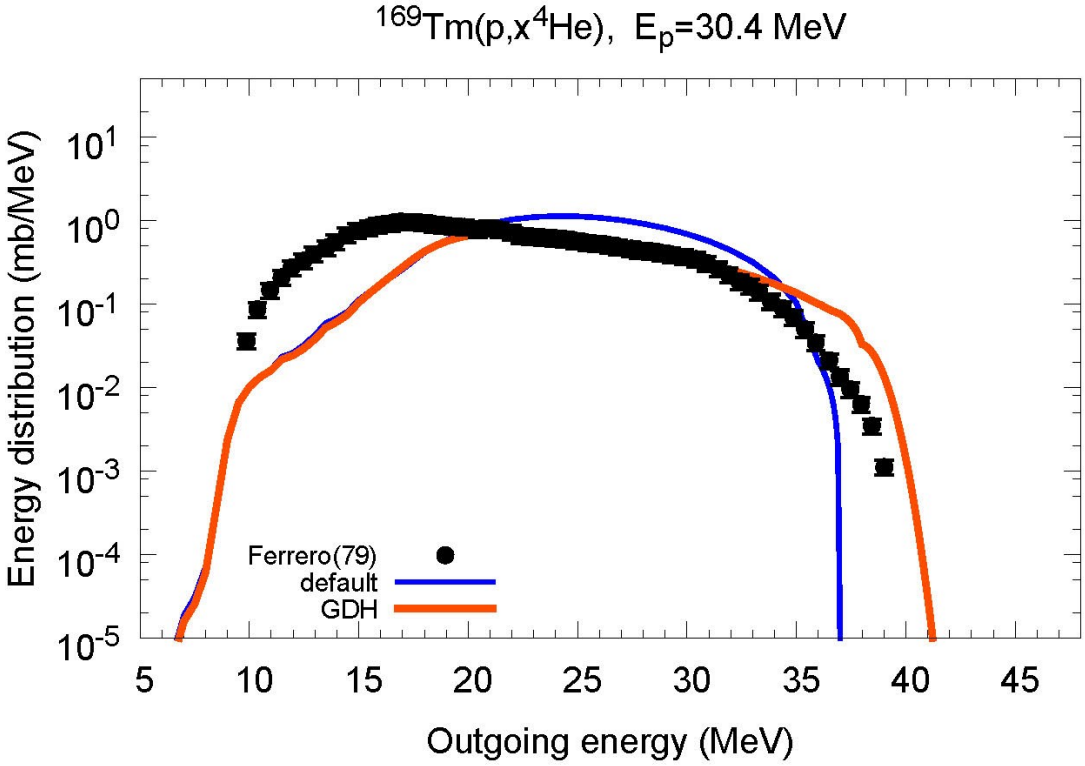
^{169}Tm(p,x^{4}He), E$_p$=30.4 MeV
Energy distribution (mb/MeV)
Outgoing energy (MeV)
Ferrero(79)
default
GDH

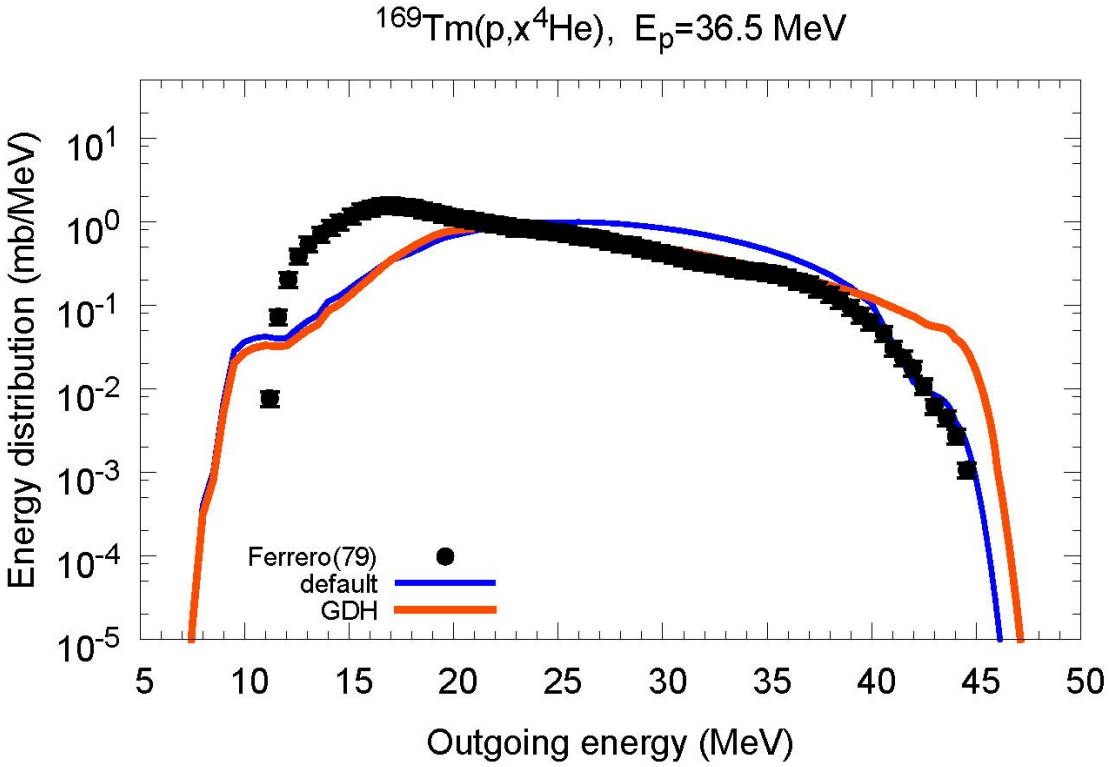
^{169}Tm(p,x^{4}He), E$_p$=36.5 MeV
Energy distribution (mb/MeV)
Outgoing energy (MeV)
Ferrero(79)
default
GDH

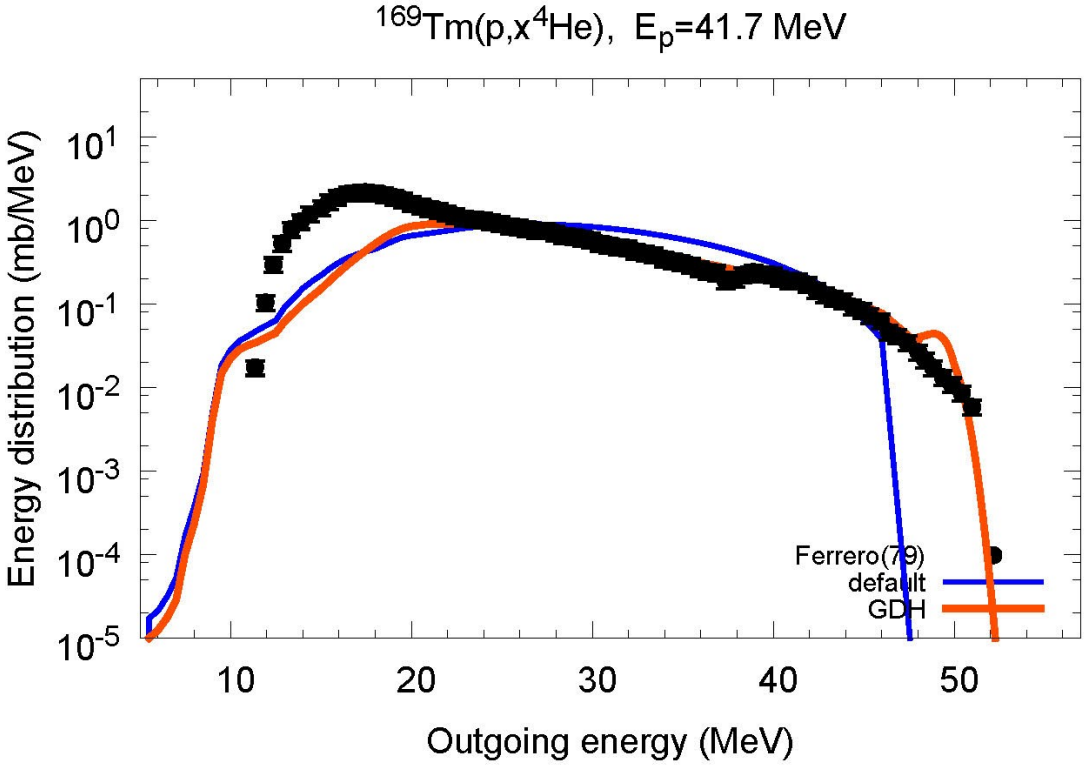
^{169}Tm(p,x^{4}He), E$_p$=41.7 MeV
Energy distribution (mb/MeV)
Outgoing energy (MeV)
Ferrero(79)
default
GDH

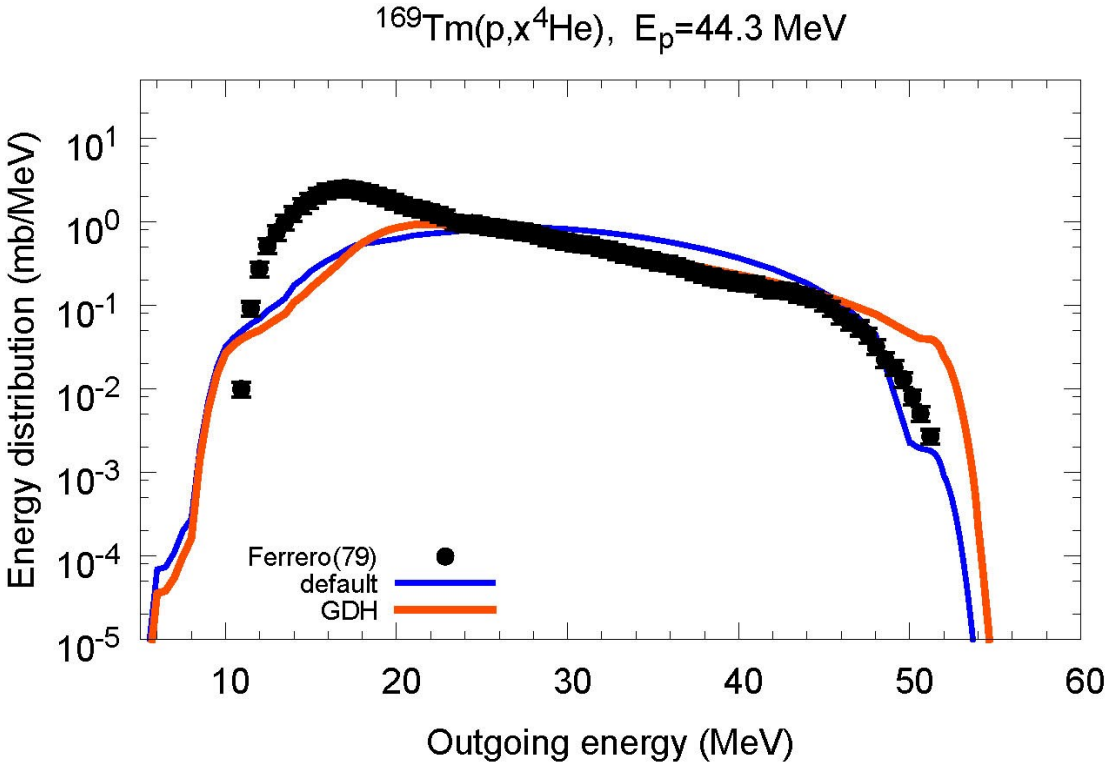
^{169}Tm(p,x^{4}He), E$_p$=44.3 MeV
Energy distribution (mb/MeV)
Outgoing energy (MeV)
Ferrero(79)
default
GDH

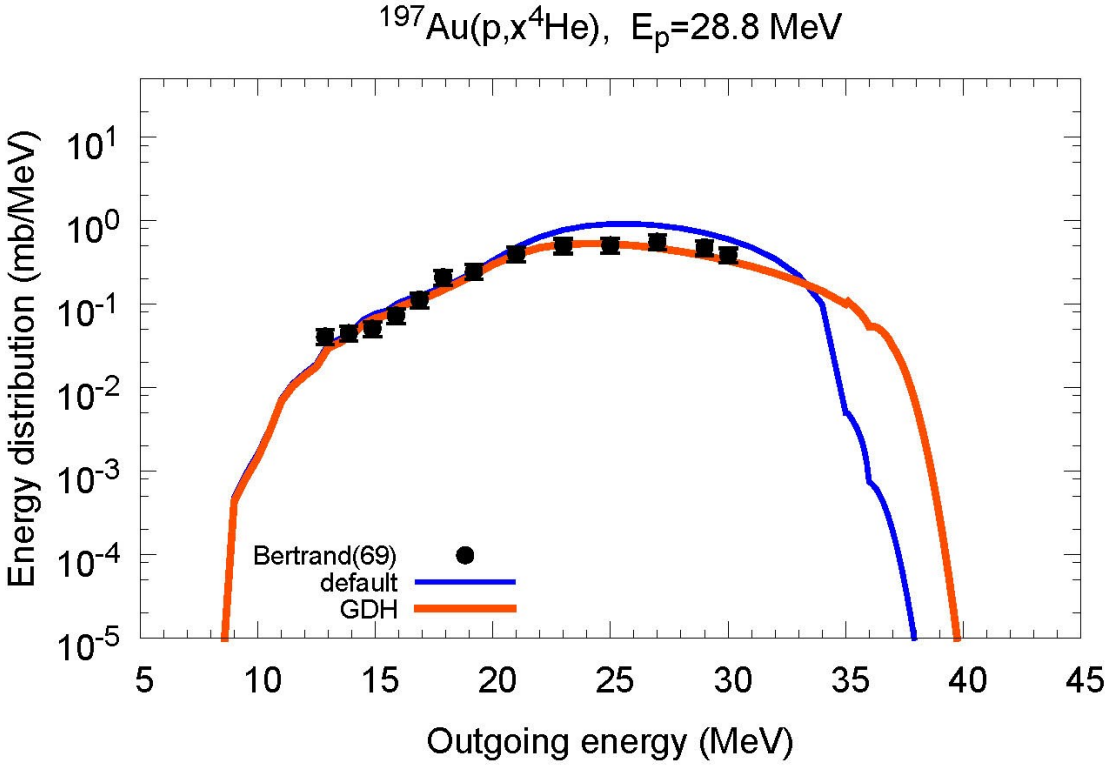
^{197}Au(p,x^{4}He), E$_p$=28.8 MeV
Energy distribution (mb/MeV)
Outgoing energy (MeV)
Bertrand(69)
default
GDH

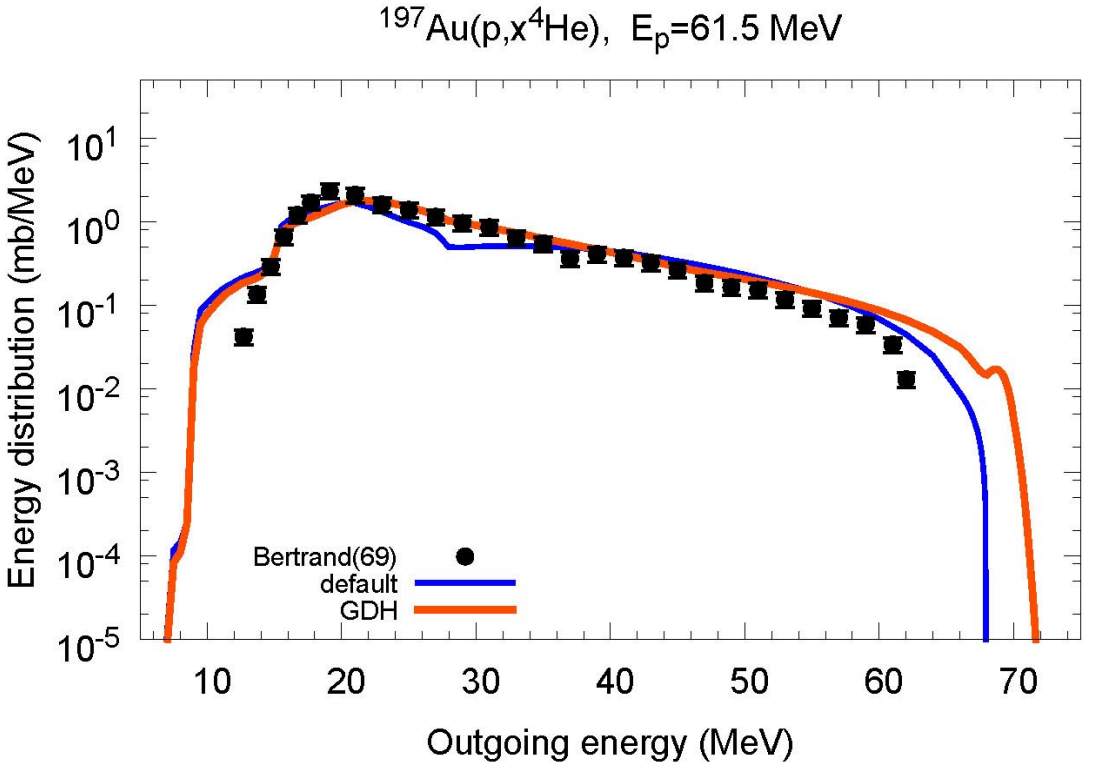
^{197}Au(p,x^{4}He), E$_p$=61.5 MeV
Energy distribution (mb/MeV)
Outgoing energy (MeV)
Bertrand(69)
default
GDH

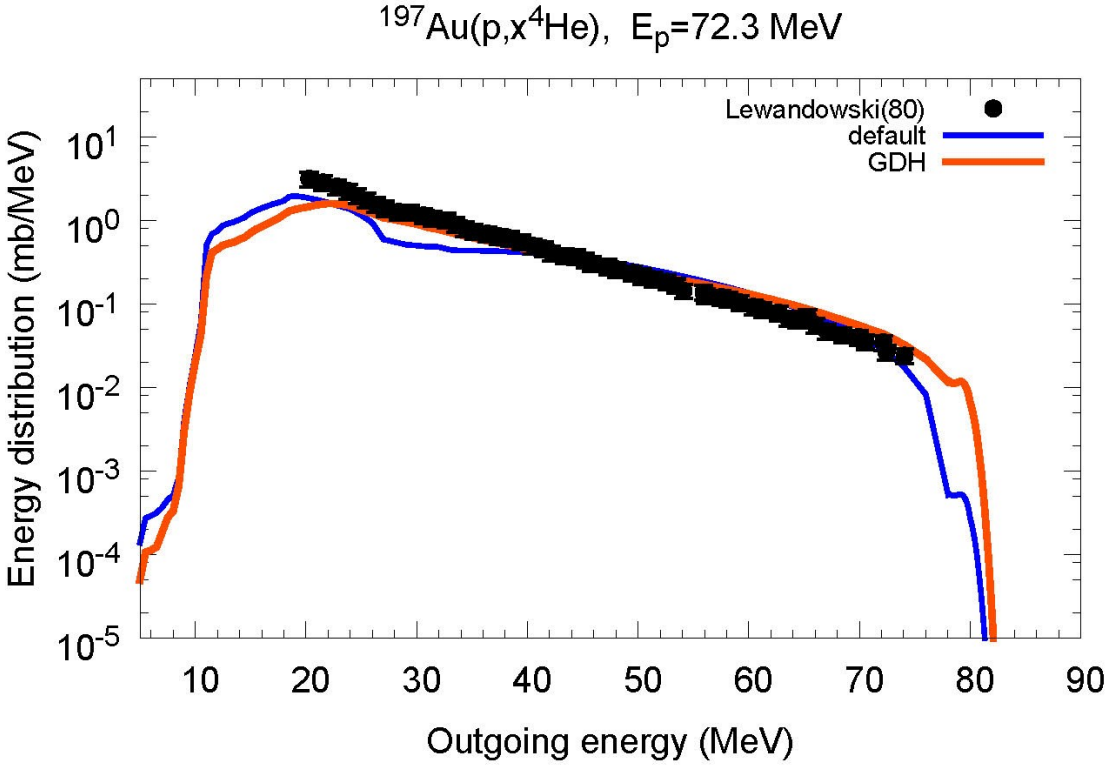
^{197}Au(p,x^{4}He), E_p=72.3 MeV
Lewandowski(80)
default
GDH
Energy distribution (mb/MeV)
Outgoing energy (MeV)

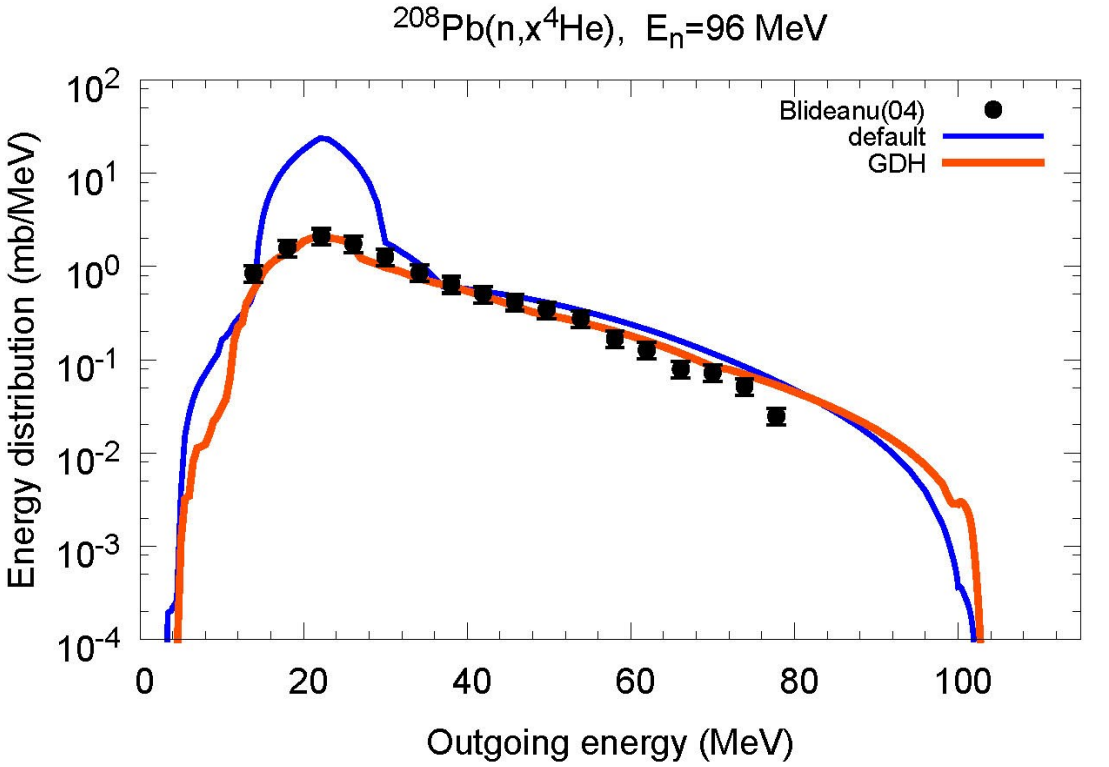
^{208}Pb(n,x^{4}He), E_n=96 MeV
Blideanu(04)
default
GDH
Energy distribution (mb/MeV)
Outgoing energy (MeV)

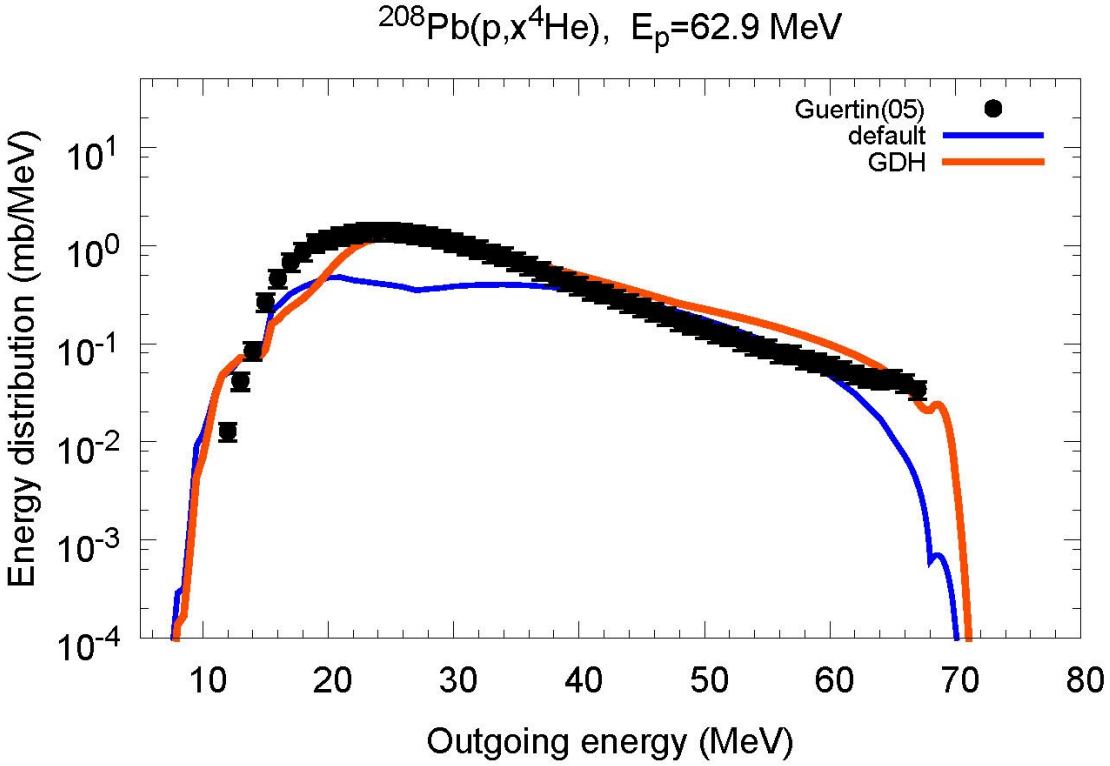
^{208}Pb(p,x^{4}He), E$_p$=62.9 MeV
Guertin(05)
default
GDH
Energy distribution (mb/MeV)
Outgoing energy (MeV)

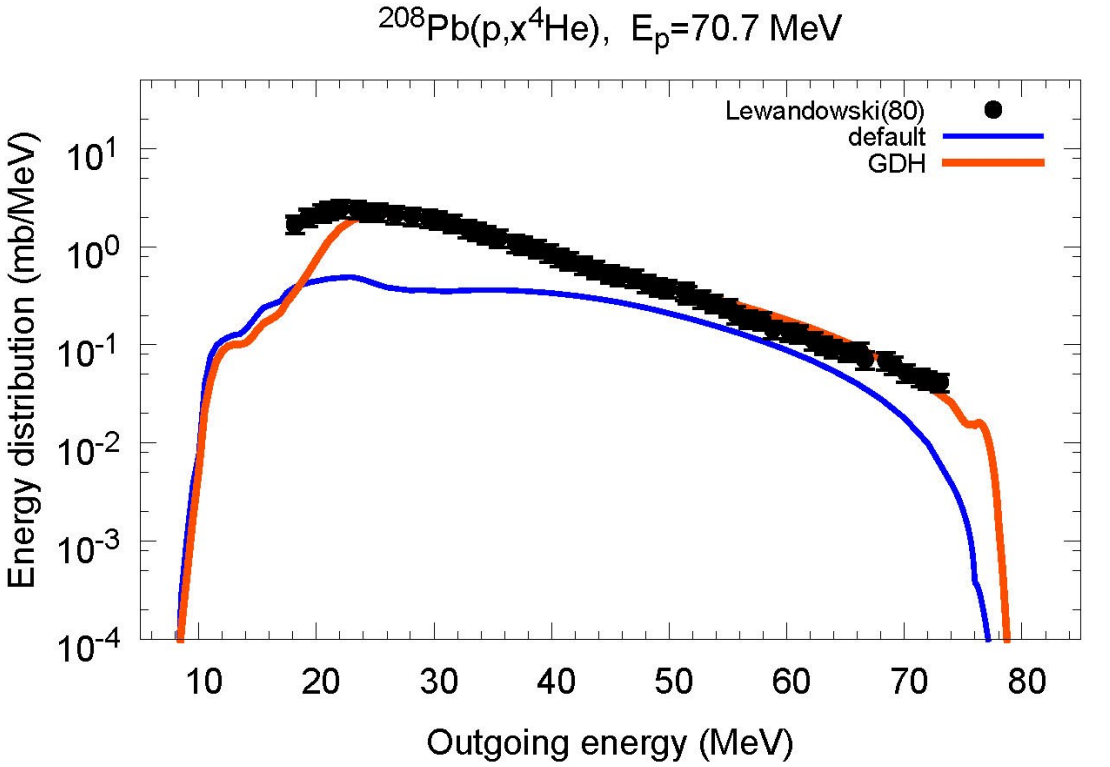
^{208}Pb(p,x^{4}He), E$_p$=70.7 MeV
Lewandowski(80)
default
GDH
Energy distribution (mb/MeV)
Outgoing energy (MeV)

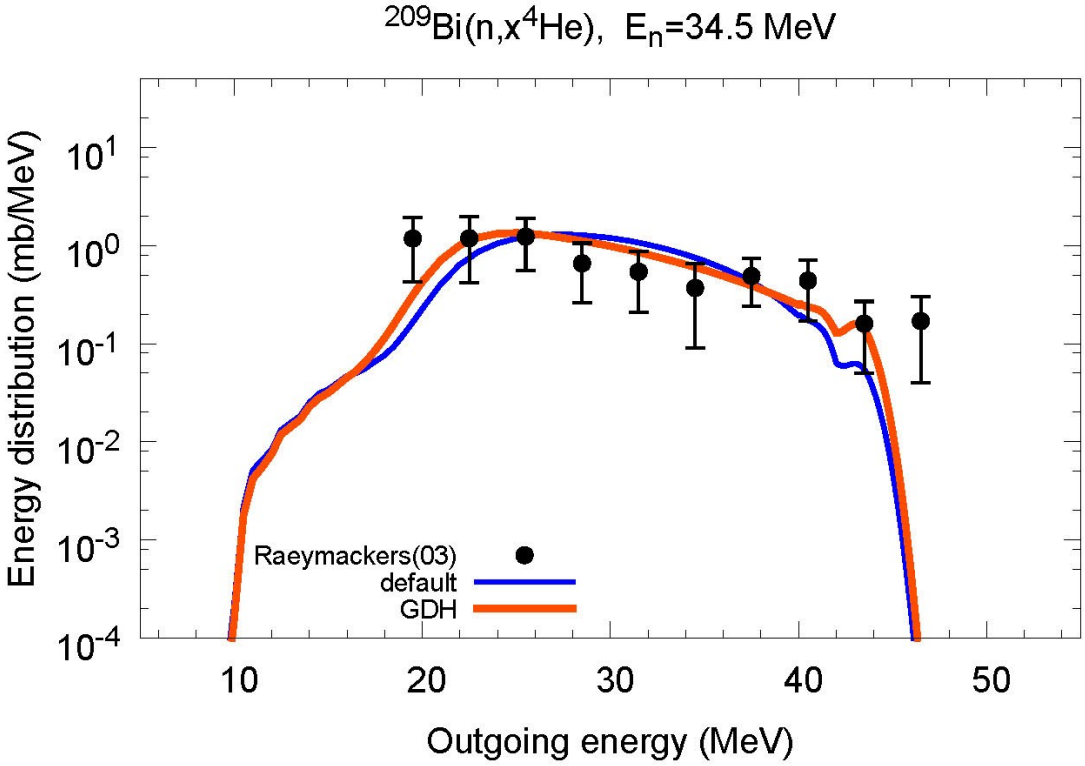
^{209}Bi(n,x^{4}He), E$_n$=34.5 MeV
Energy distribution (mb/MeV)
Outgoing energy (MeV)
Raeymackers(03)
default
GDH

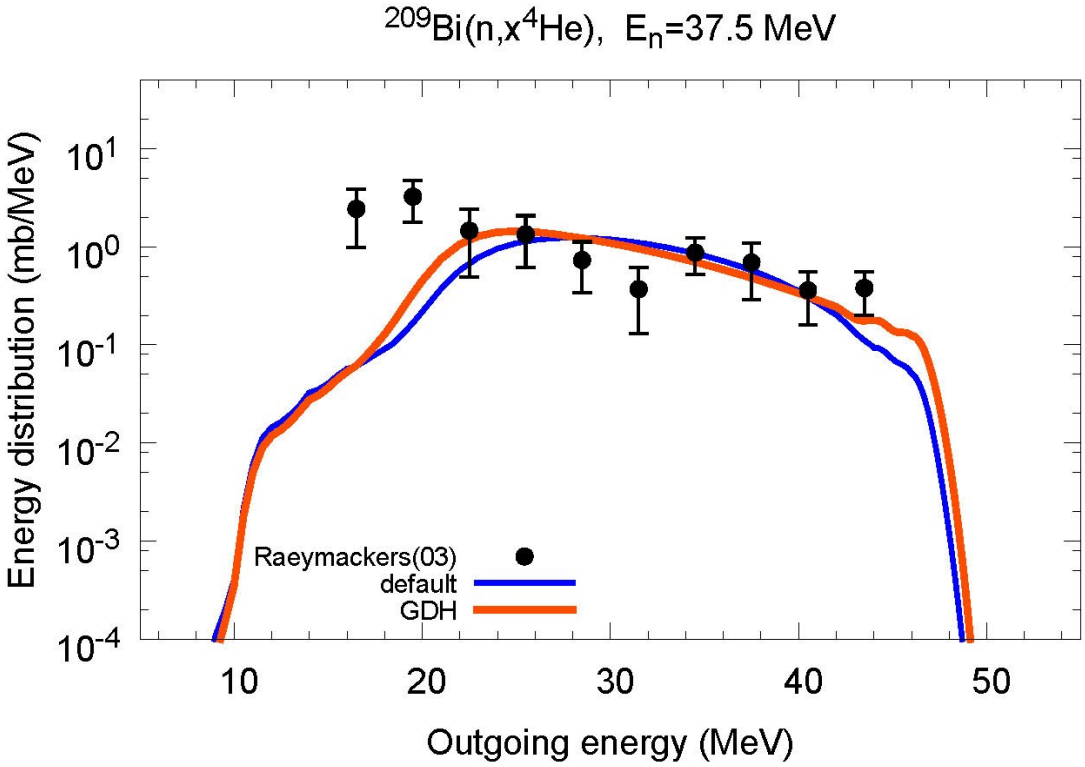
^{209}Bi(n,x^{4}He), E$_n$=37.5 MeV
Energy distribution (mb/MeV)
Outgoing energy (MeV)
Raeymackers(03)
default
GDH

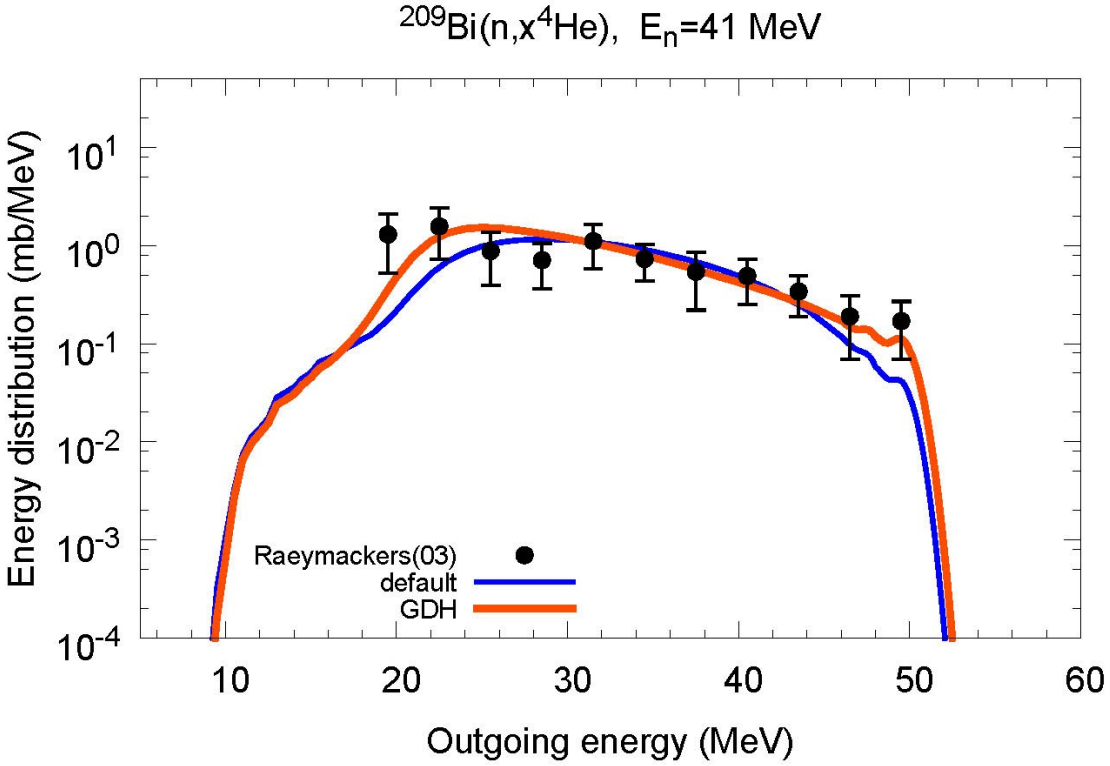
^{209}Bi(n,x^{4}He), E_n=41 MeV
Energy distribution (mb/MeV)
Outgoing energy (MeV)
Raeymackers(03)
default
GDH

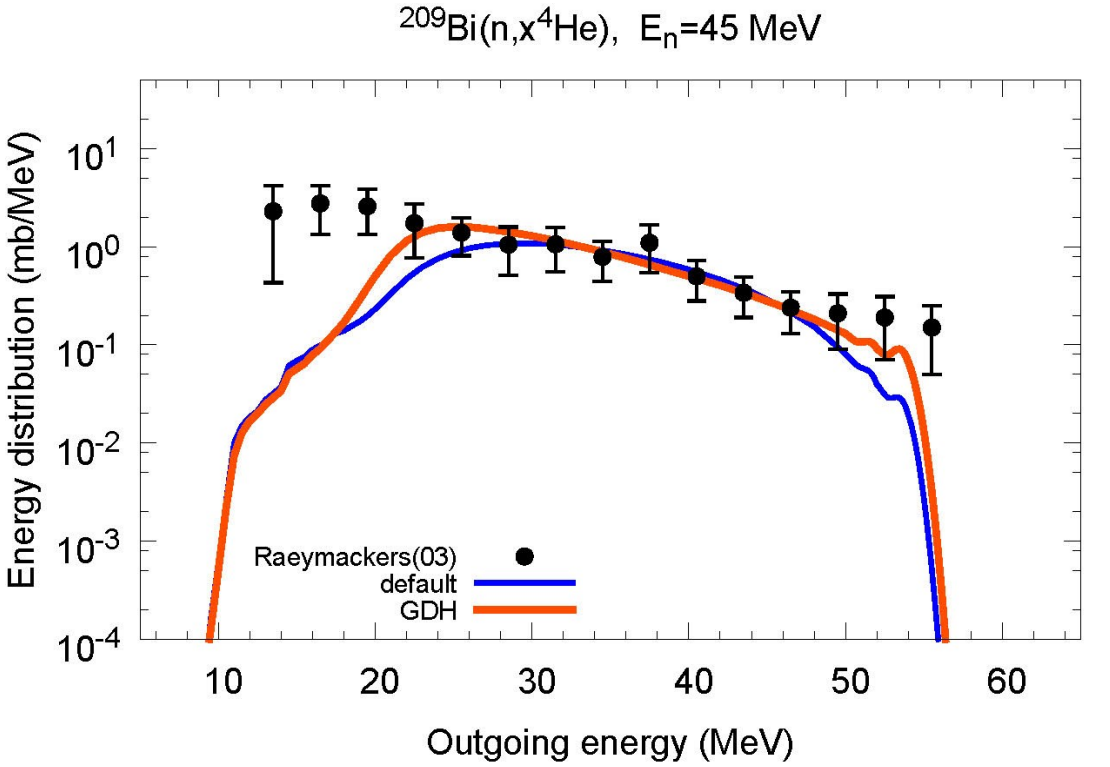
^{209}Bi(n,x^{4}He), E_n=45 MeV
Energy distribution (mb/MeV)
Outgoing energy (MeV)
Raeymackers(03)
default
GDH

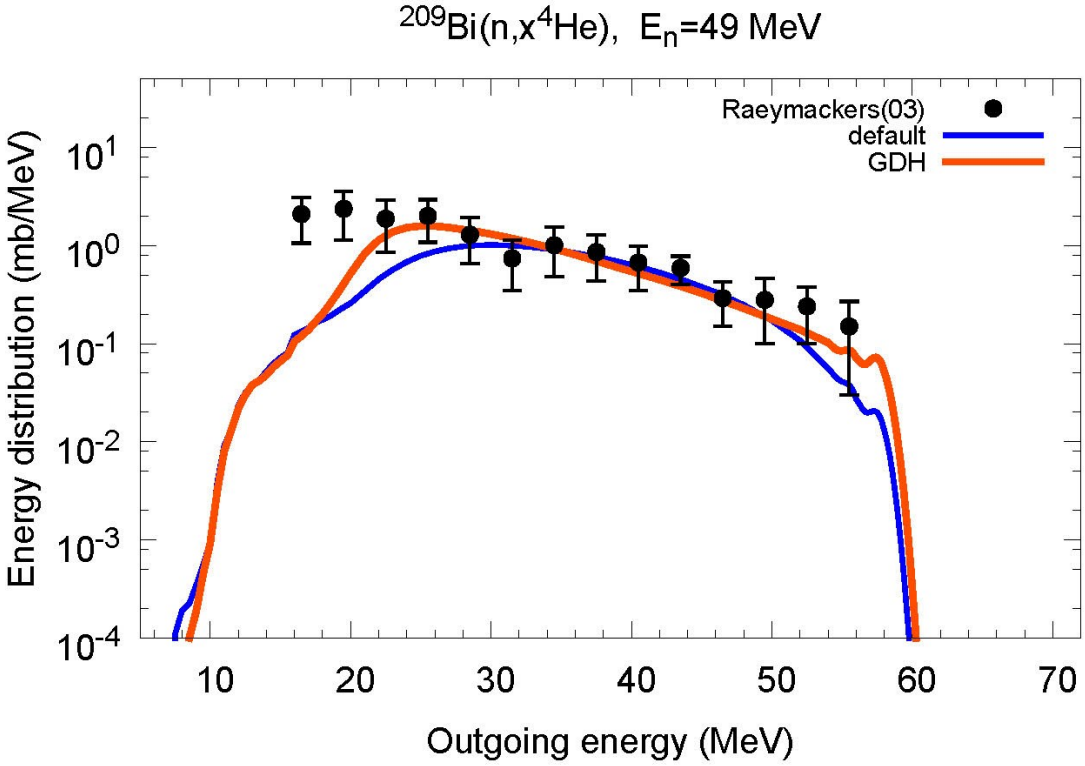
^{209}Bi(n,x^{4}He), E$_n$=49 MeV
Raeymackers(03)
default
GDH
Energy distribution (mb/MeV)
Outgoing energy (MeV)

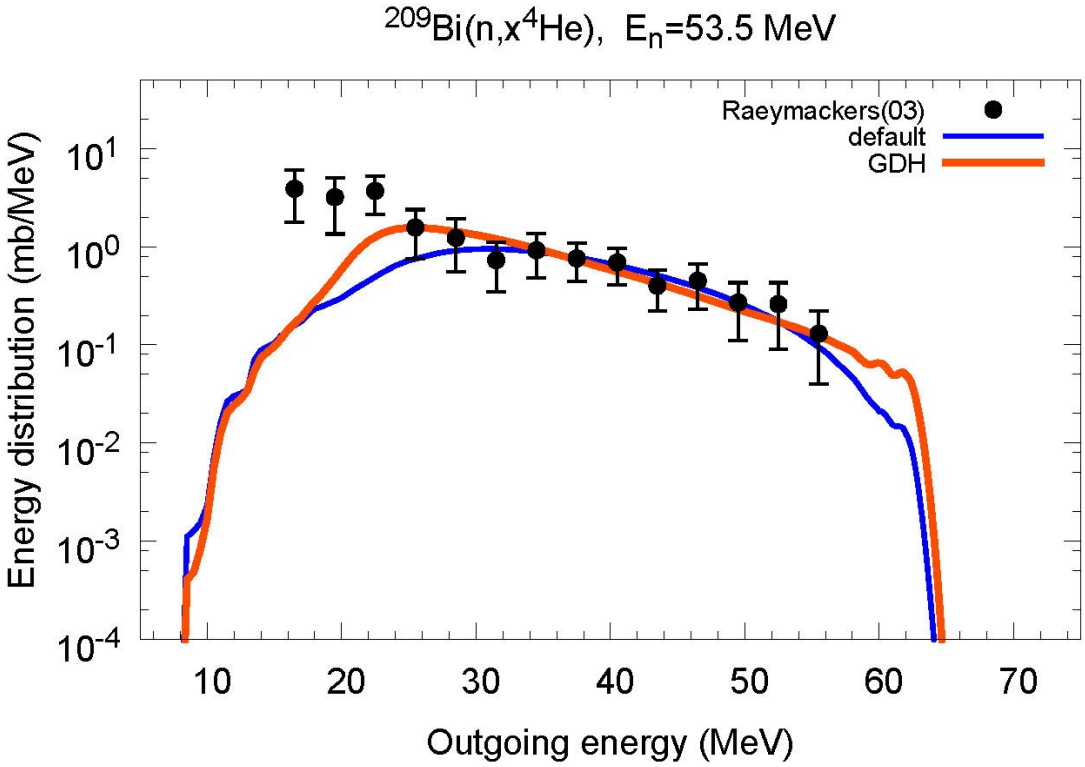
^{209}Bi(n,x^{4}He), E$_n$=53.5 MeV
Raeymackers(03)
default
GDH
Energy distribution (mb/MeV)
Outgoing energy (MeV)

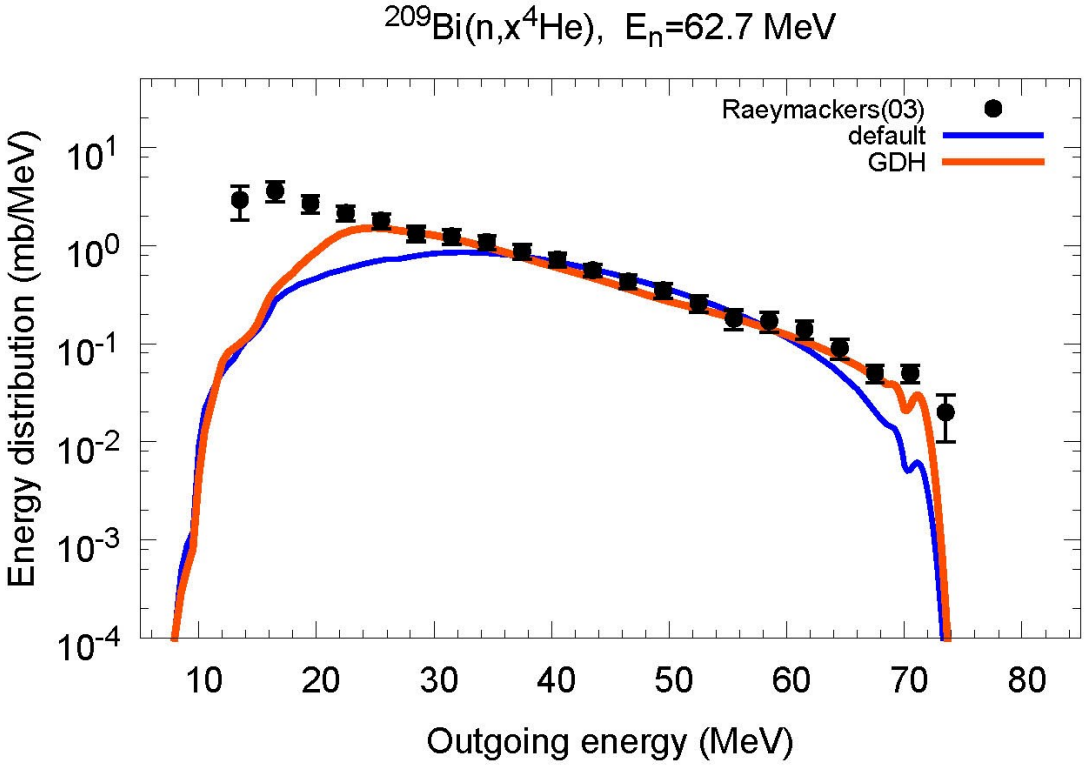
^{209}Bi(n,x^{4}He), E_n=62.7 MeV
Raeymackers(03)
default
GDH
Energy distribution (mb/MeV)
Outgoing energy (MeV)

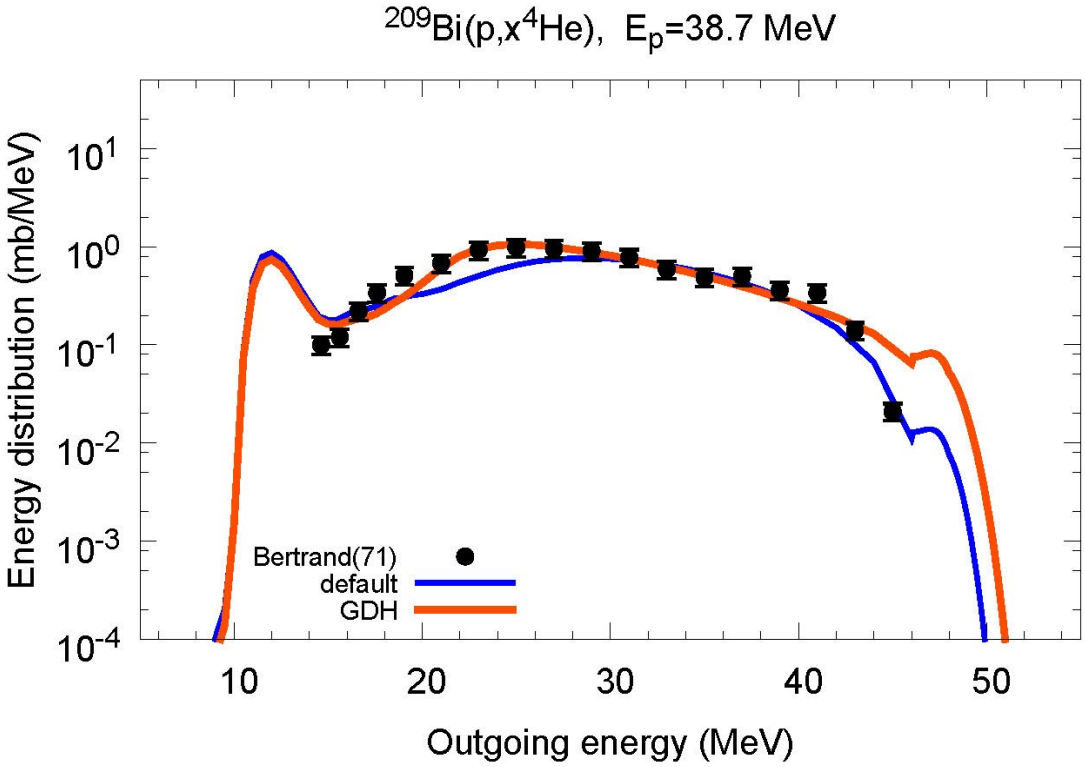
^{209}Bi(p,x^{4}He), E_p=38.7 MeV
Bertrand(71)
default
GDH
Energy distribution (mb/MeV)
Outgoing energy (MeV)

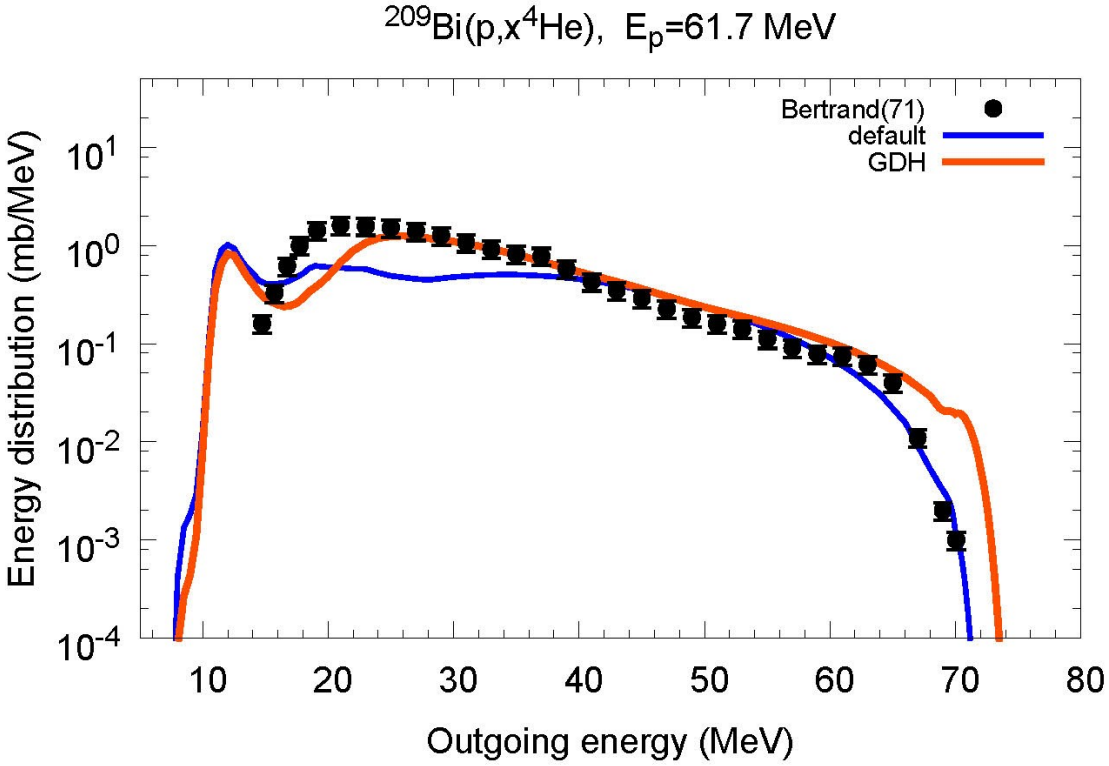
^{209}Bi(p,x^{4}He), E$_p$=61.7 MeV
Bertrand(71)
default
GDH
Energy distribution (mb/MeV)
Outgoing energy (MeV)

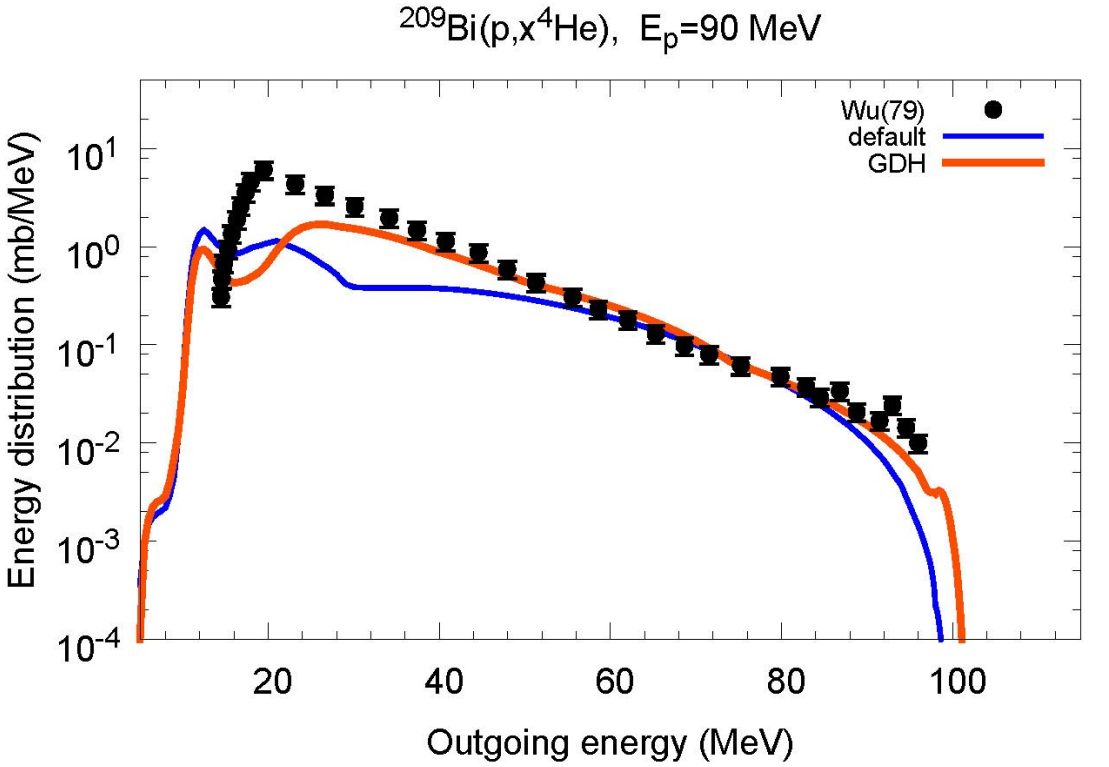
^{209}Bi(p,x^{4}He), E$_p$=90 MeV
Wu(79)
default
GDH
Energy distribution (mb/MeV)
Outgoing energy (MeV)

KIT Scientific Working Papers
ISSN 2194-1629

www.kit.edu